Sediment Dynamics of a Shallow Exposed Surfing Headland

A thesis submitted for the requirements
for the Degree of

Doctor of Philosophy

in Earth Sciences

at the University of Waikato

by

David John Phillips

November 2004

Raglan headland 1955 (Source: Geosmart, 5 April 1955).

ABSTRACT

A study of the wave, current and sediment dynamics was conducted at a shallow and exposed world-class surfing headland at Raglan, on the west coast of New Zealand to determine the mechanism for sustaining the sandy seabed. The location features a large-scale headland with titano-magnetite iron sand dominant on the seabed, adjacent to a rocky reef and boulder shoreline. Field experiments were conducted at the headland involving (i) wave, current and suspended sediment measurements, (ii) side-scan sonar surveys, (iii) hydrographic surveys and (iv) seabed sampling and ground truth observations by divers. Waves and currents were numerically modelled using the 3DD model suite (Black, 2001), with model outputs showing a strong comparison to the measured field data.

The results show that the mechanism responsible for maintaining the sandy seabed at the Raglan headland is a combination of sediment transport around the headland to the east (i.e. west coast littoral drift system), and a local re-circulating sediment pathway transporting sediment in the west direction. Sediment moves continually around the headland supplying the littoral system at the headland, and not in "slugs' as reported for other large protruding headlands. The net sediment flux was approximately 275000 m^3/yr flowing east inshore and 100000 m^3/yr to the west offshore. The difference of 175000 m^3/yr flows from the headland littoral cell into the northwards flowing longshore transport system of the west coast. This compares well to the previous estimate of 175000 m^3/yr of net transport along the coast.

The alignment of the Raglan headland provides an environment where waves of a high oblique angle generate strong wave-driven currents in the surf-zone, flowing inshore along the headland in an easterly direction. Alternatively, a westerly flowing current is generated by the interaction of wave-driven forces and topographic steering where alignment of the headland changes. Numerical model outputs show the presence of recirculating eddy flows in four cells, which compare very closely to the

compartmentalisation of the headland characterised by the main surf breaks, with the width and velocity of the current flows depending on both the size of the swell and the level of the tide. Large wave events at low tide generate the strongest currents flowing east along the headland inshore, whilst at high tide the westerly current also reaches its greatest velocity, and the eddy flows are at their most prevalent. The large inshore currents flowing along the headland decrease the surfability of a headland and make the break difficult if not impossible to surf. However, the large scale and variation in topographic alignment of the Raglan headland can allow access for surfers in the zones of lower wave height and decreased current velocity (e.g. Whale Bay reef). It is recommended that the affect of strong currents on surfability be considered in the design of artificial surfing reefs if amenity of the structure is to be maximised.

The wave-orbital interaction with the hydrodynamically 'rough' substrate on the rocky boulder reef creates a greater turbulent flow over these beds. Sediment is unable to settle in this zone and is scoured or winnowed away to leave the rocky bed exposed. The regions further shoreward are influenced by the easterly flowing currents more often eroding sand away in the absence of sufficient upstream inputs to maintain the sediment flux. The location of the interface between the sand and rocky seafloor corresponds to the point where the long-term mean currents change from flowing easterly to flowing westerly along the headland. Side scan sonar surveys showed the interface generally followed the shape of the headland and remained fairly stable in position. This is confirmed by the bathymetric surveys where despite significant volume changes in the quantity of sand being transported or deposited at the headland, the seabed level fluctuates about a stable long-term equilibrium position of the bed (quasi permanent position). This is supported by the long-term habitation and zonation of marine organisms on the sub-tidal reef edge, demonstrating an upper level of seabed movement. The characteristics of the seabed in the study area reflect the presence of the surf zone and strong unidirectional currents to the east, and show re-circulating sediment pathways flowing to the west.

I would like to acknowledge the following people who contributed to my thesis (Raglan headland and fieldwork site in the background):

DEDICATION

I would like to dedicate this work to my dad (Thomas D. Phillips), who passed away before I had finished this thesis. Thanks so much dad for the love, support, encouragement and interest in my work.

ACKNOWLEDGEMENTS

I would like to thank most importantly my wife (Fi) for her love, advice, support and encouragement on the journey that is a doctorate thesis, especially a part-time PhD on top of a full-time job, and for being such a wonderful mother to our son (Tommy) whilst I undertook this project and spent many days and nights away at the field site, university and at the computer. To my Mum, Peter, Sally, Mike, Bev, Pete and the rest of my whanau (family) I appreciate your interest in the thesis and thankyou so much for the

encouragement you gave me to complete this project. It was great to have you help with the fieldwork Mike. I give sincere thanks to my employers at UNITEC and both Jonathan Leaver and Prof. Graham Smith, and the staff of the School of Civil and Environmental Engineering for the support and opportunity to upgrade my qualifications and grow as a person. I would also especially like to thank Prof. Kerry Black for acting as my supervisor and for maintaining the role after leaving the University, and Prof. Terry Healy for taking up the position and editing the thesis when Kerry departed. Thanks guys, I greatly appreciate the time and expertise you both gave me. Your level of excellence is a true inspiration. Thanks also to Dr Shaw Mead who got me stoked to go on this journey and helped along the way. Thanks dude sure was a great experience. Thanks also to Kerry and Shaw for allowing me to continue using the numerical model 3DD and for the use of the ASR Ltd office computers, and the flat for accommodation in Raglan. Kiaora to the Tainui iwi at Raglan for endorsing the research at the headland. Thanks to Dirk Immenga for the technical work in the field and for venturing out so many times to the "wild" west coast that often provided very challenging fieldwork conditions. It certainly was an experience dodging the boat around large breaking waves and diving in zero visibility under the waves. Thanks also to Dr Brett Beamsley, James Beam, Brad Scarfe, Hayden Easton, Dr Scott Stephens and other graduate students who assisted over the years with fieldwork and advice, Dr Richard Gorman for helping solve my Matlab and Tseries problems, and to Shaw and Angela for allowing me to stay so many times at their house at Raglan. Kiaora to you all, Dave. And of course thanks must go to the waves at Raglan for providing me with so many great surf sessions after the work was done, which was not only great fun but also allowed me to observe and experience the dynamics of the headland first hand.

TABLE OF CONTENTS

LIST OF FIGURES

LIST OF TABLES

CHAPTER ONE

PERSPECTIVES OF A SURFING HEADLAND

1.1 INTRODUCTION

1.1.1 *Raglan – Surfing Perspectives*

My interest in the headland at Raglan began many years ago, when I made my first surfing trip to a town that had a left hand point break of world class surfing reputation (Fig. 1.1). A surfer feels a great adrenaline rush when they see a perfect peeling wave, and to actually ride that energy is an even greater soulful or stoked feeling. I have a similar inspirational feeling to be studying and attempting to understand what is essentially *taonga*[1] to the surfing and wider community of Raglan and New Zealand.

[1] *Taonga* Elements of the natural world that are greatly treasured by the Maori culture.

The inspiration and vision came from Professor Kerry Black, who with the support of Professor Terry Healy, initiated a research program (The Artificial Reef Program) that focused on the potential of surfing reefs to not only provide surfing waves, but also to protect the coast from erosion. Recognition that nature could provide specific examples of utilising ocean energy for surfing waves and a research team that pursues excellence, were the driving forces for my interest in this study.

Figure 1.1: Waves peeling along the headland at Raglan (Source: J and M Milek, 2000).

This thesis focuses not only on the surfing aspects of the headland, but also on the understanding of the coastal processes in this environment. The resulting data and insight will lead to greater scientific and engineering knowledge, of application both for coastal protection and the future development of artificial surfing reefs, such as the large scale submerged headland constructed at Narrowneck on the Gold Coast of Australia.

1.1.2 *Dynamics of a surfing headland*

The circulation and sediment dynamics on the headland promontory formed from the Karioi andesitic cone near Raglan have never been studied, yet the passage of sand bypassing these headlands is fundamental to an understanding of sediment movement along much of New Zealand's west coast.

The coastal processes of waves on beaches are well known (e.g. Beer, 1997; Komar, 1998; Short, 1999). Cases of extreme erosion are seen in large storm events; however methods to prevent this erosion are still being debated. Occasionally extreme measures such as evacuation of residents or the moving of houses inland is required to protect property and human life, but mostly coastal protection with rocks (riprap) or other structures is undertaken (Herbich, 2000; Kamphuis, 2000). In addition, construction and dredging around the coasts has placed pressure on the coastal marine environment. These methods can be classified as "end of the pipe solutions", but without a good understanding of the movement of the sand around headlands the most appropriate strategy in this environment is difficult to ascertain.

Previous studies on New Zealand's west coast have shown that the total longshore drift and net sediment movement is to the north (e.g. Mattews, 1977; Gibb, 1979; Hicks and Hume, 1993; McComb, 2002). However, there has been no previous research undertaken at Raglan on the effect that this natural headland feature has on the littoral transport and sediment dynamics of the coast. Observations show that longshore currents are strong and directed 'east' along the headland when large waves are present. Such currents would be expected to transport large quantities of sediment around the headland. Thus, the general aim to be addressed in this thesis is to investigate how headlands such as at Raglan maintain the sand bed in the presence of strong shoreward currents and potentially large net sediment fluxes that occur during large swell events.

1.2 *OBJECTIVES OF THESIS*

The specific objectives of the study are to:

1. Investigate the currents and sediment movement around the surfing headland near Raglan, by recording currents and suspended sediment concentrations during a range of wave conditions on cross-shore transects.

2. Undertake side-scan sonar and hydrographic surveys of the seabed to distinguish sedimentary characteristics and determine changes in the pattern of the seafloor sediments and rock surfaces.

3. Numerically model the wave-driven flows at the headland to develop theory on wave and current characteristics along the headland.

4. Assess the effect of currents on surfability of headlands and artificial reefs, including implications for future designs.

1.3 *RESEARCH PROCEDURES*

In order to achieve the listed objectives a range of field experiments were undertaken to determine the stability, sediment dynamics and characteristics of the seabed at Indicators (a breaking wave section) on the Raglan headland. The experimental procedures include:

1. Undertaking field experiments and the recording of waves and currents simultaneously with sediment concentration in the water column, both inside and outside the surf zone, across a line transect at Indicators (Fig. 1.2). This was accomplished using a bottom-frame supporting a current/wave recorder and wave pressure sensors (S4) and a series of sediment traps mounted at 3 different elevations above the bed. Together these instruments measure the waves, currents and suspended sediment load. The data were analysed by

relating waves, currents and the wave orbital motion to suspended sediment load.

2. Undertaking side-scan sonar surveys to determine characteristics of the seafloor and examine variability in the location of the sand/rock interference. These were conducted both seasonally and over a specific time period of swell duration, to determine the immediate effect on the bed. The side scan also recorded bedforms on the seafloor, which are prime indicators of sediment transport.

3. Undertaking bed level monitoring through the use of hydrographic surveys to provide bathymetric maps of the seabed. A Trimble Real Time Kinematic (RTK) Geographic Positioning System (GPS), was utilised to gather this data, and maps were produced and bed level change analysed using the SURFER software.

4. Numerical computer modelling using the software model suite 3DD (Black, 2001a) for the purpose of determining the wave and current characteristics at the headland.

1.4 THESIS STRUCTURE

Chapter 1 describes the motive and background for the study, thesis objectives, structure and methodology, glossary of surfing terms, contribution and relationship to the scientific knowledge and related programmes, and a general description of the study site on the headland south of Raglan.

Chapter 2 provides a literature review of the geomorphology, sediment dynamics and seabed characteristics of headlands, with a particular focus on surfing headlands and their wave and sediment characteristics. Scientific information on the west coast of New Zealand is also reviewed, to obtain an understanding of the sand characteristics, coastal processes and systems that are apparent on this coast.

The application of artificial headlands and surfing reefs in the coastal environment are also investigated. Parts of this chapter on currents and surfability of headlands were peer reviewed/refereed and published as:

Phillips, D.J., Mead, S.T., Black, K.P. and T.R. Healy., 2003. Surf Zone Currents and Influence on Surfability. *Surfing Reefs 2003*. The 3rd International Conference. Raglan, New Zealand. pp. 60-82 (Appendix 1 contains the fully reproduced paper).

Chapter 3 describes the seabed characteristics of the headland, focusing on the seafloor sediment texture and habitation of marine organisms. Parts of this chapter were peer reviewed/refereed and published as:

Phillips, D.J., Black, K.P. and T.R. Healy., 2001. Seabed Characteristics of a Dynamic Exposed Headland. *Coasts and Ports 2001*, Gold Coast, Australia. pp. 400-405 (Appendix 2 contains the fully reproduced paper).

Chapter 4 comprises the results of bathymetric surveys undertaken to determine the temporal and spatial seafloor volume changes at the headland. Bathymetric charts of the seabed are produced using highly accurate Real Time Kinematic Global Positioning Systems (RTK GPS) and a KNUDSON depth sounder. Conclusions are made from the analysis of field data showing changes to the level of the seabed at the headland. This chapter was peer reviewed/refereed and published as:

Phillips, D.J., Black, K.P. and T.R. Healy., 2003. Sandy Seafloor Volume Changes off a High Energy Headland Boulder Beach, Raglan, New Zealand. *Coasts and Ports 2003*, Auckland, New Zealand. CD Publication: Paper No. 115, 8 p. ISBN: 0-473-09801-6 (Appendix 3 contains the fully reproduced paper).

and aspects of the fieldwork methodology were peer reviewed/refereed and published as:

Scarfe, B.E., Black, K.P., Chong, A.K., de Lange, W.L., Phillips, D.J. and S.T. Mead., 2002. The Application of Surveying Techniques to Artificial Surfing Reef Studies. *Trans Tasman Surveyor. Journal of the New Zealand Institute of Surveyors*, 5, 29-40. (Appendix 3 contains the fully reproduced paper).

Chapter 5 comprises the results of repetitive side-scan sonar surveys that identify the location, orientation and size of bedforms and seabed characteristics, and define any temporal and spatial change in the rock/sand boundary at the headland. Parts of the chapter were peer reviewed/refereed and published as:

Phillips, D.J., Black, K.P. and T.R. Healy., 2001. Seabed Characteristics of a Dynamic Exposed Headland. *Coasts and Ports 2001,* Gold Coast, Australia. pp. 400-405 (Appendix 2 contains the fully reproduced paper).

A conference presentation on parts of the chapter included:

Phillips, D., Black, K., Hume, T., and T.R. Healy., 1999. Seabed Characteristics of a Large Surfing Headland. New Zealand Marine Sciences Society Annual Conference, 1-3 September. University of Victoria, Wellington, NZ (Appendix 6 contains the abstract).

Chapter 6 comprises the results of the wave and current measurements at the headland. Parts of this chapter were peer reviewed/refereed and published as:

Phillips, D.J., Mead, S.T., Black, K.P. and T.R. Healy., 2003. Surf Zone Currents and Influence on Surfability. *Surfing Reefs 2003*. The 3rd International Conference, Raglan, New Zealand. pp. 60-82. CD Publication, ISBN: 0-473-09801-6 (Appendix 1 contains the fully reproduced paper).

Phillips, D., Black, K., Hume, T., and T.R. Healy., 1999. Sediment Dynamics Along a Surfing Headland. *Coasts & Ports 99: Challenges and Directions for the New Century,* Perth, Australia. Vol. 2, pp. 513-518. (Appendix 4 contains the fully reproduced paper).

Chapter 7 comprises the results of the sediment trap data and discusses the sediment transport pathways at the headland. Parts of this chapter were peer reviewed/refereed and published as:

Phillips, D., Black, K., Hume, T., and T.R. Healy., 1999. Sediment Dynamics Along a Surfing Headland. *Coasts & Ports '99,* Perth, Australia. pp. 513-518 (Appendix 4 contains the fully reproduced paper).

A poster paper and conference presentation on parts of the chapter included:

Phillips, D.J., Black, K.P. and Healy, T.R. 2000. Sediment Transport along a Surfing Headland at Raglan, New Zealand. Poster Paper, ICS 2000, Rotorua, New Zealand. (Appendix 5 contains the fully reproduced poster paper).

Phillips, D. and K. Black., 1998. Sediment Dynamics along a Shallow West Coast Headland., 1998. New Zealand Marine Sciences Society Annual Conference, 8-11 July. University of Otago, Dunedin, NZ (Appendix 6 contains the abstract).

Chapter 8 comprises the outputs of the computer numerical modelling. Comparisons are made between the conclusions from field experiments and the numerical model outputs.

Chapter 9 comprises calculations based on the field data and numerical modelling to determine the characteristics and quantity of sediment in the headland littoral system (i.e. net sediment flux).

Chapter 10 comprises a discussion that integrates all the data and describes the mechanism for sustaining sediment at the headland. A refereed journal paper is intended to be submitted from this chapter, including the numerical modelling and sediment flux results.

Chapter 11 presents the conclusions of the study, including understanding the hydrodynamics and sediment transport, mechanism for sustaining sand at the headland, implications for surfers and artificial surfing reefs, and recommendations for future work.

1.5 *GLOSSARY OF SURFING TERMS*

This glossary has been adapted from J. Kala Kukea (Walker, 1974) and Scarfe (2003), to provide an understanding of surfing terms used in this thesis for those unfamiliar with surfing terminology.

Back-off
The termination of the broken wave's white water due to the wave's movement over an inshore trench or deep, diverging orthogonals, or a loss of energy caused by movment over a long, shallow reef.

Bank
An area of the seabed contoured so that waves break over it in favourable form.

Blown-out
A rough choppy surface condition caused by a wind blowing with sufficient velocity to spoil the waves for surfing.

Board surfing
Surfing in which a surfboard is utilised by the surfer.

Body surfing

Surfing in which no extra equipment except possibly swim fins are utilised.

Break

The surf riding area; the breaking area.

Breaking area

That area outlined by the initial breaking point, the peel-lines, and the shoreward limit of advance of white water.

Channel break

A surf site adjacent to an easily distinguishable natural or artificial channel.

Chop

Short-crested waves that spring up quickly in a moderate breeze.

Close-out

A long-section of the wave crest which breaks instantly. A section in which the peel-rate exceeds the maximum speed of the surfer. A distinguishable section in which the peel-angle equals zero. Short, fast sections that a surfer is able to ride under would not be considered a “close-out”.

Peak

An easily distinguishable high point along a wave’s crest line. It usually occurs just prior to a wave’s initial breaking point.

Peel

The wave’s breaking point. A wave is said to peel right or left depending upon the lateral direction the breaking point moves when viewed in the direction of wave advance.

Peel-angle

Peel angle is defined as the angle between the trail of the broken whitewater and the crest of the unbroken wave as it propagates shoreward. Peel angles range between 0° and 90°, with low angles creating fast surfing waves and high angles creating slow waves. An angle of 0° is described as a "closeout".

Peel-line

The path described by the breaking point along the bottom as the wave proceeds shoreward. The outside boundary of the white water seen in aerial photographs very nearly describes the peel-line.

Point break

A surf site adjacent to a point of land, headland or promontory.

Reef

An area of rock or reef seabed contoured so that waves break over it in favourable form.

Riding distance

The distance travelled from the surfer's 'take-off point' to the end of the ride.

Rip

A narrow strong current flowing outward from the shore, caused by waves that can be used by a surfer to get out to the 'take off point' of the break.

Section

A distinguishable portion of a breaking wave where the peel-rate is fairly constant. Sections are classified as fast or slow, depending upon the peel-rate.

Shore-break

A surf site very close to shore. Shore breaks usually have short-rides that terminate at or near the beach.

Stoked

A feeling of great joy and happiness. A sensation experienced after surfing a great wave.

Surf reef

An area of the seabed contoured so that waves break over it in favourable form**.**

Take-off point

The region of a surf break where surfers catch waves. It usually occurs just seaward of the initial breaking point.

Tube

That portion of the breaking wave between the breaking point and the point where the white water defines the fully broken wave. For a plunging breaker, the tube becomes greater as the peel-angle decreases. This type of wave is the most desired by surfers as "tube riding" provides the greatest thrill.

Wall

A nearly vertical wave face. A wave is often said to be "walling up" as its forward face approaches the vertical and can be surfed at a greater velocity.

Wave crest

The highest point of a wave.

Wave-crest line

The lateral line described by the wave crest at any instant in time. Wave patterns are distinguished by crest-lines in aerial photographs (i.e. wave orthogonals).

Wave face

The water surface in front of the wave's crest. In most cases for surfing waves, the face is the water surface from the wave crest forward to the point where the water surface is nearly horizontal.

Wave height

Surfing wave height is often considered the most important variable at a surfing break. Oceanographers measure wave height from the crest to the trough of the wave. Groups of surfers develop their own definitions of wave heights, which can be slightly larger or smaller than crest-to-trough distances. In the scientific study of surfing waves, the oceanographic method is used.

Wave line-up

The relationship between the wave's direction of advance and its breaking characteristics at a particular surf site. A good wave line-up implies that the direction of the wave advance corresponds well with the bottom topography at the particular surf site and results in well-formed surfing waves.

Wave lip

The wave's upper leading edge in the breaking region.

Wave shoulder

That surfable portion of the wave outside the white water.

Wave steepness

In traditional oceanographic terms it is the ratio of wave height to wave length (H/L). To the surfer, it refers to the attitude or slope of the wave's face. A steep wave would be one with a nearly vertical face.

1.6 *SCIENTIFIC CONTRIBUTION & ASSOCIATED INVESTIGATIONS*

This project began as part of a larger research programme within the Centre of Excellence of the National Institute of Water and Atmospheric Research and the Earth Sciences Coastal Marine Group of the University of Waikato, funded by the foundation for Research Science and Technology. The 6-year research programme addressed the circulation and sediment dynamics of estuaries and beaches in a range of wave/current environments. Known as "Wave and Sediment Dynamics in Estuarine and Coastal Systems" (WSD), the programme consisted of 4 objectives: (i) wave generation (ii) hydrodynamics (iii) sediment dynamics and (iv) numerical modelling. These inter-related objectives have the ultimate aim of developing an improved understanding of physical systems and comprehensive numerical models of the processes.

The results of this study will provide input into the broader programme so that coastal engineers and regional managers (with regulatory responsibility for the marine environment) are able to better understand the implications of altering or utilising coastal systems). The Centre of Excellence was disestablished in 2000, and although the results will still benefit coastal engineers and regional managers, the focus of the project shifted to become part of the Artificial Reef Program (ARP) in the Coastal Marine Group, of the University of Waikato. The ARP was also disestablished in 2001, with the research continuing within the Coastal Marine Group at the University of Waikato.

1.7 STUDY SITE DESCRIPTION

1.7.1 *Introduction*

The Indicators surf break at Raglan was selected as the study site for the focus of the fieldwork due its position on the downdrift (north) side of the headland, the orientation of the surf break, boat access and the consideration of safety to surfers (Fig. 1.2). The transect location was selected at the eastern end of the surf break so

that equipment could be deployed away from the group of surfers who tend to sit further west along the headland where the waves first break (i.e. the take-off point). For some fieldwork such as sediment sampling or side-scan sonar surveys, an extended area over the headland was used for sampling or data collection.

Figure 1.2: The Indicators surf break on the headland near Raglan (Source: www.ragtimeblue.co.nz, 20 April 2001).

1.7.2 Raglan headland

1.7.2.1 Site description

The headland at Raglan is one of the largest on New Zealand's west coast stretching some 13 km from Ruapuke Beach and Papanui Point in the south to the Raglan Harbour entrance (Fig. 1.3). It is one of a succession of headlands and long sandy beaches that characterise this coast. The headland comprises the flanks of the Karioi volcanic cone and is known locally as the Raglan headland. The seabed

at Indicators consists of a mobile west coast titano-magnetite "black sand" adjacent to a boulder and reef shoreline (Figs. 1.4 to 1.7).

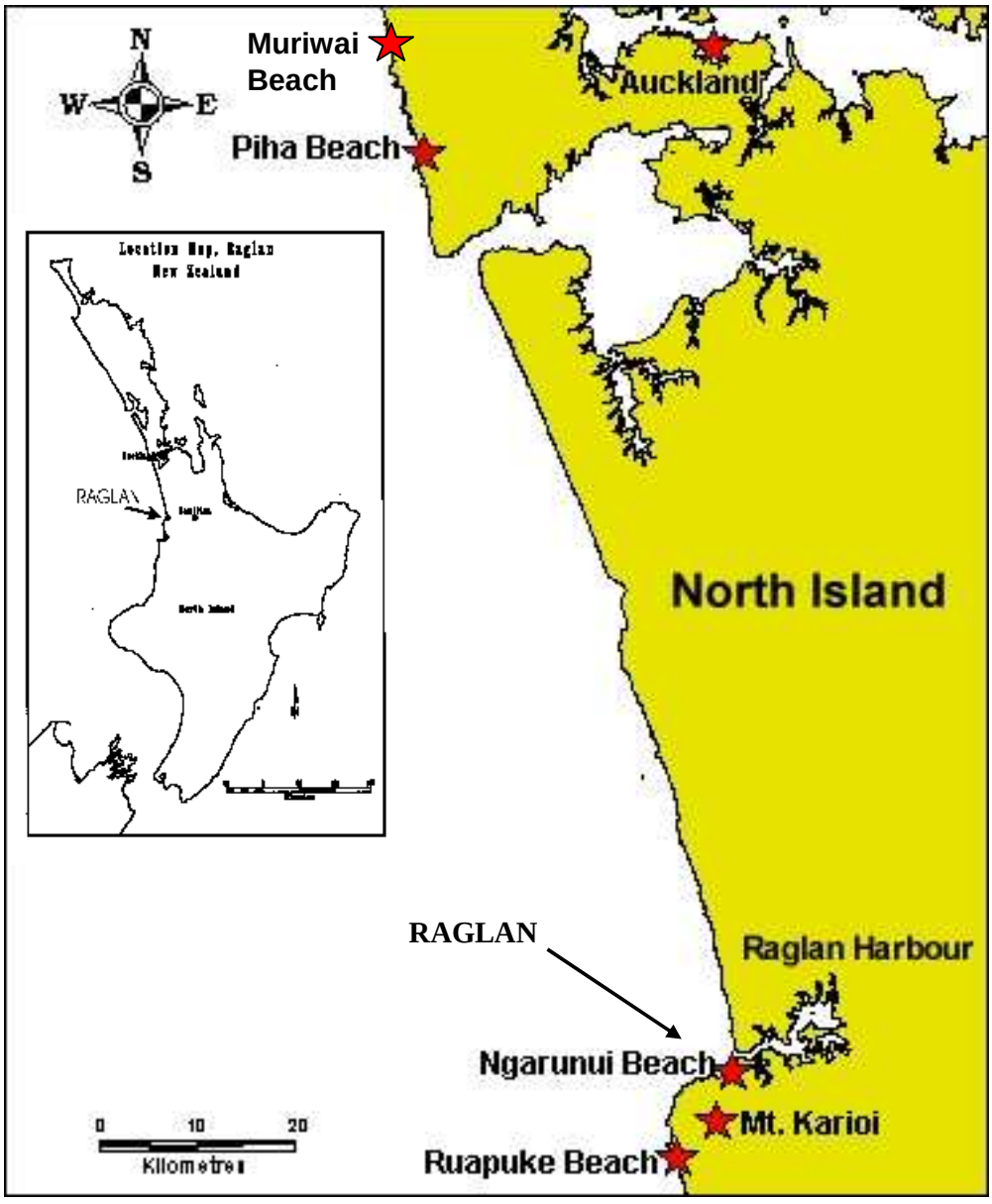

Figure 1.3: Location map of Raglan, New Zealand (Source: Hutt, 1997).

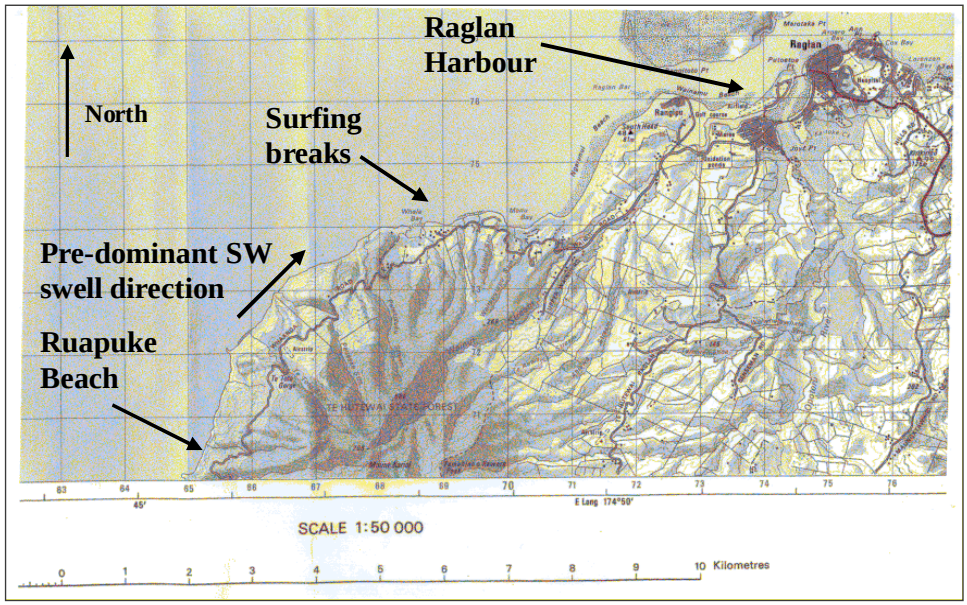

Figure 1.4: Map of the Raglan headland (Source: NZ Topographical Map, Land Information New Zealand).

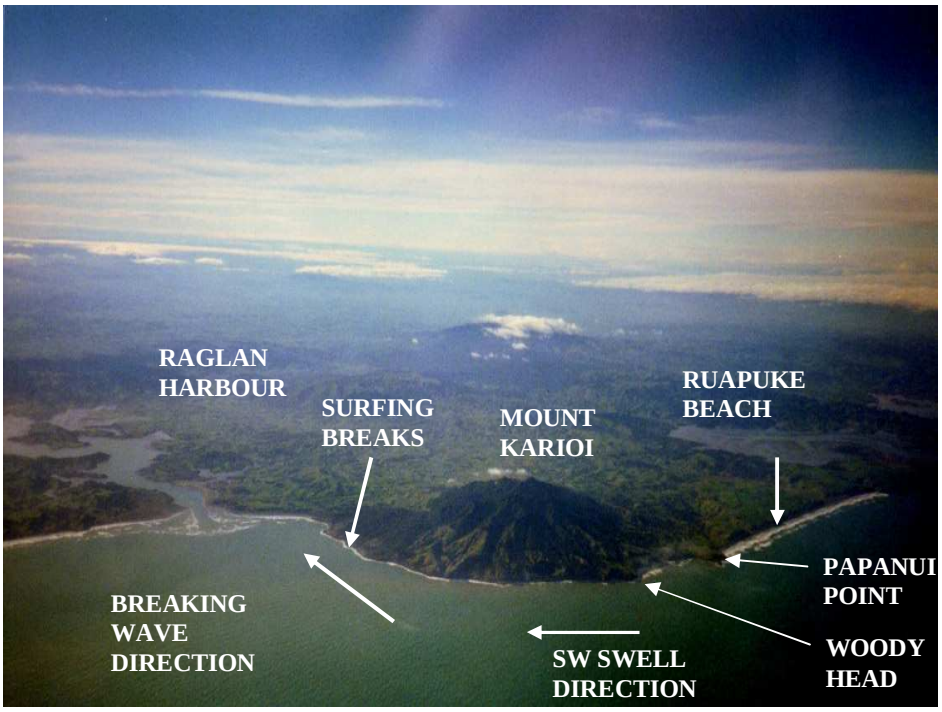

Figure 1.5: The headland south of Raglan from Ruapuke Beach to Raglan Harbour, formed from the Mt Karioi volcanic cone (Source: Author, 10 July 2000).

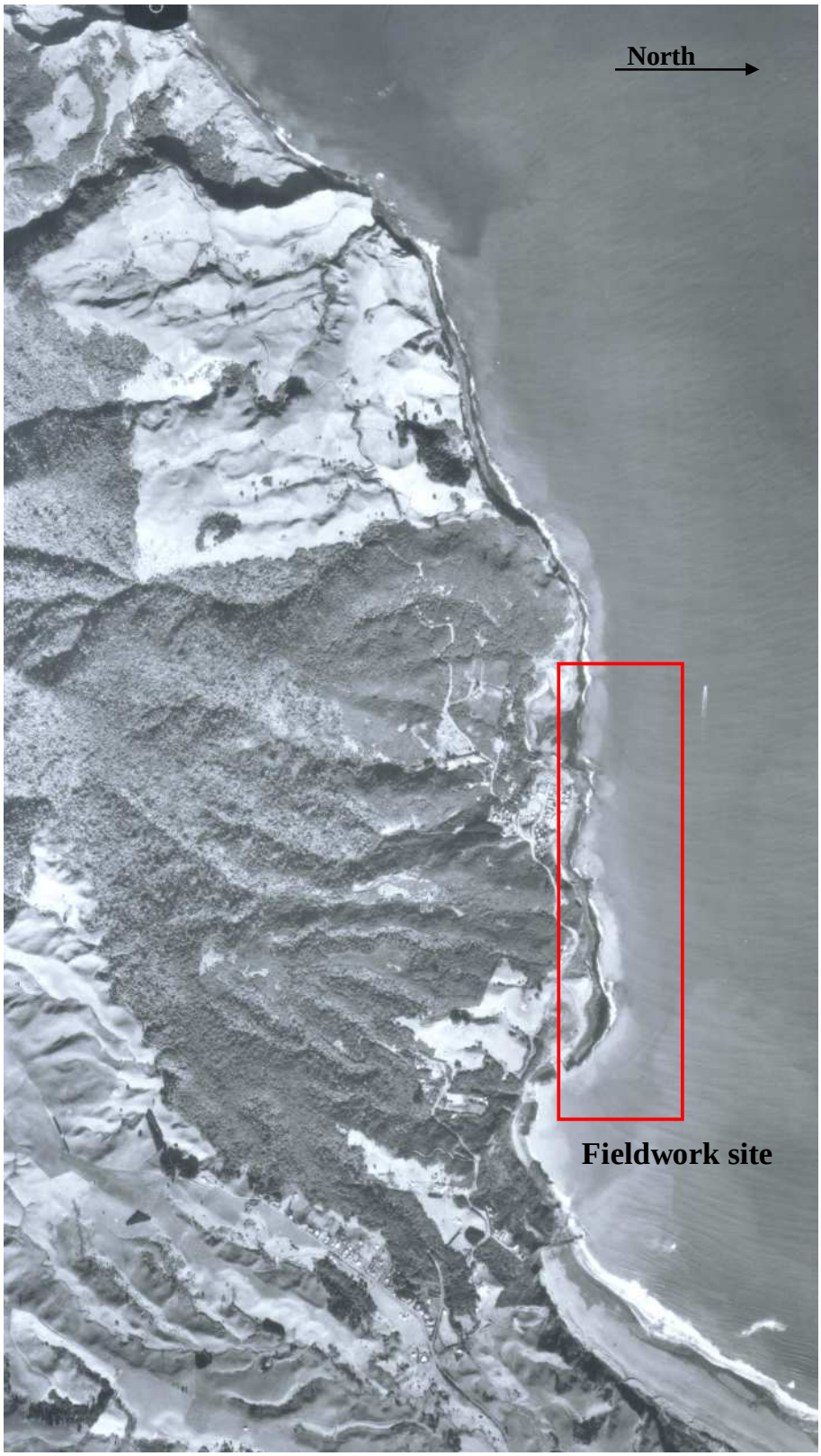

Figure 1.6: Aerial photo of the Raglan headland showing the fieldwork site at a scale of 1:27500 (Source: GeoSmart, 13 February 1993).

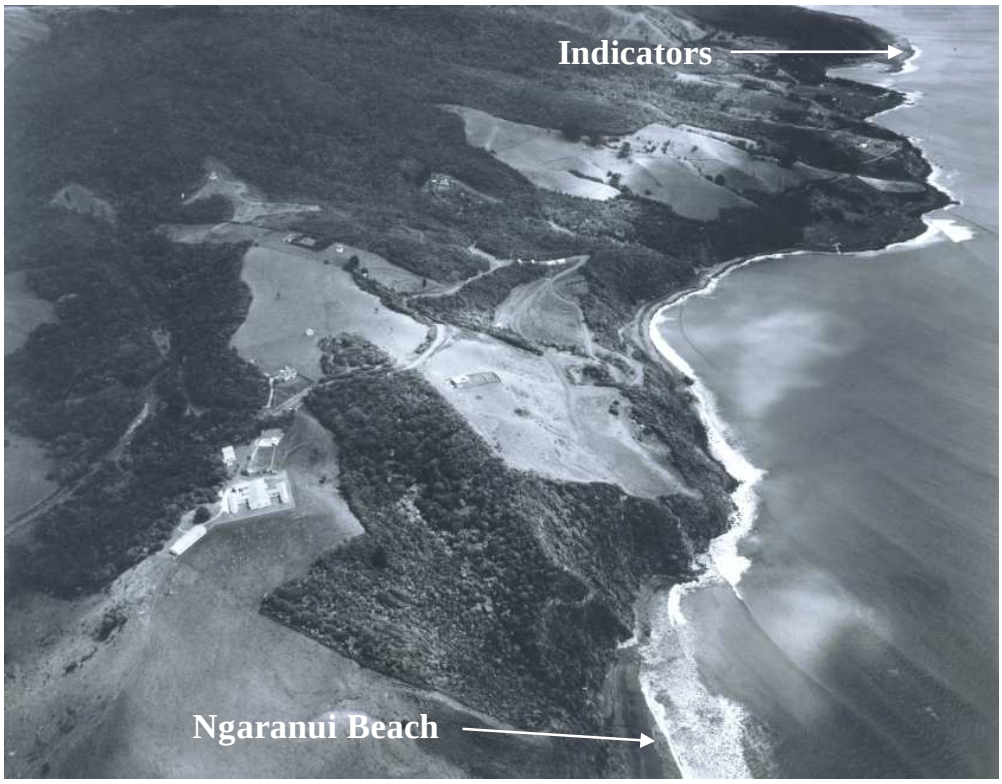

Figure 1.7: Historical aerial oblique photo of the Raglan headland from Indicators to Ngaranui Beach in the foreground, showing the variation in alignment along the coastline (Source: GeoSmart, 7 February, 1969).

1.7.2.2 Headland geomorphology

The headland at Raglan was formed as a result of the geomorphic evolution of Mt Karioi, which was an active volcano during a short period in the late Pliocene times and is the northwestern-most volcano of the Alexandra Volcanic Lineament (Briggs *et al.*, 1993)(Fig. 1.8). The seabed consists of a mobile west coast "black sand" that originates from the Taranaki volcanic region (Briggs, 1989), and is finer grained and denser (2710 kg/m^3)(Appendix 8) than typical quartz "white sand".

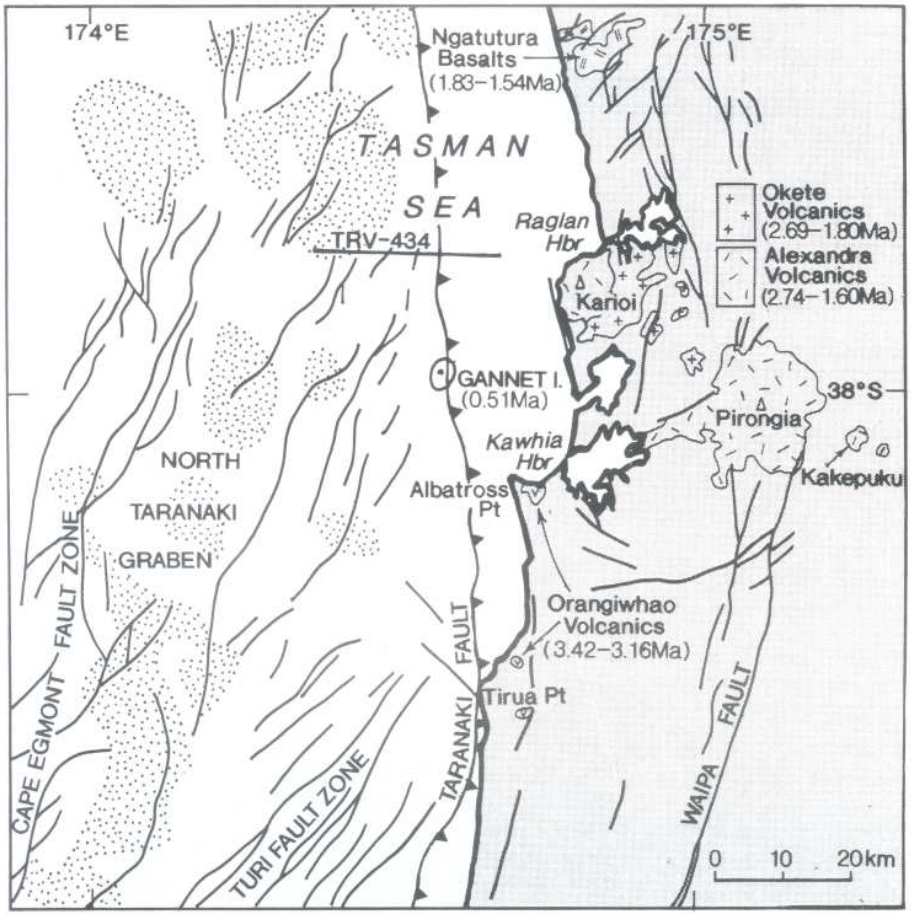

Figure 1.8: Part of western North Island and Tasman Sea showing the Okete Volcanics and Mount Karioi near Raglan Harbour (Source: Briggs et al., 1997).

The headland is armoured by rocks that are eroded from the Karioi and Okete volcanic formations (Figs. 1.9 to 1.12), which are predominately basaltic andesites derived from eruptions and lava flows (Goles *et al.*, 1996). The sizes on the shoreline vary from small rocks to large boulders up to 1.5 m in diameter, nestled amongst reef formations of solid rock.

Figure 1.9: Rocks and reef looking eastwards from Indicators across the lagoon (low tide) to Whale Bay (Source: Author, 12 May 2001).

Figure 1.10: Rocks and reef at Whale Bay looking westwards to Indicators (low tide)(Source: Author, 12 May 2001).

Figure 1.11: Rock boulders and reef at Whale Bay, Raglan (Source: Author, 12 May 2001).

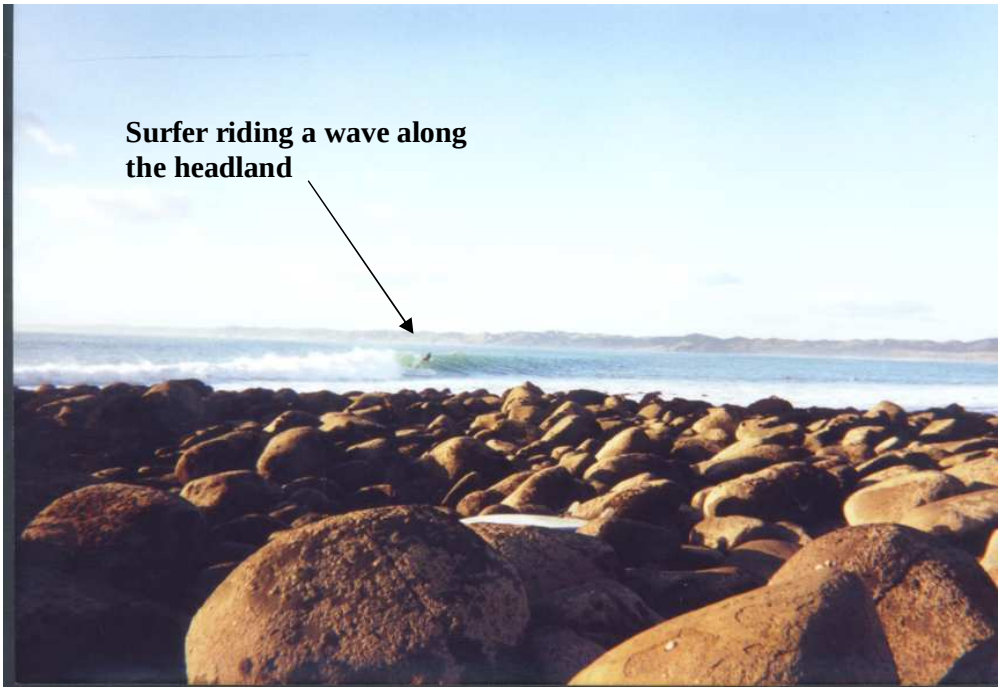

Figure 1.12: Rock boulders at Indicators looking northwards along the transect alignment, with a surfer riding past (eastwards) on a breaking wave (Source: Author: 12 May 2001).

CHAPTER TWO

BACKGROUND ON SURFING HEADLANDS

2.1 SURFING HEADLANDS

2.1.1 *Introduction*

The saying that "headlands draw the waves" was known by many an old seafarer and was used in reference to the fact that wave energy is concentrated on these promontories, therefore building larger waves (Cotton, 1942; Bird, 1968; Deacon, 1968; Fig. 2.1a). Headlands may be large and extend across a section of the continental shelf or they may be small and protrude a few hundred metres at a favourite beach (Hume *et al.,* 1997; Fig. 2.1b). However, Hume describes how headlands play a significant role by isolating beaches from sediment inputs or by modifying the currents along the shore. In this chapter this phenomenon is investigated and the background knowledge of surfing headlands and their associated flow and sediment dynamics discussed. Scientific information on the west coast environment of New Zealand is reviewed to obtain an understanding of the sand characteristics, coastal processes and systems that are apparent on this coast. The geomorphology of headlands and seabed morphology are investigated,

including bedform classification and effect of seabed roughness on sediment transport. The application of artificial headlands and surfing reefs are also discussed, including the effect that currents have on the 'surfability' of waves.

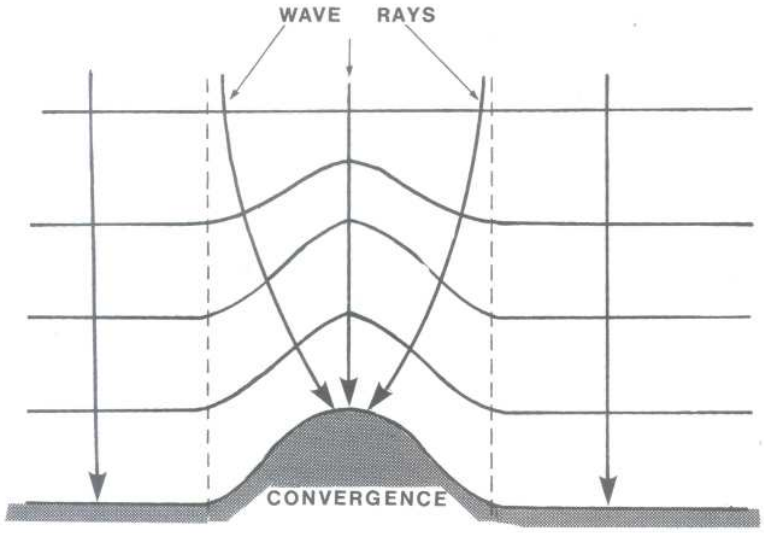

Figure 2.1a: Headland refracting waves towards itself. Zones of convergence have substantial wave activity (Source: Beer, 1997).

Figure 2.1b: The headland at Angourie Point, Australia with breaking waves. (Photo source: Dart, W., 2000. Tracks magazine).

2.1.1.1 Definition of a surfing headland

"Surfing headlands" are shallow and exposed coastal features that provide a specific form of breaking wave allowing a board-rider to ride on the unbroken wave face. Walker (1974) describes headlands or promontories as one of a number of environments in which surfing waves are generated, which include reefs or shoals, beaches, and channels (Fig. 2.2). The form of breaking waves is affected by several factors, which includes not only the shape of the seabed, wave height, period and angle of approach (Dally, 1989; Beer, 1997; Sayce, 1997, Sayce *et al.*, 1999), but also the wind strength and direction *(*Galloway *et al.*, 1989; Moffat and Nichol, 1989; Button, 1991).

Mead and Black (2001c), outlined a variety of properties that define world-class surfing breaks in a category of their own, but it is the seabed shape that has the largest influence on the form of a breaking wave and therefore the quality of a surfing break. For example, at Pambula on the New South Wales south coast, Australia, the sandbars that create fast peeling waves vary in position and depth depending on the fluctuating quantity of river flow and make the surf spot inconsistent (Warren, 1999; Fig 2.3). The steepness of the wave (breaking intensity) is directly related to the gradient of the seabed, with steeper seabeds in the shoaling zone producing steeper wave faces (Sayce *et al.*, 1999; Mead and Black, 2001a and 2001b; Scarfe *et al.*, 2003). The plunging form of wave breaking is the most desirable for surfing, as it produces the steepest surfable face and therefore the highest board speed. This may also provide an opportunity for the surfer to ride under the crest of the breaking wave inside the 'tube' (Fig. 2.4).

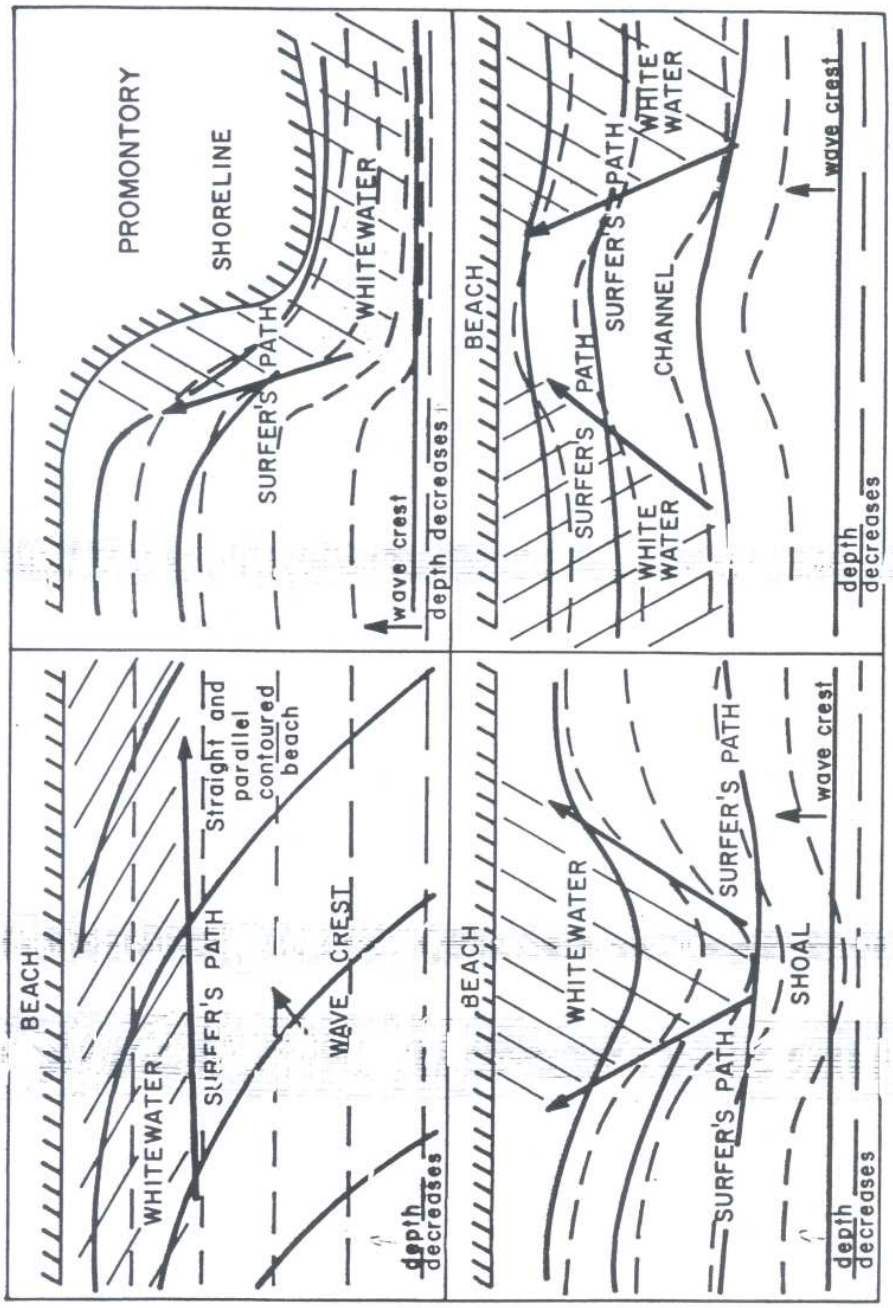

Figure 2.2: Basic surf site configurations including beach, shoal, channel and promontory (Source: Walker, 1974).

Figure 2.3: Waves breaking in the lee of the headland at Pambula, Australia that break inconsistently due to variation in the shape of the seabed as river outflow fluctuates (Photo source: Dart, W., 2000. Tracks magazine).

Figure 2.4: Surfer inside the "tube" at Cloudbreak, Fiji (Photo source: Dart, W., 2000. Tracks magazine).

The seabed features of a surfing headland are configured to produce waves that peel around the headland promontory, enabling maintenance of a steep unbroken wave face that creates sufficient board-speed to perform manoeuvres. The 'peel angle' is defined as the angle between the trail of the broken white water and the crest of the unbroken part of the wave as it propagates shoreward (Walker, 1974). The speed of the surfing wave is determined by the peel angle, which can range between 0^o and 90^o. A small peel angle results in fast surfing waves and large angles in slow surfing waves. For high quality surfing, the waves must peel fast, which means the peel angles are low (Walker, 1974; Hutt, 1997; Dally, 2001b; Hutt *et al.*, 2001).

Kirra Point in Australia, a natural rocky headland with an attached groyne, is regarded as one of the world's renowned surf sites and has a peel angle of 35^o that is near the limit of 'surfability' (Hutt *et al.*, 2001). This 'surfability' relates to how small the peel angle can get before it becomes impossible for a surfer to stay on the unbroken wave face ahead of the breaking section. This is termed a 'close-out'. On the other hand, as the peel angle increases towards the maximum 90^o, peel speed is reduced until it becomes too slow to be considered good for surfing (Mead and Black, 2002).

The peel angle is influenced by the shape and orientation of the seabed, because waves break in relation to specific depth contours (dependent on wave height) (Komar, 1998; Hutt *et al.*, 2001). On a headland refraction can alter the waves and have a significant affect on the peel angle and type of surfing waves generated. Refraction changes the direction of wave propagation causing wave crests to align more parallel with the seabed contours (Kamphuis, 2000), and can influence the morphology of landforms as waves refract around discrete headlands and islands (Sanderson *et al.*, 2000). The orientation of the headland in relation to the pre-dominant swell direction can cause significant refraction to occur as waves bend into the headland. The peel angle and surfability for a specific swell can therefore change depending on the direction of this swell (Figs. 2.5a and 2.5b).

As waves pass into shallow water they slow down according to $C = \sqrt{gh}$ where C = speed, g = gravity and h = *water depth*, increase in wave height and decrease in wavelength (Komar, 1998). As a wave approaches a headland, the part of the wave closest to the land slows more rapidly than the part that is in deeper water, thereby causing the wave crest to bend. Because refraction begins to occur with the water depth is around 0.5 the wavelength (Komar, 1998), the amount that wave crests bend depends on the wave period. Long period swells bend significantly, compared to short period waves such as small chop, which do not refract a great amount (e.g. Dyer, 1986; Ingmanson and Wallace, 1989; Mead, 2000; Mead and Black, 2001c).

Point breaks at headlands can therefore have excellent quality surf compared to the rest of the coast as only the low frequency swell refracts around the headland to create the breaking waves. Refraction also causes the wave height to decrease due to the divergence of energy associated with the curved wave front passing around the headland. The 'headland effect' (Mead and Black, 2001b) is demonstrated at surf breaks such as large headland at Shipwreck Bay (Ahipara), with either a very large swell or a very long period swell required to bend around the headland and create surfing waves (Bhana, 1988; Fig. 2.6). A combination of both large wave heights and long period swell produces the best waves.

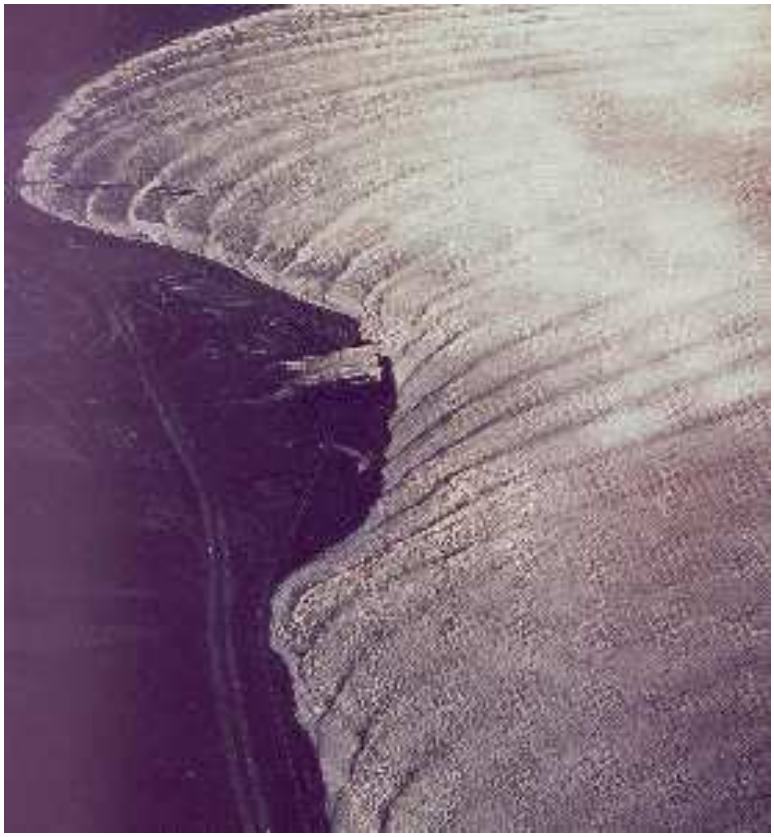

Figure 2.5a: Waves refracting into the headland at Rincon Point, California (Photo source: Surfer magazine, 1986).

Figure 2.5b: Waves refracting into the headland at Rincon Point, California (Photo source: Dart, W., 2000. Tracks magazine).

Figure 2.6: Map of Shipwreck Bay, Ahipara showing the swell and wave directions and the amount of refraction that occurs for waves to break along the headland (Source: New Zealand Topographical Map, Land Information NZ).

Many examples of surfing headlands exist throughout the world. These include famous sites at Burleigh Heads, Lennox Heads (Fig. 2.7), Byron Bay, Noosa Heads and Kirra Point in Australia (Warren, 1999), Malibu and Rincon in the USA (Fig. 2.8), Chicama in Peru, and Raglan in New Zealand.

Figure 2.7: Waves peeling down the headland at Lennox Head, Gold Coast, Australia (Photo source: Dart, W., 2000. Tracks magazine).

Figure 2.8: Rincon Point in California with surf breaking along the Headland (Photo source: Dart, W., 2000. Tracks magazine).

2.1.1.2 Surfing at the Raglan headland

Raglan is considered a world class surfing site and is known as one of New Zealand's most consistent breaking waves (Bhana, 1988). It is comprised of seven surf breaks compartmentalized along the large-scale headland, with each having its own distinctive form of breaking wave, creating variability in wave and current characteristics depending on the orientation and bathymetry at the different locations. The breaks are comprised of various components and wave characteristics as described by Mead and Black (2001c). At the tip of the headland is Outsides, which comprises a large wedge, pinnacle and ridge. The wave characteristics are moderate to very steep, hollow with moderate to fast sections. Further east along the headland is Indicators (Fig. 2.9), the predominant site of field experiments for this thesis. Surfing wave components include a large wedge and ridge, moderate to steep waves that are hollow with fast sections. The Valley breaks inside Indicators and comprises a large wedge and ridge, with steep to very steep waves, that are hollow and break with fast to very fast sections. Whale Bay is the slowest of the surfing waves with a moderate peel angle and moderate to

steep waves. The components are a large wedge, ridge and pinnacle. The furthest break down the headland is Manu Bay, which has a large wedge and ridge, which produces low to very steep waves with hollow and fast sections.

There are a range of gradients and peel angles at the various breaks, which provide the necessary components of seabed shape and refraction that produce high quality surfing waves. Hutt *et al.* (2001), describes how at Outsides the peel angle is 45-60^{o}, with a seabed gradient of 1:20, Indicators 50-65^{o} and 1:25, The Valley 50^{o} and 1:30, Whale Bay 60-80^{o} and 1:40, and Manu Bay with 55-75^{o} and 1:30 (Fig. 2.10).

Figure 2.9: Waves breaking along the Indicators headland at Raglan. (Image from www.asrltd.co.nz)

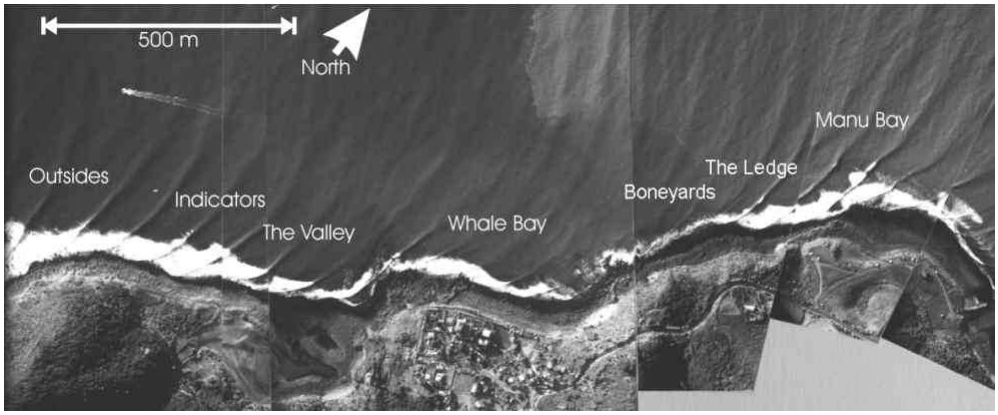

Figure 2.10. Aerial photo of the Raglan surfing breaks (Hutt et al., 2001).

Generally there are three types of surfing breaks creating waves by either refraction; where this is the dominant control on the wave alignment at the break point and therefore the relating peel angles, peakiness; where a peaky swell with height gradients along the wave crests determines the peel angles and corresponding break speeds, or at a headland; where peel angles are determined by the orientation of the depth contours to the incoming swell (Walker, 1974; Hutt, 1997; Hutt *et al.*, 2001). A surfing site may display all three characteristics depending on the wave conditions, but sites can be classified by the dominant control on peel angles for the given wave conditions. At the Raglan headland, refraction is the dominating type of break during swells to a moderate size, but in very large swells refraction at the break point is more limited, and peel angles are more dependent on the orientation of the incoming swell to the headland, as the depth contours are approximately parallel to the shoreline.

2.1.2 Headland geomorphology

Headlands are dominant controlling factors in the sedimentary processes that shape coastlines (Melville, 1984). The geomorphology of a surfing headland requires a large-scale coastal structure that may be a point of land or promontory, which is both exposed to swell and provides shallow water for waves to break. In comparison a deeper water headland at Cape Rodney, New Zealand, as modelled by Hume *et al.* (1997), showed little wave shoaling in the water surrounding the

headland, and minor refraction and focusing on the headland. In both cases though, pronounced headlands as they are often described, retreat slowly due to their resistant strata and rock formations (Guilcher, 1958). Solid and massive igneous rocks, most metamorphic rocks, and some limestones are very resistant to wave attack and hence are found in headlands (Cotton, 1974; Shih and Komar, 1994; Komar, 1998).

Figure 2.11: Aerial view of Point Danger to Kirra Point breakwater at the top of the picture, Gold Coast, Australia (Source: Gold Coast City Council, 23-4-96).

A good example is on the northern NSW-southern Queensland coast in Australia that comprises a series of sandy embayments, separated by bedrock headlands (Short, 1999), which provide surfing conditions of a world class standard (Warren, 1999). The Gold Coast, commencing at Point Danger, in general terms consists of a major embayment, but within this general embayment, there exist four more subdued bays, each generated by a "hard" headland at Greenmount,

Kirra Point where the headland has been extended by a groyne (Fig. 2.11), Currumbin and Burleigh Heads (Hutt *et al.*, 1998). These headlands can be considered similar to the set-up at Raglan, where a hard structure allows waves to break along these sections of coast.

Figure 2.12: Waves breaking into Shipwreck Bay, Ahipara, Northland, after refracting around the headland (Source: Author, 20-2-02).

The shoreline of the headland may be armoured by either rock boulders or rocky reef (Ingman and Wallace, 1989). Examples of this type of structure in New Zealand are the headland at Raglan, Ahipara (Shipwreck Bay; Fig. 2.12) and sections of the Taranaki coastline (Thornton, 1995). The seabed may be comprised of either reef, rock or sand, or could be a combination of two (e.g. Taranaki – boulder and sand) or all of these materials (e.g. Raglan).

2.1.3 Artificial headlands

There are many devices that have in the past (Department of Public Works, 1960; U.S. Army Corps., 1973) or are presently being used to protect the coast (Fleming, 1990; Silvester and Hsu, 1997). These include seawalls, groynes, detached breakwaters, beach nourishment, dune revegetation, training walls to stabilise river entrances, submerged reefs and artificial headlands (Herbich, 2000). Artificial headlands have been both investigated and implemented as a means of protecting coastlines from significant erosion (e.g. Magoon and Edge, 1978; Silvester, 1985; Silvester and Hsu, 1997), in an attempt to simulate the crenulate-shaped bays formed by nature (e.g. Leblond, 1979; Lesnik, 1979; Phillips, 1985; Epps, 1987; Quevauviller, 1987; Kimberly, 1989; Klein and Menzies, 2001). This method of coastal protection can be termed 'headland control', where headlands are designed to minimise the effect of storm waves on the coast (Hsu *et al.*, 1989).

The early use of seawall or rock revetments, and later rock groynes, led to the construction of detached and offshore breakwaters that were virtually seawalls constructed in deeper water than the previous tips of groynes (Short, 1999). These structures were either built longer than groynes or with spaces that allow the diffraction of waves behind them, so building salients that are meant to protect the coast at specific points. These forms of coastal protection focused on methods that accumulate littoral sediment behind or inside the structures as it is transported along the coast, and have not always been successful in their intent (Flores and Mazza, 1971; Foster, 1972).

Breakwaters acting as headlands for the formation of sandy beaches, is a concept that has been used historically and to this day for the stabilisation of erosion (Silvester and Hsu, 1997). If the most persistent or predominant waves on a sedimentary coast have a resultant direction that is oblique to the headland alignment (Kobayashi and Entin, 2001), a shape is gradually reached which is in equilibrium with the waves and most likely to be crenulate in shape (Ho, 1971). The size and orientation of the headland breakwater, therefore has a direct relationship with the berm orientation that is created (Chew *et al.*, 1974).

Different shaped structures (i.e. groyne type or T-shaped headland) have also been shown to have different current patterns, with rip currents developing along the groyne-type headland and currents re-circulating in the lee of the T-shape headland (Saito *et al.,* 1996). These types of currents also have an influence on the sediment transport near the structure (Walker *et al.,* 1991).

Research by Silvester (1960 and 1976) and Hsu *et al.* (1993), proposed that artificial headland control is a more viable method of coastal protection, with bays formed that are much larger than the small compartments between groynes, which can be classified as pseudo-bays. Initially the logarithmic spiral was the preferred geometric shape of the bays formed between headlands. This shape was difficult to apply in practice and found to be inaccurate, especially for the down-coast segment that is straighter, with a parabolic shape now seen as more applicable (Silvester and Hsu, 1997). Artificial headlands act partly as groins to hold sand in embayments, but also from their shape generate a wave refraction pattern to emulate that of small "pocket" beaches, so that the sand is encouraged to remain within the embayment between the artificial headlands (Healy and Harada, 1997) (Fig. 2.13).

Figure 2.13: Artificial Headlands on the Ibaraki Coast Source: *Japanese Coasts and Ports (1994) Committee on Coastal Engineering, Japan Society on Coastal Engineering, p.62.*

This form of coastal protection has been used in the stabilisation of the Te Atatu Peninsula, in Auckland by Healy and White (Auckland City Council, 2000). The design involves the use of constructed headlands (10 m diameter mounds consisting of a clay core with rip-rap armour rock exterior, ranging from 20 - 40 m from the mean high water mark), to refract waves around them and naturally trap sediment (Fig. 2.14). The use of an artificial headland at Narrowneck on the Gold Coast, Australia, was described by Jackson and McGrath (1995) as the preferred method of beach protection along with nourishment and dune stabilisation. The structure was to be designed as a wide, visually unobtrusive, low profile artificial headland that would enhance surfing conditions and have no adverse effect on beaches to the north (downdrift). This structure known as the Narrowneck Artificial Surfing Reef which is essentially a large scale submerged headland, has since been constructed and has stabilised the beach and improved surfing conditions at the site (Black, 2001a, Black, 2001b; Fig. 2.15).

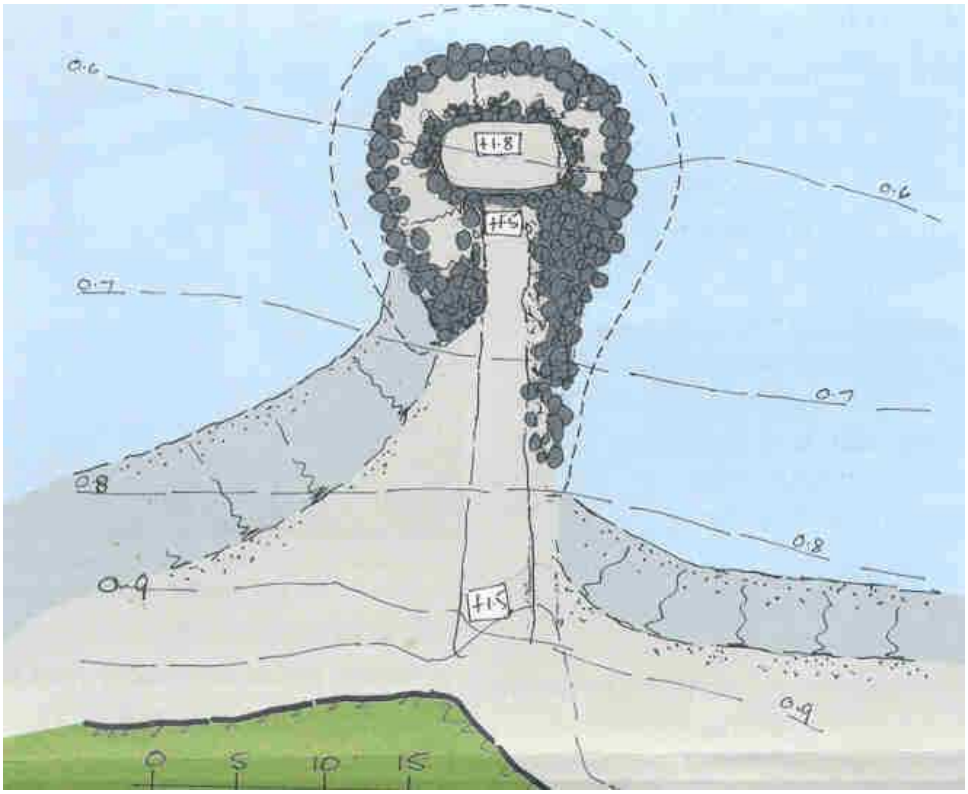

Figure 2.14: Plan of the Artificial Headlands at Te Atatu Pennisula (Source: Auckland City Council, 2000).

At coastal structures such as artificial headlands and breakwaters, currents and sediment transport may display similar characteristics to those found on surfing headlands. Surfing waves often break along the side of breakwaters or jetties in a consistent peeling manner, similar to that of natural surfing headlands (Scarfe *et al.,* 2003). Currents and sediment transport are driven by the breaking waves, with sediment transport enhanced in the zone closest to the seaward face, which may induce scouring at the toe of the structure (Baquerizo and Losada, 1998). Return currents may also be generated by obliquely incident waves reflecting from the rubble mound breakwaters (Kobayashi and Entin, 2001), through wave generated currents rotating seaward due to topographic forcing (Gourlay, 1981; Gaillard, 1988; Fig. 2.16), or due to reversing tidal currents (Furukawa, 2000).

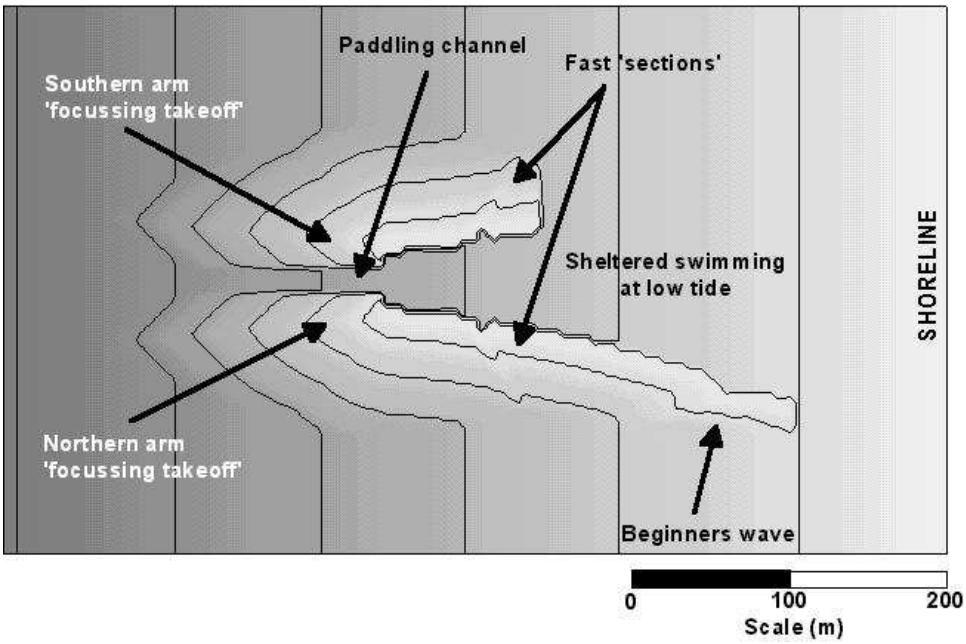

Figure 2.15: Plan of the Narrowneck artificial surfing reef, Gold Coast, Queensland, Australia. (Source: Black and Mead, 2001).

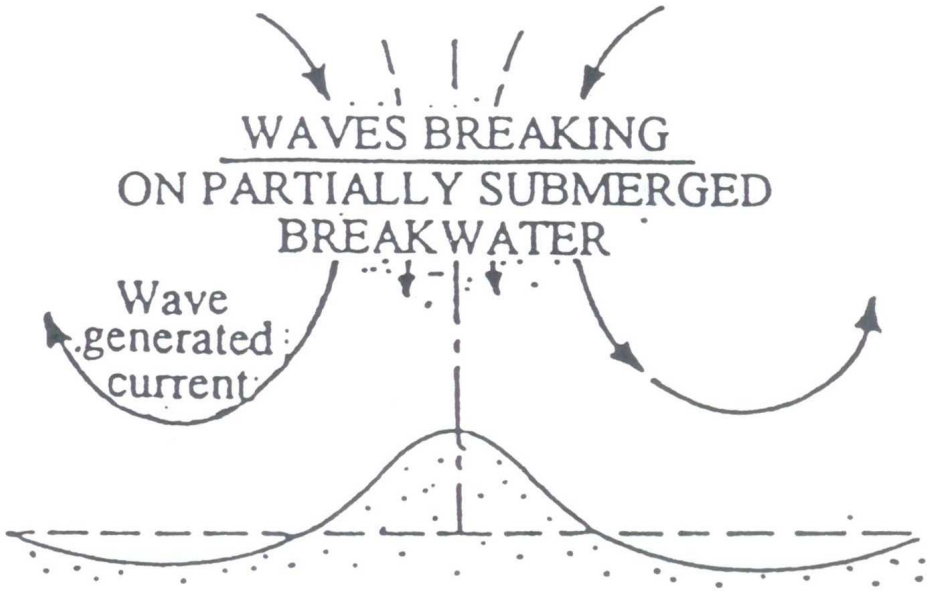

Figure 2.16: Current generated at a partially submerged breakwater (Gourlay, 1981).

2.1.4 ***Artificial surfing reefs***

Silvester (1975) commented that the crenulate-shaped bay, either as a natural or human-made feature can supply the variety of conditions demanded by the body or board surfer. Thus, stabilisation and recreation might be served by the same headland approach. This concept has previously not been embraced in the design of coastal protection, but through chance with the construction of groynes and breakwaters throughout the world, surfing waves of a quality nature were sometimes produced or enhanced following the build-up of sediment near the structure. Examples are the Kirra Point Breakwater on the Gold Coast of Australia (Fig. 2.17) and The Wedge in California, USA. On the Gold Coast, all the groynes have resulted in enhanced surfing conditions due to the beach and bar realignment and initiation of breaking at the tip of the groyne. The Tweed and Nerang River training walls (Gourlay, 1996) have created excellent surf breaks at Duranbah and the southern tip of Stradbroke Island respectively (Warren, 1999). The surfing conditions are more consistent due to the wave refraction effects of the entrance shoals and larger wave size because of the steeper nearshore seabed slope (Scarfe *at al.,* 2003).

There have, however, also been a number of surf sites adversely impacted or completely lost due to coastal construction where quality of surf was not considered as part of the design (Moffat and Nichol, 1989). An example is the Kirra Point groyne construction in 1972, which had major impacts on the sand supply and modified the nature of sand movement in the area. The groyne was constructed by the local council to stop the beach erosion at Coolangatta and Greenmount beaches and although successful in restoring these beaches, extensive erosion occurred downdrift on the Kirra Beach foreshore with approximately 100 m of land being lost to the sea (Macdonald and Patterson, 1984). This form of erosion is a common occurrence in the downdrift direction of groynes and breakwaters (Tsuchiya *et al.*, 1990). The waves at Kirra Point stopped breaking, described by Bartholomew and Baker (1996) as "something died, something actually died in the town, some spirit left the town when the groyne went in, and left a big, deep hole north of the groyne. Surfers who were the lifeblood and core of the beach culture all left the area". Some waves did break on an outer reef during large swells, but it was not until the groyne area filled with sand three years later that quality waves returned to this headland.

Figure 2.17: Waves refracting around the Kirra Point groyne, Gold Coast, Australia producing a surfing break (Source: Tracks magazine, 2000).

In the late 1990's significant research has been undertaken and published as part of the Artificial Reef's Program in the Department of Earth Sciences, University of Waikato (e.g. Andrews, 1997; Black. *et al.*, 1997; Hutt, 1997; Sayce, 1997; Mead, 2000; Black and Andrews, 2001a and 2001b). This program embraced the concept of coastal protection through the use of artificial surfing reefs (Black, 2001b and 2001c), which advanced the concept first proposed in the 1970's (Gerschler, 1978; Moffat and Nichol, 1989; Walker *et al.*, 1972; Walker, 1974; Bohnsack and Sutherland, 1985; Dally, 1989 and 1990), and more recently the constructed cable stations artificial reef in Perth, Australia (Pattiarachi, 1997 and 1999).

Further work has continued including both research (Dally, 2001a and 2001b; Evans and Ranasinghe, 2001; Mead and Black, 2002; West *et al.*, 2002; Beamsley and Black, 2003; Blenkensopp, 2003; Scarfe *et al.*, 2003), and the design and construction of projects such as multi-purpose artificial reef at Narrowneck, on the Gold Coast, Australia (Black, 1999; Black, 2001c; Black and Mead, 2001). This reef was designed as a "double-sided" submerged headland that consisted of two arms extending 450 m offshore to the reef toe in 10.4 m water depth (i.e. the reef contours are almost perpendicular to the natural seabed contours; Fig. 2.18). If the reef had been designed as originally suggested, with reef contours at around 45º to the seabed contours, refraction would have reduced wave peel angles so as to make them so small that the waves would break too fast to be surfable (Mead and Black, 2001a; Mead *et al.*, 2003). The submerged reef has successfully stabilised the beach erosion, created good quality surfing waves and enhanced marine habitat and biota (Mead and Black, 2002; Burgess *et al.*, 2003; Turner, 2003).

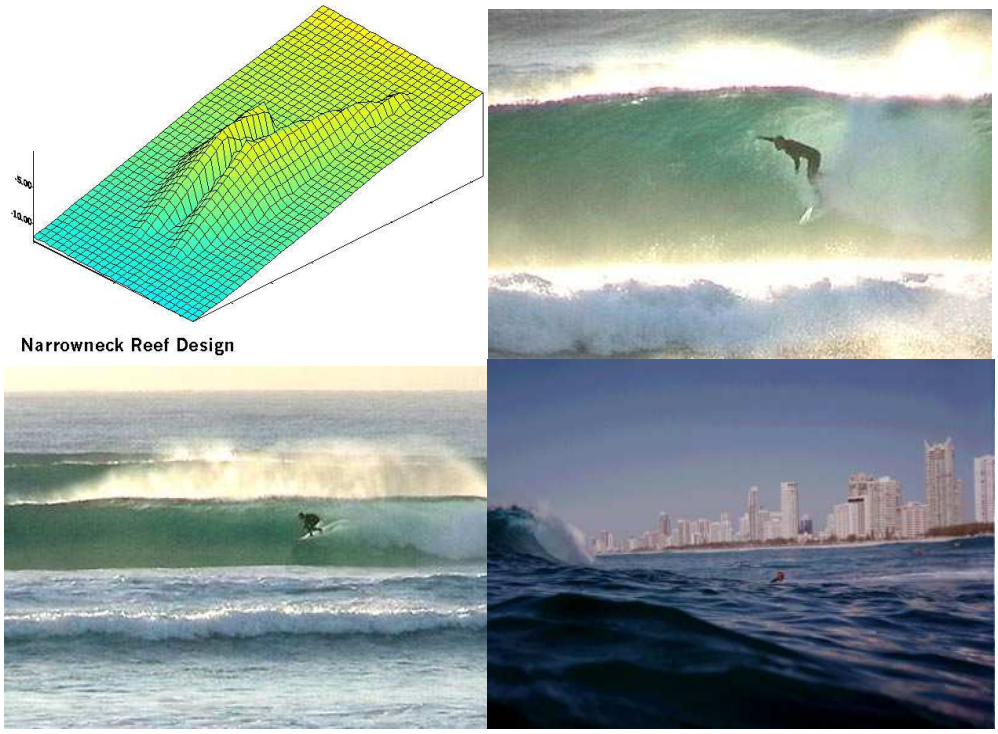

Figure 2.18: The Gold Coast multi-purpose reef (Clockwise from top left), topographical representation of the design, surfing on the reef in 1999, the view from the water 2002, July 1999 (Source: Mead and Black, 2002).

This form of coastal protection acts to mitigate the cause of the coastal erosion, rather than just dealing with the effect, as is often the case (Buckeridge, 1995). Black and Mead (2001), describe the two types of offshore reef as "dissipators" and "rotators", working with nature by modifying the natural wave transformation processes to alter nearshore currents and obviate coastal erosion processes. The reefs act to break the waves and protect the coast by reducing wave energy in the lee of the structure, whilst also rotating waves to reduce the orientation angle, resulting in reduced inshore wave-driven currents and therefore less longshore sediment transport. In both cases, this leads to reduction or elimination of the sediment movement responsible for beach erosion.

Research on natural offshore reefs and headlands, which have a beneficial impact on coastal stability, has advanced the knowledge and application of this form of protection. Black (2001b and 2001c) described offshore protection as nature's

way, and cites examples of coral-fringed islands, where the reef dissipates wave energy to protect the coast, and the many nearshore reefs found on beaches worldwide. Field studies (Mead, 2000; Mead and Black, 2001), led to the bathymetric classification of world-class surfing breaks, whilst research on the surfing headland at Raglan, led to a greater understanding of the bathymetry, wave refraction, breakpoint location and surfing characteristics in this environment (Hutt, 1997; Sayce, 1997; Sayce *et al.*, 1999; Hutt *et al.*, 2001).

Black (2001c) identified a weakness in the Narrowneck reef design as being the strong wave-driven currents generated over the reef crest. The shoreward running currents in a 3-4 m swell were predicted by Symonds and Black (2001) to exceed 1-1.5 ms^{-1}. These currents could sweep surfers caught in the breaking waves over the crest and into the shore. A design feature of the Narrowneck surfing reef to help compensate for this is the paddling channel between the two arms of the reef (Fig. 2.15), which allows surfers access to the break during moderate and large wave conditions (Black and Mead, 2001). Even though wave-driven currents are directed inshore on the outer sides of the reef, the current is reversed through the paddling channel, aiding paddling out through the channel. In addition, shoreward of the reef, a 'quiet zone' provides sheltered paddling from the beach.

The design of the Lyall Bay artificial surfing reef in Wellington, New Zealand, does not incorporate a paddling channel (Fig. 2.19). This was due to budget constraints that would not allow the construction of two separate reef arms (Mead *et al.*, 2003). The surfability of the reef could be enhanced by the incorporation of a paddling channel, especially during large swell conditions, when access to the take-off point could prove difficult.

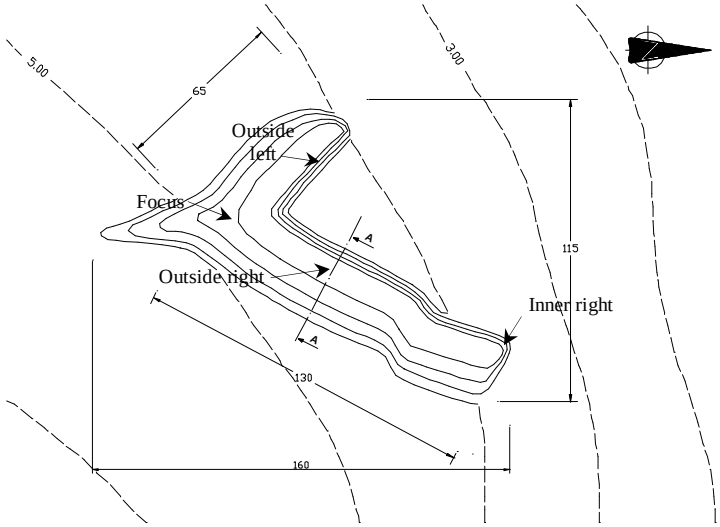

Figure 2.19: The final design of Lyall Bay Reef. (Source: Mead et al., 2003).

Design evaluations for an artificial reef in Dubai have shown that strong wave generated currents around the reef may pose a hazard for swimmers, although a re-circulating current flowing seawards will assist surfers in paddling back to the take-off site (Mocke *et al.*, 2003; Fig. 2.20). The current is rotated due to the end effect of the existing coastline orientation.

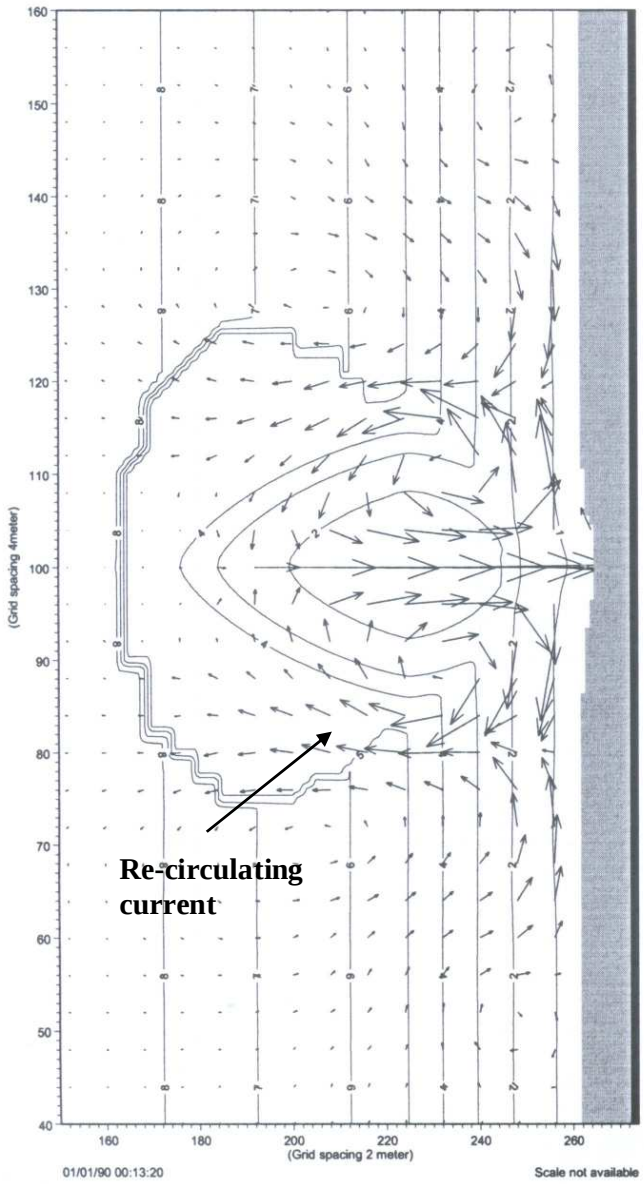

Figure 2.20: Numerical model wave–driven current field for a shore-perpendicular wave direction, showing the seaward flowing re-circulating current (Source: Mocke et al., 2003).

2.1.5 Characteristics of currents at headlands

A coast that is irregular, with occasional jutting headlands will clearly effect current flows and impede sediment transport in a way that a regular, smooth coast will not (e.g. Davies, 1972, Willmott, 1983; Xu, 1999). These headlands act as natural obstacles to the longshore sediment transport and the result is a downdrift

accumulation of sediment (Short, 1999). The effect of this accumulation on the littoral transport can depend on factors such as the scale and orientation of the headland, wave and current characteristics of the coastal environment, and the amount of sediment in the system. Classic New Zealand examples of barriers that trap sediment on the updrift side, are Kaitorete Spit, Sumner Spit and the constructed river-mouth jetties at Wanganui (Shepherd and Hesp, 2003). Shepherd and Hesp found that in contrast projecting bedrock headlands usually have steeper offshore gradients and an oblique wave approach, which results in the removal offshore or alongshore of all but the coarsest sediment sizes.

Geyer and Signell (1991) defined coastal headlands as locations where wave and current energy converge, which may generate secondary circulations as flow passes the protuberance. The flow characteristics at the headland can be significantly different from that of the overall coastline. Understanding current structure and eddy formation at headlands allows quantification of the role of these features on coastal exchange processes (Hume *et al.,* 1997). A rocky headland can provide shelter from wave energy to the lee side, with a subsequent effect on the littoral supply and drift of sediment. The headland can also act as a cell boundary where local sediment circulation is confined into compartments (Bray *et al.,* 1995; Hume *et al.,* 1997). Komar (1998) found that headlands are marked by a reversal in the longshore current, which is driven by oblique waves and, to a more limited extent longshore variations in wave height. Gourlay (1974) found similar characteristics in the lee of headlands or a structure, with wave-generated current systems that often caused local reversals of the alongshore current.

Positional stability can be provided to tidal inlets in the lee of the headland, with characteristics similar to inlets stabilised by jetties on United States shores (Hume and Herdendorf, 1990). A similar degree of protection and stability can also be predicted for sheltered beaches and littoral sections of the coast. It has been demonstrated by Hicks and Hume (1993), that ebb and flood delta morphology relates to the configuration of headlands, barriers, and bays, alignment of the tidal jets, and the degree of wave exposure (Fig. 2.21). This is particularly important on

New Zealand's headland dominated, active margin coastal setting, with exposure to a broad range of moderate to high energy wave climates, providing for a range of inlet types and associated sand bodies deposited by the flooding and ebbing tide flows (Shepherd and Hesp, 2003). A number of these ebb tide deltas in the lee of headlands create quality surfing breaks. An example is Whangamata Bar, New Zealand, which has been classified on the National Geopreservation Index as a unique bathymetric landform that should be protected (Scarfe *et al.*, 2003).

While waves are often the dominant process controlling sediment movement and beach morphology, the tidal range and tidal currents can also influence the beach and nearshore system. Headland flow characteristics may be characterised by eddy formations where tidal currents spiral about the headland and influence the sediment transport and sediment signature on the seabed (Falconer *et al.*, 1984; Black and Gay, 1987; Saunders, 1999; Hume *et al.*, 2000). They are commonly associated with oscillatory tidal currents, forming on alternate sides of the headland with the reversal of the tide (Signell and Geyer, 1991). The strongly nonlinear flow associated with the development of these eddies has substantial influence on fluid and sediment transport processes (Signell and Geyer, 1991; Geyer, 1993).

This striking feature is evident at Cape Rodney, with counter rotating eddies in the lee of the headland (Hume *et al.*, 1997). These have been shown to be phase eddies developing after peak flow in reversing tidal currents, and are characterised by strong flows along their shoreward boundaries and the seabed beneath is largely devoid of sand. A similar feature was distinguished by Saunders (1999) at Kohi Point, Whakatane, New Zealand (Fig. 2.22).

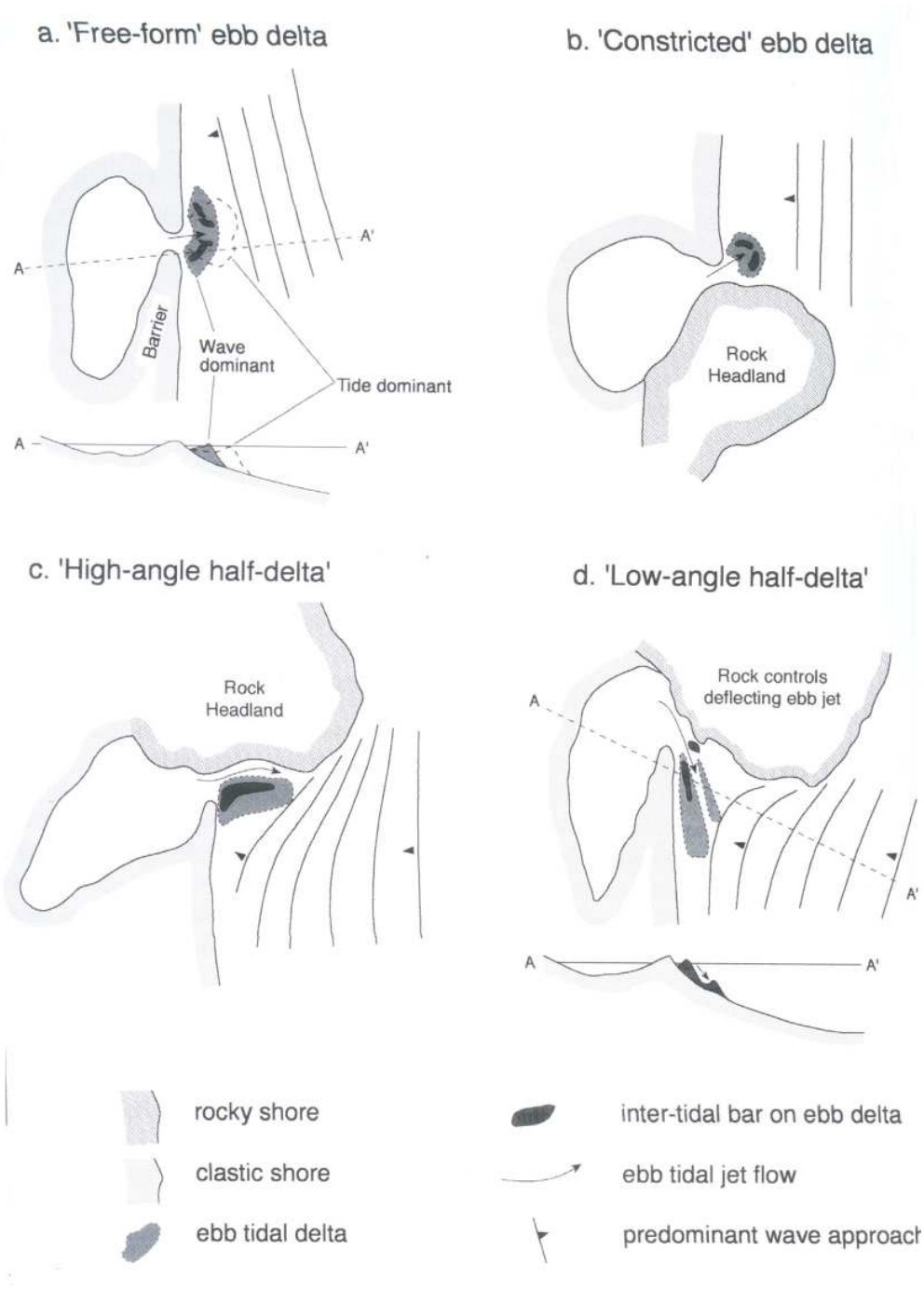

Figure 2.21: Schematic diagrams depicting the various type of ebb-tidal delta and controls on delta size and shape by barriers and rocky headlands (Source: Hicks and Hume, 1996).

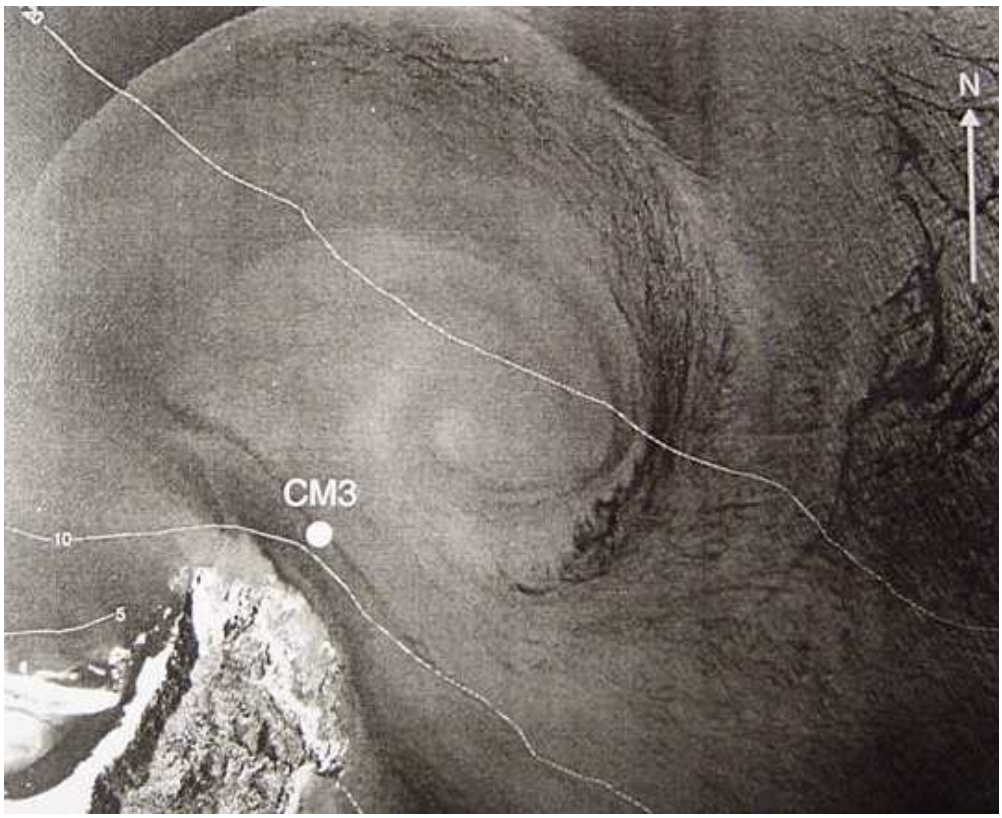

Figure 2.22: Aerial view of eddy at Kohi Point, Whakatane, New Zealand (Source: Saunders, 1999).

Davies *et al.,* (1995) identified that the size of the eddy and vorticity distribution behind coastal headlands are controlled by the value of the bottom friction parameter, although the maximum vorticity within the eddy depends upon the incident flow velocity and the horizontal dimension of the headland obstruction. Denniss *et al.* (1995) supports this conclusion and found that the size of the re-circulating current is affected by the complexity of the headland's geometry.

Headland-related residual flows, mean tidal currents, wind-driven currents, and waves all influence regional shelf circulation and sediment distribution at a cuspate foreland promontory (McNinch *et al.*, 2000). It was concluded by McNinch that the coupling of wave-driven and tidal currents supply sediment and maintain the morphology at headlands, whilst Pattiarachi (1988) found that wave action intensifies the rate and influences the direction of net sediment transport.

Although the Raglan headland is different in morphology, similar influences of the combination of wave-driven and significantly smaller tidal currents are likely to have an impact on the sediment budgets at the Raglan study site. A tidal jet is known to flow from the Raglan Harbour on the ebb tide, with a visible plume after heavy rainfall extending to the surf breaks on the headland. This flow is more likely to transport fine-grained sediment and is not likely to significantly contribute to the sustenance of sand on the headland.

Although extensive research has been undertaken on the flow characteristics at various shapes and sizes of headlands (e.g. Pingree and Maddock, 1979; Pattiaratchi *et al.,* 1986; Davies *et al.,* 1990; Freeland, 1990; Signell and Geyer, 1991; Yin *et al.,* 2003), and the effect that topography can have on current re-circulation (i.e. topographical forcing; e.g. Zimmerman, 1981; Middleton *et al.,* 1993; Davies *et al.,* 1995; Hume *et al.,* 1997; Jirka, 2001; Aiken *et al*., 2002), limited investigation has been carried out on surfing headlands where waves peel along the shoreline with a consistent breaking style. Klein *et al.* (2002) describes how minimal research has been conducted on headland bay beaches, despite Short and Masselink (1999) reporting that 51% of the worlds coastline presents this type of morphology. The term headland bay beach or embayed beaches defines a sandy shoreline bounded by rock outcrops or headlands (Klein and Menzies, 2001). There has been even less research on surfing headlands, with the literature containing minimal reference to surfing headlands in any form, with the most extensive investigations on current and sediment dynamics being undertaken by ASR Ltd, Raglan, New Zealand, in relation to the potential use of artificial surfing reefs for coastal stabilisation in the lee of headlands (e.g. Black *et al.,* 1999; Black *et al.,* 2001; Mead *et al.,* 2001).

One such surfing headland is at Noosa Heads, Australia, where processes of a different nature are prevalent, with an erosion problem on the main Noosa beach that has been identified by Black *et al.* (2001) as being primarily caused by wave crests being misaligned with the shoreline. This misalignment plus the wave-driven flows that initiate along First Point (surfing break along the headland), and bay-wide wind-driven circulation create littoral sediment transport along the

beach (Fig. 2.23a). The natural inputs of sand to the beach are also irregular and rely on large wave events that bring sand around the headland into Laguna Bay (Fig. 2.23b). It has been found that these slugs of sand are out of phase with the other coastal processes and erosion (Black *et al.,* 2001). Previous beach restoration by sand pumping techniques (Lloyd, 1980) has failed to stabilise the beach long term.

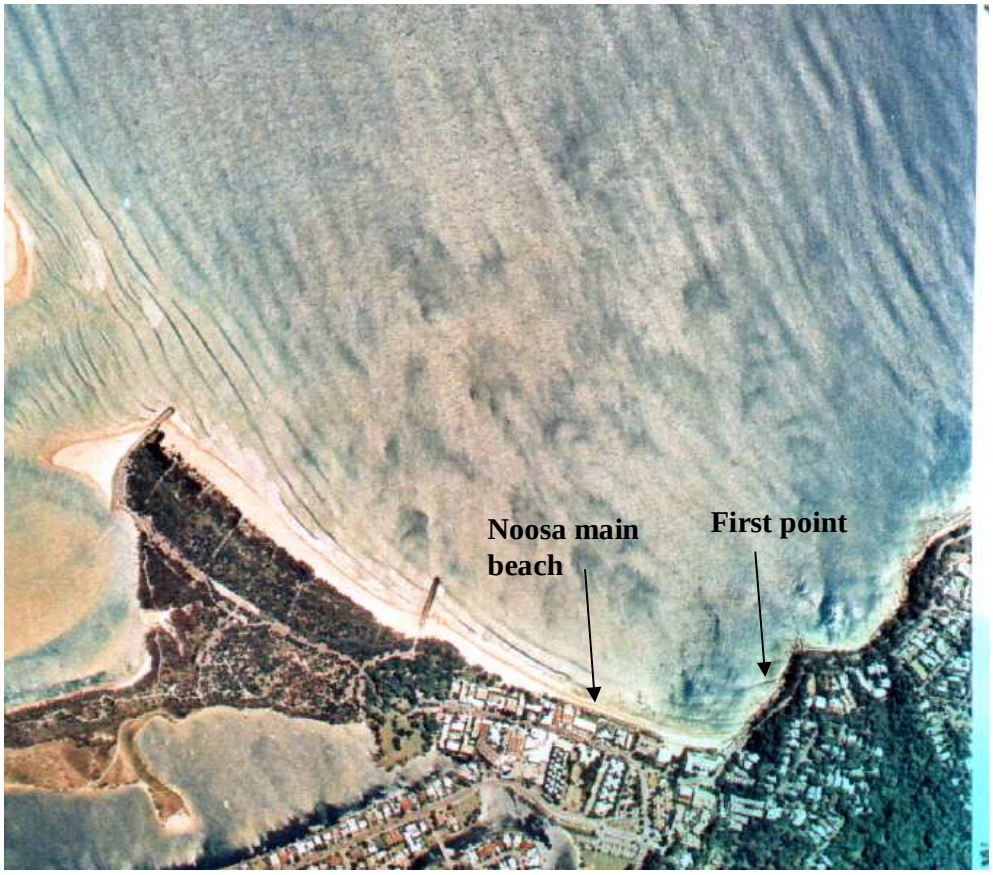

Figure 2.23a: Wave crests at Noosa Main Beach are mis-aligned with the shoreline and incompletely refracted, resulting in prevailing longshore currents to the west (Black et al., 2001).

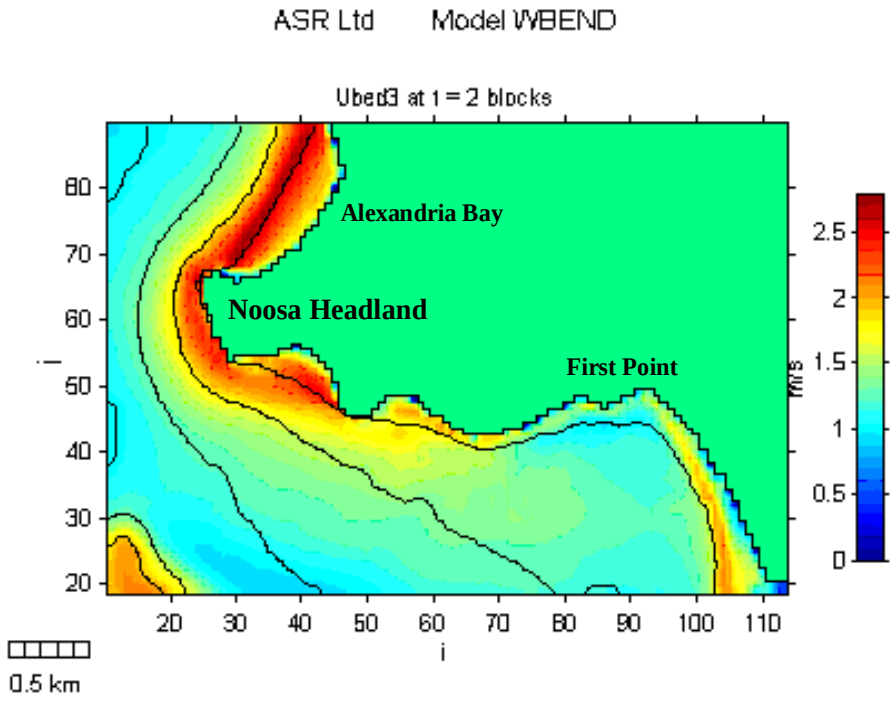

Figure 2.23b: The bottom wave orbital current pattern for a 4 m and 12 s swell from the east (Black et al., 2001).

The littoral drift system of a coastline is influenced by sand losses from beaches to coastal dune systems and tidal inlets and deltas, and ocean transport of sand beyond the nearshore active zone, causing a decrease in the amount of sand available to bypass headlands. Stephens *et al.*, (1981) found on the Australian east coast that eventually projecting headlands can prevent littoral drift into downdrift embayments, and as the embayments erode and the shoreline retreats, the headlands emerge to prevent further bypassing creating a compartmented coast. Studies on the Oregon coast have shown through the mineralogies and grain rounding on opposite sides of headlands, that these coastline features are effective in blocking longshore sand movement and therefore isolate beaches (Clemens and Komar, 1988; Shih and Komar, 1994).

In comparison, bypassing of sand on medium to high littoral drift coastlines around headlands or large groynes extending beyond the surf zone has a tendency to occur in "slugs" or pulses of sand (Short, 1999; Fig. 2.24). This slug transport creates patterns of "full" and "lean" segments which is not necessarily related to local conditions of sand supply or process (Pattearson and Patterson, 1983). Sand appears to accumulate on the updrift side of the headland or groyne to form a slug, which may pass very rapidly when activated (Short, 1999). The movement of the slug must be initiated by high wave energy, with larger or long period waves required to mobilise the sand in deeper water. The sand accumulates until the critical combination of wave height, period and direction occurs, allowing the sand to bypass the obstruction until wave conditions again become sub-critical (Chapman, 1981).

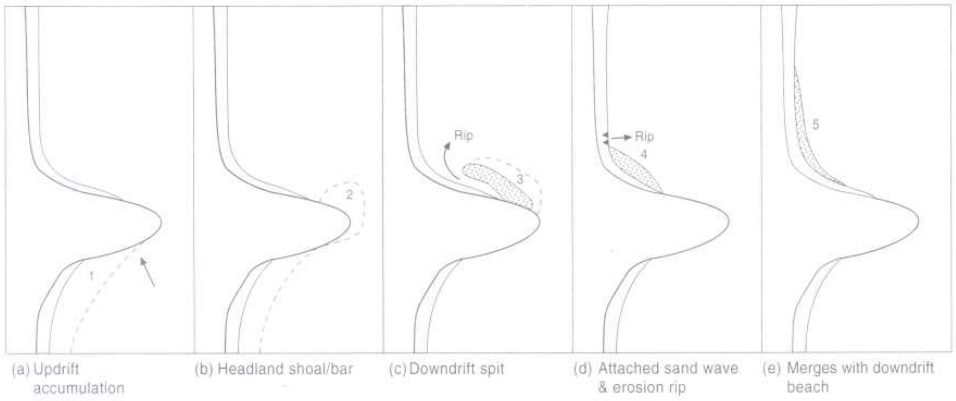

Figure 2.24: Schematic illustration of headland sand bypassing observed on the northern NSW and southern Queensland coast, eastern Australia. (a) It is assumed that longshore sand transport, perhaps assisted by beach rotation, causes sand to accumulate updrift of the headland. (b) The sand manifests itself as a substantial sub-aqueous sand wave on the tip and immediately downdrift of the headland. (c) The sand wave moves around and along the downdrift side as an elongate spit which often encloses a backing lagoon. (d) When the sand wave/spit is attached to the beach it initiates a topographically controlled rip that migrates in advance of the wave, often causing severe localised beach erosion. (e) The sand finally merges with the beach causing slight accretion. (Source: Short, 1999).

The Point Danger headland on the Gold Coast, Australia, extends significantly seaward compared to the general coastline, and into such deep water, dictating that almost all the sand input into the Gold Coast littoral system by-passes in a pulse fashion (Smith, 1982; Short, 1999), with most longshore transport taking place in depths mostly confined to less than 10 m (Pattearson and Patterson, 1983; Roelvink and Murray, 1992). In comparison, the sub-zeta bay headlands (e.g. Kirra and Burleigh Heads) are significantly smaller in size allowing sand to bypass more readily (Fig. 2.25). This can occur in comparatively mild sea conditions as long as the up-drift beach meeting the headland is reasonably full of sediment (Short, 1999).

Figure 2.25: Aerial view of Burleigh Heads, Australia showing the direction of sediment transport around the hard bedrock headland (Source: Gold Coast City Council, 23-4-96).

Storms have been found to create scour holes if sediment supply is lacking, or in areas where waves and currents interact with a nearshore reef (Pattearson and Patterson, 1983). Due its position in the wave shadow of Snapper Rocks (Point Danger headland) on the Gold Coast of Australia, areas such as Snapper Rocks Beach have a tendency to cycle between erosion and accretion depending on prevailing conditions and sand supply. Sand is contributed from large offshore shoals that move slowly under background swell conditions, or much faster in major storm conditions. Most sand appears to move in the longshore direction, rather than onshore (Pattearson and Patterson, 1983).

In general on coastlines with a predominant direction of littoral drift the downdrift beach shape in plan adopts the classic zeta shape, pitching its tightest curve immediately behind the headland (Silvester, 1976). However, Silvester found on the Gold Coast that when significant quantities of sediment bypass the local headland, the littoral drift does not follow the whole beach line but strikes across the 'hook' of the zeta embayment in a more or less straight line. In almost all cases the slug of sediment forms a bar, raised above the mean beach slope, until this melds into the zeta curve beach bar again some distance further up the beach (Smith, 1982). This bar is not a static feature but mobile over time. This sand bar system, just offshore, which promotes a smooth, well formed peeling wave with a hard plunge is a major factor contributing to the excellent surfing waves found at these headlands (Warren, 1999). This bar exists when there is a strong natural longshore transport of sand through this beach system.

However, the construction of the sand bypass system at the Tweed Rivermouth has significantly increased the quantity of sediment in the Gold Coast littoral system, and has created a longshore bar extending from Snapper Rocks to Kirra Point groyne (Turner, 2003). This essentially maintains the 'full' phase of sediment supply on a continous basis, filling the embayments and creating a breaking wave for surfing that extends for many hundreds of metres along the length of the longshore bar.

A rotating hydraulic cell that involves a recirculating eddy current in the lee of the headland has been observed along the Gold Coast (Smith, 1982). A nearly straight submerged bar of sand in the lee of the headland causes wave crest direction to reverse, which in turn drives both the currents and the sediments in the hook into their reverse flow. The cell rotates and an equilibrium recycling of the sediments within the hook occurs. At extreme periods of low tide, the cell is often perched as a lagoon on the beach, and all the sediment travels along the seaward face of the bar, until the rising tide reactivates the cell.

At St Clair Beach, a surfing headland in Dunedin, New Zealand, Dyer (1994) has observed that the primary influence on sediment transport is the longshore component of wave energy flux. This causes strong alongshore currents to flow in the nearshore zones (i.e. close to and within the surf-zone). In this case the predominant southwest swell maintains a net longshore current to the east, whilst a secondary northeast swell occurs mostly in the summer months. Because waves do not always approach from the same direction the sediment is usually transported in both directions along the beach and an equilibrium beach alignment is reached that is in dynamic balance with the wave climate, sediment supply, and the effects of sheltering due to local topography.

In this case the 'hard' rock headland at St Clair contributes to similar erosional trends identified at other areas throughout New Zealand and around the world, where the main sediment transport pathway bypasses the indented corner of the headland in the lee of the dominant wave approach (McComb *et al.*, 1999; Black *et al.*, 2001; Mead and McComb, 2001; Mead *et al.*, 2001). Erosion occurs at St. Clair typically during extended periods of strong southwest winds coincident with energetic wave conditions (Pope and Todd, 2003). Dyer (1994) observed that such conditions also had shorter period waves, and a noticeable easterly alongshore current. Under these conditions sand is likely to be transported both offshore and alongshore to the east, away from the western St.Clair corner, thereby causing the lowering of the beach profiles (Dyer, 1994). Although this seems a simple process the coastal and beach dynamics adjacent to a rocky headland such as this are complex, and arise from the combined interaction and effects of waves, sediment

supply, currents and seabed shape, and the presence of the large headland over 1 km long towards Black Head (Mead and McComb, 2001).

At Westshore Beach, located to the north of Napier City, in Hawkes Bay, New Zealand, a large headland also has a significant role in the dynamics of this section of the coast. In the presence of a headland, the local wave climate is modified, because the headland eliminates or greatly reduces the wave energy from the direction sheltered by the headland. This means that a segment of the directional wave climate is eliminated and the average direction of waves reaching the beach in the lee of the headland is rotated (Mead *et al.*, 2001). The processes have been further altered by the addition of a large breakwater at the port (Rowland *et al.*, 2003), which effectively extends the headland further into the sea. Local recirculating flows in the lee of the headland rotate in both clockwise and anticlockwise directions depending on the wave approach angle and inflowing current direction at the time (Fig. 2.26). Computer modelling suggested that these flows were altered after the breakwater was constructed and sediment is carried offshore, rather than being carried back to the headland in a closed recirculating loop. Wave-driven currents along the headland would be directed shorewards in the original condition, while this process is not able to develop with the presence of the port.

Sand is deposited in deeper water and cannot easily find its way back to the beach due to the presence of the headland eddy directing flows offshore. The port disrupts the continuous recirculating sediment pathway over the Westshore sand fillet (Mead *et al.*, 2001). Although Westshore is a different setup to that up of Raglan with no port or breakwater at the tip of the headland, an analogous recirculating loop transport system may be applicable to the dynamics of Raglan.

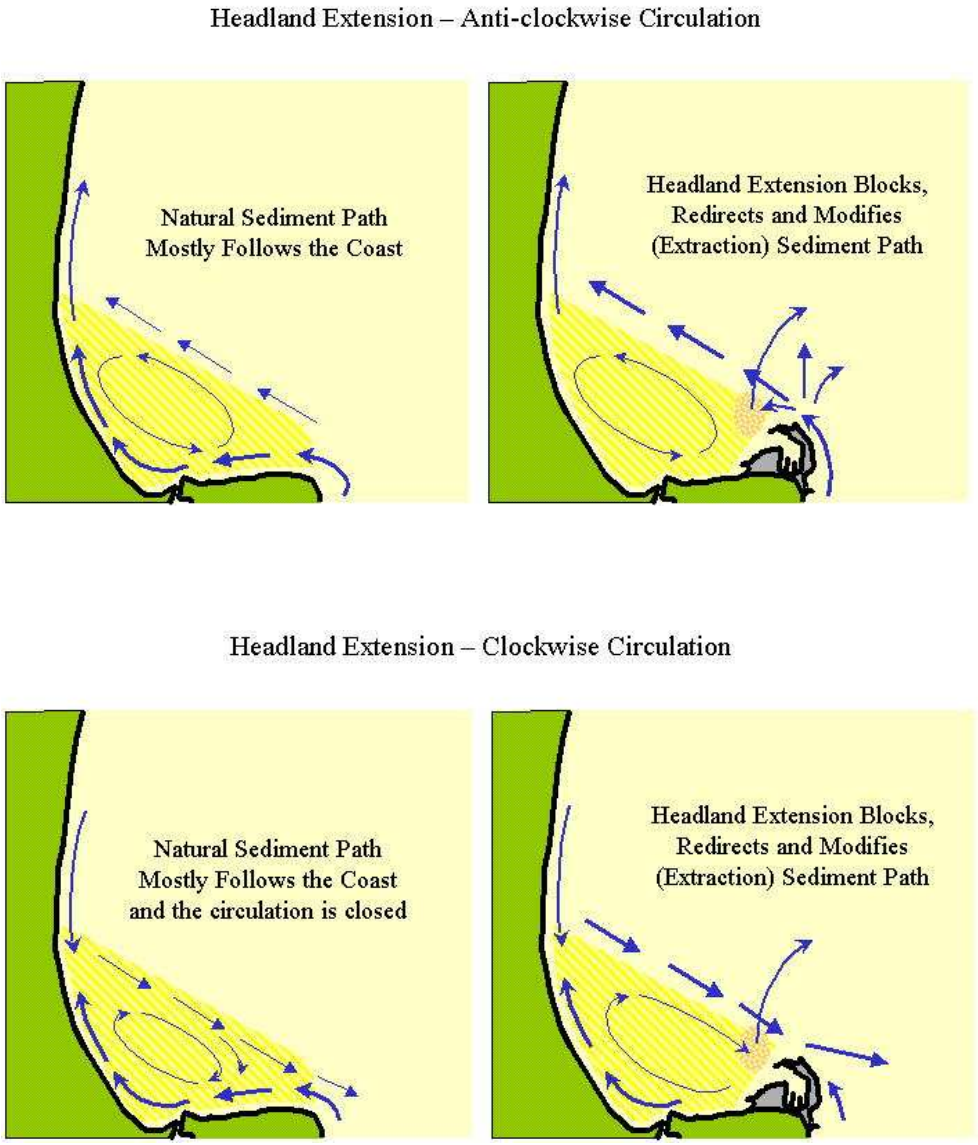

Figure 2.26: Idealised diagram of the natural recirculating systems without the headland extension and the effects of the headland extension (Port development) at Westshore Bay (Source: Mead et al., 2001).

Short (1985) describes how headland circulation can be impacted by the end effects, where in conditions with wave heights exceeding a few metres, large scale, topographically controlled rip systems called mega-rips can prevail. These can be transitional where circulation occurs when the embayment size and shape begin to increasingly influence the surf zone circulation, by initially causing longshore currents to turn and flow seaward against the headland. Cellular

circulation occurs when the topography (end effects) dominates the circulation. Longshore flow dominates within the embayment, with strong, seaward-flowing mega-rips occurring away from the headland. Hence the surf zone circulation is completely controlled by end effects. The rip intensity strengthens with increasing wave height, and can flow significantly seaward of the surf zone at high velocities (Short, 1999) and transport sediment offshore (Roy *et al.,* 1994). These large-scale cellular surf zone circulation currents were first described by Shephard and Inman (1950) and particularly McKenzie (1958).

Walker (1974) describes a similar rip current re-circulating back along a headland or point break that provides surfers with an easier paddle to the take off site at the initial break point of the waves (Fig. 2.27). This current is generated by the end effect, where a change in the orientation of the headland orientation causes the current to turn and flow back seawards. Carter *et al.* (1990) identified the presence of distinct cells along two similar headlands, where currents accelerated to a maximum along the headland flanks and then decelerated on the bay beaches where the coastal alignment changed. This clearly showed that the partitioning of wave energy or power is of fundamental importance in the transport of sediment at the headland.

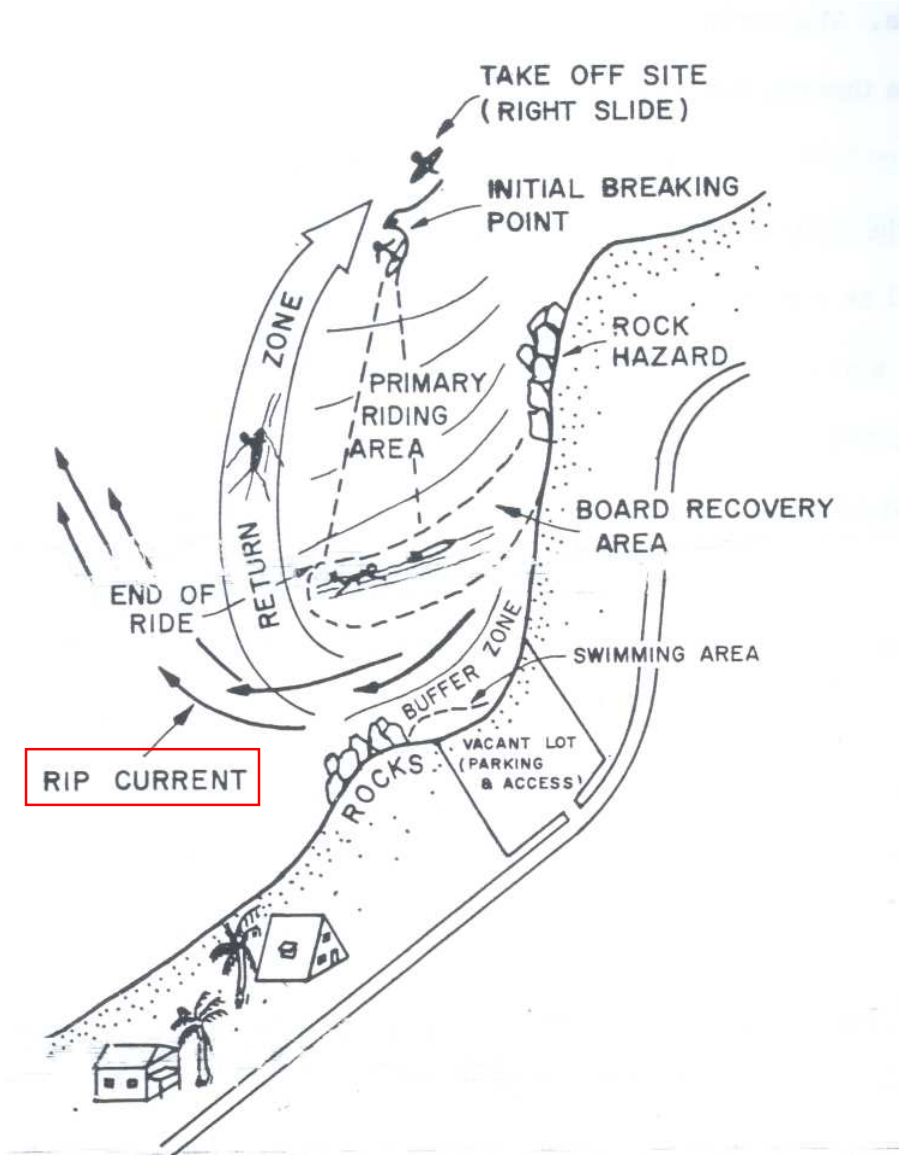

Figure 2.27: Headland or promontory surf site components (Source: Walker, 1974), showing the rip current flowing back along the headland due to topographic end effects.

2.1.6 *Wave driven currents*

Wave-induced currents transport sediment along coastlines (e.g. Guilcher, 1958; Inman *et al.,* 1968; Hallermeier, 1982; Basco, 1983; Bodge, 1989; Yoo, 1994, Komar, 1998). The rate of transport varies according to the angle or orientation at which the waves break relative to the shoreline, as well as the height and period of wave events (Kamphuis, 2000). It has also been suggested by Ebersole (2002) that a significantly greater total rate of longshore transport occurs in plunging breakers, than in spilling breakers of a similar wave height.

The two principal patterns of wave-generated currents within the nearshore area are cell circulation, and longshore currents produced by waves breaking at an angle to the shoreline (Sorenson *et al.,* 1994; Komar, 1998). Komar found that cell circulation can be generated by longshore variations in wave-breaker heights, allowing currents to flow from areas of high waves and set-up, to zones of low waves and set-up where the currents converge and turn seaward as rips. The variation can occur due to wave refraction over irregular topography, or by local sheltering of headlands, jetties and breakwaters.

It is well documented that when waves approach a shore at an oblique angle, a shore-parallel current is generated as waves break in the near-shore zone, transporting sediment along the coast (e.g. Longuet-Higgins, 1970; Komar, 1985; Fredsøe and Diegard, 1992; Schoonees and Theron, 1993; Komar, 1998; Zhang and Wu, 1999; Ashton *et al.*, 2001; Kim *et al.*, 2001). This longshore wave-driven current is less complex than the cell circulation system, and observations confirm that the current is driven by forces associated with waves breaking on a sloping beach and that ocean-currents, wind-driven currents, and tides do not in general play significant roles (although these factors can modify the current that is otherwise generated by waves; Komar, 1998). An understanding of the generation of this current has come from the analyses of the longshore component of the radiation stress of the waves, which exerts a thrust on the water within the nearshore. The velocity of the longshore current can be approximated (Komar and Inman, 1970)(Eqn 2.1) as:

$$V_l = 2.7 u_{\mathrm{m}} \sin\alpha_b \cos\alpha_b \qquad (2.1)$$

where V_l = velocity of the longshore current, u_{m} = horizontal component of the water particle velocity under waves, α_b = angle between the wave crest and a line parallel to the shoreline.

The cause of long-term erosion can relate to either changes in sediment supply (e.g. altered river or coastal cliff supply, diabathic loss offshore, upstream construction), variation in the wave climate, climate change, or changes to beach orientation due to construction (Kamphuis, 2000). The fundamental problem in a number of cases relates to an imbalanced alignment of the coast in relation to the average wave orientation, which leads to wave-driven longshore currents (Mead and Black, 2002). These currents transport sand away from the site and local erosion results. Applied investigations at a number of surfing headlands have shown in each case that the coastal orientation is out of alignment with the wave orientation, and input supply is not able to sustain the sediment losses that occur with the currents (Mead and Black, 2002). Examples are Noosa Beach (Australia), Westshore Beach (New Zealand) and Bournemouth Beach (Southern England).

Although not exactly the same as these examples, Raglan can be compared to these sections of coast that are out of alignment with the predominant wave direction, in that waves sweep along the surf breaks at the headland transporting sediment in the wave-driven currents, and potentially eroding the seabed at the headland. The orientation of the headland and the surf breaks upon it, create this environment. The angle of the wave breaking at the headland is very dependent on the swell direction at the time, with a more southwest swell flowing along the headland (very oblique angle), whilst a northwest swell is directed more normal to the headland (lower oblique angle).

2.1.7 *Influence of currents on surfing breaks*

Strong currents are something that surfers have to deal with almost every time they paddle out to a surf break (Warren, 1999). Most often, the currents are wave-driven, but tidal jets near river and estuary bar surfing breaks, and even large oceanic currents can impact on the surfability of a surfing break (Symonds and Black, 2001). This section gives examples of the different types of currents that surfers have to deal with at a variety of surf breaks, based in some cases on the observations and experience of the author and other surfers gained whilst surfing the locations. These can be compared to the currents found at Raglan to gain a better understanding of the effect of wave-driven currents at surfing breaks including 'surfability', ease/difficulty of paddling back out at artificial surfing reefs (Dally, 2001b) and bar formation and reef erosion/deposition patterns.

The strength and direction of wave-driven currents in the surf zone can influence the 'surfability' of a break. At a surfing headland strong currents flowing down-drift along the shoreline can limit access to the surf and make it difficult for a paddling surfer to get to the "take-off" location of the break, or maintain position in the line-up (Symonds and Black, 2001). In comparison currents flowing up-drift along headlands makes getting "out the back" relatively easy, although surfers can be taken out to sea past the "take-off" point by a fast flowing current. These currents are often found at surf breaks near harbours and rivermouths, with an ebb tide creating an easy paddle out in the deep channel (Warwick, 1986; Fig. 2.28). This is demonstrated at the Whangapoua bar on Great Barrier Island and Whangamata bar on the Coromandel Pennisula in New Zealand, where surfers are taken out to sea from the "take-off" zone on an outgoing tide (Bhana, 1988). However, the strong out-flowing current also means surfers must continually paddle against the flow to stay in the "take-off" area of the break.

At Omaha bar, north of Auckland, the reverse occurs where surfers must continually paddle wide from the initial break-point, as currents push over the bar taking surfers too far inside the breaking wave zone, making it difficult to catch waves. Pickard (1986) described a similar flow over Davies Reef, Australia, where 40% of the flow was due to wave forcing. The current can also increase the steepness and shoaling of the wave as it breaks, with the outgoing flow significantly 'sucking' the wave face, possibly creating a 'tubing' wave (Bhana, 1988). The ebb current is seen to compress the wavelength and concentrate the energy of the wave form which is reflected in a dramatic increase in height (Hales and Herbich, 1972). This is seen in places such as Whangapoa on Great Barrier Island, New Zealand (Fig. 2.29).

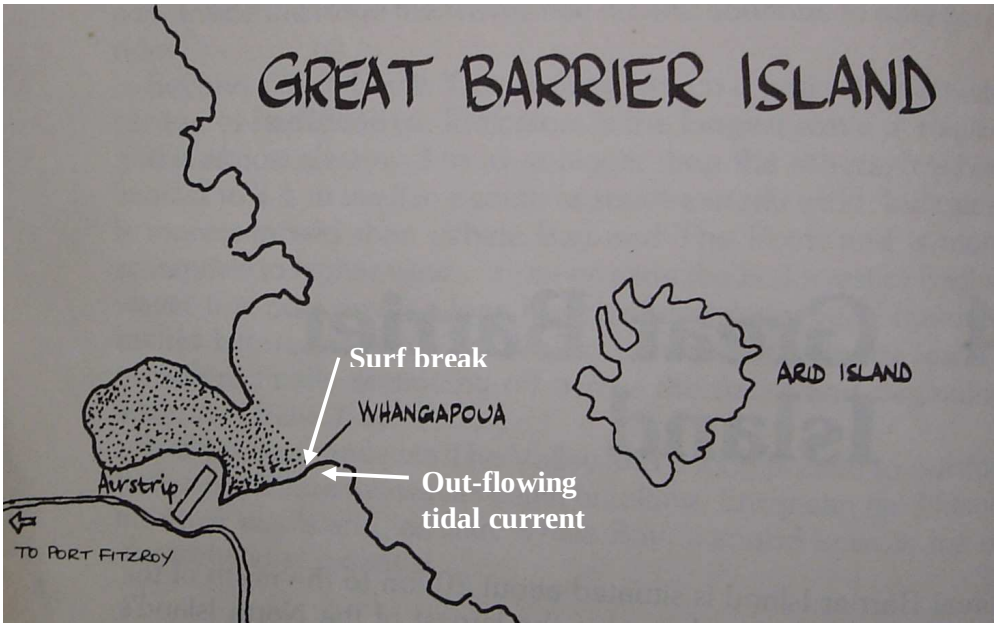

Figure 2.28: Whangapoua Estuary on Great Barrier Island showing location of surf break and tidal current (Source: Bhana, 1988).

On the Gold Coast of Australia, a number of world-class point breaks exist at the sub-zeta headlands north of the large Point Danger headland. These breaks include Greenmount, Kirra Point and Burleigh Heads (Warren, 1999). During medium to large swell events at these surfing breaks, a significant northward current flows in the direction of the waves that is very difficult to paddle against (Hutt *et al.,* 1998). This current extends significantly wide of the surf zone and

requires surfers to constantly paddle in order to maintain position in the line-up. Jumping from the rocks up-drift along the coast is often the only means of getting out to surf the break.

Figure 2.29: A 'tubing' wave breaking on the Whangapoua Bar (Source: Bhana, 1988).

In comparison the world famous break at Desert Point in Lombok, Indonesia (Fig. 2.30) has a very large wave-driven current in the breaking wave zone, but seawards of this a significant counter-current exists flowing back out to sea (Lueras, 1995). This current makes paddling "out the back" very easy, but unless a wave is caught surfers can be taken past the "take-off" point and struggle to get back to the breaking wave zone. This current may be mostly due to the flow through the Lombok straight that runs at a minimum of 7-8 knots. However, Symonds *et al.* (1995) describes the basic dynamics of wave forcing on reefs, where incident wave momentum lost through wave breaking on the reef slope is partitioned between driving cross reef currents against bottom friction and balancing an offshore-directed pressure gradient due to wave set up. The returning current at Desert Point increases in velocity as the waves become larger, which

may primarily be due to the build of a pressure gradient of the waves interacting with the reef.

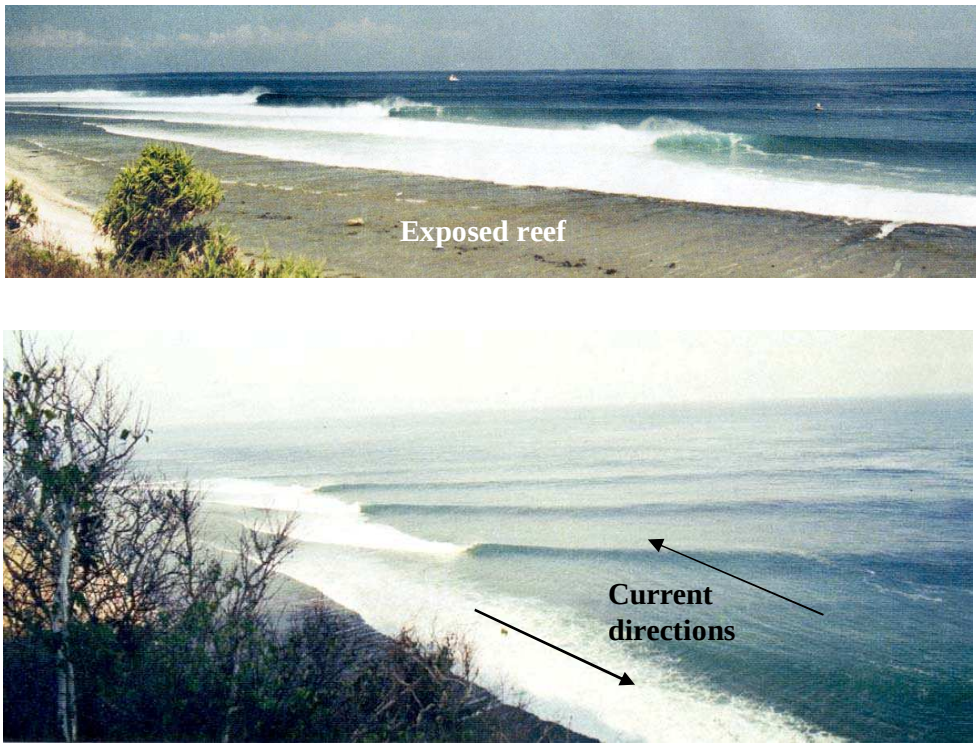

Figure 2.30: Desert Point in Lombok, Indonesia rated as the best wave in the world by Tracks surfing magazine with directions of currents along the reef (Photo source: Tracks Magazine, 2000).

In large swells where the waves break in a pattern of sets, the lull period provides the opportunity for surfers to have a chance of paddling through the surf zone. However, this is not the case when the waves break with a consistent and continuous period, providing no opportunity for access to the surf-break. In some locations such as Rincon surf break in California the out-flowing creek halfway up the headland provides a better access point as waves can be attenuated in this zone (Fig. 2.31).

At Raglan, a site at the end of the Whale Bay reef where the waves are not sweeping down the headland, but rather breaking into the reef between compartments provides a similar opportunity (Fig. 2.32). A build-up of a pressure gradient and less current velocity in this area can increase the chances of getting out to the breaking waves.

Figure 2.31: Aerial view of Rincon showing the waves refracting around the headland, and the 'creek' where easier access to the surf is available due to wave attenuation, compared to the strong currents found along the remainder of the headland (Source: Woodworth, W, Surfer Magazine, 1992).

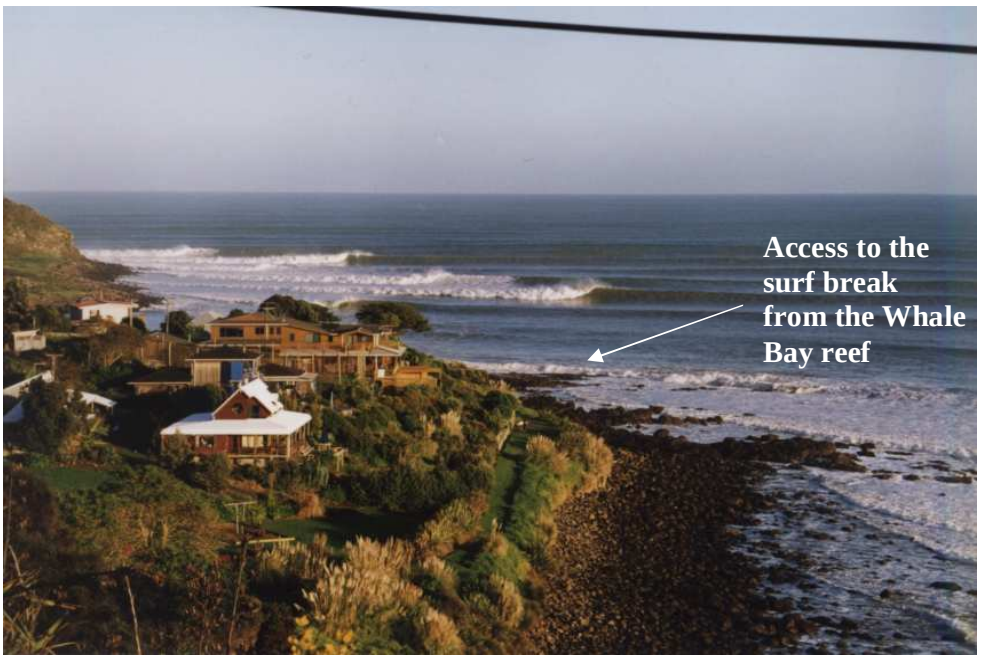

Figure 2.32: Raglan headland looking past Whale Bay to Indicators surf break, showing the access point for surfers at the Whale bay reef (Source: Author, 20-4-01).

2.2 SEDIMENT DYNAMICS

2.2.1 Introduction

Sediment dynamics is the transportation of sediment through bedload and suspension in the water column, which has been found to be coupled with waves, wind and wave-induced currents, oscillatory motions, bed topography, and the size and density of sediment (Deigard *et al.*, 1986; Fredsøe *et al.*, 1986; Nielson, 1986; Li and Davies, 1997; Komar, 1998). Therefore, suspended sediment concentrations around the surf zone are strongly related to breaker type, wave properties, the position relative to the breakpoint and bed topography (Zampol and Inman, 1989; Beach and Sternberg, 1996). Osborne and Greenwood (1992) found that wave groups rather than individual large waves transport the highest concentrations of suspended sediment, with wave groups progressively more dominant at higher elevations above the bed (Hanes and Huntley, 1986). Beach and Sternberg (1992) suggest that wave/current interactions enhance sediment

load and longshore sand transport by approximately 50-60%, over the transport forced by waves alone.

An exponential relationship exists for the time-averaged vertical distribution of suspended sediment as well as a decreasing grain size with elevation above the bed (Fredsøe and Diegaard, 1992). The description of time-averaged suspended-sediment concentration profiles under waves can be broken down into two steps. The first is specification of the amount of sediment in suspension; the second is specification of the distribution of sediment throughout the water column (Nielson, 1986). The suspended-sediment reference concentration, which is the time-averaged concentration of suspended-sediment "at the bed", relates to the first step, and the second step typically, although not necessarily, relates to sediment diffusivity (Green and Black, 1999).

The amount of sediment suspended in the water is directly related to the grain size of the sediment, the wave-orbital induced stress on the seabed and turbulence. Consequently, higher concentrations of suspended sediments are expected during larger wave events, and also in regions that experience higher wave energy or shallower water depths (Deigard *et al.*, 1986). To calculate and estimate suspended sediment concentration profiles and near-bed reference concentrations various equations and models have been developed. Eddy diffusivity must be considered in the calculation, and has been found that the application of a vertically constant eddy diffusivity (Equation 2.2) represents surf zone data well for time periods over many wave cycles (Nielson, 1986).

$$C_z = C_o \exp^{(-z/ls)} \qquad (2.2)$$

where

C_z = concentration of sediment at elevation z

C_o = concentration of sediment at the bed

and the mixing length ls is the length scale of sediment motion, which is given by ε_s/w

ε_s = eddy diffusivity

w = settling velocity

Mocke and Smith (1992) found that Equation 2.2 describes the time-averaged concentration profile in the surf zone well, and that there is an indication that it describes surf zone concentrations well over relatively long periods.

There remain, however, many questions concerning sediment suspension, sediment interactions with flow, turbulence and boundary layers and ultimately the use of empirical equations to calculate and model concentrations and represent their profiles. Black *et al.* (1997) describes how although numerical simulation of complex circulation patterns over the bed have been effective in modelling suspended sediment processes, difficulties arise in modelling concentrations as they are not spatially-uniform. Black and Rosenberg (1992b) concluded that the dynamic nature of the processes involved in the initiation of sediment movement, sediment suspension and transport and the small scale in which these processes are involved make their measurement extremely difficult.

2.2.2 New Zealand west coast littoral sediment transport

The west coast of New Zealand has been aptly named the untamed coast by Harvey (1998), due its rugged nature and exposure to the elements of strong winds and large surf (Fig. 2.33).

Figure 2.33: West coast of North Island, New Zealand (Source: Harvey, 1998).

Investigations of west coast littoral sediment transport have shown that net sediment movement is to the north, with approximately 175,000 m^3/yr of net littoral drift on the coastline at Raglan (Matthews, 1977; Gibb, 1979; Hicks and Hume, 1993). These studies focused on the total longshore drift up the coast, not on the headland environment that exists south of Raglan. Stokes (1991) concluded that the large reservoir of sediment that occurs on the north side of the Raglan Harbour entrance are associated with a prolonged period of northerly littoral drift. Further south of Raglan at New Plymouth, a net northeasterly flux was found, although sediments were found to respond to local and temporal perturbations which give rise to reversing and circulating fluxes. A total of 220,000 m^3/yr is known to migrate around the Paritutu headland (McComb *et al.*, 1999).

Scarfe *et al.* (2002) undertook a series of detailed hydrographic surveys over a one-year period of the seabed at Manu Bay, Raglan, to identify fluctuations in the

level of the bed and to identify features that modify shoaling and breaking of waves. The results showed that up to 0.5 m of sediment can be eroded or accreted per month from sand bars as they move onshore and offshore (Scarfe, 2002a). This significant change in the shape of the seafloor over time was found to affect the preconditioning of breaking waves, with meso-scale focus components appearing and disappearing as successive swells accumulated or scoured sediment around the reef.

In New Plymouth McComb and Black (2001) found that erosion from a placed sediment mound did not occur as a contiguous body, and rocky areas adjacent to the mound did not become inundated with sand. The data suggested that littoral transport to and from the placement region is primarily by sediment suspension, rather than bedload. Douglass (1996) describes how sediment is mobilised by wave-orbital motion through wave-orbital velocity asymmetry under finite-amplitude waves. This is most likely in the energetic wave climate that was observed at New Plymouth, with significant wave heights of up to 4.47 m and persistent long-period (12-14 second) swells. However McComb and Black (2001) conclude that velocity asymmetry is not the fundamental cause of erosion, but rather sediment suspension by waves and net transport by the variable coastal currents. A 100^{o} range in wave directions was recorded, although 72 % of data were within a 40^{o} directional window with the mean direction of wave advance being 116^{o}. Near-bed currents had a broad directional distribution and reached a maximum velocity of 0.29 ms^{-1}, with a mean value of 0.57 ms^{-1}. No direct relationship between mound erosion and the current regimen was found. The relatively slow dissipation of the mound, despite high sediment entrainment potential, is attributed to the gradual re-establishment of the pre-placement sedimentary equilibrium under a dynamic and multi-directional sediment flux.

The rock/sand boundaries adjacent to the placed mound off New Plymouth showed remarkable stability, distinguished through the use of time-series side-scan sonograph images. The side-scan also indicated that persistent regions of sandy sediments often coincide with seabed depressions and the western flanks of raised bathymetric features. This feature was also found by Scarfe *et al.* (2002) at

Manu Bay, Raglan where scouring and infilling around the reefs is evident with certain reef features acting as groins to trap sand (Fig. 2.34). It is therefore apparent that the seabed topography influences the sediment transport, and raised features present an obstacle for the sediments in transit (McComb and Black, 2001).

At New Plymouth it can be concluded that the rocky subtidal regions are not conducive to the long-term settlement of the mobile littoral sediments under the present nearshore sedimentary budgets. The wave-orbital interaction with the hydrodynamically 'rough' substrate possibly creates a greater turbulent flow over these beds making settlement of sediment less likely (e.g. Nelson, 1996; Green *et al.*, 1998). This may also be the case at Raglan as identified by Scarfe (2002), where the rocky reef boundaries and outcrops are clearly defined and distinguishable from the sandy seabed.

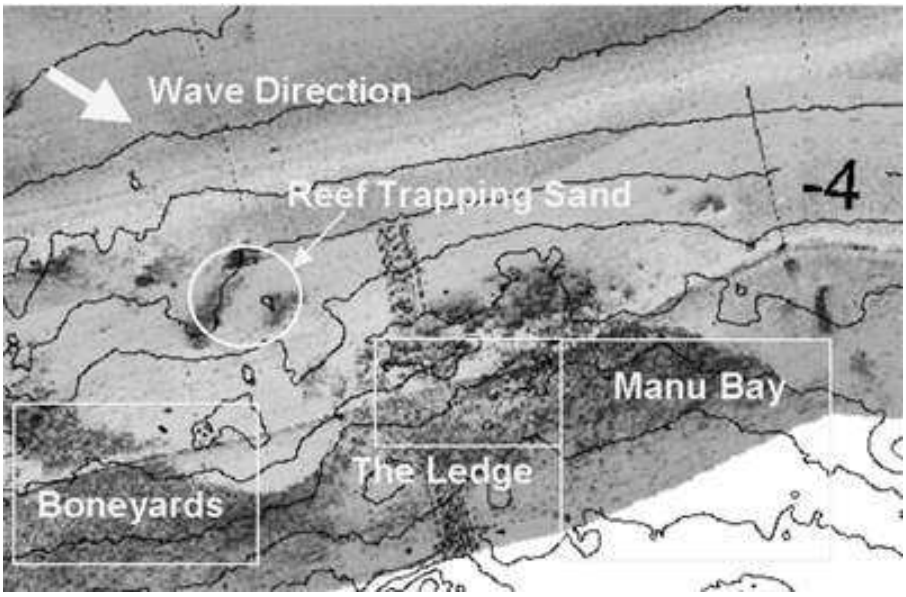

Figure 2.34: Side Scan image of Raglan (Phillips et al., 2001) with 1 m contours. The sand-reef boundary and the offshore reefs trapping sand are evident (Scarfe, 2002).

Hicks and Hume (1996) describe how ebb tidal deltas are major and dynamic elements of the littoral sediment budget at tidal inlets, and they can strongly influence coastal processes in the vicinity of the tidal inlet, for example, by-passing of littoral drift and partial wave sheltering of the adjacent shore. The

Raglan tidal delta was classified as a "free form" delta that is "bat-winged" in shape with a single spit, is longshore-elongated and reasonably symmetrical. These features are common on the large headland-bound open-coast inlets on the high-energy west coast with its exposed shoreline experiencing significant littoral drift (e.g. Kawhia, Kaipara, Manukau, Hokianga).

The primary factors controlling the shape of the ebb delta are the tidal outflow, shoreline configuration, wave energy and wave direction. A distinctive feature of the New Zealand inlets, as at Raglan, is the importance of bedrock headlands (Hicks and Hume, 1996). The relative exposure to waves can be influenced by the headland, which in the case of Raglan may provide some shelter from the south-westerly swell. The tidal outflow is also a significant factor and at Raglan a balance exists between this flow and the large waves limiting the offshore extent of the delta by driving delta sediment shoreward and also spreading it alongshore. The influences from the ebb-delta may have an effect on the Raglan headland dynamics with its proximity to the delta, with possible flow to the headland shown by visible evidence of a plume (Hutt, 1997). However this flow is not expected to significantly affect the stability of the bed at the headland.

2.2.2.1 West coast wind and wave climate

The coastline of New Zealand is comparatively long in proportion to land area and also very diverse (Buckeridge, 1995). The country's elongated shape and north-south orientation straddling the circumpolar westerlies and its temperate to subtropical climate and varied geology provide a wide range of coastal environments (e.g. Healy and Kirk, 1982; Hume *et al.,* 1992). The west coast of New Zealand is one particular coastal environment that is characterised by a succession of headlands and long sandy beaches. There has been very little data collected on the high-energy New Zealand west coast wave climate (Hume *et al.*, 1997), apart from short-term experiments (e.g. Hutt, 1997; McComb *et al.,* 1999; Scarfe, 2002) and data from the offshore Maui oil platform (e.g. Ewans and Kibblewhite, 1992).

The west coast of the North island of New Zealand is characterised as having a high-energy wave climate with exposure to waves ranging from the southwest through to the north. The predominant wind and swell direction on the west coast is from the southwest (Heath, 1982), confirmed through numerical modelling by Laing (1993). The wind patterns are characterised by the eastward migration of anticyclones and low-pressure troughs. Anticyclones (high-pressure systems) account for settled conditions, which occur about 25 % of the time, with the remainder of the weather determined by cyclones (low-pressure systems) (Maunder, 1970; Harris, 1990). McComb *et al.*, (2000) describe how the path of anticyclones across New Zealand exhibit a seasonal variation, with anticyclonic influences extending further south over the summer / autumn months. Patterns are further modified in response to El Nino-Southern Oscillation (ENSO) events, whereby an El Nino event typically results in a west-southwest anomaly superimposed over the 'normal' wind conditions, causing strengthened and more frequent west-southwesterly winds. For a La Nina event the opposite is generally true, with an east-northeasterly wind field anomaly.

The wave environment is dominated by west and southwest swell and storm waves generated in the temperate latitude belt of westerly winds, with the larger swell generated in the south (Pickrill and Mitchel, 1979). Wave data collected at the Maui oilfield over a 10-year period (September 1976 – April 1987) was analysed by Kibblewhite *et al.,* (1982) over a 5-year period from 1977 – 81, and found a higher wave climate in the winter months. The occurrence of significant wave height in the <1, 1 – 2, 2 – 3, 3 – 4, 4 – 5, and >5m ranges is approximately 3%, 25%, 35%, 25%, 8% and 4%, respectively. The importance of southwest swell arriving from distant shores in the south of the Tasman Sea and the Southern Ocean, with a wave period of approximately 12 seconds was identified by Ewans and Kibblewhite (1992), in a spectral analysis of the Maui wave data.

Numerical hindcast data (WAM model time-series) is available for a site 5 km off the coast near Raglan (38.001^{o}S, 174.737^{o}E; Fig. 2.35)(Data source: R. Gorman, National Institute of Water and Atmospheric Research (NIWA), Hamilton; Gorman, 2000; Gorman and Laing, 2000) for a 15-year period (1979 – 1993)

giving averaged wave statistics (Table 2.1), along with the joint probability of significant wave height and direction (Table 2.2). This data clearly shows that the most waves approach from the WSW with an average heading of 71.07^{o}, followed by waves from the SW and W directions. The average peak spectral period is 11.21 seconds, with a maximum of 19.82 seconds, and the average significant wave height is 1.66 m. The largest waves (i.e. >3.5 m) approach from the WSW quarter and range from 0.23 m to 9.15 m (McComb *et al.*, 2000).

McComb and Black (2001) describe the west coast as open and exposed to the Tasman Sea, experiencing a high-energy wave climate that varies from short-term waves (1-4 m at 4-8 s periods) to long-period (12-18 s) swell, with inshore heights of up to 6 m. The nearshore circulation is similarly variable and responds to regional flows as well as wave-driven components plus a strong influence from the sub-tidal reefs. As at Raglan the New Plymouth coast has an irregular bathymetry with a heterogenous seabed substrate of sand and large rocky reefs.

Table 2.1: Mean statistics of significant wave height, peak spectral wave period and wave direction for the WAM 15-year numerical hindcast for a site 5 km offshore of Raglan. (Data source: R. Gorman, NIWA, Hamilton).

	Average	**Standard Deviation**	**Minimum**	**Maximum**
Significant wave height (m)	1.66	0.79	0.23	9.15
Peak spectral wave period (s)	11.21	2.24	3.23	19.82
Mean wave direction towards (deg)	71.07	22.62	-	-

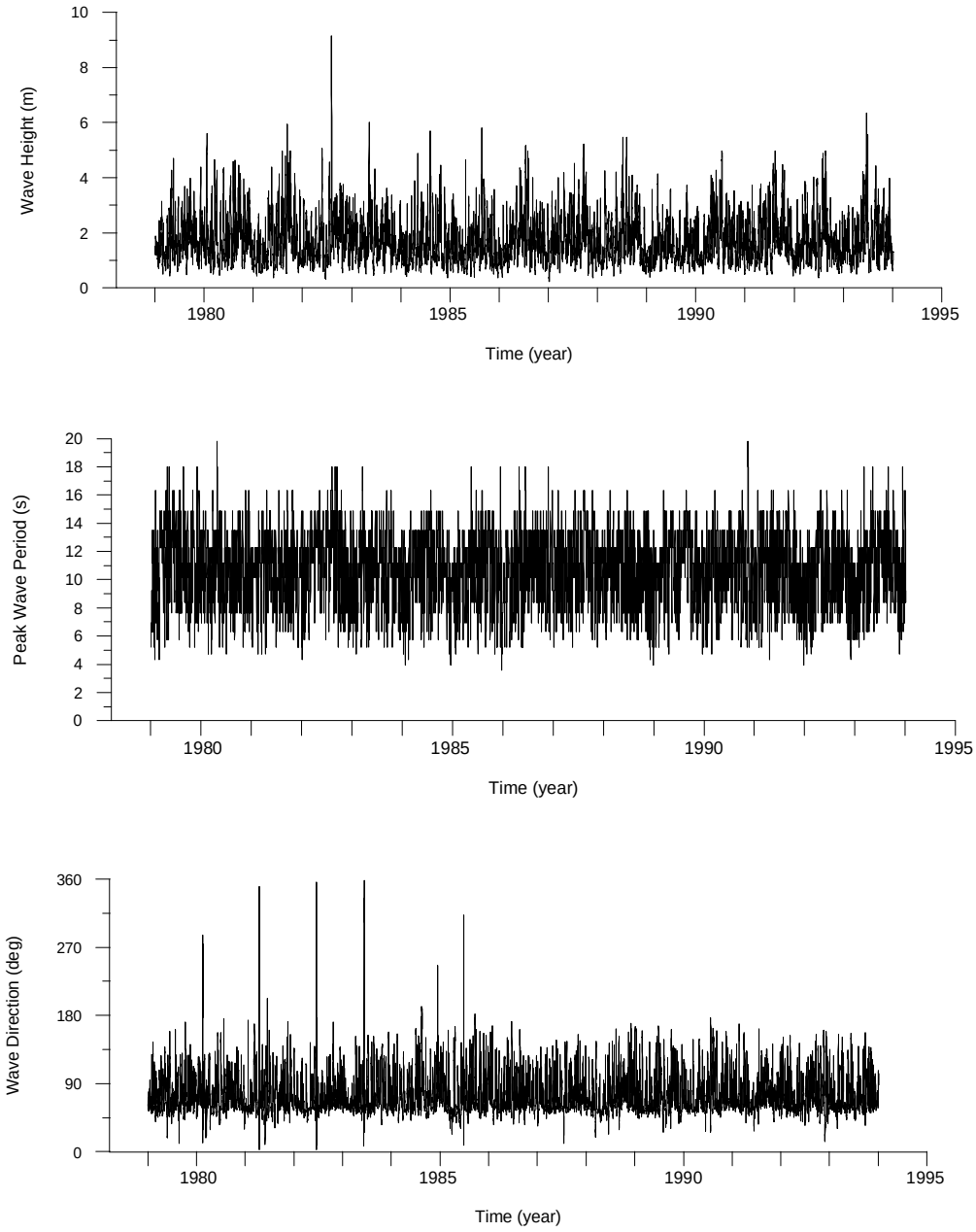

Figure 2.35: 15-year time-series of significant wave heights, peak spectral wave periods and mean wave directions (i.e. 'going to') from the WAM hindcast of wave and wind statistics (Source: R. Gorman, NIWA, Hamilton). Model output is for a site 5 km offshore of the coast near Raglan (38.001S, 174.737E).

Table 2.2. Joint probability of occurrence of significant wave height (m) and mean wave direction (from) for the WAM hindcast data 5 km offshore of Raglan. (Data source: R. Gorman, NIWA, Hamilton).

	<0.2	**<0.5**	**<1.0**	**<1.5**	**<2.0**	**<2.5**	**<3.0**	**<3.5**	**<4.0**	**<5.0**	**<10.0**	**Total**
NNE	0	0	0.01	0	0	0	0	0	0	0	0	0.01
NE	0	0	0.01	0	0	0	0	0	0	0	0	0.01
ENE	0	0	0.01	0	0	0	0	0	0	0	0	0.01
E	0	0	0.01	0	0	0	0	0	0	0	0	0.01
ESE	0	0	0.01	0	0	0	0	0	0	0	0	0.01
SE	0	0	0.02	0	0	0	0	0	0	0	0	0.02
SSE	0	0	0.01	0	0	0	0	0	0	0	0	0.01
S	0	0.01	0.02	0	0	0	0	0	0	0	0	0.03
SSW	0	0.03	0.16	0.07	0	0	0	0	0	0	0	0.27
SW	0	0.42	7.52	9.12	4.54	1.91	0.9	0.26	0.14	0.08	0.01	24.93
WSW	0	0.22	7.78	13.6	11.1	7.25	4.61	2.46	1.1	0.66	0.11	48.87
W	0	0.06	1.99	4.39	3.8	2.39	1.41	0.82	0.31	0.25	0.04	15.46
WNW	0	0	1	1.83	1.76	1.29	0.49	0.24	0.07	0.05	0	6.75
NW	0	0.01	0.42	0.85	0.72	0.45	0.14	0.07	0.03	0.01	0	2.69
NNW	0	0.01	0.24	0.36	0.17	0.03	0.01	0	0	0	0	0.81
N	0	0	0.08	0.03	0	0	0	0	0	0	0	0.12
SUM	0	0.78	19.3	30.2	22.1	13.3	7.57	3.85	1.65	1.06	0.16	100

2.2.2.2 West coast research

The New Zealand coast arguably contains a greater range of beach and nearshore environments within close proximity than any coastline in the world (Brander, *et al.,* 2003). Brander describes that a comprehensive understanding of the New Zealand coast is yet to be realised, with large areas of the New Zealand coast remaining unstudied. This is due to a lack of data and research motivated by management issues in regions of high population, economic and recreational value.

In general the west coast has been studied far less extensively than the east coast of the country (Hume *et al.,* 1992), due a distinct difference in the wave climates of the respective coasts. The wave climate of the west coast classifies the coast as a high-energy environment, in comparison to the low-energy east coast wave climate (Pickrill and Mitchell, 1979). Typically the larger waves associated with high-energy beaches limit the collection of field data due to obvious logistical constraints of working in energetic conditions, where the deployment and retrieval of equipment can be dangerous and the probability of equipment damage is exceedingly high (Brander *et al.,* 2003).

Research on the west coast has been undertaken on the Auckland beaches of Muriwai and Piha (Smith and Ovenden, 1992; Tonkin and Taylor, 1998; NIWA, 1999; Short and Brander, 1999; Brander and Short, 2000; Dahm, 2002), Taranaki relating to Fitzroy Beach (Matthews, 1977; McClennan, 1982), the New Plymouth Port (Westgate) (Heath, 1982) and recently extensive work in relation to dredge disposal works (McComb *et al.,* 1999; McComb and Black, 2000; McComb, 2001). Studies have also been undertaken for the Maui gas field (Kibblewhite *et al.,* 1982; Ewans and Kibblewhite, 1992), the Wanganui coastline using remote video imagery (Shand and Bailey, 1999; Shand *et al.,* 1999), the coastline around Wellington, Kapiti and the Cook Strait (Gibb, 1978; Lewis, 1979; Morris, 1984; Carter and Lewis, 1995). More recently, work has been undertaken by ASR Ltd related to the west coast Telstra-Saturn cable-crossing project, with an extensive summary published on research along this coast (McComb *et al.,* 2000).

Research on the west coast of New Zealand had not previously included the surfing headland at Raglan, until investigations were initiated as part of the Artificial Reef Program at the University of Waikato (Black, 2001b). Studies included extensive investigation of surfing related parameters (bathymetry, wave refraction, wave peel angles, etc)(Hutt, 1997; Sayce, 1997; Hutt *et al.*, 1999; Sayce *et al.*, 1999; Mead, 2000). There has however been no previous research undertaken at Raglan on the effect that this natural feature has on the currents and sediment dynamics of the coast.

2.3 SEABED CHARACTERISTICS

2.3.1 Introduction

Characteristics of the seabed form an integral component in the understanding of the dynamics and processes acting upon an environment. It can be difficult to quantify wave and current-driven transport around headlands by field measurements of these parameters alone, particularly over long time scales (years), due to their spatial variability and because sediment transport increases dramatically during intense, infrequent, episodic storm and large swell events (Hume *et al.*, 1997). Storms may still mask the underlying dominant processes, but the seabed is likely to still reflect the long-term signature of the forcing processes. This may include sites of deposition and scour, sorting of grain size, sediment transport pathways, rock/sand boundaries and breaking wave zones.

It was found at Cape Rodney, Northland, New Zealand that waves entrain sediment about the headland and leave a signature of small bedforms on the substrate, but have no obvious influence on the overall distribution of sediment facies (Hume *et al.*, 1997). Rather the tidal currents had a major influence on the nature and distribution of the sedimentary facies. Hume found that the sediment transport and sediment signature on the seabed is generated by phase eddies causing significant asymmetrical flows and current residuals, that show the signature of bed winnowing in the strongest flows. Unlike the west coast with its

northerly moving "river of sand", this area has a limited supply of sand and appears only minor amounts bypass the large headland.

On the seabed of a headland the sediment grain size varies depending on the sediment source, the wave-energy level, and the general slope of the shoreline. The sediment source is obviously the main controlling factor, but further winnowing of relatively fine sediment by wave action leads to a coarsening of the sediment with increased wave energy (Komar, 1998). However the offshore slope is also important with higher gradients enabling coarser sediment to be maintained in suspension (Komar, 1998).

2.3.1.1 TITANO-MAGNETITE (BLACK) SAND SEDIMENTS

Beach sediment may be composed of any material that is available in significant quantities, and is of a suitable size to remain on the beach (Komar, 1998). Ultimately the composition of the beach sediment reflects the type of rocks from which the sediment is derived (Allen, 1985). The west coast "black sand" is fine grained and consists of 38% heavy minerals (titano-magnetite, augite, horneblend) and 62% lighter minerals (feldspars) (Bartholomeusz, 1985). It is denser (2850 kg/m^3)(Bartholomeusz, 1985) than quartz "white sand" and originates from the Taranaki volcanic region (Briggs, 1989), and is thought to be derived from inland sources to the south-west, transported by rivers and streams to the sea and subsequently moved by littoral processes to the northeast (Mclennan, 1982). It contains trace elements such as titanium and is a source of iron ore, which is mined for use in the production of iron and steel.

2.3.1.2 SEABED MORPHOLOGY

Waves and currents ensure that a mobile seabed will frequently create bedforms, which in the case of the energetic environment found at the Raglan headland distinguish any variation on the seabed due to the presence of waves or strong currents. These structures have a large range of shapes and sizes, and the terms to describe them include bars, dunes, anti-dunes, ripples, megaripples, sand waves

and ribbons (Boothroyd, 1978; Dyer, 1986; Nielson, 1992; van Rijn, 1993). Bedforms are generated on the seafloor under flow conditions ranging from unidirectional currents, non-steady currents (tidal inlet flows) and wave orbitals, or may be a combination of these variables (e.g. waves and currents)(Osborne and Vincent, 1993). The type and size of bedforms that result from these forces on the seabed depends on fluid factors (i.e. density and viscosity), the strength, variability and direction of the flow, the bottom configuration (e.g. depth, slope, etc) and the sediment characteristics (i.e. shape – especially angularity, size and density)(Allen, 1985).

The threshold of sediment mobility has been derived using a number of methods (Komar, 1998; Nielson, 1992), which use parameters such as the sediment size and density, and bed-shear velocity due to currents or waves to calculate a dimensionless mobility parameter (Nielson, 1992). Nielson describes how the natural range of sediment sizes and flow regimes lead to the formation of different types of bedforms, and quantifies if the flow is too low to cause appreciable sediment movement (i.e. $\theta \leq 0.05$), the bed topography will be dominated by relict bedforms from previous more rigorous events, or if no such events have occurred recently (eg: in deep water unaffected by strong currents), the topography will be dominated by bioturbation. Intermediate strength flows ($0.05 \leq \theta \leq 1.0$) create an active bed that will be covered in bedforms, which are more or less in equilibrium with the flow conditions.

The orientation of the bedforms has also been shown to reflect the direction of the flow (Komar, 1998). Hume *et al.*, (1997) illustrated a distinctive correlation between wave orthogonal orientation and the bedform alignment at Cape Rodney, New Zealand. The wave signature was reflected in megaripples of the course gravels, which showed an alignment different on the lee side of the headland (after wave refraction) to that on the open side of the headland facing the wave approach direction.

Boothroyd (1978) developed a classification scheme for bedforms based on size (Table 2.3). The scheme demonstrates how generally, the length of ripples (crest

to crest) increases with decreasing grain size for a specific flow strength, due to the decreasing angle of repose as grain size decreases (Allen, 1985), and the strength of the flow (Clifton, 1976; van Rijn, 1993; Nielsen, 1992). At Raglan, despite the strong flow and highly-mobile seabed, bedform magnitudes are therefore likely to be limited by the generally fine grade of sediments that are present.

To initiate particle motion for the creation of ripples the near-bed peak velocity must be 1.2 times the critical velocity (van Rijn, 1993). Rijn found that megaripples have large amplitude to wave length ratios (η/λ), depending on the grain size, but amplitudes are rarely greater than 0.5 m when length is restricted to 6 m.

Wave-induced ripples can be distinguished from uni-directional current ripples by their shape, with wave ripples having profiles that are symmetrical and rounded, and do not slope at the angle of repose (Nielsen, 1992; van Rijn, 1993). Their crests tend to be long and straight, and ripple height and spacing is very uniform. Ripples formed under unidirectional flow tend to be asymmetrical, with the steep side of the ripple crest facing with the direction of the current and normally sloping at the angle of repose (Nielsen, 1992). A progressive sequence of bedforms is produced under waves as the magnitude of the wave orbital diameter increases (Dyer, 1986; Nielsen, 1992).

The general sequence is,

Flat bed -> rolling grain ripples -> vortex ripples -> flat sheet (sheet flow)

Table 2.3: Bedform classification developed by Boothroyd (1978).

Characteristics	**Ripples**	**Megaripples**	**Sand Waves**
Spacing	up to 0.6 m	0.6 – 6 m	> 6 m
η/λ ratio	Variable	Relatively large	Relatively small
Geometry	Highly variable	Sinuous to highly 3-dimensional, prominent scour and pits in trough	Straight to sinuous, uniform scour in troughs
Characteristic flow velocity (U)	Low (25-30 < U < 40-50 cm s^{-1}	High (70-80 < U < 100-150 cm s^{-1}	Moderate (30-40 U < 70-80 cm s^{-1}
Velocity asymmetry	Negligible to substantial	Negligible to substantial	Usually substantial

Sand waves are long wavelength bedforms (> 6 m) that are normally associated with unidirectional currents and have been observed in the continental shelf area all over the world (van Rijn, 1993), as well as in New Zealand (e.g. Lewis, 1979; Black and Healy, 1982; Bradshaw *et al.*, 1994; Hume *et al.*, 1997). Sheets, waves or lenses of fine sediments that overlay coarser sediments are termed sand ribbons and are usually very active and wave events are often observed to redistribute them. They can be kilometres long and up to 1 m thick.

2.3.1.3 West coast morphology

The north island west coast has both induced bedforms (e.g. ripples – sand waves), as well as sand ridges and sand ribbons that have been identified on the South Taranaki Bight in < 60 m water depth by Lewis (1979). Bedforms and sand waves were found to be symmetrical and have continuous crests, and are sinusoidal in nature. The “black sand” ridges are generally shore parallel, 4-11 m high, separated by flat seafloor and are several hundred metres to several kilometres apart.

Megaripples with wavelengths of 1-3 m were found on coarse sediment up to a depth of 50 m depths off Wanganui (Lewis, 1979). Generally shore-parallel sand ribbons, composed of fine sand, were evident between the sand ridges and occasionally overlaying the coarse grain megaripples (McComb *et al.*, 2000). The sand ribbons in the troughs of the ridges are up to 1 m deep and overlay the coarser sediment of the troughs. In common with sand ribbons elsewhere in the world (Lewis, 1979, Allen, 1985) and in New Zealand (Black and Healy, 1982; Beamsley, 1996; Hume *et al.*, 1997) the fine light sand sheets are clearly moving over the coarser substrate with a high potential for variability in seabed level (McComb *et al.*, 2000).

Carter and Lewis (1995) identified that general reef outlines were maintained in the south Wellington region, but the patch margins were less stable and are frequently modified by scour or accretion. The driving forces behind these changes are tides, swell, and storm-forced currents. This is in comparison to experiments on the downstream coast beyond Port Taranaki, that indicated long term stability of sandy patches within and between the rock reef (McComb, 1999). The seabed offshore of New Plymouth comprises rocky reefs and boulders with large patches of sand, similar to that found at Raglan.

The stability in New Plymouth could be due to the more sheltered nature of this reef, than found at Raglan, where the more shoreward regions over the rocky seabed are presumably disrupted by along-headland, wave-driven currents more often. The sandy bed at Raglan is more likely to be winnowed away, being unable to exist over the long term where strong wave-driven flows down the headland cause strong net transport.

2.3.2 *Effect of bed roughness on sediment suspension*

Bed roughness is a major control on suspended sediment concentration (Nielson, 1986; Clifford *et al.*, 1993). The bedforms and seabed composition have a significant influence on the flow, modifying near-bed flows, enhancing the entrainment and resuspension of sediment (e.g. Greenwood *et al.*, 1990; Clifford

et al., 1993; Davies *et al.*, 1995; Hume *et al.*, 1999; Kyotoh *et al.*, 2000), as well as influencing the timing and spatial distribution of sand resuspension (Aagard and Greenwood, 1995). Black and Oldman (1999) demonstrated that enhanced seabed roughness leads to an increase in sediment suspension, which over long periods leads to winnowing of finer fractions of the sediments.

McComb *et al.* (1999) identified a high sediment flux over rocky regions, maintaining the rocky character in this zone through the wave-orbital interaction with the hydrodynamically 'rough' substrate creating a greater turbulent flow over these beds. This is supported by Bastos *et al.* (2002), who found at the tip of a headland that bedrock exposed on the seabed was associated with scouring and maximum values of bed shear stress. Bastos identified two conceptually distinct regions: (a) an inner zone, with increasing gradients of sand transport and bed shear stress towards the headland; and (b) an outer zone, in which sand transport is away from the headland, associated with a decrease in the bed shear stress. These zones merge into a bed shear stress (sand bedload transport) convergent zone, which enhances the formation of sandbanks around headlands. In the inner zone maximum current speeds winnow sediment to define a parting zone between the outer zone, where erosion does not occur as current speeds are not at a maximum (Bastos *et al.*, 2002). These zones relate to the development of eddies, pressure gradient forces, changing patterns in the shear stress and sediment transport rates. Aagaard and Greenwood (1999) also found that sediment transport is promoted by large shear stress values, which increase the phase-coupling between oscillatory velocity and sediment concentration.

Measurements of turbulent eddy viscosities within 1 km of Bass Point (a 4 km wide headland near Sydney, Australia) indicate the presence of a relatively high level of turbulent energy, apparently caused by the complex subsurface topography near the point (Middleton *et al.*, 1993). As many rocky promontories and headlands have complex subsurface topography extending several hundred metres offshore the effect on flow patterns at these features compared to smooth bottom bathymetery could be pronounced.

The reef and boulder rock shoreline at Raglan therefore could have a significant role in the suspension of sediment in this zone of high bed roughness. The sand is sent flying up into suspension as it gets to the rock seafloor and is swept away where entrainment is enhanced by the greater bed roughness (Hume *et al.,* 1995).

2.4 CONCLUSION

The literature review on surfing headlands and their associated flow characteristics has shown that published research on surfing headlands specifically is not extensive, with some of the most comprehensive research related to the science of waves and understanding the components that create world class surfing waves (e.g. Walker, 1974; Dally, 2001b; Hutt *et al.,* 2001*;* Mead and Black, 2001a; Scarfe *et al.,* 2003). However, analogies can be made to natural and engineered areas of the coast that have been more comprehensively investigated. These include large coastal headlands of various shapes and sizes (e.g. Pinegree and Maddock, 1979; Pattiarachi *et al.,* 1986; Davies *et al.,* 1990; Ashton *et al.,* 2001; Hume *et al.,* 1997; Hume *et al.,* 2000) and the effect that topographic forcing can have on current re-circulation (e.g. Zimmerman, 1981; Middleton *et al.,* 1993; Aiken *et al.,* 2002), embayed beaches between headlands (Short, 1999; Klein, 2002), breakwaters and jetties (Gourlay, 1974 and 1981; Scarfe *et al.,* 2003), artificial headlands (Healy and Harada, 1997; Silvester and Hsu, 1997) and artificial reefs (Black and Mead, 2001; Black, 2001c; Mocke *et al.,* 2003).

Geyer and Signell (1991) defined coastal headlands as locations where wave and current energy converge, which may generate secondary circulations as flow passes the protrubence (i.e. spiraling tidal eddy flows)(Black and Gay, 1987; Geyer, 1993; Saunders, 1999). Gourlay (1974) found in the lee of headlands or structures wave-generated current systems that often caused local reversals of the alongshore current. Saito *et al.* (1996) reported strong rip currents along artificial headlands as well as recirculating currents in the lee of the structure, which strongly influenced sediment transport (Walker *et al.,* 1991).

Research related to surfing headlands has often been in conjunction with the study of hydrodynamics and sediment transport related to issues of erosion in the coastal region near the headland. Examples include the Gold Coast and Noosa Heads in Australia, Dunedin in New Zealand, and Bournemouth in England (e.g. Chapman, 1981; Pattearson and Patterson, 1983; Black *et al*., 2001). The erosion problems in areas downdrift of the headlands are often related to the high oblique angle at which the waves break along the shoreline, essentially creating a "large groyne" effect. This high breaking wave angle due to improperly refracted waves leads to significant sediment transport, especially in large surf conditions (Komar, 1998). Komar describes how these longshore currents as well as cell circulation are the two principal patterns of wave-generated currents within the nearshore area. The rate of transport can vary depending not only on the orientation at which the waves break relative to the shoreline, but also the height and period of wave events. This coastal process is well documented in the literature (e.g. Longuet-Higggins, 1970; Komar, 1985; Fredsøe and Deigaard, 1992; Komar, 1998). Pattiarachi (1998) also found that wave action not only intensifies the rate, but also influences the direction of net sediment transport. Cell circulation can occur as currents flow from areas of high waves and set-up, to zones of low waves and set-up where the currents converge and turn seaward as rips. The variation can occur due to wave refraction over irregular topography, or by local sheltering of headlands, jetties or breakwaters (Komar, 1998). Examples of recirculating currents and sediment pathways at headlands include Cape Rodney and Napier in New Zealand (Hume *et al.,* 2000; Mead *et al.,* 2001) and the Gold Coast, Australia (Smith, 1982).

The presence of a re-circulating rip current at a surfing headland was identified by Walker (1974), who found that a change in the headland orientation created a return flow back seawards allowing surfers an easier paddle back to the "take-off" point of the break. Short (1985) describes this as the 'end effect' where headland circulation is impacted or completely controlled by the topography where longshore currents turn and flow seaward. The rip intensity has been found to increase with wave height (Short, 1999) and can transport significant sediment offshore (Roy *et al.,* 1994). Modelling for an artificial reef by Mocke *et al.* (2003)

showed similar re-circulating currents in the lee of the structure, whilst Symonds *et al.* (1995) found that a pressure gradient due to waves breaking on a natural reef may generate return flow. Carter *et al.*, (1990) reported that currents which had accelerated to a maximum along the flanks of a headland, decelerated on the bay beaches where the coastal alignment changed, showing that the partitioning of wave energy or power is of fundamental importance in the transport of sediment at the headland. A decrease of wave energy where the alignment changed allowed deposition of sediment in this zone.

The strong alongshore current also has a significant effect on the 'surfability' of a break, with surfers being pushed rapidly along the headland whilst attempting to get out to the 'take-off point' or maintain their position in the line-up (Symonds and Black, 2001). However, in comparison a re-circulating or 'outflowing' tidal current, or a lower velocity current due to a change in headland alignment can assist the surfer in access to a particular break, whilst wave height can also significantly increase where currents flow against the breaking wave direction (Hales and Herbich, 1972). This factor was considered in the design of the Narrowneck artificial reef where a paddling channel was included in the design to counter the strong over the crest currents that were predicted during large swell events (Black and Mead, 2001).

A rocky headland provides shelter from wave energy to the lee side, with a subsequent effect on the littoral supply and drift of sediment. The headland can act as a natural obstacle to the longshore sediment transport and the result is a downdrift accumulation of sediment (Short, 1999), or may act as a cell boundary where local sediment circulation is confined into compartments (Bray *et al.*, 1995). Short (1999) found that the bypassing of sand on medium to high littoral drift coastlines around headlands or large groynes extending beyond the surf zone has a tendency to occur in 'slugs' (or pulses of sand). This transport creates phases of 'lean' and 'full' segments, with activation of the 'slug' initiated by high wave energy, due to larger or long period waves (Chapman, 1981). Sand was found to pass more readily on smaller headlands such as Burleigh Heads on the Gold Coast, Australia.

The literature shows that a significantly lower amount of research has been undertaken on New Zealand's west coast when compared to the east coast, due to a distinct difference in the wave climates of the respective coasts limiting the collection of field data (Hume *et al.,* 1992; Brander *et al.,* 2003). However, a number of previous investigations at Raglan focused primarily on the investigation of components of the headland that relate to artificial surfing reef development (e.g. Mead and Black, 2001; Hutt *et al.,* 2001, Scarfe *et al.,* 2002), with minimal research undertaken on the effect that this natural feature has on the currents and sediment dynamics of the coast. The most significant was by Scarfe *et al.* (2002) at Manu Bay, Raglan where it was found that the bed level fluctuated approximately 0.5 m per month, influencing the shoaling and breaking of waves. Research undertaken at New Plymouth 120 km south of Raglan in a similar coastal environment on the west coast of New Zealand, provides significant findings that are relevant to this thesis (e.g. Mattews, 1977; McClennan, 1982; McComb *et al.,* 1997 and 1999; McComb and Black, 2001).

The wave climate of the west coast classifies the coast as a high-energy environment, in comparison to the low energy east coast wave climate (Pickrill and Mitchell, 1979). The predominant wind and waves are from the southwest direction (Heath, 1982), and the direction of littoral transport is to the north with approximately 175,000 m^3/yr of net littoral drift on the coastline at Raglan (Gibb, 1979, Hicks and Hume, 1993; Mattews, 1977; McComb *et al.,* 1999). McComb *et al.* (1999) reported that along with a net northeasterly sediment flux at New Plymouth, sediments were shown to respond to local perturbations that give rise to reversing and circulating fluxes.

Bed roughness has been found to be a major control on suspended sediment concentration (Nielson, 1986; Clifford *et al.,* 1993), with the boulder and reef shoreline armouring the Raglan headland likely to have a significant role in the sediment dynamics of the headland. McComb *et al.* (1999) identified that the character of the rocky reef regions at New Plymouth, was maintained through the wave-orbital interaction with the hydrodynamically 'rough' substrate creating a greater turbulent flow over these beds making settlement of sediment less likely.

Bastos *et al*. (2002) showed that sand transport was greatest closer to the headland where current velocity and bed shear stress was greatest, with sand transport away from the headland where bed shear stress decreased. These zones relate to the development of eddies, pressure gradient forces, changing patterns in the shear stress and sediment transport rates.

CHAPTER THREE

SEABED CHARACTERISTICS

3.1 INTRODUCTION

Effective coastal management requires an adequate understanding of physical coastal processes and their effects. More particularly, it demands an appreciation of the physical processes acting on the coast and the dynamic response of coastal landforms as those forces are applied (Brookes and Green, 2000). To fully understand the response of a dynamic exposed headland, as found at Raglan, it is therefore important to determine the characteristics of the seabed and textures of the seafloor sediments.

Surface sediments provide information about the energy of the environment as well as the long-term processes and movement of materials, or sediment transport pathways, sources and sinks. Sediments in the coastal zone may be composed of any material that is available in significant quantities and is of a suitable grain size to remain on the beach (Komar, 1998). On the seabed of a headland the sediment grain size varies depending on the sediment source, the wave-energy level, and the general slope of the shoreline. The sediment source is obviously the main controlling factor, but further winnowing out of relatively fine sediment by wave

action leads to a coarsening of the sediment with increased energy (Black, 1992; Black and Oldman, 1999).

The west coast "black sand" is fine grained and denser (2850 kg/m^3) than quartz "white sand" (Bartholomeusz, 1985). It originates from the Taranaki volcanic region (Briggs, *et al.,* 1989), and can be classified as from Taranaki andesitic origin, thought to be derived from inland sources to the south west, transported by rivers and streams to the sea and subsequently moved by littoral processes to the northeast (McClennan, 1982). It contains trace elements such as titanium and is a source of iron ore, which is mined for use in the production of iron and steel. The 'black' sand consists of 38% heavy minerals (titano-magnetite, augite, hornblende) and 62% lighter minerals (feldspars) (Bartholomeusz, 1985).

This chapter focuses on the interpretation of seafloor sediments through the analysis of substrate type, grain size and sediment texture, as well as an assessment of visual observations of the seabed and rocky boulder reef, and classification of marine organisms inhabiting the sub-tidal reef zone.

3.2 FIELD PROGRAMME

The composition of the seabed was sampled to a distance of 500 m offshore using SCUBA equipment and a Birge Ekman seabed sampler on the 11-6-98 and 26-4-01. The divers collected the samples from positions fixed by Global Positioning Systems (GPS) using Mt Eden grid as the coordinate system, in locations covering the entire Indicators headland from Outsides to Whale Bay (Fig. 3.1). The grab samples were collected using plastic sampling containers (Fig. 3.2), whilst the Birge Ekman sediment sampler was deployed on a rope over the side of the boat, and upon impact with the seabed the trap opens and closes shut when the rope is pulled to retrieve the sample (Fig. 3.3). A grab sample is collected from the seabed as the trap closes.

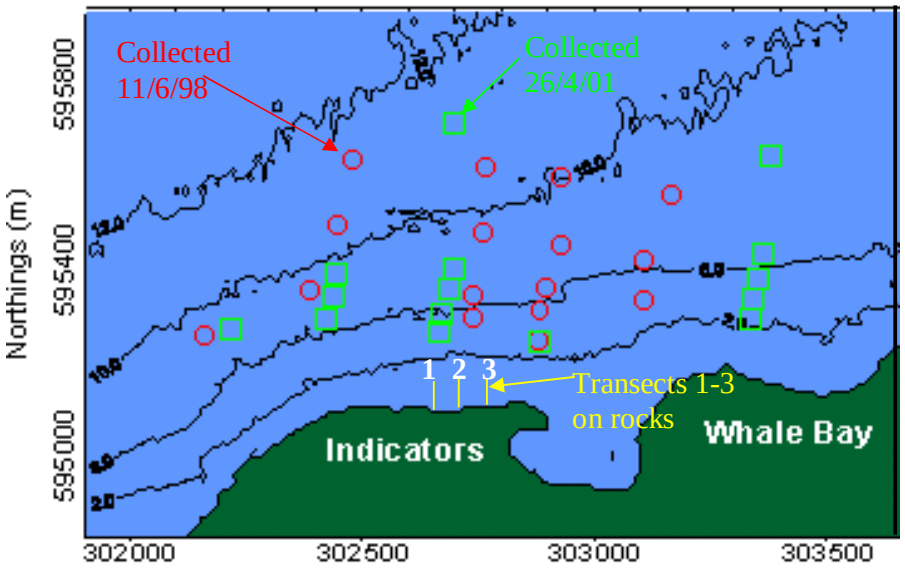

Figure 3.1: Map of sediment sampling sites, and location of the 3 transects on the rock shoreline (Mt Eden Grid).

These samples allowed the determination of the grain size gradient at the headland, which was subsequently plotted as a contour map using the software SURFER. This process was carried out to monitor any change in the grain size characteristics over the headland both temporally and spatially.

Figure 3.2: Diver surfacing with a seabed sample (Source: Author 11-06-98).

Transects were undertaken along the boulder shoreline at Indicators in 3 locations to measure the size of the rocks armouring the headland (Fig. 3.1). The transects were carried out at low tide so that the rocks sizes could be measured from the low water mark to the berm above the high tide mark and were 25 m apart (Fig. 3.4). The position of the transects were located using a hand held GARMIN etrex GPS receiver accurate to approximately 3 m (Mt Eden Grid). Transect 1 (595 152.21 N, 302837.62 E to 595101.65 N, 302831.80 E), Transect 2 (595154.32 N, 302860.45 E to 595105.32 E, 302855.12) and Transect 3 (595158.62 N, 302 883.26 E to 595114.64 N, 302878.41 E).

Figure 3.3: The Birge Ekman seabed sampler being deployed from the boat (Source: Author: 26-4-00).

Figure 3.4: The rock shoreline at Indicators where the 3 transects were located from the low tide mark (weed covered rocks) to the berm above above the high tide mark (Source: Author, 12-8-99).

3.2.1 *Sediment sample analysis*

Sediment samples were analysed using the University of Waikato Rapid Sediment Analyser (RSA) to obtain hydraulic grain size and settling velocity distributions (Lewis and McConchie, 1994). The amount of sediment settling to the bottom of the 1.9 m fall tube over a specified time is measured by a balance, which is connected to a Macintosh computer with a software package written at the University of Waikato. The automated RSA requires sub-samples between 20–30 g (de Lange *et al.*, 1997) requiring collected samples to be of a large enough size for settling velocity to be determined. This form of automated settling tube analysis measures grain sizes based on the concept that particles which fall in fluid at the same velocity are considered to be of equivalent size (Greilach *et al.*, 1995).

The Gibbs *et al.* (1971) equation is used to calculate the grain size from the settling velocity:

$$r = \frac{0.055804V^2\rho_f + \sqrt{0.003114V^4\rho_f^2 + \left[g(\rho_s - \rho_f)\right]\left[4.5\eta V + 0.008705V^2\rho_f\right]}}{\left[g(\rho_s - \rho_f)\right]} \qquad (3.0)$$

Where

V = velocity ($cm.s^{-1}$)

G = gravitational acceleration ($cm.s^{-2}$)

η = dynamic viscosity (poise)

ρf = density of fluid ($g.cm^{-3}$)

ρ_s = density of sphere ($g.cm^{-3}$)

r = sphere radius (cm)

To calculate the settling velocity (ms^{-1}) from a known sphere size Equation 3.1 can be used:

$$w = \frac{-3\eta\sqrt{9\eta^2 + gr^2\rho_f(\rho_s - \rho_f)(0.015476 + 0.19841r)}}{\rho_f(0.011607 + 0.14881r)} x1/100 \qquad (3.1)$$

3.3 RESULTS

3.3.1 *Textural Analysis*

The shoreline of the Raglan headland is armoured by boulders ranging in size from 0.01 m to 1.5 m (Figs. 3.5 and 3.6), and interdispersed rocky reef outcrops that are particularly evident in the Whale Bay region of the headland. The boulders and areas of reef provide shoreline stability and protection from the breaking waves that regularly break along this section of the coast. The 3 transects along the Indicators surf break from the low to high tide marks, show that the boulders have a mean size of 0.3 m at Transect 1, 0.28 m at Transect 2, and 0.25 m at Transect 3 (Figs. 3.7, 3.8 and 3.9). Transect 1 is the most westward and shows a larger mean rock size towards the tip of the headland where the waves are of a greater size. A random variation in sizes across the shoreline is evident, with large sized rocks (0.7 – 1.0+ m) distributed over the shore face, with the upper 10 m of the berm zone consisting of small to medium sized rocks (0.01 - 0.4 m). The large rocks were often surrounded by medium sized rocks in the 0.1 - 0.3 m range (Fig. 3.10), whilst in the high tide zone small pebbles in the 0.01 - 0.02 range were inter-dispersed in clusters amongst the larger rocks (Fig. 3.11). Observations have also shown that the rocks become rounder in shape further along the headland from the initial break point at Indicators.

Figure 3.5. Rocks armouring the headland above the low tide mark at Indicators (tape measure marking transect 2). Size of the rocks varies from 0.01 m to 1.5 m. (Source: Author 12-8-99).

Figure 3.6: Large rock (1.5 m) on the Raglan shoreline at Indicators. (Source: Author, 12-8-99).

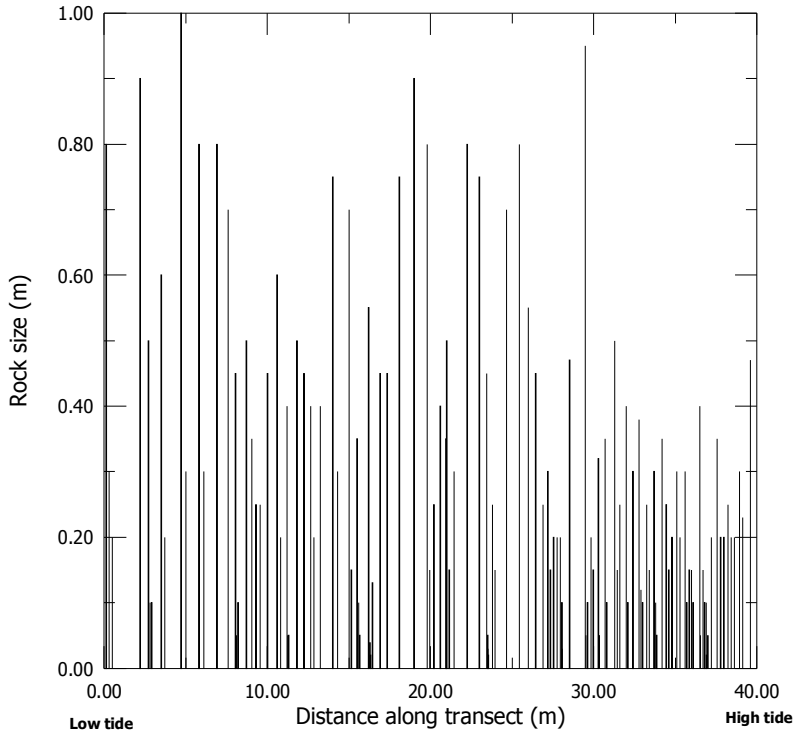

Figure 3.7: Rock sizes (m) along a transect (Transect 1) at Indicators from the low tide to the berm of the shoreline measured on the 12-8-99.

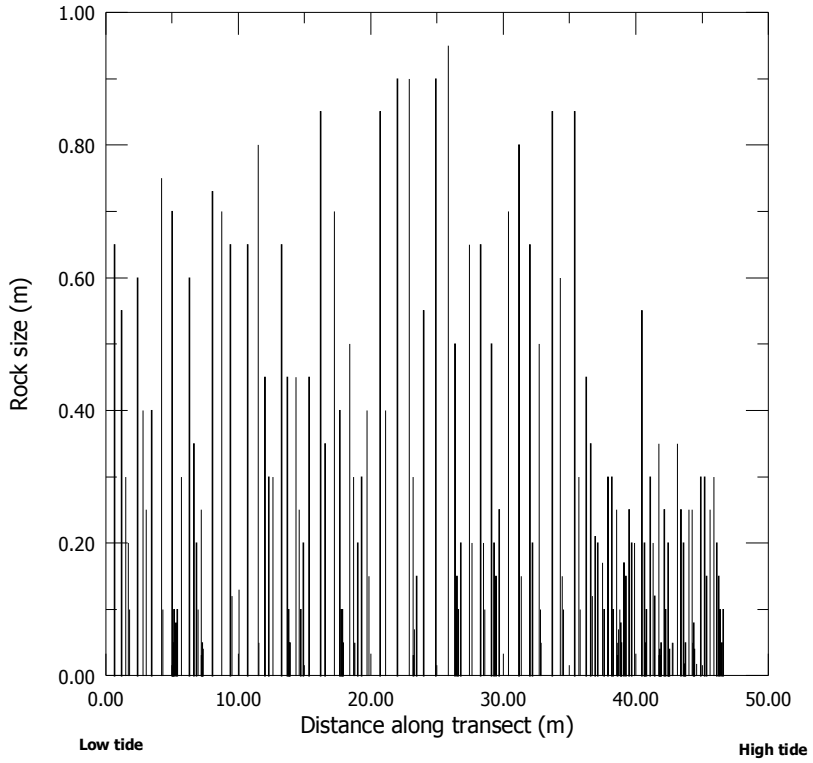

Figure 3.8: Rock sizes (m) along a transect (Transect 2) at Indicators from the low tide to the berm of the shoreline measured on the 12-8-99.

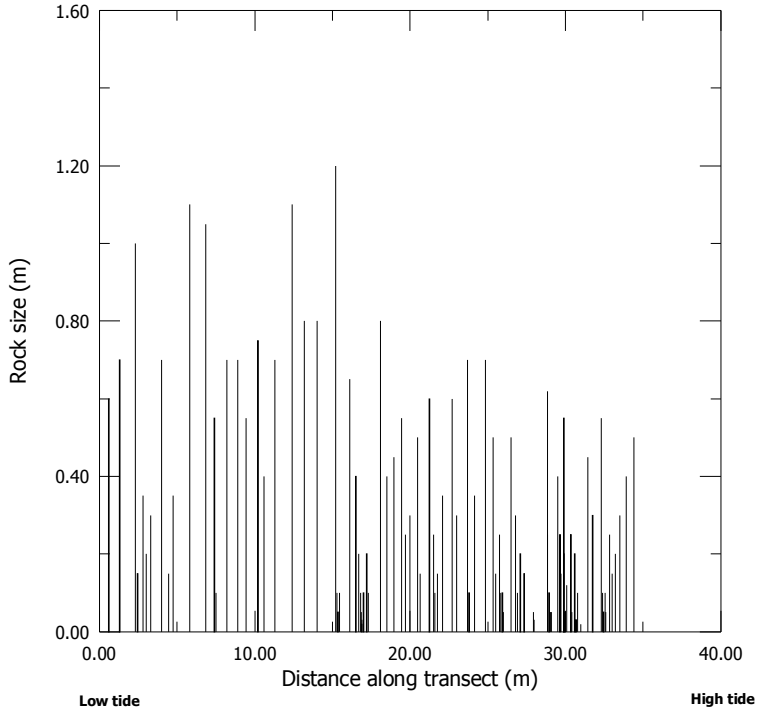

Figure 3.9: Rock sizes (m) along a transect (Transect 3) at Indicators from the low tide to the berm of the shoreline measured on the 12-8-99.

Figure 3.10: Rocks in the 0.1-0.3 m range surrounding the larger rocks at the headland (Source: Author, 12-8-99).

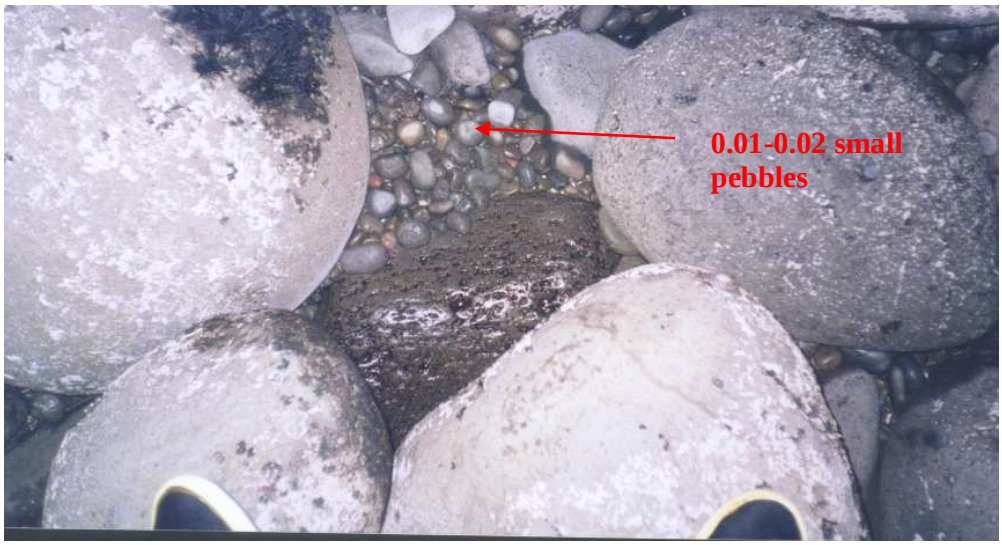

Figure 3.11: Small rocks (pebbles) in the 0.01-0.02 m range clustered amongst the larger rocks at the headland in the high tide zone (Source: Author, 12-8-99).

Bed sediments were well sorted and graded from 0.28 mm inshore to 0.14 mm offshore (Fig. 3.12). The largest-sized grains were located at the tip of the headland where the waves first break (high energy zone), decreasing slightly down the headland. There was not a significant variation in the sediment grain size and its location at the headland, from the sampling in June 1998 to that in April 2001 (Tables A7.1, A7.2, A7.3 and A7.4). The sediment can be classified from particle size analysis as predominantly slightly gravely sand. The 1998 samples were more sandy in grain size and more finely skewed than the 2001 samples, which were more coarsely skewed with more gravely sand. This shows the removal of finer material in 2001 due to the presence of a large swell prior to sampling (Chapter 6).

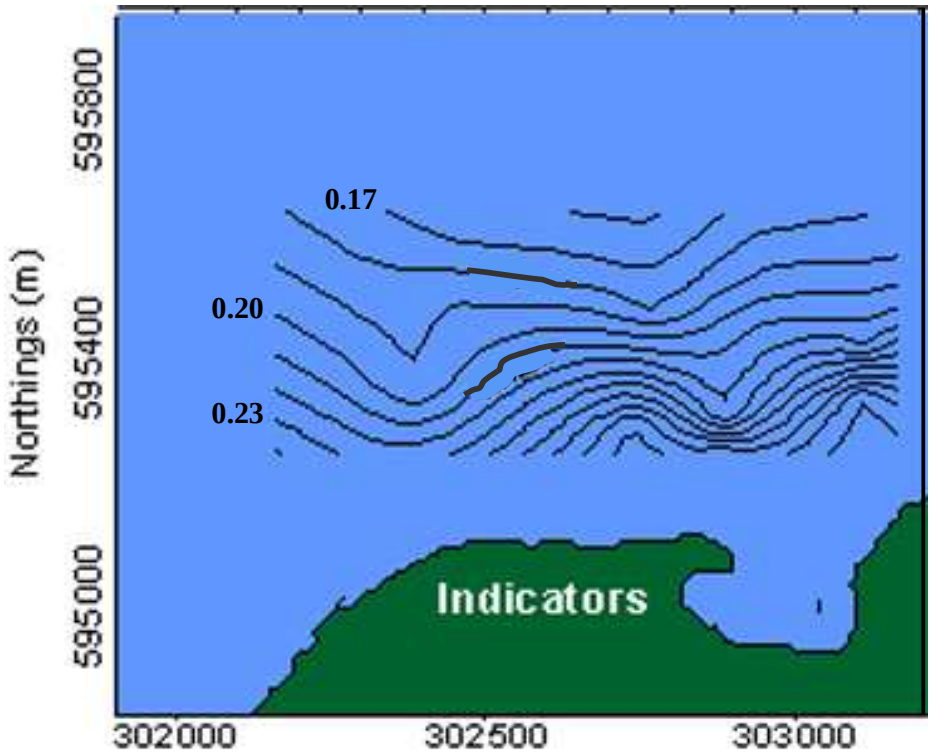

Figure 3.12: Median Grain Size (mm) distribution at Indicators (a surf break along the Raglan headland), sampled on 11-6-98. Contour interval 0.01 mm.

Local sorting is characterised by predominantly well-sorted sediments, although the sorting is slightly more significant closer to the shoreline in the breaking wave zone (Fig. 3.13). A zone of slightly poorer sorting is visible offshore from the Indicators headland, which may be a zone of sediment accumulation that is less subjected to wave action. The skewness is characterised by less fines inshore, although in the zone between the Indicators and Whale Bay surf breaks finer material is evident, most likely due to decreased wave action in this area (Fig. 3.14).

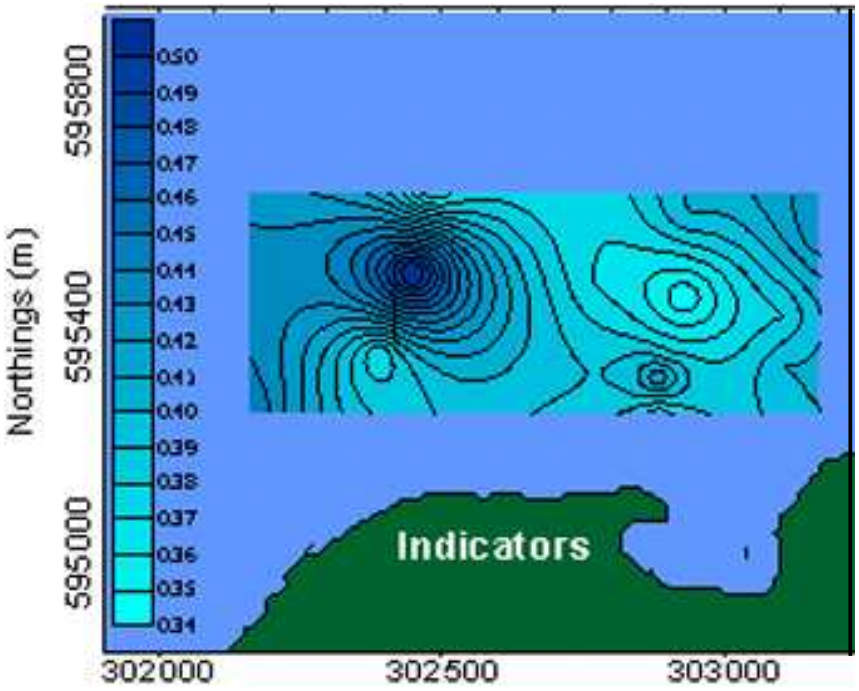

Figure 3.13: Sorting distribution at Indicators (a surf break along the Raglan headland), sampled on 11-6-98. Contours are spaced at 0.01 phi intervals.

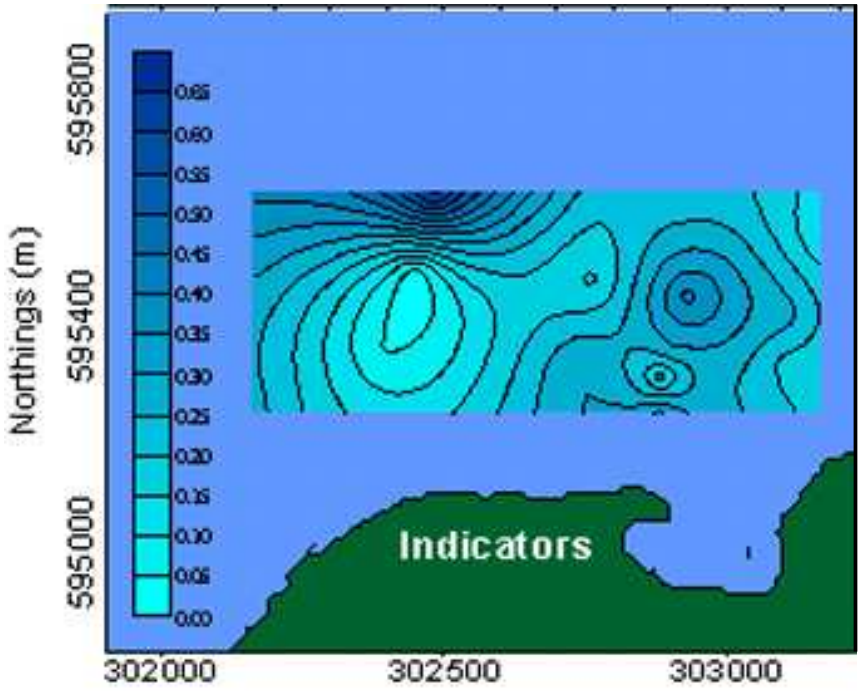

Figure 3.14: Skewness distribution at Indicators (a surf break along the Raglan headland), sampled on 11-6-98. Contours are spaced at 0.05 chi intervals.

3.3.2 *Observations of seafloor characteristics and marine organisms*

Observations by divers using SCUBA at Whale Bay showed that the reef at sub-tidal depths in the range of 5-8 m (MSL) is comprised of boulders (approximately between 0.5 m and 1.5 m in diameter) that are invariably cemented together by calcareous encrusting algae (possibly *Coralline* sp.), light pink to patches of white in colour. Apart from an area of approximately 0.15 and 0.20 m around the base of the fused boulders that was relatively scoured and free of life, the surface of the boulder reef is inhabited by a variety of marine organisms, many of which are adults. For example, in some areas the tops of many boulders are covered with large brown algae of the *Carpophyllum* genera (Morton and Miller, 1968). Other boulders provided habitat for a mixture of encrusting sponges, notably, large colonies of *Polymastia glanulosa* and *Cliona celata* (some colonies covered the top surface of entire boulders). Large greenshell mussels (*Perna canaliculus*) can be found on boulders, as well as other *kaimoana*[2] species that are known to occupy the sub-tidal reef including paua (*Haliotis iris*), kina (*Evechius chloroticus*) and the catseye (*Turbo smaragdus).* Various types of seaweed were found inhabiting the rocks (Fig. 3.15). At Indicators a zone of approximately 10 m was visible in the boundary zone between the rock reef and sandy seafloor where no seaweed inhabited the rocks. This demonstrates a region where the sand is scoured or deposited more frequently.

[2] *Kaimoana* Maori word meaning seafood.

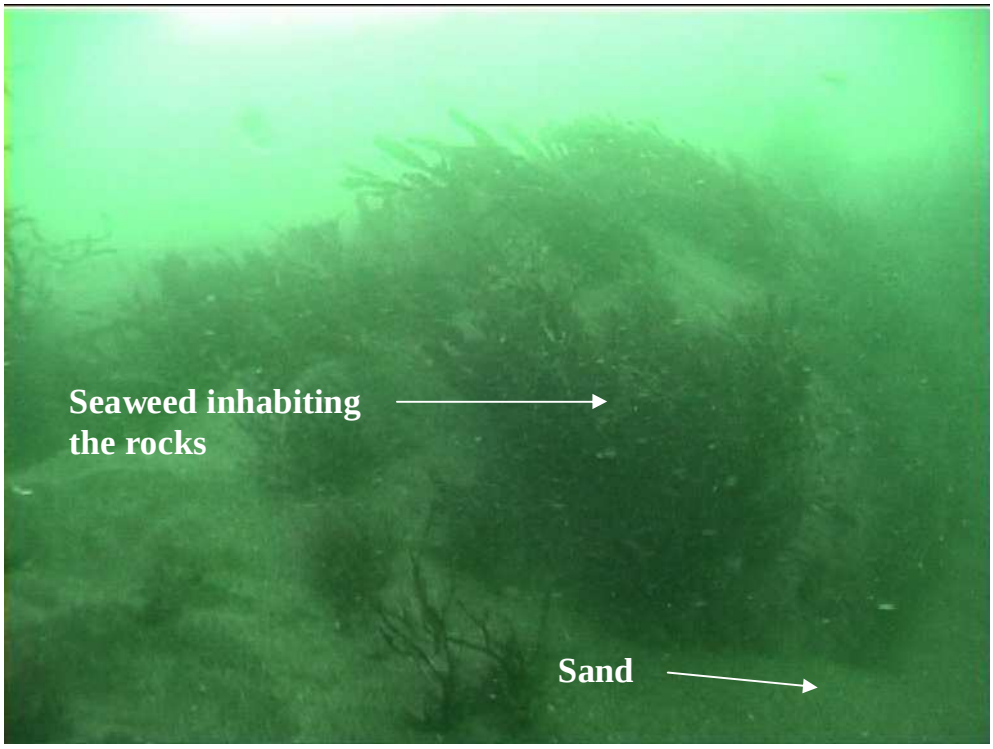

Figure 3.15: Seaweed inhabiting rocks on the seafloor with mobile sand around the base (Source: Author, 11-6-98).

During sediment sampling in 2001 a stainless steel frame from a previous field experiment in 1998 (Chapter 6) was discovered. The frame was not retrieved at the completion of the fieldwork due to large swell conditions. The interesting discovery was that of a cluster of green shell mussels (*Perna canaliculus)*, living on the top centrepiece of the frame, at a height of approximately 0.6 m above the current bed level (Fig. 3.16). The age of the mussels has been dated (S. Mead, *pers comm.)* as approximately 1-2 years old based on the 70 mm length (Fig. 3.17). The survival of these mussels over this period demonstrates that the bedlevel has not been over this height for a significant time period.

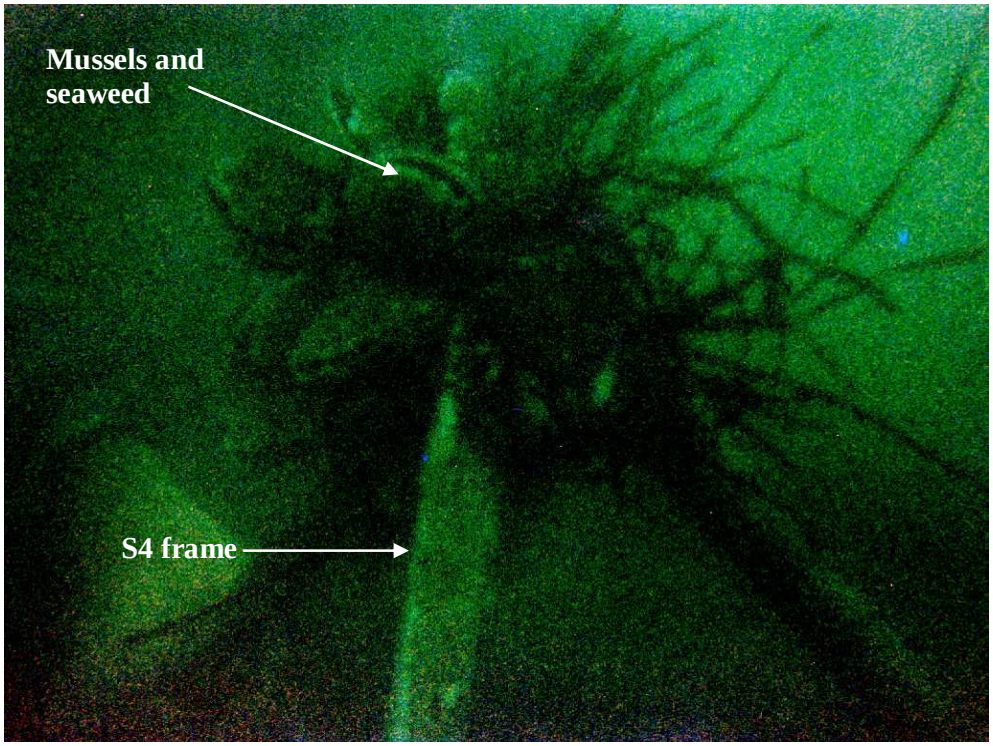

Figure 3.16: Frame on the seabed from previous experiment in 1998 with large green shell mussels (Perna canaliculus) inhabiting the top of the structure (Source: Author, 26-4-01).

Figure 3.17: Mussels (Perna canaliculus) taken from the frame on the seabed photographed next to a New Zealand 50 cent coin (Source: Author, 26-4-01).

These observations are very interesting when the proximity to the sandy seabed and the large wave exposure of the area are considered (waves of up to 4 m break fairly regularly along this stretch of coast, and annually even larger events can be expected). These observations suggest that the division between the boulder reef and the sandy seabed is fairly stable and not subject to regular smothering by wave induced sediment movements. The presence of adult representatives of many species along the reef edge suggests that this habitat has remained stable for a period of years, rather than several weeks or months if intermittent smothering was the case.

3.4 SUMMARY

It is evident from the results that the wave signature is strongly present in the seafloor sediment textures at the headland. This is a characteristic also found by Hume *et al.* (1997) during experiments about a large coastal headland. Sediment samples identified that the largest sized grains were located closer to the high-energy surf zone of the headland, where the waves are shoaling and peeling along the reef. This is supported by Shepard and Hesp (2003), who found that projecting headlands usually have steeper offshore gradients and oblique wave approach, which results in the removal offshore or alongshore of all but the coarsest grains. The rocks at Indicators also became rounder in shape further along the headland from the initial break point.

Sediments can be classified as mostly slightly gravelly sand and were well sorted, and slightly less well sorted further offshore, whilst the skewness showed less fines inshore at the headland, which is most likely due to increased wave energy winnowing away finer sediment (Komar, 1998). Possible zones of sand deposition were identified between the Indicators and Whale Bay surf breaks and further offshore from Indicators nearer the tip of the headland. Visual observations have shown long-term habitation and zonation of the sub-tidal reef edge and on an un-retrieved S4 frame by adult marine organisms, which could demonstrate an upper level in the seabed movement and a degree of stability in the bed level.

CHAPTER FOUR

BATHYMETRIC SURVEYS

4.1 INTRODUCTION

The previous chapter analysed the type, size and texture of seafloor sediments found at the Raglan headland, which were significantly influenced by the presence of the surf-zone. This chapter focuses on the changes in the seafloor topography temporally and spatially at the Indicators surf break of the headland.

Hydrographic surveying to chart the Indicators seafloor was undertaken during the study period using a LEICA SR530 RTK-GPS (Real Time Kinematic – Global Positioning System) and a KNUDSEN MP 320 depth sounder, to quantify any variation in the seafloor level and allow calculation of sediment volume that had either accreted or eroded from the site. The surveys were repeated on five occasions at different times of the year, to distinguish variation both before and after a period of swell and seasonally to gauge long-term temporal variation. Experiments of a similar nature were carried out by Scarfe (2002a), at Manu Bay, Raglan to understand how surfing waves transform in this zone. Previously attempts had been made by the author to drive sedimentation rods into the seabed

to measure the change in bed level, but this proved unsuccessful in the energetic wave conditions and was considered a hazard for surfers.

4.2 EXPERIMENTAL METHODOLOGY

Experimental RTK-GPS was validated and utilised to measure a water level correction for depth soundings as part of the hydrographic surveying at the Raglan headland (Scarfe, 2002b). This system created precise bathymetric charts identifying small and large scale features and changes in the bed level. Scarfe (2002b) proposed a new theory to overcome problems with measuring separate heave and tide correction. These problems arise because heave and tide are combined to correct a sounding for the water level at any one instant. The new method identifies that a water level correction (WLC) that reduces a sounding to the local datum is required. To alleviate this issue measuring the water level where a sounding is undertaken removes errors caused by tidal corrections from remote locations.

These issues arose in the hydrographic surveying at the field area because accurate tidal corrections are difficult to obtain, as no permanent tide station exists in the area. To undertake an accurate survey the equipment must be calibrated and specifically deployed in relation to a local datum. At Raglan as in many coastal locations, tide gauges tend to be located in harbours and port embayments where the tide phase and amplitude can be significantly different to that of the open coast (Scarfe *et al.,* 2002).

Data were compiled into bathymetry grids using SURFER surface mapping system (Golden Software, Inc.). The kriging method of interpolation was selected for grid creation. Kriging is a geostatistical gridding method that has proven useful and popular in many fields (Golden Software, Inc., 1996). It produces contour and surface plots from irregularly spaced data such as that produced from digitising charts and bathymetry surveys. Kriging attempts to express trends that are suggested in the data, so that, for example, high points might be connected

along a ridge, rather than isolated by bull's-eye type contours (Golden Software, Inc., 1996). Kriging is an exact interpolator, i.e: this method of gridding honours data points exactly when the data point coincides with the grid node being interpolated. Validation tests comparing survey data with grids created using kriging have shown that the method is very accurate and that errors associated with grid creation are based on the accuracy of the depth sounding equipment.

4.3 SURVEY ERRORS

A high update low latency RTK GPS is required to measure a water level correction, with a high enough rate (> 5 Hz) to calculate 3D positions, so that waves can be modelled. The timing of the position must be matched precisely (< 50 ms) to the sounding. Scarfe *et al.* (2002) describes how most receivers output a position around two-seconds after it is true because of the time taken to transmit carrier phase observations from the reference GPS to the rover. This latency can be corrected using techniques presented by Scarfe (2002b) but ideally the GPS should have negligible latency. Trimble's MS750 RTK GPS has a low latency (20 ms) mode that predicts the reference GPS's carrier phase observations a few seconds in advance. This is possible, as the reference GPS observations do not change significantly over a short time. There is a small loss in accuracy from ±2-3 cm (horizontal) to ±3-5 cm but this is acceptable within the error budget of a hydrographic survey. The 5 Hz Leica SR530 RTK was successfully used for the Raglan experiments providing accurate bathymetric survey data using synchronized mode. Analysis of cross-lines for the survey yielded a 95% confidence interval of depth accuracy of 0.17 m.

4.4 FIELD PROGRAMME

Hydrographic surveys were undertaken on the 10-7-01, 3-9-01, 6-11-01, 29-01-02 and 8-02-02 over an 88,000 m^2 area at the Raglan headland. Fieldwork constraints limited the survey area to this region, which does not allow definitive demonstration of the variation of the seabed over the entire Raglan headland, but does give evidence of the temporal and spatial variation within the survey area.

Hutt (1997) undertook a detailed hydrographic survey as part of a large experiment at the headland, producing a bathymetric chart of the area (17-01-98). This survey covered the entire headland but was not as accurate as the survey undertaken for this study with a positional accuracy of approximately 1 m. Over 80,000 depth fixes were measured in a rectangular region of 2 km^2. Positioning for this survey was established using GPS with a real-time correction from a differential GPS unit. Results of the survey have been compared to the more recent surveys.

The surveys for this study were undertaken using the University of Waikato Mac Boat (Fig. 4.1) and Taitimu, and hydrographic survey equipment that included a KNUDSEN MP 320 depth sounder with an accuracy of $\pm$1 cm. Surveys were undertaken on days when the swell and wave conditions were generally low with a flat sea, although this could not always be achieved with some small swell present for some of the surveys. The RTK GPS is capable of removing this swell from the data when processed, due to high the number of stored positions, enabling a nominal sea level to be calculated. High tide was selected as the ideal time to undertake the surveys as less shoaling of waves takes place in the deeper water of the surfing headland. The hydrographic data allowed the calculation of the sediment volume changes in the survey area, including analysis of a 500 m transect from 595200 mN, 302880 mE to 595700 mN, 303000 mE (Mt Eden Grid)(Fig. 4.2).

Figure 4.1: The University of Waikato Survey vessel (MacBoat) used for Hydrographic Surveys on the 10-7-01 and 3-9-01 (Source: Author, 10-7-01).

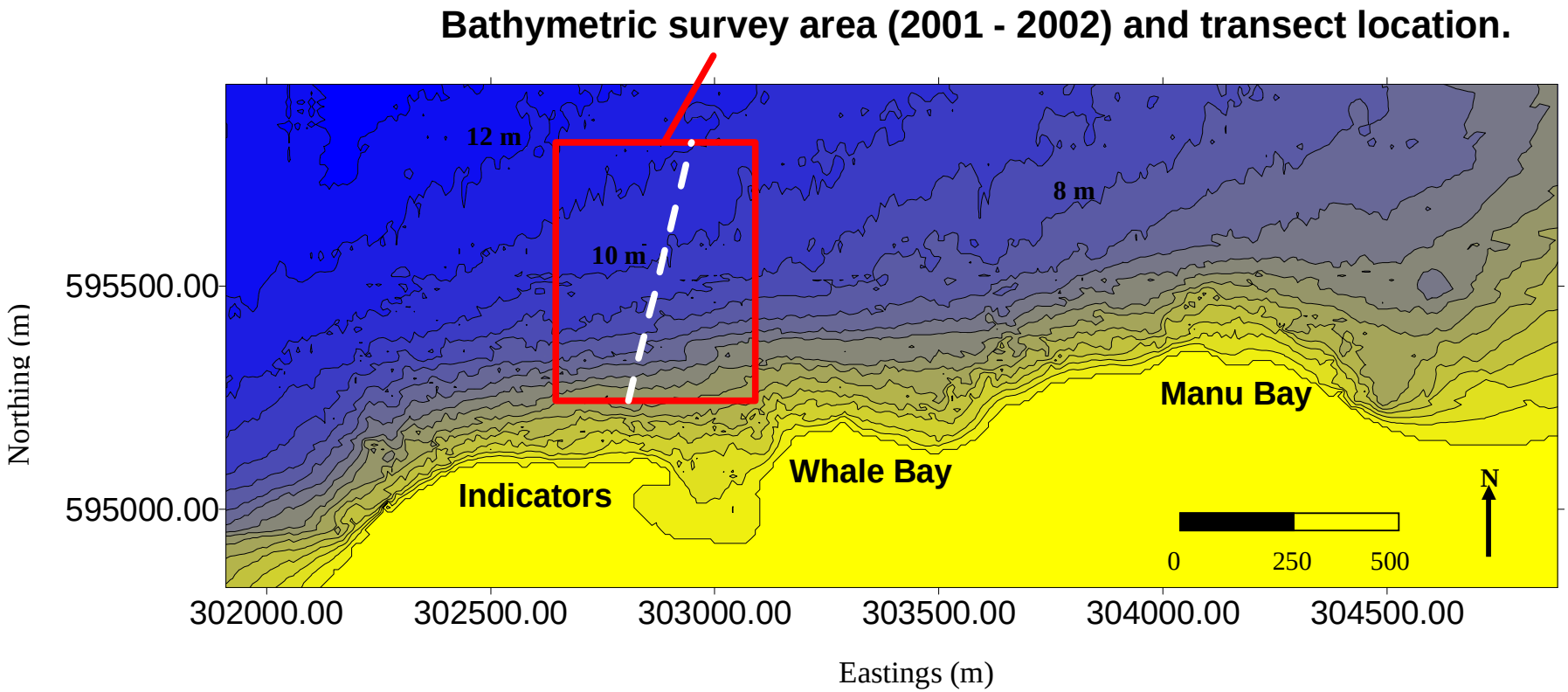

Figure 4.2: Bathymetric map of the Raglan headland in 1996 (Mt Eden Grid)(Source: Hutt, 1997) with the area of the surveys undertaken in 2001/2002 and the transect location (1m contour interval).

4.5 RESULTS

The 500 m transect through the survey area shows the variation in bed level over the 6 hydrographic surveys (Fig. 4.3), whilst Figure 4.4 shows the upper and lower envelope of bed-level over the observation period. Along the transect the mean bed levels vary from a minimum range of 0.1 m for the offshore 250 m part of the transect (>8 m), to a maximum of 0.5 m variation for the inshore area. This demonstrates the stability of the bed offshore with greater variation in the surf zone nearer the headland. The surveys showed that the depth contours graded on a 1 in 45 slope for the first 250 m of the transect, then levelled to a 1 in 85 grade for the remaining 250 m of the transect. The steeper inshore gradient is suitable for surfing wave conditioning and breaking at the headland.

A mean bed level below Chart Datum (CD) was calculated from all the transect data for each survey, to quantify the variation over the survey period (Table 4.1). The mean of this data was 7.64 m and ranged from a minimum of 7.47 m on the 8-02-02, to a maximum of 7.86 m on the 3-09-01, which is a maximum variation of 0.43 m along the 500 m transect. The volume difference in bed levels between surveys over the total area was calculated using the SURFER software and shown as $\pm$ m^3 of variation. This data correlated well to the mean bed levels, where higher bed levels also had larger positive increases in volume and vice versa for the low mean bed levels. The lowest volume change was +69 m^3 between 29-01-02 and 8-02-02, and the highest was -17990 m^3 between the 10-07-01 and 3-09-01. This is a maximum height difference of -0.21 m if averaged over the full survey region of 88,000 m^2.

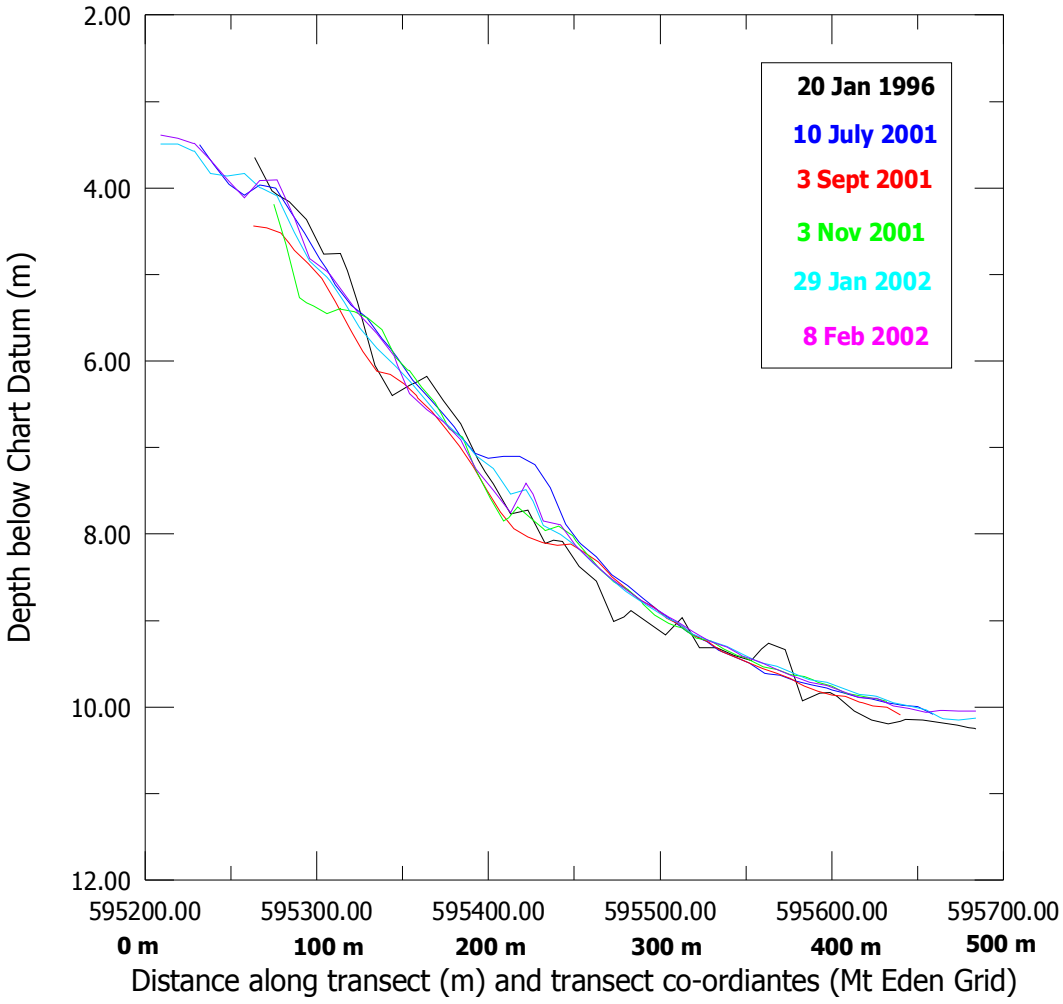

Figure 4.3: Seabed level along a 500 m transect, from 6 bathymetric surveys undertaken (20-01-96 to 8-02-02).

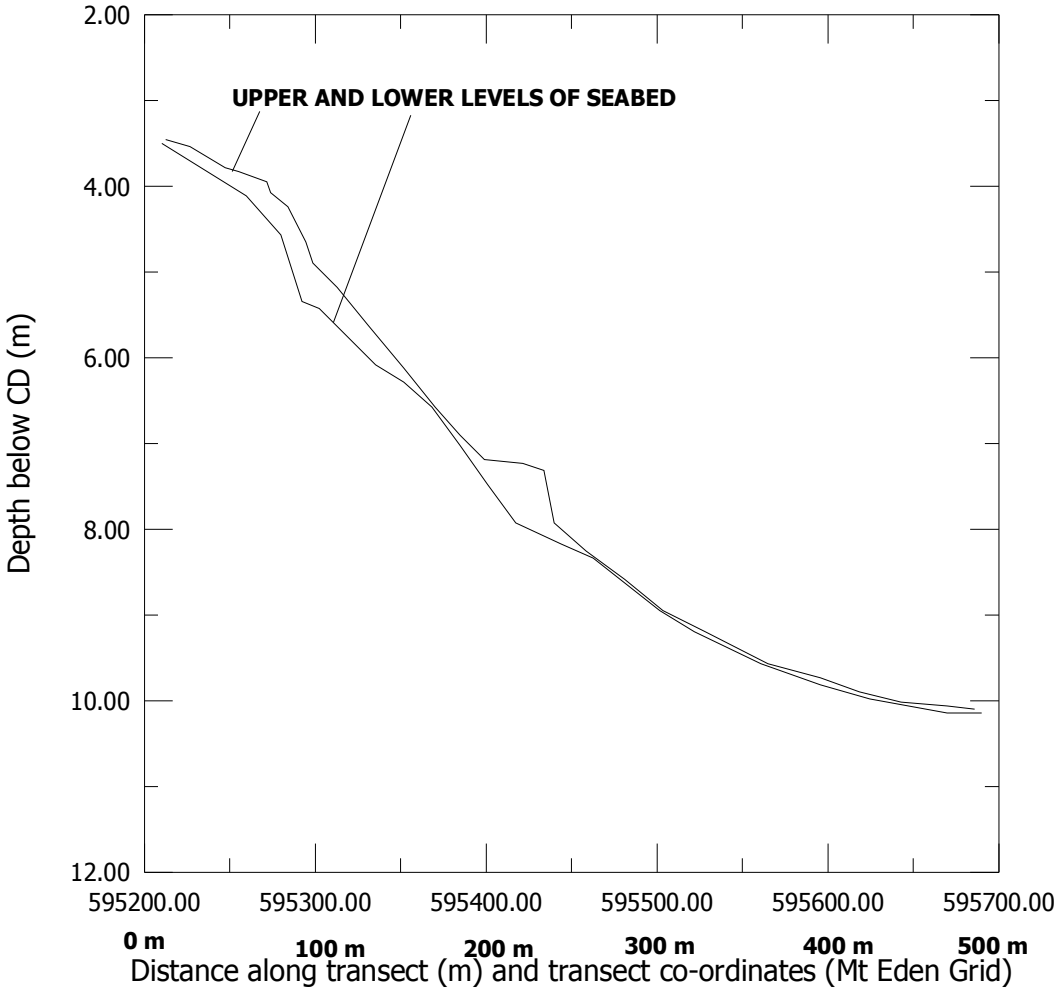

Figure 4.4: The upper and lower bed-level envelope from the bathymetric surveys (10-7-01 to 8-02-02)(ie: excludes lower accuracy survey 20-01-96).

The data demonstrate that the lowest bed level occurred in winter when swells tend to be at their largest size on the west coast, however wave heights of over 4 m measured on a number of occasions throughout September and October 2001 (Chapter 6) did not result in a significant lowering of the bed level, but rather a maintenance of the bed near this low level. This shows the bed is capable of maintaining an equilibrium level in the presence of large wave driven currents that

would be expected to transport large quantities of sand from adjacent to the shoreline.

Bathymetric maps of the bed level differences between hydrographic surveys on 10-07-01 to 3-09-01 (Fig. 4.5a: Map A), 3-09-01 to 6-11-01 (Fig. 4.5b: Map B), 6-11-01 to 29-01-02 (Fig. 4.5c: Map C) and 29-01-02 to 8-02-02 (Fig 4.5d: Map D) show a range of variation in seabed level. Sedimentary troughs and mounds are most visible on all the maps inshore in the breaking wave zone of the survey area.

- Map A shows significant erosion of sediment inshore (0.7 m) but grading to 0.2 m of erosion offshore over the majority of the survey area. In the centre a mound of sand visible in the July survey was eroded away, whilst bands (20 m wide) of erosion and accretion occurred in the vicinity of two submerged reefs (one showing 1.0 m erosion further offshore and the other 0.5 m accretion inshore).

- Map B shows a fairly stable bed offshore ranging between $\pm$0.3 m variation, whilst in the nearshore area mixed erosion and accretion was more significant at $\pm$0.7 m. The most significant area of deposition occurred in an area updrift of the Whale Bay reef.

- Map C showed the bed had eroded up to 1.4 m offshore to the northwest, grading inshore to 1.8 m of accretion in the Whale Bay reef area. Sand may have deposited in this area as in Map B due to smaller wave heights and lower current velocities in this zone, and the topographic barrier of the reef (Chapter 2).

- There was less variation in Map D than that of the other three maps, with a stable bed offshore and pockets of erosion and accretion in the inshore area up to 0.7 m. This result corresponds well to the side scan survey undertaken at this time that showed minimal variation in the rock/sand boundary and features of the seafloor (Chapter 5).

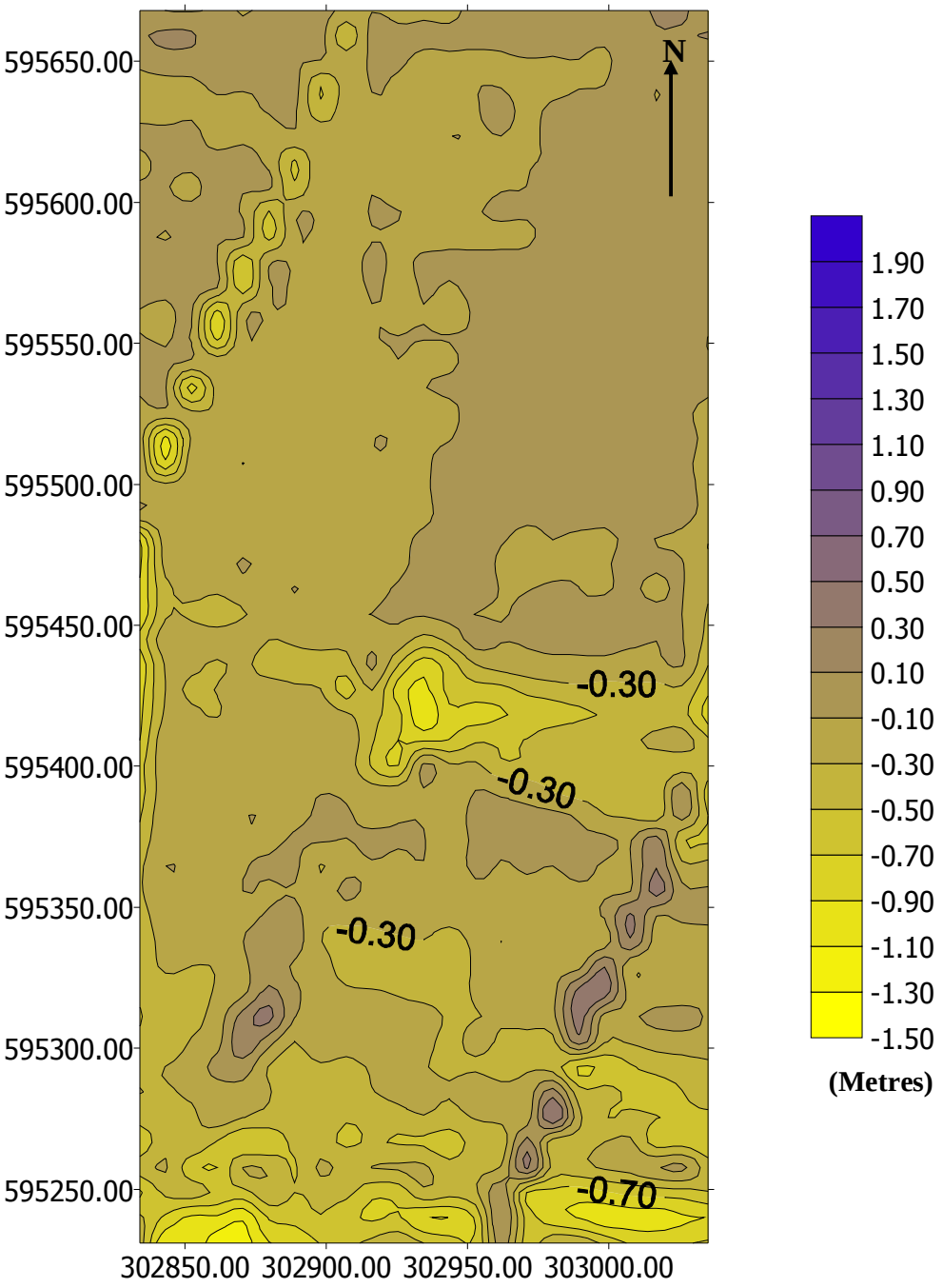

Figure 4.5a: Bathymetric map of the volume difference between hydrographic surveys on 10-07-01 and 3-09-01 plotted in SURFER.

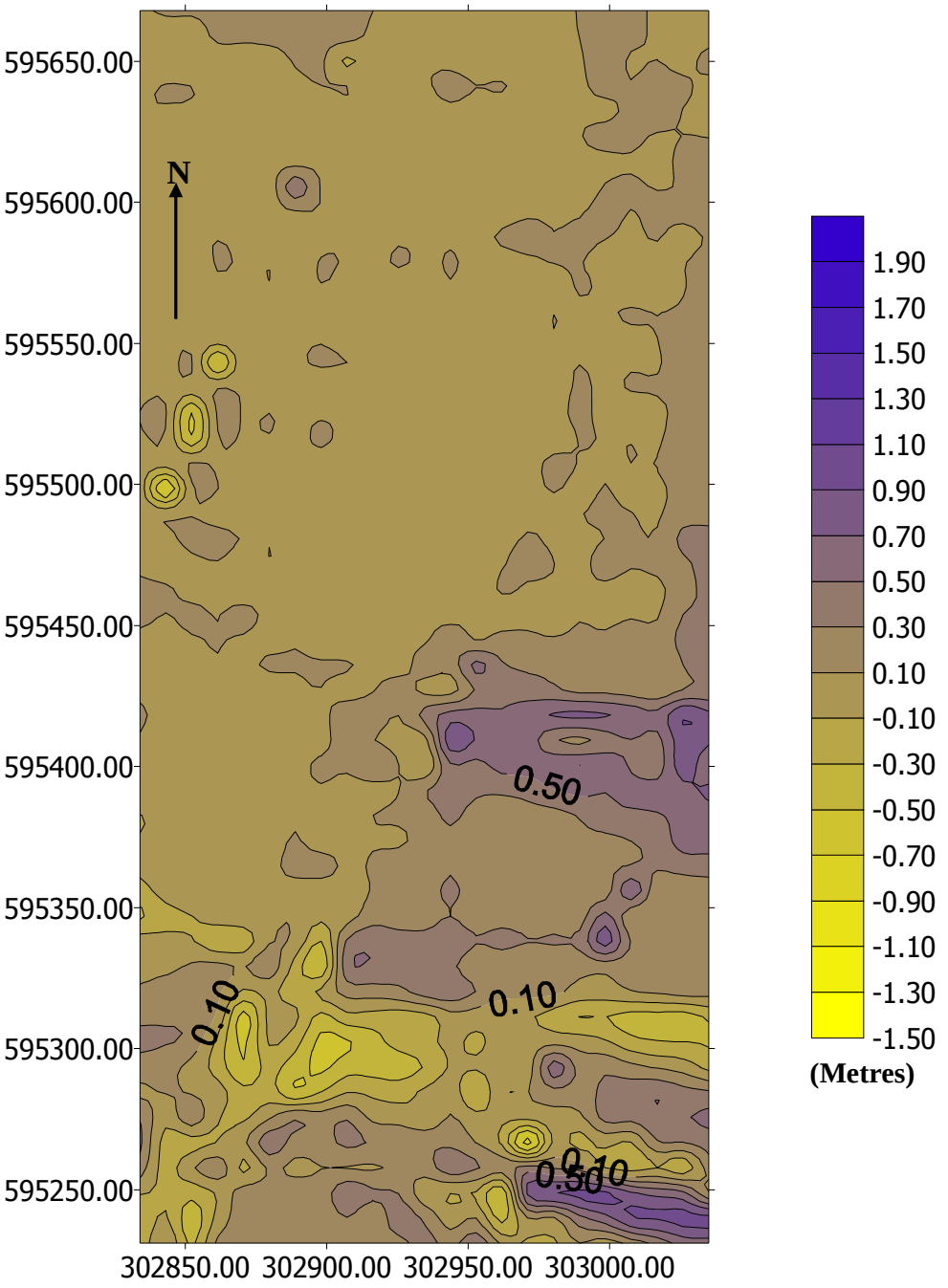

Figure 4.5b: Bathymetric map of the volume difference between hydrographic surveys on 3-09-01 and 6-11-01 plotted in SURFER.

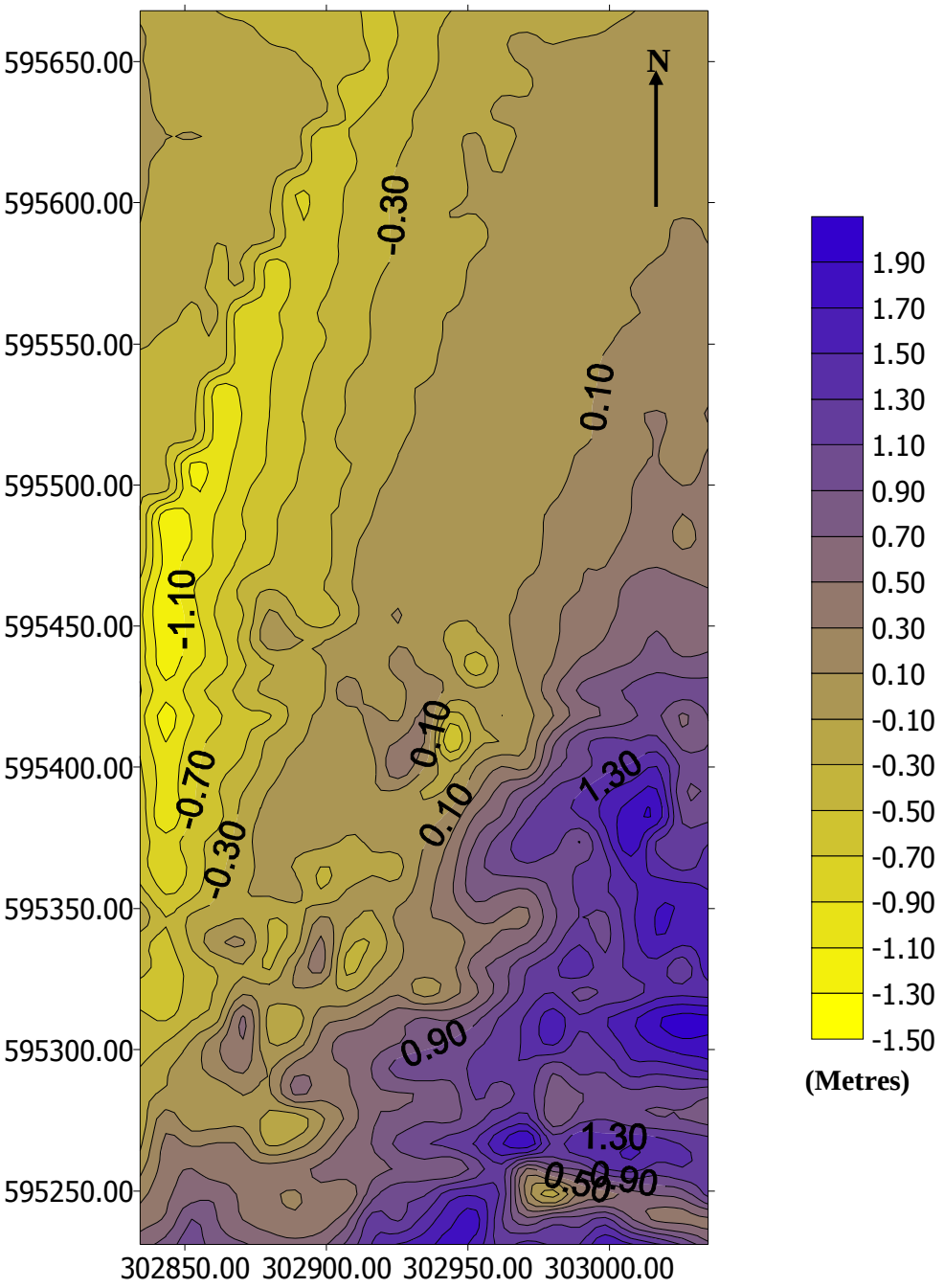

Figure 4.5c: Bathymetric map of the volume difference between hydrographic surveys on 6-11-01 and 29-01-02 plotted in SURFER.

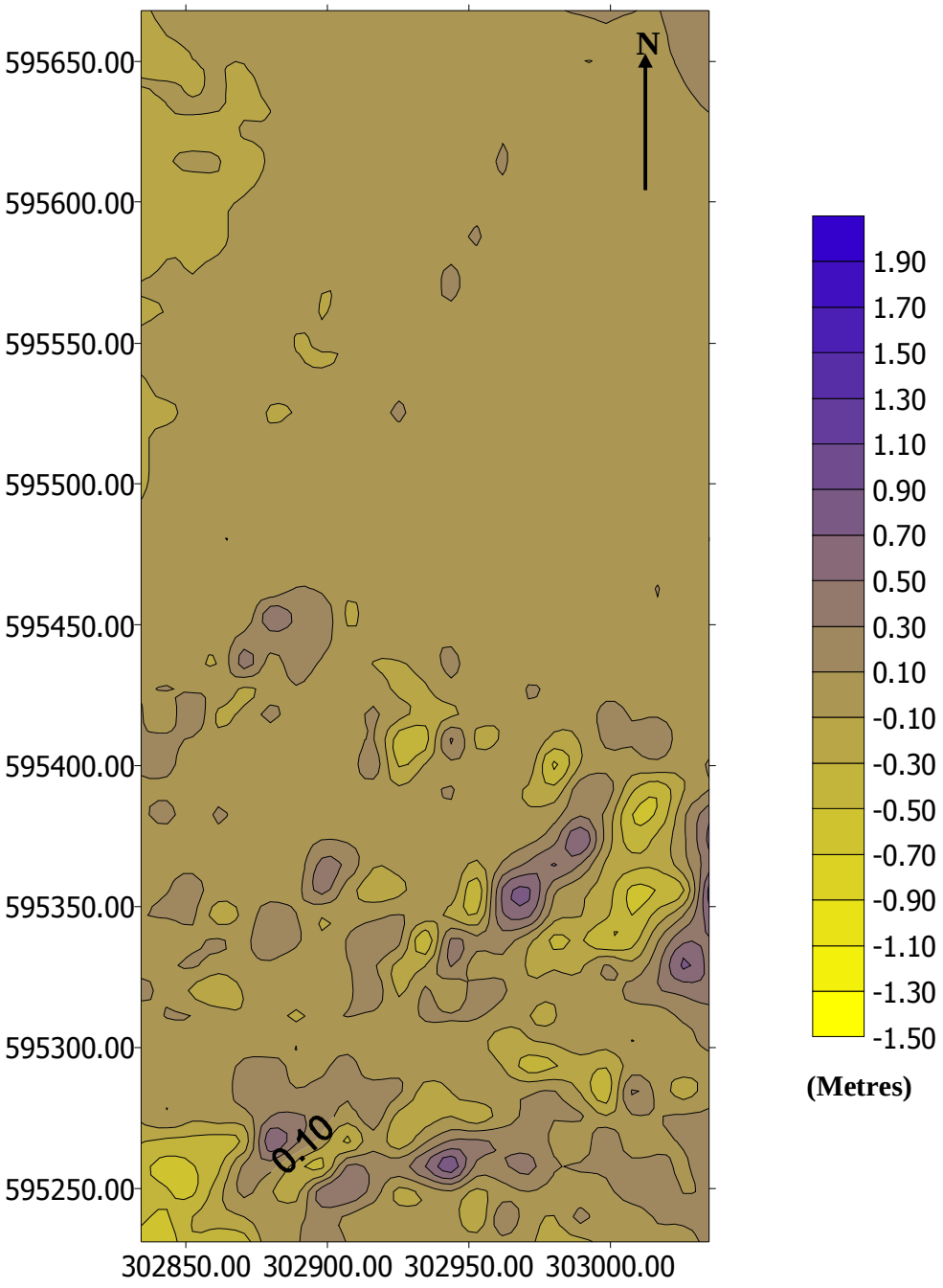

Figure 4.5d: Bathymetric map of the volume difference between hydrographic surveys on 29-01-02 and 8-02-02 plotted in SURFER.

Table 4.1: Mean seafloor elevation along the transect for the surveys, and the volume changes (m^3) over the survey area (87837 m^2), from bathymetric survey to the subsequent survey and vertical height difference (m).

Survey Date	Mean Bed Level (below Chart Datum) (m)	Volume Difference Over Total Survey Area (87837m^2) (m^3)	Vertical Height Difference Over Total Survey Area (m)
20-01-96	8.05		
10-07-01	7.51	-3330	-0.04
3-09-01	7.86	-17990	-0.21
6-11-01	7.83	+902	+0.01
29-01-02	7.48	+12780	+0.15
8-02-02	7.47	+69	+0.0008
Mean *	7.64		
Max Range *	0.43		

* Mean and Maximum range do not include the lower accuracy 20-01-96 data.

4.6 SUMMARY

Fieldwork constraints limited the nearshore survey area to 88,000 m^2 of the Raglan headland, which does not allow definitive demonstration of the variation of the seabed over the entire headland environment, but the data does however give evidence of the temporal and spatial variation within the measured area. The repeated bathymetric surveys at the Indicators surf break have shown that a range of variation occurred (both accretion and erosion) in the level of the bed over the survey period between 10-7-01 and 8-02-02. The mean seabed levels along a 500 m transect for all the bathymetric surveys varied by up to 0.5 m, although isolated mounds and scour holes were found up +1.8 m and -1.4 m respectively. Calculation of the mean levels of the seabed for each survey shows a minimum

level of 7.47 m below Chart Datum, a maximum of 7.86 m and a mean of 7.64 m. This is a maximum variation of 0.43 m, and interestingly is 0.22 m each side of the calculated mean level, which suggests that the bed appears to have an equilibrium level or range about which the variation occurs. This is supported by observations described in Chapter 3, where an upper level was designated by the long-term habitation of adult marine organisms on underwater boulders and the rock reef.

Significantly greater variation was found in the bed level within the first 250 m of the transect closest to the shore, where the gradient is steeper and breaking waves are located. Bathymetric maps of the difference in bed levels between surveys show a more complex erosion and accretion pattern in this zone, when compared to the offshore region. The bed offshore was more stable with considerably less variation in level. Interestingly a zone of sand deposition was located at the change in the bed gradients of the seabed (1 in 45 to 1 in 85) near the submerged Whale Bay reef, that was particularly apparent in the July 2001 survey but eroded away on the next survey on September 2001. This area of accretion is very apparent in the volume difference maps (Figure 4.4b and 4.4c).

The level of the bed may be regulated by the seasonal wave climate, which is supported by the survey in early September 2001 when the bed was found to be at its lowest level. This is a period in late winter when the west coast of New Zealand has very large southwest swells occurring (Heath, 1982), whilst in summer the bed was at its highest level (January and February 2002). Large swells in September and October 2001 (Chapter 6) maintained the bed at this low level, but did not further decrease the level. This demonstrates that despite the presence of large waves and the associated movement of sand, the bed is able to remain fairly stable in level, with the possible existence of a sedimentary equilibrium balancing the inputs and outputs at the headland.

The difference in the January – February 2002 surveys showed minimal variation in the volume of sediment on the bed with +69 m^3 of change over the survey area, after a period of waves with a mean height of 1.2 m and one event reaching 3.5 m

(Chapter 6). The bathymetric map of the difference in the bed level shows a fairly stable environment offshore, with mixed deposition and erosion inshore at the headland. This demonstrates that sediment was transported in the nearshore region where the breaking waves are found, but significant loss of sediment from the littoral system did not occur despite the large wave event. This factor shows that for the bed level to change for a longer period of time, the sedimentary equilibrium of inputs and outputs must alter at the headland.

CHAPTER FIVE

SIDE SCAN SONAR SURVEYS

5.1 INTRODUCTION

Characteristics of the seabed, such as the occurrence of bedforms form an integral component in the understanding of the dynamics and processes acting upon an environment. It can be difficult to quantify wave and current-driven transport around headlands by field measurements of these parameters alone, particularly over long time scales (years), due to their spatial variability and because sediment transport increases dramatically during intense, infrequent, episodic storm and large swell events (Hume *et al.*, 1997). Storms may still mask the underlying dominant processes, but the seabed is likely to still reflect the long-term signature of the forcing processes. This may include sites of deposition and scour, sorting of grain size, bedforms, sediment transport pathways, rock/sand boundaries and breaking wave zones (Fig. 5.1).

In the previous chapter the variation in the level of the bed was analysed at the Raglan headland, whilst this chapter focuses on the use of side scan sonar surveys to delineate the rock/sand boundary (Fig. 5.2) and characteristics of the seafloor such as rock outcrops, the type of substrate (i.e. sand, mud), and seabed morphology (i.e. bedforms - ripples, mega-ripples, sand-waves and their position and size). These surveys were completed both seasonally and pre and post a swell event to differentiate any changes in the characteristics of the seabed.

Figure 5.1: Waves breaking along the headland at Raglan influencing the seabed characteristics (Source: www.ragtimeblue.co.nz).

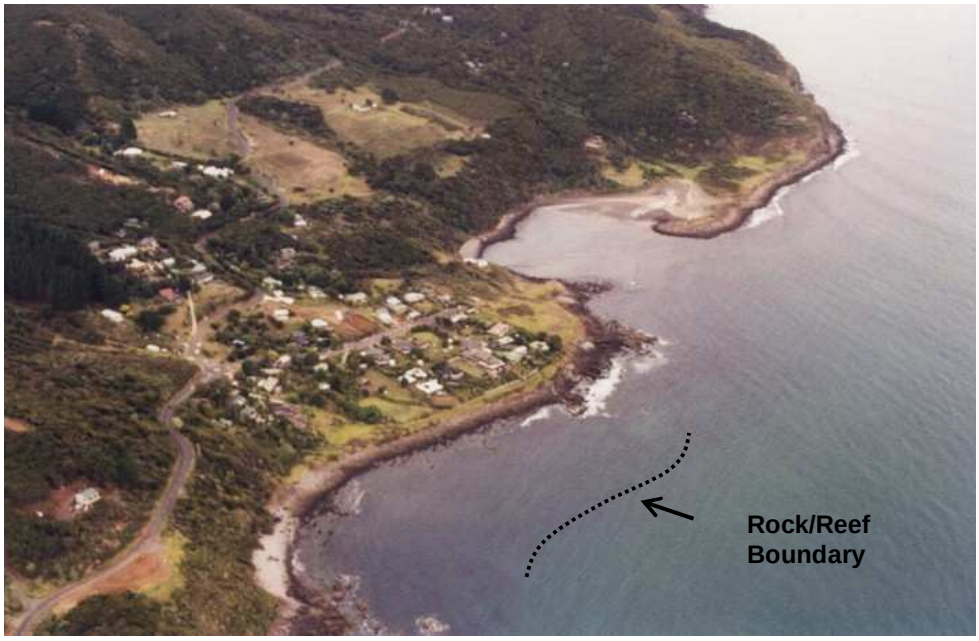

Figure 5.2: Aerial view of the headland at Raglan showing the boulder and reef shoreline (Source: Author, March 2001).

5.2 SIDE-SCAN SONAR SURVEYS

5.2.1 *Methodology and field programme*

The side-scan sonar system consists of a transducer "fish" towed behind a vessel, which emits a sound pulse that is aimed at, at reflects off, the seafloor. The return signal received by the transducer is transformed to an image depending on the strength of the return signal. Thus acoustically "hard" matter returns a strong signal, whilst sand surfaces return a weaker signal. The image of the reflected sound is processed and may be printed as a hard copy, or viewed and analysed in a digital medium. For the surveys in this study a Klein 595 side-scan sonar system was used with a single frequency 100 kHz transducer. The Klein side-scan is a dual frequency echo sounder operating on 100 kHz and 500 kHz. For the surveys it was run on 100 kHz.

Vessel position fixing was achieved using Differential Global Positioning System (DGPS) for some of the surveys with a base station satellite receiver set up each day at Manu Bay on a known benchmark (595314.90 N, 304039.00 E) (Fig. 5.3). Establishment of the benchmark was by Hutt (1997) on a permanent fence post using the South Head Trig, Number 48 (596707.55 N, 306348.22 E). This system uses a radio link through a VHF modem between the base station and the boat to improve positional accuracy, through a process of differential correction. Positional accuracy of approximately 1 m is achieved with this method. In the later surveys the base station located at Gulf Harbour marina in Whangaparoa was used for the surveys, which also has an accuracy of approximately 1 m. This method does not require a local base station.

The vessel survey tracks were programmed into the software package Hydro (Trimble Navigation Ltd) as "run lines". Four "run lines" were used for the Raglan surveys starting at Manu Bay and finishing at the surf break Outsides just past Indicators (Fig. 5.4). The output of the side-scan was selected to cover a distance of 140 m across (70 m each side of the transducer), and the "run-lines" were

planned to ensure overlapping coverage of the seafloor. The programme DELPH MAP® was subsequently used in the post-processing of the side-scan data to edit position and depths. For one of the surveys only an analog output was available, due to insufficient space on the University of Waikato survey vessel Mac Boat for the ISIS® computer capable of storing the digital copy (10-6-98).

Figure 5.3: The base station set up over the benchmark at Manu Bay looking out towards the Indicators surf break (Source: Author, 10-6-98).

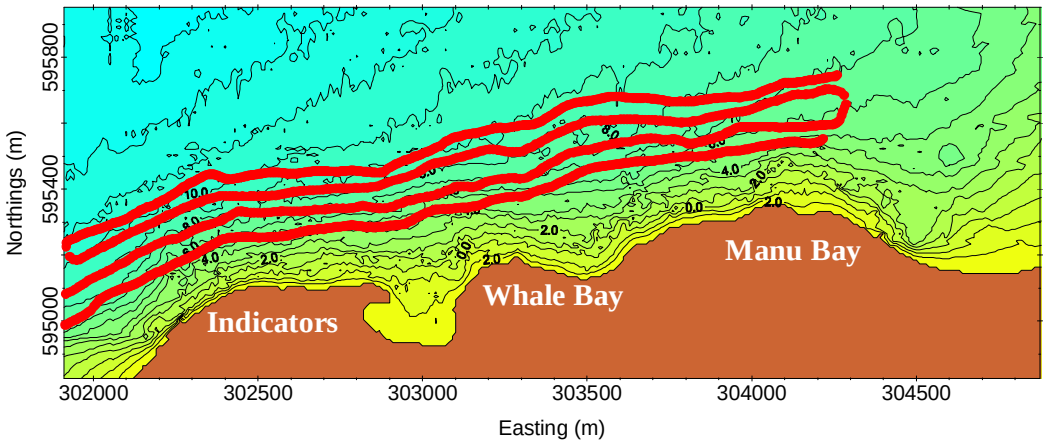

Figure 5.4: Map showing the position of the 'run-lines' used for all the side-scan sonar surveys at the field area (shown on a contour map with 1 m intervals of the study area from Hutt, 1997)(Mt Eden Grid).

For the other surveys (11-4-00, 27-4-01, 24-1-02, 12-2-02 and 15-7-02) digital capability recording was also possible using the chartered vessel Islay Mist II and the purpose designed University of Waikato survey vessel Taitimu (Figs. 5.5 and 5.6), although a computer failure on the 11-4-00 corrupted the digital copy of the scan. The ISIS® data analysis software digitises, stores and processes side-scan sonar signals and combines the sonar imagery with navigation inputs to geocode the data in real-time.

Figure 5.5: The University of Waikato survey vessel Taitimu (Source: D. Immenga 13-8-01).

Figure 5.6: The Klein side-scan sonar setup inside Taitimu (Source: D. Immenga 13-8-01).

During the surveys the vessels were operated at a speed of approximately 5 knots, with minor corrections being made to allow for wind and tide drift. The side-scan tow-fish was lowered below the boat and ideally set at one-third of the water depth from the bottom (Fig. 5.7). In shallow zones or where known rock outcrops existed, care was taken to not damage the transducer on the bottom.

Digital scans were processed and plotted in DELPH MAP® which is a mosaicing package that builds a georeferenced visual database of images, vectorised sonar feature extractions and other spatial data. DELPH MAP® is designed to support the ISIS® data acquisition systems with geocoding, image merging and mosaicing capabilities, and combined with swath bathymetry into a single software environment.

For presentation of the geocoded mosaics the software MAP INFO, ARC VIEW and SURFER were used. These allowed presentation of the seabed interpretation

and comparison of the rock/sand boundary position, as well as other features such as bedform location and size. The seabed characteristics are presented showing the zones of mega-ripples and their relative sizes and other distinctive features of the bed. Analog outputs were used to interpret the bedforms, whilst for the analog traces a section of the coastline at Whale Bay was selected for detailed analysis and manual analysis undertaken to plot the variation in the rock/sand boundary.

Figure 5.7: Side-scan sonar fish ready for deployment (Source: Author, 27-4-01).

Two of the side-scan sonar surveys were undertaken before and after a significant large swell event (H_s=3.5 m) at Raglan (24-1-02 and 12-2-02), to identify variation in the seabed features, whilst all other surveys were undertaken seasonally for the purpose of ascertaing temporal variation in the characteristics of the bed. These surveys were always conducted when the swell was as close to flat as possible, with some small swell on a few occasions. The flat conditions meant that fishing boats were present making the most of the conditions and thus boat noise appears on some of the scans when passing the survey vessel. High tide was selected as the ideal time to undertake the surveys as shoaling of waves at the time are less likely to influence the survey.

In March 2001, a flight was made to provide aerial photos of the headland and to delineate the underwater rock/sand boundary that was visible at this time, due to good water clarity following a period of minimal rainfall. Although the aerial photos were not to scale visual comparison with the boundary shown in the side scan surveys was possible.

5.3 RESULTS

The successive side scan sonar surveys at the Raglan headland have shown that the rock/sand interface generally follows the shape of the headland, with a series of reefs protruding seaward (shore-normal) from the main reef structure. This is verified in the aerial photographs of the headland at Indicators and Whale Bay (Figs. 5.8 and 5.9). The side scan sonagraph of the survey in January 2002 provides an example of the position of the interface and outlines the location of the reefs protruding offshore from the headland (Fig. 5.13). Megaripples were most common closer to the headland at the rock/sand boundary where large breaking waves and associated strong unidirectional alongshore currents are found (Fig. 5.10). They were sinusoidal and asymmetrical in shape and aligned with the orientation of the waves and currents that sweep in an easterly direction down the headland (Table 5.1). Ground truth observations by divers confirmed their presence with wavelengths of up to 3.5 m (crest to crest) and heights of 0.5 m.

These megaripples are created by the strong unidirectional current flow driven by the breaking waves as the water depth is shallow (3-8 m), which would not allow the creation of megaripples to the size measured by wave orbital motion (Boothroyd, 1978). The Boothroyd classification system shows that megaripples in the 0.6-6 m range are generated by currents in the 0.7-1.5 ms^{-1} range (Table 2.3), which were found in the measured data (Chapter 6) and numerical modelling (Chapter 8) at the headland. The asymmetrical shape also shows formation by unidirectional flow (Nielson, 1992), with the steep side of the crest confirmed by divers to be facing with the direction of the current flow. Both the Indicators (Site D) and Whale Bay (Site A) sites analysed showed similar characteristics of large

megaripples inshore, and further offshore (Site C) the orientation showed a possible offshore flowing current with smaller megaripples. At Whale Bay (Site B) the orientation of the bedforms shows a current flowing back into the seaward end of the Whale Bay reef area and sediment deposition in this area, which may be due to the protruding reef creating a barrier to the flow.

Figure 5.8: Aerial view of "Indicators" surf break, edge of the lagoon and the underwater rock/sand boundary (Source: Author, 25-03-01).

Figure 5.9: Aerial view of Manu Bay with the submerged rock/sand interface visible (Source: Author 25-03-01).

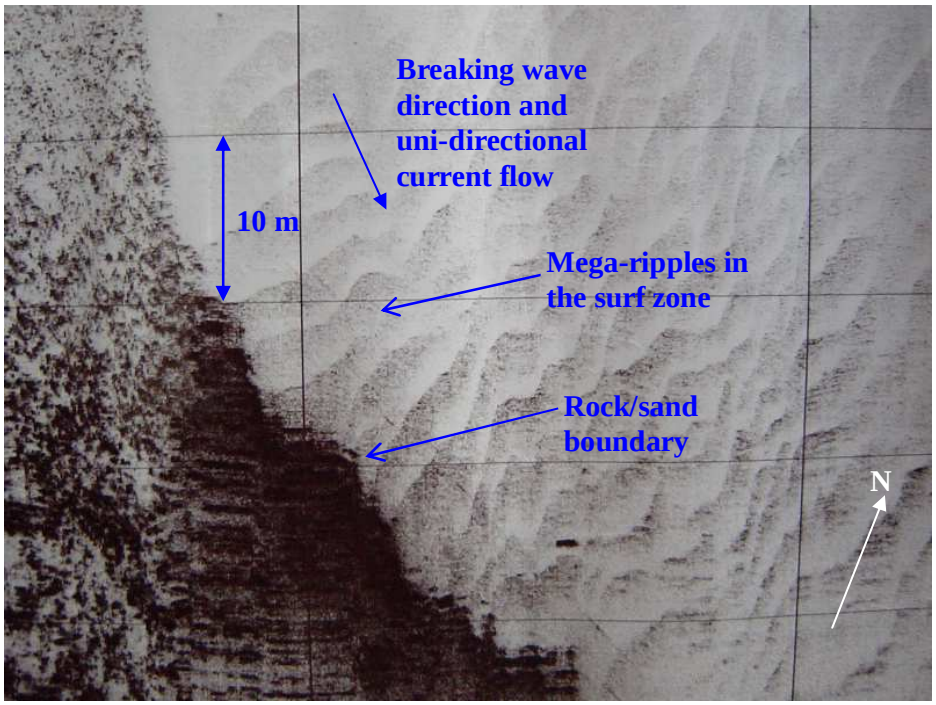

Figure 5.10: Side scan image (11-7-00) of large sinusoidal megaripples at Whale Bay.

The percentage sand cover on the rocky reef was measured (Table 5.2) and shows similarity across all the surveys, although the most significant cover was found on the rocks when the rock/sand boundary was furthest seaward (April 2001 survey following a large 6 m swell event). This could demonstrate accretion of sediment on the reef in proportion to where the boundary is located (i.e. lower bed level and potential shoreward movement of the boundary with recovering of the exposed rocks). This is also identified in Chapter 6 where soon after the large swell event sediment recovered the freshly exposed rocks.

The side scan sonagraph on the 24-01-02 is characterised by large megaripples and a disrupted bed, showing the presence of large waves and strong currents inshore at the headland, whilst further offshore the bedforms show the presence of a possible offshore flowing current. Between these zones a less distinguishable pattern exists, that was also identified by divers using scuba. Bathymetric surveys (Chapter 4) of the lower Indicators surf break area on the 29-01-02, showed the bed was at its highest level in this summer period with significant accretion in the nearshore region. The side scan reflects this finding with sand drifts visible in the same area (Fig. 5.11), and the rock/sand interface at a slightly higher level than previous scans (Figs. 5.13 and 5.14). The shore-normal reefs suggest they may act as a barrier to longshore sediment transport, however sediment seems to both cross and flow through gaps in the reefs, and may have more of a localised effect on the sediment dynamics.

Table 5.1: Megaripple characteristics at 4 sites (Indicators and Whale Bay shown on Fig. 5.13) on the Raglan headland from all the side-scan sonar surveys.

Scan Date and location	Ripple length λ (m)	Ripple height η (m)	Angle θ (deg)	Transport direction (deg)	Description
(A) Whale Bay					
10-6-98	2.0	0.4	45^o	135^o	tsp/assym
27-4-00	2.2	0.4	35^o	120^o	tsp/assym
27-4-01	2.5	0.5	50^o	140^o	tsp/assym
24-1-02	3.5	0.5	40^o	130^o	tcop/assym
12-2-02	3.5 relict with 0.1 overlain	0.5 0.03	40^o 80^o	130^o 170^o	tcop/assym tsp/symm
15-7-02	3.8	0.5	45^o	135^o	tsp/assym
(B) Whale Bay					
10-6-98	1.0	0.15	105^o	190^o	tcop/assym
27-4-00	1.2	0.1	110^o	200^o	tcop/assym
27-4-01	Poor sonagraph clarity – not identifiiable				
24-1-02	0.8	0.1	125^o	215^o	tco/assym
12-2-02	0.8 relict with 0.1 overlain	0.1 0.03	125^o 90^o	215^o 180^o	tco/assym tsp/symm
15-7-02	1.3	0.2	100^o	190^o	tcop/assym
(C) Indicators					
10-6-98	3.0	0.4	40^o	130^o	tsp/assym
27-4-00	3.5	0.5	20^o	110^o	tsp/assym
27-4-01	3.5	0.5	35^o	125^o	tsp/assym
24-1-02	3.2	0.5	20^o	110^o	tcop/assym
12-2-02	3.0 relict with 0.1 overlain	0.5 0.02	20^o 60^o	110^o 150^o	tcop/assym tsp/symm
15-7-02	3.6	0.5	30^o	120^o	tsp/assym
(D) Indicators					
10-6-98	1.0	0.2	60^o	330^o	tsp/assym
27-4-00	3.0	0.5	30^o	300^o	cuspate/ass
27-4-01	2.5	0.4	35^o	305^o	cuspate/ass
24-1-02	2.0	0.3	40^o	310^o	cuspate/ass
12-2-02	2.0 relict with 0.1 overlain	0.3 0.02	40^o 75^o	310^o 165^o	cuspate/ass tsp/assym
15-7-02	2.0	0.3	45^o	315^o	cuspate/ass

- tsp (transverse sinuous in phase)
- tcop (transverse catenary out of phase)
- assym (assymetrical shape)
- symm (symmetrical shape)

Table 5.2: Percentage sand cover measured at Indicators (E) and Whale Bay (F)(Fig. 5.13) on the rocky boulder and reef shoreline from the side-scan sonagraphs (10-6-98 to 15-7-02).

Survey Date	Indicators % cover (E)	Whale Bay % cover (F)
10-6-98	15	10
27-4-00	17	15
27-4-01	30	26
24-1-02	14	13
12-2-02	21	20
15-7-02	18	16

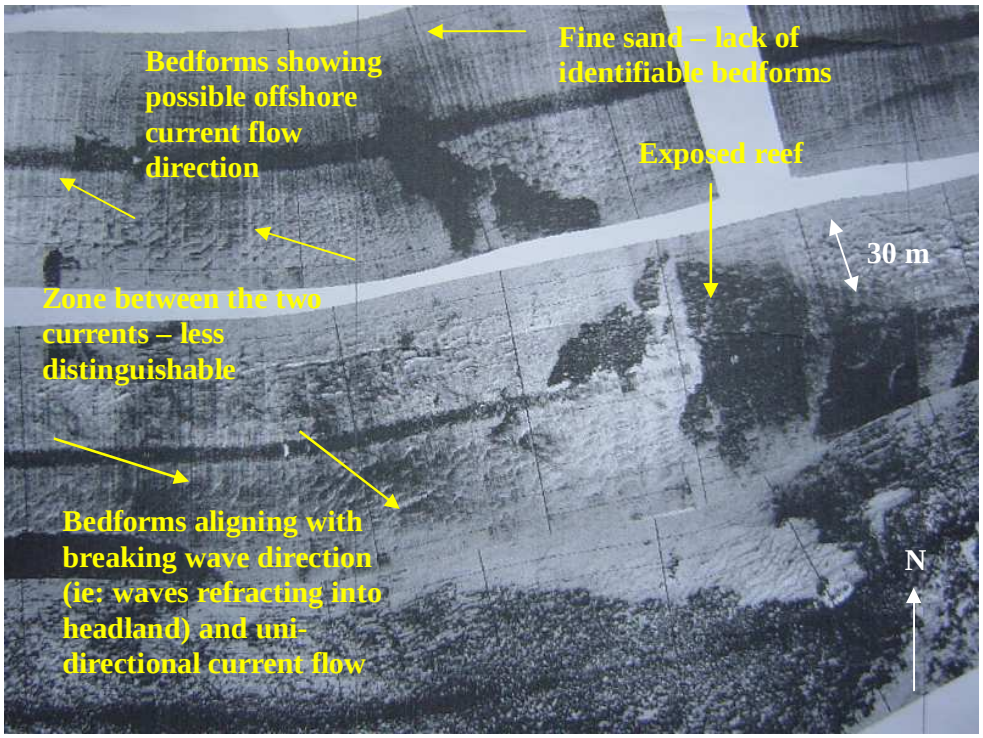

Figure 5.11: Side scan sonagraph image of the survey on 24-01-02 west of the Whale Bay reef area showing the large bedforms, evidence of easterly sand movement in large wave conditions, whilst offshore smaller bedforms show a possible offshore flowing current.

The side scan survey on the 12-2-02 showed a significantly smoother bed with large remnant megaripples overlain with small symmetrical bedforms (approx. 100 mm crest to crest; Fig. 5.12). The swell over this period (Chapter 6) appears to have not significantly affected the bed, with the small bedforms visible at all the analysed sites (Table 5.1), imposed on relic larger bedforms. The small symmetrical bedforms reflect the small swell over this period, where a 1 m average wave height was recorded with significantly lower current velocities than during large (>3 m) swell (Chapter 6). This finding corresponds well to the results of the bathymetric surveys (Chapter 4), where the bed level was found to have remained fairly stable.

Figure 5.14 shows the outline of the rock/sand interface for the 12-02-02 survey and is overlain with the boundary from the 24-01-02 survey. The idealised outlines show the rock/sand boundary did not vary significantly in position with some smaller rocks visible in the February survey that were covered by sand in the January survey.

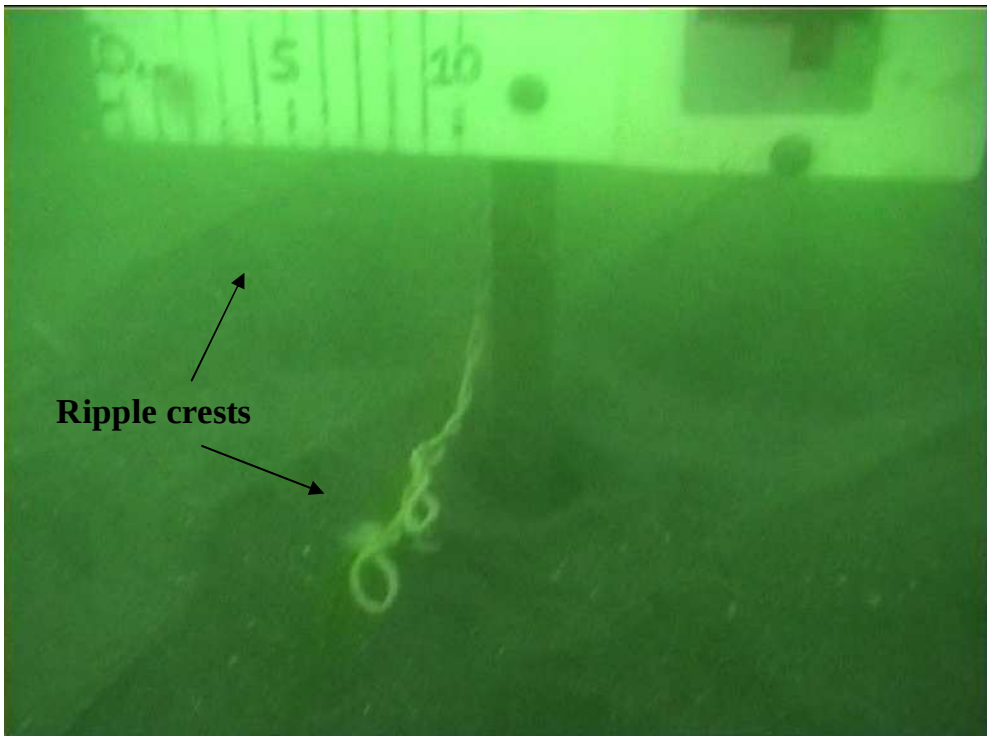

Figure 5.12: Bedforms (symmetrical) on the seafloor (100 mm crest to crest) at the Indicators surf break of the headland on the 12-2-02 (Source: Author, 12-2-02).

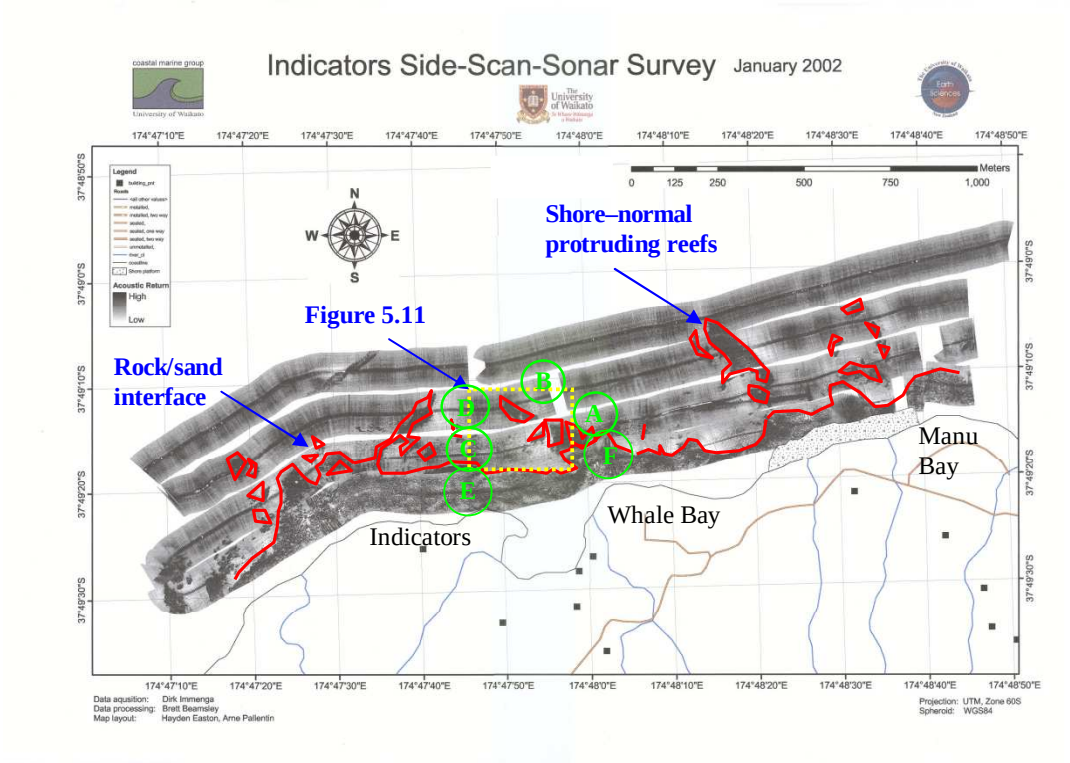

Figure 5.13: Side scan sonagraph on the 24-01-02 of the Raglan headland illustrating the reef location (outlined in red), shore-normal protruding reefs, location of Figure 9.13, Sites A to D where detailed bedform analysis has been undertaken and the data presented in Table 5.1, and Sites E and F where percentage sand cover has been measured and presented in Table 5.2.

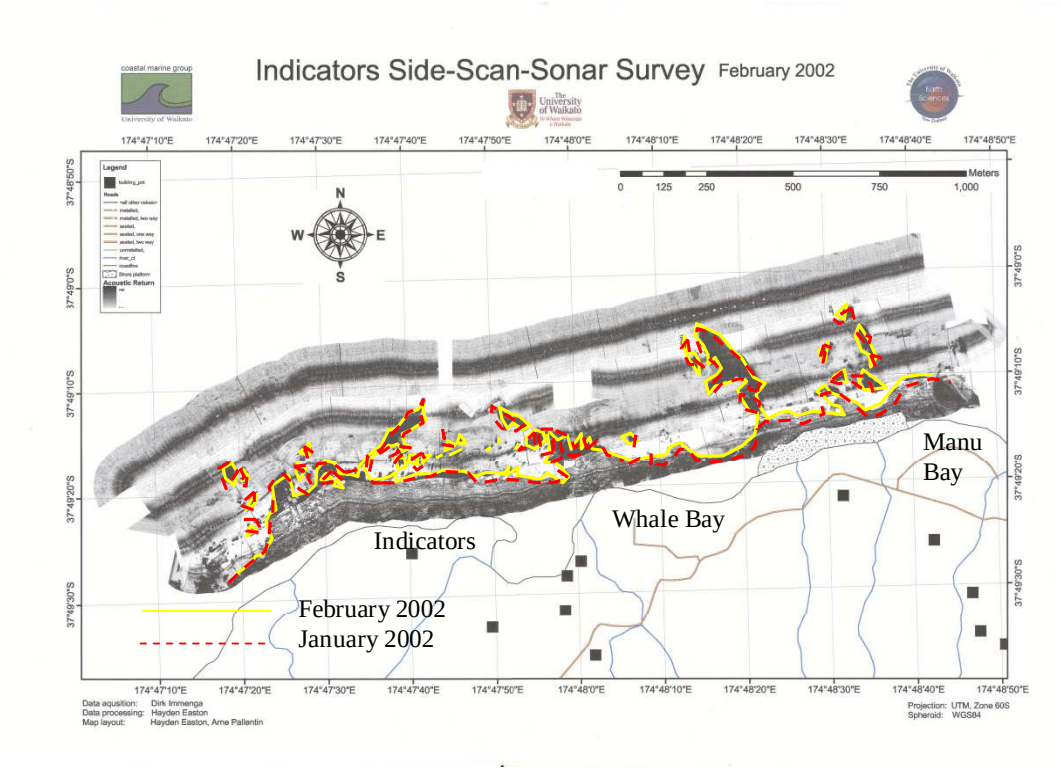

Figure 5.14: Side scan sonagraph on the 12-02-02 of the Raglan headland with the outline of the rock/sand interface shown in yellow, overlain with the 24-01-02 survey in dashed red.

The succession of side-scan sonar surveys from 10-6-98 to 15-07-02 (Fig. 5.15) has shown the rock/sand interface to not vary significantly in position along the headland, whilst the rocky reefs protruding from the headland and offshore appear to become covered by sand accretion and also erode more readily. The rocky reef/sand boundary varies in position depending on the recent swell conditions, with a maximum variation over all the surveys at Indicators of 50 m. The rocky reef/sand boundary does not however maintain this distance long term except where a possible variation occurs in the sedimentary balance of the littoral system. The boundary has been found to return to an equilibrium level (quasi-permanent position), which was also identified in the bathymetric surveys (Chapter 4) and indirectly by the habitat zonation of adult marine organisms (Chapter 3).

Long-term variation in the level of the seabed is demonstrated by the June 1998 and April 2000 surveys that showed more sand at the headland than the later surveys, with sand covering both the reefs that protrude from the headland and various rock features. The sedimentary equilibrium of the system at this time was therefore likely to have consisted of more sand than for the following surveys, where the reefs were more exposed. Aside from this significant variation in the bed characteristics, the bathymetrically higher reefs typically maintained their rocky nature, with lower level rocks becoming inundated with sandy sediment or exposed more readily, and sand patches varying in size.

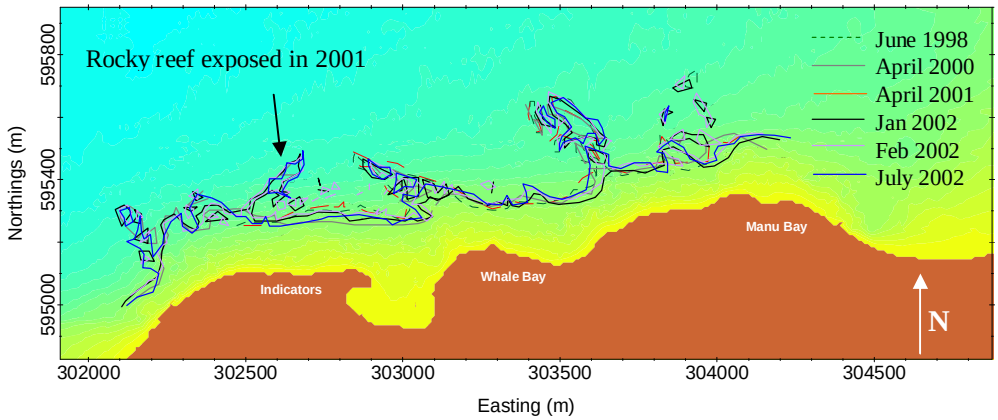

Figure 5.15: Diagram of Raglan showing the underwater rock/sand interface position for all of the side-scan surveys and the rocky reef exposed in 2001.

An example includes the shore-normal rocky reef at the Indicators surf break which was covered with sand, with only small rocks exposed in the early surveys (10-6-98, 27-4-00; Figs. 5.15 and 5.16a), but the 27-4-01 and all the subsequent surveys showed this reef to be more exposed (Fig. 5.16b). This demonstrates that a significant quantity of sediment was transported from this area of the headland and has not accreted to recover the reef, which was also found in the bathymetric surveys (Chapter 4).

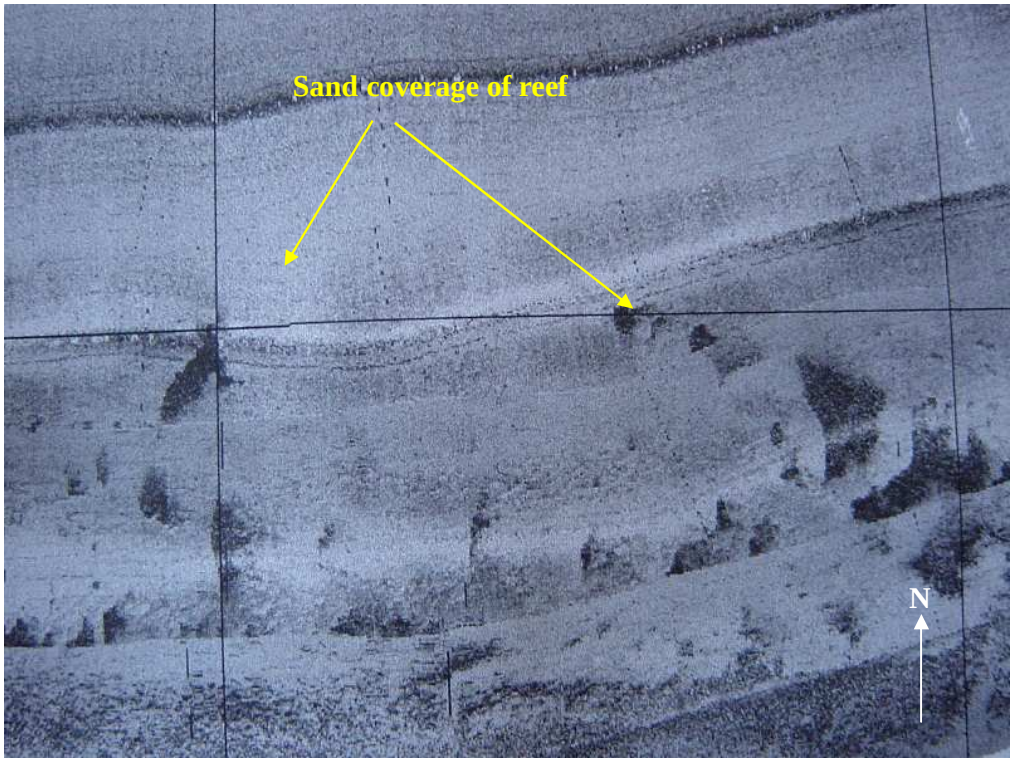

Figure 5.16a: Side scan sonagraph image on the 11-4-00 showing the reefs at Indicators and Whale Bay covered with sand.

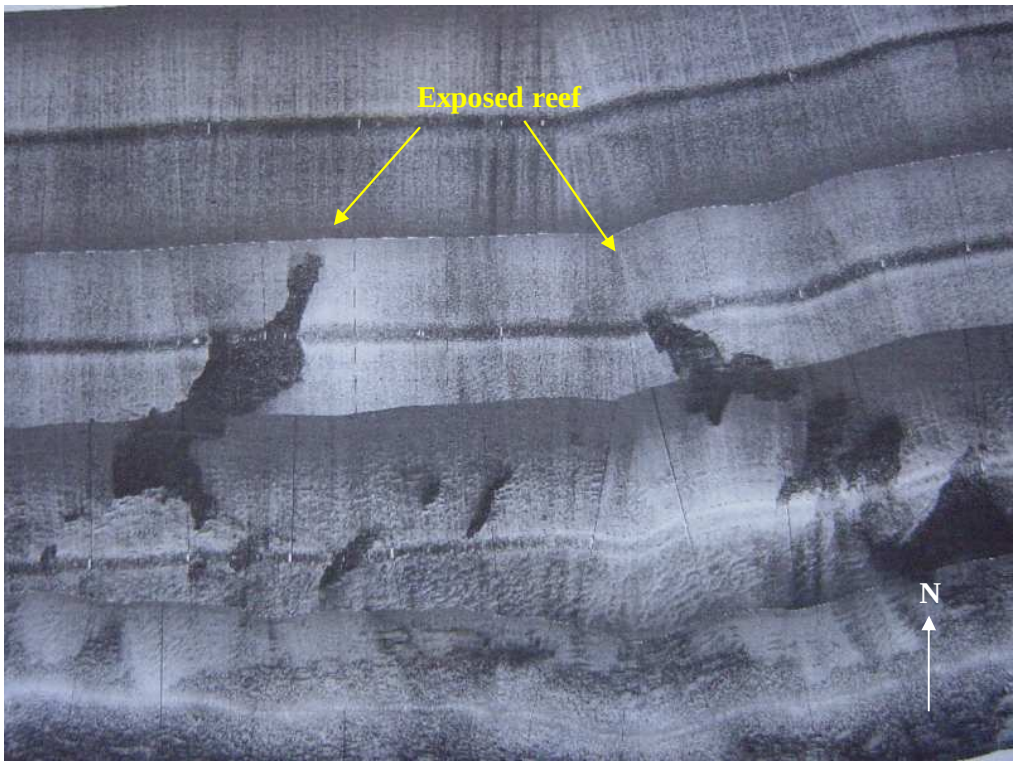

Figure 5.16b: Side scan sonagraph image on the 15-07-02 showing the greater area of exposed reef at Indicators and Whale Bay.

The author observed during the summer period (2000/2001), that the west coast had very low levels of sand on the beaches, with numerous rocks exposed at Ruapuke, Ngarunui and Muriwai beaches (Fig. 1.3). The field site had also shown variation in surf conditions that might be due to a predominantly lower bed level (S. Mead, pers comm.). The side scan survey on the 27-4-01 showed that the rock/sand interface was more seaward than previous surveys, where a 30 m difference in the boundary was found at Whale Bay.

However, the side scan on the 27-04-01 was undertaken after a very large swell (6 m), and observations by the author using scuba diving equipment showed fresh rock exposed at the Indicators reef boundary that was approximately 30 m further seaward from the coast than during field experiments in 1998 (Fig. 5.17). Interestingly, bathymetric surveys correspond well (Chapter 4), showing a maximum bed level variation of mean data along a transect of 0.5 m, which

correlates to a distance of 20-30 m variation of the rock/sand interface found in the side scan sonar surveys for the known gradient of 1 in 45 inshore at Indicators.

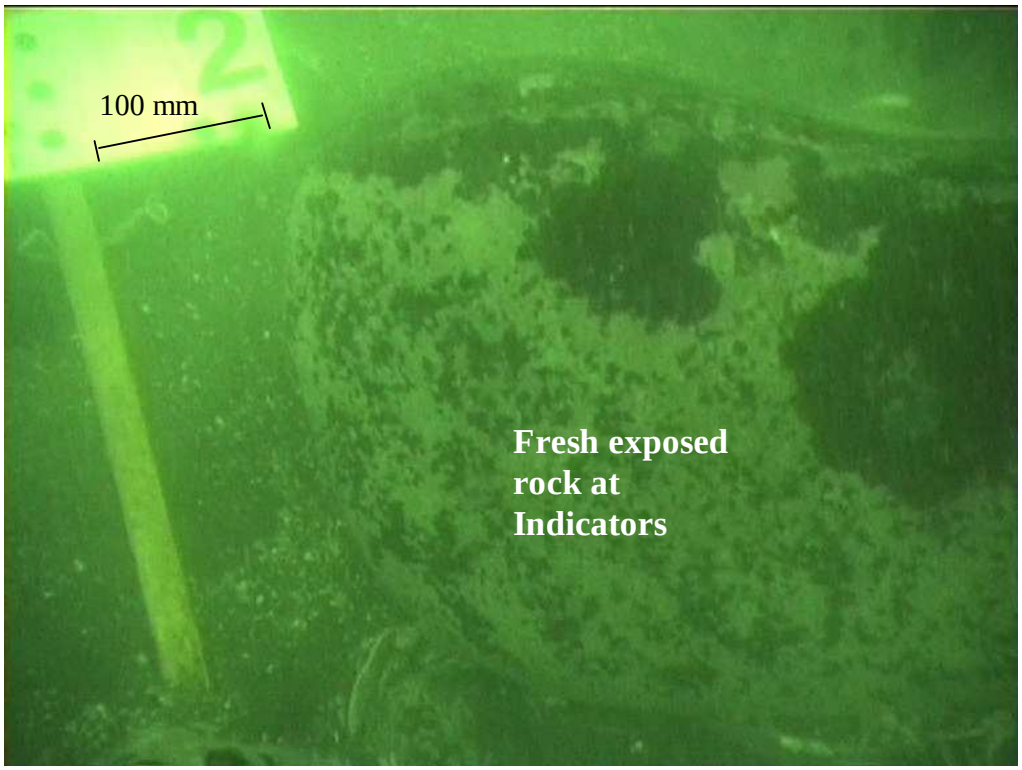

Figure 5.17: Fresh rock exposed on the seabed at the Indicators surf break (Source: Author 27-4-01).

One week later the same inshore location had accreted sediment and covered the exposed rock again. Significant sand coverage of the rocks was noticeable on the sonagraph. Sea conditions during this week were characterised by a much smaller groundswell (1-1.5 m) than the previous large swell, which appears to have transported sediment back onto the sub-tidal reef and boulders. Accretion of sand can be seen on both sides of the reef in the January 2002 survey, however the reef was still exposed and shows that either the sedimentary budget had changed, or settlement to recover the reef may be difficult due to the increased turbulence created by the rocks. McComb (2002) found that a dredged sediment mound placed near rocky reefs off New Plymouth did not inundate and cover the reefs, but

was transported in suspension from the area, and did not settle on the reef due to greater bed shear stress and turbulence in this region.

The boundary had moved slightly inshore over the summer of 2002 which correlates well to the results of the bathymetric surveys (Chapter 4) where the bed levels were also at their highest at this time. The survey on the 15-07-02 shows the presence of large megaripples inshore along the headland (Table 5.1), with a reef at the western end more exposed than normal, and at Manu Bay an accretion of sand covering rock outcrops. This shows the movement of sand in an easterly direction along the headland, but the rock/sand interface is still fairly stable and considerable sand is present along the entire headland. The erosion is likely to have occurred as wave driven currents present in a large swell at the Outsides surf break, identified in numerical modelling (Chapter 8) would have transported sand from this breaking wave zone.

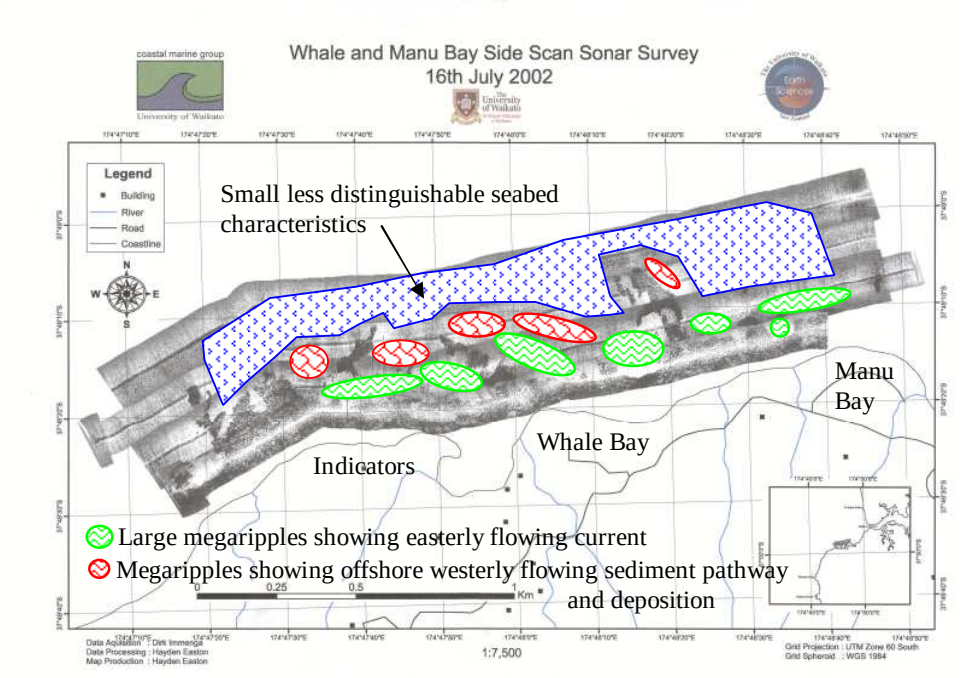

Figure 5.18: Side scan sonagraph of the Raglan headland on 15-7-02, outlining the rock/sand boundary, reefs and seabed features.

Zones of large megaripples (2-3.5 m crest to crest) have been identified from the side scan sonagraphs and shown on Figure 5.18. The well-defined megaripples that are common close to the rock/sand interface where breaking waves and strong unidirectional currents are found have continuous crests, assymmetrical shape and are sinusoidal in nature (Table 5.1). Further offshore, the ripples were smaller and less distinguishable but suggest an offshore flowing current and zones of sediment deposition.

The bedforms at Whale Bay (Table 5.1) show a pattern (Fig. 5.19) that correlates well to the rotating of the westerly flowing current identified in the modelling (Chapter 8). Essentially regions such as this at Whale Bay, in the lee of the shore-normal protruding reefs may provide a sink where the sediment accumulates and is available for transport back along the headland in an easterly direction in larger swells, which forms part of the dynamic equilibrium in the nearshore littoral system.

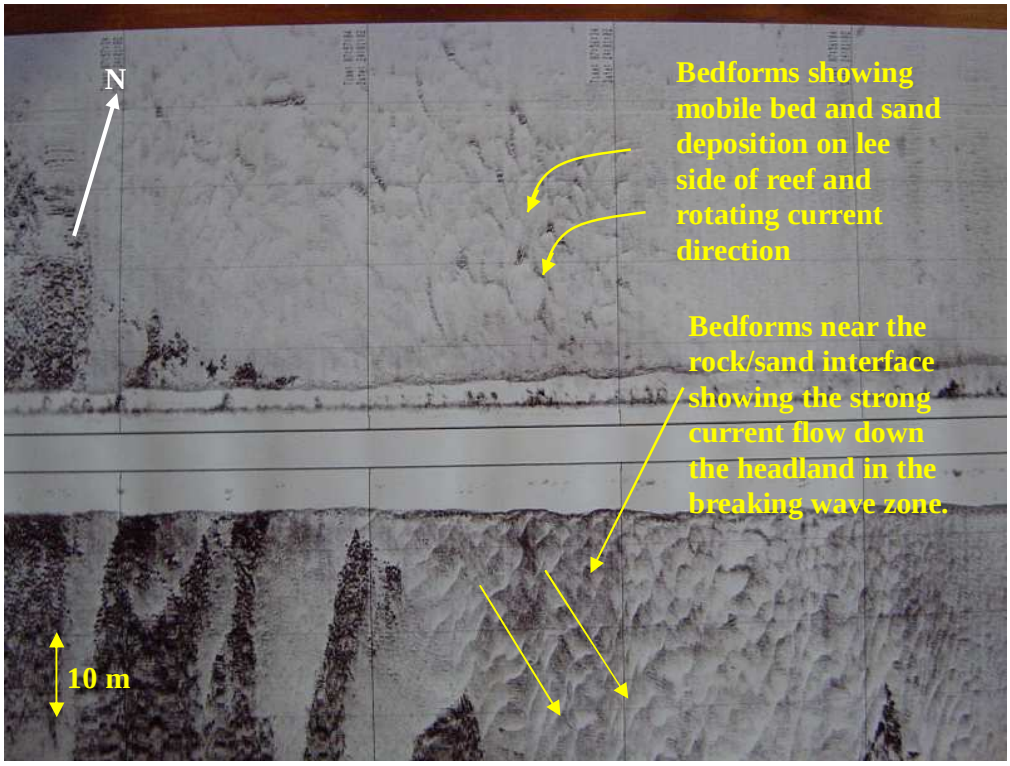

Figure 5.19: Side scan sonagraph image of the seabed at Indicators and Outsides surf breaks showing the disrupted pattern and sand accumulation on the 24-1-02.

5.4 SUMMARY

The results of the successive side scan sonar surveys at the field site has shown that the seabed is very dynamic in nature, with sediment being both accreted and scoured at the headland, and covering and uncovering rock outcrops. However, the sediment facies (i.e. rock/sand boundary and areas of sandy and rocky bed) have remained relatively stable in position. A long-term variation in the amount of sand in the sedimentary regime at the headland was found, with more rocks and reef area exposed offshore in later surveys from the 27-4-01 than was previously found. This result corresponds well to the results of the bathymetric surveys conducted at the headland (Chapter 4). The stability shows dynamic equilibrium in the nearshore sedimentary budget, which was also found by McComb (2001) at New Plymouth 120 km south of Raglan in a similar seabed environment. McComb showed that the time-averaged volumes of sediment entering the littoral cell were found to be equivalent to those leaving it. Carter and Lewis (1995) identified a similar result in the energetic coastal environment near Wellington where sandy areas were positionally stable over tens of years, but variation was found in the volume and depth of sand cover.

Wave data (Chapter 6) shows that seabed features correspond to swell conditions found at the field site with large bedforms generated by the strong wave driven unidirectional currents common near the rock/sand interface, where the waves are shoaling and peeling along the reef. The large bedforms have continuous crests and are sinusoidal in nature (transverse sinuous in phase) and were verified by ground truth observations by divers to be of wavelengths up to 3.5 m (crest to crest) and heights of 0.5 m. The large bedforms are asymmetrical in shape and using the Boothroyd (1978) classification system are generated by the strong easterly flowing unidirectional currents, and are similar to those identified by Lewis (1979) in the South Taranaki Bight, on the west coast of New Zealand. Further offshore at Indicators smaller asymmetrical bedforms were identified suggesting a current flow and associated sediment transport in an offshore westerly direction, whilst offshore at Whale Bay the bedform orientation correlates well to the rotating of a

westerly flowing current identified in the modelling (Chapter 8), where sand is deposited and accumulates to be available for wave-driven transport in an easterly direction during large swell.

The rock/sand boundary generally followed the shape of the headland but showed variation in its position over time, whilst reefs protruding offshore from the Raglan headland varied more significantly in their sand coverage. Similar characteristics were found by Carter and Lewis (1995) where general outlines were maintained, but the patch margins were less stable and were frequently modified by scour or accretion. The side scan sonagraphs suggest that the shore-normal reefs provide a topographical barrier, which can influence the sediment transport by presenting an obstacle for sediments in transit, with the side scan surveys showing areas of sediment accretion or erosion around the reefs. Sedimentation can occur on the up-drift side as the waves and currents transport sediment into this region, and to a lesser extent on the downstream side suggesting some transport of sediment in a westerly direction. This feature was also found by Scarfe *et al.* (2002) at Manu Bay, Raglan where scouring and infilling around the reefs was evident, with certain reef features acting as groins to trap sand.

The surveys suggest that sand was transported both over the rocky beds of the inshore region, through gaps in the offshore protruding reefs and over the raised features with sediment in suspension. Significant sand cover was found on the rocks when the boundary was furthest seaward and could demonstrate accretion of sediment on the reef in proportion to where the boundary is located (i.e. lower bed level and potential shoreward movement of the boundary with recovering of the exposed rocks). This was identified in Chapter 6 where soon after a large swell event sediment recovered the freshly exposed rocks.

This variation in the rock/sand boundary appears to be influenced by the seasonal sediment supply (identified by the bathymetric surveys, Chapter 4), sedimentary equilibrium, as well as recent wave events, and it changes in position very rapidly in response to the prevailing conditions. The rock/sand boundary was found to

have moved 30 m seaward in the April 2001 survey from its position in the 2000 survey, which may have been largely due to a recent large swell (6 m) event, with fresh rock exposed. The rocks soon began to cover with the subsequent smaller swell (observed by the author diving using scuba), but all the surveys from this point showed the offshore reefs to be more exposed than previously found. A zone of approximately 10 m was identified where no seaweed inhabited the rocks (Chapter 3), and demonstrates a region where sand accretes or erodes more frequently. A maximum variation was found in the position of the rock/sand boundary of 50 m from the high bed levels in 2000 to the furthest seaward point in 2001. This is comparable to the 50 m adjustment found by McComb (2001) on the New Plymouth coast, with an associated bed level decrease of 0.3 m. A value of 0.1 m was typical in this study, whilst bathymetric surveys (Chapter 4) also found 0.1 m offshore from the Raglan headland, but up to 0.5 m variation in mean bed levels inshore in the surfzone. An upper level in the boundary was identified (Chapter 3) where adult marine organisms were found inhabiting the reef fringe, and suggests long-term stability of the interface with possible intermittent covering and uncovering of the rocks.

The exposed rock was therefore unable to recover in sand due to either the inability of sand to settle on the reef through the increased turbulence over the rocks, which was also found by McComb (2001), or a possible change in the sedimentary equilibrium. Low seabed levels were observed by the author in the months before the side scan at beaches in the region, and a decrease in the amount of sand in the sedimentary system at the headland may have existed. Bathymetric surveys at this time showed a lower bed level (Chapter 4), corresponding well to the side scan sonagraphs.

CHAPTER SIX

WAVE AND CURRENT MEASUREMENTS

6.1 INTRODUCTION

A large multi-faceted field experiment was previously undertaken at Raglan in 1996. This research on the surfing headland, has led to a greater understanding of the bathymetry, wave refraction, breakpoint location and surfing characteristics in this environment (Hutt, 1997; Mead, 2000; Sayce, 1997; Sayce *et al.*, 1999). However limited analysis was undertaken on the hydrodynamics of the headland. This chapter focuses on the measurement of waves and currents at the headland, providing data that can be related to the physical changes to the seabed identified in the previous chapters.

6.2 METHODOLOGY

Field experiments at Indicators were conducted to measure waves and currents at sites along a 150 m cross-shore transect (Fig. 6.1). Bottom-mounted frames supporting a wave-recording current meter and sediment traps were deployed from a boat at each site (Fig. 6.2).

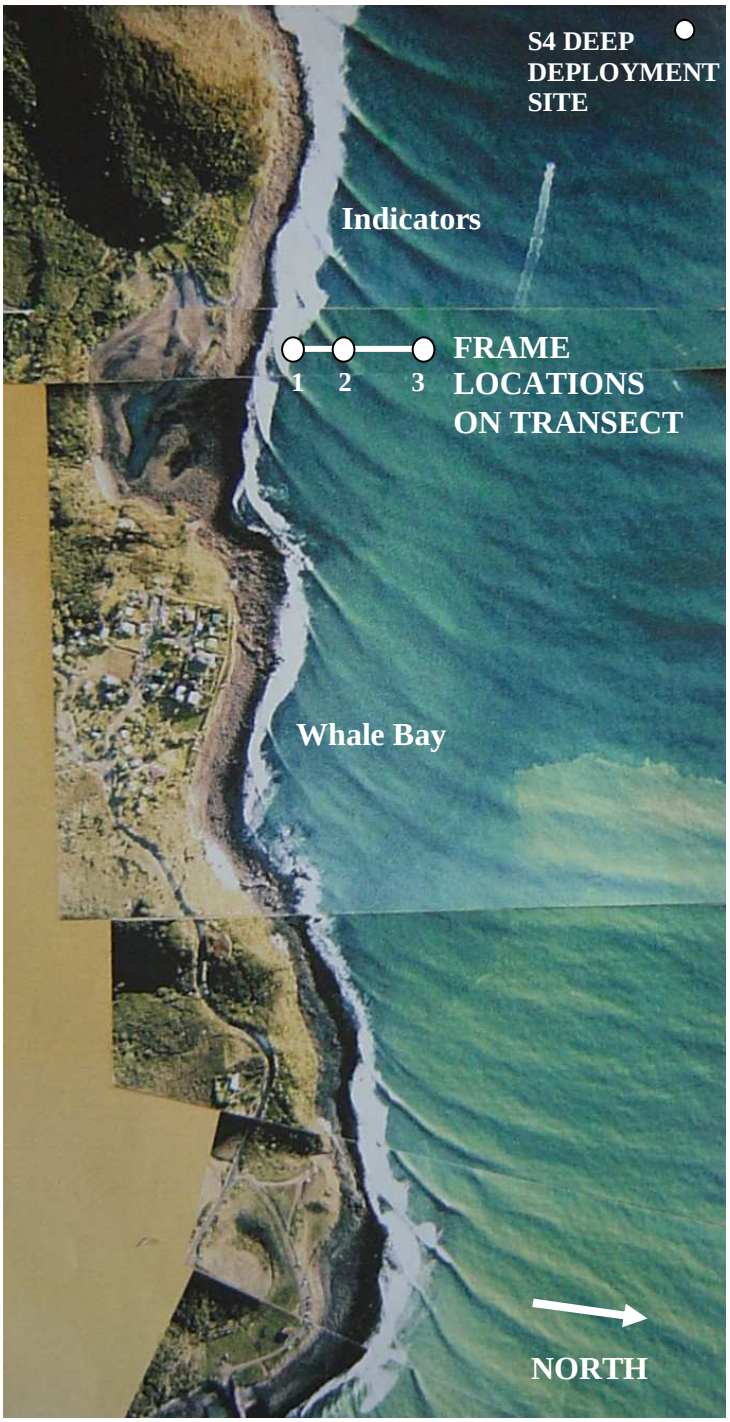

Figure 6.1: Aerial photograph showing the headland, wave refraction, plume and the position of the transect (Site 1, 2 and 3)(Not to Scale)(Source: Hutt, 1997).

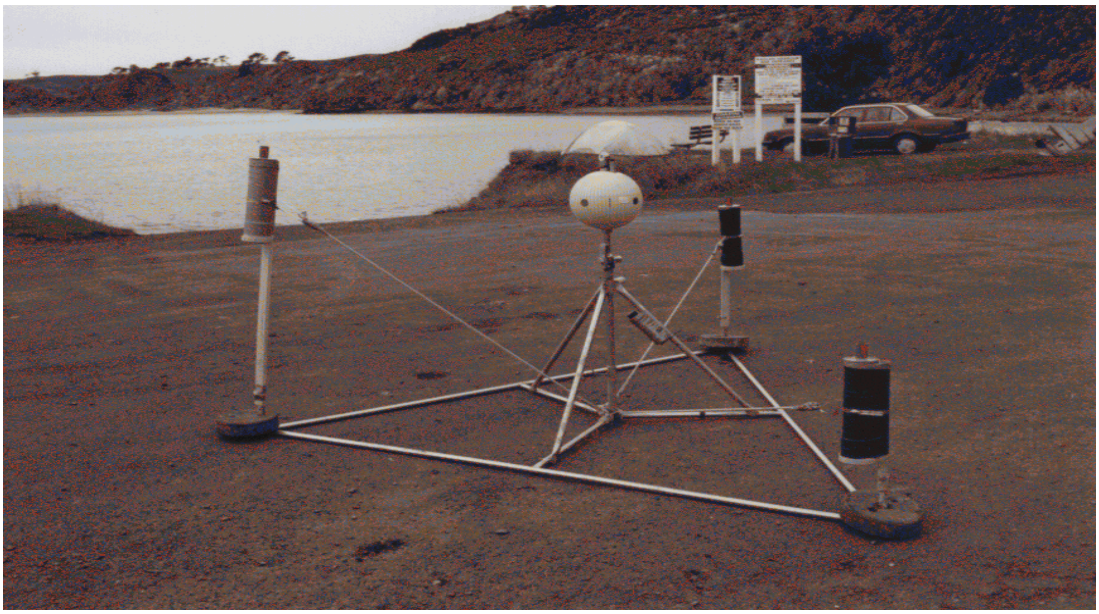

Figure 6.2: Frame with S4 current meter and sediment traps attached (Source: Author, 11-06-98).

Data were logged at 2 Hz by the S4 current meters in bursts ranging from 9 minutes to 18 minutes every hour. The burst data were analysed in the MATLAB® programme T-SERIES[1] to extract significant wave heights and direction, current speed and direction, and bed orbital velocities. T-SERIES is a set of routines for reading and plotting time series data, including spectral and zero down-crossing analysis on time series data, such as that recorded by the S4. The recorded mean currents were resolved through the transect with positive being defined as directed "east along the headland". Positive along the transect was offshore. Pressure data and velocities (U and V) were both utilised for calculation of wave statistics depending on the logging capability of each S4 current meter. Wave data was vertically attenuated in T-SERIES analysis and H_{sig} was computed from spectra as this form of analysis better describes the energy distribution of sea and swell waves (Komar, 1998).

The InterOcean S4 current meter combines an electromagnetic meter for measuring current velocity and a pressure sensor for measuring depth at 2 Hz. The device is

[1] Tseries – R. Gorman, National Instititute of Water and Atmospheric Research

fully self-contained, with its own power supply. Software for communication and down-loading is provided by the manufacturer, InterOcean Systems Inc (APPIBM). The S4 was mounted on a high-grade stainless steel frame that was held on the seabed with heavy weights. Position of each frame was recorded using GPS (Global Positioning System) surveying equipment.

Horizontal current measurement is made by means of two pairs of symmetrically placed titanium electrodes located on the equator of the S4 shell which sense the potential gradient generated by water flowing through the electromagnetic field set up by the current meter. The speed at which water flows through this field is proportional to the voltage created. Direction of the water flow is determined relative to magnetic north by means of an internal flux-gate compass.

6.3 FIELD PROGRAMME

6.3.1 *Field experiment 1: 11 February 1998*

This experiment was undertaken at the Indicators headland, along a cross-section just above the lagoon. At the time only one S4 current meter was available for use in the field, which meant that this piece of equipment on a frame had to be used multiple times throughout the day, in different site locations. A base-station was set up at the Manu Bay benchmark, to provide differential GPS positions for the frame locations. The swell was 2 m with similar sized waves breaking along the headland (Fig. 6.3). The S4 current meters were programmed to log continuously at 2 Hz over the deployment period.

Figure 6.3: Waves breaking during the experiment along the headland (Source: Author 11-02-98).

The first deployment was designated Site 1, and was located approximately 15-20 m from the rock/sand boundary. The boundary was located by a person diving to the seafloor confirming the approximate position of the change in the seabed (595242.90 N, 302842.93 E). This position was approximately 80 m from the shoreline at high tide with a water depth of 6.5 m. Waves were breaking close to the frame location at this time, but the boat was able to get into the site during gaps in the wave sets to deploy the equipment.

The frame was deployed from the boat to the seafloor and orientated into the incoming swell direction, and weights were attached to the frame to anchor it in position (Fig. 6.4). The stability was checked during passing waves and then the caps were removed from the traps at 1200 hrs. The frame was deployed in this location for 1.5 hours, at which time the traps were capped (1330 hours). Sediment traps are discussed in more detail in Chapter 7.

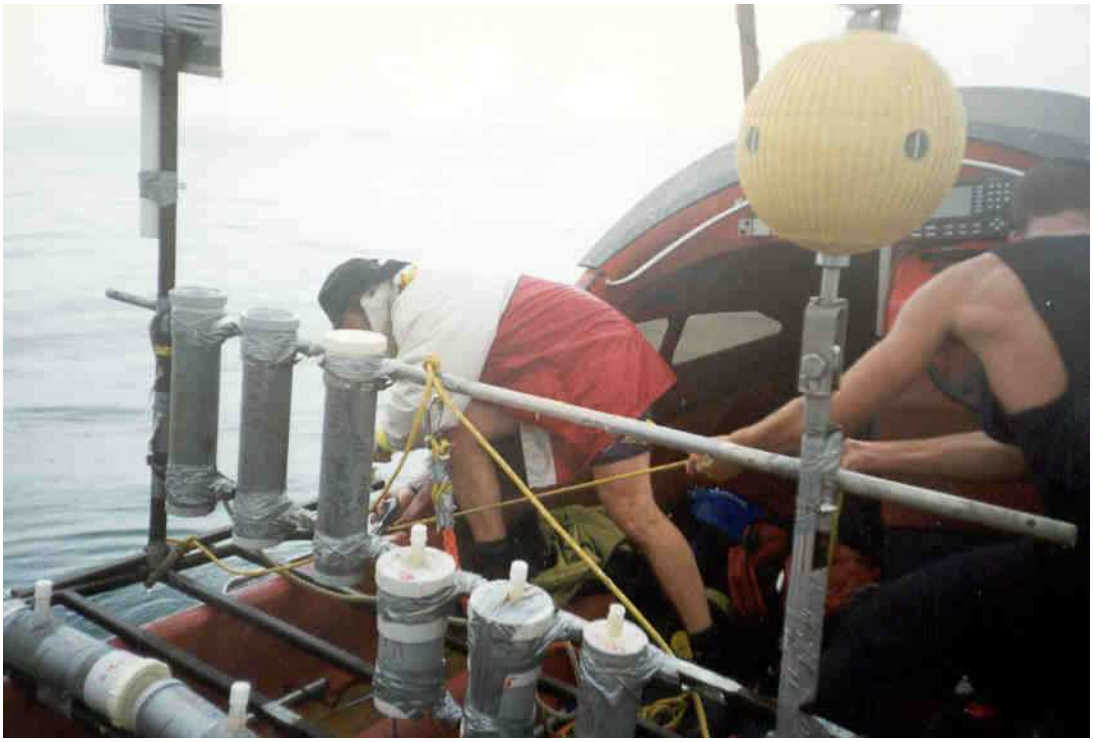

Figure 6.4: Frame, sediment traps and current meter on the back of the boat being made ready for deployment (Source: 11-02-98).

The frame was then dragged 25 m to the next site, by a rope attached to the boat, with a diver ensuring it did not get stuck on rock outcrops as it moved across the seabed. Traps for Site 2 were uncapped at 1340 hours and capped at 1500 hours. The frame was then dragged a further 50 m to the Site 3 location, traps uncapped at 1505 hours and capped at 1635 hours.

Deployment positions:

- Site 1: 595242.52 N, 302882.84 E
- Site 2: 595288.02 N, 302880.66 E
- Site 3: 595325.56 N, 302910.75 E

It was decided that this experiment would form a test procedure in this surf zone environment for the frame deployment at the headland, and although comparison can be made to the data it has not been presented or used for analysis, but rather as a check for the viability of the methodology. As the experiment was successful a larger deployment was planned that would include multiple frames and S4's, for a period of approximately 2 weeks incorporating a large swell.

6.3.2 *Field experiment 2: 12 - 24 June 1998*

This experiment was undertaken again at the Indicators headland, along the same cross-section just above the lagoon as previously used in the first experiment. The weather maps indicated a large swell approaching from the south-west with a period of small swell proceeding this event. This was therefore seen as an ideal time to deploy instruments at the headland as it would be impossible when large waves would be breaking at the headland. Three frames were set up on shore with sediment traps set at elevations of 0.6 m, 0.9 m and 1.3 m above the bed, and weights attached (Fig. 6.2). The poles were securely fastened to ensure as least possible sway in the surf conditions. The water visibility was very poor with a 0.5 m swell generating small waves at the surf break of Indicators.

The location of the rock/sand boundary was checked from the previous experiment by a diver. It was found to be in the same position, and it was decided to deploy the first frame 3 m from this boundary on the sand bed. The lowest and highest traps were orientated perpendicular to the swell direction, and it was ensured that the frame was stable in the waves before the traps were uncapped at 1141 hours. It was high tide at this time and the water depth was 6.5 m. The ADW current meter (which measured pressure in addition to velocity) was used at this site. The visibility was 0.2 m and the seabed had 0.5 m height bedforms, with crests orientated approximately perpendicular out from the headland.

Site 2 was in 7.0 m of water approximately 40 m from Site 1, with the bed showing the same characteristics as at Site 1. The DW current meter (measured velocity only) was deployed at this site at 1221 hours. A DW current meter was also deployed at Site 3 at 1307 hours, 100 m from Site 2 along the transect. The water depth was 10.0 m and the bed was firmer packed with small wavy and uneven angled bedforms apparent. Data were logged by the S4 current meters at 2 Hz in bursts of 18 min every hour at Site 1, 9 min every 2 hours at Site 2, and 9 min every 4 hours at Site 3.

Deployment positions:

- Site 1: 595250.60 N, 302859.63 E
- Site 2: 595278.39 N, 302854.80 E
- Site 3: 595374.00 N, 302823.00 E

The frames were retrieved after 12 days when the swell had become small enough to enable the boat into the surf zone after a period of very large swell (Fig. 6.5). However, 2 of the 9 traps and two frames could not be retrieved in the mild swell conditions (although the traps could be capped) and so a subsequent trip was made in more favourable swell conditions to recover the missing traps. The frames had been significantly buried in sand and so they had to be left in place. The traps had collected a substantial quantity of fine-grained silt/mud particles due to land run-off through the nearby entrance to Raglan Harbour, and so the sediment was passed through a 45 micron sieve so that the mud was not included in the total mass.

Figure 6.5: Large surf conditions during the experimental period and the transect location (Source: Author 20-6-98).

6.3.3 *Field experiment 3: 20 April to 4 May 2001*

The transect from the first two experiments was again the location for the deployments for this experiment. A long period ground swell was predicted to continue breaking at the headland providing data for medium swell conditions (Fig. 6.6). A total of four instruments were available with three sediment traps to also be placed on the rocks of the shoreline at low tide, to gather further sediment data (Fig. 6.7). It was hoped to use the same positions for the frames as the last experiment but when the rock/sand boundary was checked by divers it was found to have moved further seaward. A very large swell (approx. 6 m) had produced massive waves the previous weekend and had taken away significant quantities of sand from the headland. Fresh rock was very visible with no marine life found, identifying rock that had previously been covered with sand (Fig. 6.8).

The first deployment site was therefore moved 30 m further seaward to where the frame could be deployed on sand that was inter-dispersed amongst rocks. The frames were set up on shore with sediment traps set at 0.6 m, 0.9 m and 1.3 m, the same as the previous experiment. Anchors on chains were attached from the corners of the frame and used to hold the frame in position. The swell was 1-1.5 m with larger sized waves (2 m) breaking on the sets. The presence of these size waves meant the gear had to put in very quickly so the boat could move out of the surf zone before the next set. The instruments were deployed in 5.3 m of water at 1040 hours, with a water visibility of 0.5 m.

Figure 6.6: Surf conditions during the deployment period (Source: Author 21-4-01).

Figure 6.7: Sediment trap sitting amongst the rocks on the shoreline at low tide (Source: Author: 20-4-01).

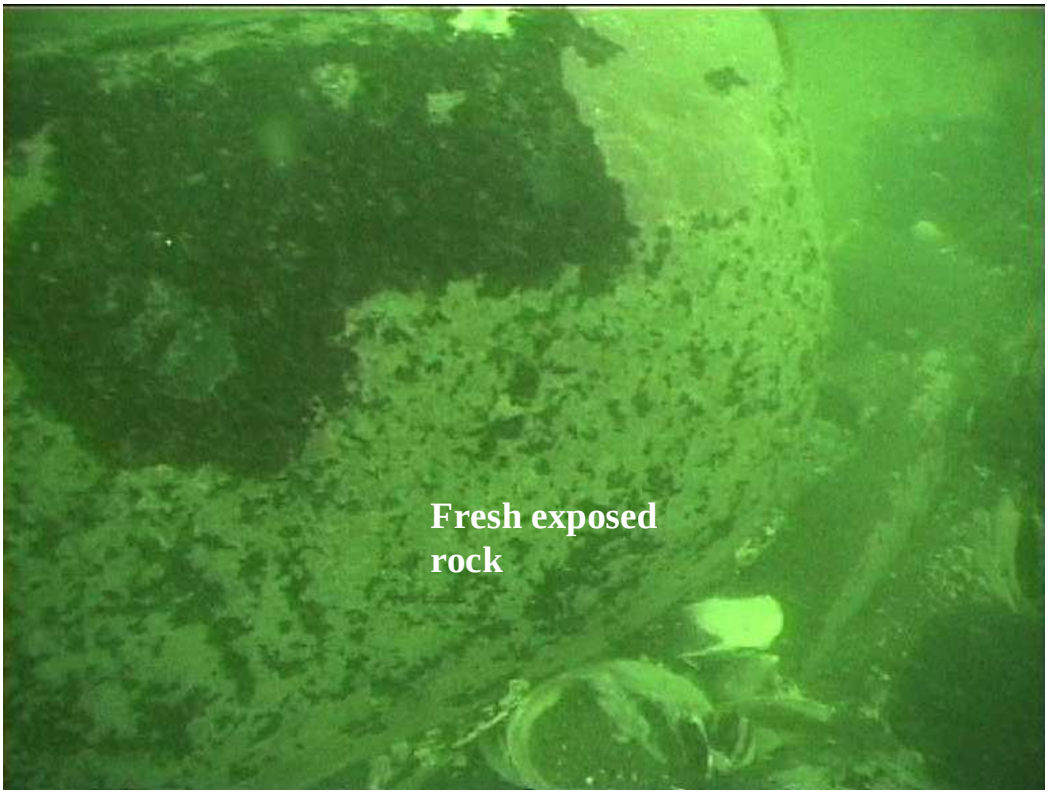

Figure 6.8: Fresh rock exposed after a very large swell (Source: Author 20-4-01).

The second frame was deployed a further 45 m seaward in 5.6 m of water at 1125 hours. Inter-dispersed sand and rocks were also found in this location. The third site was 35 m further along the transect, and the instruments were deployed at 1145 in 6.5 m of water. This location was characterised by sand on the bed, and >2 m wavelength megaripples crest to crest with a height of >0.3 m. The final deployment was a further 35 m along and also on sand, but with smaller bedforms. The water depth was 6.5 m and the deployment time was 1220 hours.

Frame deployment positions:

- Site 4: 595281.55 N, 302877.21 E
- Site 5: 595309.03N, 302913.76 E
- Site 6: 595343.04N, 302923.65 E
- Site 7: 595371.26 N, 302946.70 E

The sediment traps were deployed on the rock shoreline on the 21-4-01 at 1530 hours, in three locations using the same alignment as the underwater transect. The cylindrical plastic traps were orientated long-ways and attached to heavy weights, before being wedged in between rocks on the shoreline. They were placed from the low tide mark to below the high tide level.

Sediment traps on rocks deployment positions:

- Rocks 1: 595124.79 N, 302831.77 E
- Rocks 2: 595134.04 N, 302828.85 E
- Rocks 3: 595150.68 N, 302837.65 E

The traps on the rocks were monitored during the duration of the experiment to check both that they were still in place and not damaged, and that were not full of sediment. The traps were changed at low tide on the 24-4-01, the samples placed in plastic bags and the traps returned to their sampling position.

The frames deployed in the sea were checked on the 26-4-01 using scuba. The frame had buried slightly and big megaripples could be seen in the surrounding region. The traps at Site 1 were capped at 1100 hours, and all replaced with new traps which were uncapped at the same time. Site 2 traps were capped at 1130 hours and replaced. The frame was also slightly buried and 100 mm ridges were identified that were possibly sitting on large megaripples. The traps at Site 3 were capped at 1200 hours and 100 mm ridges were again evident on possibly large megaripples. The large bedforms may have been remnant from the previous large swell. At Site 4 the traps were replaced at 1230 hours and the bed level was still the same under the frame, with no megaripples identified, but small ridges (< 100 mm) were found at the site. Seabed samples were also collected at all the sites near the frames. At Indicators the sand had accreted back onto areas where fresh rock had been sighted a week ago (specifically the previous Site 1 close to the headland). The ripples in this area appeared to be orientated north/south with 100 mm between slight ridges.

The trap on the rocks at Site 1 required repairs to its nozzle on the 28-4-01. The swell had been flat for a few days but was expected to rise. A small swell broke at the headland till the 4-5-01 when it was decided to retrieve the instruments. The traps were capped at Site 1 at 0900 hours, Site 2 at 0945 hours, Site 3 at 1010 hours and at Site 4 at 1040 hours. The old frame from experiment 3 (Site 2) was visible and photos taken (250 mm of the top triangle), with mussels (*Perna canaliculus*) inhabiting the structure (Chapter 3).

6.4 S4 DEEP WATER (>10 m) DEPLOYMENTS

6.4.1 *Introduction*

The long-term deployment of an S4ADW current meter in deep water depth (>10 m) was required to provide data that would quantify the typical swell size and direction experienced at Raglan. This data could then be utilised in the numerical modelling process providing data on the characteristics of the incoming swell at the boundary of

the model. This data could then be related to current meter data collected closer to the shoreline, allowing calibration of the models.

6.4.2 *Field programme*

A frame and S4 was deployed on the 31-3-00 in deep water out from the headland at Raglan, in the location (595409 N, 302840 E)(Fig. 6.1) in 10 m of water at low tide. The S4 was dived on using SCUBA on the 14-4-00 and was still in position and had not buried. The S4 was then retrieved on the 6-5-00 in poor visibility, which made finding the frame difficult but was located successfully with the use of a 10 m search rope. The S4 was connected to the computer and the data downloaded, but an error had occurred in the logging and data was unusable. The S4 needed to be sent for servicing and could not re-deployed at the present time.

Further deep-water deployments were made in September to December 2001. The data from 11/10/01 to 26/10/01 was unusable due to an error but the remainder of the data was logged successfully. A further deployment was made on the 29-1-02 and retrieved on the 8-2-02, for use in the side-scan and bathymetry experiments being conducted at this time.

6.5 RESULTS

6.5.1 *Fieldwork experiment 2 (11-06-98)*

Wave heights during the study period were small during the first 5 days (0.5-1.2 m), and then increased to over 3 m during a large swell and remained above 1.5 m for the remainder of the deployment (Fig. 6.9a). Heights were larger in size closer to the shoreline, reducing from Site 1 to Site 2 and Site 3 (Figs. 6.9a, 6.9b and 6.9c). The currents were directed mostly in a cross-offshore direction of approximately 300^{o}, which changed to easterly along the headland (approx. 50^{o}; Fig. 6.10) and increased dramatically to the maximum speed of 0.8 ms^{-1} (Fig. 6.11), as swell size peaked at

3.25 m. Current velocities also decreased further offshore from Site 1 to Site 3, aside from during a period of northwest swell when the velocity increased at Site 3 (Figs. 6.11a and 6.11b). Wave direction was higher inshore averaging 127^{o} due to refraction in the shallower water depth (Figs. 6.12a and 6.12b). During the large >3 m swell the wave direction decreased to 110^{o} as the larger waves swept straighter down the headland, which a trend also identified by Hutt (1997). Peak spectral periods ranged from a minimum of 6 seconds to a maximum of 21 seconds, with an average of 13 seconds over the measurement period (Fig. 6.13). This shows that predominantly long period swell refracts around the Raglan headland to create the breaking waves. It is noted that not all the measured data has been included as graphs in the text but can be found in Appendix 11.

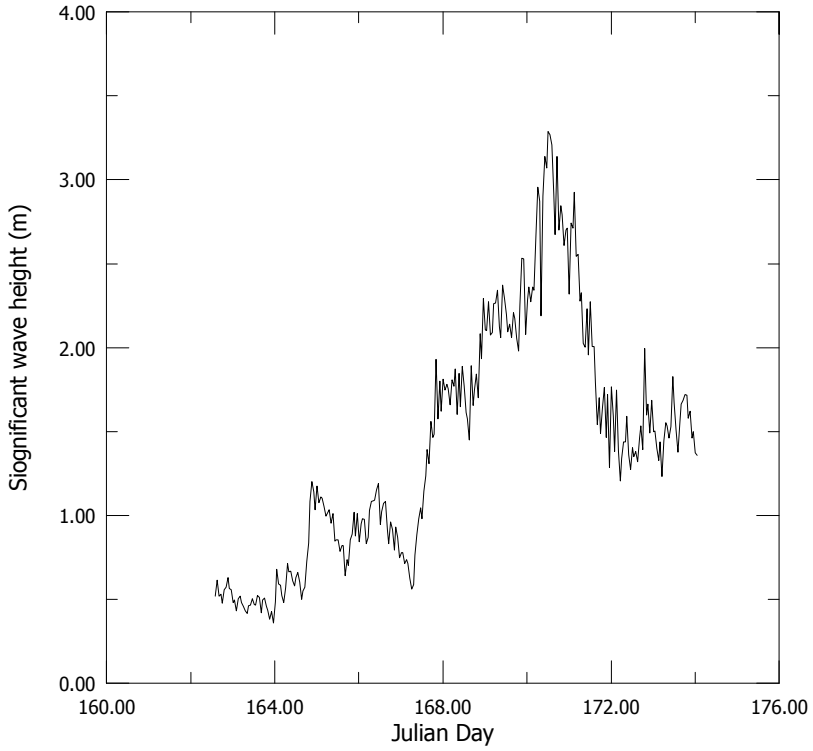

Figure 6.9a: Significant wave heights measured at Site 1 over the June 1998 experiment duration.

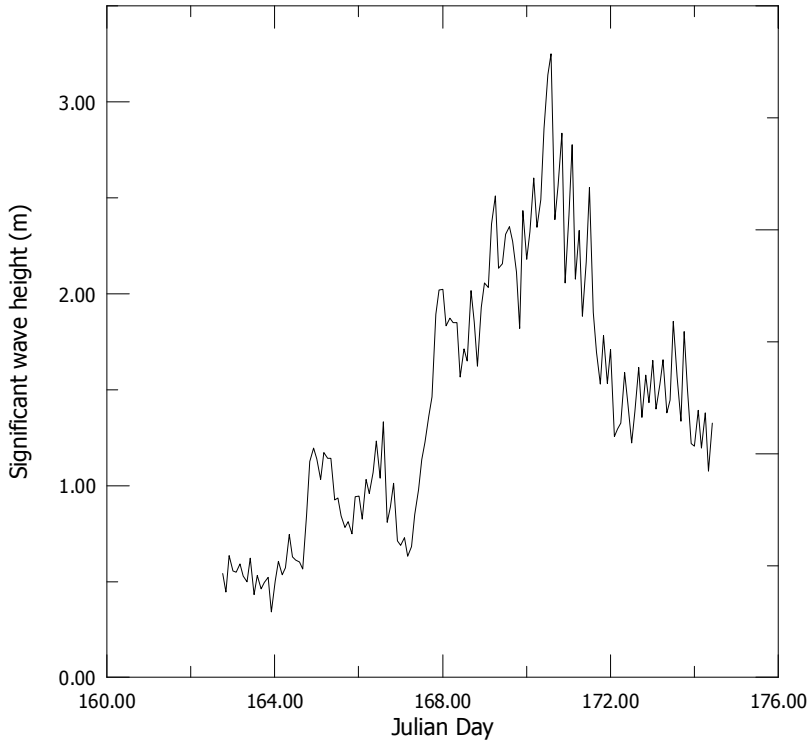

Figure 6.9b: Significant wave heights measured at Site 2 over the June 1998 experiment duration.

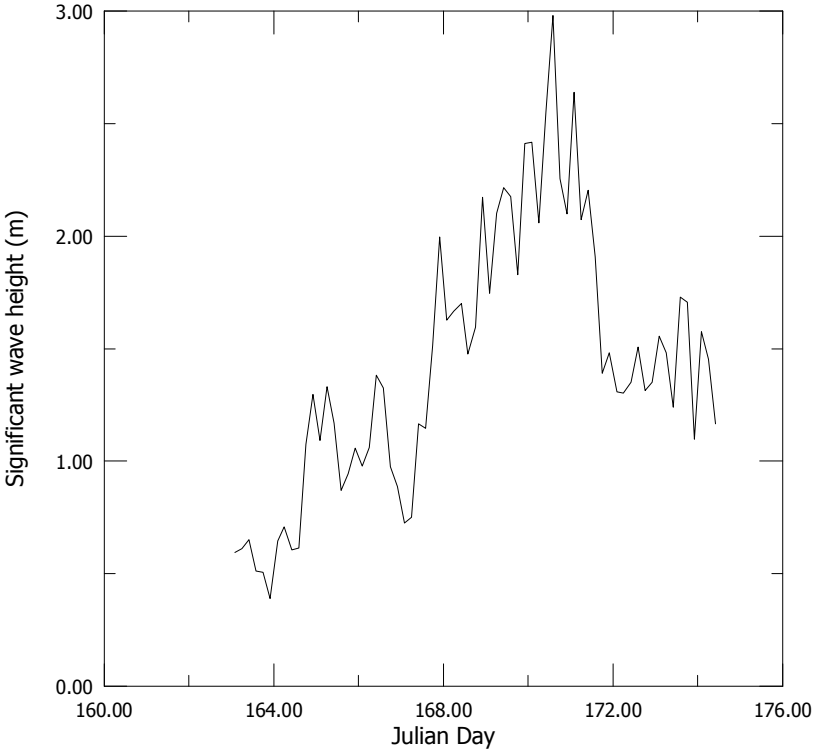

Figure 6.9c: Significant wave heights measured at Site 3 over the June 1998 experiment duration.

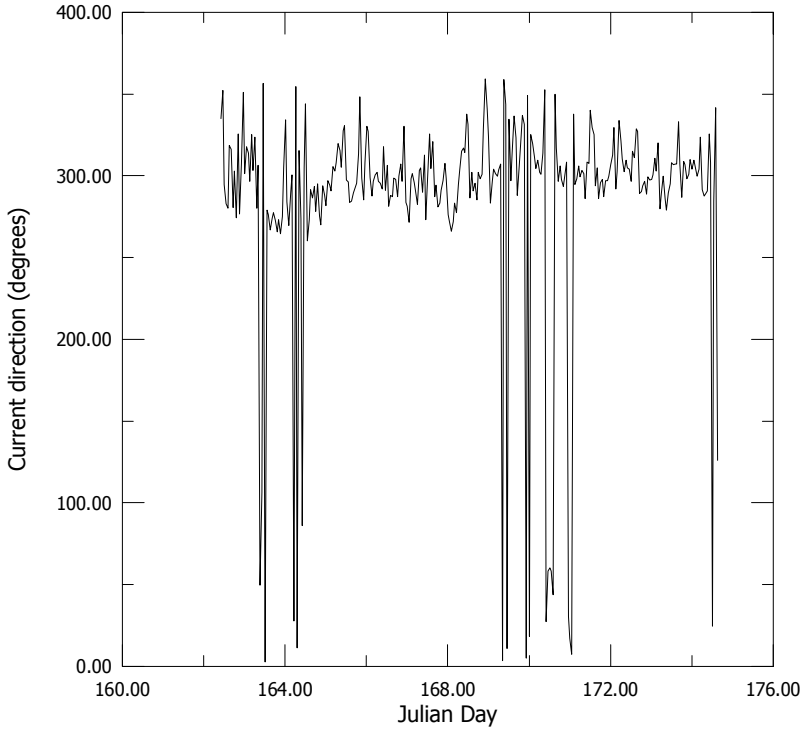

Figure 6.10: Current direction (towards) measured at Site 1 over the June 1998 experiment duration.

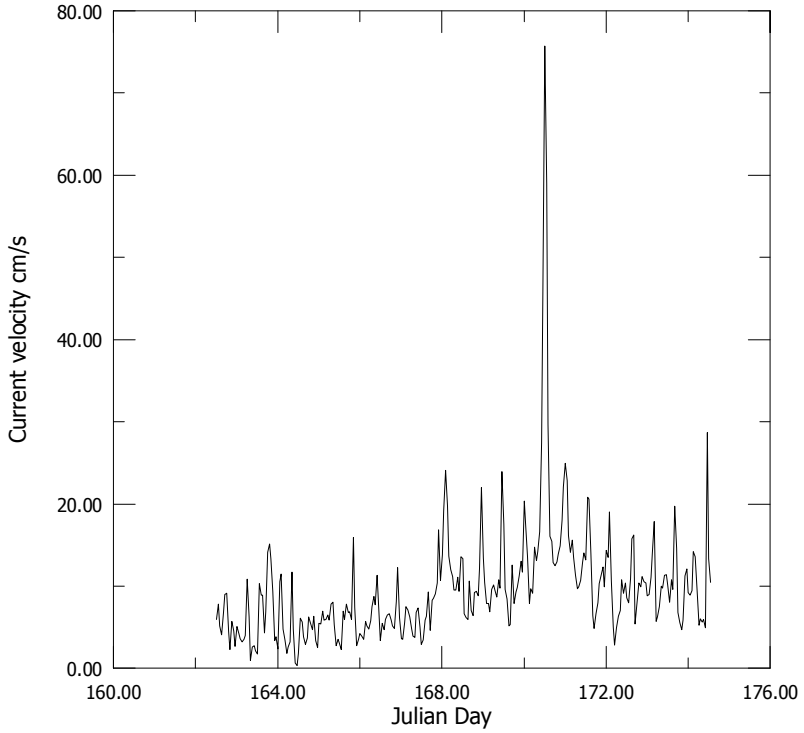

Figure 6.11a: Current velocity measured at Site 1 over the June 1998 experiment duration.

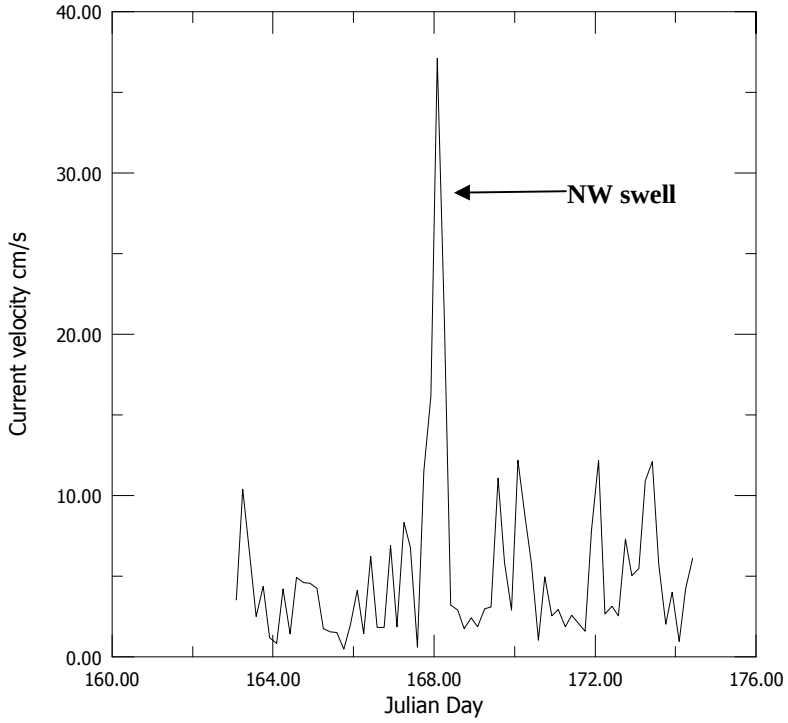

Figure 6.11b: Current velocity measured at Site3 over the June 1998 experiment duration.

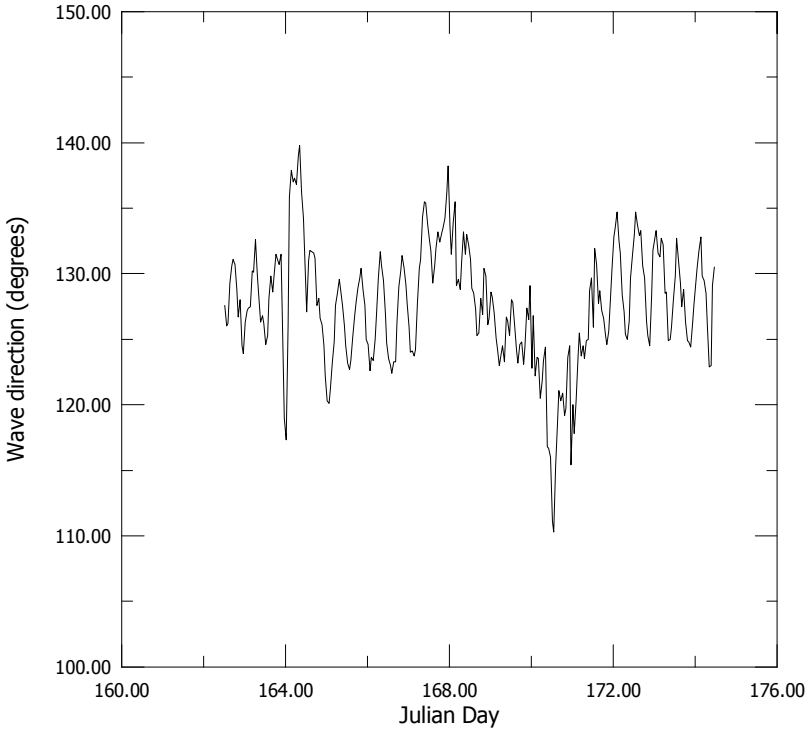

Figure 6.12a: Wave direction (mean)(towards) measured at Site 1 over the June 1998 experiment duration.

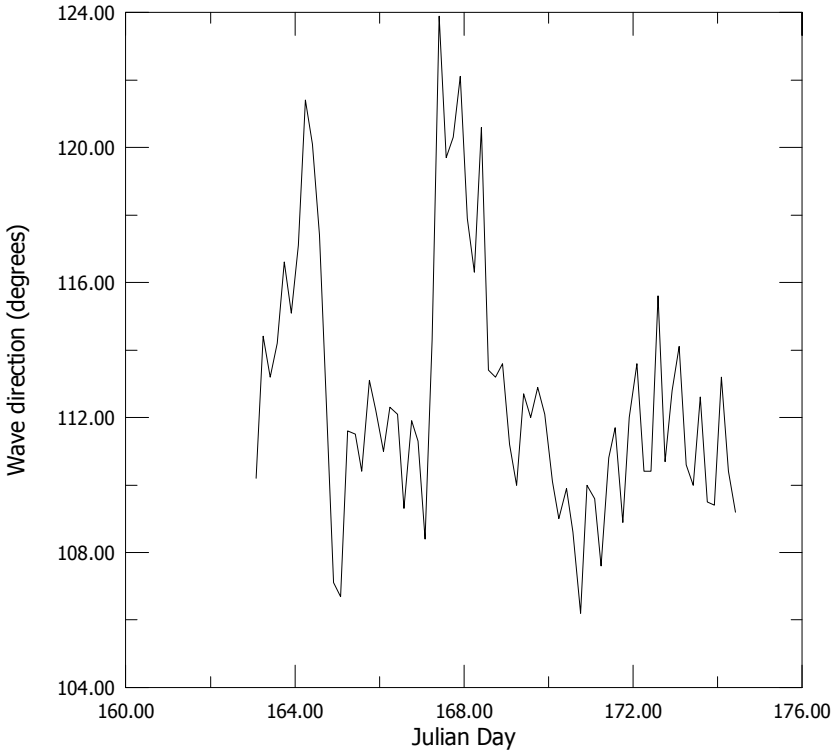

Figure 6.12b: Wave direction (mean)(towards) measured at Site 3 over the June 1998 experiment duration.

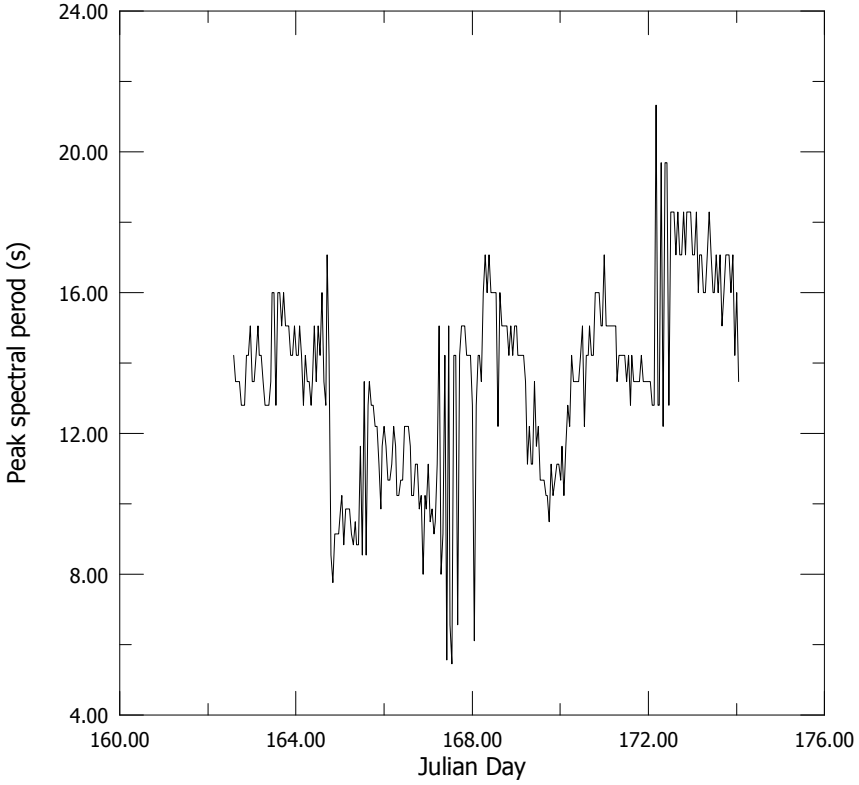

Figure 6.13: Peak spectral wave period measured at Site 1 over the June 1998 experiment.

The mean burst-averaged currents when resolved perpendicular to the transect were mostly negative in the west direction at all sites (Fig. 6.14). A strong negative flow occurred during a northwest swell around day 168. Positive (east along the headland) flows were experienced from days 169 to 172 with a large eastward flow being recorded at the innermost site (Site 1) of around 0.8 $m.s^{-1}$ on day 170 when the largest waves were present (Fig. 6.14). In these large swell conditions, burst-averaged currents at Site 1 were generally directed parallel with the headland. Maximum bed orbital velocities were up to 2.5 $m.s^{-1}$ (Fig. 6.15). A strong tidal oscillation (low to high tide) in the current during this period is also evident.

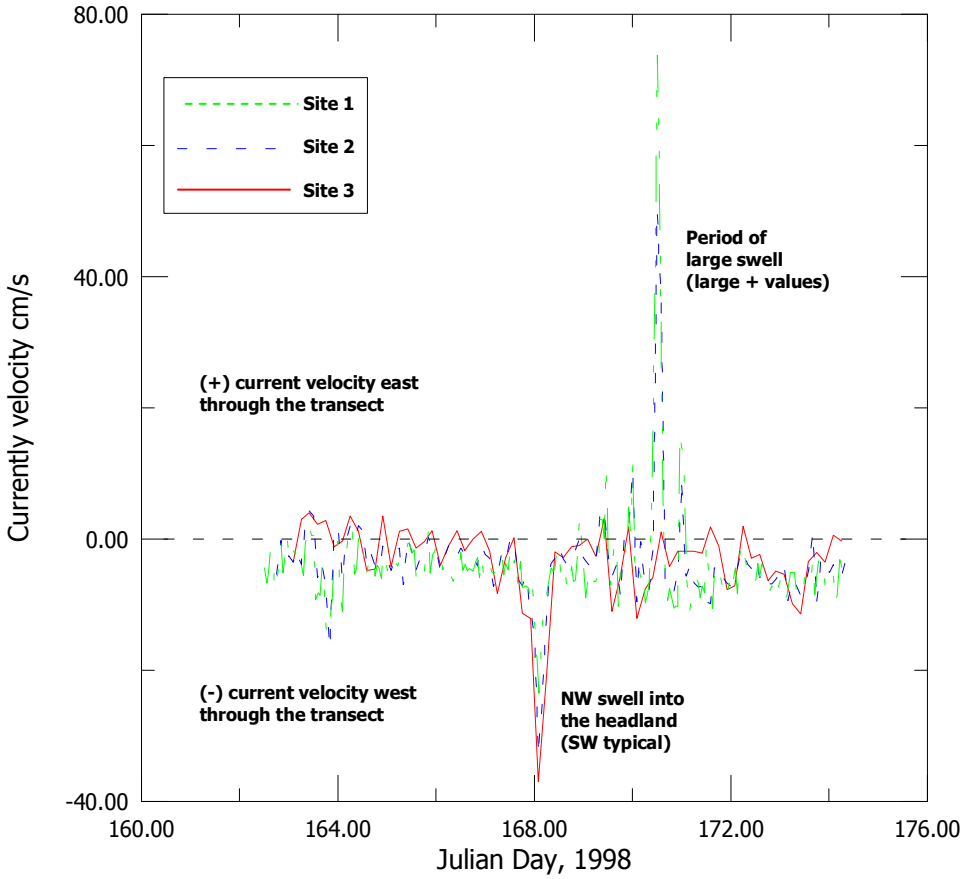

Figure 6.14: Current velocity through the transect, with positive values east along the headland, and negative west along the headland.

Time-averaged currents during the experimental period were cross-offshore at all sites, even though large easterly directed currents were recorded during the >3 m wave event

(Table 6.1). The current component through the transect is negative (directed west along the headland) at all sites. The heading was -30^{o} (relative to the transect angle of 343^{o}) at Site 1, -60^{o} at Site 2 and -78^{o} at Site 3. Thus, the currents were directed more normal to the transect offshore at Site 3.

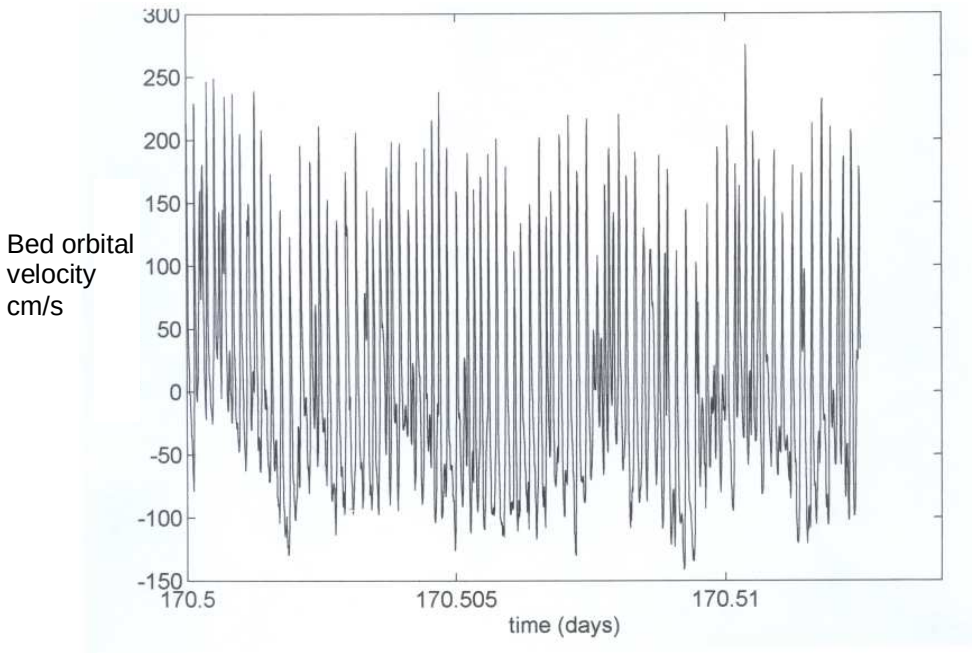

Figure 6.15: Bed orbital velocity measured at Site 1 during June 1998 (burst 195 of raw data when wave heights were at their most significant).

Table 6.1: Time-averaged currents through (U) and along (V) the experimental transect.

Sites	U (av) (through) m s^{-1}	V (av) (along) m s^{-1}	Current dir (av) degrees (relative to 343^{o})
1	-0.038 (WSW)	0.066 (NNW)	-30
2	-0.034 (WSW)	0.020 (NNW)	-60
3	-0.032 (WSW)	0.007 (NNW)	-78

Experience of the author surfing at the break and observations over the experimental period of surfers attempting to paddle against the currents during large waves indicate that flows are strongly east along the headland in the surf zone. The surfers were often swept several hundred metres while attempting to paddle out beyond the breaking wave zone. In comparison surfers sitting on their surfboards outside the breaking wave zone could be seen to drift back in a westerly direction along the headland back to the take-off point (Fig. 6.16). In periods of onshore westerly to southwesterly winds, a choppy sea surface could be seen as the wind flowed against the out-flowing westerly current (Fig. 6.17). Wind blowing against the direction of current flow is well documented and more commonly seen at harbour mouths on strong ebb tides (Goff *et al.*, 2003).

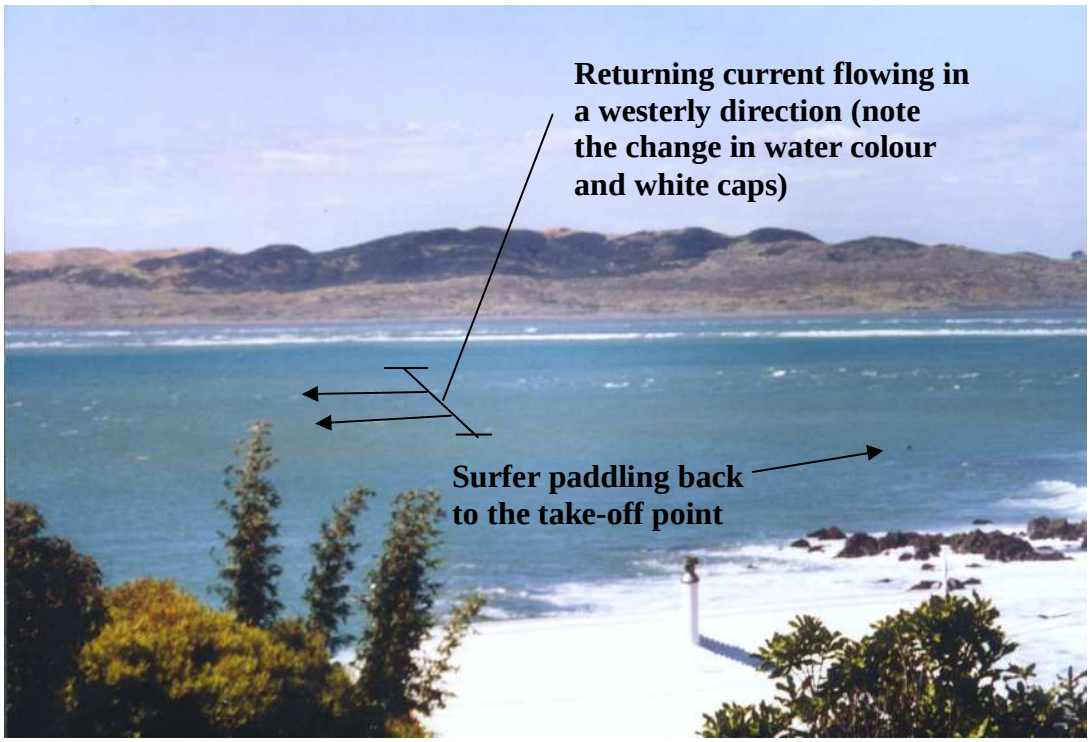

Figure 6.16: Current flowing in a westerly direction at Whale Bay back along the headland in a distinct band characterised by a change in water colour. A surfer is seen paddling back to the take-off point wide of the inshore wave-driven easterly flowing current (Source: Author, 17-6-98).

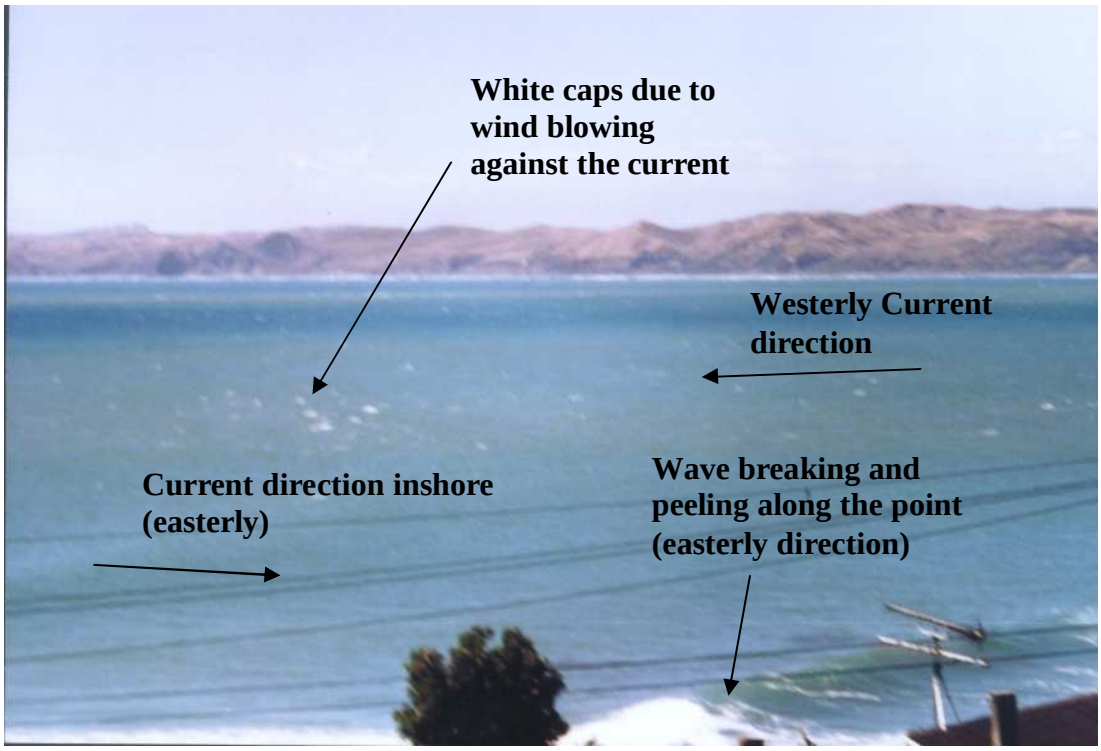

Figure 6.17: Breaking wave at Whale Bay generating an easterly flowing current inshore with white caps visible due to a westerly wind blowing against the current (Source: Author, 17-6-98).

6.5.2 *Fieldwork experiment 3 (20-04-01)*

Two distinct swells were recorded during the deployment period, with the 2.0 m peak decreasing over 5 days to a low of 0.4 m for 2 days, before the second swell arrived and peaked at 1.4 m and then decreased slowly to 0.7 m over 4 days (Fig. 6.18). Interestingly the strongest mean burst-averaged currents were recorded during the 1.4 m swell, attaining 0.14 ms^{-1} at site 1, whilst a maximum current velocity of 0.08 ms^{-1} was measured during the 2 m swell (Fig. 6.19). This is most likely due to the variation in swell direction during the experimental period, where the larger swell was from a southwest direction, whilst the 1.4 m swell was from a northwest direction which causes waves to break with less refraction into the headland (Fig. 6.20), providing faster peeling waves and stronger associated currents. The peak spectral period ranged from a minimum of 8.5 seconds to 20 seconds, averaging 14

seconds and shows a similar trend to Experiment 1 where long period swell was found at the field site (Fig. 6.21). Current directions were also similar to Experiment 1 being cross-offshore in a westerly direction averaging 280^{o}, with easterly flows during larger swell or north-west swell breaking straighter into the headland (Fig. 6.22). Wave heights and current velocity were found to decrease from inshore to the sites further offshore, as also seen in Experiment 1. All measured data has not been plotted due to the similar trends that have been identified. However the data can be found in Appendix 11.

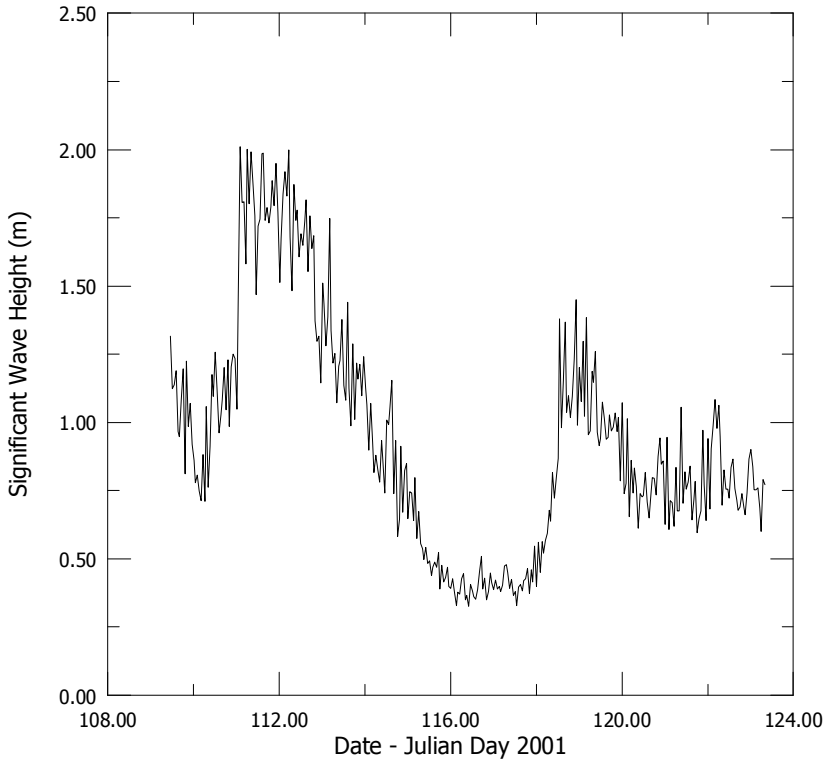

Figure 6.18: Wave heights measured at Site 1 over the September 2001 experiment duration.

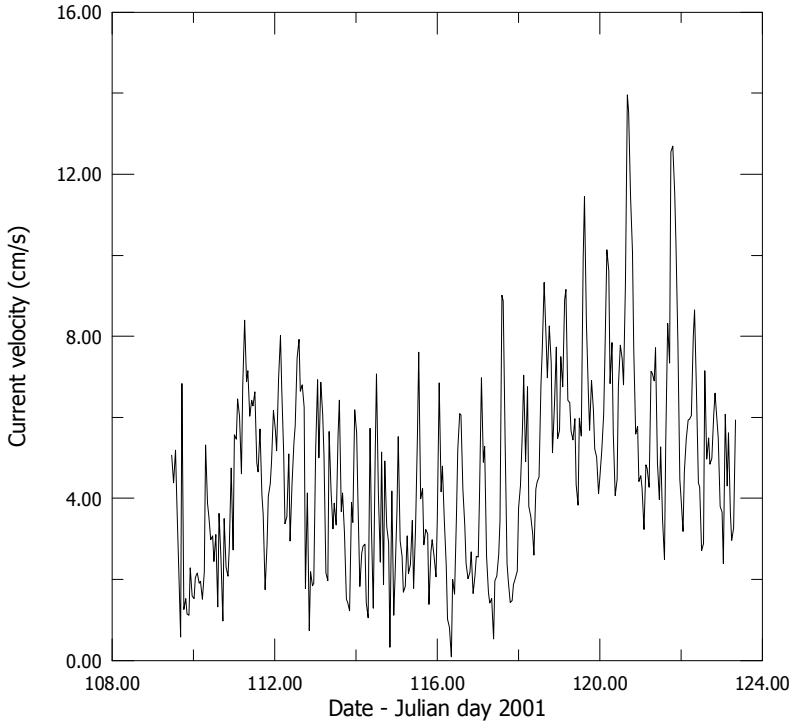

Figure 6.19: Current velocity measured at Site 1 over the September 2001 experiment duration.

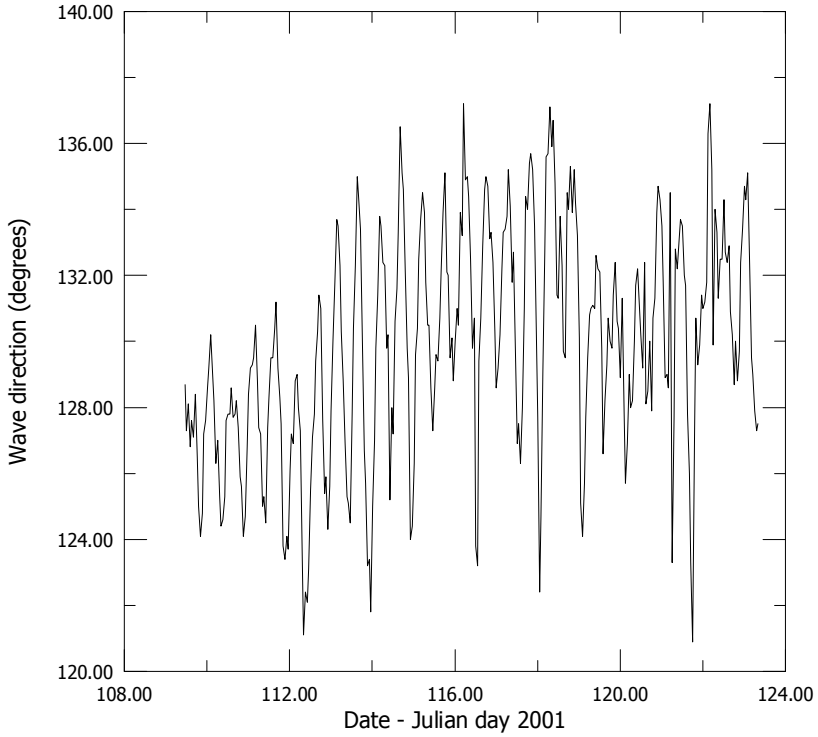

Figure 6.20: Wave directions (towards) measured at Site 1 over the September 2001 experiment duration.

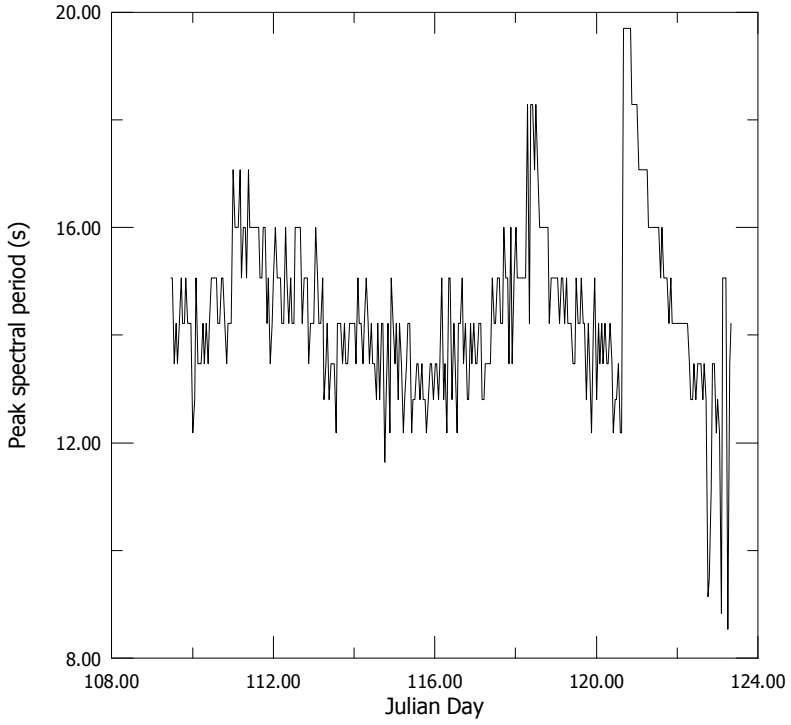

Figure 6.21: Peak spectral period measured at Site 1 over the September 2001 experiment duration.

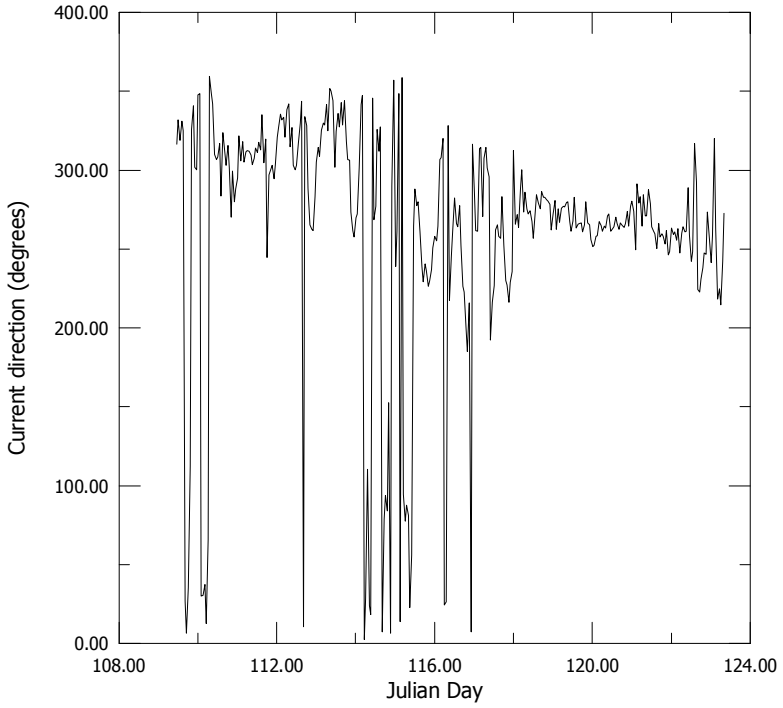

Figure 6.22: Current direction (towards) measured at Site 1 over the September 2001 experiment duration.

Although the swell did not reach the same large size as that found in Experiment 1, similar trends can be seen in the analysis of data from this further experiment. A strong tidal oscillation is again apparent in the data, with wave size and direction, current speed and direction, all varying between low and high tide levels. At Indicators high tide causes less refraction of the waves and the waves tend to be smaller in size, which was also found by Hutt (1997). The mean burst-averaged currents when resolved perpendicular to the transect were again mostly negative and directed westerly along the headland at all the measuring sites (Table 6.2), ranging from -0.027 ms^{-1} at Site 1, -0.025 ms^{-1} at Site 2 and -0.020 ms^{-1} at Site 3. The current directions through the transect are negative (directed westerly along the headland) at all sites. The heading was -55^{o} (relative to the transect at 343^{o}) at Site 1 increasing to -63^{o} at Site 3 (Table 6.2). Both the current velocities and directions showed a similar trend to those found in Experiment 1.

Table 6.2: Time-averaged currents through (U) and along (V) the experimental transect (20-4-01). The mean current direction is given (towards).

Sites	U (av) (through:) m s^{-1}	V (av) (along) m s^{-1}	Current dir (av) Degrees (Relative to 343^{o})
1	-0.027 (WSW)	0.019 (NNW)	-55
2	-0.025 (WSW)	0.018 (NNW)	-54
3	-0.020 (WSW)	0.010 (NNW)	-63

6.5.3 *S4 deep water (>10 m) deployments*

Wave heights measured over the survey period showed a range of conditions varying from 0.2 m to 4.8 m from the 31-8-01 to 19-11-01 (Fig. 6.23a) and 0.45 m to 3.5 m from 29-01-01 to 8-02-02 (Fig. 6.23b). Between the hydrographic surveys on the 3-09-01 and the 6-11-01 (Chapter 4) the wave heights averaged 1.8 m with 3 wave

events reaching over 4 m. In 2002 the wave data averaged 1.2 m with a maximum of 3.5 m.

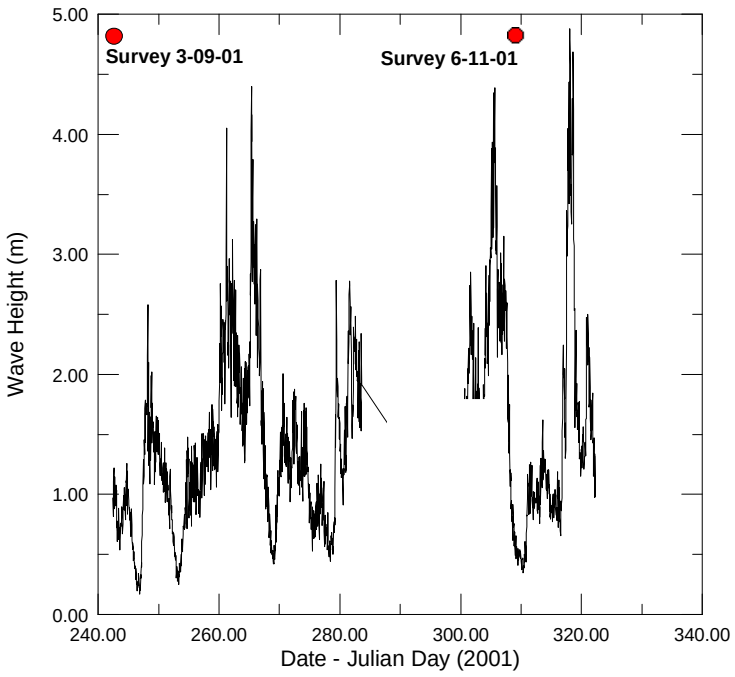

A)

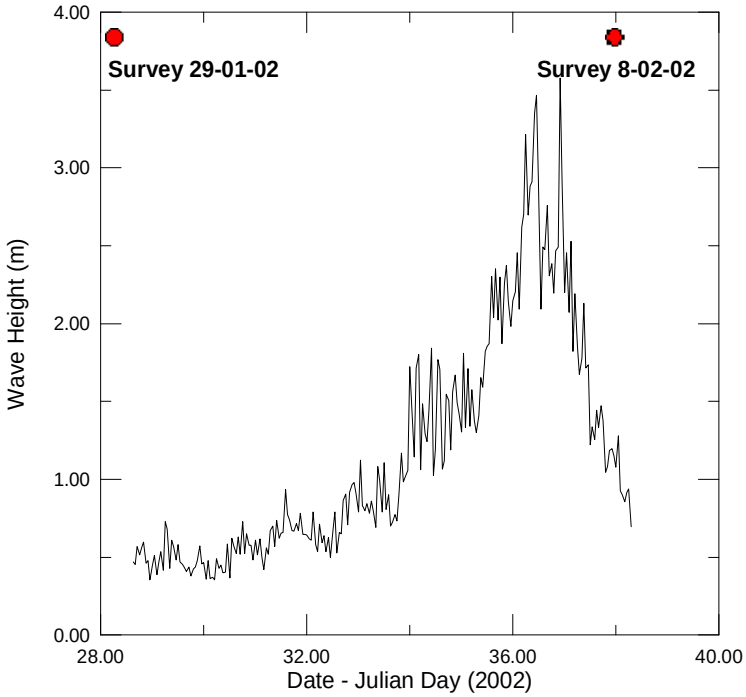

B)

Figure 6.23: (A) Measured wave heights (H_{sig}) from an S4 deployment at Raglan from 31-08-01 to 19-11-01 and (B) 29-01-02 to 8-02-02. Dates of the hydrographic surveys undertaken are also shown (Chapter 4).

6.6 SUMMARY

On the measurement transect which stretched from within 3 m of the sand rock interface to 150 m offshore, a broad range of conditions including north-west and south-west large swell (peaking at 3.25 m) and low waves were recorded. Although not comprehensive, it can be assumed that these conditions represent many of conditions that would be experienced over an annual period, as reported in Chapter 2. Overall, it was found that the measured bed orbital velocities were up to 2.5 ms^{-1}. These would have the ability to suspend large quantities of sediment, which could then be carried along the headland by the strong currents (up to 0.8 ms^{-1}). Wave heights and current velocities decreased further seaward from the shoreline and breaking wave zone. The peak spectral periods showed with an average of 13.5 seconds that long period swell is commonly found at the headland, due to shorter period swell not refracting around the large scale headland.

Experience of the author surfing at the break and observations of surfers attempting to paddle against the currents during large waves indicate that flows are strongly east along the headland in the surf zone. Surfers are often swept several hundred metres while attempting to paddle out beyond the breaking zone. Further offshore outside the surf zone surfers sitting on their surfboards can be seen drifting in a westerly direction suggesting an offshore flowing current. Further evidence of the currents was shown in Figure 6.16 and 6.17, where discoloured water and whitecaps on the water surface (as the wind blew against the current) distinguished the westerly flow further offshore from the headland.

The currents averaged over the deployment period at the three measurement sites were mostly in a westerly direction at the headland. Mean currents were only easterly along the headland during large swell, particularly at the most shoreward site, whilst further offshore a westerly returning current was found. The more shoreward regions over the rocky seabed are presumably disrupted by easterly wave-driven currents more often. Indeed, the location of the interface between the sand and rocky bed may

relate to the location where long-term mean currents change from being directed up to directed down the headland. The sandy bed is winnowed away, being unable to exist over the long term where strong wave-driven flows down the headland cause strong net transport.

CHAPTER SEVEN

SEDIMENT TRANSPORT

7.1 INTRODUCTION

The measurement of suspended sediment, particularly in field settings, is important in the documentation of sediment transport and deposition (Wren, 2000). The process of sediment suspension has been well studied for quartz "white sand" beaches eg: (Fredsøe and Deigard, 1992), but sand transport on "black sand" headlands has not been studied in any detail. The seabed at Indicators (a surf break located along the Raglan headland) consists of a mobile west coast "black sand" adjacent to a boulder and reef shoreline. Previous studies on the west coast have shown that net sediment movement is to the north (Mattews, 1977; Gibb, 1979; Hicks and Hume, 1993; McComb, 2001).

The previous chapter presented the results of wave and current measurements at the Raglan headland where a strong relationship between wave height and current intensity was found, whilst this chapter focuses on the sediment transport in this environment.

7.2 METHODS

7.2.1 *Sediment trap design and calibration*

Initial experiments were carried out at Ngarunui Beach (Fig. 7.1) to gain an understanding of the equipment and gauge the performance and reliability of S4 frames and sediment traps in the surf zone environment of the west coast (Fig. 7.1). Sediment traps were selected as the most suitable method for collecting samples in the surf zone (Fig. 7.2). Traps have been shown to be a cost effective and relatively accurate method of obtaining sediment samples in the coastal environment (e.g. Kraus, 1987; Flint, 1998; McComb, 2002). The high wave climate of the west coast and potentially large sediment fluxes, as well as difficulty in servicing the traps in the surf zone, meant that the sediment traps being used in the deployments needed sufficient storage capacity and the ability to prevent possible sediment escape from the trap after settlement. Nozzles were therefore fitted to the traps to increase the aspect ratio and prevent re-entrainment of the sediment.

Cylindrical sediment traps (90 mm x 300 mm) with smaller-diameter, raised inlet nozzles (18 mm x 50 mm) were used in the experiments (Fig. 6.2). The smaller inlet nozzle was required to allow the trap an extended filling period and to reduce any risk of sediment being re-suspended from the trap in the large wave conditions. There is general acceptance that cylinders most accurately measure natural suspended sediment concentrations as long as a suitable aspect ratio (height of the trap to the diameter of the collection orifice) is used e.g. (Hargrave and Burns, 1979; Bloesch and Burns, 1980; Gardner, 1980; Butman, 1986; Baker *et al.*, 1988). The use of the nozzle greatly increases the aspect ratio of the traps to 20:1. There is some concern about the use of sediment traps in extreme environments (White, 1990), although recent studies by Flint (1998) and McComb *et al.* (1999) confirmed their value in moderate to high-energy surf zones.

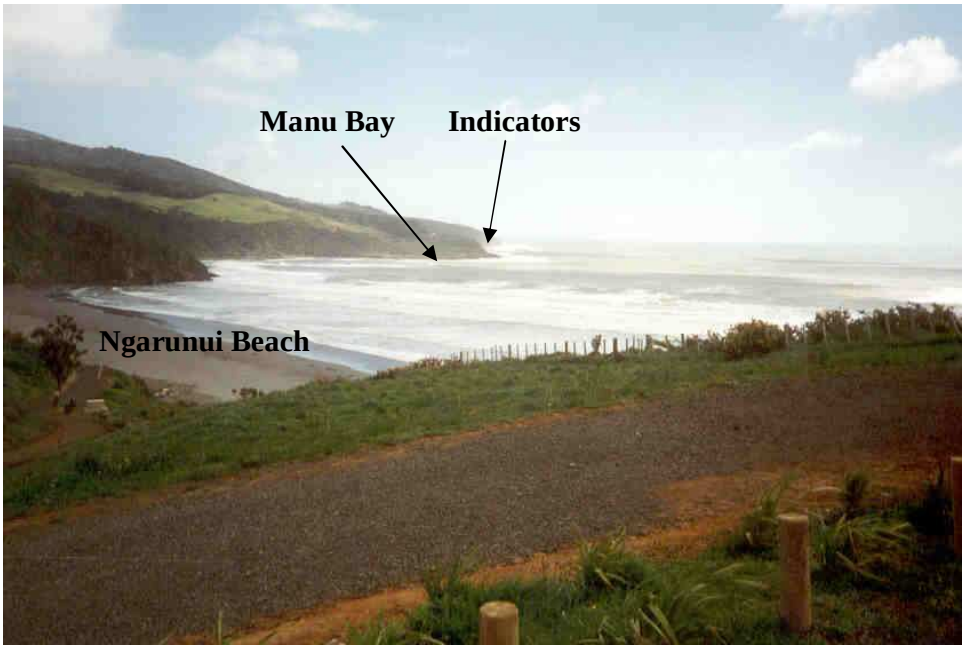

Figure 7.1: Ngarunui Beach looking southwest to the Raglan headland (Source: Author, 10 July 1997).

Figure 7.2: S4 frame on Ngaranui Beach prior to deployment with sediment traps at different heights and orientations to allow testing of the various shapes and orientations (Source: Author, 9 July 1997).

These experiments tested the strength and viability of the nozzles and traps, as well as comparing the quantities of sediment collected by placing two traps the same size and aspect at the same height on the frame.

7.2.2 *Laboratory sample analysis*

In the laboratory, sediment samples were taken from the traps, oven-dried and weighed for the total mass of sediment. The traps had collected a substantial quantity of fine-grained silt/mud particles due to land run-off through the nearby entrance to Raglan Harbour and so the sediment was passed through a 45 micron sieve so that the mud was not included in the total mass. An RSA fall tube was used for analysis of settling velocity as described in Chapter 3 (Particle size distribution).

7.2.3 *Calculation of suspended sediment concentrations*

Time-averaged sediment concentrations (C_z) over the deployment period for each trap at elevation z were calculated as,

$$f = M / A \ t \qquad (7.0)$$

where f = downward flux ($kg.m^{-2}.s^{-1}$); M = mass of sample collected (kg); A = area of the aperture of the trap (m^2); t = duration of the sampling period (s). The time-averaged concentration ($kg.m^{-3}$) is then,

$$C_z = f / W \qquad (7.1)$$

where w = mean settling velocity ($m.s^{-1}$).

Near-bed reference concentrations were obtained by fitting the trapped concentrations to a logarithmic profile given by,

$$C = C_0 e^{-z/l_s} \qquad (7.2)$$

where C_o = near-bed reference concentration (kg.m^{-3}); l_s = the mixing length (m). The mass of the collected samples was determined by weighing each sample after being oven dryed (Fig. 7.3).

Figure 7.3: Samples being dryed in the oven before weighing (Source: Author, 14 April 1998).

7.3 FIELD PROGRAMME

Sediment trap data was collected during the deployment of S4 current meter frames as described in Chapter 6.

7.4 RESULTS

7.4.1 *Fieldwork experiment 1 (12-06-98)*

The sediment concentrations collected in the traps from all three locations decreased with elevation above the bed, and with distance offshore along the transect (Fig. 7.4). The near-bed reference concentrations at z=0 above the bed (Eqn 7.2) decreased from 1.75 kg.m^3 inshore at Site 1 to 0.17 kg.m^3 offshore at Site 3 (Table 7.1).

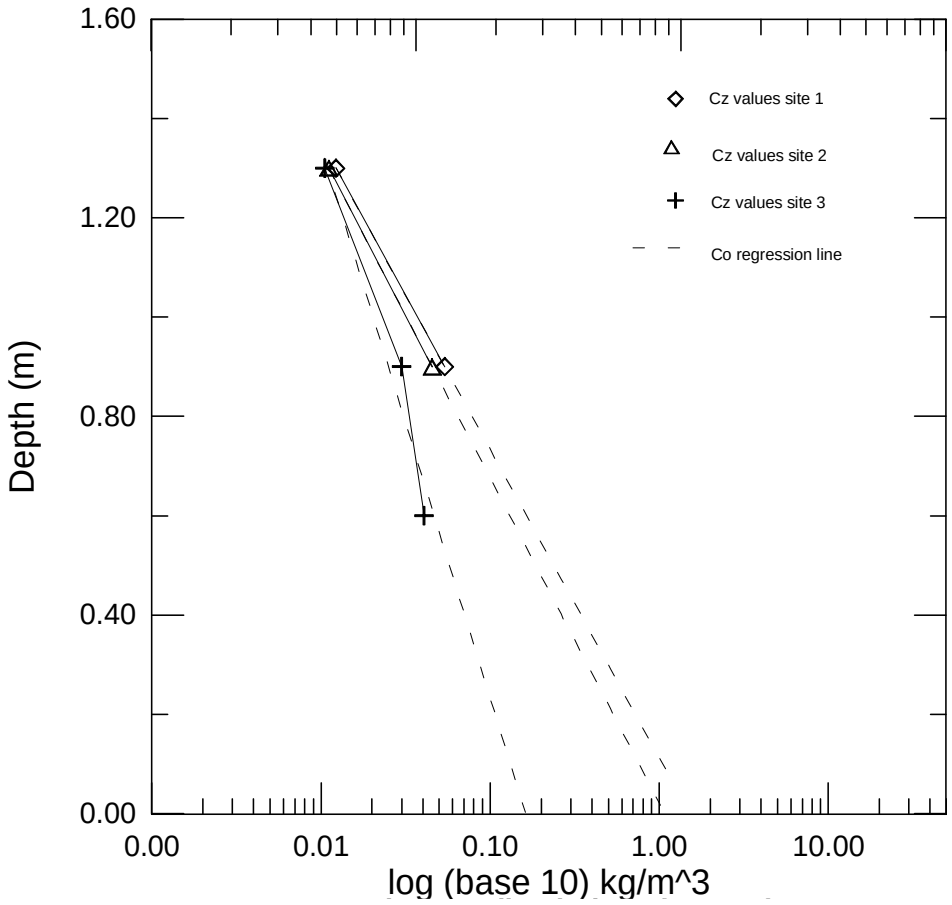

Figure 7.4: Time-averaged sediment concentrations at elevations (C_z) and best-fit regression lines for determination of near-bed reference concentrations (C_o).

Table 7.1: Sediment trap measurements at sites (#) 1-3. z is trap entrance elevation, M is the total trapped mass, w is the median fall velocity, t is the deployment duration, A is the trap entrance area, C_z is the concentration at the trap entrance, and C_o is the near-bed reference concentration.

#	z m	M kg	w m s^{-1}	t s	A m^2	C_z $kg.m^3$	C_o $kg.m^3$
1	1.3 0.9	0.134 0.592	0.042	1031460	2.54 x 10^{-4}	0.012 0.054	1.75
2	1.3 0.9	0.107 0.440	0.037	1031940	2.54 x 10^{-4}	0.011 0.045	1.1
3	1.3 0.9 0.6	0.088 0.251 0.341	0.032	1031880	2.54 x 10^{-4}	0.011 0.03 0.041	0.17

7.4.2 *Fieldwork experiment 2 (20-04-01)*

The sediment concentrations and grain size collected in the traps from all three locations decreased with elevation above the bed, and with distance offshore along the transect (Figure 7.4). The near-bed reference concentrations at z=0 above the bed decreased from 1.0 $kg.m^3$ inshore at Site 1, 0.8 $kg.m^3$ at Site 2, 0.6 $kg.m^3$ at Site 3 and 0.3 $kg.m^3$ offshore at Site 4 (Table 7.2).

The traps on the rocks at the bed level collected small quantities of sediment, which was typically of a larger grain size than the traps on the frames (e.g. Rocks 1 median size: 0.32 mm) Significant broken shell and small gravels were found at Rocks 1 (furthest inshore) and 2, decreasing to Rocks 3, which continues the trend from the trap data of largest sized grains being closest to the shore. Despite being covered with water for significantly less time than the trap at Rocks 3, the traps at Rocks 1 and 2 showed that sediment can settle in amongst the rocky boulders, although the shell and gravels are likely to be from a nearby source in the boulder

area and limited in supply. The traps collected 0.0042 kg at Rocks 1 and 0.0034 kg at Rocks 2 over the experimental period. The sediment is likely to be raised from in-between the boulders by the turbulence created by the breaking waves. The traps at this low level were able to collect this sediment that would not attain a significant height from the bed and therefore remain in the local area.

The trap at Rocks 3 near the low tide mark was covered with water for a considerably longer period of the day yet collected a similar mass of sediment (0.0031 kg), but did have a smaller grain size with no small gravels or shell. The C_o values calculated using *t* excluding the time the trap was exposed, were lower than those measured over the sandy beds, with values of 0.01 $kg.m^3$ at Rocks 1, 0.006 $kg.m^3$ at Rocks 2 and 0.004 $kg.m^3$ at Rocks 3. This demonstrates that over the rocky bed there may be limited transport of sediment at this low level which could be due to a lack of local sediment and distance from the sandy beds, and/or more conclusively, an inability in settle in this turbulent environment which makes quantification more difficult.

The difference between the *Co* values at Rocks 3 at the low tide mark, and Frame 1 located 30 m seaward of the rock/sand boundary, was significant despite the trap at Rocks 3 being covered for a large part of the tidal cycle. McComb (2001) found in New Plymouth, that greater suspended sediment loads were found at higher levels in the water column over rocky beds than at low levels, when compared to loads across sandy substrate. The sand is therefore transported in suspension over the rocky beds at a higher level, which may be reflected in the low quantity of sediment collected in the traps at Raglan.

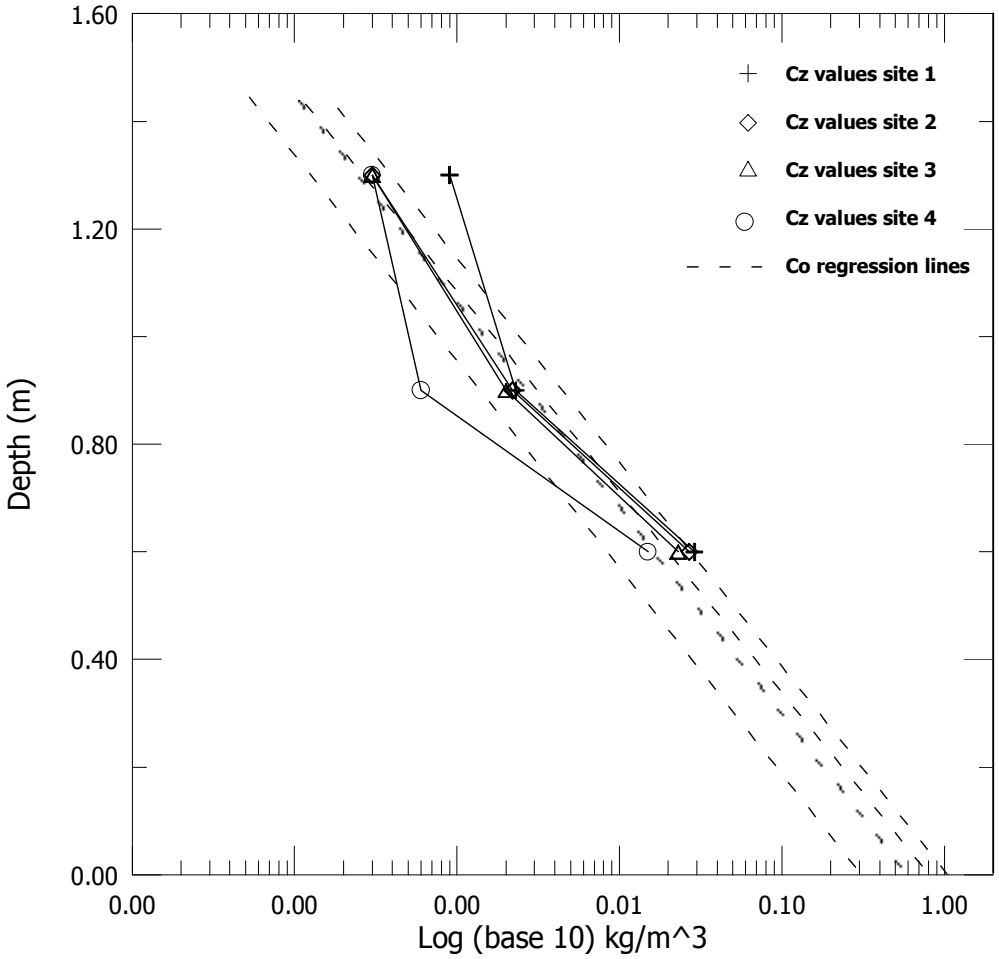

Figure 7.5: Time-averaged sediment concentrations at elevations (C_z) and best-fit regression lines for determination of near-bed reference concentrations (C_o).

Table 7.2: Sediment trap measurements at sites (#) 1-4. z is trap entrance elevation, M is the total trapped mass, w is the median fall velocity, t is the deployment duration, A is the trap entrance area, C_z is the concentration at the trap entrance, and C_o is the near-bed reference concentration.

#	z m	M kg	w ms^{-1}	t s	A m^2	C_z $kg.m^3$	C_o $kg.m^3$
1	1.3 0.9 0.6	0.022 0.058 0.738	0.037	1203600	5.73 x 10^{-4}	0.0009 0.0023 0.029	1.00
2	1.3 0.9 0.6	0.007 0.052 0.654	0.035	1203600	5.73 x 10^{-4}	0.0003 0.0022 0.027	0.80
3	1.3 0.9 0.6	0.0064 0.044 0.454	0.029	1203900	5.73 x 10^{-4}	0.0003 0.0023 0.02	0.60
4	1.3 0.9 0.6	0.0036 0.0085 0.218	0.021	1203600	5.73 x 10^{-4}	0.0003 0.0006 0.015	0.3
Rocks							
1	0	0.0405	0.044	302400	2.54	0.012	0.01
2	0	0.0342	0.035	604800	x 10^{-4}	0.0064	0.006
3	0	0.0314	0.029	1008000		0.0042	0.004

7.5 SUMMARY

Averaged near-bed reference concentrations calculated using measured data from two field experiments at the Raglan headland were significant, and ranged from a maximum of 1.75 kg.m^3 inshore to 0.17 kg.m^3 offshore in Experiment 1 (12-6-98). In Experiment 2 (20-04-01) the maximum was 1.0 kg.m^3 inshore to 0.30 kg.m^3 offshore, whilst on the rocks the concentration varied from 0.01 kg.m^3 at the high tide mark, to 0.004 kg.m^3 at the low tide mark. These concentrations show that greater sediment transport is found in the breaking wave zone along the headland where the highest orbital velocities and significant turbulence are found. Significantly lower near-bed reference concentrations of sediment across the rocks armouring the shoreline shows that sand is unable to settle in this turbulent zone and is likely to be transported in suspension over the rocky beds at a higher level. Distance from a local sediment source, i.e. sandy seabed may also contribute to the lower concentration values found on the rocks.

CHAPTER EIGHT

NUMERICAL MODELLING

8.1 INTRODUCTION

Numerical models have become an essential component of coastal studies. They can be used to predict wave, tide and current scenarios that otherwise are impossible to measure in reality (Komar, 1998). Current patterns can be utilised to predict sediment movements and budgets, in an area of the coast under investigation (Lou and Ridd, 1997). The bathymetry forms an important component of the modelling process, which therefore requires accurate hydrographic surveying methodology to provide valid results. Complex theoretical and empirical formulae that represent physical coastal processes are the basis of the model outputs, with radiation stress being a particularly important mechanism that drives currents at Raglan. A more detailed description is found in Appendix 9.

There are a range of hydrodynamic models and types of solutions being used to numerically model coastal scenarios, with the most common being classified as wave ray, mild slope, iterative finite difference and Lagrangian methods (Hutt, 1997). One of the more recent models is WBEND, with a finite difference numerical solution scheme, developed by Black and Rosenberg (1992a) to investigate wave refraction, shoaling and frictional dissipation for both monochromatic waves and wave spectra. The model was calibrated with laboratory and field measurements, and was found

suitable for general application to irregular bathymetry and variable wave conditions (Black and Rosenberg, 1992a).

The two previous chapters presented the results of measured waves, currents and sediment transport, whilst this chapter focuses on the numerical modelling of the waves and currents at the headland, using the 3DD model suite (Black, 2001a). Model outputs are presented for a range of wave heights, periods and directions. The model was set up with a 20 m x 20 m grid size with a total of 140 cells along the x axis (i) and 94 along the y axis (j). The orientation was with the open sea to the left (western boundary) and the coast to the right (eastern boundary)(i.e. the same as the natural orientation found at Raglan). The boundary conditions were set up for the model, with a file created for each that could be loaded up by the model i.e. north, west and east. These set the water at constant level with different magnitudes for each of the low, mid and high tide scenarios modelled e.g. 0.5 m for low tide. However, the southern boundary was set up with a sea level set to a selected internal cell as land dominates along this boundary.

8.2 MODEL CALIBRATION

Calibration for this study involved input of boundary information including wave height, period and direction into the WBEND model and adjusting the friction coefficient, as well as height and angle eddy viscosities until the model accurately predicted known wave data measurements collected during the field experiments, at those positions where instruments were placed (Chapter 6). The model WBEND has been previously calibrated and validated at this field site by Hutt (1997), Sayce (1999), and Scarfe (2002). The calibration in these cases involved the use of extensive field data and the model was found to very accurately predict the measured data (Hutt and Black, 2001). The field program was undertaken when good quality waves were breaking at the field site, and included aerial photography and the deployment of nine pressure-sensing instruments spread over the study site to

measure waves and currents. This knowledge was used as the basis for the modelling in this study to investigate the hydrodynamics of the headland.

As confidence already existed in the model capability at the field site, two separate events (2 m and 3 m swell) were selected to compare the measured and predicted data at three sites along the fieldwork transect, as a validation for the previous calibration at high and low tides (Table 8.1 and 8.2). The accuracy of the model during the large 3 m swell was considered most important, as this is when the greatest sediment transport would be likely to occur. This validation confirmed the accuracy of the model at both high and low tides, and provided an acceptable comparison between the measured and predicted data. The variable factors (coefficients) were found to be very similar to that of previous calibrations, being friction coefficient (0.002), height eddy viscosity (0.28) and angle eddy viscosity (0.06).

Table 8.1. Calibration of observed and modelled data for wave height and wave direction based on data measured at the field site in 1998 (relative to True North).

	Position along transect at Indicators surf break					
Wave Height (m) and Direction (Deg)	0 (m) 595 250.60 N 302 859.63 E		40 (m) 595 278.39 N 302 854.80 E		130 (m) 595 374.00 N 302 823.00 E	
3m Swell	Low Tide	High Tide	Low Tide	High Tide	Low Tide	High Tide
Observed value	3.0 128	2.7, 121	3.0, 126	2.6, 118	2.8, 114	2.3, 109
Modelled value	2.9, 131	2.5, 124	2.8, 128	2.4, 122	2.8, 117	2.3, 112
2m Swell						
Observed value	2.2, 128	2.0, 125	2.2, 124	2.0, 121	2.1, 113	1.9, 112
Modelled value	2.2, 131	2.0, 123	2.2, 128	2.0, 120	2.0, 114	1.9, 110

Table 8.2. Calibration data of observed and modelled data for current speed and current direction based on data measured at the field site in 1998 (relative to True North).

	Position along transect at Indicators surf break					
Current Speed (m/s) and Direction (Deg)	0 (m) 595 250.60 N 302 859.63 E		40 (m) 595 278.39 N 302 854.80 E		130 (m) 595 374.00 N 302 823.00 E	
3m Swell	Low Tide	High Tide	Low Tide	High Tide	Low Tide	High Tide
Observed value	0.8, 60	0.13, 232	0.5, 68	0.2, 230	0.1, 247	0.1, 247
Modelled value	0.9, 61	0.3, 221	0.65, 60	0.4, 221	0.2, 241	0.2, 238
2m Swell						
Observed value	0.3, 65	0.13, 238	0.1, 219	0.1, 228	0.11, 245	0.1, 250
Modelled value	0.3, 75	0.14, 219	0.1, 209	0.2, 224	0.2, 237	0.1, 236

The output files from WBEND were then used in the model 3DD for validation of the current velocities and directions at known positions, to get a comparison between measured and predicted data, at both high and low tide (Table 8.2).

8.3 MODEL INPUTS AND OUTPUTS

The model was run using the following wave height, period and direction (relative to the model grid) combinations, at both high, mid and low tide (1 m, 12 s, 25^{o}; 2 m, 12 s, 25^{o}; 3 m, 14 s, 25^{o}; 4 m, 16 s, 25^{o}; 2 m, 12 s, 0^{o}; 1 m, 10 s, -25^{o}), to determine the wave and current characteristics along the headland. This was similar to the parameters used by Hutt (1997), Sayce (1997) and Scarfe (2002) in previous modelling at the field site, which were found to best represent the prevailing conditions (Chapter 2). Hutt (1997) found through calibration of the model suite 3DD, that a wave direction of zero degrees at the boundary (due east) aligns best with the predominant wave direction (from approximately southwest). This direction was found from long-term data to be the most common swell direction at the field site (Chapter 2). As the grid has been rotated 25^{o} anticlockwise, the input angle must also be rotated by this margin to be relative to the grid.

8.4 MODEL PRESENTATION

Model output presentation is undertaken using the PLOT3DD graphics routine. It is a Windows-based high quality graphical support routine written in Matlab for the 3DD suite. The software has been developed by Dr Richard Gorman, of the National Institute of Water and Atmospheric Research (NIWA) over more than 10 years duration. This package allows for pseudo-colour, vectors, 3-dimensional projections, time series and movies.

8.5 WAVE CHARACTERISTICS

Trends related to the waves and refraction at the Indicators surf break identified by Hutt (1997) and Scarfe (2002), were reconfirmed with the modelling undertaken for this study using the software WBEND. These include more refraction at low tide than found at high tide, as waves are able to more readily interact with the seabed in the shallower water, slow down and refract into the headland (Fig. 8.1 and 8.2). A difference of approximately 10^{o} was found at Indicators between low and high tide levels. In larger swells (>4 m) the waves tend to sweep straighter down the headland when compared to smaller swells where more refraction takes place. Swells from the northwest direction break straighter into the surfing headland, with significantly less refraction and have high peel angles creating fast breaking waves (Fig. 8.3). At low tide the shallower water also leads to greater shoaling of the waves with an increased wave height, whilst at high tide wave size can decrease in size (Fig. 8.4). These factors can all influence the current direction and current velocity, varying the amount of sediment transport and quantity of deposition or scour at the headland.

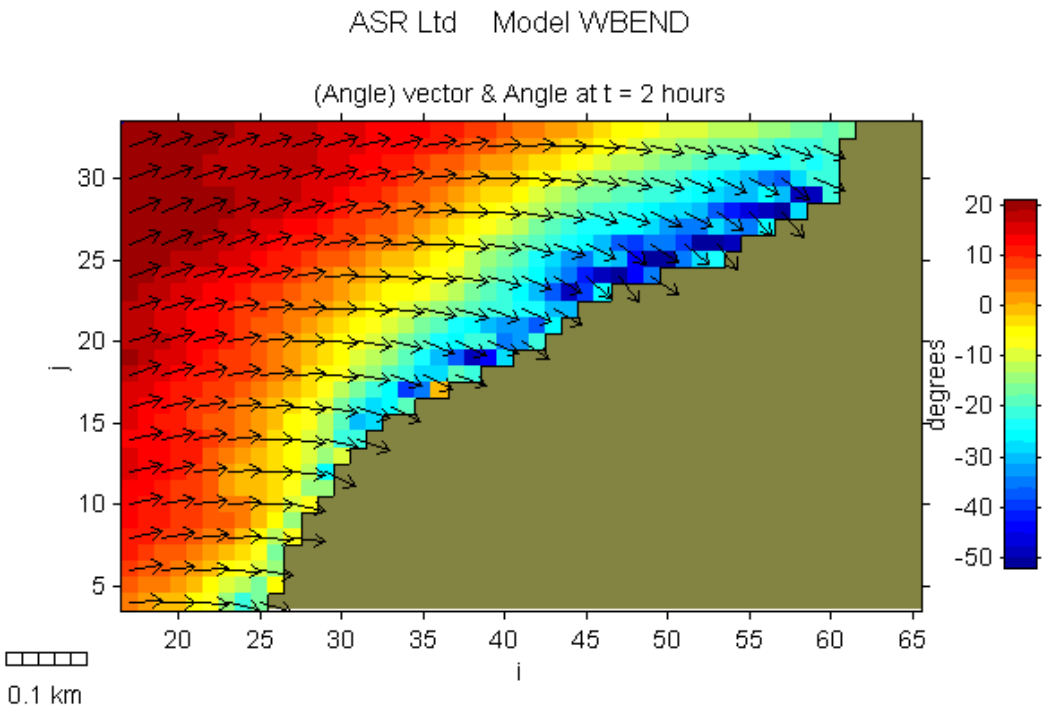

Figure 8.1: Wave refraction at the Indicators surf break at low tide for a 2 m swell, 12 second period from the southwest direction.

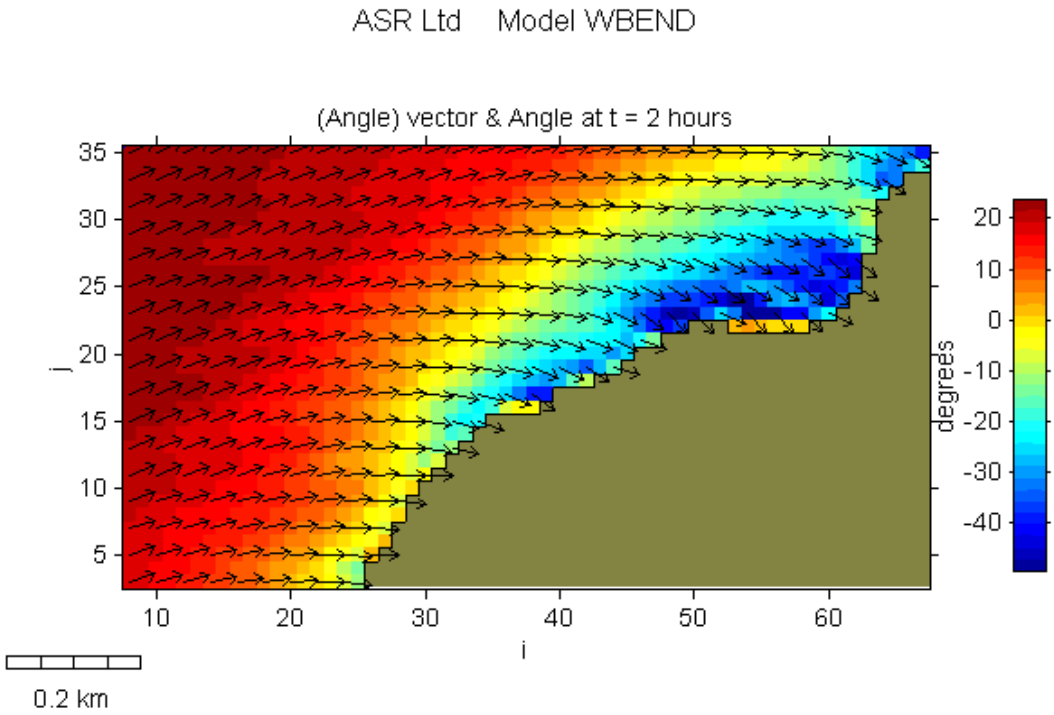

Figure 8.2: Wave refraction at the Indicators surf break at high tide for a 2 m, 12 sec period swell from the southwest direction.

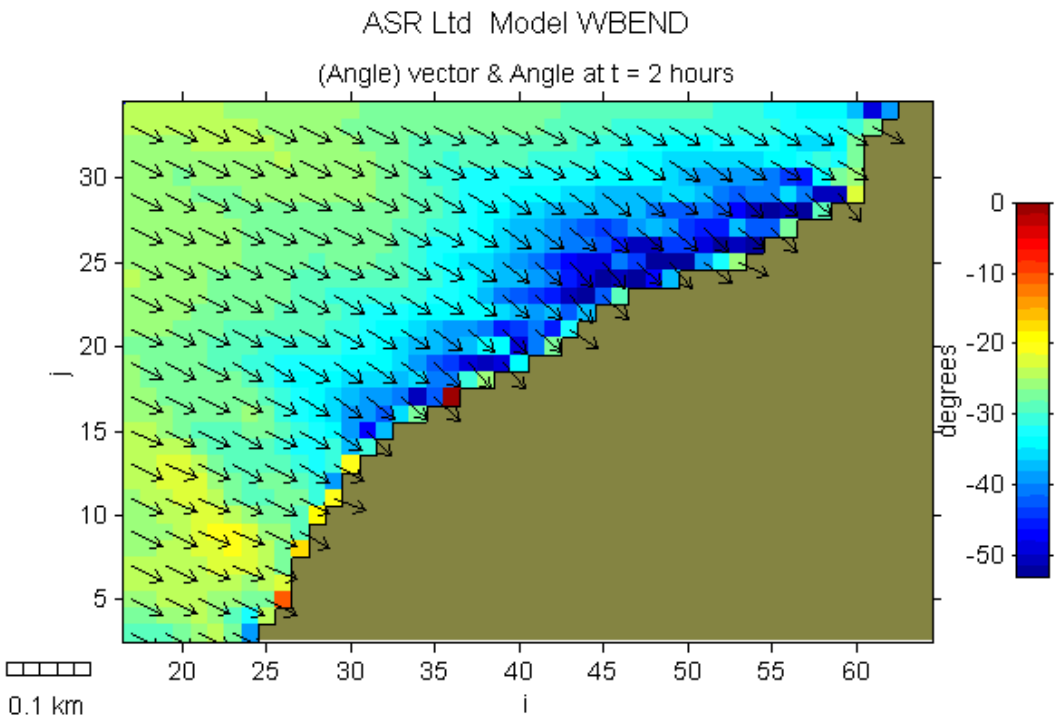

Figure 8.3: Wave refraction at the Indicators surf break at high tide for a 1 m, 10 sec period swell from the northwest direction.

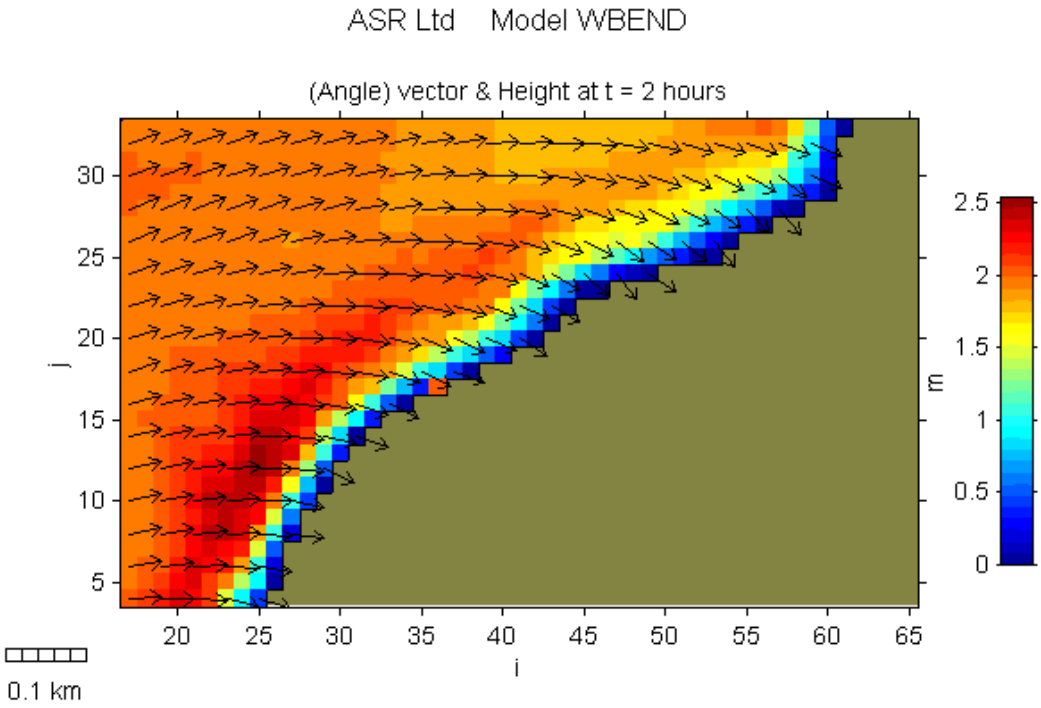

Figure 8.4: Wave shoaling along the Indicators surf break at low tide for a 2 m 12 sec period southwest direction swell.

8.6 CURRENT AND CIRCULATION CHARACTERISTICS

The 3DD suite was used for modelling the current characteristics at the Raglan headland, with data extracted from the model outputs at 5 sites in a transect perpendicular to the headland orientation (Table 8.3). Site 1 (model grid cell 42, 24) was selected on the rocky boulder shoreline (approximately 30 m from the rock/sand boundary in Experiment 1), so that an understanding could be gained into the current characteristics across the rocks. Sites 2 to 5 are in the same positions as the experimental fieldwork transect, with Site 2 (42, 27) approximately 30 m seaward from the rock/sand boundary, Site 3 (42, 28) and Site 4 (42, 29) a further 30 m seaward respectively, and Site 5 (41, 31) most seaward a further 50 m (Fig. 8.5). Plots of the outputs are used for identification of the current patterns and for comparison between the different scenarios modelled.

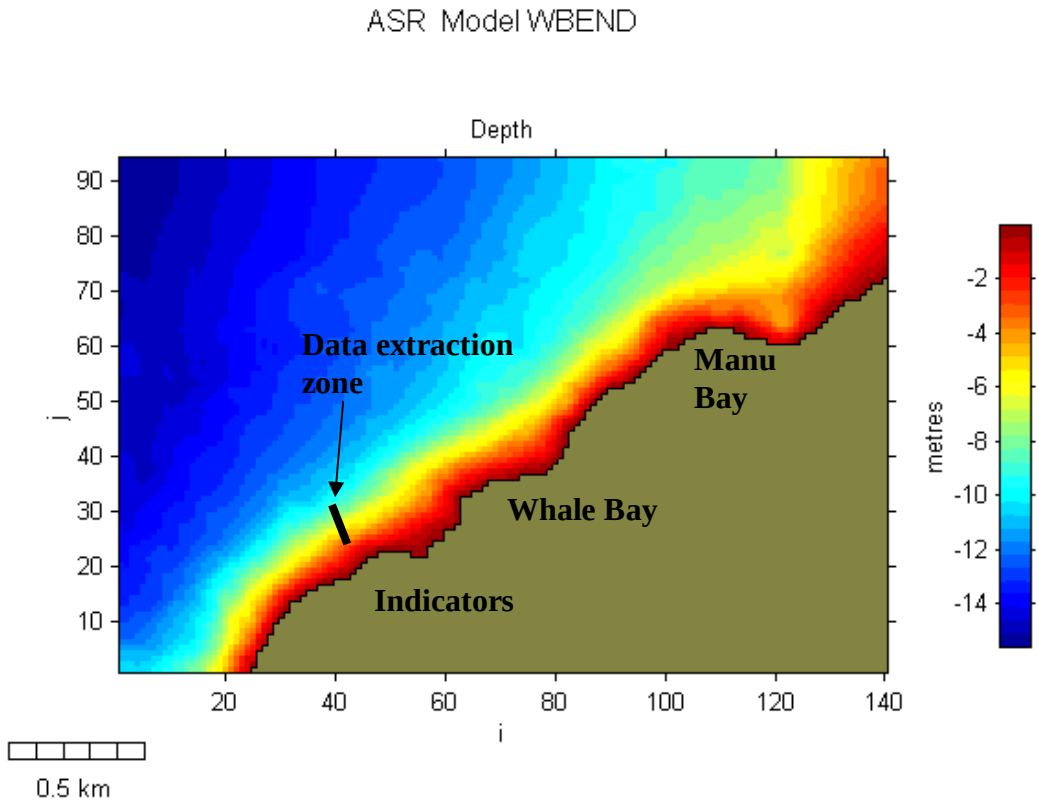

Figure 8.5: Contour map of the study site showing the location of the data extraction zone where 5 points were analysed (Site 1: 42, 24; Site 2: 42, 27; Site 3: 42, 28; Site 4: 42, 29; Site 5: 41, 31).

The extracted data from Site 1 shows the current flows east along the headland in the surf-zone above the rock boulders for all of the scenarios (mostly in the range 75-90^{o}), and ranges in velocity from 1.4 ms^{-1} in the 4 m southwest swell to 0.1 ms^{-1} at high tide in the 1m northwest swell. The 1 m northwest swell attained a maximum current velocity at low tide of 0.27 ms^{-1} inshore at Site 1, with a easterly directed current of 90^{o} (Fig. 8.6). At Sites 2-5 the current varied from 0.07-0.15 ms^{-1} and was directed west at the headland on all occasions, increasing in angle at high tide. Figure 8.6 of a 1 m northwest swell shows zones of higher velocity different to that seen with a typical southwest swell, due to the straighter angle that the waves approach the shoreline. A strong eddy can be seen rotating at Indicators and Whale Bay.

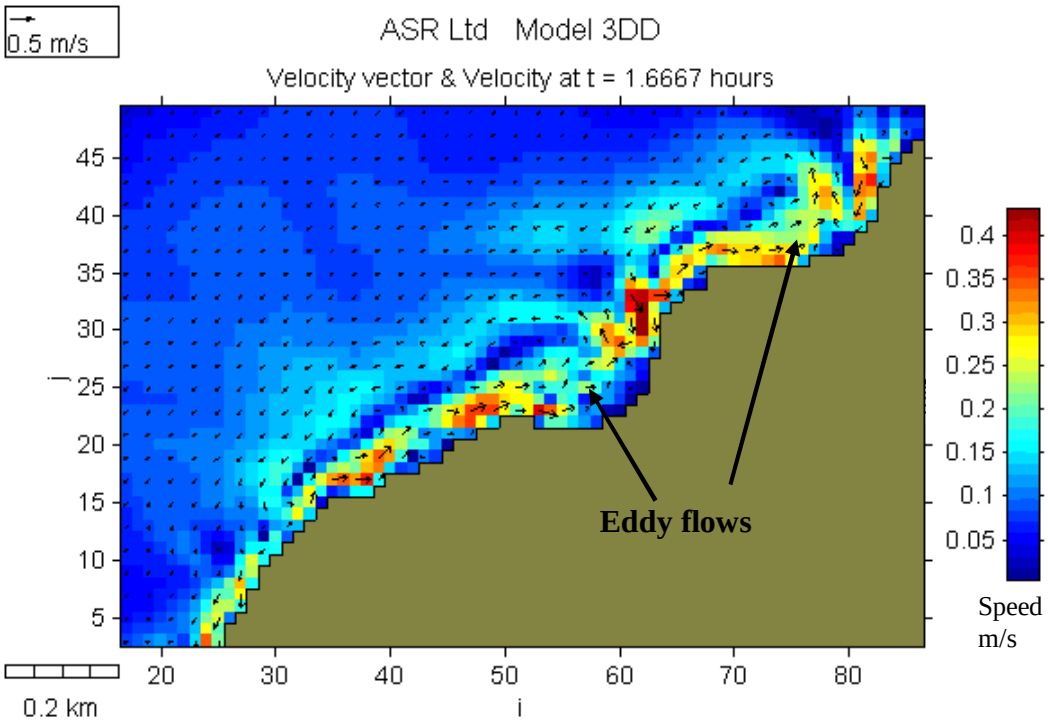

Figure 8.6: Model 3DD plot for a 1 m NW swell at high tide with a 10 sec period, showing current direction and velocity and eddy flow at Indicators and Whale Bay.

Table 8.3: Numerical model output data for current speed (ms^{-1}) and and current direction (degrees True North) for typical wave conditions at Raglan (eg: 1 m wave height, 12 sec period, SW swell direction).

	Site 1 Cell 42, 24		Site 2 Cell 42, 27		Site 3 Cell 42, 28		Site 4 Cell 42, 29		Site 5 Cell 41, 31	
	Speed (ms^{-1})	Dir (deg)	Speed (ms^{-1})	Dir (deg)	Speed (ms^{-1})	Dir (deg)	Speed (ms^{-1})	Dir (deg)	Speed (ms^{-1})	Dir (deg)
1m 12 s SW										
Low Tide	0.23	75	0.09	219	0.12	237	0.13	256	0.13	256
Mid Tide	0.12	70	0.09	253	0.12	237	0.14	247	0.14	247
High Tide	0.05	35	0.12	270	0.13	267	0.13	267	0.13	267
2m 12s SW										
Low Tide	0.7	80	0.22	103	0.09	213	0.26	260	0.26	260
Mid Tide	0.5	78	0.18	226	0.28	241	0.35	259	0.35	259
High Tide	0.24	70	0.22	252	0.30	256	0.35	263	0.35	263
3m 14s SW										
Low Tide	1.02	79	0.83	87	0.55	86	0.48	277	0.48	277
Mid Tide	1.05	78	0.36	97	0.08	216	0.37	258	0.37	258
High Tide	0.8	74	0.29	226	0.43	239	0.56	256	0.56	256
4m 16s SW										
Low Tide	1.2	81	1.40	85	1.22	58	0.23	33	0.23	33
Mid Tide	1.4	80	1.16	87	0.79	61	0.46	272	0.46	272
High Tide	1.4	78	0.24	85	0.28	214	0.74	258	0.74	258
2m 12s W										
Low Tide	0.8	82	0.47	96	0.13	92	0.20	256	0.20	231
Mid Tide	0.7	88	0.14	208	0.28	219	0.34	251	0.34	226
High Tide	0.65	90	0.25	242	0.30	223	0.32	253	0.32	228
1m 10s NW										
Low Tide	0.27	90	0.07	201	0.14	225	0.15	253	0.15	228
Mid Tide	0.18	92	0.11	256	0.13	236	0.12	261	0.12	236
High Tide	0.10	30	0.13	273	0.13	245	0.10	262	0.12	242

In comparison the 1 m SW swell with a 12 sec period attained a slightly lower maximum velocity at low tide of 0.23 ms^{-1} at 75^{o} (Fig. 8.7), which decreased in velocity and angle at high tide to 0.05 ms^{-1} at 35^{o} (Fig. 8.8). Further offshore at Sites 2-5 the current was again westerly varying between 0.09-0.14 ms^{-1} and 219-270^{o}.

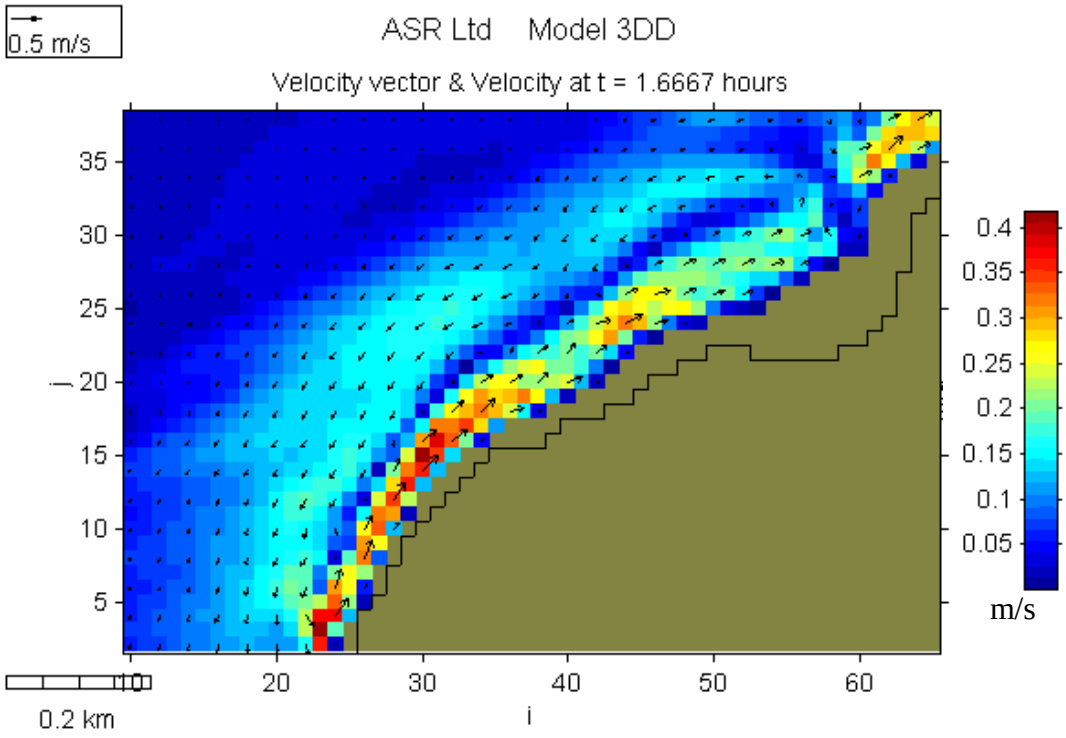

Figure 8.7: Model 3DD plot for a 1 m SW swell at low tide with a 12 sec period, showing current direction and velocity at Indicators.

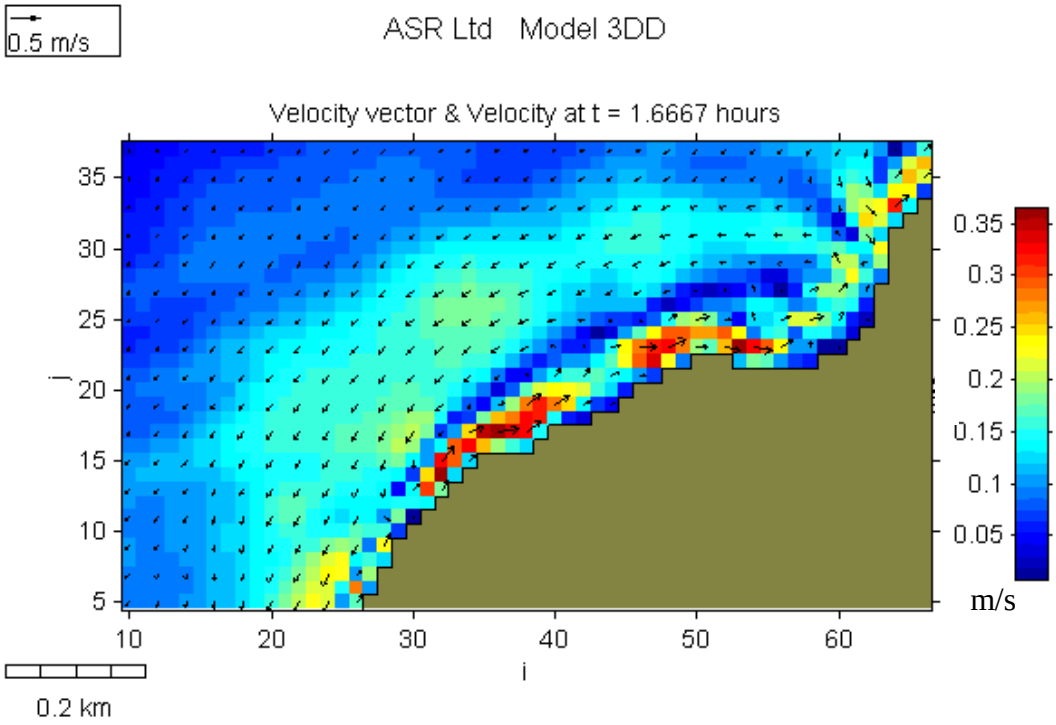

Figure 8.8: Model 3DD plot for a 1 m SW swell at high tide with a 12 sec period, showing current direction and velocity at Indicators.

In the 2 m SW swell with a 12 sec period the current in the surf-zone at Site 1 varies from a maximum at low tide of 0.7 ms^{-1} at 80^{o}, decreasing at high tide to 0.24 ms^{-1} at 70^{o} (i.e. lower refraction; Fig. 8.9 and Fig. 8.10). At site 2 the current is east along the headland (103^{o}) when the tide is low, attaining a velocity of 0.22 ms^{-1}, then changing to a westerly direction at both mid and high tides. The current at all other sites on all tides was westerly (0.26-0.35 ms^{-1}) with an increasing angle at high tide, which varied from 226-263^{o}. A more distinct eddy can be seen at high tide when compared to low tide, spiraling out from the change in headland orientation at Whale Bay (Fig. 8.10).

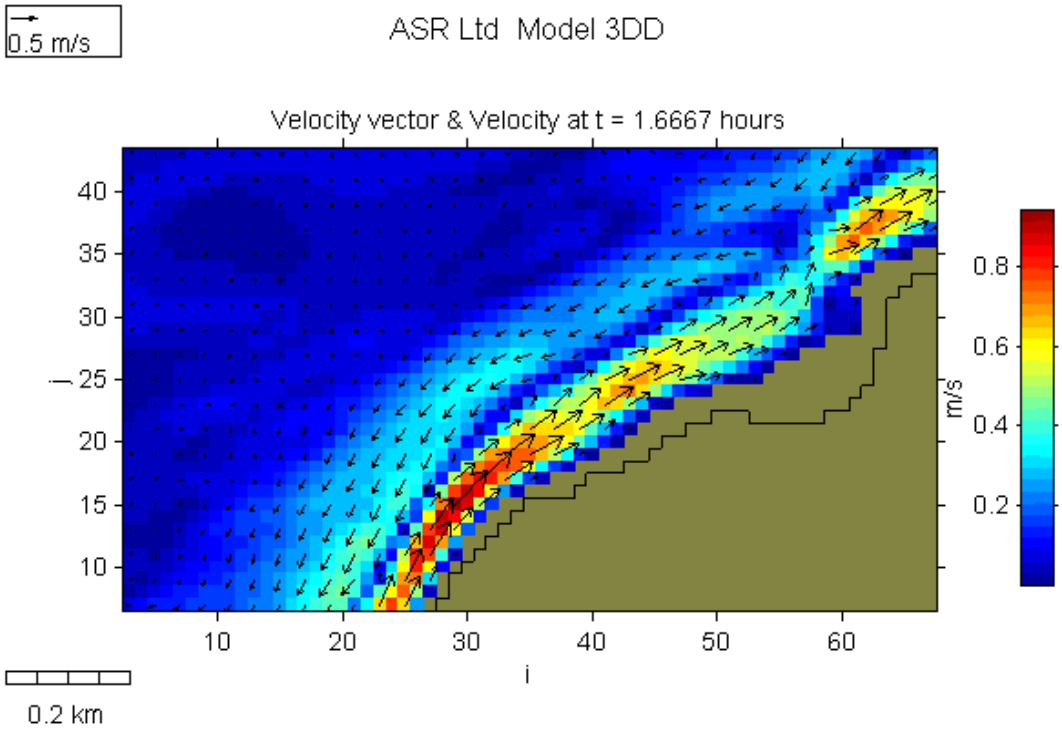

Figure 8.9: Model 3DD plot for a 2 m SW swell at low tide with a 12 sec period, showing current direction and velocity at Indicators.

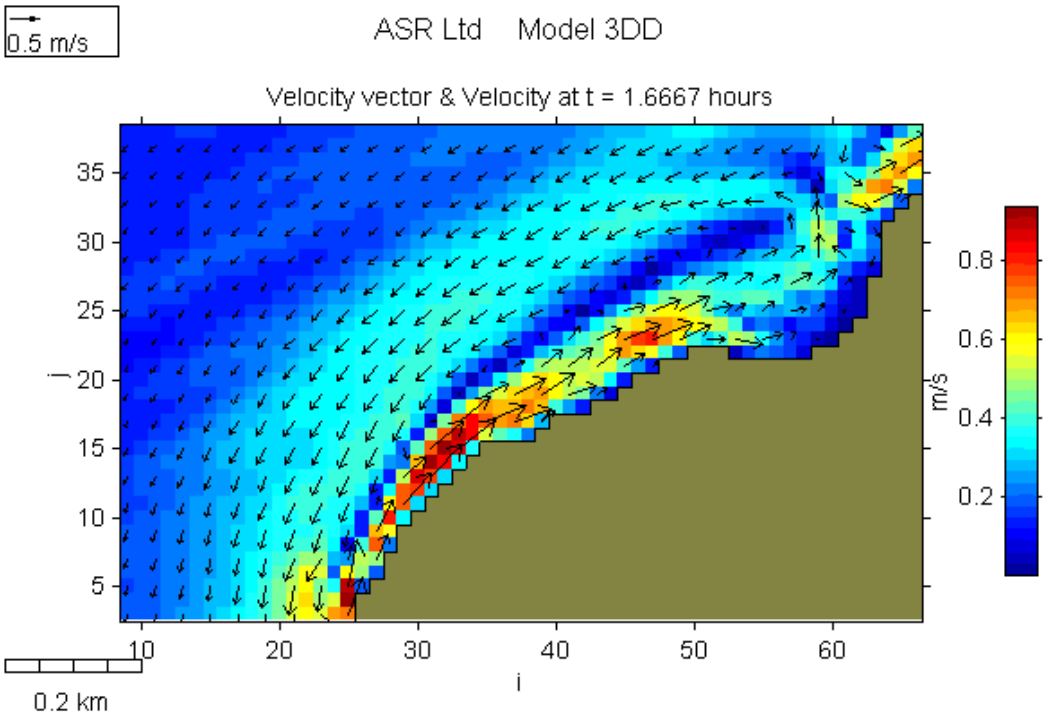

Figure 8.10: Model 3DD plot for a 2 m SW swell at high tide with a 12 sec period, showing current direction and velocity at Indicators.

The 2 m west swell with a 12 sec period displayed similar characteristics to the 2 m southwest swell, although an easterly current direction was maintained at Site 3 at low tide (Fig. 8.11), flowing at 0.13 ms^{-1} at an angle of 92°. The current at Site 1 attained 0.8 ms^{-1} decreasing to 0.65 ms^{-1} at high tide (Fig. 8.12), and the angle varied from 82° at low tide to 90° at high tide. Site 2 had a larger current flowing easterly along the headland at 0.47 ms^{-1}, compared to 0.22 ms^{-1} for the southwest swell. The data shows the current was larger inshore at the headland, due to the lower oblique angle at which the west swell would have reached the shore (i.e. lower refraction). Figures 8.11 and 8.12 again demonstrate a trend visible on all the model outputs, where the current spiraling seawards from the headland at high tide, is significantly greater than at low tide.

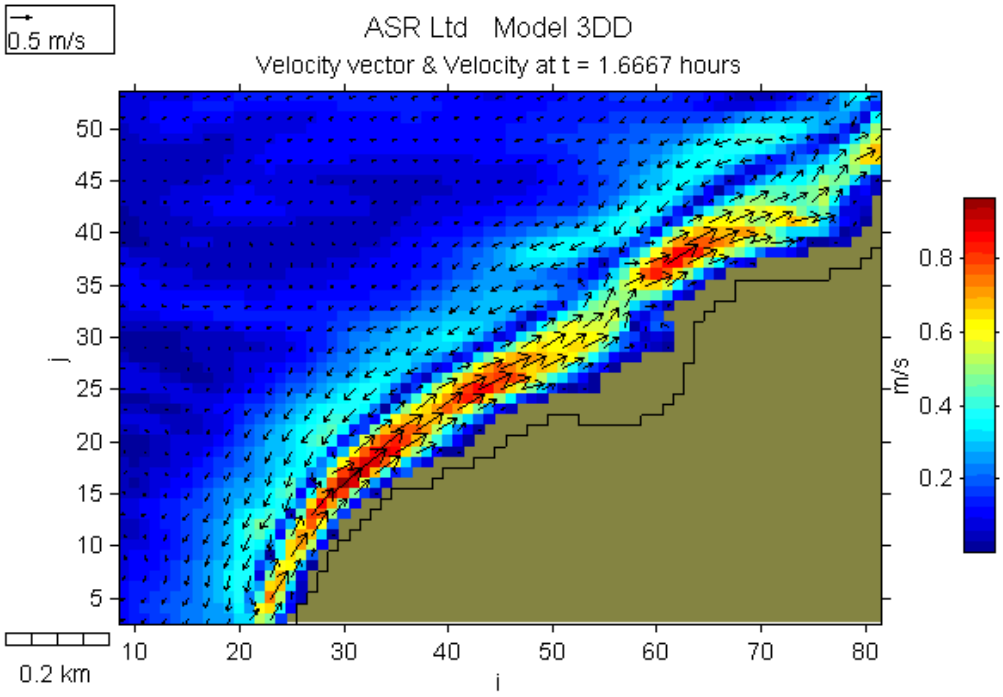

Figure 8.11: Model 3DD plot for a 2 m west swell at low tide with a 12 sec period, showing current direction and velocity at Indicators and Whale Bay.

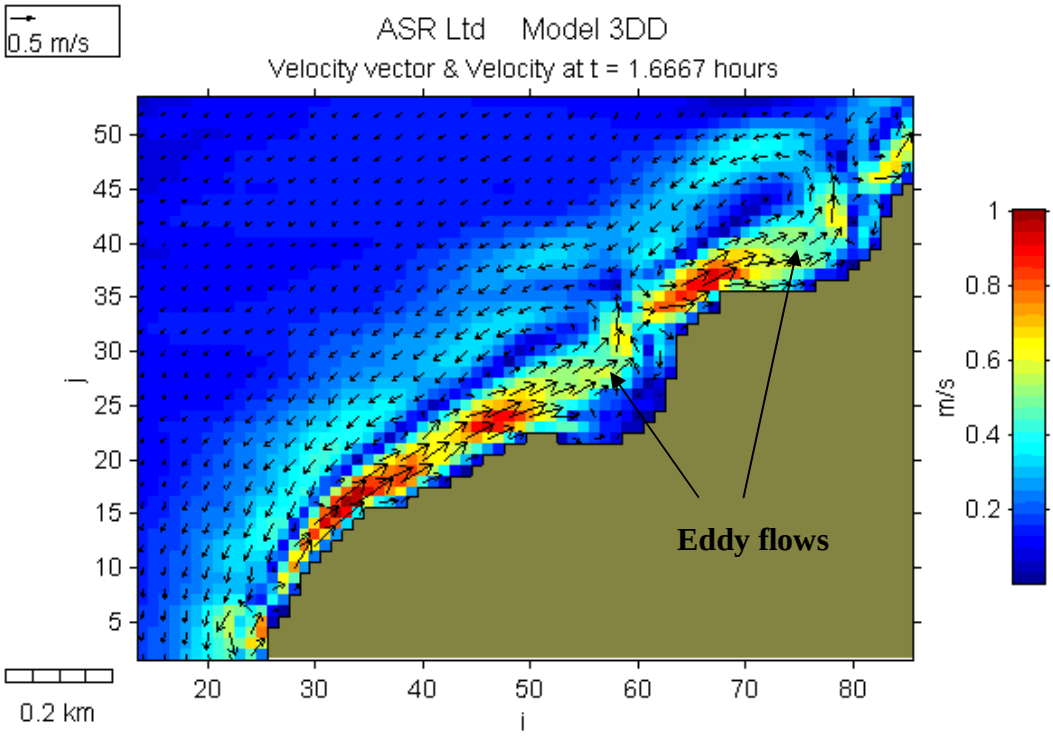

Figure 8.12: Model 3DD plot for a 2 m west swell at high tide with a 12 sec period, showing current direction and velocity at Indicators and Whale bay.

The larger 3 m swell with a 14 sec period produced significantly stronger currents both east and west along the headland at low and high tides (Fig. 8.13 and Fig. 8.14). The maximum velocities were 1.02 ms^{-1} at Site 1 at low tide and 1.05 ms^{-1} at mid tide, whilst Site 3 decreased to 0.8 ms^{-1}, all flowing east at the headland. Interestingly a current velocity of 2 ms^{-1} was found in an easterly direction at Outsides, which is where visible scouring was evident in the side scan sonagraphs following a large swell (Chapter 5). A current was maintained in an easterly direction at the headland at Sites 2-5 at low tide, and at site 2 at mid tide. For the remainder of the mid and high tide recordings, the current was directed west at velocities varying from a minimum of 0.31 ms^{-1} to a maximum of 0.56 ms^{-1}. The model run of 3 m waves produced currents at Site 2 of 0.8 ms^{-1} velocity at a direction of 62^{o}, which correlate very closely to the data from the field experiment in 1998.

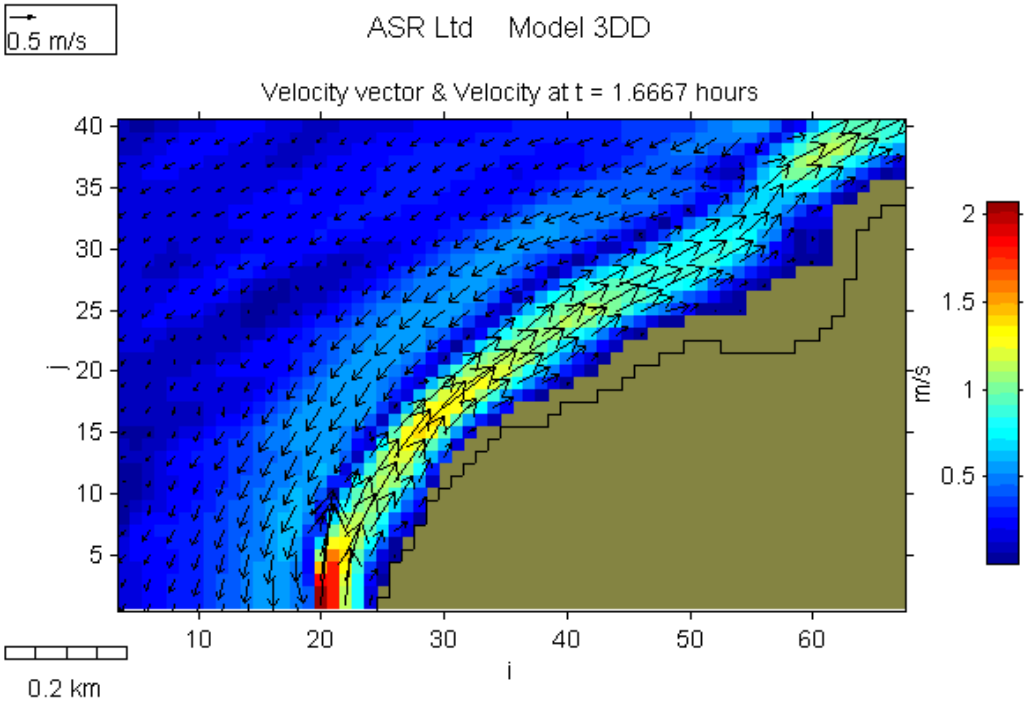

Figure 8.13: Model 3DD plot for a 3 m SW swell at low tide with a 14 sec period, showing the current direction and velocity at Indicators.

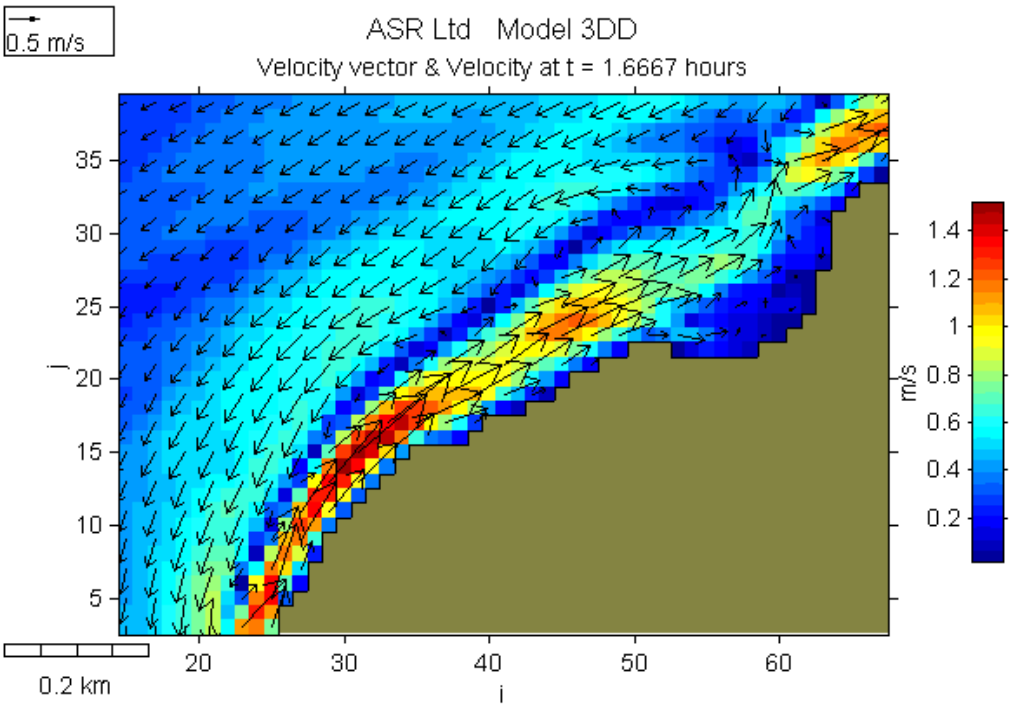

Figure 8.14: Model 3DD plot for a 3 m SW swell at high tide with a 14 sec period, showing the current direction and velocity at Indicators.

The largest of the modelled swells at 4 m from the southwest with a 16 sec period produced currents that peaked at 1.4 ms^{-1} at mid and high tides at Site 1, and low tide at Site 2. The currents inshore were again to the east, but further offshore reversing to westerly. The currents at low and mid tides were always easterly except for Sites 4 and 5 at mid tide, whilst at high tide the current was easterly at Site 1 and 2 and westerly at Sites 3, 4 and 5. The increased velocity flowing in an east direction along the headland at this swell size has been confirmed by both observations of surfers being swept down the headland, and field data collected in the 1998 experiment (Chapter 6).

Plots of the current velocities and directions for various sizes of waves show the presence of not only the strong easterly flow during large swells and the returning current, but also 4 eddy flows at various locations along the headland. These eddies spiral the current flow back along the headland (westerly direction) in zones where changes in orientation of the headland generate a return current. Some current shear can be seen on the model outputs as the two opposing flows pass each other, but the most important factor in the returning current flow appears to be change in the topography. The eddies appear to divide the Raglan headland into 4 distinct cells with divisions at Indicators, Whale Bay, The Pinnacles, The Ledge (Manu Bay) and the end of Manu Bay/Ngarunui Beach (Figs. 8.15 to 8.18). The figures show the currents at the headland both at low and high tides, on depth and velocity contours to identify the depths at which the currents flow and characteristics of the current velocity. Interestingly the model outputs show the current eddy flowing back into the Whale Bay region on the lee side of the shore-normal reef that was also evident in the side scan sonagraphs in this region (Chapter 5).

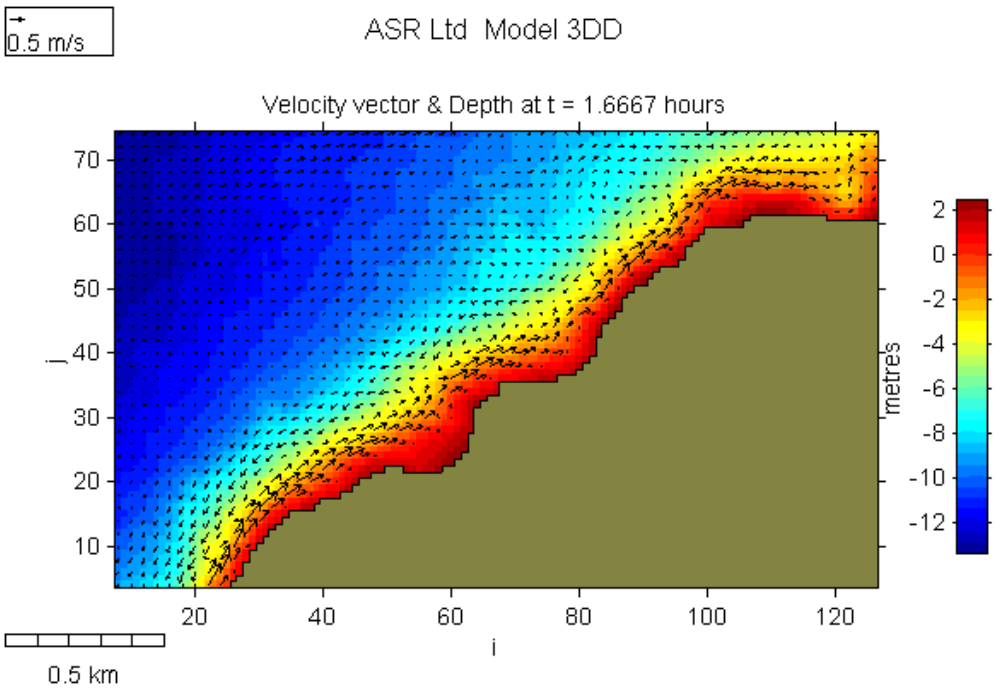

Figure 8.15: Model 3DD plot for a 2 m SW swell at low tide with a 12 sec period, showing current direction and velocity vectors on depth contours at the Raglan headland.

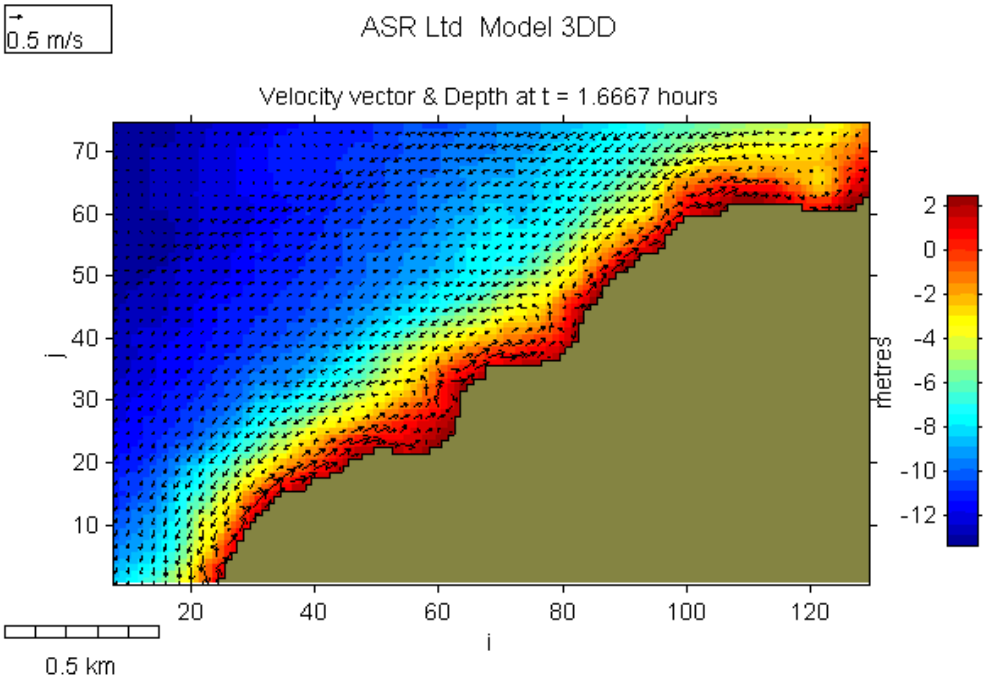

Figure 8.16: Model 3DD plot for a 2 m SW swell at high tide with a 12 sec period, showing current direction and velocity vectors on depth contours at the Raglan headland.

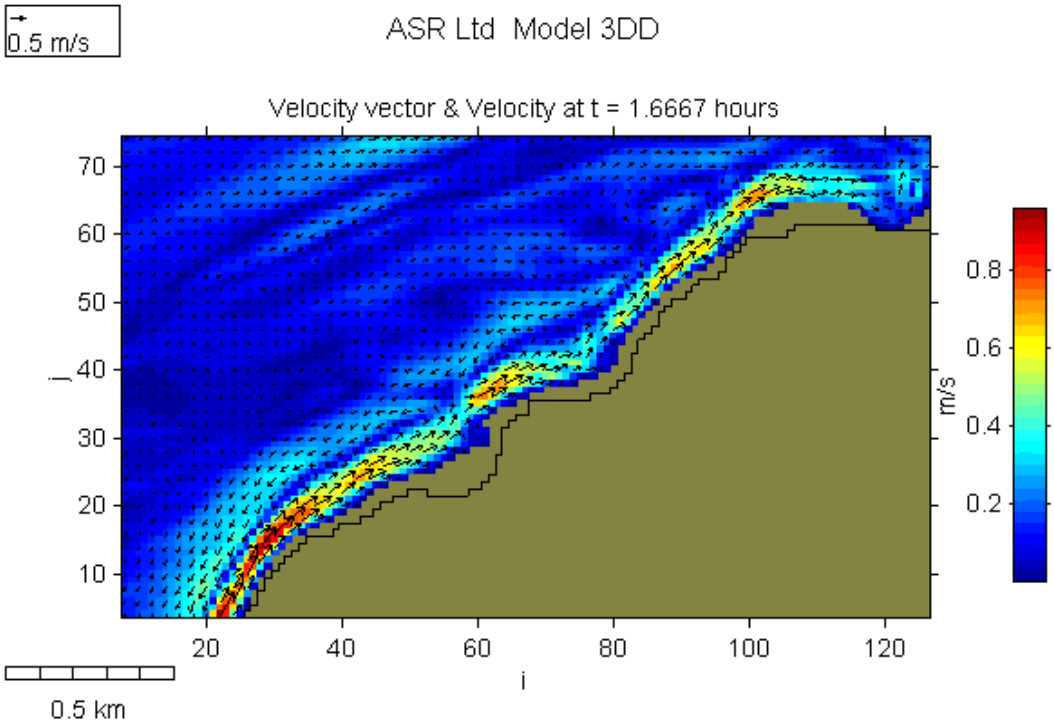

Figure 8.17: Model 3DD plot for a 2 m SW swell at low tide with a 12 sec period showing current direction and velocity vectors and contours at the Raglan headland.

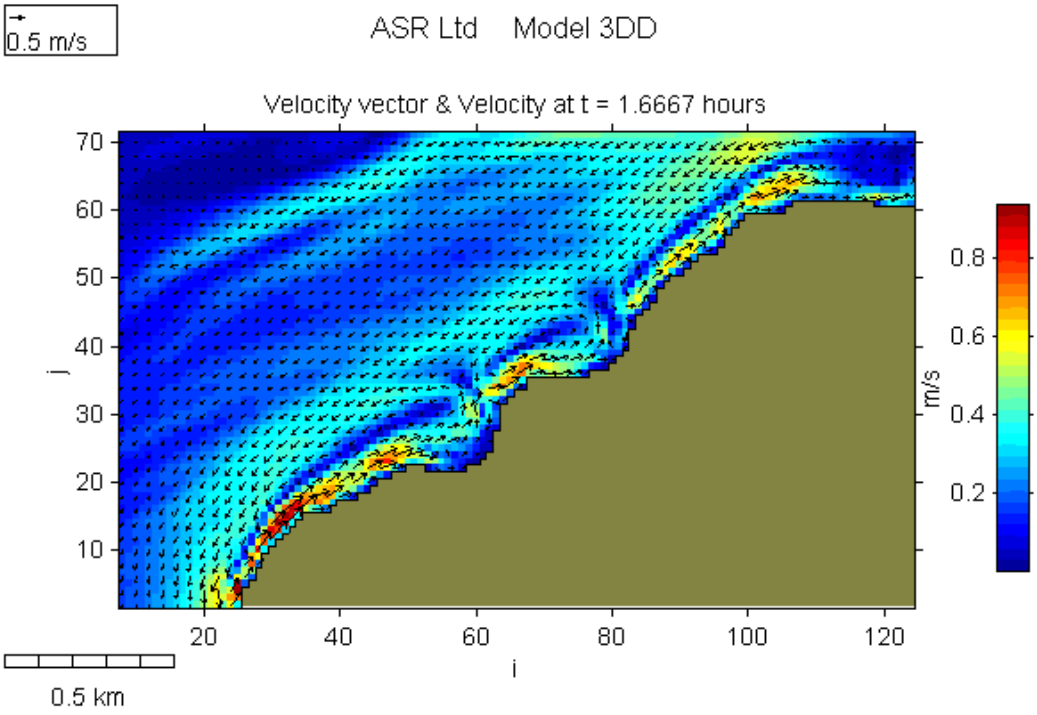

Figure 8.18: Model 3DD plot for a 2 m SW swell at high tide with a 12 sec period showing current direction and velocity vectors and contours at the Raglan headland.

The cells at Indicators and Whale Bay are very distinct, due to the significant changes in the coastal alignment in these zones, whilst at "The Ledge" a change can be seen in the current direction, but as the headland sweeps around in this location there is not the same topographical change to build a pressure gradient. However, "The Ledge" at Manu Bay breaks at low tide with a heavy barrelling wave, generated by the sudden rise in seafloor level in this location. This increased bathymetric level of rocky reefs run perpendicular to the headland in this location provides a barrier to the current flow at low tide, generating a spiraling eddy (Fig. 8.19). Surfers know when surfing "The Ledge", that the current can hold you at the breakpoint, rather than being taken in an easterly direction along the headland.

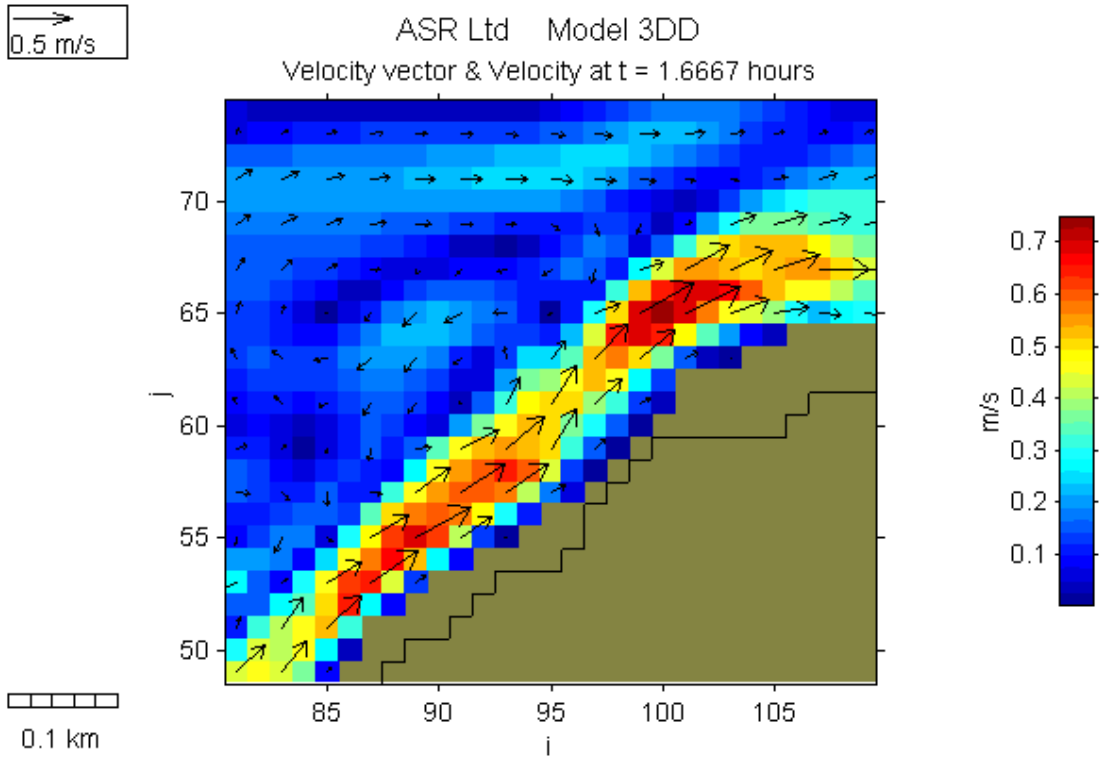

Figure 8.19: Model 3DD plot for a 2 m SW swell at low tide with a 12 sec period showing current direction and velocity at the Ledge, Manu Bay.

At Manu Bay a distinct eddy flow can also be seen re-circulating in an anti-clockwise westerly direction (Fig. 8.20). This flow is more prevalent at high tide as water

pushes back out of the Manu Bay region. At low tide there is some re-circulation, but the current tends to flow out from the shoreline of the headland.

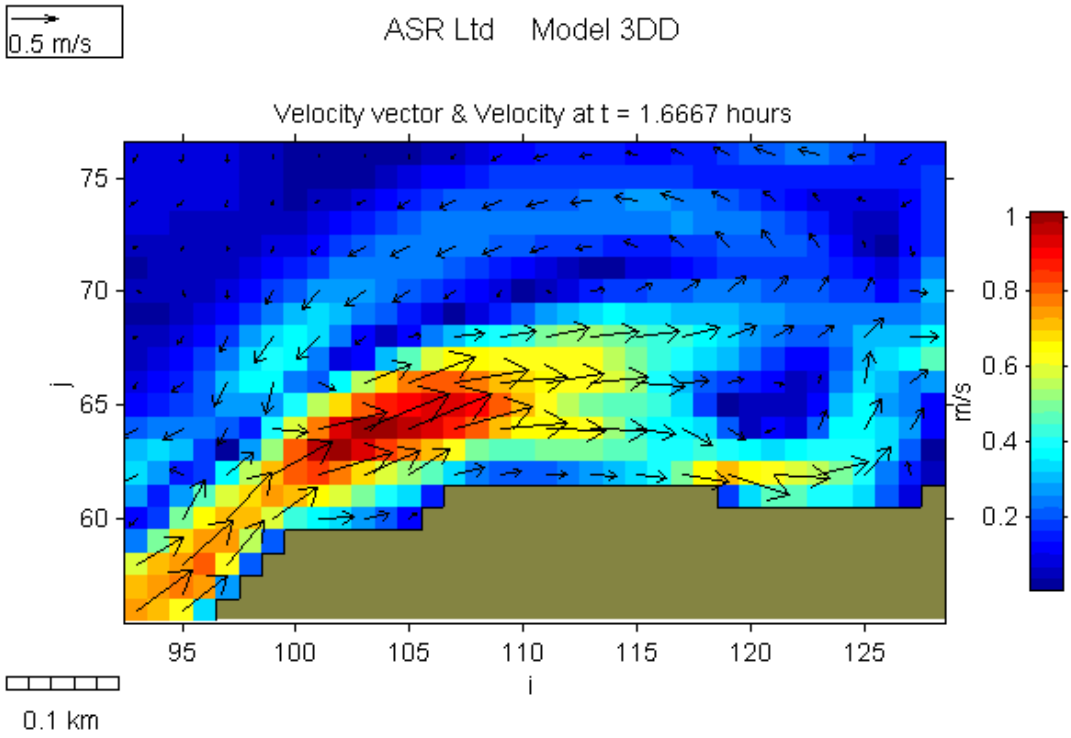

Figure 8.20: Model 3DD plot for a 2 m West swell at high tide with a 12 sec period, showing current direction and velocity at Manu Bay.

8.7 SUMMARY

The analysis of the model output data has identified the presence of strong inshore currents flowing easterly along the headland, with a lower velocity offshore returning current in a westerly direction. A zone exists between the currents, where a lower velocity current can be found flowing in a westerly direction, with some current shear evident between the two opposing flows.

The width and velocity of the currents along the headland depend on the size of the swell and the level of the tide. At low tide the current flowing eastwards is at its highest velocity, whilst at high tide the westerly current also reaches its greatest velocity. Variation occurs in both the current velocity and direction due to a change in tide level. The direction of the current flow can alter completely in direction from low tide (east) to high tide (west), as shown by the 2 m swell output at Site 1 where the current changes from 78^{o} to 227^{o}. The current is therefore changing from one where the breaking waves dictate the direction to one where the westerly directed flow along the headland is able to dominate.

During smaller swells (1-2 m) the current flowed in a westerly direction for all the results, apart from a 0.22 ms^{-1} current flowing east along the headland (78^{o}) in the 2 m waves, measured at the furthest inshore site at low tide. The less typical west and northwest swells that are usually of a smaller wave size with a shorter period than the predominant southwest swells, showed a stronger nearshore easterly current in a 2 m west swell at low tide, but overall similar current velocities and directions were again found in the 1 and 2 m waves modelled. During large swells (4 m) the model outputs show the current flows eastward along the headland inshore, attaining 1.4 ms^{-1} across the rocky boulder shoreline, whilst offshore attaining a maximum of 0.74 ms^{-1} flowing back up the headland in a westerly direction.

Model outputs of the current velocities and directions for various sizes of waves show the presence of four eddy flows, in zones where changes in orientation of the headland and topographic steering generate a return current. The eddies appear to divide the Raglan headland into distinct cells with divisions at Indicators, Whale Bay, The Pinnacles, The Ledge (Manu Bay) and the end of Manu Bay/Ngarunui Beach. The cells at Indicators and Whale Bay are very distinct and support the bedforms described from the side scan sonagraphs (Chapter 5). Coastal alignment significantly changes in these zones, whilst at "The Ledge" the increased bathymetric level of rocky reefs aligned perpendicular to the headland, provide a barrier to the current flow at low tide, generating a spiraling eddy. The ability of headlands to divide littoral systems into cells has been well documented (e.g. Komar, 1998; Short, 1999), but in this case the variation in alignment along the large scale headland appears to induce topographic forcing that drives the recirculating current, as well as a variation in wave height that generates cell circulation. This characteristic has been found at surfing headlands (Walker, 1974), headlands with embayed beaches (Short, 1999), breakwaters acting as headlands (Gourlay, 1981), and artificial reefs (Mocke *et al.*, 2003).

CHAPTER NINE

SEDIMENT FLUX

9.1 INTRODUCTION

The ability of the sandy seabed to be sustained at the Raglan headland is dependant on the input and output of sand to the littoral system. Komar (1998) defines the net longshore transport of sediment as the summation of the movement under all wave trains arriving at the shore, accounting for the different transport directions. This chapter therefore focuses on the calculation of a net sediment flux using data collected in field experiments at the Raglan headland (Chapters 6 and 7), and utilises the results of the numerical modelling (Chapter 8) to determine the characteristics and quantity of sediment in the headland littoral system.

9.2 METHODOLOGY

As time series of concentration were not measured during the experiment (only averaged concentrations from the trap were recorded), a near-bed reference concentration (C_o) was calculated using the measured orbital currents using the methodology of Black and Rosenberg (Black and Rosenberg, 1991). To examine the importance of correlation between suspended sediment concentration and current intensity on net sediment fluxes, a weighted current U_c was determined as,

$$U_c = \frac{\sum_{i=1}^{N} U_i C_{oi}}{\sum_{i=1}^{N} C_{oi}} \qquad (9.1)$$

where U_i = burst-averaged current; C_{oi} = calculated burst-averaged near-bed reference concentration; N = number of burst-averaged observations. The weighted current is indicative of the direction of net sediment flux.

The data measured in the field experiments has been used to calculate a total net flux of sediment that is transported both in an easterly and westerly direction along the headland (Table 9.3). The program SFLUX 3DD (Black, pers comm.) that applies the Black and Rosenberg method was utilised to determine the net sediment flux over the period of the input data. The program uses the bed orbital velocity, grain size and density, mean period, current velocity and current direction to calculate a cross-shore and long-shore sediment flux (Figure 9.1), which are summed to provide the total sediment flux and direction of transport. The net flux was determined using the data from the 1998 experiment as a very large >3 m swell event occurred during this period (Chapter 6). The greatest sediment transport occurs at the headland in these large wave events, and it was considered an important factor to use this data for the calculation of the sediment flux.

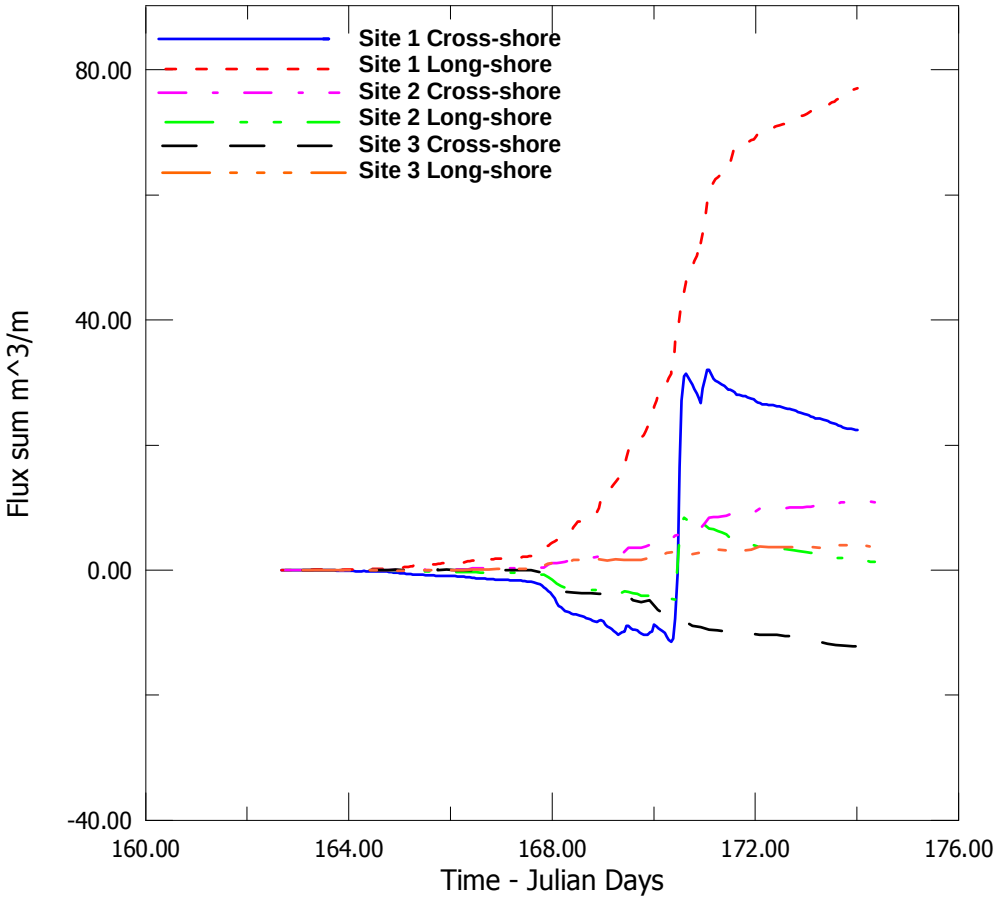

Figure 9.1: Sum of cross and longshore sediment flux from SFLUX 3DD using the 1998 experimental data.

The data used in the calculations was collected over 11.5 days and consisted of a range of swell sizes including large and small waves, and has been assumed in the analysis to be representative of a typical year. The measured data had an average wave height of 1.4 m, compared to 1.6 m identified in Chapter 2, from a year of numerically modelled data offshore at Raglan. Some correlation is therefore possible in the data, but it is noted that there may be variation in the total net sediment flux through the use of this data and the values are therefore classified as a best estimate from the available data.

9.3 RESULTS

The weighted current, which is indicative of the direction of net sediment flux, shows that when the time-averaged currents are weighted by C_o (Eqn 9.1), the currents from the 1998 experiment change their orientation to easterly and are 0.044 $m.s^{-1}$ at Site 1 and 0.130 $m.s^{-1}$ at Site 2 (Table 9.1). However, the weighted current remains negative (directed westerly) at Site 3 and is –0.034 $m.s^{-1}$.

Table 9.1: Time-averaged currents through (U) the experimental transect (12-6-98). U_c is the current magnitude through the transect after weighting by the near-bed reference concentration.

Sites	U (av) (through) $m\ s^{-1}$	U_c magnitude $m.s^{-1}$
1	-0.038 (westerly)	0.044 (easterly)
2	-0.034 (westerly)	0.130 (easterly)
3	-0.032 (westerly)	-0.034 (westerly)

The mean currents when weighted by C_o (Eqn 9.1) on the 20-4-01 also changed orientation at Site 1 to easterly attaining 0.004 ms^{-1}, whilst remaining westerly at Site 2 and 3 (Table 9.2). The smaller swell measured over the deployment period (Chapter 6) resulted in lower velocity currents and associated lower *Co* values (Chapter 7) than the first field experiment (12-6-98), when the large >3 m swell generated a large current. However, in both field experiments easterly flows were found inshore and westerly further offshore. The westerly-directed current was stronger at Site 3 than at Site 2 and shows a transition zone between the two flows that is also apparent in the modelling results (Chapter 8).

Table 9.2: Time-averaged currents through (U)) the experimental transect (20-4-01). U_c is the current magnitude through the transect after weighting by the near-bed reference concentration.

Sites	U (av) (through) m s^{-1}	U_c magnitude $m.s^{-1}$
1	-0.027 (westerly)	0.004 (easterly)
2	-0.025 (westerly)	-0.005 (westerly)
3	-0.020 (westerly)	-0.0018 (westerly)

The results of the analysis using SFLUX 3DD showed that at Site 1 nearest the rock/sand boundary, a net sediment flux of 80.3 m^3/m was determined flowing at 91^o, Site 2 further offshore had 10.9 m^3/m at 83^o and at Site 3 a net flux of 12.8 m^3/m at 343^o (Appendix 10). The data shows a large easterly-directed flux at the inshore site nearest the rocks with a smaller flux flowing in the same direction further offshore. The most offshore site had a slightly larger flux than at Site 2, but in comparison was cross-offshore in a westerly direction along the headland. These values can be extrapolated to daily rates of flux for the headland, which showed 7.1, 0.94 and 1.14 m^3/m/day at Sites 1 to 3 respectively.

The width of the current flows in both westerly and easterly directions along the headland were determined from numerical model outputs to calculate the total net sediment flux in each zone (Fig. 9.2). These were chosen to best represent the width of currents for average swell conditions at the headland. These included the rocky bed region (80 m width) and area seaward of the rock/sand boundary where Site 1 was located (60 m width). The total flux for this zone flowing east along the headland was 259200 m^3/yr. Further offshore the next zone where Site 2 was located (50 m wide) had a total flux also flowing east along the headland of 17150 m^3/yr. The summation of these two inshore flows provides a total of 276350 m^3/yr of net sediment flux flowing east along the headland, which can be rounded to approximately 275000 m^3/yr.

Table 9.3: Net sediment flux calculated from measured data (1998 experiment) using SFLUX 3DD.

	Site 1	Site 2	Site 3
Period (days)	11.3	11.6	11.2
Net flux over measurement period (m^3/m)	80.3	10.9	12.8
Direction (deg) (towards)	91	83	343
Flux per day (m^3/m/day)	7.1	0.94	1.14
Flux per year (m^3/m/year)	2592	343	416
Width of flow (m)	60 + 0.5 of 80 m for rocks* = 100	50	250
Total net flux (m^3)	259200 (east direction)	17150 (east direction)	104000 (west direction)

* McComb (2002) found the relationship of sediment collected in traps over rocks to those over sandy beds at New Plymouth south of Raglan, to be a ratio of approximately 0.5. Wave and current data was not measured in the rocky bed region during the experiments at Raglan, therefore this ratio has been used in calculations.

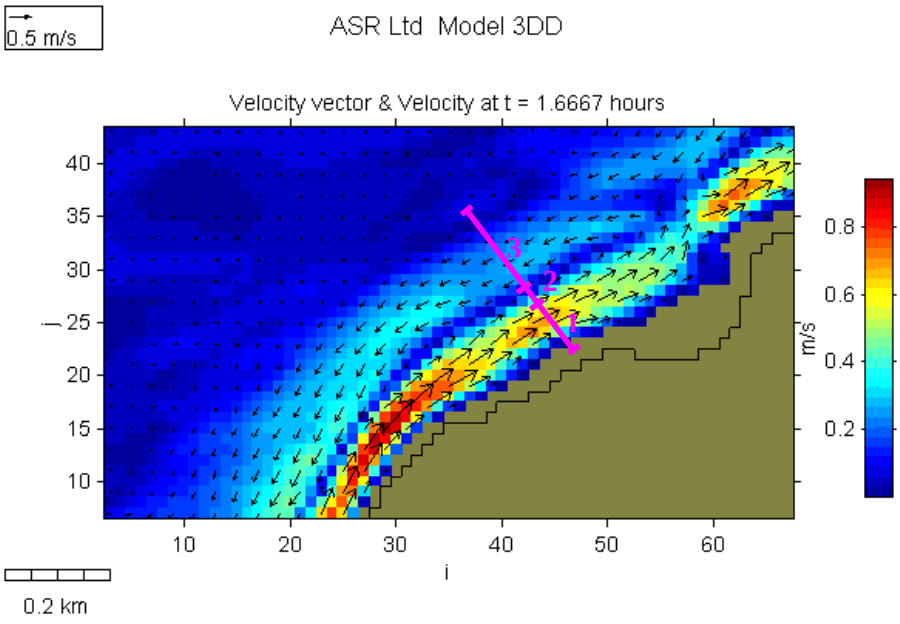

Figure 9.2: Model 3DD plot of current direction and velocity at Indicators for a 2 m SW swell at low tide with a 12 sec period, showing the width of each zone of current flow 1,2 and 3.

In comparison the region where Site 3 was located (250 m wide), has a flux of 104000 m^3/yr flowing in a west direction at the headland in the re-circulating sediment loop. This can be rounded to approximately 100000 m^3/yr of sediment transport. Subtracting this quantity from the total easterly flowing headland flux of 275000 m^3/yr provides a net sediment flux flowing from the headland littoral system of 175000 m^3/yr. This quantity corresponds well to the approximately 175000 m^3/yr of sediment that has been reported (Gibb, 1979; Hicks and Hume, 1993) to travel northwards up the coast in the longshore littoral drift in the general vicinity of Raglan.

9.4 SUMMARY

The measured currents flowed in an eastward direction inshore along the shoreline, with the velocity and width of the current increasing during large swell events at the Indicators surf break of the Raglan headland (Chapter 6 and 8). Further offshore the currents were directed westward along the headland. The direction of net sediment flux, was eastward along the headland inshore and westward further seaward, when time-averaged currents are weighted by C_o which is indicative of the direction of net sediment transport (Eqn 9.1). This infers the presence of a sediment circulation loop that sustains the sandy beds by transporting sediment in a westerly direction most of the time, with only the largest wave events disrupting this pattern close to the shore.

The results of the analysis using SFLUX 3DD to determine a net sediment flux at the field site showed that at Site 1 nearest the rock/sand boundary, a net sediment flux of 80.3 m^3/m was determined flowing at 91^o, Site 2 further offshore had 10.9 m^3/m at 83^o and at Site 3 a net flux of 12.8 m^3/m at 343^o. The flow directions correspond well to the directions of transport determined using the weighted current, with easterly flow inshore and westerly further offshore. The values of net flux can be extrapolated to daily rates of flux for the headland, which showed 7.1, 0.94 and 1.14 m^3/m/day at Sites 1 to 3 respectively.

The results of the numerical modelling allows the rate of flux per day to be applied to an average width of flow, which gives a total of approximately 275000 m^3/yr of net sediment flux flowing easterly along the headland, whilst in comparison further offshore a flux of approximately 100000 m^3/yr back along the headland was determined in the re-circulating sediment transport loop (westerly direction). The balance of these flows provides a net sediment flux flowing from the headland littoral system of 175000 m^3/yr. This quantity corresponds well to the 175000 m^3/yr of sediment that has been estimated (Gibb, 1979; Hicks and Hume, 1993) to travel northwards up the coast in the longshore littoral drift at Raglan.

CHAPTER TEN

DISCUSSION

10.1 INTRODUCTION

In this chapter the results of the fieldwork investigations, data analysis, numerical modelling, and sediment flux calculations are discussed and summarised in terms of the mechanism for sustaining sand on the seabed at the field site.

10.2 BED SUSTAINING MECHANISM

The analysis of the fieldwork data and numerical model outputs has identified the presence of strong inshore currents flowing easterly along the headland generated by breaking waves, with a lower velocity offshore returning current in a westerly direction. Figure 10.1 shows the currents with a wave breaking to the east inshore generating the nearshore current to the east, and further offshore the west flowing current is visible as a zone of discoloured water and whitecaps on the water surface as the wind blows against the current. A zone exists between the stronger easterly flow and the westerly flow where a lower velocity westerly flow can be found. Bastos *et al.* (2002), found similar characteristics at a headland with two distinct zones consisting of a strong inshore current and lower offshore flowing current. The

presence of these currents has been verified through observation of surfers in the line-up and experience of the author surfing the waves at Raglan, whereby the inshore currents sweep the surfers in an easterly direction along the headland for hundreds of metres during large waves, and further offshore the westerly current can assist with paddling to the 'take-off' point of the break.

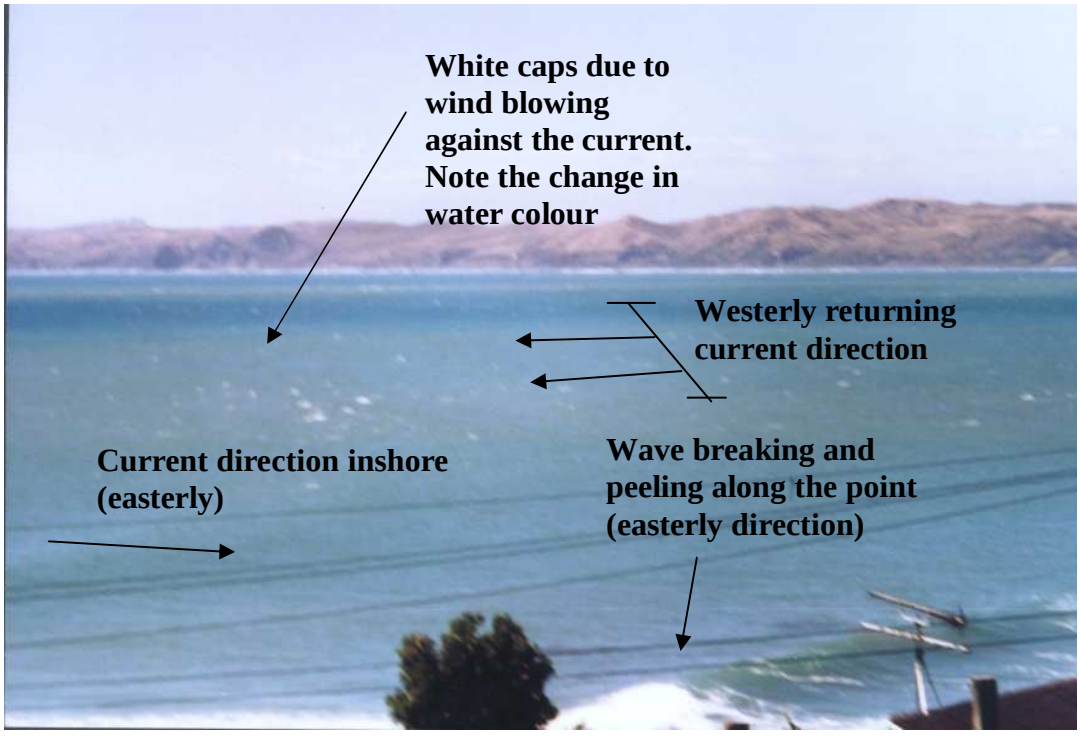

Figure 10.1: Current flowing in a westerly direction at Whale Bay back along the headland in a distinct band characterised by a change in water colour. Breaking wave at Whale Bay generating an easterly flowing current inshore with white caps visible due to a westerly wind blowing against the westerly flowing current further offshore (Source: Author, 17-6-98).

During large swells (4 m) the model outputs show the current flows easterly along the headland inshore attaining 1.4 ms^{-1} across the rocky boulder shoreline at Indicators, whilst offshore attaining a maximum of 0.74 ms^{-1} flowing back in a westerly direction. The width and velocity of the currents depend on the size of the swell and the level of the tide. At low tide the easterly flowing current is at its highest velocity, whilst at high tide the westerly current also reaches its greatest velocity. At Indicators the waves are known by surfers to shoal more at low tide with greater refraction than

at high tide, increasing the velocity of the wave-driven current. This is supported by the data from both the experimental fieldwork and the numerical modelling. Hutt (1997) identified the same trends in previous work on the Raglan headland. The waves at low tide are also more likely to be breaking closer to the sandy bed adjacent to the rock/sand boundary, with decreased turbulence and friction than found over the rocky reef, depending on the size of the waves.

It has been found by Howse (2000) that the roughness elements of rocky platforms influence the velocity and turbulence structure under oscillatory wave motion, which is supported by a study encompassing the wider New Plymouth coast 120 km south of Raglan (McComb *et al.*, 1999). The wave-orbital interaction with the hydrodynamically 'rough' substrate found at Raglan (up to 1.5 m basalt boulders) creates a greater turbulent flow over these beds (e.g. Nelson, 1996; Green *et al.*, 1998). Sediment is unable to settle in this zone and is scoured or winnowed away to leave the rocky bed exposed. Bastos *et al.*, (2002) found that at the tip of a headland bedrock exposed on the seabed was associated with scouring and maximum values of bed shear stress and increasing gradients of sand transport.

Variation occurs in both the current velocity and direction due to a change in tide level. The direction of the current can alter completely in direction from low tide (east) to high tide (west), as shown by the 2 m swell output at Site 1 where the current changes from 78^{o} to 227^{o}. The current is therefore changing as the tide rises from one where the breaking waves dictate the direction to one where the westerly directed current flow is able to dominate. During smaller swells (1-2 m) the current flowed westerly at the headland for all the results, apart from a 0.22 ms^{-1} current flowing easterly along the headland (78^{o}) in the 2 m waves, measured at the furthest inshore site at low tide. The less typical west and northwest swells that are usually of a smaller wave size with a shorter period than the predominant southwest swells, showed a stronger nearshore current in a 2 m west swell at low tide, but overall similar westerly flowing current velocities and directions were again found in the 1 and 2 m waves modelled.

These results demonstrate that for the average significant wave height for Raglan, which is 1.66 m with a 11.2 sec period (Chapter 2) the boundary position is likely to be fairly stable, as the current direction is only likely to be easterly inshore over the rocky boulders. This is supported by the results of the experiment on 20-04-01 where the weighted current (current multiplied by C_o) which is indicative of the direction of net sediment transport, showed a very low current velocity to the east (0.004 ms^{-1}) at the inshore site and to the west at the 2 sites further offshore. However, in comparison during the experiment on the 12-6-98 the weighted current was easterly at the 2 inshore sites (0.044 ms^{-1} and 0.130 ms^{-1}) and westerly further offshore. A significantly larger swell (>3.5 m) was measured over this deployment period that attained burst-averaged current velocities of 0.8 ms^{-1}, whilst the 2001 experiment attained a maximum of 0.14 ms^{-1}. The variation in these values demonstrates the significantly greater sediment transport that occurs during large swell events, verified by the difference in C_o values at the inshore site of 1.75 kg/m^3 and 1.0 kg/m^3 in 1998 and 2001 respectively. The position of the rock/sand boundary is likely to correspond with the position where currents change from east to west direction.

The successive side-scan sonar surveys undertaken at the headland have shown the seabed at Raglan is highly mobile and significantly influenced by the large waves that break along the headland generating strong unidirectional currents. The main sediment facies (i.e. areas of rocky reefs and sandy beds) have remained fairly stable in position, which suggests the sedimentary budgets are in equilibrium at the headland. Healy (1975) first introduced the concept to New Zealand of a “dynamic equilibrium beach” which appears to be applicable to the littoral system at the Raglan headland. McComb (2001) identified a similar equilibrium at New Plymouth south of Raglan.

The rock/sand boundary or interface on the seabed generally follows the shape of the headland and does not vary significantly in position long-term, whilst shore-normal

reefs and localised rocks were found to accrete or scour more readily, but still maintained their general position. Similar findings were found in other west coast studies (Carter and Lewis, 1995; McComb and Black, 2001). The location of the rock/sand boundary varies depending on recent swell conditions, with the rocky beds maintained by the strong wave-driven currents that flow east along the headland in large wave events. The boundary has been found to alter rapidly during a large swell event. Fresh rock was visible 30 m further seaward prior to the 2001 fieldwork experiment, than where the boundary had been in 1999 following a recent large (6 m) swell event in the previous week. However, the rocks recovered over the following week in the subsequent smaller swell.

The raised topography of the shore-normal reefs was found to influence the circulation patterns and sediment transport, suggesting compartmentalisation of the headland into cells, which was also shown in the numerical model outputs. The reefs provide a topographical barrier where sedimentation can occur on the upstream side as the waves and currents transport sediment into this region, and to a lesser extent on the downstream side through the westerly flowing current. However, the reefs may not necessarily impede all the sediment transport, but have a more localised effect on the sediment dynamics of the headland, with sand also transported both through gaps in the reef and carried over through suspension. This feature was also found by Scarfe *et al.* (2002) at Manu Bay, Raglan where scouring and infilling around the reefs is evident with certain reef features acting as groins to trap sand. McComb and Black (2001) obtained a similar result where seabed topography influenced currents and sediment transport leading to reversing and circulating fluxes, and raised features presented an obstacle for sediments in transit but did not prevent downstream transport.

The signature of wave generated unidirectional currents was very evident in the seabed characteristics with large (2-3.5 m) bedforms in the breaking wave zone close to the headland, whilst further offshore evidence of westerly flowing currents and re-circulating sediment pathways were visible. Verification of the megaripples using

ground truth observations by divers showed wavelengths up to 3.5 m (crest to crest) and heights of 0.5 m. Sediment samples collected at the headland can be classified as mostly slightly gravely sand, with the largest sized grains located at the tip of the headland where the waves first break (high energy zone), decreasing slightly down the headland. Sediment trap samples from both field experiments had grain sizes that both decreased further offshore and with elevation above the bed, and the rocks were rounder in shape further along the headland from the initial break point. These results demonstrate that the signature of waves and wave-generated currents is strongly present in the seabed features of the headland, which has also been found by Hume *et al.* (1997) during experiments about a large coastal headland.

The greatest percentage sediment cover over the rocks was shown by the sonagraphs to be when the boundary was furthest seaward, and is most likely due to the lower seabed level found at this time and potential shoreward movement of the boundary, with recovering of the rocks with sand in moderate swell conditions. The seabed is therefore very dynamic in nature, with sediment being both accreted and scoured at the headland, and covering and uncovering rock outcrops depending on the swell conditions at the time. The long-term habitation and zonation of marine organisms on the sub-tidal reef edge demonstrates an upper level of seabed movement. An un-retrieved S4 frame from 1998 was found to have mussels *(Perna canaliculus)* of approximately 1-2 years old inhabiting the top of the frame in 2001, showing that sand had not been permanently at this level. This has been verified with highly accurate bathymetric surveys to determine the temporal and spatial changes of the seabed adjacent to the boulder reef. The results of the surveys demonstrate that wave-climate is the predominant factor controlling the level of the bed, which can lead to a seasonal variation (i.e. higher bed level in summer when waves are typically smaller).

The seabed level along a 500 m transect when averaged levels from each bathymetric survey were compared varied by up to 0.5 m, although variation in isolated mounds and scour holes was found of up +1.8 m and -1.4 m respectively, whilst further offshore the bed showed considerably less variation. The levels correlated well to the

volume changes at the headland (i.e. lower level with prior loss of sand volume), and the bed appears to have an equilibrium level or range about which the variation occurs which is supported by the long-term habitation of the adult marine organisms on the underwater boulders and the rock reef. Significantly greater variation was found in the bed level within the first 250 m of the transect closest to the shore, where the gradient is steeper and breaking waves are located. Bathymetric maps of the difference in bed levels between surveys show a more complex erosion and accretion pattern in this zone, when compared to the offshore region. Sediment was found to accrete fairly uniformly over the entire survey area during periods of smaller wave conditions, and specific deposition was found in the lower energy zone between Indicators and Whale Bay surf breaks, demonstrating compartmentalization between these areas of the headland. Carter *et al.*, (1990) reported similar findings with currents that had accelerated to a maximum along the flanks of a headland, decelerating on bay beaches where alignment changed, showing that partitioning of wave energy is important for deposition of sediment. This sediment is likely to be available for re-suspension into an unsaturated current flow, for transport along the headland during large swells. The implication is therefore that mobile sediment is being transported or deposited during varying swell conditions at the headland, but a long-term equilibrium position exists, which is likely to be delineated by where the long-term mean currents change from being directed west to directed east at the headland.

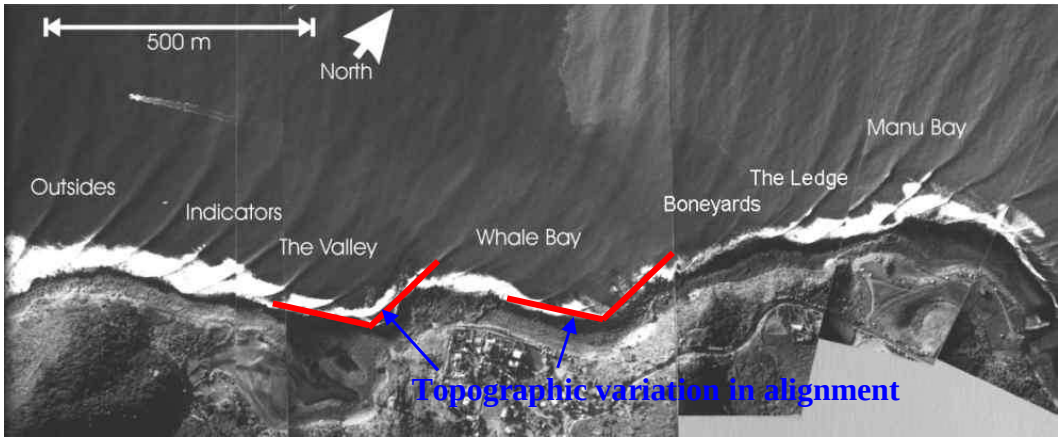

Figure 10.2: Aerial photo of the Raglan surfing breaks and topographic variation in the shoreline alignment (Hutt, et al., 2001).

The large scale and orientation of the Raglan headland (13 km from Ruapuke Beach to the Raglan Harbour entrance) allows only the low frequency swells to refract around the headland to create surfing waves, a feature that makes headland breaks particularly sought after by surfers since waves will be 'cleaner' on headlands than on other parts of the coast. Mead and Black (2001c) found that there are 7 different breaks at Raglan, comprised of various components and wave characteristics with their own distinctive form of breaking wave, i.e. different peel angles and breaking intensity (Fig. 10.2).

The numerical modelling has shown that these different surf breaks or compartments are also significant in the current and sediment dynamics of the headland. The re-circulating current results from topographic steering and the build-up of a pressure gradient due to variation in the shoreline alignment at different locations along the headland. These locations can be divided into 4 cells and compare very closely to the compartmentalisation of the headland characterised by the different surf breaks (Fig. 10.3). Variation also occurs in wave height in these regions that can generate cell circulation as currents flow from areas of high waves to those with low waves (Fig. 10.2). The eddy flows are more prevalent at high tide, and the results indicate there is some current shear between the easterly and westerly flowing currents as the two travel past each other. The effect that topographic forcing can have on current re-circulation and cell circulation due to a variation in wave set-up has been well documented in a number of publications (e.g. Zimmerman, 1981; Middleton *et al.*, 1993; Komar, 1998; Aiken *et al.*, 2002). Symonds *et al.*, (1995) found that pressure gradients can be found as waves break on a reef generating a return flow due to wave set-up. The model has demonstrated these factors have a role in the current re-circulation at Raglan, with the radiation stress component being a particularly important mechanism.

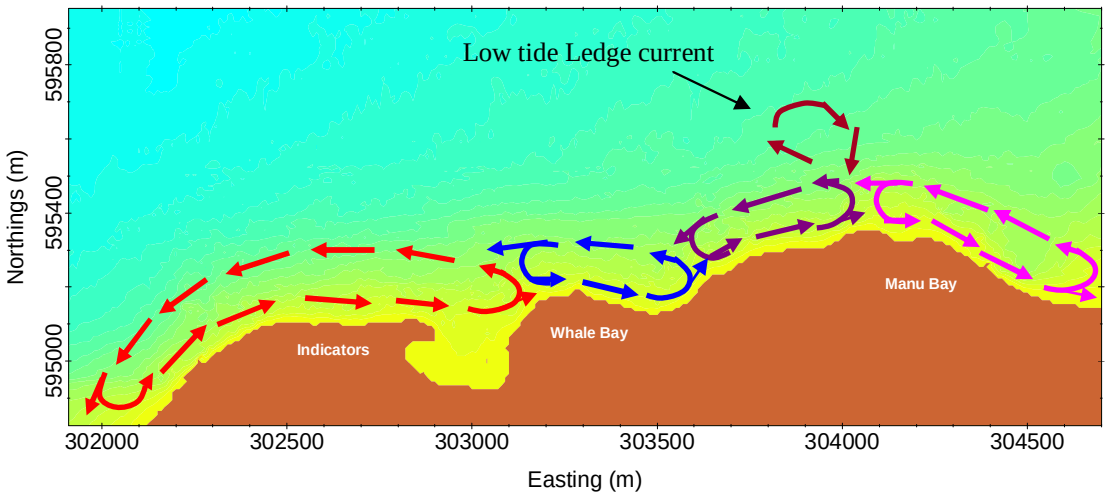

Figure 10.3: Idealised diagram of Raglan showing the 4 cells operating at the headland, and the low tide eddy flowing back onto the Ledge.

The shallow and exposed nature of surfing headlands provide long peeling waves allowing a board-rider to ride on the unbroken wave face. The seabed shape and refraction of the waves in relation to depth contours, is the greatest influence on the quality of the surf break, although due to headlands oblique orientation to the waves, strong wave-driven currents are often present. It is well documented that when waves approach a shore at an oblique angle, a shore-parallel current is generated as waves break in the near-shore zone, transporting sediment along the coast (Fredsøe and Diegard, 1992; Komar, 1998). Headlands such as the Raglan headland can be classified as sections of the coast where the alignment substantially varies from the predominating coastline orientation, where the higher oblique angle of the shoreline generates large wave-driven currents. This is confirmed by the field measurements, numerical modelling and observations of surfers paddling in the surf-zone at Raglan, that make the break difficult if not impossible to surf in large swell conditions. These currents provide a strong sediment transport mechanism that may preclude beach formation, and in the case of Raglan maintain exposure of the rocky bed.

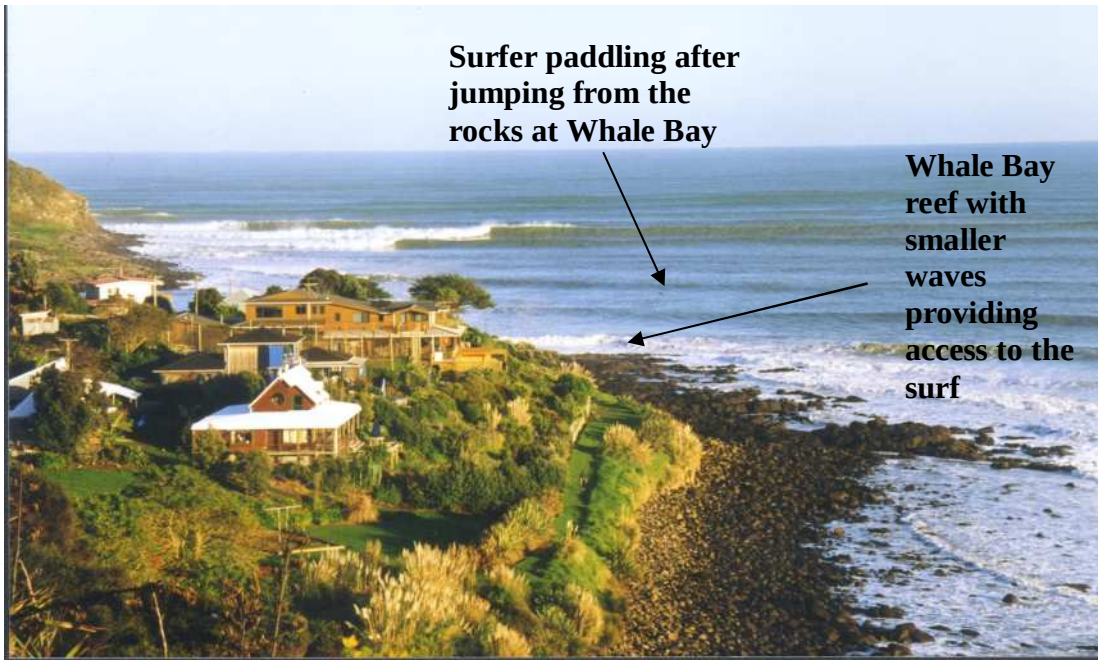

Figure 10.4: Whale Bay looking west to Indicators showing change in alignment at Whale Bay reef and smaller waves, and surfer paddling to the 'line-up' after jumping from the rocks (Source: Author, 9 September 2002).

However, the large scale of the Raglan headland and compartmentalisation into different zones, can provide not only a variety of surf breaks and current patterns, but deposition of sediment can also be found in these zones (e.g. Whale Bay reef) due to smaller waves, lower currents and the presence of the reef acting as a barrier to the sediment transport. Carter *et al.*, (1990) reported similar findings where a decrease of wave energy where headland alignment changed allowed deposition of sediment in this zone. The presence of these zones also increases the surfability in a range of conditions, as potential access for surfers through the surf zone is available (Fig. 10.4).

Currents at surfing headlands have been previously studied in relation to sediment transport and dynamics of the adjoining coast, and have a major influence on the seabed stability of the headland, e.g. Kirra Point, Greenmount, Noosa Heads – all in Queensland, Australia (Chapman, 1981). Wave-driven currents during large swell events have been commonly found to transport large quantities of sediment along the coast (Komar, 1998). This is usually in the form of slugs of sand moving around the

headland (Short, 1999). This does not however appear to be the case at Raglan, where the large rounded shape of the headland allows sediment to pass more readily along the coast, when compared to the more protruding nature of headlands that are known to trap sediment upstream (e.g. Point Danger, Gold Coast).

Raglan is similar to smaller scale headlands that allow sediment to pass on a more regular basis such as Burleigh Heads and Greenmount on the Gold Coast (Smith, 1982). Indeed, the individual surf breaks or compartments at Raglan (i.e. Indicators), could be considered as being more like Burleigh Heads in relation to scale and length of surfing ride. The west coast also has consistent waves throughout the year with a significant number of swells in the 2-3 m range and less frequent larger swells, all capable of transporting sediment. This results in a constant supply of sediment to the headland, rather the 'lean' and 'full' nature found at many other protruding headlands. The results have shown that sediment is not able to settle in the surf-zone where strong wave-driven currents as well as increased turbulence in this rocky region are prevalent. At the onset of a large swell, sediment is eroded from the headland to a point where the currents change from easterly to westerly. The bed then recovers to a point correlating with the swell size and amount of sediment available for deposition, and attains a dynamic equilibrium in the sedimentary regime, i.e. balance between time-averaged input and output volumes of sediment in the littoral cell.

On the Gold Coast of Australia significant quantities of sediment are winnowed away and transported from the headlands if insufficient sediment supply is available. Storms have been found to create scour holes if sediment supply is lacking, or in areas where waves and currents interact with a nearshore reef (Pattearson and Patterson, 1983). Due its position in the wave shadow of Snapper Rocks on the Gold Coast, Australia, areas such as Snapper Rocks beach before the construction of the Tweed River sand-bypass system had a tendency to cycle between erosion and accretion depending on prevailing conditions and sand supply. The mass balance between saturated and unsaturated flows and the strength of the current is therefore a

significant factor in the stability of the headland. This determines whether accretion or erosion occurs either along the entire headland or varies spatially in different zones. This is also the case at Raglan, although the bed appears to be more stable due to the more consistent surf conditions (i.e. size and direction) predominantly from the west-southwest direction, rather than the small surf conditions with the odd larger swell event on the Gold Coast. Raglan does not experience the boom and bust sediment level that has been found on the Gold Coast headlands, where large swells transporting slugs of sand are required to replenish the seabed of the headland.

McComb and Black (2001) found at New Plymouth, south of Raglan that despite high sediment entrainment potential, stability of the bed is attributed to sedimentary equilibrium under a dynamic and multi-directional sediment flux. The data suggested that littoral transport is not the fundamental cause of erosion, but rather sediment suspension by waves and net transport by the variable coastal currents. At Raglan strong wave-driven currents are prevalent and sediment is also suspended by waves and transported by currents flowing either east or west along the headland. Inshore along the headland the net sediment flux was found to be in an easterly direction at the headland, measuring 2592 m^3/m/yr closest to the rock/sand boundary and 416 m^3/m/yr in a westerly direction further offshore. The combination of a re-circulating system and sedimentary equilibrium between the two flux flows are most likely responsible for the stability of the bed in this unique surfing headland environment at Raglan. Sedimentary equilibrium is also supported by both the bathymetric and side-scan survey results. The bed is maintained whilst sediment is also transported from the littoral cell at the headland into the northerly littoral flow up the coast. A net sediment flux of approximately 275000 m^3/yr flows easterly along the headland and approximately 100000 m^3/yr in a westerly direction at the headland, providing 175000 m^3/yr of sediment flux to the northwards flowing longshore littoral transport system (estimated by Gibb (1979) and Hicks and Hume (1993) at approximately 175000 m^3/yr; Fig. 10.5).

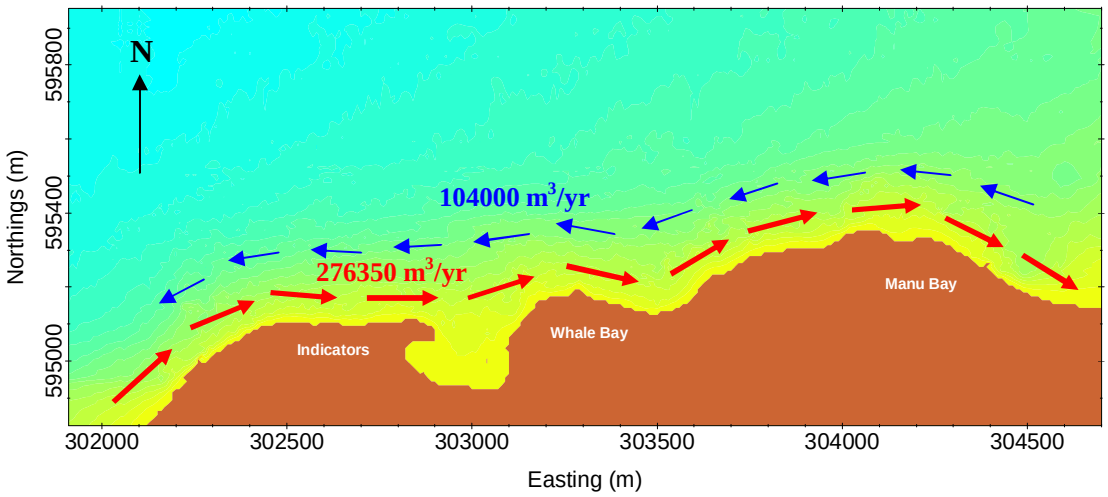

Figure 10.5: Idealised diagram of Raglan showing the two directions of current flow along the headland and the quantity of net sediment flux. Red arrows depicting the inshore easterly flow and the blue the westerly offshore current.

The current flowing both easterly along the headland and westerly in a anti-clockwise recirculating gyre at the headland, supported by both field data and numerical modelling can be confirmed as the mechanism most likely responsible for sustaining the sandy bed at the headland, in the presence of strong shoreward currents and large net sediment fluxes that occur during large swell events. Similar re-circulating sediment pathways have been found on headlands such as the rotating hydraulic cell that generates an escape current flowing in reverse (inshore) to the normal littoral drift on the Gold Coast headlands, which provides an equilibrium recycling of sediments (Smith, 1982). Also, at Westshore on the New Zealand east coast local re-circulating flows in the lee of the headland have been found to rotate in both clockwise and anticlockwise directions depending on the inflowing current direction at the time (Mead *et al.*, 2001). The presence of rip currents flowing seaward due to changes in coastal orientation and 'end effects', has been described by both Short (1999)(rip currents flowing from embayed headlands) which are capable of transporting significant quantities of sediment seaward in their flow (Roy *et al.*, 1994), and Walker (1974) who investigated various aspects of surfing breaks and showed returning currents assisted surfers in paddling back to the 'take-off point' of

the break. Komar describes reversing longshore currents driven by oblique waves and cell circulation due to variation in wave set-up, whilst recirculating current flows have been found at breakwaters which can be compared to headlands (e.g. Gourlay, 1981), as well as artificial surfing reefs where submerged headlands act in the same manner as a surfing headland with currents generated that flow seaward in a recirculating direction (Mocke, 2003).

CHAPTER ELEVEN

CONCLUSIONS

An experimental study of the wave, current and sediment dynamics has been conducted at a surfing headland at Raglan, New Zealand. The main findings of the study are summarised in terms of the objectives of the thesis:

- The results show that the mechanism responsible for maintaining the sandy seabed in the presence of energetic wave conditions and strong wave-driven currents, is a combination of sediment transport around the headland to the east, i.e. west coast littoral drift system, and a local re-circulating sediment pathway transporting sediment in the west direction. Sediment moves continually around the headland supplying the littoral system at the headland, and not in "slugs' as reported for other large protruding headlands (e.g. Komar, 1998; Short, 1999).

- The net sediment flux calculated from 12 days of field data, which was inferred as representative of a typical year of waves at the Raglan headland was approximately 275000 m^3/yr flowing east inshore and approximately 100000 m^3/yr to the west offshore. The difference of 175000 m^3/yr flows from the headland littoral cell into the northwards flowing longshore transport system of the west coast. This compares well to the previous estimate of 175,000 m^3/yr (Gibb, 1978; Hicks and Hume, 1993) of net transport along the coast. The values of net sediment flux, along with the combined evidence of the bathymetric and side-scan surveys, shows that a sedimentary equilibrium may exist that has balanced input and output volumes of sand in the littoral cell sustaining sand on the seabed of the headland.

- The alignment of the Raglan headland provides an environment where waves of a high oblique angle generate strong wave-driven currents in the surf-zone, flowing inshore along the headland in an easterly direction. Alternatively, the westerly flowing current is generated by the interaction of wave-driven forces and topographic variation along the length of the large-scale headland, where change in the alignment of the shoreline and submerged reefs build a pressure gradient and create topographic steering of the currents. Variation in wave height also generates cell circulation as currents flow from areas of high waves to those of low wave set-up. The presence of both the easterly and westerly flowing currents is confirmed by observations of surfers in the 'line-up' and experience of the author surfing at the headland.

  Similar currents have been reported at surfing headlands where variation in alignment assisted surfers to paddle back to the 'take-off' point of the surf break (Walker, 1974), at headlands with oblique waves breaking in relation to the shoreline and variation in wave set-up (Komar, 1998), in the lee of headlands and breakwaters (Gourlay, 1974), at headlands where 'end effects' create current re-circulation (Short, 1995 and 1999), topographic forcing (Hume *et al.,* 1997; Middleton *et al.,* 1993; Aiken *et al.,* 2002), and at reefs where incident wave momentum is partitioned between driving cross reef currents against bottom friction and balancing an offshore-directed pressure gradient due to wave set-up (Symonds *et al.,* 1995). The presence of both a strong inshore current over rocky beds to an offshore returning flow, were reported by Bastos *et al.* (2002) to be related to the development of eddies, pressure gradient forces, and variation in bed shear stress at a headland.

- Numerical model outputs confirm the current re-circulation due to topographic steering and show the presence of four cells, which compare very closely to the compartmentalisation of the headland characterised by the main surf breaks. The model outputs also showed the width and velocity of the current flows depend on the size of the swell and the level of the tide. Large wave events at low tide generate the strongest currents flowing east along the headland inshore, whilst at

high tide the westerly current also reaches its greatest velocity, and the eddy flows are at their most prevalent. Greater shoaling of waves at low tide increases the velocity of the wave-driven current.

- The wave-orbital interaction with the hydrodynamically 'rough' substrate found at Raglan on the rocky boulder reef (up to 1.5 m basalt boulders) creates a greater turbulent flow over these beds. Sediment is unable to settle in this zone and is scoured or winnowed away to leave the rocky bed exposed. The more shoreward regions over the rocky seabed are influenced by the easterly flowing currents more often, eroding sand away in the absence of sufficient upstream inputs to maintain the sediment flux. The location of the interface between the sand and rocky seafloor corresponds to the point where the long-term mean currents change from flowing easterly to flowing westerly along the headland. This location varies depending on recent swell conditions, i.e. size and duration of the swell. The sandy bed is winnowed away, being unable to exist over the long term where strong wave-driven flows down the headland cause large net sediment transport. Near bed reference concentrations confirm that significantly greater sediment transport occurs in large wave events at the headland, and are highest nearer the shoreline of the headland, i.e. breaking wave zone.

- Shore-normal reefs protruding from the headland do not provide a significant barrier to longshore sediment transport, but are likely to influence the current circulation and sediment dynamics found in the compartments of the headland. The side-scan sonagraphs and bathymetric surveys showed areas of sedimentation on the upstream and downstream sides of the reefs, which occurs through variation in both wave height, and current speed and direction in these zones as shown in the numerical model outputs. Similar findings were reported by both Scarfe *et al.* (2002) at Raglan and at New Plymouth 120 km south of Raglan by McComb *et al.* (1999), who also reported reversing and circulating fluxes in these regions. Carter *et al.* (1990) also found deposition at a headland where wave energy and currents had decreased due to a change in coastal alignment.

- Bathymetric surveys have shown that despite significant volume changes in the quantity of sand being transported or deposited at the headland, the seabed level fluctuates about a stable long-term equilibrium position of the bed (quasi permanent position). This is supported by the long-term habitation and zonation of marine organisms on the sub-tidal reef edge, demonstrating an upper level of seabed movement.

- Side scan sonar surveys showed the underwater rocky reef/sand boundary generally followed the shape of the headland and remained fairly stable in position, fluctuating a maximum of 30 m after a large 6 m swell event, but recovering in the subsequent smaller swell. Generally the sediment facies, i.e. areas of rocky and sandy bed remained positionally stable, with the edge of the rock/sand boundary and patch margins being more readily eroded or accreted. The characteristics of the seabed in the study area reflect the presence of the surf zone and strong unidirectional currents, and show the presence of re-circulating sediment pathways flowing to the west. The orientation and position of mega-ripples, and sediment grain size and distribution is strongly related to the location of the breaking waves and wave driven currents. The largest sized sediment grains were located at the tip of the headland where the waves first break (high energy zone), decreasing both easterly and offshore from the headland, and with elevation above the bed.

STUDY RELEVANCE TO SURFING AND ARTIFICIAL REEF DESIGN

Surfability of a headland can be significantly decreased in large surf conditions where strong inshore currents along the headland make the break difficult if not impossible to surf. However, the large scale and variation in topographic alignment of the Raglan headland not only compartmentalises the current and sediment circulation into cells, but also allows access for surfers in the zones of lower wave height and decreased current velocity, e.g. Whale Bay reef. It is recommended that the affect of strong current velocities on surfability of artificial surfing reefs must be considered in the design process if amenity of the structure is to be maximised. This may include possible methods of access for surfers such as paddling channels, e.g. Narrowneck

reef, Gold Coast) and recirculating currents that not only make getting 'out the back' to the 'take-off point' easier, but assist in maintaining a stable sandy seabed adjacent to the reef.

FURTHER RESEARCH

This study investigated the mechanism for sustaining the sandy seabed at the Indicators surf break of the Raglan headland. The study has shown that investigation of the current and sediment dynamics of surfing headlands such as the large scale headland found at Raglan is limited and further research into the following areas would be of scientific interest:

- Research on the current and sediment dynamics of various surfing headlands that have a range of breaking wave types (i.e. 'tubes' to 'mal' waves) relative to the shape of the seabed and scale/orientation of the headlands. Comparison of the dynamics of these coastal features could then be undertaken.

- Detailed analysis of the role that shore-normal submerged reefs have on influencing the current and sediment dynamics would be of interest, especially if structures such as "The Ledge", which create heavy "tubing" waves, are recreated in artificial surfing reef construction.

- Research into the effect of the turbulence generated by the rocky boulder reef armouring the shoreline, would lead to a better understanding of entrainment and deposition in these regions.

- A larger scale study encompassing the entire headland from Ruapuke beach to Raglan Harbour would be of valuable scientific interest as very limited research has been undertaken in this west coast environment. It would provide an understanding of the role that the interaction between the headland and harbour have on this coastal system, and the influence on the beach stability at Ngarunui Beach which has suffered from erosion in the past.

12 REFERENCES

Aagard, T. and B. Greenwood., 1995. Suspended sediment transport and morphological response on a dissipative beach. *Continental Shelf Research,* 15(9), 1061-1086.

Aagard, T. and B. Greenwood., 1999. *Directionality of cross-shore sediment transport in the surf-zone under high-energy conditions.* Proceedings of Coastal Sediments '99, Long Island, New York. pp. 1003-1018.

Aiken, C.M., Moore, A.M. and J.H. Middleton., 2002. The nonnormality of coastal ocean flows around obstacles, and their response to stochastic forcing. *Journal of Physical Oceanography,* 32(10), 2955-2978.

Allen, J.R.L. 1985. *Principles of physical sedimentology.* George Allen and Unwin Publishers, London. 272 p.

Andrews, C., 1997. Sandy shoreline response to sub-tidal and sub-aerial reefs, breakwaters and islands. Unpublished Master of Science Thesis, Earth Sciences Department, University of Waikato. 137 p.

Ashton, A. Murray, A.B. and O. Arnault., 2001. Formation of coastline features by large-scale instabilities induced by high-angle waves. *Nature,* 414(6861), 296-300.

Auckland City Council., 2000. Growing New Beaches. Vision Hauraki Gulf, July 2000 Newsletter, Issue 16. 10 p.

Baker, E.T., Milburn, H.B. and D.A. Tennant., 1988. Field assessment of sediment trap efficiency under varying flow conditions. *Journal of Marine Research,* 46, 573-592.

Baquerizo, A. and M.A. Losada.,1998. Longitudanal current induced by oblique waves along coastal structures. *Coastal Engineering,* 35(3), 211-230.

Bartholomew, W. and T. Baker., 1996. *Bustin' down the door.* Harper Collins Publishers Ltd, Australia. 368 p.

Bartholomeusz, W.G., 1985. Beach and nearshore sediment data for the New Plymouth beach restoration study. Central Laboratories Report 2-85/11. MWD, Lower Hutt. 59 p.

Basco, D.R., 1983. Surfzone currents. *Coastal Engineering,* 7(2), 331-355.

Bastos, A.C., Kenyon, N.H. and M. Collins., 2002. Sedimentary processes, bedforms and facies, associated with a coastal headland: Portland Bill, Southern UK. *Marine Geology,* 187(3-4), 235-258.

Beach, R.A. and R.W. Sternberg., 1992. Suspended sediment transport in the surf zone: response to incident wave and longshore current interaction. *Marine Geology*. 108, 275-294.

Beach, R.A. and R.W. Sternberg., 1996. Suspended-sediment transport in the surf-zone: response to breaking waves. *Continental Shelf Research,* 16(15), 1989-2003.

Beamsley, B. J., 1996. Shoreface wave height reinforcement and frictional dissipation off Waihi Beach, with emphasis on seabed characteristics and numerical modelling. Unpublished MSc Thesis, University of Waikato. 125 p.

Beamsley, B.J. and K.P. Black., 2003. The effect of offshore reefs on inshore surfing conditions. *Proceedings of the 3rd International Surfing Reef Symposium*, Raglan, New Zealand. pp. 99-144. CD publication, ISBN: 0-473-09801-6.

Beer, T., 1997. *Environmental Oceanography.* CRC Press, Florida. 367 p.

Bhana, M., 1988. *The New Zealand Surfing Guide.* Heinemann Reed, NZ. 137 p.

Bird, E.C.F., 1968. *Coasts: An Introduction to Systematic Geomorphology.* Australian National University Press, Canberra. 246 p.

Black, K.P. and T.R. Healy., 1982. *Sediment transport investigations in a New Zealand tidal inlet.* Proceedings of 18th Coastal Engineering Conference (ASCE), Cape Town, Republic of South Africa. Volume 3, 2436-2457.

Black. K.P. and S.L. Gay., 1987. Eddy formation in unsteady flows. *Journal of Geophysical Research,* 92, 9514-9522.

Black, K.P. and M.A. Rosenberg., 1991. Suspended sediment load at three time scales. *Coastal Sediments'91 Conference,* ASCE, Seattle, WA, pp. 313-327.

Black, K.P., 1992. Evidence of the importance of deposition and winnowing of surficial sediments at a continental shelf scale. *Journal of Coastal Research,* 8, 319-331.

Black, K.P. and M.A. Rosenberg., 1992a. Natural stability of beaches around a large bay. *Journal of Coastal Research,* 8(2), 385-397.

Black, K.P. and M.A. Rosenberg., 1992b. Semi-empirical treatment of wave transformation outside and inside the breaker line. *Coastal Engineering,* 16, 313-345.

Black, K.P., 1995. The hydrodynamic model 3DD and support software. *Occasional Report No. 19.* Department of Earth Sciences, University of Waikato, 53 p.

Black, K.P., Andrews, C., Green, M., Gorman, R., Healy, T., Hume, T., Hutt, J., Mead, S. and A. Sayce., 1997. Wave dynamics and shoreline response on and around surfing reefs. *Proceedings of the 1st International Surfing Reef Symposium*, Sydney, Australia. pp. 1-10.

Black. K.P. Hutt, J.A., and S.T. Mead., 1998. Narrowneck Reef – Report 2: Surfing Aspects. Technical report prepared for the Gold Coast City Council. Centre of Excellence in Coastal Oceanography and Marine Geology, University of Waikato and National Institute of Water and Atmospheric Research, 120 p.

Black, K.P., 1999. *Designing the shape of the Gold Coast reef: Sediment dynamics.* Coasts and Ports 1999, Perth, Australia. pp. 58-63.

Black, K.P. and J.W. Oldman., 1999. Wave mechanisms responsible for grain sorting and non-uniform ripple distribution across two moderate energy, sandy continental shelves. *Marine Geology,* 162, 121-132.

Black. K.P., S.T. Mead, P. McComb, A. Jackson and K. Armstrong., 1999. New Plymouth Foreshore Redevelopment: Reef and Beach Feasibility Study. Report prepared for New Plymouth City Council by the Department of Earth Sciences, University of Waikato, 57 p.

Black, K.P., 2001a. 3DD computational marine and freshwater laboratory. ASR Ltd, PO Box 13048, Hamilton, New Zealand.

Black, K.P., 2001b. Natural and artificial reefs for surfing and coastal protection. *Journal of Coastal Research,* Special Issue No. 29, pp. 1.

Black, K.P., 2001c. Artificial surfing reefs for erosion control and amenity: Theory and Application. *Journal of Coastal Research,* Special Issue No. 34, 1-14.

Black, K.P. and C.J. Andrews., 2001a. Sandy shoreline response to offshore obstacles, Part 1: Salient and tombolo geometry and shape. *Journal of Coastal Research*, Special Issue No. 29, pp. 82-93.

Black, K.P. and C.J. Andrews., 2001b. Sandy shoreline response to offshore obstacles, Part 1: Discussion of formative mechanisms. *Journal of Coastal Research*, Special Issue No. 29, pp. 94-101.

Black, K.P. and S.T. Mead., 2001. Design of the Gold Coast reef for surfing, public amenity and coastal protection: Surfing aspects. *Journal of Coastal Research, Special Issue 29,* 115-130.

Black, K.P. Mead, S.T. and J. Mattew., 2001. Design and Approvals for an Artificial Reef for Protection of Noosa Main Beach: Detailed Investigations and Modelling. Final Report for Noosa Council and ICM Ltd, June 2001. 298 p.

Blenkensopp, C., 2003. The effect of micro-scale bathymetric components (steps) on wave breaking and implications for artificial surfing reef construction tolerances. *Proceedings of the 3rd International Surfing Reef Symposium,* Raglan, New Zealand. pp. 139-155. CD publication, ISBN: 0-473-09801-6.

Bloesch, J. and N.M. Burns., 1980. A critical review of sedimentation trap technique. *Schweizerische Zeitschrift fur Hydrologie,* 42, 15-55.

Bodge, K.R., 1989. A literature review of the distribution of longshore sediment transport across the surf zone. *Journal of Coastal Research,* 5(2), 307-328.

Boothroyd. J.C., 1978. Mesotidal Inlets and Estuaries. Chapter 6, In: Davies, R.A. (ed.) *Coastal Sedimentary Environments,* Ed. R.A. Davie. Springer, New York. pp. 287-360.

Bohnsack, J.A. and D.L. Sutherland., 1985. Artificial reef research: a review with recommendations for future priorities. *Bulletin of Marine Sciences,* pp. 23-34.

Bradshaw, B.E., Healy, T.R., Nelson, C.S., Dell, P.M. and W.P. de Lange., 1994. Holecene sediment lithofacies and dispersal systems on a storm-doinated, back-arc shelf margin: The east Coromandel coast, New Zealand. *Marine Geology,* 119, 75-98.

Brander, R.W. and A.D. Short., 2000. Morphodynamics of a large-scale rip current system, Muriwai Beach, New Zealand. *Marine Geology,* 165, 27-39.

Brander, R.W., Osborne, P.D. and K. Parnell., 2003. High-energy beach and nearshore processes. In: Goff, J.R, Nichol., S.L and H.L Rouse. (eds). *The New Zealand Coast – Te Tai O Aotearoa.* Dunmore Press, Palmerston North, New Zealand. 312 p.

Bray, M.J., Carter, D.J. and J.M. Hooke., 1995. Littoral cell definition and budgets for central southern England. *Journal of Coastal Research,* 11(2), 381-400.

Briggs, R.M., Itaya, T., Lowe, D., and A. Keane., 1989. Ages of Pliocene – Pleistocene Alexandra and Nagatutra Volcanics, Western North Island, New Zealand. Some geological implications. *New Zealand Journal of Geology and Geophysics,* 32, 417-427.

Briggs, R.M., 1993. Distribution, form, and structural control of the Alexandra Volcanic Group, North Island, New Zealand. *New Zealand Journal of Geology and Geophysics,* 26, 47-55.

Briggs, R.M., Rosenberg, M.D., deLange, P.J., Itaya, T., King, P.R. and R.C. Price., 1997. Geology and geochemistry of Gannet (Karewa) Island, Tasman Sea: a rift-

related nephelinitic ring. *New Zealand Journal of Geology and Geophysics,* 40, 263-273.

Brookes, H.D. and M.O. Green., 2000. Determination of wave climate for the Auckland region, New Zealand. *Journal of Coastal Research Special Issue 34,* 23-29.

Buckeridge, St.J.S., 1995. Coastal protection in New Zealand: A systems approach. *The Proceedings of the Institution of Professional Engineers New Zealand Annual Conference,* Palmerston North, New Zealand. pp. 252-256.

Burgess, S.C., Black, K.P., Mead, S.T. and M.J. Kingsford., 2003. Considerations for artificial surfing reef's as habitat for marine organisms. *Proceedings of 3rd International Surfing Reef Symposium,* Raglan, New Zealand. pp. 289-302. CD publication, ISBN: 0-473-09801-6.

Butman, C.A., 1986. Sediment trap biases in turbulent flows: results from a laboratory flume study. *Journal of Marine Research,* 11, 381-400.

Button, M., 1991. Laboratory Study of Artificial Reefs. Bachelor of Engineering Dissertation, Department of Civil and Environmental Engineering, University of Western Australia. 107 p.

Carter, L. and K. Lewis., 1995. Variability of the modern sand cover on a tide and storm driven inner shelf, South Wellington, New Zealand. *N.Z Journal of Geology and Geophysics,* 38, 451-470.

Carter, R.W.G., Jennings, S.C. and J.D. Orford., 1990. Headland erosion by waves. *Journal of Coastal Research,* 6(3), 517-529.

Chapman, D.E.M., 1981. Coastal erosion and sediment budget, with special reference to the Gold Coast Australia. *Coastal Engineering,* 4, 207-227.

Chew, S.Y., Wong, P.P. and K.K. Chin., 1974. Beach development between headland breakwaters. *Proceedings of 14th International Costal Engineering Conference, (ASCE),* 4, 4667-4681.

Clemens, K.E. and P.D Komar., 1988. Oregon beach-sand compositions produced by the mixing of sediments from multiple sources under a transgressing sea. *Journal of Sedimentary Petrology,* 58, 519-529.

Clifford, N.J., French, J.R. and J. Hardisty., 1993. *Turbulence: Perspectives on flow and sediment transport.* John Wiley and Sons, Chichester, England. 360 p.

Clifton, H. E., 1976. *Wave-Formed Sedimentary Structures – A Conceptual Model.* In: Beach and Nearshore Sedimentation, Eds. Davis and Ethington. Society of Economic Paleontologists and Mineralogists, Special Publication N0. 24.

Cotton, C.A., 1942. *Geomorphology, An introduction to the study of landforms.* Whitcombe and Tombs Ltd. 505 p.

Cotton, C.A., 1974. *Bold Coasts.* A.H. and A.W. Reed, Wellington. 354 p.

Daborn, G. R. and B. Dickie., 1997. Community based Environmental Management: Whaingaroa (Raglan) Harbour and Water Catchment. *Proceedings of the Combined Australasian Coastal Engineering and Ports Conference*, Christchurch, New Zealand, 1997. pp. 485-490.

Dahm, J., 2002. Muriwai. Coastal Hazard Management Strategy. Report for Auckland Regional Council and Rodney District Council. 85 p.

Dally, W.R., 1989. Quantifying Beach 'Surfability'. *Proceedings Beach Technology Conference,* Tampa, Florida. pp. 154-159.

Dally, W.R. 1990. Stochastic modeling for surfing climate. *Proceedings of 22nd International Conference on Coastal Engineering,* Delft, The Netherlands. ASCE, New York. pp. 516-529.

Dally, W.R. 2001a. Improved stochastic models for surfing climate. *Journal of Coastal Research,* Special Issue, 29, 41-50.

Dally, W.R. 2001b., 2001b. The maximum speed of surfers. *Journal of Coastal Research,* Special Issue, 29, 33-40.

Davies, J.L., 1972. *Geographical Variation in Coastal Development.* Longman Group Ltd, London. 204 p.

Davies, P.A., Besley, P. and D.L. Boyer., 1990. An experimental study of flow past a triangular cape in a linearly stratified fluid. *Dynamics of Atmospheres and Oceans,* 14, 497-528.

Davies, P.A., Dakin, J.M., and R.A. Falconer., 1995. Eddy formation behind a coastal headland. *Journal of Coastal Research,* 11(1), 154-167.

Deacon, G.E.R., 1968. *Oceans. An atlas-history of man's exploration of the deep.* Paul Hamlyn London. 258 p.

Deigard, R., Fredscoe, J. and I.B. Hedegaard., 1986.Suspended sediment in the surf zone. *Journal of Waterway, Port, Coastal, and Ocean Engineering,* 109(1), 115-127.

deLange, W.P., Healy, T.R. and Y. Darlan., 1997. Reproducibility of sieve and settling tube textural determinations for sand-sized beach sediment. *Journal of Coastal Research,* 13(1), 73-80.

Denniss, T. Middleton, J.H. and R. Manasseh., 1995. Re-circulation in the lee of complicated headlands: a case study of Bass Point. *Journal of Geophysical Research,* 100(C8), 16087-16101.

Department of Public Works., 1960. *Bank and shore protection in California highway practice.* State of California Department of Public Works, Division of Highways. 423 p.

Douglass, S.L., 1996. Nearshore Placement of Sand. *Proceedings of the 25th International Conference on Coastal Engineering,* ASCE, pp. 3708-3721.

Dyer, K.R., 1986. *Coastal and Estuarine Dynamics.* Chischester, Wiley. 342 p.

Dyer, M.J., 1994. Beach profile change at St. Clair Beach, Dunedin. Unpublished MSc Thesis, University of Cantebury. 150 p.

Ebersole, B.A. 2002., Large-scale laboratory measurements of longshore sediment transport under spilling and plunging breakers. *Joirnal of Coastal research, 18(1), 118-135.*

Epps, W.R., 1987. The influence of headland alignment on the plan shape of modelled zeta-form beaches. *Australian Geographical Studies,* 25(2), 47-53.

Ewans, K.C. and A.C. Kibblewhite., 1992. Spectral features of the New Zealand deep-water ocean wave climate. *New Zealand Journal of Marine and Freshwater Research.* 26, 323-338.

Evans, P. and R. Ranasinghe., 2001. Artificial surfing reefs: A paradigm in coastal protection. *Proceedings of Coasts and Ports 2001, 15th Australasian Coastal and Ocean Engineering Conference,* Gold Coast, Australia. pp. 128-133.

Falconer, R.A., Wolanski, E. and L. Mardapitta-Hadjipandeli., 1984. *Numerical simulation of secondary currents in the lee of headlands.* Proceedings of the 19th Coastal Engineering Conference (ASCE), Houston, Texas. pp. 2414-2433.

Fleming, C.A., 1990. *Principles and effectiveness of groynes.* In Pilarczyk, K.P. (Ed.)., Coastal Protection. Proceedings of the short course on coastal protection. Delft University of Technology. A.A. Balkema, Roterdam. pp. 121-156.

Flint, S.B., 1998. Sediment Trapping in the Nearshore Coastal Environment. Unpublished MSc Thesis, University of Waikato. 198 p.

Foster, D.N., 1972. Breakwater Stability: Kirra Beach. Technical Report No. 72/13, Water Research Laboratory, University of New South Wales, Australia. 80 p.

Flores Lira, M.A. and A.J., Maza., 1971. *New Type of structures for littoral drift control.* Proceedings of the 14th Congress of the International Association for Hydraulic Research, Vol. 4, pp. 177-182.

Fredsøe, J., Anderson, O.H. and S. Silberg., 1986. Distribution of suspended sediment in large waves. *Journal of Waterway, Port, Coastal, and Ocean Engineering,* 111(6), 1041-1059.

Fredsøe, J. and Deigaard, R., 1992. *Mechanics of coastal sediment transport.* Advanced Series on Ocean Engineering, World Scientific. 369 p.

Freeland, H.J., 1990. The flow of a coastal current past a blunt headland. *Atmosphere-Ocean,* 28(3), 288-302.

Furukawa, K., 2000. The role of a man-made headland in generating patches in coastal waters of Isle Bay, Japan. *Estuarine, Coastal and Shelf Science,* 50, 33-37.

Gaillard, P., 1988. Numerical modelling of wave-induced currents in the presence of coastal structures. *Coastal Engineering,* 12, 63-81.

Galloway, G.S., Collins, M.B., and A.D. Moran, 1989. Onshore/offshore wind influence on breaking waves: An empirical study. *Coastal Engineering,* 13, 305-323.

Gardner, W.D., 1980. Field assessment of sediment traps. *Journal of Marine Research,* 38, 41-52.

Gerschler, T., 1978. Reefer madness. Surfing, 14(5), 83-85.

Geyer, W.R. and S. Signell., 1991. Measurements and modelling of the spatial structure of nonlinear tidal flow around a headland. Tidal Hydrodynamics, John Wiley and Sons, Inc, 883 p.

Geyer, W.R., 1993. Three-dimensional tidal flow around headlands. *Journal of Geophysical Research,* 98(C1), 955-966.

Gibb, J. G., 1978. The problem of coastal erosion along the "golden coast", western Wellington, New Zealand. Water and Soil Division, Ministry of Works and Development, Wellington. Technical Publication No. 10, 67 p.

Gibb, J.G., 1979. Late Quaternary Shoreline Movements in New Zealand. Unpublished PhD Thesis, Victoria University of Wellington. 216 p.

Gibbs, R.J., Mathews, M.D. and D.A. Link., 1971. The relationship between sphere size and settling velocity. *Journal of Sedimentary Petrology,* 41(1), 7-18.

Goff, J.R., Nichol, S.L. and H.L. Rouse., 2003. *The New Zealand coast: Te Tai Aotearoa.* Dunmore Press, Palmerston North, New Zealand. 312 p.

Golden Software, Inc., 1996. *Surfer Surface Mapping System, Version 6.03.* Golden Software, Incorporated, Colorado, USA.

Goles, G.G., Briggs, R.M. and Rosenberg, M.D., 1996. Late Pliocene stratigraphic succession and volcanic evolution of Karioi volcano, Western North Island, New Zealand. *New Zealand Journal of Geology and Geophysics,* 39, 283-294.

Gorman , R. and K.P. Black., 1997. Harbour wave studies with a hybrid explicit-implicit hydrodynamics model. *Pacific Coasts and Ports '97 Conference,* Christchurch, New Zealand, pp. 631-636.

Gorman, R.G., 1997. TSERIES – A Matlab system for time-series analysis. Operating Manual, National Institute of Water and Atmospheric Research, New Zealand. 65 p.

Gorman, R.M. 2000. The New Zealand coastal wave climate: 1979-1993 WAM hindcast. National Institute of Water and Atmospheric Research Internal Report 66, Hamilton.

Gorman, R.M. and A.K. Laing., 2000. Bringing wave hindcasts to the New Zealand coast, *Journal of Coastal Research Special Issue*, 34, 30-37.

Gourlay, M.R., 1974. Wave set-up and wave-generated currents in the lee of breakwater or headland. *Proceedings 14th Conference in Coastal Engineering,* Copenhagen, Denmark. ASCE, New York. Vol. , pp. 1976-2987.

Gourlay, M.R., 1981. Beach processes in the vicinity of offshore breakwaters. *Proceedings of the 5th Australasian Conference on Coastal and Ocean Engineering, Perth, Australia.* pp. 129-134.

Gourlay, M.R., 1996. *History of coastal engineering in Australia.* In: Kraus, N.C. (ed). History and heritage of coastal engineering. American Society of Civil Engineers (ASCE), New York. 603 p.

Green, M.O. and K.P. Black., 1999. Suspended-sediment reference concentration under waves: Field observations and critical analysis of two predictive models. *Coastal Engineering,* 38, 115-141.

Green, M.O. Hewitt, J.E. and S.F. Thrush., 1998. Seabed Drag Coefficient over Natural Beds of Horse Mussels (Atrina zelandica). *Journal of Marine Research,* 13(1), 111-133.

Greenwood, B., Osborne, P.D., Bowen, A.J. and D.G. Hazen., 1990. Nearshore sediment flux and bottom boundary dynamics: The Canadian Sediment Transport Programme (C-Coast). *Proceedings Coastal Engineering*, Vol. 3, 2227-2240.

Greilach, P.R., Black, K.P., Parry, G.D. and M. Forsyth., 1995. Scallop dredging and sedimentation in Port Phillip Bay. Victorian Institute of Marine Sciences, Working Paper No. 29. 52 p.

Guilcher, A., 1958. *Coastal and submarine morphology.* Methuen and Co. Ltd, London. 274 p.

Hales, L.Z. and J.B. Herbich., 1972. *Tidal inlet – Ocean wave interaction.* Proceedings of 13th Coastal Engineering Conference (ASCE), Vancouver, B.C., Canada. pp. 669-688.

Hallermieir, R.J., 1982. Bedload and wave thrust computations of alongshore sand transport. *Journal of Geophysical Research,* 87(C8), 5741-5751.

Hanes, D.M. and D.A. Huntely., 1986. Continuous measurements of suspended sand concentration in a wave dominated nearshore environment. *Continental Shelf Research,* 6(4), 585-596.

Hargraves, B.T. and N.M. Burns., 1979. Assessment of Sediment Trap Efficiency. *Journal of Limnology and Oceanography,* 24(6), 1124-1137.

Harris, T.F., 1990. Greater Cook Strait: form and flow. DSIR Marine and Freshwater, Wellington, 212 p.

Harvey, B., 1998. Untamed Coast. Auckland's Waitakere Ranges and west coast beaches. Exisle Publishing Ltd, Auckland. 208 p.

Healy, T.R., 1975. The equilibrium beach – a model for real estate development and management of the coastal zone in northeast New Zealand. *Proceedings of the International Geographical Union Regional Conference,* Massey University, New Zealand. pp. 319-324.

Healy, T.R. and K. Harada., 1997. Towards the Concept of "At One with Nature" in Japenese Coastal Engineering and Environment. *Proceedings of the Combined Australasian Coastal Engineering and Pacific Coasts and Ports Conference*, Christchurch, NZ. pp. 275-278.

Healy, T.R., and R.M. Kirk., 1992. Coasts. In: Soons, J.M. and M.J. Selby., (ed.) *Landforms of New Zealand,* Longman Paul, Auckland,. pp. 81-104.

Heath, R.A., 1982. What drives the mean circulation on the New Zealand west coast continental shelf. *New Zealand Journal of Marine and Freshwater Research,* 16, 215-226.

Herbich, J.B., 2000. *Handbook of Coastal Engineering.* McGraw-Hill, New York. USA.

Hicks, D.M. and T.M. Hume., 1993. Morphologies and sand volumes of flood and ebb tidal deltas on the New Zealand coast. Proceedings of the *11th Australasian Conference on Coastal and Ocean Engineering.* Instituition of Engineers, Australia, Townsville, pp. 665-670.

Hicks, D.M. and T.M. Hume., 1996. Morphology and Size of Ebb Tidal Deltas at Natural Inlets on Open-sea and Pocket-bay Coasts, North Island, New Zealand. *Journal of Coastal Research,* 12(1), 47-63.

Ho, S.K., 1971. Crenulate Shaped Bays. Thesis No. 346, Asian Institute of Technology, Bangkok, Thailand. 180 p.

Howse, B., 2000. Bed roughness of reefs and the relationship of sediment flux to benthic reef ecology. Unpublished M.Sc. thesis, University of Waikato. 184 p.

Hsu, J.R.C., Silvester, R. and Y. Xia., 1989. Applications of headland control. *Journal of Waterway Port Coastal and Ocean,* 115, 299-310.

Hsu, J.R.C., Uda, T. and R. Silvester., 1993. Beaches downcoast of harbours in bays. *Coastal Engineering,* 19(1-2), 163-181.

Hume. T.M. and C.E. Herdendorf., 1990. Morphologic and Hydrologic Characteristics of Tidal Inlets on a Headland Dominated, Low Littoral Drift Coast, Northeastern New Zealand. *Journal of Coastal Research Special Issue 9,* 527 – 563.

Hume, T.M., Bell, R.G., de Lange, W.P., Healy, T.R. Hicks, D.M. and R.M. Kirk., 1992. Coastal Oceanography and Sedimentology in New Zealand, 1967-91. *New Zealand Journal of Marine and Freshwater Research,* 26, 1-36.

Hume, T.M., Green, M.O., Beamsley, B., de Lange, W.P. and M. Hicks., 1995. Seabed Morphology/Roughness Affect Coastal Processes. *Proceedings of Coastal Dynamics '95,* Gdansk, Poland. pp. 254-259.

Hume, T.M., Bell, R.G., Parnell, K.E. and R.M. Kirk., 1997. Coastal physical sciences. In: Davey, F. and R. Pridmore. (eds). *The New Zealand Knowledge Base: Earth Sciences.* Ministry of Science and Technology, Wellington. pp. 52-58.

Hume, T.M., Vennell, R. and K.P Black., 1997. Sounding out the currents: Acoustic mapping of current structure at a coastal headland. Water and Atmosphere, 5(2), 19-21.

Hume, T.M., Black, K.P., Oldman, J.W. and R. Vennell., 1997. Signatures of Wave and Current Forcing on the Seabed about a Large Coastal Headland. *Pacific Coasts and Ports '97*. Christchurch, New Zealand. pp. 319-324.

Hume, T.M., Green, M.O. and J.W. Oldman., 1999., What Happens at the Seabed off a Headland During a Tropical Cyclone. *Proceedings of Coastal Sediments '99.* Long Island, New York. pp. 1836-1851.

Hume, T.M., Oldman, J.W. and K.P. Black., 2000. Sediment facies and pathways of sand transport about a large deep water headland, Cape Rodney, New Zealand. *New Zealand Journal of Marine and Freshwater Research,* 34, 695-717.

Hutt, J.A., 1997. Bathymetry and Wave Parameters Defining the Surfing Quality of Five Adjacent Reefs. Unpublished MSc Thesis, University of Waikato, New Zealand. 169 p.

Hutt, J.A. Black, K.P. Jackson, A. and J. McGrath., 1998. Narrowneck Reef. Report 1: Surf Zone Experiments. Centre of Excellence in Coastal Oceanography and University of Waikto report prepared for Gold Coast City Council, 1998, 63 p.

Hutt, J.A. and K.P. Black., 2001. Numerical Model Validation Against Surfing Reef Measurements. New Zealand Marine Sciences Society Conference. Hamilton, NZ, August 2001. pp. 46.

Hutt, J.A., Black, K.P. and S.T Mead., 2001. Classification of surf breaks in relation to surfing skill. *Journal of Coastal Research,* Special Issue 29, 66-81.

Inman, D.L., Komar, P.D. and A.J. Bowen., 1968. *Longshore transport of sand.* Proceedings of the 11th Conference on Coastal Engineering (ASCE), London, England. pp. 298-306.

Ingman, D.E. and W.J. Wallace., 1989. *Oceanography.* Wadsworth Publishing Company, California, USA. 513 p.

Jackson, L.A. and McGrath, J.E., 1995. Proposed Headland for Surfers Paradise. *12th Australian Conference on Coastal and Ocean Engineering.* Melbourne, Australia. pp. 21-24.

Jirka, G.H., 2001. Large scale flow structures and mixing processes in shallow flows. *Journal of Hydraulic Research,* 39(6), 567-573.

Kamphuis, W.J., 2000. *Introduction to coastal engineering and management.* Advanced series on ocean engineering – Volume 16. World Scientific Publishing Ltd. 437 p.

Kibblewhite, A.C., Bergquist, P.R. and M.R., Gregory., 1982. *Maui Development Environmental Study.* Report on Phase II 1977-1981. The University of Auckland. 169p.

Kim, H., O'Conner, B.A., Park, I. and Y. Lee., 2001. Modeling effect of intersection angle on near-bed flows for waves and currents. *Journal of Waterway, Port¸Coastal and Ocean Engineering,* 127(6), 308-318.

Kimberly, M.M., 1989. Fitting a logarithmic spiral to the shoreline of a headland-bay beach. *Computers and Geosciences,* 15(7), 1089-1108.

Klein, A.H.F. and J.T. Menzies. 2001. Beach morphodynamics and profile sequence for a headland bay coast. *Journal of Coastal Research,* 17(4), 812-835.

Klein, A.H.F., Filho, L.B. and D.H. Schumacher., 2002. Short-term beach rotation processes in distinct headland bay beach systems. *Journal of Coastal Research,* 18(3), 442-458.

Kobayashi, N. and A. Entin., 2001. Obliquely incident wave reflection and run-up on steep rough slope. *Journal of Coastal Research,* 17(4), 919-930.

Komar, P.D., 1985. Computer models of shoreline configuration: Headland erosion and the graded beach revisted (sand movement). *In:* Woldenberg,. M.J., (ed). *Models in Geomorphology.* Allen and Unwin. London. pp. 155-170.

Komar, P. D., 1998. *Beach Processes and Sedimentation*. 2nd edition, Prentice-Hall Inc., New Jersey. 544p.

Komar, P.D. and D.L. Inman., 1970. Longshore sand transport on beaches. *Journal of Geophysical Research,* 75, 5914-5927.

Kraus, N.C., 1987. Application of portable traps for obtaining point measurements of sediment transport rates in the surf zone. *Journal of Coastal Research,* 3(2), 139-152.

Kyotoh, H., Fujii, S. And D.V. To., 2000. Currents induced by long waves propagating towards a beach over a wavy bed. *Journal of Fluid Mechanics,* 413, 317-343.

Laing, A.K., 1993. Estimates of wave height for New Zealand waters by numerical modelling. *New Zealand Journal of Marine and Freshwater Research,* 27, 157-175.

Leblond, P.H., 1979. An explanation of the logarithmic spiral plant shape of headland-bay beaches. *Journal of Sedimentary Petrology,* 49(4), 1093-1100.

Lesnik, J.L., 1979. An Annotated Bibliography on Detached Breakwaters and Artificial Headlands. Miscellaneous Report No. 79-1. U.S. Army, Corps of Engineers. Coastal Engineering Research Centre, Fort Belvoir, Va. 22060. 81 p.

Lewis, K. B., 1979. Storm Dominated Inner Shelf, Western Cook Strait, New Zealand. *Marine Geology,* 31, 31-43.

Lewis, D.W and D. McConchie., 1994. *Analytical Sedimentology.* Chapman and Hall, New York. 197 p.

Li, Z. and A.G. Davies., 1997. Effect of grain size gradation and reference concentration of sediment transport beneath large waves. *Proceedings of Coastal Dynamics '97,* pp. 245-254.

Longuet-Higgins, M.S., 1970. Longshore currents generated by obliquely incident sea waves. *Journal of Geophysical Research,* 75(33), 203-248.

Lou, J. and P.V. Ridd., 1997. Modelling of suspended sediment transport in coastal areas under waves and currents. *Estuarine, Coastal and Shelf Science,* 45, 1-16.

Lloyd, R.J., 1980. Noosa beach restoration scheme. Proceedings of the 7th Coastal Engineering Conference (ASCE), Sydney, Australia. pp. 1619-1635.

Lueras, L. 1995. Surfing Indonesia: A search for the world's most perfect waves. Periplus Action Guide, California, USA. 152 p.

Macdonald, H.V. and D.C Paterson., 1984. *Beach response to coastal works, Gold Coast, Australia.* Proceedings of the 19th Coastal Engineering Conference (ASCE), Houston, Texas. pp. 1522-1538.

Magoon, O.T. and B.L. Edge., 1978. Stabilisation of Shorelines by Use of Artificial Headlands and Enclosed Beaches. *Coastal Zone 78*. pp. 1367-1370.

Marsh, S.W., Vincent, C.E. and P.D. Osborne., 1999. Bedforms in a laboratory wave flume: An evaluation of predictive models for bedform wavelengths. *Journal of Coastal Research,* 15(3), 624-634.

Mattews, E., 1977. Movement of Sand on some Western Taranaki Beaches. Unpublished M.Sc. thesis, University of Auckland. 135 p.

Maunder, W., 1970. The climate of New Zealand – physical and dynamic features. In: World survey of climatology, H.E. Landsberg (Ed.), Elsevier, London.

McClennan, N.R. 1982. Fitzroy Beach Processes and Quantitative Estimation of Littoral Drift. Unpublished M.Sc. Thesis, Earth Sciences Dept., University of Waikato. 200 p.

McComb, P.J., Black, K.P., Atkinson, P.N., Healy, T.R. and R.G. Bell., 1997. High-resolution wave transformation on a coast with complex bathymetry. *Pacific Coasts and Ports'97*, Christchurch, New Zealand (Vol. 2), pp. 995-1000.

McComb, P., Black, K., Healy, T. and P. Atkinson., 1999 Coastal and Sediment dynamics at Port Taranaki, New Zealand; a large, multi-faceted field experiment. *Coastal Structures '99*, Santander, Spain, pp. 823-8329.

McComb, P., Beamsley, B. and S. Mead., 2000. Telstra Saturn Cable Crossings Report. ASR Ltd. 120 p.

McComb, P., 2001. Coastal and Sediment Dynamics in a High Energy Rocky Environment. Unpublished PhD thesis. University of Waikato. 286 p.

McComb, P. J. and K.P. Black., 2001. Dynamics of a Nearshore Dredged-Sand Mound on a Rocky, High-Energy Coast. *Journal of Coastal Research Special Issue 34*, 550-563.

McKenzie, P., 1958. Rip-current systems. *Journal of Geology*, 66, 103-113.

McLean, S. R., 1981. The Role of Non-Uniform roughness in the Formation of Sand Ribbons. *Marine Geology*, 42; 49-74.

McNinch, J.E. and R.A. Luettich., 2000. Physical processes around a cuspate foreland: implications to the evolution and long-term maintenance of a cape-associated shoal. *Continental Shelf Research*, 20, 2367-2389.

Mead, S.T., 2000. Incorporating High Quality Surfing Breaks into Multi Purpose Reefs. Unpublished PhD Thesis, University of Waikato, New Zealand. pp 209+ appendices.

Mead, S. T. and K. P. Black., 2001a. Functional Component Combinations Controlling Surfing Wave Quality at World-Class Surfing Breaks. *Journal of Coastal Research Special Surfing Issue 29*, 21-32.

Mead S.T., and K.P. Black., 2001b. Predicting the Breaking Intensity of Surfing Waves. *Journal of Coastal Research Special Surfing Issue No. 29*, 51-65.

Mead, S. T. and K. P. Black., 2001c. Field Studies Leading to the Bathymetric Classification of World-Class Surfing Breaks. *Journal of Coastal Research Special Surfing Issue 29*, 5-20.

Mead, S. T., K. P. Black and P. McComb., 2001. Lyall Bay Surfing Reef Feasibility Study. Report for the Lyall Bay Surfing Reef Charitable Trust, Wellington. 248 p.

Mead, S. T., and P. McComb., 2001. Issues and Options Report: Assessment of a Long-Term Solution to Erosion Control at St Clair Beach, Dunedin. Report to the Dunedin City Council, November 2001. 28 p.

Mead, S.T., Black, K.P. and P. McComb., 2001. Westshore Coastal Process Investigation. Technical Report for Napier City Council, September 2001. 194 p.

Mead, S.T. and K.P. Black., 2002. Multi-Purpose Reefs Provide Multiple Benefits – Amalgamating Coastal Protection, High-Quality Surfing Breaks and Ecological Enhancement to Maximise User Benefits and Development Opportunities. *Proceedings for Surfing Art Science Issues Conference 2 (SASIC 2)*, Ventura, California. pp. 47-63.

Mead, S. T., K. P. Black, J. Frazerhurst and B. Scarfe., 2003. The Impacts of Wave Focussing on Surfing Reef Design on Continental Shelf to Sub-Tidal Reef Scales. *3rd International Artificial Surfing Reef Symposium*, Raglan, New Zealand. pp. 115-137.

Melville, G., 1984. Headlands and offshore islands as dominant controlling factors during late quaternary barrier formation in the Forster-Tuncurry area, New South Wales, Australia. *Sedimentary Geology.* 39, 243-271.

Middleton, J.H., Griffin, D.A. and A.M. Moore. 1993. Oceanic circulation and turbulence in the coastal zone. *Continental Shelf Research,* 13(2-3), 143-168.

Mocke, G.P. and G.G. Smith., 1992. Wave breaker turbulence as a mechanism for sediment suspension. *Coastal Engineering,* 2, 2279-2292.

Mocke, G., Smit, F., Fernando, S. and K. Al Zahed., 2003. Coastal protection and amenity value of an artificial reef for Dubai. *Proceedings of the 3rd International Surfing Reef Symposium*, Raglan, New Zealand. pp. 180-195.

Moffat and Nichol Engineers., 1989. The Patagonia Surfing Reef Feasibility Study. Report prepared for The Surfrider Foundation, Huntington Beach, California, Long Beach, California. Job No. 2521. 16 p.

Morris, R. W. and Associates., 1984. Kapiti Borough Council Coastal Investigations, Report No. 3a. Report for the Kapiti Borough Council prepared by Morris and Associates Consulting Engineers, New Plymouth, February 1984. 67 p.

Morton, J.E and M.C. Miller., 1968. *The New Zealand Seashore.* William Collins Sons and Co. Ltd, Glasgow, Great Britain. 638 p.

Nelson, R.C., 1996. Hydraulic Roughness of Coral Reef Platforms. *Applied Ocean Research,* 18, 265-274.

Nielson, P., 1986. Suspended Sediment Concentration Under Waves. *Coastal Engineering,* 10, 23-31.

Nielson, P., 1992. Mechanics of Coastal Sediment Transport. *Advanced Series on Ocean Engineering, Vol. 3.* World Scientific, Singapore. 324 p.

NIWA., 1999. Piha Beach. Coastal Physical Processes, Effect of Human Activities and Future Management. Report prepared for Waitakere City Council, July 1999. 48 p.

Osborne, P.D. and B. Greenwood., 1992. Frequency Dependent Cross-Shore Suspended Sediment Transport on a Non-Barred Shoreface. *Marine Geology,* 106, 1-24.

Osborne, P.D. and C.E. Vincent., 1993. Dynamics of large and small scale bedforms on a macrotidal shoreface under shoaling and breaking waves. *Marine Geology,* 115, 207-226.

Pattiarachi, C. 1988. Wave influence on coastal sand transport paths in a tidally dominated environment. *Ocean and Shoreline Management,* 11, 449-465.

Pattiarachi, C., James, A. and M. Collins., 1986. Island wakes and headland eddies: A comparison between remotely sensed data and laboratory experiments. *Journal of Geophysical Research,* 90(C1), 783-794.

Pattiarachi, C., 1997. Design studies for an artificial surfing reef at Cable Stations, Perth, Western Australia. *1st International Surfing Reef Symposium,* Sydney, Australia. pp. 87-90.

Pattiarachi, C., 1999. Design studies for an artificial surfing reef at Cable Stations, Perth, Western Australia. *Coasts and Ports '99,* Perth, Western Australia. pp. 485-489.

Pattearson, C.C. and D.C. Patterson., 1983. Gold Coast longshore transport. *Proceedings of 6th Austalian Coastal and Ocean Engineering Conference*, Surfers Paradise, Queensland, Australia. pp. 251-256.

Phillips, J.D., 1985. Headland-bay beaches revisted: an example from Sandy Hook, New Jersey. *Marine Geology,* 65(1-2), 21-31.

Phillips, D., Black, K., Hume, T., and T. Healy., 1999. Sediment Dynamics Along a Surfing Headland. *Coasts and Ports 99,* Perth, Australia. Vol. 2, pp. 513-518.

Phillips, D.J., Black, K.P. and T.R. Healy., 2000. Sediment Transport along a Surfing Headland at Raglan, New Zealand. Challenges for the 21st Century in Coastal Sciences, Engineering and Environment. Poster Paper, ICS 2000, Rotorua, New Zealand.

Phillips, D.J., Black, K.P. and T.R. Healy., 2001. Seabed Characteristics of a Dynamic Exposed Headland. *Coasts and Ports 2001*, Gold Coast, Australia. pp. 400-405.

Phillips, D.J., Black, K.P. and Healy, T.R., 2003. Sandy Seafloor Volume Changes off a High Energy Headland Boulder Beach, Raglan, New Zealand. *Coasts and Ports 2003*. Auckland, New Zealand. CD Publication, Paper No. 115. 8 p. ISBN: 0-473-09832-6.

Phillips, D.J., S.T. Mead., Black, K.P. and Healy, T.R., 2003. Surf Zone Currents and Influence on Surfability. *Artificial Surfing Reefs 2003*. The 3rd International Conference, Raglan, New Zealand. pp. 60-82. CD publication, ISBN: 0-473-09801-6.

Pickard, G.L., 1986. Effects of wind and tide on upper layer currents at Davies Reef, Great Barrier Reef. *Australian Journal of Marine and Freshwater Research*, 37, 545-566.

Pickrill, R.A. and J.S. Michell., 1979. Ocean Wave Characteristics Around New Zealand. *New Zealand Journal of Marine and Freshwater Research*, 13 (4), 501-520.

Pingree, R.D. and L. Maddock., 1979. The tidal physics of headland flows and offshore tidal bank formation. *Marine Geology*, 32, 269-289.

Pope, P. and D. Todd., 2003. Dunedin City, New Zealand - Coastal reserves conservation programme: Programme development and overview. *Proceedings of Coasts and Ports*, Auckland, New Zealand. On CD, Paper No. 150. 7 p.

Quevauviller, P. 1987. Evolution and stabilization of headland-bay beaches. *Journal of Shoreline Management*, 3(4), 269-284.

Rowland, J., Burling, M. and D. Hoy., 2003. Analysis of wave conditions and vessel motions at the Port of Napier, New Zealand. *Proceedings of Coasts and Ports*, Auckland, New Zealand. CD Publication, Paper No. 128. 8 p. ISBN: 0-473-09832-6.

Roelvink, J.A. and R.J. Murray., 1992. Southern Gold Coast Littoral Sand Supply. Prepared for Queensland Government. Delft Hydraulics. 67 p.

Roy, P.S., Cowell, P.J., Ferland, M.A. and B.G. Thom., 1994. Wave dominated coasts. In Carter, R.W.G. and C.D. Woodroffe. (eds) *Coastal Evolution, Late Quaterbary Shoreline Morphodynamics*. Cambridge University Press, Cambridge, 121-186.

Saito, K., Uda, T., Yokota, K., Ohara, S., Kawanakajima, Y. and K. Uchida., 1996. *Observation of nearshore currents and beach changes around headlands built on the Kashimanda Coast, Japan.* Proceedings of the 25th Coastal Engineering Conference (ASCE), Orlando, Florida. pp. 4000- 4006.

Sanderson, P.G., Eliot, I., Hegge, B. and S. Maxwell., 2000. Regional variation of coastal morphology in southwestern Australia: a synthesis. *Geomorphology,* 34 (1-2), 73-88.

Saunders, H.A., 1999. Coastal Processes Influencing Beach Erosion at West End, Ohope. Unpublished MSc Thesis, University of Waiakto. 229 p.

Sayce, A.J., 1997. Transformation of Surfing Waves Over Steep and Complex Reefs. Unpublished Thesis, University of Waikato. 158 p.

Sayce, A., Black, K.P., and R. Gorman., 1999. Breaking Wave Shape on Surfing Reefs. *Proceedings Coasts and Ports '99,* Vol. 2, pp. 596-603.

Scarfe, B.E., 2002a. Categorising Surfing Manoeuvres Using Wave and Reef Characteristics. Unpublished MSc Thesis, Department of Earth Science, University of Waikato. 190 p.

Scarfe, B.E. 2002b. Water Level Corrections (WLC) Using RTK-GPS. *The Hydrographic Journal,* 104, 17-23.

Scarfe, B.E., Black, K.P., Chong, A.K., de Lange, W.L., Phillips, D.J. and S.T. Mead., 2002. The Application of Surveying Techniques to Artificial Surfing Reef Studies. *Trans Tasman Surveyor. Journal of the New Zealand Institute of Surveyors,* 5, 29-40.

Scarfe, B.E., Elwany, M.H., Black, K.P. and S.T Mead., 2003. Surfing conditions around jetties. Scripps Instituition of Oceanography Technical Report. University of California, San Diego, USA. 101 p.

Scarfe, B.E., Elwany, M.H., Mead, S.T. and K.P Black., 2003. The science of surfing waves and surfing breaks. *Proceedings of 3rd International Surfing Reef Symposium,* Raglan, New Zealand. pp. 37-59. CD Publication, ISBN: 0-473-09801-6.

Schoonees, J.S. and A.K. Theron., 1993. Review of the field-database for longshore sediment transport. *Coastal Engineering,* 19(1-2), 1-25.

Shand, R.D. and D.G. Bailey., 1999. A review of net offshore bar migration with photographic illustrations from Wanganui, New Zealand. *Journal of Coastal Research,* 15(2), pp. 365-378.

Shand, R.D., Shepard, M. J. and D.G. Bailey., 1999. An inter-site comparison of net offshore bar migration characteristics and environmental conditions. *Journal of Coastal Research,* 15(3), pp. 750-765.

Shepard, F.P. and D.L. Inman. 1950. Nearshore water circulation related to bottom topography and wave refraction. *Transactions of the American Geophysical Union,* 31, 196-212.

Shepherd, M. and P. Hesp., 2003. Sandy barriers and coastal dunes. In: Goff *et al.* (eds). *The New Zealand Coast – Te Tai O Aotearoa.* Dunmore Press, Palmerston North, New Zealand. 312 p.

Shih, S. and P.D. Komar., 1994. Sediments, beach morphology and sea cliff erosion within an Oregon coast littoral cell. *Journal of Coastal Research,* 10(1), 144-157.

Short, A.D., 1985. Rip current type, spacing and persistance, Narrabeen Beach, Australia. *Marine Geology,* 65, 47-71.

Short, A.D., 1999. *Handbook of Beach and Shoreface Morphodynamics.* John Wiley and Sons Ltd. 379 p.

Short, A.D. and R.W. Brander., 1999. Regional variations in rip density. *Journal of Coastal Research.* 15(3), pp. 813-822.

Short, A.D. and G. Masselink., 1999. Embayed and structurally controlled beaches. In: Short, A.D. 1999. (Ed.) *Handbook of beach and shoreface morphodynamics.* Wiley, Chichester. pp. 142-161.

Signell, R.P. and W.R. Geyer., 1991. Transient Eddy Formation Around Headlands. *Journal of Geophysical Research,* 96(C2), 2561-2575.

Silvester, R., 1960. Stabilisation of Sedimentary Coastlines. *Nature,* 188(4749), 467-469.

Silvester, R., 1975. What Makes a Good Surfing Beach. *Proceedings of the 2nd Australian. Coastal and Ocean Engineering,* pp. 30-37.

Silvester, R., 1976. Headland Defence of Coasts. *Proceedings of the 15th Conference on Coastal Engineering,* American Society of Civil Engineers. Vol. 2. pp. 1394-1406.

Silvester, R., 1985. Natural headland control of beaches. *Continental Shelf Research,* 4(5), 581-596.

Silvester, R., 1990. *Scour around breakwaters and submerged structures.* Herbich, J.B. (Ed.). Handbook of Coastal and Ocean Engineering. Gulf Publishing Company, Houston. pp. 959-996.

Silvester, R. and J. R. Hsu., 1997. *Coastal Stabilisation: Innovative Concepts.* World Scientific. Singapore. 578 p.

Smith, A.W., 1982. Littoral transport into zeta bays, Gold Coast Beach Renourishment Program Report No. 59. 32 p.

Smith, R.K. and R. Ovenden., 1992. Report on survey information, Piha Beach, 1981 to 1992. Consultancy Report No. 6142. New Zealand Department of Scientific and Industrial Research, Hamilton. 10 p.

Sorenson, O.R., Hemming, A.S., Madsen, P.A. and R. Diegaard., 1994. *Wave breaking and induced nearshore circulations.* Proceedings of the 24th International Conference (ASCE), Kobe, Japan. pp. 2583-2594.

Stephens, A.W., Roy, P.S. and M.R. Jones., 1981. Geological Model of Erosion on a Littoral Drift Coast. *5th Australian Conference on Coastal and Ocean Engineering,* Perth, Australia. pp. 171-176.

Stokes, S., 1991. Tectonic Volcanic Implications of Provenance Changes in the Later Neogene Coastal Sand Deposits of the Kaihu Group, South Auckland, New Zealand. *New Zealand Journal of Geology and Geophysics,* 34, 51-59.

Symonds, G., Black, K.P. and I.R. Young., 1995. Wave driven flow over shallow reefs. *Journal of Geophysical Research,* 100(C2), 2639-2648.

Symonds, G. and K.P. Black., 2001. Predicting Wave-driven Currents on Surfing Reefs. *Journal of Coastal Research Special Surfing Issue 29,* 102-114.

Thornton, J., 1995. *The Reed field guide to New Zealand geology.* Reed Books, Auckland. 226 p.

Tonkin and Taylor Ltd., 1998. Beach Monitoring Report for Long Bay, Muriwai and Piha. Report for the ARC, 7p + apps.

Tsuchiya, Y., Yamashita, T. And R. Silverster.,1990. *Beach erosion due to large coastal structure and its control.* Proceedings of 22nd Coastal Engineering Conference (ASCE), Delft, The Netherlands. pp. 2726-2737.

Turner, I.L., 2003. Applications of coastal imaging technology to coastal engineering and coastal management in Australia. *Coasts and Ports,* Auckland, New Zealand. CD Publication, Paper No. 29. 9 p. ISBN: 0-473-09832-6.

U.S. Army Corps of Engineers., 1973. *Shore Protection Manual*. Coastal Engineering Research Centre, U.S. Govt. Printing Office, Washington, D.C.

van Rijn, L.C. 1993. *Principles of Sediment Transport in Rivers, Estuaries and Coastal Seas.* Delft Hydraulics, Aqua Publications. pp. 13-86.

Walker, D.J., Dong, P. and K. Anastasiou., 1991. Sediment transport near groynes in the nearshore zone. *Journal of Coastal Research,* 7(4), 1003-1011.

Walker, J.R., Palmer, K.Q. and J.K. Kukea., 1972. Recreational surfing on Hawaiian reefs. *Proceedings of the 13th Coastal Engineering Conference.* (ASCE), pp. 2609-2628.

Walker, J.R., 1974. Recreational Surf Parameters. LOOK Laboratory Report TR-30, University of Hawaii, Department of Ocean Engineering, Honolulu, Hawaii. 311 p.

Warren, M., 1999. Atlas of Australian surfing. Harper Sports, Australia. 272 p.

Warwick, W., 1986. Guide to surfriding in New Zealand. International Specialised Book Services. 85 p.

West, A.S., Cowell, P., Batjies, J.A., Stive, M.J.F., Doorn, M. and J.A. Roelvink., 2002. Wave focusing surfing reefs – a new concept. *Surfing Art Science Issues Conference 2, (SASIC2,* Ventura, California. pp. 31-41.

White, J., 1990. The Use of Sedeiment Traps in High-Energy Environments. *Journal of Marine Geophysical Research*, 12, 145-152.

Willmott, A.J., 1983. The influence of a coastal headland on oceanic boundary currents. *Geophysical and Astrophysical Fluid Dynamics*, 23(4), 272-299.

Wren, D.G., Barkdoll, B.D., Kuhnle, R.A. and R.W. Derrow., 2000. Field techniques for suspended-sediment measurement. *Journal of Hydraulic Engineering*, 126(2), 97-104.

Xu, J.P., 1999. Local wave climate and long-term bed shear stress characteristics in Monterey Bay, California. *Marine Geology*, 159(1-4), 341-353.

Yin, J., Chen, Y., and R.A. Falconer., 2003. Steady shallow-water current and solute transport around a semi-conical headland. *Environmental Fluid Mechanics*, 3, 221-234.

Yoo, D., 1994. Wave –induced longshore currents in the surf zone. *Journal of Waterway, Port, Coastal and Ocean Engineering*, 120(6), 557-575.

Zampool, J.A. and D.L. Inman., 1989. Discrete measurements of suspended sediment. In: Seymour, R.J. (Ed.) Nearshore Sediment Transport. pp. 259-272. Plenum Press, New York.

Zimmerman, J.T.F., 1981. Dynamics, diffusion and geomorphological significance of tidal residual eddies. *Nature*, 290, 549-555.

Zhang, J.E. and T.Y. Wu., 1999. Oblique long waves on beach and induced longshore currents. *Journal of Engineering Mechanics*, 125(7), 812-826.

APPENDIX 1: Published paper

SURF ZONE CURRENTS AND INFLUENCE ON SURFABILITY

Phillips, D.J., Mead, S.T., Black, K.P. and T.R. Healy., 2003. Surf Zone Currents and Influence on Surfability. *Surfing Reefs 2003.* The 3rd International Conference. Raglan, New Zealand. pp. 60-82 .

Surf Zone Currents and Influence on Surfability

David Phillips[1,2], Shaw Mead[2], Kerry Black[2], Terry Healy[3]

[1]UNITEC Institute of Technology, Private Bag 92025, Auckland.
[2]ASR Ltd, PO Box 13048, Hamilton, New Zealand
[3]Coastal Marine Group, Department of Earth Sciences, University of Waikato.
P.O. Box 11-115, Hamilton.
Email: dphillips@unitec.ac.nz

Abstract

Surfing headlands are shallow and exposed coastal features that provide a specific form of breaking wave allowing a board-rider to ride on the unbroken wave face. The seabed shape and refraction of the waves in relation to depth contours provide the greatest influence on the quality of the surf break. The large scale and orientation of the Raglan headland allows only the low frequency swells to refract around the headland to create seven different surfing breaks. Each represents a compartmentalization of the shoreline along the headland. This creates variability in wave and current characteristics depending on the orientation and bathymetry at different locations. This provides not only potential access points through the surf-zone (ie: smaller currents), but greater surfability in a range of conditions that is not possible on small scale headlands.

Headlands with surfing waves can be classified as mis-aligned sections of the coast, where the higher oblique angle of the breaking surf generates strong wave-driven currents. These currents are far greater than that found on coastlines in equilibrium with the dominant swell direction, where comparatively insignificant longshore drift is found. The strength and direction of wave-driven currents in the surf zone can influence the surfability of a break. At a surfing headland strong currents flowing

downdrift along the shoreline make it difficult for a paddling surfer to get to the "take-off" location of the break, or maintain position in the line-up. In comparison currents flowing updrift along headlands makes getting "out the back" relatively easy, although surfers can be taken out to sea past the "take-off" point by a fast flowing current.

Field experiments at Raglan, on the west coast of New Zealand have been conducted to measure current speed and direction during a large swell event. Observations of surfers attempting to paddle through the breaking-wave zone, confirms the strength of the wave-driven currents with surfers being swept rapidly down the headland. Results from the experiments at Raglan, have shown strong currents in the inshore breaking wave zone with burst-averaged velocities attaining 0.8 ms^{-1}, and maximum bed orbital velocities of up to 2.0 ms^{-1}. Interestingly, further offshore the currents have been found to flow in a re-circulating gyre back up the headland. Comparisons are made from observations of waves and currents found at other surfing headlands around the world. The effect that strong currents may have on the surfability of artificial surfing reefs needs to be considered in the design process, if the surfing amenity is to be maximised for large surf conditions.

1. INTRODUCTION

The saying that "headlands draw the waves" was known by many an old seafarer and was used in reference to the fact that wave energy is concentrated on these promontories, therefore building larger waves (Deacon, 1968) (Fig. 1). These larger waves are sought-after by surfers throughout the world, but the associated strength and direction of wave-driven currents in the surf zone can influence the surfability of a break. Significantly strong currents flowing downdrift along the shoreline do not allow a paddling surfer the opportunity to get to the "take-off" location of the break, or maintain position in the line-up.

Figure 1: The headland at Angourie Point, Australia with breaking waves. (Photo source: Tracks magazine).

2. SURFING HEADLANDS

Surfing headlands are shallow and exposed coastal features that provide a specific form of breaking wave allowing a board-rider to ride on the unbroken wave face. The form of breaking waves is affected by several factors, which includes not only the scale of the headland, shape of the seabed, wave height and period (Dally, 1989; Sayce, 1997), but also the wind strength and direction (Button, 1991; Galloway *et al.*, 1989; Moffat and Nichol, 1989)(Fig. 2). Mead and Black (2001a, b), found that there are a variety of properties that put world-class surfing breaks in a category of their own, but it is the seabed shape that has the largest influence on the form of a breaking wave and therefore the quality of a surfing break.

Figure 2: Waves breaking in the lee of the headland at Pambula, Australia.

Refraction changes the direction of wave propagation causing wave crests to align more parallel with the seabed contours (Komar, 1998). This is important for surfing because it alters the peel angle. The closer aligned the crest lines and the isobaths become, the greater velocity the surfer must attain to successfully ride the wave (Walker *et al.*, 1972). On a headland refraction can alter the waves and have a significant affect on the peel angle and type of surfing waves generated. The orientation of the headland in relation to the pre-dominant swell direction can cause significant refraction to occur as waves bend into the headland. The peel angle and surfability for a specific swell can therefore change depending on the direction of this swell (Fig. 3). Refraction is therefore considered the dominant factor controlling surfing wave quality at a headland (Hutt, 1997).

Figure 3: Waves refracting around a headland at Rincon, California to create high-quality surfing waves.

As waves pass into shallow water they slow down, increase in wave height and decrease in wavelength (Komar, 1998). As a wave approaches a headland, the part of the wave closest to the land slows more rapidly than the other part that is in deeper water. This causes the wave to bend. Because refraction begins to occur with the water depth is around 0.5 the wave length (Komar, 1998), the amount that waves bend into the coast depends on the wave period. Long period swells bend significantly, compared to short period waves such as small chop, which do not 'feel' the bottom until relatively shallow water and therefore cannot bend into large embayments (Mead, 2000). Point breaks at headlands can therefore have excellent quality surf compared to the rest of the coast, as only the low frequency swell refracts around the headland to create the breaking waves. Refraction also causes the wave height to decrease, as the more the waves refract around a headland the more they decrease in height (Komar, 1998). The 'headland effect' (Mead and Black, 2001b) is demonstrated at surf breaks such as large headland at Shipwreck Bay (Ahipara), with either a very large swell or a very long period swell required to bend around the headland and create surfing waves (Figs. 4 and 5) – a combination of both large wave heights and long period swell produces the best waves.

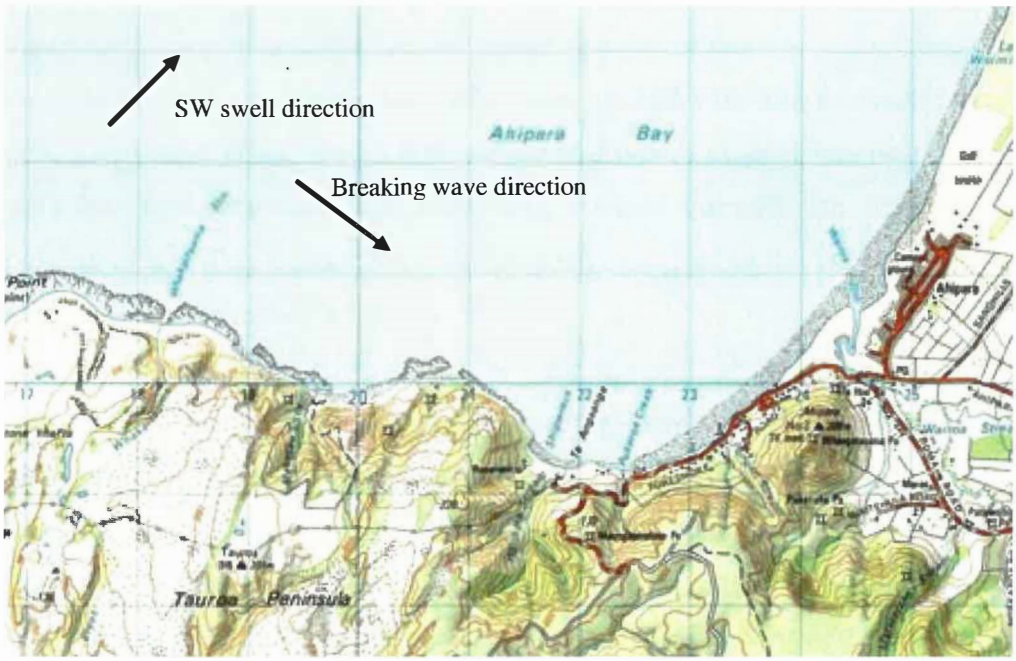

Figure 4: Map of Shipwreck Bay, Ahipara showing the swell and wave directions and the amount of refraction that occurs for waves to break along the headland.

Figure 5: Surfing waves breaking at Shipwreck bay, Ahipara.

3. CURRENTS INFLUENCE ON SURFING BREAKS

Strong currents are something that surfers have to deal with almost every time they paddle out. Most often, the current are wave-driven, but tidal jets near river and estuary bar surfing breaks, and even large oceanic currents can impact on the surfability of a surfing break. This section gives examples of the variety of different current surfers have to deal with.

It is well documented that when waves approach a shore at an oblique angle, a shore-parallel current is generated as waves break in the near-shore zone, transporting sediment along the coast (Fredsøe and Diegard, 1992; Komar, 1998). Headlands can be classified as mis-aligned sections of the coast, where the higher angle generates strong wave-driven currents. Currents at surfing headlands have been previously studied in relation to sediment transport and dynamics of the adjoining coast, and have a major influence on the seabed stability of the headland (eg: Kirra Point, Greenmount, Noosa Heads – all in Queensland, Australia).

Currents also have an influence on the surfability of a surf-break at a headland by limiting access to the surf and the ability to get into and maintain position in the line-up. Black and Symonds (2001) found that strong wave-driven currents occur over reefs when the reef is: (i) narrow; (ii) detached; (iii) fully submerged; and (iv) smooth with low frictional resistance. At a headland the wave-driven currents flow along the headland and make it very difficult to surf in large conditions.

However, currents can work in the favour of the surfer when flowing out towards the "take-off" zone, as seen at surf breaks near harbours and rivermouths, with an ebb tide creating an easy paddle out in the deep channel. This is demonstrated at the Whangamata bar on the Coromandel Pennisula in New Zealand, where surfers are taken out to sea from the "take-off" zone on an outgoing tide. However, the strong out-flowing current also means surfers must continually paddle against the flow to stay in the "take-off" area of the break. At Omaha bar, north of Auckland, the reverse

occurs where surfers must continually paddle wide from the initial break-point, as currents push over the bar taking surfers too far inside the breaking wave zone, making it difficult to catch waves. The current can also increase the shoaling of the wave as it breaks, with the outgoing flow significantly "sucking" the wave face, possibly creating a "tubing" wave. This is seen in places such as Whangapoa on Great Barrier Island, New Zealand.

On the Gold Coast of Australia, a number of world-class point breaks exist at the sub-zeta headlands north of the large Point Danger headland (Fig. 6). These breaks include Greenmount, Kirra Point (Fig. 7) and Burleigh Heads. During medium to large swell events at these surfing breaks, a significant northward current flows in the direction of the waves that is very difficult to paddle against. This current extends significantly wide of the surf zone and requires surfers to constantly paddle in order to maintain position in the line-up. Jumping from the rocks up-coast is often the only means of getting out to surf the break.

Figure 6: Aerial view of Point Danger to Kirra Point breakwater at the top of the picture, Gold Coast, Australia.

Figure 8: Kirra Point, breaking along the headland from the groyne. (Photo source: Tracks Magazine).

Bathymetric surveys and analysis by Black *et al.* (1998) showed that Kirra and Burleigh Heads have steep seabed gradients down to depths of ~6 m formed by large sand banks running parallel to the headland. These linear sand banks are probably "break point" bars formed by the interaction of wave breaking and the stream-like rip currents that travel down these headlands when a large swell is running. The seabed gradient reduces below 6 m and could be part of the reason for the wide streaming current down the headland. The surfing headlands are also of a small scale when compared to the overall size of the coastline in the area.

In comparison the world famous break at Desert Point in Lombok, Indonesia (Fig. 9) has a very large wave-driven current in the breaking wave zone, but seawards of this a significant counter-current exists flowing back out to sea (J. Frazerhurst pers comm.). This current makes paddling "out the back" very easy, but unless a wave is caught surfers can be taken past the "take-off" point and struggle to get back to the breaking wave zone. This current may be mostly due to the flow through the Lombok straight that runs at a minimum of 7-8 knots.

Figure 9: Desert Point in Lombok, Indonesia rated as the best wave in the world by Tracks surfing magazine. (Photo source: Tracks Magazine).

3.0 SURFING ON THE RAGLAN HEADLAND

Raglan is considered a world class surfing wave and is known as one of New Zealand's most consistent breaking waves (Bhana, 1988) (Fig. 10). It is located on the west coast of the country, and is comprised of seven surf breaks, with each having its own distinctive form of breaking wave (Fig. 11). The large scale of the Raglan headland (13 km from Ruapuke Beach to the Raglan harbour entrance) creates an environment where not only is there a variety of surf breaks, but each represents a compartmentalization of the shoreline along the headland. This creates variability in wave and current characteristics depending on the orientation and bathymetry at different locations.

Figure 10: Waves breaking along the Indicators surf break at Raglan (Source: www.ragtimeblue.co.nz).

The breaks are comprised of various components and wave characteristics (ie: different peel angles) as described by Mead and Black (2001a, b) and Scarfe (2002). At the tip of the headland is Outsides with wave characteristics that are moderate to very steep, hollow with moderate to fast sections. Further down the down the headland is Indicators, the predominant study site of field experiments presented here, which has moderate to steep waves that are steep to hollow with fast sections. The Valley breaks inside Indicators and has steep to very steep waves that are hollow and break with fast to very fast sections. Whale Bay is the slowest of the surfing waves with a moderate peel angle and moderate to steep waves. The next break is Boneyards, which is also slower with less power than the other Raglan breaks. Between Boneyards and Manu Bay is the Ledge, which can produce the hollowest and fastest tubes on the headland when the conditions are right. The furthest break

down the headland is Manu Bay, which produces moderate to steep waves with occasional short hollow and fast sections. It must be noted that these are general descriptions, and under swell conditions different from the predominant SW swell, and during different phases of the tide, all breaks can produce significantly different waves than those described above.

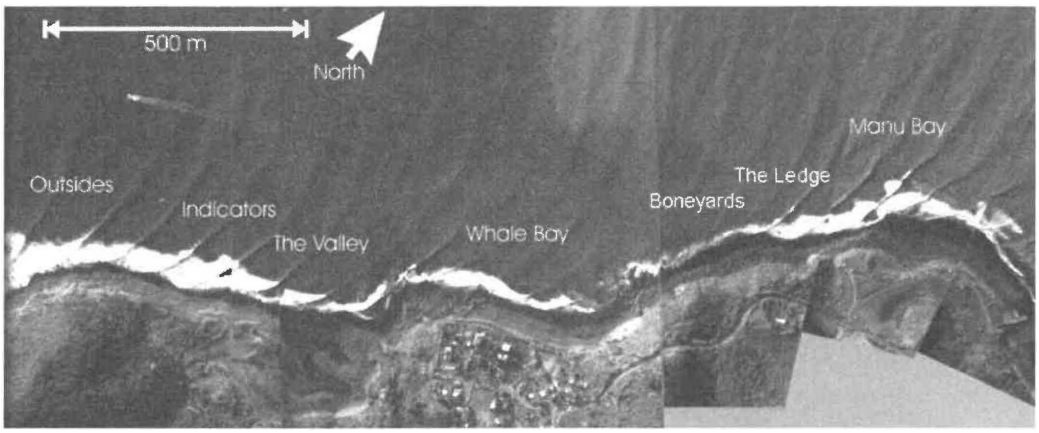

Figure 11: Aerial photo of the Raglan Surfing Breaks (Hutt, et al., 2001).

3. RAGLAN FIELD EXPERIMENTS

A large multi-faceted field experiment was previously undertaken at Raglan in 1996. This research on the surfing headland, has led to a greater understanding of the bathymetry, wave refraction, breakpoint location and surfing characteristics in this environment (Hutt, 1997; Mead, 2000; Sayce, 1997; Sayce *et al.,* 1999). The latest field experiments have been conducted to measure current speed and direction, as well as sediment flux during moderate and large swell events at Raglan. Bottom mounted frames were deployed from a boat and anchored to the seabed with weights, for stability and to maintain their position in the surf-zone (Fig. 12). The frames were fitted with S4 current meters and programmed to record burst data at a set interval per hour. The retrieved data was analysed in the Matlab programme tseries, providing burst-averaged data over the deployment period.

Figure 12: S4 current meter mounted on a frame ready for deployment in the surf zone.

Observations were also made of surfers attempting to paddle through the breaking-wave zone, confirming the strength of the wave-driven currents with surfers being swept rapidly down the headland for hundreds of metres. In large swells where the waves break in a pattern of sets, the lull period provides the opportunity for surfers to have a chance of paddling through the surf zone. However, this is not the case when the waves break with a consistent and continuous period, providing no opportunity for access to the surf-break.

In some locations such as Rincon surf break in California the out-flowing creek halfway up the headland provides a better access point as waves can be attenuated in this zone. At Raglan, a site at the end of the Whale Bay reef where the waves are not sweeping down the headland, but rather breaking into the reef between compartments provides a similar opportunity. A build-up of a pressure gradient and less current velocity in this area can increase the chances of getting out to the breaking waves.

4. FIELDWORK RESULTS

During large swell conditions the results from the experiments at Raglan (Fig. 13), have shown strong currents in the inshore breaking wave zone with burst-averaged velocities attaining 0.8 ms^{-1}, and maximum bed orbital velocities of up to 2.0 ms^{-1} (Phillips *et al.,* 1999). The currents were directed down the headland in an easterly direction (50^0) and increased dramatically to the maximum value, as swell size peaked at 3.25 m. The combination of increased swell size and a dropping tide, meant the current direction at the headland decreased to 110^0 as the waves swept straighter down the headland.

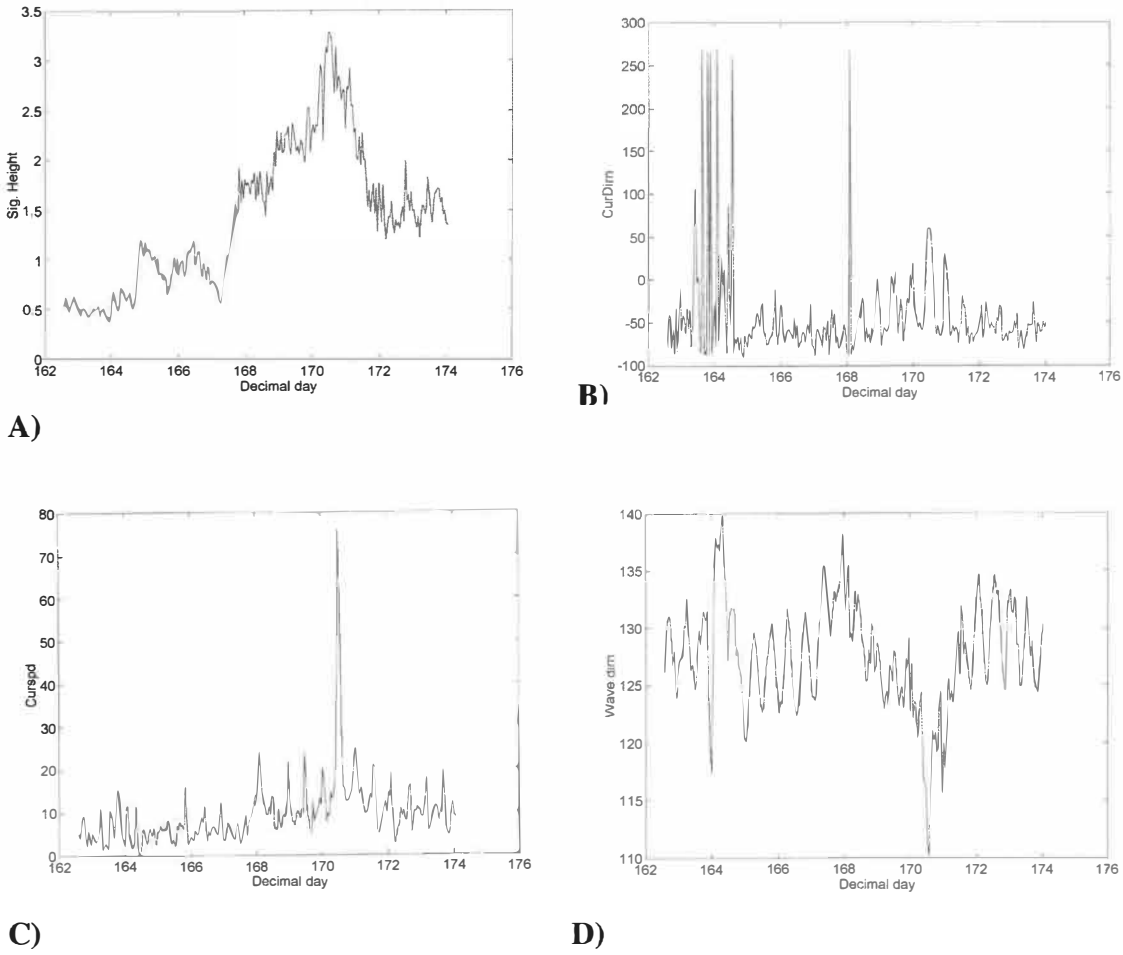

Figure 13: Graphs of data from field experiments A) Wave height (m); B) Current direction (degrees); C) Current speed (cms^{-1}); D) and Wave direction (degrees).

Interestingly, Phillips *et al.,* (1999) found that further offshore the currents have been found to flow in a re-circulating gyre back up the headland. These currents are significantly lower in velocity than the inshore flow, but can allow surfers an easier paddle back to the "take-off" point, although novice surfers have been known to experience difficulties being taken out to sea. Obviously surfers must first cross the fast flowing inshore current in the breaking wave zone, if this out-flowing conveyor is to have any advantage in surfing the break. As the size of the surf increases, the strength and width of the inshore wave-driven current also increases making surfing the site more difficult, if not impossible in 4-5 m swell.

5. ARTIFICIAL SURFING REEFS

Artificial surfing reefs (ASR's) exhibit many of the characteristics that generate strong wave-driven currents that could adversely affect surfing conditions at the break, i.e. they are (i) narrow; (ii) detached; (iii) fully submerged; and (iv) smooth with low frictional resistance (Symonds and Black, 2001). Design of artificial reefs need to consider the impacts of these currents if surfing amenity is to have optimum enhancement. Black and Mead (2001), describes the two types of offshore reef as "dissipators" and "rotators", working with nature by modifying the natural wave transformation processes to alter nearshore currents and obviate coastal erosion processes. The reefs act to break the waves and protect the coast by reducing wave energy in the lee of the structure, whilst also rotating waves to reduce the orientation angle, resulting in lower inshore wave-driven currents and therefore less longshore sediment transport. The reduced inshore currents also provide surfers with the opportunity to get to the take-off point of the break, increasing the surfability of the reef.

The Narrowneck surfing reef on the Gold Coast, Australia, is essentially a submerged headland, i.e. the reef contours are almost perpendicular to the natural seabed

contours (Fig. 14). This orientation was required due to the large depth in which the reef is located (10.5 m deep on the offshore toe of the reef) in order to compensate for the large amount of refraction that occurs as the waves bend up on to the reef. If the reef had been designed as originally suggested, with reef contours at around 45° to the seabed contours (Fig. 15), refraction would have reduced wave peel angles so as to make them so small that the waves would break too fast to be surfable (Mead and Black, 2001b; Mead, these proceedings).

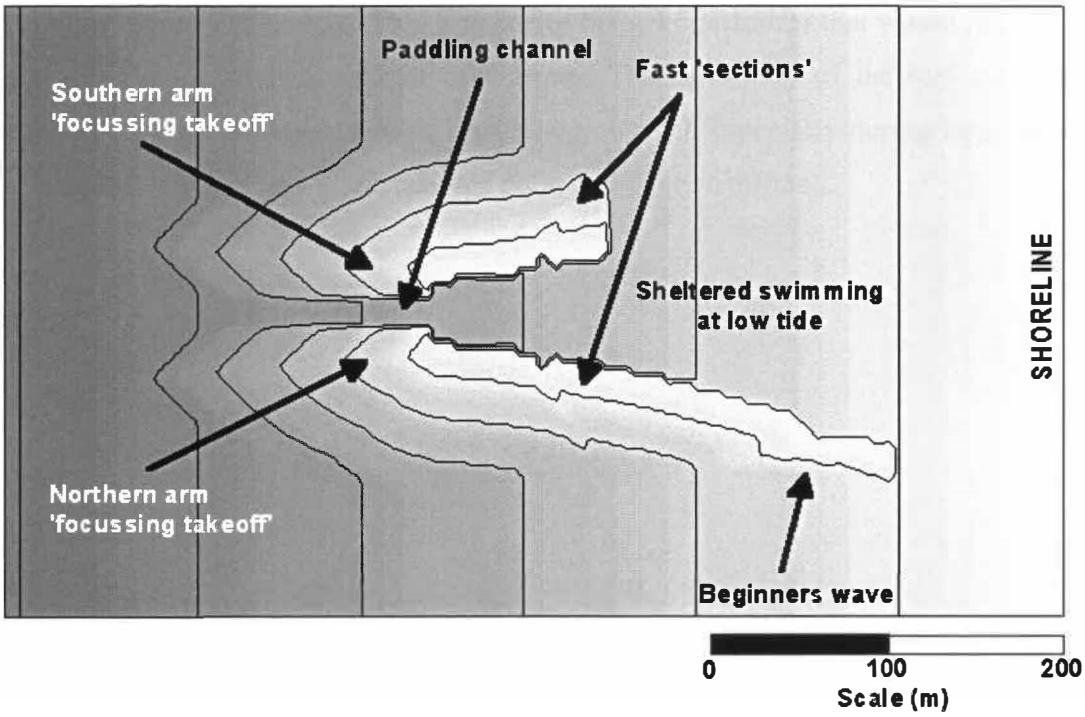

Figure 14: Narrowneck Reef (Black and Mead, 2001b).

Black (2001) identified a weakness in the Narrowneck reef design as being the strong wave-driven currents generated over the reef crest. The shoreward running currents in a 3-4 m swell, were predicted by Symonds and Black (2001) to exceed 1-1.5 ms^{-1}. These currents could sweep surfers caught in the breaking waves over the crest and into the shore. A design feature of the Narrowneck surfing reef to help compensate

for this is the paddling channel between the two arms of the reef (Fig. 14), which allows surfers access to the break during moderate and large wave conditions (Black and Mead, 2001b). Even though wave-driven currents are directed inshore on the outer sides of the reef, the current is reversed through the paddling channel, aiding paddling out through the channel. In addition, shoreward of the reef, a 'quiet zone' provides sheltered paddling from the beach (Fig. 14).

The design of the Lyall Bay ASR in Wellington, New Zealand, does not incorporate a paddling channel (Fig. 16). This was due to budget constraints that would not allow the construction of two separate reef arms. The surfability of the reef could be enhanced by the incorporation of a paddling channel, especially during large swell conditions, when access to the take-off point could prove difficult.

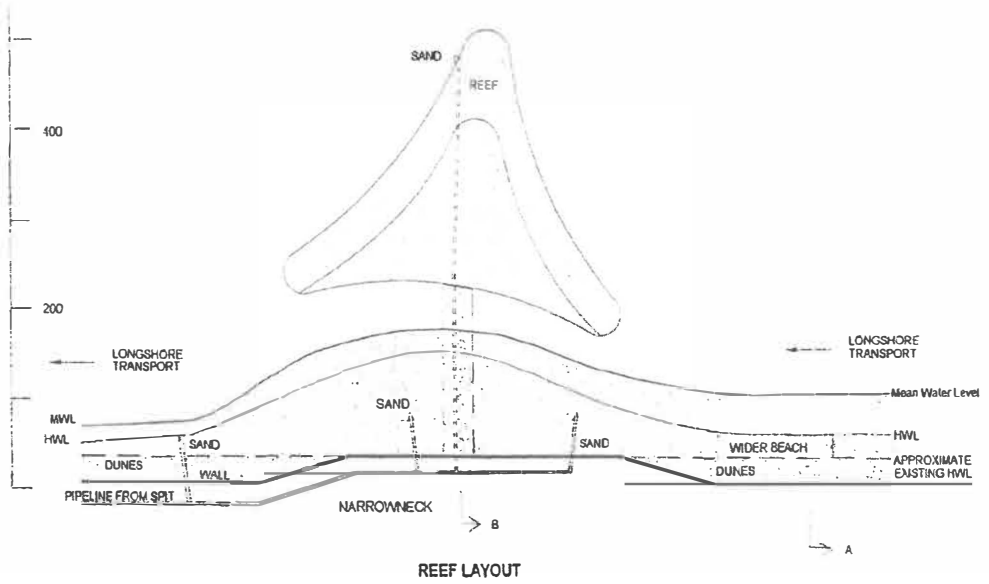

Figure 15. Early concept design of the Narrowneck surfing reef (Jackson et al., 1997).

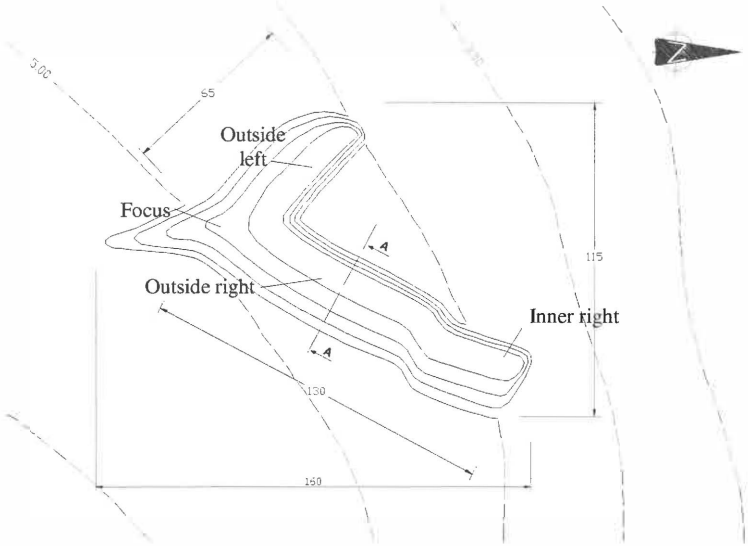

Figure 16. The final design of Lyall Bay Reef. (From Mead et al., 2003).

5. DISCUSSION

Headlands in small to moderate surf conditions can be classified as relatively easy to access when compared to beaches with similar surf conditions. Surfers must paddle through the breaker zone on a beach, whilst they must only get through a much narrower zone on a headland. However, this is not the case when large surf conditions prevail producing strong wave-driven currents in the surf-zone that significantly decreases the surfability of a break. This is due to the increased velocity of the wave-driven currents as the surf size becomes larger. Headlands are essentially mis-aligned sections of the coast, where the higher oblique angle generates strong wave-driven currents, when compared to a coastline in equilibrium with the dominant swell direction where the longshore flows are insignificant.

At some headlands where strong ebb-tidal outflow is found such as Whangamata bar, Coromandel Pennisula and Whangapoa on Great Barrier Island, New Zealand, the current assists surfers in not only getting to the take-off point but in creating barreling

waves in this zone. However, difficulties can be experienced with continual paddling required to stay in position in the line-up, but this far outweighs having to watch perfect surf if no access can be obtained. Indeed, currents will always be something that surfers have to contend with, since they are an integral part of the surf zone.

The field experiments provided data for a 3 m swell at the Raglan headland. This data supported visual observations of surfers attempting to paddle out at the break, who were washed rapidly down the headland in strong currents. The data did, however, show a counter current further offshore that rotates back up the headland (Phillips *et al.,* 1999), but this current does not significantly increase the surfability as surfers must first paddle through the surf-zone to get to this area. On some natural headlands the morphology and bathymetry can allow greater surfability, such as a change in orientation or a deeper zone where the waves attenuate and currents decrease in velocity. The out-flowing creek at Rincon, California, is a classic example of this scenario. The scale of the headland is therefore important, as large scale headlands may provide the variability in coastline needed for different breaks with a mixture of peel angles and wave characteristics.

In the design of artificial surfing reefs the surfability of the break due to wave-driven currents must be considered if the amenity is to be maximized, especially during large surf conditions. Black (2001) described a limitation in the Gold Coast reef at Narrowneck, from wave-driven currents flowing over the reef and pushing surfers into the lagoon. However the reef does include a paddling channel between the two arms of the reef allowing better access to the take-off point in larger surf conditions by reversing the current direction. Future designs of artificial reefs should consider the impacts of currents on surfability as an integral factor, especially if big wave surfing is to be a component specified for the reef by the client. This has certain attractions to sponsors who may be interested in contributing funding to the project. However, features such as a paddling channel need to be considered, and may limit the ability to include greater surfability in the design of the reef.

6. CONCLUSION

Surfing headlands are shallow and exposed coastal features that provide long peeling waves allowing a board-rider to ride on the unbroken wave face. The seabed shape and refraction of the waves in relation to depth contours, is the greatest influence on the quality of the surf break, although due to headlands oblique orientation to the waves, strong wave-driven currents are often present. The large scale and orientation of the Raglan headland allows only the low frequency swells to refract around the headland to create surfing waves, a feature that makes headland breaks particularly sought after by surfers since waves will be 'cleaner' on headlands than on other parts of the coast. The large size of the Raglan headland also creates seven surf breaks, with each having its own distinctive form of breaking wave (i.e: different peel angles and breaking intensity). Each represents a compartmentalization of the shoreline along the headland. This creates variability in wave and current characteristics depending on the orientation and bathymetry at different locations. This provides not only potential access points through the surf-zone (ie: smaller currents), but greater surfability in a range of conditions that is not possible on small scale headlands.

Headlands can be classified as mis-aligned sections of the coast, where the higher oblique angle of the shoreline generates large wave-driven currents. This is confirmed by measurements in the surf-zone that have shown strong wave-driven currents at the Raglan surfing headland, that make the break difficult if not impossible to surf in large swell conditions. In a 3 m swell, burst-averaged velocities attained 0.8 ms^{-1}, and maximum bed orbital velocities of 2.0 ms^{-1}. A rotating gyre at the headland provides a counter-current further offshore that flows back up the headland. This current does not, however, assist surfers when the swell is very large (4-5+ m), as the downstream current inshore is too strong to cross.

Observations from a variety of other surf breaks around the world, provides further evidence of the influence that currents in the surf zone can have on the surfability of a

break. These can sometimes be positive influences with out-flowing currents providing an easier paddle out for surfers to the break-point. The consideration of currents and the effect on surfability of an artificial surf break should be a component that is considered in the overall design of a reef if the amenity value is to be maximized, especially during large swell events.

7. ACKNOWLEDGEMENTS

Technical assistance by Dirk Immenga was greatly appreciated. Graduate students of the school are thanked for their help in the field.

8. REFERENCES

ASR Ltd. 2001. *Lyall Bay Surfing Reef Feasibility Study.* Volume 3 – Appendices.

Bhana, M. 1988. *The New Zealand Surfing Guide.* Heinemann Reed, NZ.

Black. K.P. Hutt, J.A., and S.T. Mead, 1998. *Narrowneck Reef – Report 2: Surfing Aspects.* Technical report prepared for the Gold Coast City Council. Centre of Excellence in Coastal Oceanography and Marine Geology, University of Waikato and National Institute of Water and Atmospheric Research, 120 p.

Black, K.P. and S.T. Mead. 2001a. Artificial Surfing Reefs for Erosion Control and Amenity: Theory and Application. Challenges for the 21st Century in Coastal Sciences, Engineering and Environment. *Journal of Coastal Research Special Issue No. 34* (ICS 2000 New Zealand).

Black, K.P. and S.T. Mead. 2001b. Design of the Gold Coast Reef for Surfing, Public Amenity and Coastal Protection: Surfing Aspects. *Journal of Coastal Research, Special Surfing Issue.* Special Issue No. 29.

Button, M., 1991. Laboratory Study of Artificial Reefs. Bachelor of Engineering, Department of Civil and Environmental Engineering, University of Western Australia, 1991. 107 pp.

Dally, W.R., 1989. Quantifying Beach 'Surfability. *Proceedings Beach Technology Conference,* Tampa, Florida, February, 1989.

Deacon, G.E.R.1968. *Oceans. An Atlas-History of Man's Exploration of the Deep.* Paul Hamlyn London.

Fredsøe, J. and Deigaard, R. 1992. *Mechanics of coastal sediment transport.* Advanced Series on Ocean Engineering, World Scientific. 369 pp.

Galloway, G.S., Collins, M.B., and A.D. Moran, 1989. Onshore/Offshore Wind Influence on Breaking Waves: An Empirical Study. *Coastal Engineering,* 13: 305-323.

Hutt, J.A., 1997. *Bathymetry and Wave Parameters Defining the Surfing Quality of Five Adjacent Reefs.* Unpublished Thesis, University of Waikato, New Zealand.

Komar, P. D., 1998. *Beach Processes and Sedimentation.* 2nd edition, Prentice-Hall Inc., New Jersey. 544p.

Mead, S.T. 2000. *Incorporating High Quality Surfing Breaks into Multi Purpose Reefs.* Unpublished Doctoral Thesis, University of Waikato, New Zealand.

Mead, S. T. & K. P. Black, 2000a. *Field Studies Leading to the Bathymetric Classification of World-Class Surfing Breaks.* Special Issue of the Journal of Coastal Research on Surfing p5-20.

Mead, S. T. & K. P. Black, 2000b. *Functional Component Combinations Controlling Surfing Wave Quality at World-Class Surfing Breaks.* Special Issue of the Journal of Coastal Research on Surfing p21-32.

Mead, S.T. & K.P. Black. 2002. Multi-Purpose Reefs Provide Multiple Benefits – Amalgamating Coastal Protection, High-Quality Surfing Breaks and Ecological Enhancement to Maximise User Benefits and Development Opportunities. *Proceedings for Surfing Art Science Issues Conference 2 (SASIC 2),* Ventura, California, 9 November 2002.

Moffat and Nichol, 1989. *The Patagonia Surfing Reef Feasibility Study.* Report prepared for The Surfrider Foundation, Huntington Beach, California, by Moffat and Nichol Engineers, Long Beach, California. Job No. 2521, September, 1989.

Phillips, D., Black, K., Hume, T., & Healy, T. (1999). Sediment Dynamics Along a Surfing Headland. Proceedings of Coasts & Ports 99*:* Perth, Australia. Vol. 2, pp. 513-518.

Sayce, A.J., 1997. *Transformation of Surfing Waves Over Steep and Complex Reefs.* Unpublished Thesis, University of Waikato, New Zealand.

Sayce, A., Black, K.P., and R. Gorman, 1999. Breaking Wave Shape on Surfing Reefs. *Proceedings Coasts and Ports '99,* Vol. 2, 596-603.

Symonds, G. and K.P. Black. 2001. Predicting Wave-driven Currents on Surfing Reefs. *Journal of Coastal Research, Special Surfing Issue.* Special Issue No. 29.

Walker, J. R., R. Q. Palmer & J. K. Kukea, 1972. Recreational Surfing on Hawaiian Reefs. *Proc. 13th Coastal Engineering Conference*, 1972.

APPENDIX 2: Published paper

SEABED CHARACTERISTICS OF A DYNAMIC EXPOSED HEADLAND

Phillips, D.J., Black, K.P. and T.R. Healy., 2001. Seabed Characteristics of a Dynamic Exposed Headland. *Coasts and Ports 2001,* Gold Coast, Australia. pp. 400-405.

Seabed Characteristics of a Dynamic Exposed Headland

David Phillips[1,2], Kerry Black[3], Terry Healy[1]

[1]Coastal Marine Group, Department of Earth Sciences, University of Waikato
P.O. Box 11-115, Hamilton. New Zealand.
[2]UNITEC Institute of Technology, Private Bag 92025, Auckland. New Zealand.
[3]ASR Ltd, PO Box 13048, Hamilton, New Zealand
Email: dphillips@unitec.ac.nz

Abstract

Experiments were conducted at Raglan, a surfing headland on the west coast of New Zealand, to determine the stability and characteristics of the "black sand" seabed and the adjacent boulder reef. Sediment sampling and successive side-scan sonar surveys were undertaken to determine seabed and bedform character, sand coverage, and the stability of the rock/sand interface at the underwater boundary of the boulder reef.

The sonagraphs showed areas of megaripples, which were most common closer to the headland at the rock/sand boundary, and contained the signature of recent swell conditions. Ground truth observations by divers confirmed their presence with wavelengths of up to 3 m (crest to crest) and heights of 0.5 m. Further offshore, the ripples became less distinguishable and were smaller and appeared to have no dominant orientation. The seabed was also firmer-packed in these areas with fine mud coating the seafloor. Sediment samples showed that the largest-sized grains were located at the tip of the headland where the waves first break (high energy zone), decreasing slightly down the headland. Bed sediments were well sorted and graded from 0.28 mm inshore to 0.14 mm offshore. Numerical model predictions show that grain size is strongly related to bed orbital velocity and the presence of the surf zone.

The rock/sand boundary on the seafloor generally followed the shape of the headland and showed considerable variation over time, with sediment covering and uncovering rock outcrops. The seabed is very dynamic in nature, with sediment being both accreted and scoured at the headland. A change in position seems to occur quite rapidly dependent on recent swell conditions. Long term habitation by adult marine organisms at the sub-tidal reef edge demonstrates a possible upper level of sediment movement.

Previous experiments identified strong down-headland currents during large swell events, mean cross-offshore currents and a local re-circulating sediment pathway that is responsible for maintaining the stability of the bed. The characteristics of the seabed appear to support this theory, with sand being transported from the headland during large swell and therefore moving the rock/sand boundary seaward. During the subsequent smaller swell, the mean cross-offshore current and local sediment re-circulation transport the sand back onto the headland in an attempt to attain an equilibrium position of the bed.

1. INTRODUCTION

Effective coastal management requires an adequate understanding of physical coastal processes and their effects. More particularly, it demands an appreciation of the physical processes acting on the coast and the dynamic response of coastal landforms as those forces are applied (Brookes & Green, 2000). To fully understand the response of a dynamic exposed headland, as found at Raglan, on the west coast of New Zealand (Fig. 1), it is therefore important to determine the stability and characteristics of the seabed.

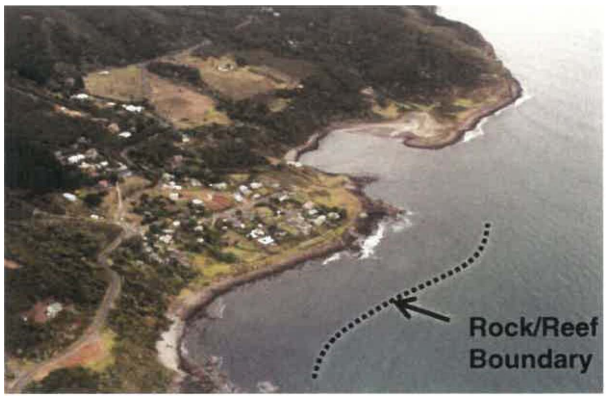

Figure 1: Aerial view of the headland at Raglan showing the boulder and reef shoreline.

Raglan, is one of the largest headlands on the west coast stretching some 13 km from Ruapuke to Raglan Harbour entrance in the central North Island. It is one of a succession of headlands and long sandy beaches that characterize this coast. The sea bed consists of a mobile west coast "black sand" adjacent to a boulder and reef shoreline that is well known for providing world class surfing waves (Fig. 2).

Figure 2: Waves breaking along the Indicators headland at Raglan. (Image from www.asrltd.co.nz)

The rocks are part of the Karioi and Okete volcanic formations, which are predominately basaltic andesites derived from eruptions and lava flows (Goles, Briggs & Rosenberg, 1996). The west coast "black sand" is fine grained and denser than quartz "white sand" and originates from the Taranaki volcanic region. It contains trace elements such as titanium and is a source of iron ore, which is mined for use in the production of iron and steel .

Previous studies on the west coast have shown that net sediment movement is to the north (Gibb, 1979), with the dominant wind and swell direction on the west coast being from the southwest (Heath, 1982). The main surfing breaks at Raglan face to the north, which causes a large amount of wave refraction to occur as the swells wrap around the headland. This orientation means the headland is only exposed to low frequency swells in storms, as the high frequency shorter period swells are not able to refract into the surfing breaks of the headland. Refraction along with the seabed shape are two of the main components for high quality surfing waves (Mead & Black, 2001). The shallow rock armoured headland (Fig. 3), at Raglan provides these variables, with the dichotomy being: What is the character of the seabed in this environment and is it variable in its nature?

Figure 3. Rocks armouring the headland above the low tide mark. Size of the rocks varies from 0.001 m to 1.5 m.

Phillips (1999), concluded that there is a strong relationship between wave height and current intensity, and therefore the average suspended sediment concentration transported along the headland. Experimental results demonstrated that local re-circulating pathways are present on the headland and appear to be responsible for maintaining the sandy bed in the presence of energetic wave conditions (Fig. 2).

Observations along the sub-tidal reef edge, where the rock meets the sand, made during field experiments in February 1998, showed species of kaimoana including paua (*Haliotis iris*), kina (*Evechinus chloroticus*) and the catseye (*Turbo smaragdus*). A single large boulder on the edge of the reef was found to be completely covered by large greenshell mussels (*Perna canaliculus*) (Mead, *pers obs*.).

These observations are very interesting when the proximity to the sandy seabed and the large wave exposure of the area are considered (waves of up to 4m break monthly along this stretch of coast, and annually even larger events can be expected). These observations suggest that the division between the boulder reef and the sandy seabed is fairly stable and not subject to regular smothering by wave induced sediment movements. The presence of adult representatives of many species along the reef edge suggests that this habitat has remained stable for a period of years, rather than several weeks or months if intermittent smothering was the case.

2. METHODS

Field experiments at Raglan were conducted to determine the stability and characteristics of the "black sand" seabed and the adjacent boulder reef. Sediment grain size, bedform location and size, rock/sand boundary, bed level and the physical properties were measured. Successive side-scan sonar survey's were undertaken in June 1998, Nov 2000 and April 2001 to determine seabed and bedform character, sand coverage, and

the stability of the rock/sand interface at the underwater boundary of the boulder reef. Sediment samples were collected on two occasions by divers in the experimental area, up to 500m offshore, for grain size analysis. There was a 3 year duration between collection of these samples to distinguish any change in sediment characteristics over this time. Visual observations were also made at the time of sampling to confirm bedforms and any variation in bed characteristics.

In the laboratory, sediment samples were analysed in a fall tube (Rapid Sediment Analyser) for settling velocity and particle grain size. The headland at Raglan was numerically computer modelled using the software WBEND (Black & Rosenberg, 1992). Bathemetry was used from a previous hydrographic survey of the headland by Hutt (1997), for input into the numerical model. Comparisons were made of the rock/reef boundary position by digitising the side scan sonagraph images in SURFER.

3. RESULTS

The side-scan surveys showed areas of megaripples, which were most common closer to the headland at the rock/sand boundary (Fig. 4). Ground truth observations by divers confirmed their presence with wavelengths of up to 3 m (crest to crest) and heights of 0.5 m. The well defined megaripples have continuous crests and are sinusoidal in nature. They are both symmetrical and asymmetrical in shape, and show the signature of recent swells. Further offshore, the ripples became less distinguishable and were smaller and appeared to have no dominant orientation. The seabed was also firmer-packed in these areas with fine mud coating the seafloor. The mud is generated by run-off during rainfall into the Whaingaoroa (Raglan) Harbour, and is transported by a tidal jet through the harbour entrance, to the headland. The annual suspended sediment discharging into the harbour has been estimated at 54,000 tonnes.y^{-1} (Daborn & Dickie, 1997).

The time-series scans also demonstrated that the rock/sand boundary on the seafloor generally followed the shape of the headland and showed considerable variation over time. This is demonstrated in Figure 5, with a variation of approximately 40 m at Whale Bay from scan 1 to scan 2, and then from scan 2 to scan 3. The percentage sand coverage on the rock reef was at its least in scan 1, increasing to scan 2 and at its greatest in scan 3.

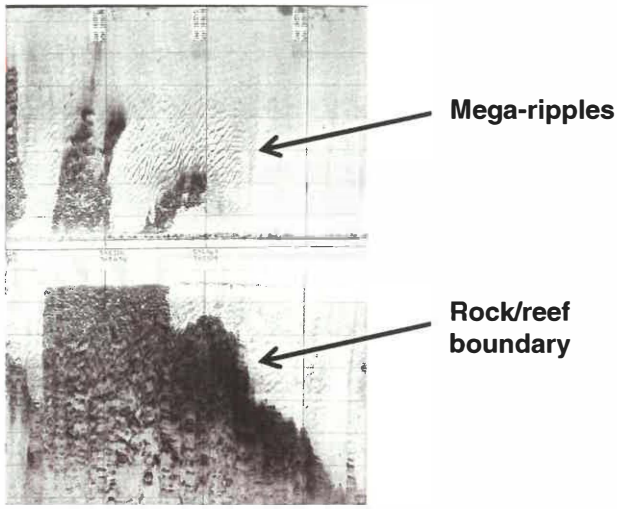

Figure 4. Side-scan map of Whale Bay from Survey 1 (June 1998), showing the rock/sand boundary and the megaripples in close proximity to this zone.

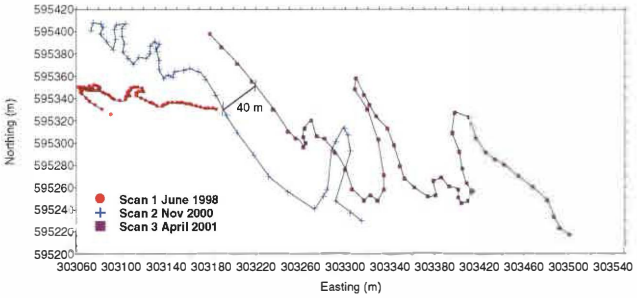

Figure 5. Digitised map drawn in Surfer of side-scan surveys in June 1998, Nov 2000 and April 2001 at Whale Bay, showing the changing position of the underwater rock/sand boundary.

Bed sediments were well sorted and graded from 0.28 mm inshore to 0.14 mm offshore (Fig. 6). The largest-sized grains were located at the tip of the headland where the waves first break (high energy zone), decreasing slightly down the headland. Their was not a significant variation in the sediment grain size and its location at the headland, from the sampling in May 1999 to that in April 2001. The sediment can be classified from particle size analysis as predominantly sand, with some samples being slightly gravely sand, due to the presence of small amounts of shell.

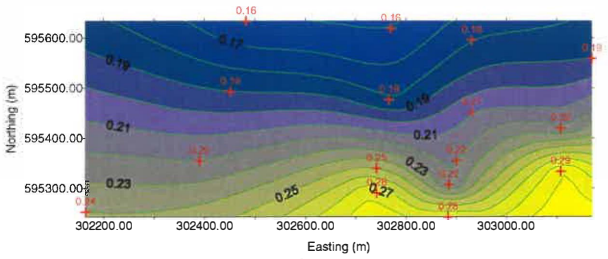

Figure 6: Sediment Grain Size Contour Map and sampling sites at Indicators (a surf break along the headland), sampled in May 1999.

The wave models (1m to 4m swell height) showed distinctive shoaling of waves in the zones known to be the best spots for surfing (Fig. 7). The bed orbital velocity numerical models

showed increased velocities in relation to the surf zone areas (Fig. 8). The resulting currents in the surf zone can be seen to directly relate to seabed characteristics delineated on the side scan sonar maps, with distinctive bedforms in areas close to the rock reef boundary where wave shoaling and the largest currents occur.

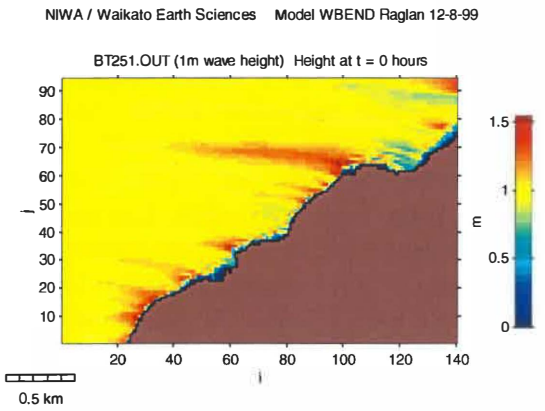

Figure 7. Wbend computer model output of the wave heights of the Raglan headland using a 1m swell.

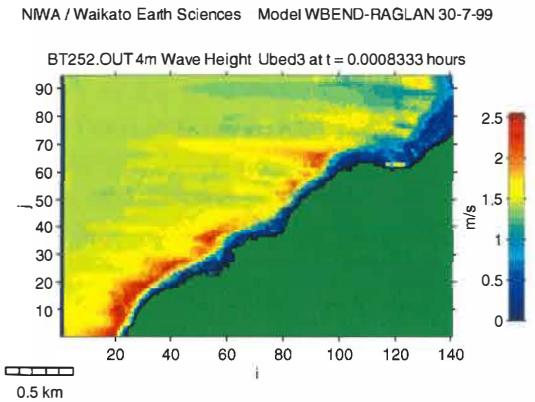

Figure 8. Wbend computer model output of the bed orbital velocities of the Raglan headland using a 4m swell.

The reef at sub-tidal depths in the range of 5-8 m (MSL) is comprised of boulders (approximately between 0.5 m and 1.5 m in diameter) that are invariably cemented together by calcareous encrusting algae (possibly *Coralline* sp.), light pink to patches of white in colour. Apart from an area of approximately 0.15 and 0.20 m around the base of the fused boulders that was relatively scoured and free of life, the surface of the boulder reef is inhabited by a variety of marine organisms, many of which are adults. For example, in some areas the tops of many boulders are covered with large brown algae of the *Carpophyllum* genera. Other boulders provided habitat for a mixture of encrusting sponges, notably, large colonies of *Polymastia glanulosa* and *Cliona celata* (some colonies covered the top surface of entire boulders).

During sediment sampling a stainless steel frame from a previous experiment by Phillips (1999) was discovered. The frame was not retrieved at the completion of the fieldwork in May 1998 due to large swell conditions. The interesting discovery was that of a cluster of green shell mussels (*Perna canaliculus)*, living on the top centrepiece of the frame, at a height of approximately 0.6m above the current bed level. The age of the mussels has been dated (S. Mead, *pers comm.)* as approximately 1-2 years old. The survival of these mussels over this period demonstrates that the bedlevel has not been over this height for a significant time period.

4. OBSERVATIONS

Observations made during recent field experiments after a very large swell (6 m), showed fresh rock exposed at the reef boundary (Phillips, *pers obs.*). The boundary was found to be approximately 30-40 m further seaward from the coast than during experiments in 1998. This swell appears to have transported away considerable sediment from the headland. It should be noted that this was a 1 in 5 year large swell event. One week later the same location had accreted sediment with relatively smaller patches of rock left exposed. Sea conditions during this week were characterized by a much smaller groundswell than the previous large swell, which appears to have transported sediment back onto the sub-tidal reef and boulders. The side scan survey undertaken on April 2001 confirms this observation, with what appears to be large drifts of sediment visible over the headland.

It has also been observed this summer (2000/2001), that the west coast has very low levels of sand on the beaches, with numerous rocks exposed at both Ruapuke, Raglan and Muriwai beaches (Phillips, *pers obs.*). The headland at Raglan has also shown some variation in surf conditions that might be due to a predominantly lower bed level as a result of low seasonal supply of sediment (Mead, *pers comm.*).

5. DISCUSSION

It is evident from the results that the wave signature is strongly present in the seabed features of the headland, including the location of the rock/sand interface, grain size, and bedform characteristics. The side-scan sonographs have identified megaripples which were aligned with the direction of the waves. This is a characteristic also found by Hume (1997) during experiments about a large coastal headland. Gallagher, Elgar, & Thornton (1998) found that megaripples are aligned on a natural beach so that the sediment transport normal to the bedform crest is

maximised, and not necessarily in the direction of the vector sum of the currents. This may also be the case at Raglan, where numerical models have shown that bed orbital velocities are at their greatest in the breaking wave zone close to the reef.

The models showed over a variety of swell size conditions (1 - 4 m), that seabed characteristics were strongly related to the presence of the surf zone, bed orbital velocities and the resulting currents. These currents have been shown to attain 0.8 $m.s^{-1}$ by Phillips (1999), while maximum bed orbital velocities were up to 2.0 $m.s^{-1}$. Mean currents were directed up the headland (cross-offshore), but strong currents down the headland were present during large swell events. The results of this previous experiment, indicated that the sandy bed is maintained by local, re-circulating sediment pathways and is not strongly dependent on the west coast net northward drift of sand.

Sediment samples identified that the larger sized grains were also located closer to the high energy surf zone of the headland. This is also where the most defined bedforms were located close in to the rock/reef boundary, where the waves are shoaling and peeling along the reef. They have continuous crests and are sinusoidal in nature. They are similar to those identified by Lewis (1979) in the South Taranaki Bight, on the west coast of New Zealand.

The rock/sand boundary boundary generally followed the shape of the headland but showed considerable variation in its position over time. Similar characteristics were found by Carter and Lewis (1995), where general outlines were maintained, but the patch margins were less stable and are frequently modified by scour or accretion. The driving forces behind these changes are tides, swell, and storm-forced currents. This is in comparison to experiments on the downstream coast beyond Port Taranaki, that indicated long term stability of sandy patches within and between the rock reef (McComb, 1999). This difference could be due to the more sheltered nature of this reef, than found at Raglan, where the more shoreward regions over the rocky sea bed are presumably disrupted by down-headland, wave-driven currents more often. The sandy bed is winnowed away, being unable to exist over the long term where strong wave-driven flows down the headland cause strong net transport.

The time-series side scan sonagraphs demonstrate the dynamic nature of the seabed, with sediment being both accreted and scoured at the headland. This variation and change in the rock/sand boundary appears to be influenced by the seasonal sediment supply, recent weather and swell conditions, and seems to change in position very rapidly. The rock/sand boundary was found to have moved 30-40 m seaward from its position in 1999, which may have been largely due to a recent large swell (6 m) event, with fresh rock exposed. The rock soon began to cover with the subsequent smaller swell.

The relative quantity of percentage sediment coverage on the rocks and reef was found to vary over each side scan survey. The greatest cover was found when the boundary was furthest seaward and could demonstrate accretion of sediment on the reef in proportion to where the boundary is located. The combination of strong currents and re-circulation of sediment on the headland supports this theory, whereby post a large swell event when sediment has been transported away, the re-circulating sediment pathway returns sediment onto the freshly exposed rock.

Visual observations have shown long term habitation of the sub-tidal reef edge by adult marine organisms, which could demonstrate an upper level in the seabed movement. This variation in bed movement will be accurately determined in the near future, with repetitive hydrographic surveys, both seasonally and pre/post swell events.

6. CONCLUSIONS

A series of 3 detailed side-scan sonar surveys delineated the rock and sand regions of the seafloor, and demonstrated that the rock/sand boundary generally followed the shape of the headland, but was found to vary considerably in its position over time. The seabed is very dynamic in nature, with sediment being both accreted and scoured at the headland, and covering and uncovering rock outcrops.

This variation and change in the rock/sand boundary appears to be influenced by the seasonal sediment supply and by recent weather and swell conditions. A change in position seems to occur quite rapidly. These seabed characteristics correlate particularly well with the previously determined theory, that strong wave driven currents during large swell events transport sand from the headland whilst local re-circulating pathways return it in an attempt to attain an equilibrium position. Long term habitation by adult marine organisms at the sub-tidal reef edge

demonstrates a possible upper level of sediment movement.

The surveys also identified zones of megaripples on the seafloor, most commonly located close to the rock/sand boundary. The bedforms have continuous crests and are sinusoidal in nature, and contained the signature of recent swell conditions. Ground truth observations by divers confirmed their presence with wavelengths of up to 3 m (crest to crest) and heights of 0.5 m.

Bed sediments were sampled in 1998 and 2001 to a distance of 500 m offshore, and both times the results showed minimal variation. The sediment can be categorised as well-sorted sands with median grain size grading from 0.28 mm inshore to 0.16 mm offshore. On both occasions the larger grains were located closer to the high energy surf zone of the headland. Numerical model predictions show that grain size is strongly related to bed orbital velocity and the presence of the surf zone.

7. ACKNOWLEDGEMENTS

Technical assistance by Dirk Immenga was greatly appreciated. Graduate students of the school are thanked for their help in the field.

8. REFERENCES

Mead, S., McComb, P. B. & Black, K. 2001 *Report prepared for Telstra Saturn*. Expert Evidence. ASR Ltd..

Black, K.P. & Rosenberg, M.A. 1992. *Semi-imperical treatment of wave transformation outside and inside the breaker line*. Coastal Eng. 16: 313-345.

Brookes, H.D. & Green, M.O. 2000. *The Determination of a Wave Climate for the Auckland Region, New Zealand.* New Zealand Coastal Society Seminar. 12-13 October.

Carter, L. & Lewis, K. 1995. *Variability of the modern sand cover on a tide and storm driven inner shelf, South Wellington, New Zealand.* N.Z Journal of Geology and Geophysics. 38: 451-470.

Daborn, G. R. & Dickie, B. 1997. *Community based Environmental Management: Whaingaroa (Raglan) Harbour and Water Catchment.* Proc. Combined Australasian Coastal Engineering and Ports Conference, Christchurch, New Zealand, 1997.

Gallagher, E.L., Elgar, S. & Thornton, B. 1998. *Megaripple migration in a natural surf zone*. Nature. Vol: 394.

Gibb, J.G. 1979. *Late Quaternary shoreline movements in New Zealand.* Unpublished PhD thesis, Victoria University of Wellington, New Zealand.

Goles, G.G., Briggs, R.M. & Rosenberg, M.D. 1996. *Late Pliocene stratigraphic succession and volcanic evolution of Karioi volcano, Western North Island, New Zealand.* New Zealand Journal of Geology and Geophysics. Vol. 39: 283-294.

Heath, R.A. 1982. *What drives the mean circulation on the New Zealand west coast continental shelf.* New Zealand Journal of Marine and Freshwater Research. *16: 215-226.*

Hume, T. M., K. P. Black, J. W. Oldman and R. Vennell, 1997. *Signatures of Wave and Current Forcing on the Seabed about a Large Coastal Headland.* Proc. Combined Australasian Coastal Engineering and Ports Conference, Christchurch, New Zealand, 1997.

Hutt, J. 1997. *Bathymetry and wave parameters defining the surfing quality of five reefs.* Unpublished Master of Science Thesis, Earth Sciences Department, University of Waikato, New Zealand.

Komar, P.D. 1976. *Beach Processes and Sedimentation.* Prentice-Hall, Inc. New Jersey. 429p.

Lewis, K.B. 1979. *Storm Dominated Inner Shelf, Western Cook Strait, New Zealand*. Marine Geology 31: 31-43

McComb, P., Black, K., Healy, T. & Atkinson, P. 1999 *"Coastal and Sediment dynamics at Port Taranaki, New Zealand; a large, multi-faceted field experiment."* Proceedings of Coastal Structures '99 Conference, Santander, Spain, 823-8329.

Mead, S.T. and K. P. Black, 2001. *Functional component combinations controlling surfing wave quality at world class surfing breaks.* Journal of Coastal Research, Special Surfing Issue (in press).

Phillips, D., K. P. Black, T. Hume, & T. Healy, 1999. *Sediment Dynamics Along a Surfing Headland.* Proceedings of Coasts & Ports 99, Vol. 2, pp. 513-518.

APPENDIX 3: Published papers

SANDY SEAFLOOR VOLUME CHANGES OFF A HIGH ENERGY HEADLAND BOULDER BEACH, RAGLAN, NEW ZEALAND

Phillips, D.J., Black, K.P. and T.R. Healy., 2003. Sandy Seafloor Volume Changes off a High Energy Headland Boulder Beach, Raglan, New Zealand. *Coasts and Ports 2003,* Auckland, New Zealand. CD Publication: Paper No. 115, 8 p. ISBN: 0-473-09801-6.

THE APPLICATION OF SURVEYING TECHNIQUES TO ARTIFICIAL SURFING REEF STUDIES

Scarfe, B.E., Black, K.P., Chong, A.K., de Lange, W.L., Phillips, D.J. and S.T. Mead., 2002. The Application of Surveying Techniques to Artificial Surfing Reef Studies. *Trans Tasman Surveyor. Journal of the New Zealand Institute of Surveyors,* 5, 29-40.

SANDY SEAFLOOR VOLUME CHANGES OFF A HIGH ENERGY HEADLAND BOULDER BEACH, RAGLAN, NEW ZEALAND

David Phillips[1,3], Kerry Black[2], Terry Healy[3]
[1]UNITEC Institute of Technology, Private Bag 92025, Auckland, New Zealand. dphillips@unitec.ac.nz
[2]ASR Ltd, PO Box 13048, Hamilton, New Zealand. k.black@asrltd.co.nz
[3]Coastal Marine Group, Department of Earth Sciences, University of Waikato.
P.O. Box 11-115, Hamilton, New Zealand. t.healy@waikato.ac.nz

Abstract: Highly accurate bathymetric surveys were conducted over an 87837 m^2 area at Raglan, a surfing headland on the west coast of New Zealand to determine the temporal and spatial changes of the iron-sand rich seabed adjacent to a boulder reef. The surveys show that the wave climate and sedimentary equilibrium are the factors controlling the level of the seabed, with a seasonal variation apparent in the results (ie: lower bed level in winter). The greatest variation in the bed level was found in the inshore region, whilst further offshore the bed showed minimal variation. Compartmentalisation between surf breaks at the headland was identified through deposition of sand in the lower energy zone at the upper end of Whale Bay. The mean seabed levels along a 500 m transect varied a maximum value of 0.47 m and levels correlated well to the volume changes at the headland.

Keywords: Raglan, surfing headland, bathymetry, volume changes, sediment.

INTRODUCTION

Along the west coast of New Zealand, the pre-dominant southwest winds and swell drive a net sediment movement that is to the north (Gibb, 1979), with approximately 175,000 250,000 m^3/yr^{-1} of net littoral drift. The Gibb study focused on the total longshore drift up the coast, not on the headland environment that exists at Raglan, a surfing headland. Stokes (1991) concluded that the large reservoir of sorted sands that occurs on the north side of the Raglan Harbour entrance is associated with the erosion of a large body of rock and a prolonged period of northerly littoral drift. In comparison a similar amount of 220,000 m^3 of sand per year, is known to travel past the Port Taranaki main breakwater at New Plymouth, some 120 km south of Raglan on the same coast (McComb *et al.,* 1999).

On the seabed of a headland the sediment grain size varies depending on the sediment source, the wave-energy level, and the general slope of the shoreline. The sediment source is obviously the main controlling factor, but further winnowing out of relatively fine sediment by wave action leads to a coarsening of the sediment with increased energy (Black *et al.*, 1999, Mead and Black, 2001). The west coast "black sand" is fine grained and denser than quartz "white sand". It originates from the Taranaki volcanic region (Briggs, *et al.,* 1989), and can be classified as from Taranaki andesitic origin, thought to be derived from inland sources to the south west, transported by rivers and streams to the sea and subsequently moved by littoral processes to the northeast (McClennan, 1982). It contains trace elements such as titanium and is a source of iron ore, which is mined for use in the production of iron and steel. The 'black' sand consists of 38% heavy minerals (titano-magnetite, augite, hornblende) and 62% lighter minerals (feldspars) (Bartholomeusz, 1985 – cited in McComb *et al.,* 1999).

Previous measurements have shown that large wave-driven currents flow northeastward around the headland during large swells from the southwest, generating a current gyre with an offshore return flow. This flow has been described as a re-circulatory system (Phillips *et al.,*

1999) that maintains the sandy seabed at the headland. The present paper examines the changes in the seafloor topography temporally and spatially within the survey area at the headland, induced by these intermittent wave-driven currents.

METHODS

Highly accurate hydrographic surveying to chart the Indicators seafloor was undertaken over the study period using RTK-GPS (Real Time Kinematic – Global Positioning System) and a depth sounder. This allowed calculation of the sediment volume changes, including analysis of a 500 m transect from 595200 mN, 302880 mE to 595700 mN, 303000 mE (Mt Eden Grid)(Fig. 1). The surveys were undertaken on the 10-07-01, 3-09-01, 6-11-01, 29-01-02 and 8-02-02. The results of a bathymetric survey in January 1996 by Hutt (1997) have also been compared to the more recent surveys. This earlier survey did however use lower accuracy equipment.

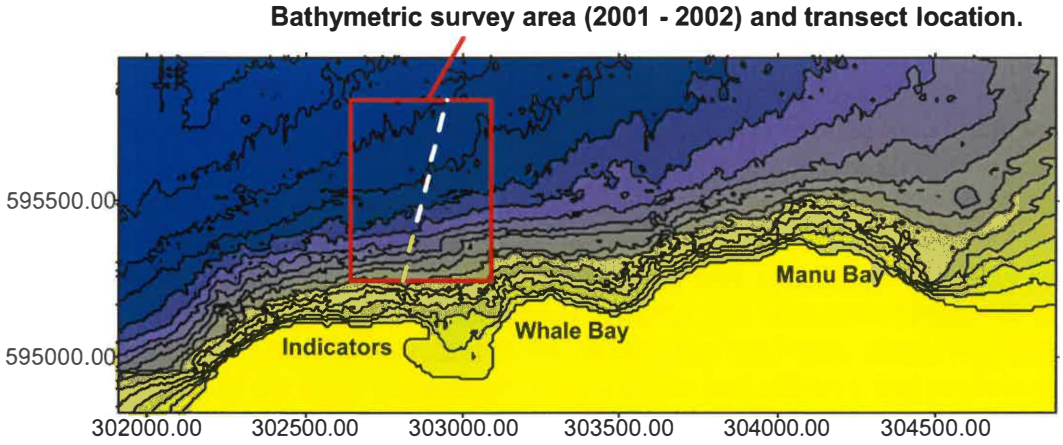

Figure 1: Bathymetric map of the Raglan headland in 1996 (source – Hutt, 1997) with the area of the surveys undertaken in 2001/2002 and the transect location.

Experimental RTK-GPS was validated and utilised to measure a water level correction for depth soundings (Scarfe, 2002). The 5 Hz Leica SR530 RTK was successfully used for the Raglan experiments in synchronized mode. Analysis of cross-lines for the survey yielded a 95% confidence interval of depth accuracy of 0.17 m. Data were compiled into bathymetric grids using Surfer© surface mapping system (Golden Software, Inc.) and analysed for variation in the bed level. The surveys were undertaken from the University of Waikato boat Taitimu on days when the swell and wave conditions were low, although this could not always be achieved, with 0.5 m swell present for some of the surveys. The RTK-GPS is capable of removing this swell from the data when processed, due to the high frequency response of the instrument. High tide was selected to undertake the surveys, as less shoaling of waves takes place in the deeper water of the surfing headland. No tide gauge is needed as the instrument corrects the depths relative to the satellite geodetic datum.

An S4 Interocean current meter was deployed at 303685 mN 595808 mE, on 3-07-01 to measure wave heights and tides to 19-11-01. The meter was serviced over this period and it was found that data in July, August and October (15 days of data) was logged unsuccessfully due to a malfunction in the instrument. A meter was also deployed from 29-01-02 to 8-02-02.

RESULTS

The surveys showed that the depth contours graded on a 1 in 45 slope for the first 250 m of the transect, then levelled to a 1 in 85 grade for the remaining 250 m of the transect (Fig. 3). The steeper inshore gradient is suitable for surfing wave conditioning and breaking at the headland. Wave heights measured over the survey period showed a range of conditions varying from 0.2 m to 4.8 m from the 31-8-01 to 19-11-01 (Fig. 2a) and 0.45 m to 3.5 m from 29-01-01 to 8-02-02 (Fig. 2b). Between the hydrographic surveys on the 3-09-01 and the 6-11-01 the wave heights averaged 1.8 m with 3 wave events reaching over 4 m. In 2002 the wave data averaged 1.2 m with a maximum of 3.5 m.

Bathymetric maps of the volume differences between hydrographic surveys on 10-07-01 to 3-09-01 (Map A), 3-09-01 to 6-11-01 (Map B), 6-11-01 to 29-01-02 (Map C) and 29-01-02 to 8-02-02 (Map D)(Fig. 3) show significant variation in seabed level. The maps show the presence of sedimentary troughs and mounds in the inshore zone, near where the reef and boulders are located and the waves break. Map A shows significant erosion of sediment inshore (0.7 m) but grading to 0.2 m of erosion offshore over the majority of the survey area. In the centre a mound of sand visible in the July survey was eroded away, whilst bands (20 m wide) of erosion and accretion occurred in the vicinity of two submerged reefs (one showing 1.0 m erosion further offshore and the other 0.5 m accretion inshore). Map B shows a fairly stable bed offshore with mixed erosion and accretion in the nearshore area ($\pm$0.7 m). The most significant area of deposition (0.5 m) occurred in an area near the Whale Bay reef. This was again evident in Map C where erosion of 1.0 m of the bed occurred offshore to the northwest, grading inshore to 1.5 m of accretion in the Whale Bay reef area. There was less variation in Map D than that of the other three maps, with a stable bed offshore and pockets of erosion and accretion in the inshore area up to 0.7 m.

Figure 3a of a 500 m transect through the survey area shows the variation in bed level over all the hydrographic surveys, whilst Figure 3b shows the upper and lower envelope of bed-level heights over the experimental period. This data varies along the transect from a minimum range of 0.1 m for the 250 m offshore part of the transect, to a maximum of 0.5 m variation for the inshore area. This demonstrates the stability of the bed offshore with greater variation in the surf zone nearer the headland. An increase in bed level can be seen at the point where the seabed gradient changes, which is evident on all the surveys.

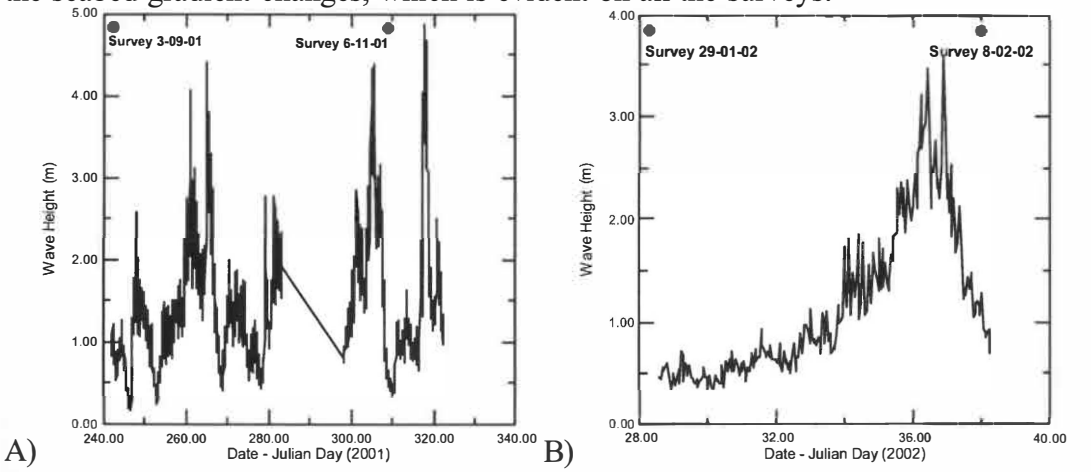

A) B)

Figure 2: (A) Measured wave heights from an S4 deployment at Raglan from 31-08-01 to 19-11-01 and (B) 29-01-02 to 8-02-02. Dates of the hydrographic surveys undertaken are also shown.

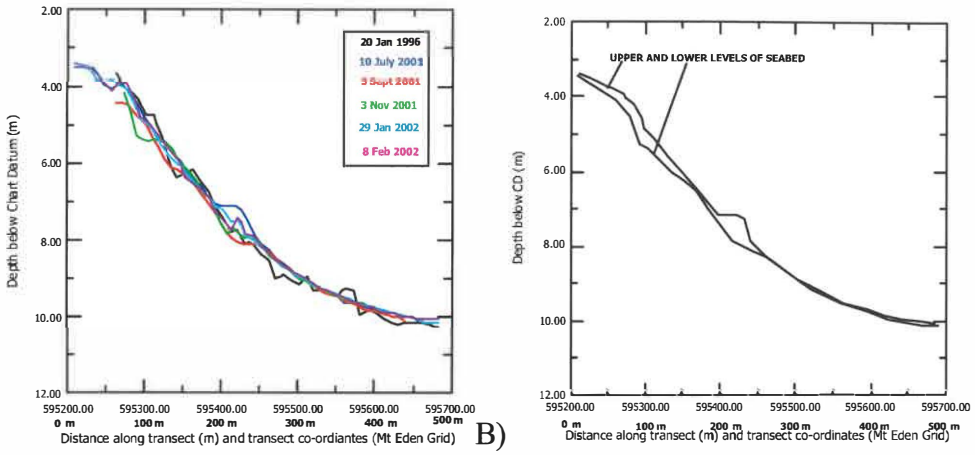

Figure 3: (A) Seabed level along a 500 m transect, from 6 bathymetric surveys undertaken (20-01-96 to 8-02-02), and (B) the upper and lower bed-level envelope from the bathymetric surveys (10-7-01 to 8-02-02)(ie: excludes lower accuracy survey 20-01-96).

A mean bed level below Chart Datum (CD) was calculated from all the transect bed level data for each survey (Table 1). The mean of this data was 7.64 m and ranged from a minimum of 7.47 m on the 8-02-02, to a maximum of 7.86 m on the 3-09-01, which is a maximum variation of 0.43 m along the 500 m transect. The volume difference in bed levels between surveys over the total area was calculated using the SURFER software and shown as $\pm$ m^3 of variation. This data correlated very well to the mean bed levels, where higher bed levels also had positive increases in volume and vice versa for the low mean bed levels. The lowest volume change was +69 m^3 between 29-01-02 and 8-02-02, and the highest was -17990 m^3 between the 10-07-01 and 3-09-01. This is a maximum height difference of –0.21 m if distributed over the full survey region of 87837 m^2 (Table 1). The data demonstrates that the lowest bed level occurred in winter when swells tend to be at their largest size on the west coast, however wave heights of over 4 m measured on a number of occasions throughout September and October 2001 did not result in a significant lowering of the bed level, but rather a maintenance of the bed near this low level. This shows the bed is capable of maintaining an equilibrium level in the presence of large wave driven currents that would be expected to transport large quantities of sand from the headland.

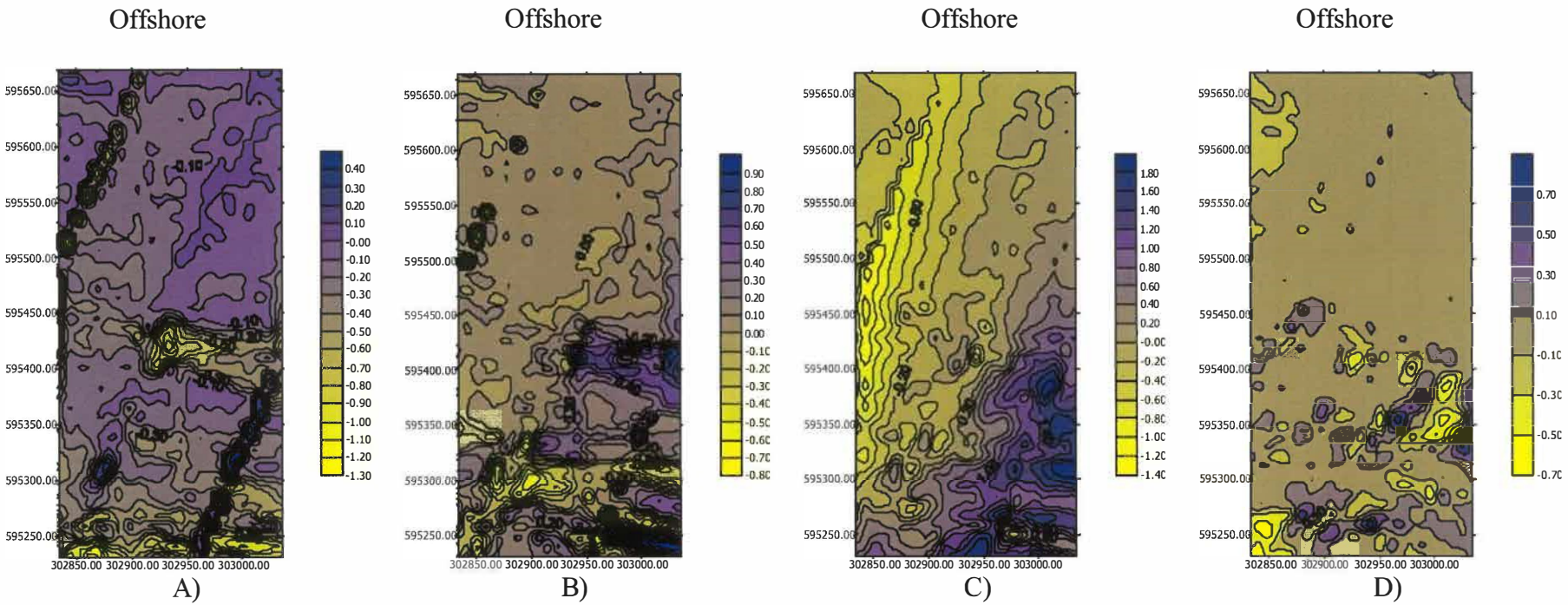

Figure 3: Bathymetric maps of the volume differences between hydrographic surveys on (A) 10-07-01 to 3-09-01, (B) 3-09-01 to 6-11-01, (C) 6-11-01 to 29-01-02 and (D) 29-01-02 to 8-02-02.

Table 1: Mean seafloor elevation along the transect for the surveys, and the volume changes (m^3) over the survey area (87837 m^2), from bathymetric survey to the subsequent survey and vertical height difference (m).

Survey Date	Mean Bed Level (below Chart Datum) (m)	Volume Difference Over Total Survey Area (87837m^2) (m^3)	Vertical Height Difference Over Total Survey Area (m)
20-01-96	8.05		
10-07-01	7.51	-3330	-0.04
3-09-01	7.86	-17990	-0.21
6-11-01	7.83	+902	+0.01
29-01-02	7.48	+12780	+0.15
8-02-02	7.47	+69	+0.0008
Mean *	7.64		
Max Range *	0.43		

* Mean and Maximum range do not include the lower accuracy 20-01-96 data.

DISCUSSION

The time-series of bathymetric surveys at the Indicators surf break has shown that significant variation occurred (both accretion and erosion) in the level of the bed over the survey period. The seabed level along a 500 m transect varied by up to 0.5 m, when the difference between the lowest and highest levels of the bed are analysed (ie: envelope of change). Calculation of the mean levels of the seabed for each survey shows a minimum level of 7.47 m below Chart Datum, a maximum of 7.86 m and a mean of 7.64 m. This is a maximum variation of 0.43 m, and interestingly is 0.22 m each side of the calculated mean level, which suggests that the bed appears to have an equilibrium level or range about which the variation occurs. This is supported by observations described in Phillips *et al.,* (2001), where an upper level was designated by the long-term habitation of adult marine organisms on underwater boulders and the rock reef. The level is most likely regulated by wave action winnowing away sediment and the re-circulating sediment pathways at the headland replenishing the lost volumes (Phillips, *et al.,* 1999).

Significantly greater variation was found in the bed level within the first 250 m of the transect closest to the shore, where the gradient is steeper and breaking waves are located. Bathymetric maps of the difference in bed levels between surveys show a more complex erosion and accretion pattern in this zone, when compared to the offshore region. The bed offshore was considerably more stable with minimal variation in level. Interestingly a zone of sand deposition was located at the change in the bed gradients of the seabed (1 in 45 to 1 in 85) near the submerged Whale Bay reef, that was particularly apparent in the July 2001 survey but eroded away on the next survey on September 2001. The reef appears to provide an area that may result in deposition through either a physical barrier or decreased current velocity. This area of accretion is very apparent in the volume difference maps (Figure 4b and 4c). Surfers use this area at Whale Bay where the headland alignment changes as an access point to the surf, and has been identified by Phillips, *et al.,* (2003) as compartmentalisation where the headland is divided into a number of different cells with re-circulating current gyres.

The level of the bed appears to be regulated by the predominant wave climate present at the time, which is supported by the survey in early September 2001 when the bed was found to be at its lowest level. This is a period in late winter when the west coast of New Zealand has very large southwest swells occurring more often than in the summer months, and the bed would have been expected to be at a low level. Large swells in the following months (September and October 2001) maintained the bed at this low level, but did not further decrease the level as

may have been expected. This demonstrates that despite the presence of large waves and the associated movement of sand, the bed is able to remain fairly stable in level, with the likely existence of a sedimentary equilibrium balancing the inputs and outputs at the headland. In comparison the bed was at its highest level in January and February 2002 during summer, when the wave climate is smaller and demonstrates a possible seasonal variation.

The difference in the January – February 2002 surveys showed minimal variation in the volume of sediment on the bed with +69 m^3 of change, after a period of waves with a mean height of 1.2 m and one event reaching 3.5 m. The bathymetric map of the difference in the bed level shows a stable environment offshore, with mixed deposition and erosion inshore at the headland. This demonstrates that sediment was transported in the nearshore region where the breaking waves are found, but significant erosion did not occur despite the large wave event. A strong correlation was found over all the surveys between the variation in bed levels and the quantity of sediment eroded or accreted within the survey area (ie: decrease in level had associated decrease in volume). This factor shows that for the bed level to change for a longer period of time the sedimentary equilibrium of inputs and outputs must alter at the headland. Large swells can alter the bed level short term and recover as found by Phillips, *et al.,* (2001), but for longer term variation the seasonal wave climate and sediment available to the system from the overall west coast littoral sediment drift are the factors most likely to affect the level of the bed.

CONCLUSION

The six bathymetric surveys (20-01-96 to 8-02-02) undertaken over a 87837 m^2 area at the Raglan headland show the greatest variation (accretion and erosion) in the bed level was found in the inshore region, whilst further offshore the bed showed minimal variation. The mean seabed levels along a 500 m transect varied a maximum value of 0.47 m and the levels correlated well to the volume changes at the headland (ie: lower level with prior loss of sand volume). The surveys show that the wave climate and a sedimentary equilibrium are the factors controlling the level of the seabed. The bed was able to maintain a fairly stable level despite the presence of large wave events and associated sediment transport, but a seasonal variation (ie: lower bed level in winter when waves are typically larger) was identified. Deposition of sand in the lower energy zone at the upper end of Whale Bay where the coastal alignment changes supports the compartmentalisation of the headland identified in Phillips, *et al.,* (2003).

ACKNOWLEDGEMENTS

Technical assistance from Dirk Immenga, Brad Scarfe and Hayden Easton was greatly appreciated and thanks to Dr Shaw Mead for comments on the paper.

REFERENCES

Black, K; Green, M.; Healy, T.; Bell, R.; Oldman, J. and Hume, T. (1999). Lagrangian Modelling Techniques Simulating Wave and Sediment Dynamics Determining Sand-Body Equilibria. Ch.1 in Computerized Modeling of Sedimentary Systems, Ed. Harff, J., Lemke, W. and Stattegger, K. 1999. Pp.3-21.

Briggs, R.M., Itaya, T., Lowe, D., and A. Keane., 1989. Ages of Pliocene – Pleistocene Alexandra and Nagatutra Volcanics, Western North Island, New Zealand. Some geological implications. *New Zealand Journal of Geology and Geophysics* 32, 417-427.

Gibb, J.G., 1979. *Late Quaternary Shoreline Movements in New Zealand.* Unpublished PhD Thesis, Victoria University of Wellington, New Zealand, 216 p.

Hutt, J.A., 1997. *Bathymetry and Wave Parameters Defining the Surfing Quality of Five Adjacent Reefs.* Unpublished MSc Thesis, University of Waikato, New Zealand. 169 p.
McClennan, N.R. 1982. *Fitzroy Beach Processes and Quantitative Estimation of Littoral Drift.* Unpublished M.Sc. Thesis, Earth Sciences Dept., University of Waikato, NZ. 200 p.
McComb, P., Black, K., Healy, T. and Atkinson, P., 1999 *"Coastal and Sediment dynamics at Port Taranaki, New Zealand; a large, multi-faceted field experiment."* Proceedings of Coastal Structures '99 Conference, Santander, Spain, pp. 823-8329.
Mead, S.T. and K.P. Black. 2001., *Lyall Bay Surfing Reef Feasibility Study.* Volume 3 – Appendices. ASR Ltd, Raglan, New Zealand.
Phillips, D., Black, K., Hume, T., and Healy, T., 1999. *Sediment Dynamics Along a Surfing Headland.* Proceedings of Coasts & Ports 99: Perth, Australia. Vol. 2, pp. 513-518.
Phillips, D.J., Black, K.P. & Healy, T.R., 2001. *Seabed Characteristics of a Dynamic Exposed Headland.* Proceedings of Coasts and Ports 2001. Gold Coast, Australia.
Phillips, D.J., S.T. Mead., Black, K.P. and Healy, T.R., (2003). *Surf Zone Currents and Influence on Surfability.* Artificial Surfing Reefs 2003. The 3rd International Conference. 23-25 June, Raglan, New Zealand.
Scarfe, B.E., 2002. Water Level Corrections (WLC) Using RTK-GPS. *The Hydrographic Journal,* April Vol. 104.
Stokes, S., 1991. Tectonic Volcanic Implications of Provenance Changes in the Later Neogene Coastal Sand Deposits of the Kaihu Group, South Auckland, New Zealand. *New Zealand Journal of Geology and Geophysics* 34, 51-59.

KEYWORDS
Raglan, surfing headland, bathymetry, volume changes, sediment.

The Application of Surveying Techniques to Artificial Surfing Reef Studies

B.E. Scarfe[1]; K. P. Black[2], A. K. Chong[3], W. L. de Lange[1], D. Phillips[4] and S. T. Mead[5]

1. **Coastal Marine Group**
   Department of Earth Sciences
   University of Waikato
   Private Bag 3105
   Hamilton, New Zealand
   bes4@waikato.ac.nz
   w.delange@waikato.ac.nz

2. **ASR Ltd.**
   P.O. Box 13048
   Raglan, New Zealand
   k.black@asrltd.co.nz
   s.mead@asrltd.co.nz
   www.asrltd.co.nz

3. **School of Surveying**
   University of Otago
   P.O. Box 56
   Dunedin, New Zealand
   chonga@otago.ac.nz

4. **Faculty of Architecture and Design School of Engineering**
   UNITEC Institute of Technology
   Private Bag 92025
   Carrington Road, Mt Albert
   Auckland, New Zealand
   dphillips@unitec.ac.nz

Note: Brad Scarfe is now at ASR Ltd., Hamilton, New Zealand.
Email: b.scarfe@asrltd.co.nz

Abstract

Interest in multi-purpose offshore reefs, or artificial surfing reefs (ASRs) is growing as more people are being informed about the benefits for surfing, erosion control and biological enhancement. Significant volumes of scientific literature have been published on the design, construction and effects on the coastal environment of human made surfing breaks. Surveying has become a key tool in research, construction and monitoring of ASRs. Spatial measurement of the seafloor shape, wave breaking locations and shoreline responses to reef is the realm of surveyors. This paper illustrates a novel application of surveying in the coastal environment.

A research methodology employed to study how surfing waves transform over complex reef bathymetry at Raglan, New Zealand is presented here. Experimental RTK-GPS was validated and utilised to measure a water level correction for depth soundings. This created one of the most precise charts of a surfing break to date. Small and large scale reef features are identified in the bathymetry that modify wave shoaling and breaking. These features create sections in the surfing ride that break with different character making for an interesting and changeable surfing wave. The breaking waves are tracked relative to the seafloor with measurements made using a modified a projective transformation of video image coordinates. The influence of the separate surfing reefs components is seen from overlaying the wave path on the bathymetry and by wave refraction modelling.

The combination of state-of-the-art surveying and oceanographic methods has increased the understanding of how surfing waves transform. In particular, the research has shown how surfing manoeuvres are controlled by the wave parameters height (H_A), peel angle (a), section length (S_L) and breaking intensity (B_I). This has enabled design criteria to be developed that incorporates a surfer's manoeuvre types into the sections of an artificial surfing break.

Introduction

Surveying techniques are utilised in many different industries and research fields. They are not limited to the traditional uses such as cadastral surveying and hydrographic surveying for navigation. Here a novel application of seabed mapping and videogrammetry is presented to show how surveying can be used in non-conventional ways. A four month field study of the Manu Bay (Plate 1) surfing break in Raglan, New Zealand was undertaken by Scarfe (2002a) to develop design criteria for artificial surfing reefs (Scarfe, *et al.,* 2002).

Interest in multi-purpose offshore reefs, or Artificial Surfing Reefs (ASRs) (Barilotti, 1998; Black, 2001a and 2001b; Black *et al.*, 1998; Black and Mead, 2001; Centre for Natural Resources, 2001; Evans and Ranasignhe, 2001; Hutt, 1997; Mead, 2001; Mead and Black, 2002; Scarfe, 1999 and 2002a; Scarfe *et al.*, 2003a; 2003b and 2003c) is growing as more people are being informed about the benefits in amalgamating amenity (e.g. surfing, sheltered swimming, diving, snorkelling, windsurfing etc.), erosion control and ecological enhancement. Significant volumes of scientific literature have been published on the design, construction and effects on the coastal environment of human made surfing breaks. Surveying has become a key tool in research, construction and monitoring of ASRs. After all, spatial measurement of the seafloor shape, wave breaking locations and shoreline responses to a reef is the realm of surveyors.

Artificial Surfing Reefs

Coastal Protection

Most coastal protection methods defend coastal development from ocean forces at the expense of recreational and/or aesthetic values. Many solutions, such as seawall and groins, are applied routinely without seeking alternative methods. Often little is understood of the coastal processes causing the erosion. Black (2001a and 2001b) and Mead (2001) have given credibility to the use of artificial surfing reefs to rotate and dissipate wave energy, modifying wave climate and current patterns to stabilise the shoreline in the lee of the submerged reef.

Surfing Enhancement

Offshore and near shore bathymetry controls how often a surfing break will have surfable waves. The seafloor can be modified to maximise the number of surfable days at a surf spot. The use of human made reefs cannot generate swell but can optimise the number of good waves by rotating wave directions, controlling shoaling as well as by creating stable seabed contours for waves to break.

The four most important wave parameters for surfing are height (H_A), peel angle (á), breaking intensity (B_I) and section length (S_L). Peel angle is defined as the angle between the trail of the broken white water and the crest of the unbroken wave as it propagates shoreward (Plate 1; Walker, 1974; Hutt, 1997; Hutt, *et al.,* 2001; Mead, 2001). Peel angles range between 0° and 90° with low angles creating fast surfing waves and high angles slow waves. An angle of 0° is described as a close out (Mead and Black, 2001b).

A group of researchers from New Zealand have been recently investigating how surfing parameters relate to artificial surfing reefs. Hutt (1997) and Hutt *et al.* (1998 and 2001) have investigated relationships between wave peel angles, wave height and surfer skill levels. They conceived a classification scheme that links surfer skill to wave height and wave character. The scheme can be used directly to determine design criteria for an artificial surfing reef. An empirically derived formula for wave breaking intensity has been found by Mead and Black (2001c). The formula, based on the orthogonal seabed gradient, is used to estimate the wave vortex ratio, or how hollow a wave will break, on an artificial surfing reef. Moores (2001) has quantified the size of a wave section that can successfully surfed by surfers of different abilities under the Hutt *et al.* (2001) skill level scheme.

The type of manoeuvres that surfers can perform is largely controlled by the wave parameters. Wave height, peel angle, breaking intensity and section length for different parts of an artificial surfing reef need to be designed to allow certain manoeuvre types. The first investigations into how different types of waves dictate manoeuvres was undertaken by Scarfe (2002a) and Scarfe *et al.* (2002).

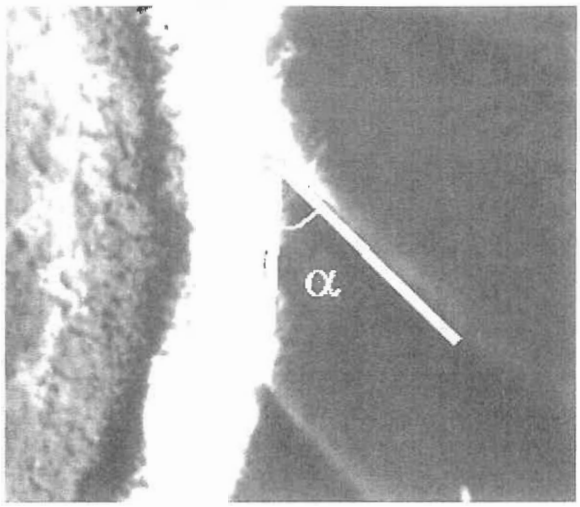

Plate 1. The peel angle, α, is defined as the angle between the trail of the broken white water and the crest of the unbroken wave as it propagates shoreward (Mead, 2001)

Biological Enhancement

It is commonly accepted that the introduction of an artificial object such as a reef into the coastal environment enhances the ecology in the area. For example, the artificial surfing reef at Narrowneck in Gold Coast, Australia has increased the bio-diversity of the marine ecosystem (Black, 2001b). Prior to reef construction the seabed supported only basic organisms and had limited diversity because of the very mobile loose sand in the area. Fish attracted to the reef within hours of the first geotixile reef bags being placed. Within two weeks, the bags were completely covered with marine organisms and plants. Now the reef supports a complete ecosystem achieving the objective of creating a new habitat for a broad range of marine life (Black, 2001).

Study Site and Research Methodology

Much of the key research on surfing waves in recent years has been done at Raglan, New Zealand just south of Auckland on the West Coast of the North Island (Andrews, 1997; Hutt, 1997; Moores, 2001; Sayce, 1997; Scarfe 2002a). The Raglan headland has a series of consistent surfing breaks that are popular for many surfers in the region (Plate 2). The breaks are made up of complex reef and boulder formations in the shallow water where waves break. In the deeper water, dynamic and changeable sand bars (Phillips *et al.*, 1999 and 2001; Scarfe, 2002a) precondition waves as they approach the surfing area.

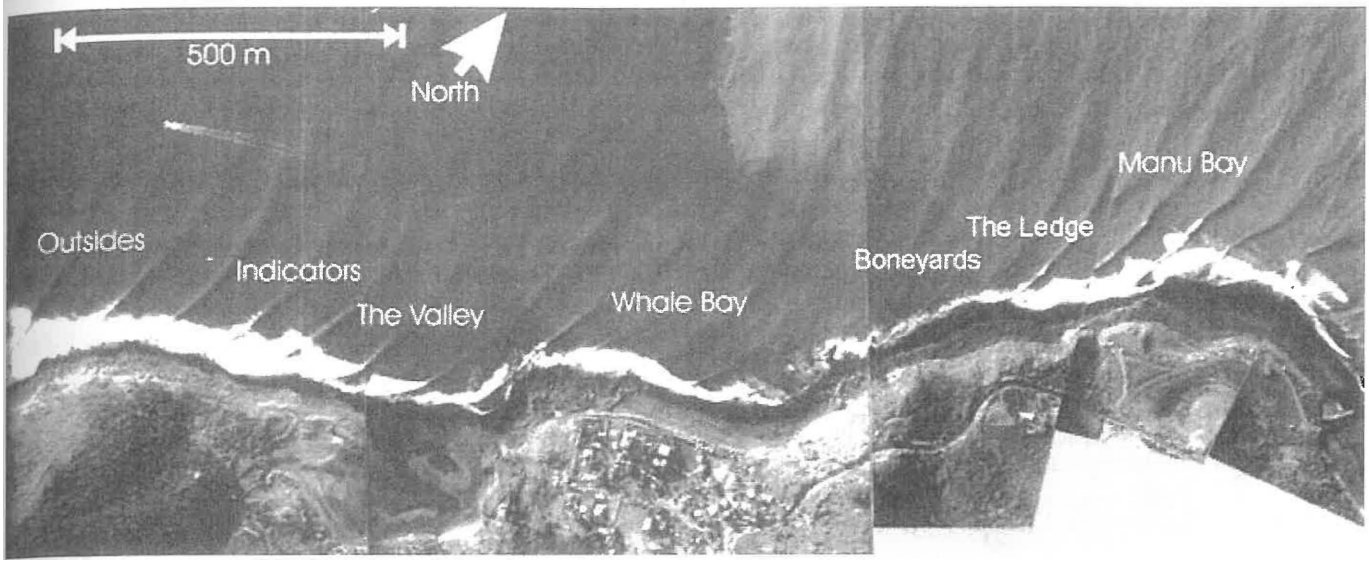

Plate 2. Aerial view of the Raglan surfing breaks (Hutt, et al. 2001).

The research methods presented here are hydrographic and photogrammetric in origin. The Manu Bay (Plate 3) seafloor was charted with experimental RTK-GPS hydrographic techniques validated by Scarfe (2002b). Side scan imaging of the seafloor by Phillips *et al.* (2001) showed the reef-sand boundaries and the presence of various scale morphological bars. Periodic surveys of sections of Manu Bay and neighbouring Indicators surf breaks quantified the scale of erosion and accretion of sediment near the reefs. Video images were used to track breaking waves and surfing rides relative to the surveyed bathymetry using a modified non-metric videogrammetry technique. Combined analysis of the wave paths with numerical modelling of the waves showed how the different components of the surf break modify wave refraction and breaking. This data allowed design criteria for different surfing wave parameters to be investigated.

Plate 3. Manu Bay, Raglan, New Zealand – Easter 2001 (photo source - A. Stringer).

Hydrographic Surveying of the Surf Break

Much information about a surfing break can be seen simply from the bathymetry since it controls wave refraction and breaking. The configuration of different reef components (Mead and Black, 2001a and 2001b) dictates the preconditioning of waves and where the waves will break. Accurate charting is essential to understanding a surfing break and running successful numerical wave refraction model scenarios. Correcting depth sounding for tide and vessel motion must be made to produce accurate charts of the coastal zone.

Raglan has a large wave climate with a significant wave height of 2-2.5 m (Scarfe, 2002a). Although surveying is done during periods of low swell there is always a small underlying swell present. Accurate tidal corrections are difficult to obtain since no permanent tide station exists nearby. Equipment must be specifically deployed and calibrated to a local datum for the survey. These issues are not exclusive to Raglan and are applicable to many coastal areas. Additionally, many tide gauges are located in harbours and port embayment where the tide phase and amplitude can be significantly different to the open coast.

A new method to overcome problems with measuring separate heave and tide correction has been proposed. Scarfe (2002b) identified problems with measuring a separate heave and tide correction because the two are combined to correct a sounding for the water level at any one instant. What is required is a water level correction (WLC) that reduces a sounding to the local datum. Measuring the water level where a sounding is made, avoids errors caused by tidal corrections from remote locations.

To measure a WLC requires high update low latency RTK GPS. The GPS must calculate 3D positions at a sufficient rate (> 5 Hz) to model the waves. The timing of the position must be matched precisely (< 50 ms) to the sounding. Most

receivers output a position about 2 s after the measurement is true because of the time taken to transmit carrier phase observations from the reference GPS to the rover. This latency can be corrected using techniques presented by Scarfe (2002b) but ideally the GPS should have negligible latency. Trimble's MS750 RTK GPS has a low latency (20 ms) mode that predicts the reference GPS's carrier phase observations a few seconds in advance. This is possible, as the reference GPS observations do not change significantly over a short time. There is a small loss in accuracy from ±2-3 cm (horizontal) to ±3-5 cm but this is acceptable within the error budget of a hydrographic survey. The 5 Hz Leica SR530 RTK GPS has been successfully used by the authors in synchronised mode. Some degradation in accuracy is expected but was not tested specifically.

Final Chart

The final chart of Manu Bay can be seen in Figure 1. The survey used a Knudsen 320MP echosounder, Trimble MS750 RTK GPS operating in low latency mode at 10 Hz and Trimble HydroPro Navigation software. Significantly more detail can be seen in the chart than from the previous survey by Hutt (1997) in 1996.

Mead and Black (2001b) categorised Manu Bay as being made up of a large scale wedge with a ridge (Figure 2). A wedge (Figure 3) is a sloping seabed that initiates wave breaking and refracts incoming waves away from the favoured orthogonal direction (Mead and Black, 2001a). The favoured orthogonal direction is the optimum wave direction for good surfing waves. The ridge (Figure 3) is a seabed ridge on a wedge or ledge aligned so that the offshore isobaths are at a greater angle to the favoured orthogonal direction than the preceding isobaths of the wedge or ledge (Mead and Black, 2001a). A ridge causes a local increase in seabed gradient and leads to a wave section with a steeper face and lower peel angles (Mead and Black, 2001a).

Small scale focusing components (Figure 3) were also observed on the wedge. These focusing features converge wave energy creating a peak in wave height with a lower seabed gradient (Mead and Black, 2001a). They often create take off zones for surfers or sections along the surfing wave.

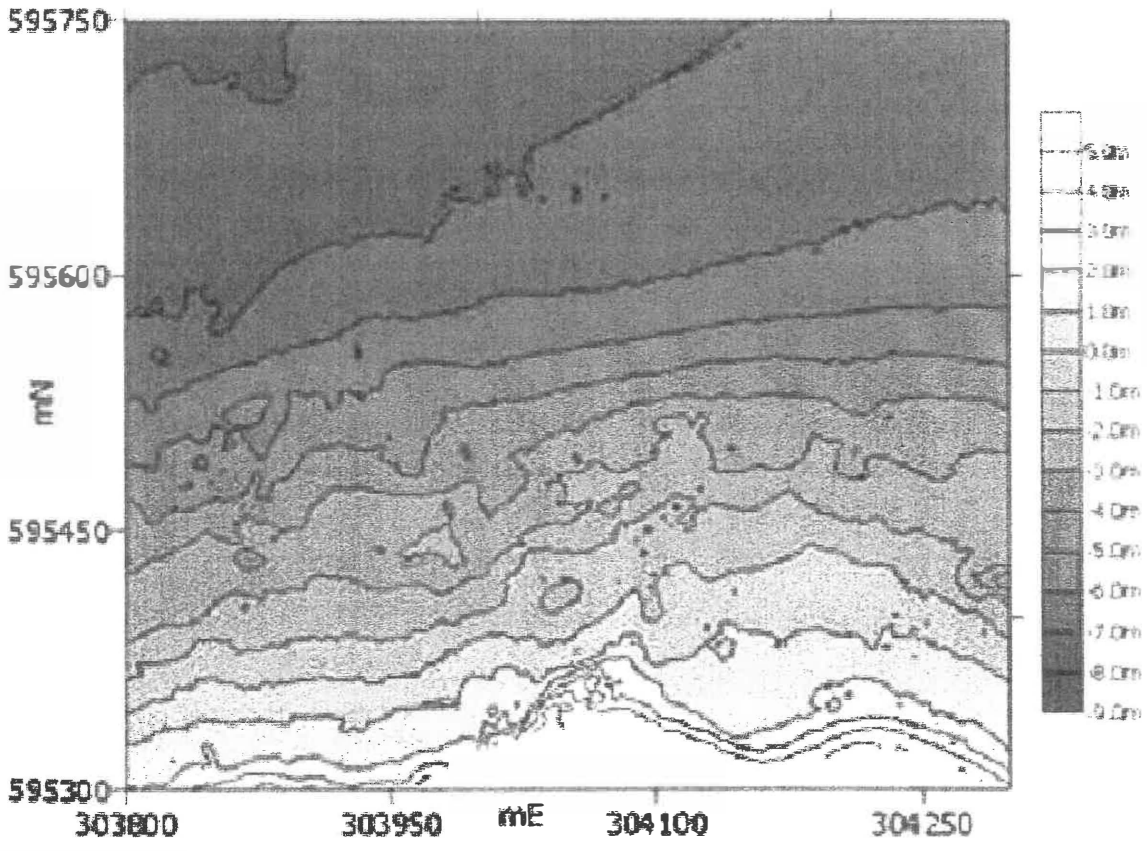

Figure 1. The Ledge and Manu Bay surfing breaks, Raglan, New Zealand. Depths relative to chart datum which is approximately lowest astronomical tide (Scarfe, 2002a).

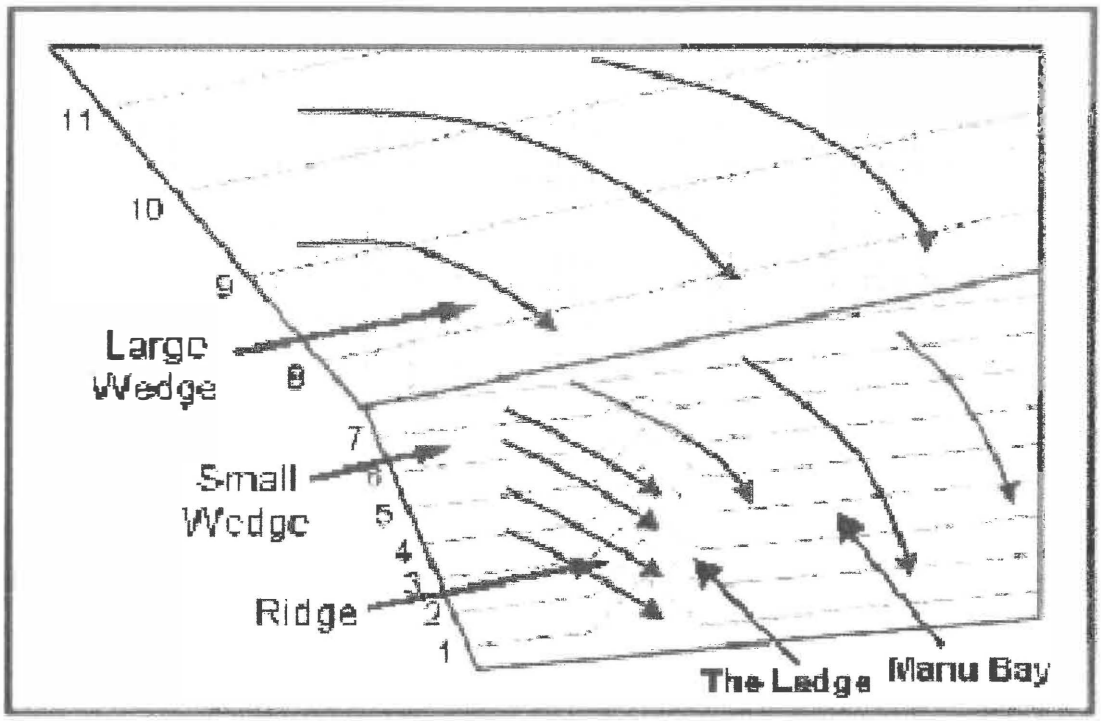

Figure 2. Schematics of Manu Bay surfing break. At a macro-scale the break is made up of a large scale wedge, small scale wedge and a ridge

Investigations of Sediment Dynamics

Investigating sediment dynamics in the coastal area involves a complete understanding of bathymetry, wave and current patterns and sediment types found at the beach. Phillips *et al.* (1999 and 2001) have been examining sediment dynamics around the Raglan surfing breaks. Among other techniques, periodic digital side scan surveys and hydrographic transects have been undertaken. The side scan images (Figure 4) appear as aerial photographs of the seafloor geology. The boundaries of reef and sand are clear. Scouring and infilling around the reefs is evident with certain reef features acting to trap sand. The side scan used was a Klien with Isis Sonar data acquisition and image processing system.

Scarfe (2002a) showed with a time series of surveys at Raglan that up to 0.5 m of sediment can be eroded and accreted per month from sand bars as they move around on shore and offshore. This significant changing the shape of the sea floor over time affects the preconditioning of surfing waves. Micro-scale focus and ridge components were seen to appear and disappear over time as successive swells accumulated or scoured around the reef.

Numerical Modelling of Waves

Numerical models are essential for coastal studies. They can be used to predict many wave, tide and current scenarios that otherwise are impossible to measure in reality. Sediment movements and budgets can be predicted based on current patterns. The models consist of many complex theoretical and empirical formulae that represent physical processes that happen at beaches. Many of these formulae include water depth making it critical to accurately chart bathymetry.

Investigations at Raglan by Scarfe (2002a) used the run rapid-solution monochromatic and spectral numerical wave refraction model Wbend (Black and Rosenberg, 1992). It was possible to simulate wave scenarios that were not observed during the field experiments. Also wave orthogonals, or changes in direction as the wave approaches the shore, were extracted allowing peel angles to be calculated.
The effect of different reef components (Figure 5 and 6) on wave refraction and shoaling was investigated for various wave conditions. The ridge component (Figure 2 and 6) creates a fast heavy wave section known as The Ledge. Numerical simulations show the wave breaks with a lower peel angle than the rest of Manu Bay because of the ridge feature.

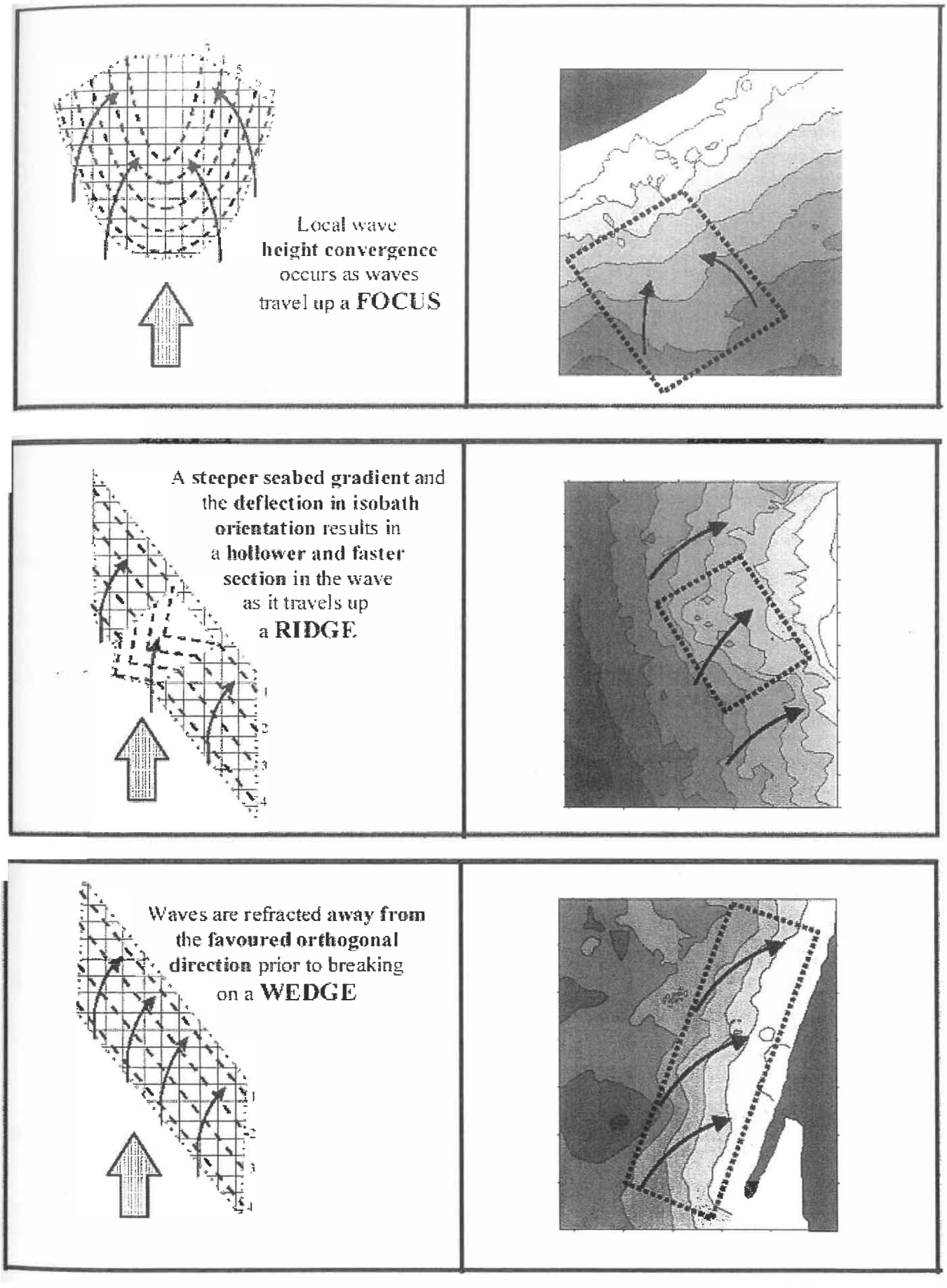

Figure 3. Schematics of a focus, ridge and wedge reef components (Mead and Black, 2001a).

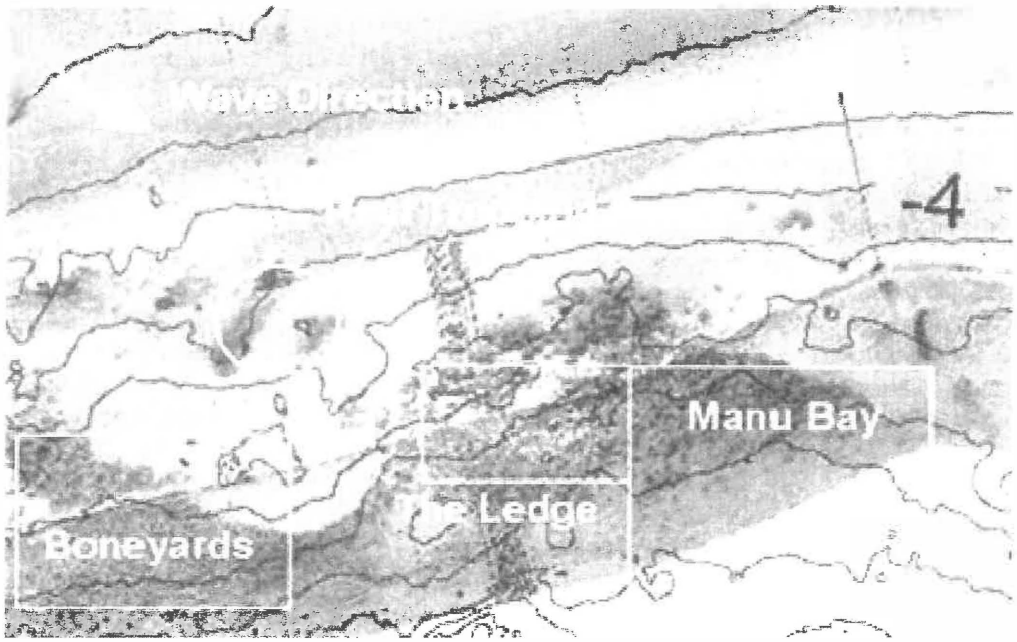

Figure 4. Side scan imaging (Phillips et al., 2001) of Raglan with 1 m contours (Scarfe, 2002a). The sediment-reef boundary is very clear and the effect of the reef on sediment accumulation and scouring is evident

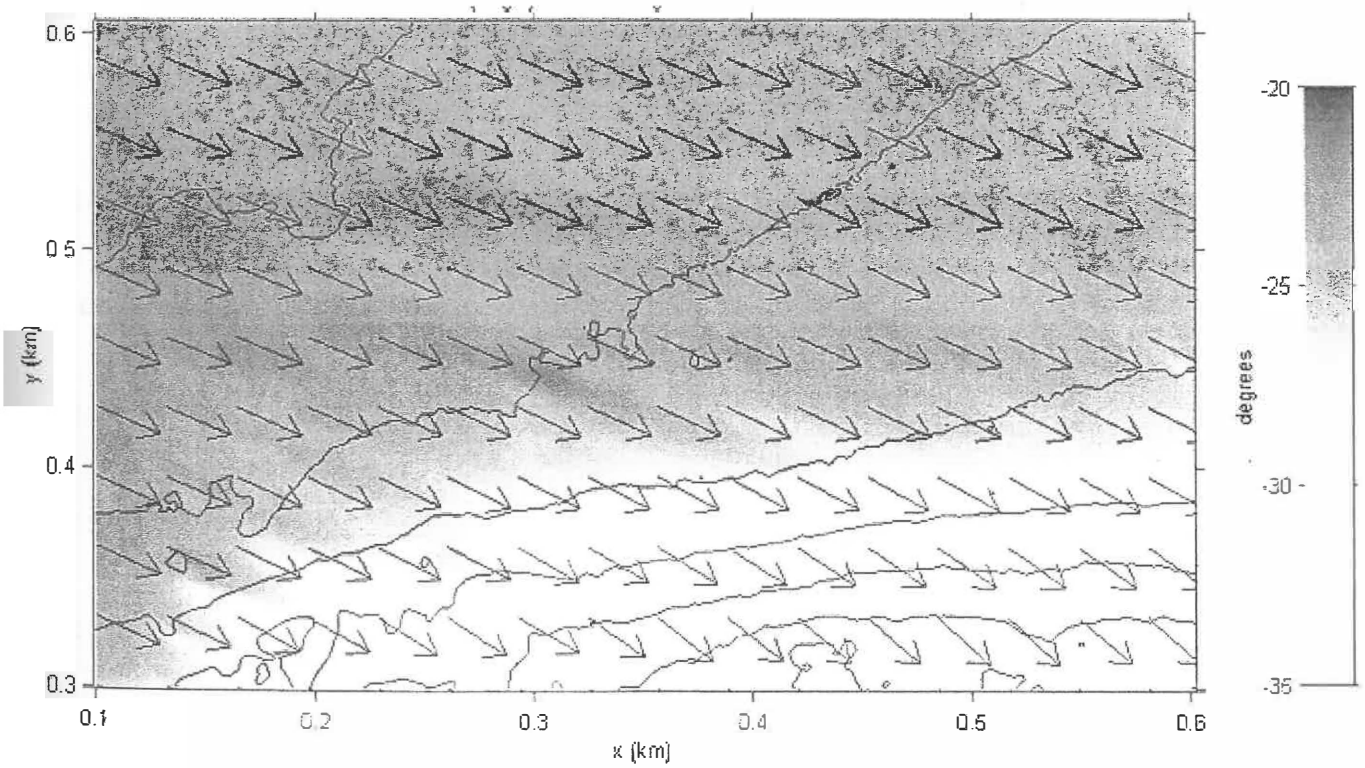

Figure 5. Numerical model simulation showing how the large wedge component on Raglan headlands shelf orientates the waves at Raglan to the favoured orthogonal direction. This simulation is of a 2.0 m, 12 second wave from 110° when the tide is 2.0 m above chart datum (Scarfe, 2002a)

Monitoring Coasts using a Modified Projective Transformation

Various researchers (Lippmann and Holman, 1989; Bailey and Shand, 1993; Kempema and Holman, 1994; Plant and Holman, 1997; Boogle, 2000; Turner, *et al.,* 2001) have used digital images to monitor shoreline evolution, beach morphology and other coastal processes. The non-metric photogrammetric techniques employed enables meaningful information to be obtained without the expertise, equipment and software required when using metric techniques. Moores (2001), Scarfe (2002a) and Scarfe *et al.* (2002) applied non-metric techniques to the study of surfing waves by extracting digital images from video footage. Moores (2001) calculated surfer speeds and the length of wave sections from relative points within the images. Scarfe (2002a) developed a modified projective transformation to precisely measure the absolute positions of breaking waves relative to the bathymetry.

When using a projective transformation it is assumed that all features on the image lie on the same plane. The rise and fall of the tide changes the plane from which measurements of wave locations should be made. This can lead to large errors when measuring absolute positions because they are projected away from the true position (Figure 7), particularly when the camera elevation is low and tide ranges are large. Therefore, the elevation of the measurement plane needs to be included in calculations for high accuracy measurements from images of the coast.

To correct to the changing object space plane as the tide rises and falls Scarfe (2002a) developed a simple extrapolation method. This method involves gathering control data when the tide is approximately low and when the tide is approximately high. When making subsequent measurements from the video images two transformations are done, one using the low tide control and one using the high tide control yielding two coordinates. The rate of change in northing and easting are determined and a corrected position (Figure 8) is calculated using Equations 1 and 2.

Scarfe (2002a) collected control data by videoing a boat equipped with RTK GPS as it navigated around the video image during low tide and high tide while the swell was low. It was clear from the video where the GPS was located on the vessel. Ten times per second a second the GPS recorded a positions which could be related to the video pixel coordinates. The timing of the GPS and video was calibrated better than a tenth of a second by videoing the GPS time. The camera mounting was purpose built to be stable over a long time even when the video camera was removed. No lens distortions have been corrected for but because the camera was zoomed fully in. This zoom-in method uses only the flattest part of the lens. If a wider angle was used then error, particularly around the image fringes could be significant.

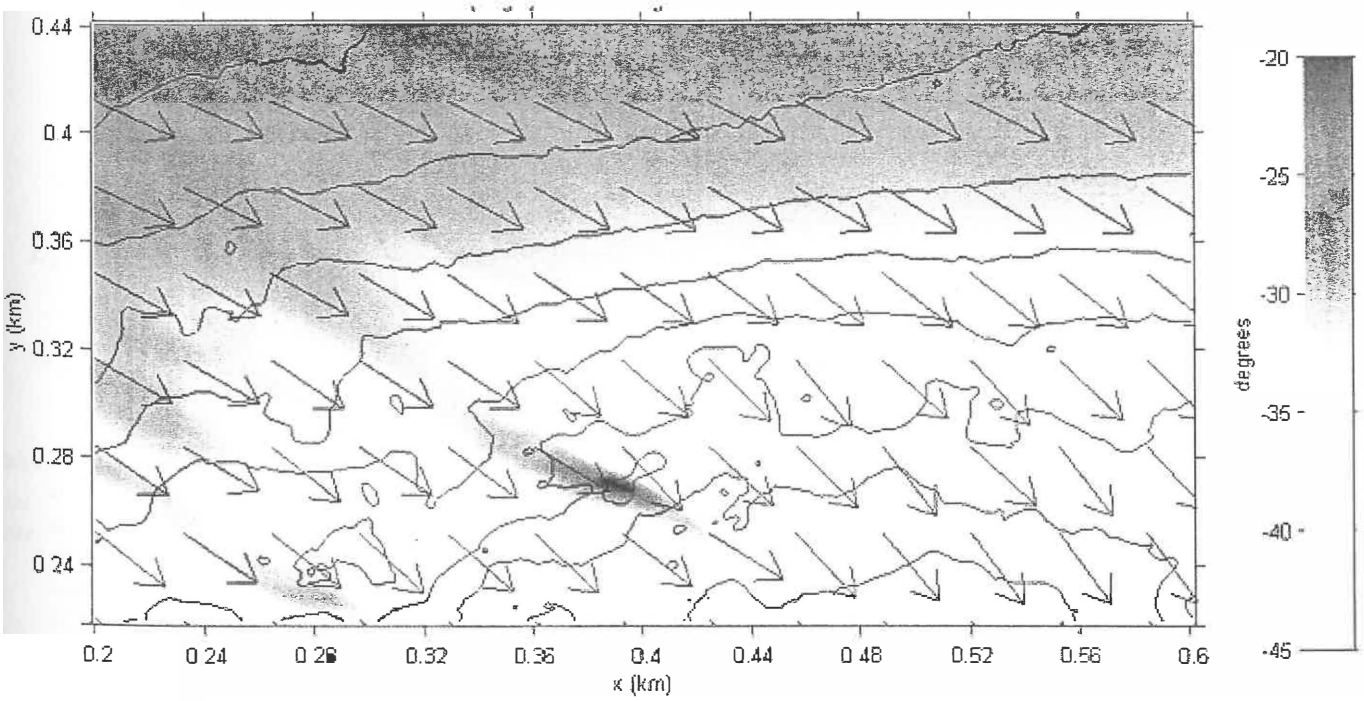

Figure 6. Numerical model simulation showing how the Manu Bay wedge cause wave refraction while waves pass over the ridge without any modification to direction. This simulation is of a 2.0 m, 12 second wave from 110° when the tide is 2.0 m above chart datum (Scarfe, 2002a)

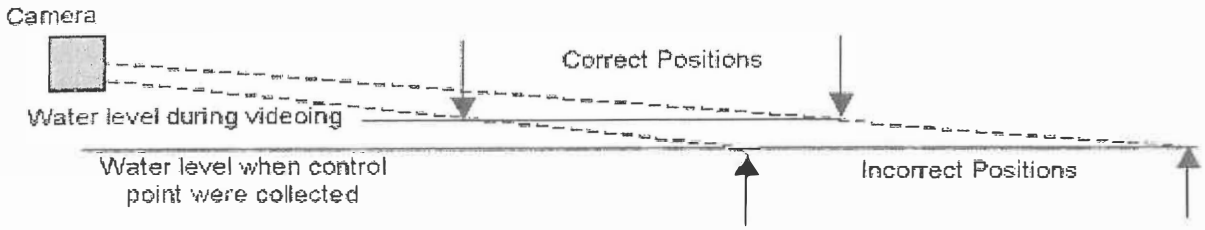

Figure 7. Effect on accuracy of positions when the water level is different from when the control points were collected. (Scarfe, 2002a)

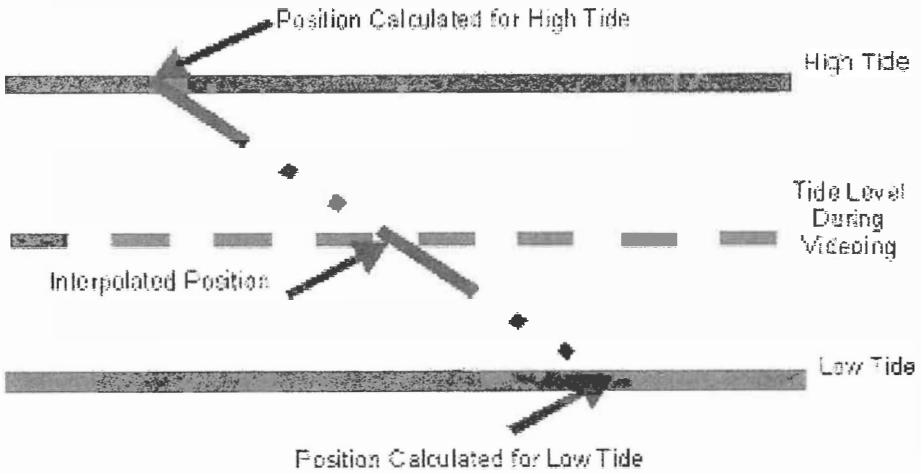

Figure 8. Interpolated position to correct for tidal fluculations (Scarfe, 2002a)

$$E_{CORR} = \frac{(E_{LT} - E_{HT}) \times (T - T_{LT})}{T_{HT} - T_{LT}} \quad (1)$$

$$N_{CORR} = \frac{(N_{LT} - N_{HT}) \times (T - T_{LT})}{T_{HT} - T_{LT}} \quad (2)$$

Where:

E_{CORR} = Corrected easting coordinate
N_{CORR} = Corrected northing coordinate
E_{LT} = Easting calculated using low tide control points
E_{HT} = Easting calculated using high tide control points
N_{LT} = Northing calculated using low tide control points
N_{HT} = Northing calculated using high tide control points
T_{LT} = Tide level above datum at low tide
T_{HT} = Tide level above datum at high tide
T = Tide level above datum at time image was taken

Images from Scarfe (2002a) of surfing at Manu Bay can be seen in Plate 4. The location of the breaking waves using the described technique were measured and plotted against the bathymetry (Figure 9). This showed how the micro-scale reef components or features create wave sections that break with varying character. Walker (1974) and Hutt (1997) used aerial photography to overlay wave break points with the bathymetry. This video technique enables more data to be obtained at a lower cost than with aerial photographs.

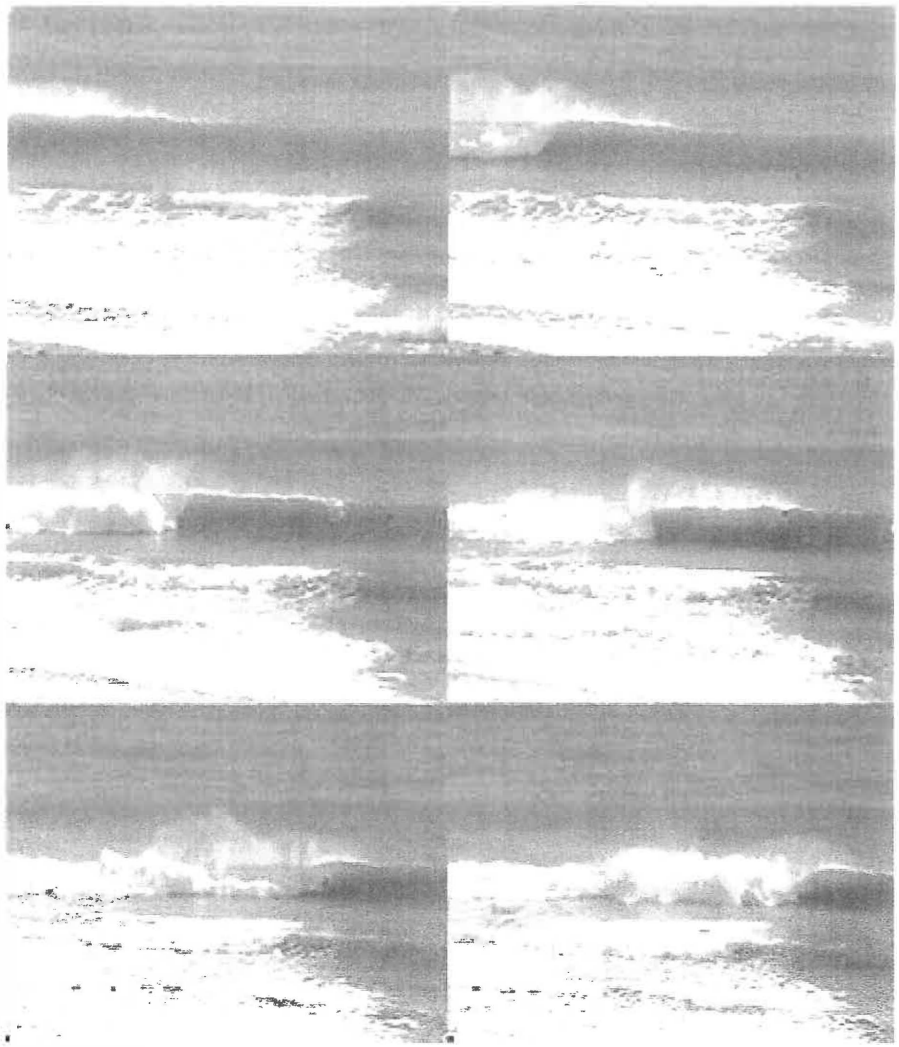

Plate 4. A sequence of a surfing wave at Manu Bay taken from digital video (Scarfe, 2002a)

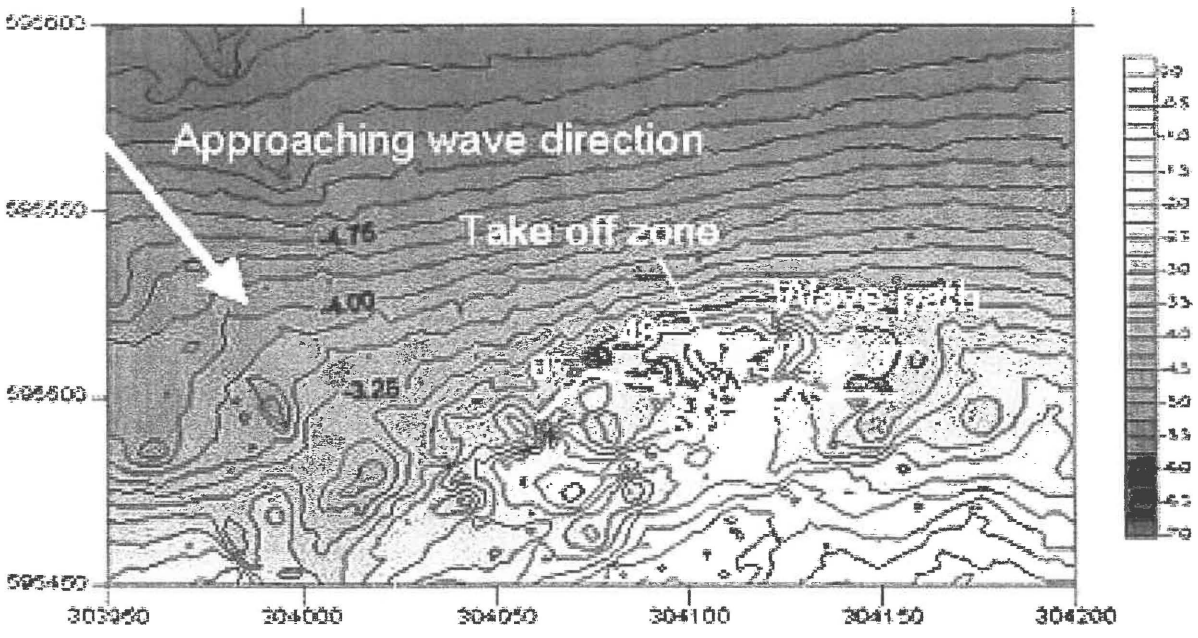

Figure 9. The path of the wave breaking in Plate 4. Micro-scale changes in peel angles that create wave sections are shown (Scarfe, 2002a)

Conclusions

Surveying techniques are utilised for many tasks. This paper shows that surveying can be an important tool for non-conventional applications. A methodology for investigating surfing waves is shown here that uses state of the art surveying coupled with oceanographic methods. The research has shown how surfing manoeuvres are controlled by the wave parameters peel angle and section length.. The outcome of the research has been the development of design criteria to incorporate a surfer's manoeuvre type into the wave sections of artificial surfing breaks. This helps to create reefs that provide an interesting and variable surfing ride that matches the skill level of the surfers who will use the reef. ASRs can be designed for beginners, intermediate, advanced and professional surfers and now there is a better understanding how surf parameters affect a surfing ride. Investigations into how manoeuvres are effected by wave height and breaking intensity were not undertaken but this knowledge would help in the design of artificial surfing reefs.

The techniques developed in this surfing study have wider application than just for artificial surfing reefs. The theory of WLC's has been successfully used here and can be applied in all types of hydrographic surveys. The accuracy, initialisation reliability and latency of positions from modern GPS equipment makes measuring WLCs possible. People are slowly adopting the use of RTK GPS to measure WLC corrections, or tide and heave, but this technique has not yet become widespread. However, the use will increase as people are exposed to the technology and software to support it improves. The modified projective transformation technique can be used in many coastal process studies where objects within the image lie on different planes. This is of particular importance when monitoring shoreline and dune evolution.

References

ANDREWS, C.J. 1997. *Sandy Shoreline Response to Offshore Reefs*. Master of Science thesis. Earth Science Department, University of Waikato.

BAILEY, D. G. and R. D. SHAND, 1993. Determining Large Scale Sandbar Evolution. *Proceedings for the first New Zealand Conference on Image Vision Computing*. August 1993. pp. 109-116.

BARILOTTI, S., 1998. Our Mother Ocean – Future Shack: An Artificial Reef Conference in San Deigo Raises a Nettlesome Question: Do Surfers have the Right to Alter the Coast for the Sake of Good Surf? *Surfer Magazine Annual Collectors Issue*. Vol. 39 no. 10 October. pp. 80-82

BLACK, K. P., 2001a. Foreword – Natural and Artificial Reefs for Surfing and Coastal Protection. In: Black, K. P., (ed.), Natural and Artificial Reefs for Surfing and Coastal Protection, *Journal of Coastal Research*, Special Issue No. 29, pp. 1.

BLACK, K. P., 2001b. Artificial Surfing Reefs for Erosion Control and Amenity: Theory and Application. *Journal of Coastal Research*, Special Issue 34. International Coastal Symposium (ICS2000). Edited by Terry Healy. pp. 1–14.

BLACK, K. P. and S. T. MEAD, 2001. Wave Rotation for Coastal Protection. *Proceedings for Coasts and Ports 2001* – The 15th Australasian Coastal Conference and Ocean Engineering Conference. pp. 120-127.

BLACK, K. P. and M. A. Rosenberg, 1992. Semi-Empirical Treatment of Wave Transformation Outside and Inside the Breaker Line. *Coastal Engineering*. 16. pp. 313-345.

BLACK, K. P., Hutt, J. A. and Mead, S.T., 1998. *Narrowneck Reef Report 2: Surfing Aspects*. Technical Report prepared for the Gold Coast City Council, June, 1998.

BOOGLE, J. A. 2000. *Video Imaging techniques for Quantitative Data on Bathymetry, Wave Period and Rips, and Qualitative Analysis of Beach Dynamics*. Master of Science Thesis, Earth Science Department, University of Waikato.

CENTRE FOR NATURAL RESOURCES, 2001. *Multi-Functional Artificial Surf Breaks: A Review*. Report published by NSW Department of Land and Water Conservation. Parramatta, Australia. 53p.

EVANS, P. and R. RANASIGNHE. 2001. Artificial Surfing Reefs: A Paradigm in Coastal Protection. *Proceedings for Coasts and Ports 2001* – the 15th Australasian Coastal Conference and Ocean Engineering Conference. pp. 128-133.

HUTT, J. A., 1997. *Bathymetry and Wave Parameters Defining the Surfing Quality of Five Adjacent Reefs*, Master of Science Thesis, Earth Science Department, University of Waikato.

HUTT J. A., K. P. BLACK and S. T. MEAD, 1998. Classification of the Degree of Surfing Difficulty for Artificial Reef Design. *2nd Annual International Artificial Surfing Reef Symposium*. San Diego. April, 1998. p. 4.

HUTT, J. A., K. P. BLACK and S. T. MEAD, 2001. Classification of Surf Breaks in Relation to Surfing Skill. In: Black, K. P., (ed.), Natural and Artificial Reefs for Surfing and Coastal Protection, *Journal of Coastal Research*, Special Issue No. 29, pp. 66-81.

KEMPEMA and HOLMAN, 1994. Longshore and cross-shore ice-drift rates, Lake Michigan. *Journal of Great Lakes Research*. Vol., 20. No. 1. pp. 196-205

LIPPMANN, T. C. and R. A. HOLMAN, 1987. Quantification of Sand Bar Morphology: A Video Technique Based o Wave Dissipation. *Journal of Geophysical Research*. Vol. 94. pp. 995-1011.

MEAD, S. T., 2001. *Incorporating High-Quality Surfing Breaks into Multi-Purpose Reefs*. Doctoral Thesis. Earth Science Department. University of Waikato.

MEAD, S. T. and K. P. BLACK, 2001a. Field Studies Leading to the Bathymetric Classification of World-Class Surfing Breaks. In: Black, K. P., (ed.), Natural and Artificial Reefs for Surfing and Coastal Protection, *Journal of Coastal Research*, Special Issue No. 29, pp. 5-20.

MEAD, S. T. and K. P. BLACK, 2001b. Functional Component Combinations Controlling Surfing Quality at World-Class Surfing Breaks. In: Black, K. P., (ed.), Natural and Artificial Reefs for Surfing and Coastal Protection, *Journal of Coastal Research*, Special Issue No. 29, pp. 21-32.

MEAD, S. T. and K. P. BLACK, 2001c. Predicting the Breaker Intensity of Surfing Waves. In: Black, K. P., (ed.), Natural and Artificial Reefs for Surfing and Coastal Protection, *Journal of Coastal Research*, Special Issue No. 29, pp. 51-65.

MEAD, S. T. and K. P. BLACK, 2002. Multi-Purpose Reefs Provide Multiple Benefits – Amalgamating Coastal Protection, High-Quality Surfing Breaks and Ecological Enhancement to Maximise User Benefits and Development Opportunities. *Proceedings for Surfing Art Science Issues Conference 2 (SASIC 2),* Ventura, California, 9 November 2002. pp. 47-63.

MOORES, A. E., 2001. *Using Video Images to Quantify Wave Section and Surfer Parameters.* Master of Science Thesis, Earth Science Department, University of Waikato.

PLANT, N. G. and R. A. HOLMAN, 1997. Intertidal Beach Profile Estimation using Video Images. *Marine Geology.* Issue 140. pp. 1-24.

PHILIPS, D., K. P. BLACK, T. HUME and T. HEALY, 1999. Sediment Dynamics Along a Surfing Headland. In: National Committee on Coastal and Ocean Engineering (Ed.), *Proceedings for Coasts and Ports 99: Challenges and Directions for the New Century.* The 14th Australasian Coastal and Ocean Engineering Conference and The 7th Australasian Port and Harbour Conference. 14-16 April, Perth, Australia. Vol. 2. pp. 513-518.

PHILLIPS, D., K. P. BLACK and T. HEALY, 2001. Seabed Characteristics of a Dynamic Exposed Headland. *Proceedings for Coasts and Ports 2001.* The 15th Australasian Coastal and Ocean Engineering Conference and The 8th Australasian Port and Harbour Conference. 25-28 September, 2001. Gold
Coast, Queensland, Australia. pp. 400-405.

SAYCE, A., K. P. BLACK and R. GORMAN, 1999. Breaking Wave Shape on Surfing Reefs. *Proceedings Coasts and Ports '99,* Vol. 2, pp. 596-603.

SAYCE, A., 1997. *Transformation of Surfing Waves on Steep and Complex Reefs.* Master of Science Thesis, Earth Science Department, University of Waikato.

SCARFE, B. E., 1999. *Hydrographic Surveying and Photogrammetry: Tools for Artificial Surfing Reef Studies.* Bachelor of Surveying Honours Dissertation, School of Surveying, The University of Otago.

SCARFE, B. E., 2002a. *Categorising Surfing Manoeuvres Using Wave and Reef Characteristics*. Master of Science Thesis, Department of Earth Science, The University of Waikato.

SCARFE, B. E., 2002b. Water Level Corrections (WLC) Using RTK GPS. *The Hydrographic Journal*, April vol. 104. pp. 17-23.

SCARFE, B. E., W. P. DE LANGE, A. K. CHONG, K. P. BLACK, AND S. T. MEAD, 2002. The Influence of Surfing Wave Parameters on Manoeuvre Type from Field Investigations at Raglan, New Zealand. *Proceedings for Surfing Art Science Issues Conference 2 (SASIC 2),* Ventura, California, 9 November 2002. pp. 74-89.

SCARFE, B. E., Elwany, M. H. S., Black, K. P., and Mead, S. T., 2003a. The influence of jetties on surfing conditions. SIO References series, Center for Coastal Studies, Scripps Institute of Oceanography, La Jolla, CA.

SCARFE, B. E., Elwany, M. H. S., Mead, S. T., and Black, K. P., 2003b. The science of surfing waves and surfing breaks: A review. Journal of Coastal Research, In Press.

SCARFE, B. E., Elwany, M. H. S., Black, K. P., and Mead, S. T., 2003c. Categorizing the type of surfing breaks around jetty structures. Journal of Coastal Research, In Press.

TURNER, I. L., T. D. T. DRONKERS, C. ROMAN, S. G. J. AARNINKHOF and J. MCGRATH. 2001. The application of video imaging at Gold Coast to quantify beach response to sand nourishment and construction of an artificial reef. *Proceedings for Coasts and Ports 2001* – the 15th Australasian Coastal Conference and Ocean Engineering Conference. pp. 55-60.

WALKER, J.R., 1974. *Recreational surfing parameters.* Technical Report, University of Hawaii, James K.K. Look Laboratory of Oceanographic Engineering, 73-30, 311p.

APPENDIX 4: Published paper

SEDIMENT DYNAMICS ALONG A SURFING HEADLAND

Phillips, D., Black, K., Hume, T., and T.R. Healy., 1999. Sediment Dynamics Along a Surfing Headland. *Coasts & Ports 99: Challenges and Directions for the New Century,* Perth, Australia. Vol. 2, pp. 513-518.

Sediment Dynamics along a Surfing Headland

David Phillips[1], Prof. Kerry Black[2], Prof. Terry Hume[2], Prof. Terry Healy[2]

[1] UNITEC Institute of Technology, Auckland, New Zealand
[2]Centre of Excellence in Coastal Oceanography and Marine Geology,
Department of Earth Sciences, University of Waikato and
National Institute of Water and Atmospheric Research
P.O. Box 11-115, Hamilton.
Phone: 64 9 849 4180 Fax: 64 9 815 4331 Email: dphillips@unitec.ac.nz

Summary: An experiment was conducted at Raglan, a surfing headland on the west coast of New Zealand, to examine how headlands maintain the sandy bed in the presence of strong currents which occur during large swell events. Waves, currents and suspended sediment settling flux were measured at 3 sites along a 150 m-cross-shore transect over a 12-day period that incorporated a large swell event. A side-scan sonar survey was undertaken to determine the extent of the sand at the headland, while sediment samples were collected out to 500 m offshore by divers. Burst-averaged currents attained 0.8 $m.s^{-1}$, while maximum bed orbital velocities were up to 2.0 $m.s^{-1}$. Mean currents over the deployment period were directed up the headland (cross-offshore) with an average of 0.035 $m.s^{-1}$, but strong currents down the headland were present during the large swell event at the shallowest site. After accounting for correlation between wave activity and suspended sediment concentration, the direction of net sediment flux was found to be down the headland (due East) at the two shallowest sites and up (due West) the headland offshore. The results indicate that the sandy bed is maintained by local, re-circulating sediment pathways. While 175,000 $m^3.yr^{-1}$ of net northward littoral drift may occur along New Zealand's west coast, headland sand presence is apparently not strongly dependent on this supply.

1 INTRODUCTION

The coastline of New Zealand is one of the longest and most diverse in the world. The country's elongated shape and north-south orientation straddling the circumpolar westerlies and its temperate to subtropical climate and varied geology provide a wide range of coastal environments (1). The west coast of New Zealand is one particular coastal environment that is characterised by a succession of headlands and long sandy beaches. One of the largest headlands is at Raglan, stretching some 13 km from Ruapuke to Raglan Harbour entrance in the central North Island (Fig. 1). The sea bed at Indicators (a surf break located along the headland) consists of a mobile west coast "black sand" adjacent to a boulder and reef shoreline.

The west coast "black sand" is fine grained and denser than quartz "white sand" and originates from the Taranaki volcanic region. It contains trace elements such as titanium and is a source of iron ore which is mined for use in the production of iron and steel. The process of sediment suspension has been well studied for quartz "white sand" beaches eg: (2), but sand transport on "black sand" beaches and headlands has not been studied in any detail.

Previous studies on the west coast have shown that net sediment movement is to the north. The study by Gibb (3) focused on the total longshore drift up the coast, not on the headland environment that exists at Raglan. There has been no previous research undertaken at Raglan on the effect that this natural feature has on the sediment dynamics of the coast. The predominant wind and swell direction on the west coast is from the southwest. The headland at Raglan faces to the north-northwest, which causes a large amount of wave refraction to occur as the swells wrap around the headland (Fig. 2) (4).

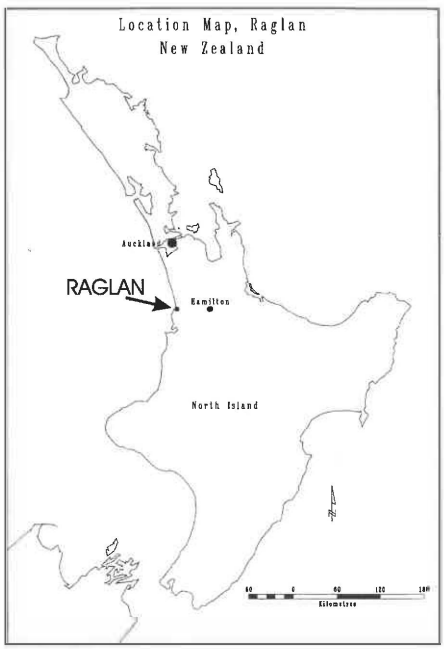

Figure 1: Raglan locality map

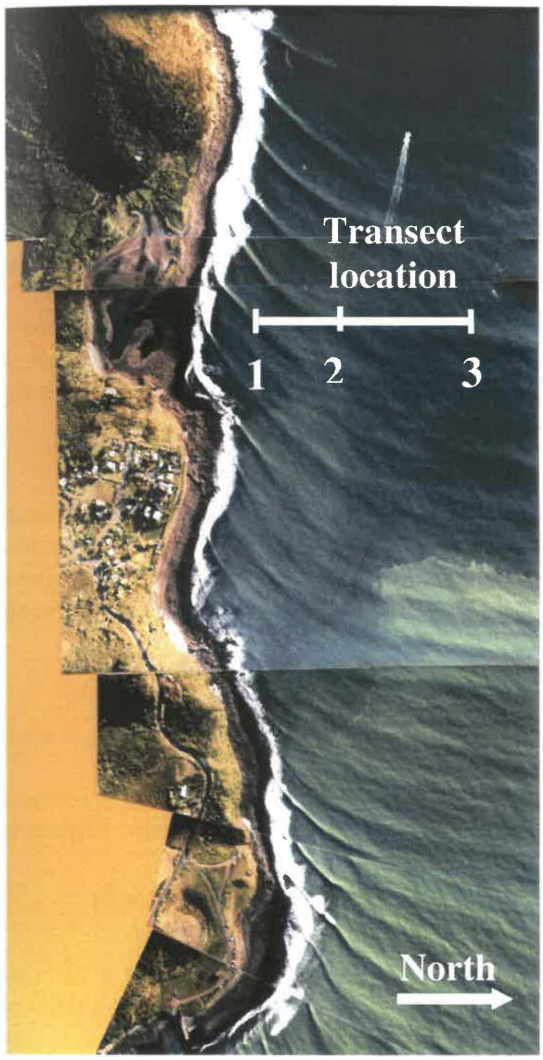

Figure 2: Aerial photograph showing the headland, wave refraction, plume and the position of the transect (Site 1, 2 and 3).

The dichotomy to be addressed is how headlands such as Raglan maintain the sand bed in the presence of strong shoreward currents that occur during large swell events. The bed can be maintained by either: (i) a net flux coming up the west coast and around the headland; (ii) local wave-driven processes in low swell causing net offshore movement which may balance the shoreward movement during large breaking wave events; or (iii) local re-circulating sediment pathways. This paper investigates the first and third options.

2 METHODS

Field experiments at Indicators were conducted to measure sediment flux at 3 sites along a 150 m cross-shore transect (Fig. 2). Bottom-mounted frames at each site supported a wave-recording current meter and sediment traps attached at heights of 600 mm, 900 mm and 1300 mm respectively (Fig. 3). The frames were deployed from a boat and then divers adjusted their orientation along the wave orthogonals to minimise the effect of the frame and instruments on the sediment traps. The frames were placed in water depths at Mean High Water of 6.5 m at Site 1, 7 m at Site 2 and 10 m at Site 3. Divers removed sediment trap caps after the frame was adjusted and replaced them before retrieval approximately 12 days later. However, 2 of the 9 traps and two frames could not be retrieved in the mild swell conditions (although the traps could be capped) and so a subsequent trip was made in more favourable swell conditions to recover the missing traps. The frames had been mostly buried in sand and so they had to be left in place.

Figure 3: Frame with S4 current meter and sediment traps attached.

Figure 4: Large surf conditions during the experiment.

Cylindrical sediment traps (90 mm x 300 mm) with smaller-diameter, raised inlet nozzles (18 mm x 50 mm) were used (5). The smaller inlet nozzle was required to allow the trap an extended filling period and to reduce any risk of sediment being re-suspended from the trap in the large wave conditions. There is general acceptance that cylinders most accurately measure natural suspended sediment concentrations as long as a suitable aspect ratio (height of the trap to the diameter of the collection orifice) is used eg: (6, 7, 8). The use of the nozzle greatly increases the aspect ratio of the traps to 20:1. There is some concern about the use of sediment traps in extreme environments (9), although recent studies by Flint (5) confirmed their value in moderate-energy surf zones.

In the laboratory, sediment samples were taken from the traps, oven-dryed and weighed for the total mass of sediment. The traps had collected a substantial quantity of fine-grained silt/mud particles due to land run-off through the nearby entrance to Raglan Harbour and so the sediment was passed through a 45 micron sieve so that the mud was not included in the total mass. A fall tube was used for analysis of settling velocity, grain size and distribution of the remaining sediment.

Time-averaged sediment concentrations (C_z) over the deployment period for each trap at elevation z were calculated as,

$$f = M / A\ t \qquad (1)$$

where f = downward flux (kg.m^{-2}.s^{-1}); M = mass of sample collected (kg); A = area of the aperture of the trap (m^2); t = duration of the sampling period (s). The time-averaged concentration (kg.m^{-3}) is then,

$$C_z = f / W \qquad (2)$$

where w = mean settling velocity (m.s^{-1}).

Near-bed reference concentrations were obtained by fitting the trapped concentrations to a logarithmic profile given by,

$$C = C_0 e^{-z/l_s} \qquad (3)$$

where C_o = near-bed reference concentration (kg.m^{-3}); l_s = the mixing length (m).

Data were logged by the S4 current meters at 2 Hz in. bursts of 18 min every hour at Site 1, 9 min every 2 hours at Site 2, and 9 min every 4 hours at Site 3. The burst data were analysed in the Matlab programme Tseries[1] to extract significant wave heights and direction, current speed and direction, and bed orbital velocities. Mean currents were resolved through the transect with positive being defined as directed "down the headland (due East)". Positive along the transect was offshore.

The observations show a strong relationship between wave height and current intensity. We would expect a similar relationship between wave height and average suspended sediment concentration. As time series of concentration were not measured during the experiment (only averaged concentrations from the trap were recorded), a near-bed reference concentration (C_o) was calculated using the measured orbital currents using the methodology of Black and Rosenberg (10). To examine the importance of correlation between suspended sediment concentration and current intensity on net sediment fluxes, a weighted current U_c was determined as,

$$U_c = \frac{\sum_{i=1}^{N} U_i C_{oi}}{\sum_{i=1}^{N} C_{oi}} \qquad (4)$$

where U_i = burst-averaged current; C_{oi} = calculated burst-averaged near-bed reference concentration; N = number of burst-averaged observations. The weighted current is indicative of the direction of net sediment flux while the mean current (unweighted) shows the direction of mean flows.

A detailed side-scan sonar survey was undertaken over the full study area while bed sediment sampling by divers out to 500 m offshore was undertaken for subsequent grain size and settling velocity analysis.

3 RESULTS

The side-scan survey showed broad areas of megaripples which were most common closer to the headland at the rock/sand boundary. The side-scan showed that the transect was located on sand with the innermost site within 3 m of the rock sand boundary.

Ground-truth observations by divers confirmed the presence of bedforms with wave lengths of up to 2 m (crest to crest) and heights of 0.5 m. Further offshore, the ripples became less distinguishable and were smaller and appeared to have no dominant orientation. The seabed was also firmer-packed in these areas with fine mud coating the seafloor. The scan also demonstrated that the rock/sand boundary on the seafloor generally followed the shape of the headland.

Bed sediments were well sorted and graded from 0.28 mm inshore to 0.16 mm offshore. The largest-sized grains were located at the tip of the headland where the waves first break (high energy zone), decreasing slightly down the headland (due East). The sediment can be classified from particle size analysis as predominantly sand, with some samples being slightly gravely sand, due to the presence of small amounts of shell.

Wave heights during the study period were small during the first 5 days (0.5-1.2 m), and then increased to over 3 m during a strong swell and remained above 1.5 m for the remainder of the deployment (Fig. 5).

The mean burst-averaged currents when resolved perpendicular to the transect were mostly negative (up the headland - due West) at all sites (Fig. 6). A strong negative flow occurred during a north-west swell around day 168. Positive (down the headland - due East) flows were experienced from days 169 to 172 with a large down-headland flow being recorded at the innermost site (Site 1) of around 0.8 m.s^{-1} on day 170 (Fig. 8) when the largest waves were present (Fig. 5). In these large swell conditions, burst-averaged currents at Site 1 were generally directed parallel with the headland. Maximum bed orbital velocities

[1] Tseries – R. Gorman, National Instititute of Water and Atmospheric Research

were up to 2.0 m.s^{-1}. A strong tidal oscillation in the current during this period is also evident (Fig. 6).

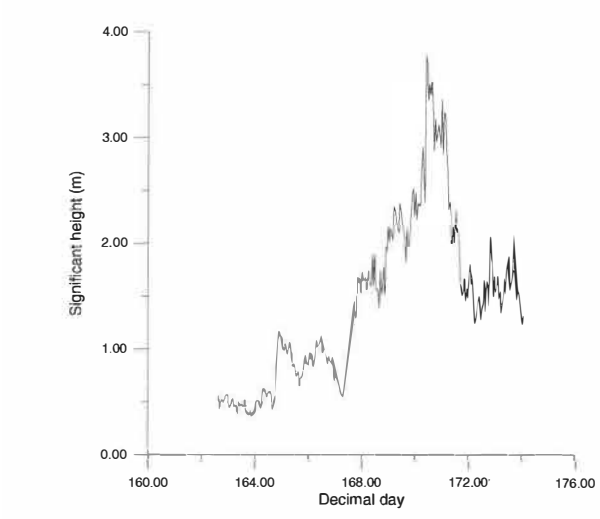

Figure 5: Wave heights measured at Site 1 over the experiment duration.

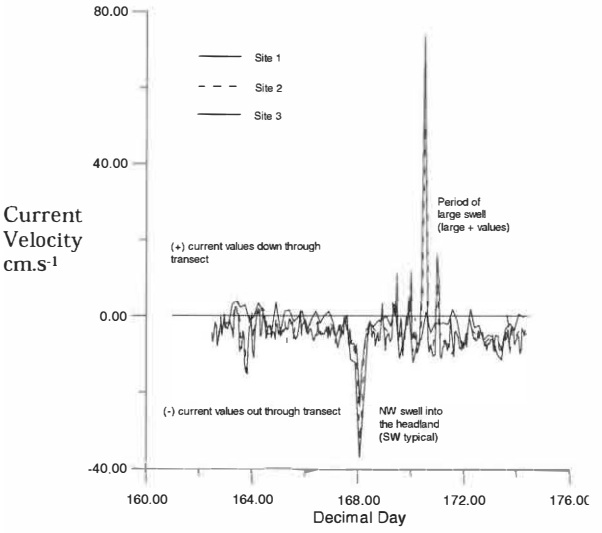

Figure 6: Current velocity through the transect, with positive values down the headland (due East), and negative up the headland (due West).

The sediment concentrations and grain size collected in the traps from all three locations decreased with elevation above the bed, and with distance offshore along the transect (Fig. 7). Near-bed reference concentrations at z=0 above the bed (eqn 3) decreased from 1.75 kg.m^3 inshore at Site 1 to 0.17 kg.m^3 offshore at Site 3 (Table 1).

Time-averaged currents during the experimental period were cross-offshore at all sites, even though large down-headland (due East) currents were recorded during the large wave event. The current component through the transect is negative (directed up the headland - due West) at all sites. The heading was -30^o (relative to the transect) at Site 1and -78^o at Site 3. Thus, the currents were directed more normal to the transect inshore at Site 3. When weighted by C_o (eqn 4), the mean currents change their orientation to down-headland (due East) and are 0.044 m.s^{-1} at Site 1 and 0.130 m.s^{-1} at Site 2 (Table 2). However, the weighted current remains negative (directed up-headland - due West) at Site 3 and is –0.034 m.s^{-1} (Table 2).

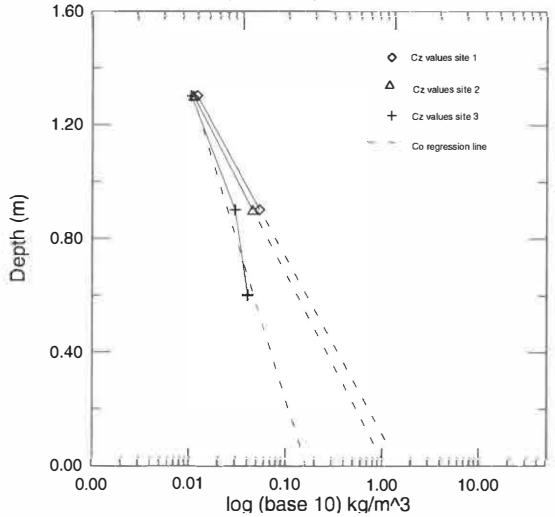

Figure 7: Time-averaged sediment concentrations at elevations and best fit regression lines for determination of near-bed reference concentrations.

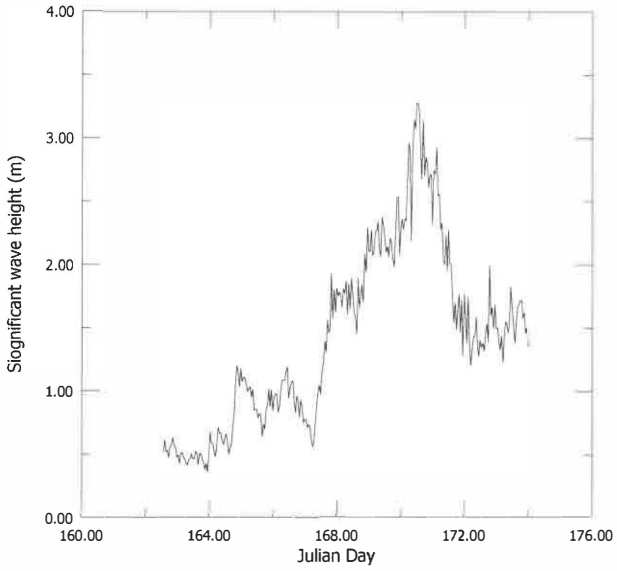

Figure 8: Current velocity at Site 1.

Table 1: Sediment trap measurements at sites (#) 1-3. z is trap entrance elevation, M is the total trapped mass, w is the median fall velocity, t is the deployment duration, A is the trap entrance area, C_z is the concentration at the trap entrance, and C_o is the near-bed reference concentration.

#	z m	M kg	w m s^{-1}	t s	A m^2	C_z kg.m^3	C_o kg. m^3
1	1.3 0.9	0.134 0.592	0.042	103, 1460	2.54 x 10^{-4}	0.012 0.054	1.75
2	1.3 0.9	0.107 0.440	0.037	103, 1940	2.54 x 10^{-4}	0.011 0.045	1.1
3	1.3 0.9 0.6	0.088 0.251 0.341	0.032	103, 1880	2.54 x 10^{-4}	0.011 0.03 0.041	0.17

Table 2: Time-averaged currents through (U) and along (V) the experimental transect. The mean current direction is given. U_c is the current magnitude through the transect after weighting by the near-bed reference concentration.

Sites	U (av) (through) $m\,s^{-1}$	V (av) (along) $m\,s^{-1}$	Current Dir (av) Degrees	U_c magnitude $m.s^{-1}$
1	-0.038	0.066	-30	0.044
2	-0.034	0.020	-60	0.130
3	-0.032	0.007	-78	-0.034

4 DISCUSSION

On the measurement transect which stretched from within 3 m of the sand rock interface to 150 m offshore, a broad range of conditions including north-west and south-west large swell and low waves was recorded. Although not comprehensive, it can be assumed that these conditions represent many of conditions that would be experienced over an annual period.

Overall, it was found that the measured bed orbital velocities have the ability to suspend large quantities of sediment that can then be carried along the headland by the strong currents. Averaged near-bed reference concentrations were of order 1 $kg.m^{-3}$, which is significant. Observations of surfers attempting to paddle against the currents during large waves indicate that flows are strongly down the headland (due East) in the surf zone. Surfers are often swept several hundred metres while attempting to paddle out beyond the breaking zone. The presence of the strong flow in the surf zone would suggest that sediment should be swept down the headland. One could then conclude that there must be a large supply of sediment coming into the region to replace the amounts being swept down, probably from littoral drift moving northward on the west coast of New Zealand (3).

Our observations, however, do not support this hypothesis. The currents averaged over the deployment period at the three measurement sites were all directed up the headland (due West). Mean currents were only down the headland (due East) during a large swell, particularly at the most shoreward site. The direction of net sediment flux, however, was positive (down the headland) at the inshore sites but remained negative offshore at Site 3.

Thus, our measurements depict an alternative mechanism for headland sediment circulation. We infer the presence of a sediment circulation loop that sustains the sandy beds by transporting sediment up the headland (due West) most of the time, with only the largest wave events disrupting this pattern at the inshore sites.

The more shoreward regions over the rocky sea bed are presumably disrupted by down-headland (due East), wave-driven currents more often. As such, sand has been swept away in the absence of sufficient upstream inputs to maintain the sediment flux. Indeed, the location of the interface between the sand and rocky bed may relate to the location where long-term mean currents change from being directed up (due West) to directed down (due East) the headland. The sandy bed is winnowed away, being unable to exist over the long term where strong wave-driven flows down the headland cause strong net transport.

Further evidence of winnowing and higher energetics is provided by the sediment sampling and side-scan. The larger-sized sediment grains and megaripples were located inshore along the headland, near the rock/sand boundary of the seafloor. This boundary generally followed the shape of the headland.

Further support for the presence of consistent up-headland flow beyond the surf zone is provided by observations of a turbid plume travelling up the headland (due West) from the entrance to Raglan Harbour (located 5000 m across the bay). The large quantity of fine mud found in the traps is evidence of wave re-entrainment of the muds and of settlement from the plume passing across the transect (Fig. 2).

5 CONCLUSIONS

Measurements of waves, currents and sediment loads were made on a cross-shore transect at Raglan, a surfing headland on the west coast of New Zealand. A detailed side-scan sonar survey delineated the rock and sand regions of the seafloor and demonstrated that the rock/sand boundary generally followed the shape of the headland. The survey also identified zones of megaripples on the seafloor, most commonly located close to the rock/sand boundary.

Bed sediments were sampled to a distance of 500 m offshore, and were well-sorted sands with median grain size grading from 0.28 mm inshore to 0.16 mm offshore. The larger grains were located closer to the high energy surf zone of the headland, where the megaripples were also identified.

A net up-headland (due West) current was determined over the sampling period with an average value of –0.035 $m.s^{-1}$ through the experimental transect. Strong currents directed down the headland (due East) developed during the largest swell event. These positive currents are wave-driven and are generally directed parallel with the headland and attain burst-averaged magnitudes of 0.8 $m.s^{-1}$, while maximum bed orbital velocities are up to 2.0 $m.s^{-1}$.

The results demonstrate that local re-circulating sediment pathways are present on the headland and appear to be responsible for maintaining the sandy bed in the presence of energetic wave conditions. Headland sand presence may not be strongly dependent on supply of sediment by longshore littoral drift along the west coast of New Zealand.

6 ACKNOWLEDGEMENTS

This project is part of the Artificial Reefs Program within the Department of Earth Sciences Coastal Marine Group of the University of Waikato and the National Institute of Water and Atmospheric Research. Technical assistance by Dirk Immenga was greatly appreciated. Shaw Mead and other graduate students of the Centre of Excellence are thanked for their help.

7 REFERENCES

Healy, T.R., and R.M. Kirk, 1982. Coasts. In: Scoons, J.M.; Selby, M.J. ed. Landforms of New Zealand, Longman Paul, Auckland,. pp. 81-104.

2 Fredscoe, J., and R. Deigard, 1992. Mechanics of coastal sediment transport. Advanced Series on Ocean Engineering, World Scientific. 369 p.

3 Gibb, J.G. 1979. Late Quaternary shoreline movements in New Zealand. Unpublished PhD thesis, Victoria University of Wellington, New Zealand.

4 Hutt, J. 1997. Bathymetry and wave parameters defining the surfing quality of five reefs. Unpublished Master of Science Thesis, Earth Sciences Department, University of Waikato, New Zealand.

5 Flint, S.B. 1998. Sediment Trapping in the Nearshore Coastal Environment. Unpublished MSc thesis, University of Waikato, New Zealand.

6 Hargrave, B.T., and N. M. Burns, 1979. Assessment of sediment trap efficiency. Liminology and Oceanography, 24(6).

7 Bloesch, J., and N.M. Burns, 1980. A critical review of sediment trap technique. Hydrology, 42(1): 15-55.

8 Butman, C.A., 1986. Sediment trap biases in turbulent flows: results from a laboratory flume study. Journal of Marine Research, 44: 645-653

9 White, J., 1990. The use of sediment traps in high energy environments. Marine Geophysical Researches, 12: 145-152.

10 Black, K.P., and M.A. Rosenburg, 1991. Hydrodynamics and sediment dynamics in wave-driven environments. Vol. 3. Sediment dynamics. Victorian Institute of Marine Sciences Technical Report No. 15, 72 pp.

11 Komar, P.D. 1976. Beach Processes and Sedimentation. Prentice-Hall, Inc. New Jersey. 429p.

APPENDIX 5: Published paper

SEDIMENT TRANSPORT ALONG A SURFING HEADLAND AT RAGLAN, NEW ZEALAND

Phillips, D.J., Black, K.P. and Healy, T.R. 2000. Sediment Transport along a Surfing Headland at Raglan, New Zealand. Poster Paper, ICS 2000, Rotorua, New Zealand.

Sediment Transport along a Surfing Headland at Raglan, NZ

David Phillips[1,2] and Kerry Black[1]

[1]Coastal Marine Group.
Department of Earth Sciences, University of Waikato.
Private Bag 3105, Hamilton.

[2]UNITEC Institute of Technology
Email: dphillips@unitec.ac.nz

SUMMARY

An experiment was conducted at Raglan, a surfing headland on the west coast of New Zealand, to examine how headlands maintain the sandy bed in the presence of strong currents which occur during large swell events. Waves, currents and suspended sediment settling flux were measured at 3 sites along a 150 m-cross-shore transect over a 12-day period that incorporated a large swell event. A side-scan sonar survey was undertaken to determine the extent of the sand at the headland, while sediment samples were collected out to 500 m offshore by divers. Burst-averaged currents attained 0.8 m.s^{-1}, while maximum bed orbital velocities were up to 2.0 m.s^{-1}. Mean currents over the deployment period were directed up the headland (cross-offshore) with an average of 0.035 m.s^{-1}, but strong currents down the headland were present during the large swell event at the shallowest site. After accounting for correlation between wave activity and suspended sediment concentration, the direction of net sediment flux was found to be down the headland at the two shallowest sites and up the headland offshore. The results indicate that the sandy bed is maintained by local, re-circulating sediment pathways. While 175,000 m^3.yr^{-1} of net northward littoral drift may occur along New Zealand's west coast, headland sand presence is apparently not strongly dependent on this supply.

INTRODUCTION

The coastline of New Zealand is one of the longest and most diverse in the world. The country's elongated shape and north-south orientation straddling the circumpolar westerlies and its temperate to subtropical climate and varied geology provide a wide range of coastal environments (1). The west coast of New Zealand is one particular coastal environment that is characterised by a succession of headlands and long sandy beaches. One of the largest headlands is at Raglan, stretching some 13 km from Ruapuke to Raglan Harbour entrance in the central North Island (Fig. 1). The sea bed at Indicators (a surf break located along the headland) consists of a mobile west coast "black sand" adjacent to a boulder and reef shoreline.

The west coast "black sand" is fine grained and denser than than quartz "white sand" and originates from the Taranaki volcanic region. It contains trace elements such as titanium and is a source of iron ore which is mined for use in the production of iron and steel. The process of sediment suspension has been well studied for quartz "white sand" beaches eg. (2), but sand transport on "black sand" beaches and headlands has not been studied in any detail. Previous studies on the west coast have shown that net sediment movement is to the north. The study by Gibb (3) focused on the total longshore drift up the coast, not on the headland environment that exists at Raglan. There has been no previous research undertaken at Raglan on the effect that this natural feature has on the sediment dynamics of the coast. The predominant wind and swell direction on the west coast is from the southwest. The headland at Raglan faces to the north-northwest, which causes a large amount of wave refraction to occur as the swells wrap around the headland (4).

The dichotomy to be addressed is how headlands such as Raglan maintain the sand bed in the presence of strong shoreward currents that occur during large swell events. The bed can be maintained by either: (i) a net flux coming up the west coast and around the headland; (ii) local wave-driven processes in low swell causing net offshore movement which may balance the shoreward movement during large breaking wave events; or (iii) local re-circulating sediment pathways. This paper investigates the first and third options (Fig. 2).

Figure 1: Raglan Locality Map

Figure 2: Map showing sandy seabed maintained by
(1) a net flux around the headland
(2) wave-driven processes in low swell causing net offshore movement
(3) local re-circulation

METHODS

Field experiments at Indicators were conducted to measure sediment flux at 3 sites along a 150 m cross-shore transect. Bottom-mounted frames at each site supported a wave-recording current meter and sediment traps attached at heights of 600 mm, 900 mm and 1300 mm respectively (Fig. 3). The frames were deployed from a boat and then divers adjusted their orientation along the wave orthogonals to minimise the effect of the frame and instruments on the sediment traps. Divers removed sediment trap cups after the frame was adjusted and replaced them before retrieval approximately 12 days later. However, 2 of the 9 traps and two frames could not be retrieved in the mild swell conditions (although the traps could be capped) and so a subsequent trip was made in more favourable swell conditions to recover the missing traps. The frames had been mostly buried in sand and so they had to be left in place.

Cylindrical sediment traps (90 mm x 300 mm) with smaller-diameter, raised inlet nozzles (18 mm x 50 mm) were used (5). The smaller inlet nozzle was required to allow the trap an extended filling period and to reduce any risk of sediment being re-suspended from the trap in the large wave conditions. There is general acceptance that cylinders most accurately measure natural suspended sediment concentrations as long as a suitable aspect ratio (height of the trap to the diameter of the collection orifice) is used eg. (6, 7, 8). The use of the nozzle greatly increases the aspect ratio of the traps to 20:1. There is some concern about the use of sediment traps in extreme environments (9), although recent studies by Flint (5) confirmed their value in moderate-energy surf zones.

In the laboratory, sediment samples were taken from the traps, oven-dryed and weighed for the total mass of sediment. The traps had collected a substantial quantity of fine-grained silt/mud particles due to land run-off through the nearby entrance to Raglan Harbour and so the sediment was passed through a 45 micron sieve so that the mud was not included in the total mass. A fall tube was used for analysis of settling velocity, grain size and distribution of the remaining sediment.

Figure 3: Frame with S4 current meter and sediment traps attached.

Data were logged by the S4 current meters at 2 Hz in, bursts of 18 min every hour at Site 1, 9 min every 2 hours at Site 2, and 9 min every 4 hours at Site 3. The burst data were analysed in the Matlab programme Tseries[1] to extract significant wave heights and direction, current speed and direction, and bed orbital velocities. Mean currents were resolved through the transect with positive being defined as directed "down the headland". Positive along the transect was offshore.

The observations show a strong relationship between wave height and current intensity. We would expect a similar relationship between wave height and average suspended sediment concentration. As time series of concentration were not measured during the experiment (only averaged concentrations from the trap were recorded), a near-bed reference concentration (C_z) was calculated using the measured orbital currents using the methodology of Black and Rosenberg (10). To examine the importance of correlation between suspended sediment concentration and current intensity on net sediment fluxes, a weighted current U_c was determined as,

$$U_c = \frac{\sum_{i=1}^{N} U_i C_{zi}}{\sum_{i=1}^{N} C_{zi}} \quad (1)$$

where U_i = burst-averaged current; C_{zi} = calculated burst-averaged near-bed reference concentration; N = number of burst-averaged observations. The weighted current is indicative of the direction of net sediment flux while the mean current (unweighted) shows the direction of mean flows.

A detailed side-scan sonar survey was undertaken over the full study area while bed sediment sampling by divers out to 500 m offshore was undertaken for subsequent grain size and settling velocity analysis.

RESULTS

The side-scan survey showed broad areas of megaripples which were most common closer to the headland at the rock/sand boundary. The side-scan showed that the transect was located on sand with the innermost site within 3 m of the rock sand boundary.

Ground-truth observations by divers confirmed the presence of bedforms with wavelengths of up to 2 m and heights of 0.5 m. Further offshore, the ripples became less distinguishable and were smaller and appeared to have no dominant orientation. The seabed was also firmer-packed in these areas with fine mud coating the seafloor. The scan also demonstrated that the rock/sand boundary on the seafloor generally followed the shape of the headland.

Bed sediments were well sorted and graded from 0.28 mm inshore to 0.16 mm offshore. The largest-sized grains were located at the tip of the headland where the waves first break (high energy zone), decreasing slightly down the headland. The sediment can be classified from particle size analysis as predominantly sand, with some samples being slightly gravely sand, due to the presence of small amounts of shell.

Wave heights during the study period were small during the first 5 days (0.5-1.2 m), and then increased to over 3 m during a strong swell (Fig. 8) and remained above 1.5 m for the remainder of the deployment (Fig. 5).

The mean burst-averaged currents when resolved perpendicular to the transect were mostly negative (up the headland) at all sites (Fig. 6). A strong negative flow occurred during a north-west swell around day 168. Positive (down the headland) flows were experienced from days 169 to 172 with a large down-headland flow being recorded at the innermost site (Site 1) of around 0.8 m.s^{-1} on day 170 when the largest waves were present (Fig. 5). In these large swell conditions, burst-averaged currents at Site 1 were generally directed parallel with the headland. Maximum bed orbital velocities were up to 2.0 m.s^{-1}. A strong tidal oscillation in the current during this period is also evident (Fig. 6).

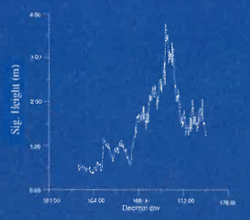

Figure 5: Wave heights measured at Site 1 over the experiment duration.

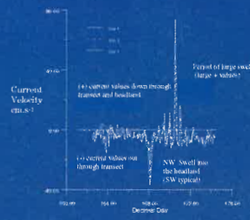

Figure 6. Current velocity through the transect, with positive values down the headland, and negative up the headland.

The sediment concentrations collected in the traps from all three locations decreased with elevation above the bed, and with distance offshore along the transect (Fig. 7). Near-bed reference concentrations at z=0 above the bed decreased from 1.75 kg.m^3 inshore at Site 1 to 0.17 kg.m^3 offshore at Site 3 (Table 1).

Time-averaged currents during the experimental period were cross-offshore at all sites, even though large down-headland currents were recorded during the large wave event. The current component through the transect is negative (directed up the headland) at all sites. The heading was ~60° (relative to the transect) at Site 1 and ~12° at Site 3. Thus, the currents were directed more normal to the transect inshore at Site 1. When weighted by C_z (eqn 1), the mean currents change their orientation to down-headland and are 0.044 m.s^{-1} at Site 1 and 0.130 m.s^{-1} at Site 2 (Table 2). However, the weighted current remains negative (directed up-headland) at Site 3 and is ~0.034 m.s^{-1} (Table 2).

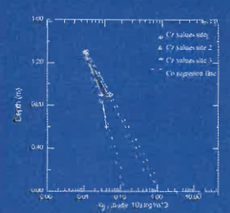

Figure 7 Time-averaged sediment concentrations at elevations and best fit regression lines for determination of near-bed reference concentrations.

Figure 8 Large surf conditions during the experiment.

Table 1: Sediment trap measurements at sites (#) 1-3. z is trap entrance elevation, M is the total trapped mass, w is the median fall velocity, t is the deployment duration, A is the trap entrance area, C_z is the concentration at the trap entrance, and C_o is the near-bed reference concentration

#	z m	M kg	w m.s^{-1}	t s	A m^2	C_z kg.m^3	C_o kg.m^3
1	1.3	0.134	0.042	103,	2.54	0.012	1.75
	0.9	0.592		1460	x 10^{-4}	0.054	
2	1.3	0.107	0.037	103,	2.54	0.011	1.1
	0.9	0.440		1940	x 10^{-4}	0.045	
3	1.3	0.088		103,	2.54	0.011	0.17
	0.9	0.251	0.032	1880	x 10^{-4}	0.03	
	0.6	0.341				0.041	

Table 2: Time-averaged currents through (U) and along (V) the experimental transect. The mean current direction is given. U_c is the current magnitude through the transect after weighting by the near-bed reference concentration.

Sites	U (av) (through) m.s^{-1}	V (av) (along) m.s^{-1}	Current Dir (av) Degrees	U_c magnitude m.s^{-1}
1	-0.038	0.066	-60	0.044
2	-0.034	0.020	-30	0.130
3	-0.032	0.007	-12	-0.034

DISCUSSION

On the measurement transect which stretched from within 3 m of the sand rock interface to 150 m offshore, a broad range of conditions including north-west and south-west large swell and low waves was recorded. Although not comprehensive, it can be assumed that these conditions represent many of conditions that would be experienced over an annual period. Overall, it was found that the measured bed orbital velocities have the ability to suspend large quantities of sediment that can then be carried along the headland by the strong currents. Averaged near-bed reference concentrations were of order 1 kg.m^{-3}, which is significant. Observations of surfers attempting to paddle against the currents during large waves indicate that flows are strongly down the headland in the surf zone. Surfers are often swept several hundred metres while attempting to paddle out beyond the breaking zone. The presence of the strong flow in the surf zone would suggest that sediment should be swept down the headland. One could then conclude that there must be a large supply of sediment coming into the region to replace the amounts being swept down, probably from littoral drift moving northward on the west coast of New Zealand (3).

Our observations, however, do not support this hypothesis. The currents averaged over the deployment period at the three measurement sites were all directed up the headland. Mean currents were only down the headland during a large swell, particularly at the most shoreward site. The direction of net sediment flux, however, was positive (down the headland) at the inshore sites but remained negative offshore at Site 3. Thus, our measurements depict an alternative mechanism for headland sediment circulation. We infer the presence of a sediment circulation loop that sustains the sandy beds by transporting sediment up the headland most of the time, with only the largest wave events disrupting this pattern at the inshore sites.

The more shoreward regions over the rocky sea bed are presumably disrupted by down-headland, wave-driven currents more often. As such, sand has been swept away in the absence of sufficient upstream inputs to maintain the sediment flux. Indeed, the location of the interface between the sand and rocky bed may relate to the location where long-term mean currents change from being directed up to directed down the headland. The sandy bed is winnowed away, being unable to exist over the long term where strong wave-driven flows down the headland cause strong net transport. Further evidence of winnowing and higher energetics is provided by the sediment sampling and side-scan. The larger-sized sediment grains and megaripples were located inshore along the headland, near the rock/sand boundary of the seafloor. This boundary generally followed the shape of the headland.

Further support for the presence of consistent up-headland flow beyond the surf zone is provided by observations of a turbid plume travelling up the headland from the entrance to Raglan Harbour (located 5000 m across the bay). The large quantity of fine mud found in the traps is evidence of wave re-entrainment of the muds and of settlement from the plume passing across the transect.

CONCLUSION

Measurements of waves, currents and sediment loads were made on a cross-shore transect at Raglan, a surfing headland on the west coast of New Zealand. A detailed side-scan sonar survey delineated the rock and sand regions of the seafloor and demonstrated that the rock/sand boundary generally followed the shape of the headland. The survey also identified zones of megaripples on the seafloor, most commonly located close to the rock/sand boundary. Bed sediments were sampled to a distance of 500 m offshore, and were well-sorted sands with median grain size grading from 0.28 mm inshore to 0.16 mm offshore. The larger grains were located closer to the high energy surf zone of the headland, where the megaripples were also identified.

A net up-headland current was determined over the sampling period with an average value of ~0.035 m.s^{-1} through the experimental transect. Strong currents directed down the headland developed during the largest swell event. These positive currents are wave-driven and are generally directed parallel with the headland and attain burst-averaged magnitudes of 0.8 m.s^{-1}, while maximum bed orbital velocities are up to 2.0 m.s^{-1}.

The results demonstrate that local re-circulating sediment pathways are present on the headland and appear to be responsible for maintaining the sandy bed in the presence of energetic wave conditions. Headland sand presence may not be strongly dependent on supply of sediment by longshore littoral drift along the west coast of New Zealand.

REFERENCES

1 Healy, T.R., and R.M. Kirk, 1982. Coasts. In: Soons, J.M.; Selby, M.J. ed. Landforms of New Zealand, Longman Paul, Auckland. pp. 81-104.
2 Fredsoe, J., and R. Deigard, 1992. Mechanics of coastal sediment transport. Advanced Series on Ocean Engineering, World Scientific, 369 p.
3 Gibb, J.G. 1979. Late-Quaternary shoreline movements in New Zealand. Unpublished PhD thesis, Victoria University of Wellington, New Zealand.
4 Hutt, J., 1997. Bathymetry and wave parameters defining the surfing quality of five reefs. Unpublished Master of Science Thesis, Earth Sciences Department, University of Waikato, New Zealand.
5 Flint, S.B. 1998. Sediment Trapping in the Nearshore Coastal Environment. Unpublished MSc thesis, University of Waikato, New Zealand.
6 Hargrave, B.T., and N. M. Burns, 1979. Assessment of sediment trap efficiency. Limnology and Oceanography, 24(6).
7 Bloesch, J., and N.M. Burns, 1980. A critical review of sediment trap technique. Hydrology, 42(1): 15-55.
8 Butman, C.A., 1986. Sediment trap biases in turbulent flows: results from a laboratory flume study. Journal of Marine Research, 44: 645-653
9 White, J., 1990. The use of sediment traps in high energy environments. Marine Geophysical Researches, 12: 145-152.
10 Black, K.P., and M.A. Rosenberg, 1991. Hydrodynamics and sediment dynamics in wave-driven environments. Vol. 3, Sediment dynamics. Victorian Institute of Marine Sciences Technical Report No. 15, 72 pp.
11 Komar, P.D. 1976. Beach Processes and Sedimentation. Prentice-Hall, Inc. New Jersey. 429p.

Coastal Marine Group
Department of Earth Sciences
University of Waikato

The University of Waikato
Te Whare Wānanga o Waikato

[1]Tseries R. Gorman, National Institute of Water an Atmospheric Research

APPENDIX 6: Conference abstracts

SEDIMENT DYNAMICS ALONG A SHALLOW WEST COAST HEADLAND

Phillips, D. and K. Black., 1998. Sediment Dynamics along a Shallow West Coast Headland., 1998. New Zealand Marine Sciences Society Annual Conference, 8-11 July. University of Otago, Dunedin, NZ.

SEABED CHARACTERISTICS OF A LARGE SURFING HEADLAND

Phillips, D., Black, K., Hume, T., and T.R. Healy., 1999. Seabed Characteristics of a Large Surfing Headland. New Zealand Marine Sciences Society Annual Conference, 1-3 September. University of Victoria, Wellington, NZ.

Sediment dynamics along a shallow west coast headland

David Phillips and Kerry Black

Centre of Excellence in Coastal Oceanography and Marine Geology,
NIWA and Department of Earth Sciences, University of Waikato
P. O. Box 11-115, Hamilton

The west coast of New Zealand is characterised by a succession of headlands and long sandy beaches. One of the largest headlands is at Raglan, stretching some 13 km from Ruapuke to Raglan Harbour entrance, in the central North Island. The sea bed at Indicators (a surf break located along the headland) consists of a mobile west coast "black sand" adjacent to a boulder and reef shoreline. Observations show that currents are strong and directed down the headland when large waves are present. Such currents would be expected to transport large quantities of sediment around the headland, but the sea bed is stable and offshore boulders are encrusted with marine organisms suggesting long-term stability of bed levels around these exposed boulders. The dichotomy to be addressed is how such headlands maintain the sand bed in the presence of potentially large net sediment fluxes. The bed can be maintained by either: (i) a net flux from around the headland (a river of sand); (ii) local wave-driven processes in low swell causing net offshore movement which may balance the shoreward movement during large breaking wave events; or (iii) local re-circulating sediment pathways. This paper examines the first two of these mechanisms. Preliminary estimates of net flux through a cross-shore transect were obtained using measurements of sediment concentrations and current strength. These are compared to previous estimates of net sediment movement along New Zealand's West Coast. In addition, observations of the sea bed using underwater video depict the suspension and movement of sediment under swell. Further experiments are to be undertaken. Side-scan sonar is to be used to delineate the rock and sand regions on the sea bed while sediment fluxes are being recorded in more detail.

Seabed Characteristics of a Large Surfing Headland

David Phillips[1,2], Kerry Black[1], Terry Hume[1], Terry Healy[1]

[1]Centre of Excellence in Coastal Oceanography and Marine Geology, Coastal Marine Group, Department of Earth Sciences, University of Waikato and National Institute of Water and Atmospheric Research. P.O. Box 11-115, Hamilton.

[2]UNITEC Institute of Technology, Auckland. Email: dphillips@unitec.ac.nz

Experiments were conducted at Raglan, a surfing headland on the west coast of New Zealand, to determine characteristics of the seabed and the adjacent boulder reef. Sediment grain size, bedform location and size, rock/sand boundary and the physical properties were measured in the local "black sands". A side-scan sonar survey was undertaken to determine the extent of the sand at the headland, including the underwater boundary of the boulder reef. Sediment samples were collected to 500m offshore by divers, for laboratory analysis.

The side-scan survey showed areas of megaripples which were most common closer to the headland at the rock/sand boundary. Ground truth observations by divers confirmed the presence of bedforms with wavelenghts of up to 2 m (crest to crest) and heights of 0.5 m. Further offshore, the ripples became less distinguishable and were smaller and appeared to have no dominant orientation. The seabed was also firmer-packed in these areas with fine mud coating the seafloor. The scan also demonstrated that the rock/sand boundary on the seafloor generally followed the shape of the headland.

Bed sediments were well sorted and graded from 0.28 mm inshore to 0.16 mm offshore. The largest-sized grains were located at the tip of the headland where the waves first break (high energy zone), decreasing slightly down the headland. The sediment can be classified from particle size analysis as predominantly sand, with some samples being slightly gravely sand, due to the presence of small amounts of shell.

The results indicate an environment that is subjected to wave induced forces, which influence the characteristics off the seabed. Numerical model predictions of bed orbital motions show that grain size is strongly related to bed orbital velocity and the presence of the surf zone. Due to the dynamic nature of the bed, further side-scan sonar surveys will be undertaken and samples collected to determine trends or variation in the seabed over time.

APPENDIX 7: Sediment Data

Table A7.1: Sediment textural data from samples collected on the 11-6-98, analysed in the University of Waikato Rapid Sediment Analyser (RSA) using the graphical method.

Sample No.	Median Grain Size (mm)	Textural description	Sorting	Skewness	Location North East
1	0.28	Slightly gravelly sand	Well sorted	Strongly fine skewed	595242.5 302882.8
2	0.22	Slightly gravelly sand	Well sorted	Fine skewed	595307.3 302884.8
3	0.22	Slightly gravelly sand	Well sorted	Fine skewed	595355.2 302899.3
4	0.21	Slightly gravelly sand	Very well sorted	Fine skewed	595451.1 302930.5
5	0.18	Slightly gravelly sand	Well sorted	Fine skewed	595595.4 302930.5
6	0.19	Sand	Well sorted	Fine skewed	595558.4 303170.3
7	0.22	Sand	Well sorted	Fine skewed	595420 303107.6
8	0.29	Slightly gravelly sand	Well sorted	Fine skewed	595333.4 303107.5
9	0.16	Sand	Well sorted	Fine skewed	595618.8 302769.4
10	0.18	Slightly gravelly sand	Well sorted	Fine skewed	595476.4 302765.7
11	0.25	Sand	Well sorted	Fine skewed	595339.5 302740.7
12	0.28	Sand	Well sorted	Strongly fine skewed	595290.5 302740.7
13	0.16	Sand	Well sorted	Fine skewed	595633.5 302481.9
14	0.19	Slightly gravelly sand	Moderately well sorted	Near symmetrical	595493.1 302450.4
15	0.22	Slightly gravelly sand	Well sorted	Strongly fine skewed	595354.4 302390.4
16	0.24	Slightly gravelly sand	Well sorted	Fine skewed	595252.6 302163

Table A7.2: Sediment textural data from samples collected on the 11-6-98, analysed in the University of Waikato Rapid Sediment Analyser (RSA) using the graphical method.

Sample No.	Median Grain Size (mm)	Sorting (Phi)	Skewness (Chi)	Location
1	0.28	0.36	0.37	595242.5 302882.8
2	0.22	0.42	0.13	595307.3 302884.8
3	0.22	0.38	0.29	595355.2 302899.3
4	0.21	0.34	0.42	595451.1 302930.5
5	0.18	0.40	0.24	595595.4 302930.5
6	0.19	0.43	0.10	595558.4 303170.3
7	0.22	0.38	0.27	595420 303107.6
8	0.29	0.40	0.18	595333.4 303107.5
9	0.16	0.37	0.21	595618.8 302769.4
10	0.18	0.37	0.14	595476.4 302765.7
11	0.25	0.39	0.30	595339.5 302740.7
12	0.28	0.39	0.30	595290.5 302740.7
13	0.16	0.36	0.68	595633.5 302481.9
14	0.19	0.52	0.02	595493.1 302450.4
15	0.22	0.37	0.05	595354.4 302390.4
16	0.24	0.45	0.27	595252.6 302163

Table A7.3: Sediment textural data from samples collected on the 26-4-01 analysed in the University of Waikato Rapid Sediment Analyser (RSA) using the graphical method.

Sample No.	Median Grain Size (mm)	Textural Description	Sorting	Skewness	Location North East
1	0.20	Slightly gravelly sand	Well sorted	Strongly fine skewed	595293 303338
2	0.18	Sand	Well sorted	Course skewed	595334 303342
3	0.14	Slightly gravelly sand	Moderately well sorted	Course skewed	595378 303351
4	0.16	Slightly gravelly sand	Moderately sorted	Strong Coarsely skewed	595431 303361
5	0.26	Slightly gravelly sand	Moderately well sorted	Strongly fine skewed	595242 302882
6	0.25	Slightly gravelly sand	Very well sorted	Fine skewed	595266 302666
7	0.17	Slightly gravelly sand	Moderately well sorted	Strongly course skewed	595420 302673
8	0.18	Slightly gravelly sand	Moderately well sorted	Strongly course skewed	595356 302685
9	0.16	Sand	Well sorted	Strongly Course skewed	595399 302697
10	0.23	Slightly gravelly sand	Moderately well sorted	Strongly fine skewed	595295 302422
11	0.19	Slightly gravelly sand	Moderately well sorted	Strongly fine skewed	595344 302438
12	0.17	Slightly gravelly sand	Moderately well sorted	Course skewed	595392 302443
13	0.15	Slightly gravelly sand	Well sorted	Strongly Course skewed	595272 302218
14	0.15	Slightly grav. sand	Very well sorted	Near symmetrical	595714 302696
15	0.14	Slightly grav. sand	Well sorted	Course skewed	595642 303382

Table A7.4 Sediment textural data from samples collected on the 26-4-01 analysed in the University of Waikato Rapid Sediment Analyser (RSA) using the graphical method.

Sample No.	Median Grain Size (mm)	Sorting (Phi)	Skewness (Chi)	Location
1	0.20	0.45	-0.02	595293 303338
2	0.18	0.42	-0.14	595334 303342
3	0.14	0.53	-0.28	595378 303351
4	0.16	0.76	-0.46	595431 303361
5	0.26	0.97	-1.20	595242 302882
6	0.25	0.31	0.19	595266 302666
7	0.17	0.67	-0.52	595420 302673
8	0.18	0.67	-0.53	595356 302685
9	0.16	0.49	-0.34	595399 302697
10	0.23	0.50	0.57	595295 302422
11	0.19	0.59	0.31	595344 302438
12	0.17	0.51	-0.21	595392 302443
13	0.15	0.45	-0.40	595272 302218
14	0.15	0.35	-0.04	595714 302696
15	0.14	0.43	-0.15	595642 303382

APPENDIX 8: Density Calculations

Form 2.7.1
DETERMINATION OF THE SOLID DENSITY OF SOIL PARTICLES
(Test 2.7.1)

Job: RAGLAN RESEARCH.
Location: RAGLAN BEACH
Depth(s): SURFACE

Sample No(s):
Tested by:
Date:

Test details*:

Test performed on fraction passing/ retained on ..... sieve

History: Natural/air-dried/oven-dried/unknown

Checked by:
Date:

Temperature of water during test, T . . . °C

Sample No.						
Gas-jar No.			T5	T3	T2	
Mass of empty gas-jar and plate	M_1	g	201.83	207.10	198.49	
Mass of gas-jar, plate and soil	M_2	g	351.75	354.70	352.74	
Mass of gas-jar, plate, soil and water	M_3	g	545.29	551.05	543.56	(.49)
Mass of gas-jar, plate and water	M_4	g	450.05	458.26	445.70	
	$M_2 - M_1$	g	149.92	147.6	154.25	
	$M_4 - M_3$	g	-95.24	-92.80	-97.79	
	$(M_2 - M_1)+(M_4 - M_3)$	g	51.68	54.80	56.46	
Solid density of soil particles $\varrho_s = \frac{M_2 - M_1}{M_2 - M_1 + M_4 - M_3} \varrho_w$		t/m³	2.89	2.69	2.73	
Average ϱ_s		t/m³	2.71			

Solid density of soil particles . . . . . t/m³

*Delete inappropriate words.

APPENDIX 9: Modelling Formula

A9.1 NUMERICAL COMPUTER MODELLING

The model WBEND was used for analysis of the wave heights and directions at Raglan and 3DD for current velocities and directions.

A9.1.1 *Model WBEND*

Model WBEND (Black and Rosenberg, 1992; Black, 1997) is a 2-dimensional numerical wave refraction model for monochromatic waves or a wave spectrum over variable topography. The model applies a fast, iterative, finite-difference solution of the wave action equations to solve for wave height, wave period, breakpoint location and longshore sediment transport. WBEND provides for:

- variable bathymetry;
- time-varying boundary conditions;
- the wave spectrum;
- options to "enhance" the wave shoaling to overcome the limitations of linear theory;
- a range of friction formulae for different physical conditions;
- third-order differential approximations to eliminate grid scale "wiggles";
- a "diffusion" scheme to parameterize diffraction;
- longshore sediment transport on beaches;
- continuity of style throughout the suite of linked models and support software;
- software tools for data input, model output manipulation and graphical presentation;
- graphical output using the Matlab routine Plot3DD[1].

A9.1.1.1 Model equations

WBEND is a two-dimensional wave propagation model that uses, as a basis for refraction, the wave action equation for the conservation of wave power in two dimensions given by,

[1] Plot3DD, Gorman, R.M. (1995)

$$\frac{\partial}{\partial x}(F\cos\theta)+\frac{\partial}{\partial y}(F\sin\theta)=-F_D \qquad \text{(A9.1)}$$

where x and y are orthogonal co-ordinates, θ is the wave angle and F_D $(= F_f + F_b)$ is a combination of the bed friction (F_f) and wave breaking (F_b) dissipation terms. F is the wave power which, for Airy waves, is

$$F = EC_g = \frac{1}{8}\rho g H^2 C_g \qquad \text{(A9.2)}$$

where E is the wave energy, C_g is the group speed, ρ is the fluid density, g is gravitational acceleration and H is the wave height.

The wave angle is obtained from the equation for conservation of wave number

$$\frac{\partial}{\partial x}(|k|\sin\theta)-\frac{\partial}{\partial x}(|k|\cos\theta)=0 \qquad \text{(A9.3)}$$

The model solves equations A4.1 and A4.3 for wave power and wave angle respectively using a shoreward marching iterative scheme (Black and Rosenberg, 1992b). Height and angle are directly obtained on a regular finite difference grid, which eliminates the need for interpolation, as required when a ray tracking procedure is used.

To obtain the wave number k, the dispersion relation for linear waves,

$$\omega^2 = gk\tanh(kh) \qquad \text{(A9.4)}$$

is solved using an iterative *Newton-Raphson* technique, given the radian frequency ω and depth h.

A formulation based on the horizontal eddy viscosity in the hydrodynamic model 3DD (Black, 1995) is used to smooth the height and angle solutions. This has the effect of spreading energy along the wave crests, similar to the process of diffraction. While solving the wave action and conservation of wave number equations, heights and angles are smoothed by the function ψ given by,

$$\psi = \varepsilon\left(\frac{\partial^2 \varphi}{\partial y^2}\right) \tag{A9.5}$$

where ε is the eddy viscosity coefficient and φ is either wave height or angle. The dominant wave direction is along the model's *x*-axis, and so the term acts primarily along the wave crests. The eddy viscosity coefficient is set by calibration. Simulations of several different environments (e.g. Black and Rosenberg, 1992b; Hutt, 1997; McComb et al., 1997) have indicated that appropriate values are in the range $0.02 < \varepsilon < 0.06$.

For monochromatic cases, the wave-energy frictional dissipation term is given by,

$$F_f = \frac{\rho C_f}{6\pi}\left(\frac{H\omega}{\sinh(kh)}\right)^3 \tag{A9.6}$$

where C_f is the friction coefficient.

For a wave spectrum, mean bed orbital velocity is obtained from the variance in the spectrum, using the linear theory transform function to relate sea surface wave height and period to bed orbital motion. The transform function is applied to each spectral estimate and then the spectrum is re-constituted to obtain total bed orbital variance. The friction term adopted in the model, expressed as a height loss H_L per unit path length *s,* becomes,

$$\frac{\partial H_L}{\partial s} = \frac{2.83 C_f H_f H_{rms} \omega_f^2 \omega_{av}}{3\pi g C_g \sinh^2(k_f h)\sinh(k_{av} h)} \tag{A9.7}$$

where H_f is the height of the wave associated with the spectral band of frequency f, radian frequency ω_f and wave number k_f given by,

$$H_f = 2.83(S_f \Delta f)^{1/2} \qquad \text{(A9.8)}$$

where S_f is the spectral energy density of the band with frequency f, and Δf is the bandwidth.

H_{rms} is the root-mean-square wave height calculated from the total variance in the spectrum as,

$$\begin{aligned} \langle \eta^2 \rangle = \sigma^2 &= \int_0^\infty S(f)df = \sum_0^{f_n} S_f \Delta f \\ H_{rms} &= 2.83\sigma \\ H_s &= 4\sigma \end{aligned} \qquad \text{(A9.9)}$$

while the average radian frequency ω_{av} is given by,

$$f_{av} = \frac{\sum H_f f}{\sum H_f} \qquad \text{and} \qquad w_{av} = 2\pi f_{av} \qquad \text{(A9.10)}$$

The summations are across all N_f frequencies in the spectrum. The corresponding wave number k_{av} is defined by the dispersion relation as,

$$\omega_{av}^2 = g k_{av} \tanh(k_{av} h) \qquad \text{(A9.11)}$$

The group speed C_g is the speed coinciding with the frequency ω_{av} and wave number k_{av}.

When solving in the model, the wave path length is assumed to consist of a series of straight line segments across each cell of width Δx for a wave travelling at angle θ. Thus the path length is

$$\Delta s = \Delta x / \cos\theta \qquad \text{(A9.12)}$$

The total height loss is summed across the model grid, row-by-row, after initially solving eqn 4.1, assuming $F_D = 0$.

Wave breaking is assessed by checking if height exceeds a depth limitation, that is if,

$$H > \gamma h \qquad \text{(A9.13)}$$

where γ is user selected and is typically of order 0.6-0.8.

A9.1.1.2 Model grids and files

The model adopts a rectangular grid for bathymetry. The x-direction is positive to the east and corresponds with increasing 'I', while the y-direction is positive northwards and corresponds with increasing 'J'. The cell (1,1) is located at the bottom left corner of the grid and the maximum coordinate cell (I_{max} , J_{max}) is at the top right corner. The model assumes the shoreline is at the eastern side of the grid (maximum I). Wave angle is defined relative to the left ("east") of the grid and is positive anti-clockwise (Cartesian axes).

Model WBEND requires three input files which are:

1. Information file
2. Wave height, period and angle file, or spectrum file
3. Bathymetry file

One information file controls the model by providing the input data and output file names.

WBEND has three types of boundary condition that can be used: the probability file listing wave events and their probability of occurrence; the spectrum file containing spectral densities and frequencies for a sea surface spectrum; and the sediment transport contour file for calculation of surf zone littoral drift. WBEND produces several output files, outlined in detail in the user's manual. The binary file, *filename.out*, was the main file used for the present study. This contains depths, wave heights, wave periods, and bottom orbital motion over the full grid for each simulated event.

In the models, wave directions to the north of east are positive and wave directions to the south of east are negative. For example, an angle in the model of –45° is at 135° True (southeast) and a model angle of +45° refers to 45° True (northeast).

A9.2 MODEL 3DD

Model 3DD (Black, 1995) is a 3-dimensional circulation, advection/dispersion and heat transfer model, for application to vertically-stratified or homogeneous ocean, continental shelf and shallow water environments. An explicit finite difference (Eulerian) solution is used to solve the momentum and continuity equations for velocity and sea level, while the temperature and salinity advection/dispersion equations are solved using either Eulerian or Lagrangian particle techniques. Shallow water wave simulations use a Boussinesq approximation, solved with a semi-implicit iterative method (Gorman and Black, 1997). Heat transfers between the ocean and atmosphere are accommodated so that thermocline development can be simulated.

3DD has a number of common and novel features, including:

- a complete momentum equation for both deep or shallow barotropic and baroclinic environments.
- flooding and drying of inter-tidal zones.

- a wide range of open boundary options, e.g. currents, sea levels, volumes, radiation conditions and sponges.

In addition:

- the model can be operated in 2 or 3 dimensions using the same input files in both cases, thereby ensuring an effortless transition.
- “side-view” (2-dimensional) simulations are catered for, so that vertical stratification can be simulated with high resolution.
- the side-view operation provides for a simplified longshore momentum balance for continental shelves.
- 3DD is supported by a range of software tools for data input, model output manipulation and graphical presentation.
- the procedures to specify the open boundaries are both simple to use and comprehensive.
- third-order accurate derivative approximations eliminate grid-scale zig-zagging.
- a body force can be applied to simulate large-scale pressure gradients associated with coastal trapped waves, other continental shelf waves or geostrophic gradients.
- shallow-water form of the Boussinesq equations provide for simulations of finite-amplitude waves around ports, beaches or harbours.
- a zero up-crossing technique is applied to find the wave heights.
- radiation stress terms are calculated within the model and can be optionally included in the simulation to model wave-driven currents.
- a special inter-tidal flooding and drying scheme prevents the development of velocity spikes on the sand banks when flooding first occurs.
- an "effective depth" formulation prevents excessive frictional resistance in very shallow water.
- a boundary slip parameter eliminates the problem of excessive damping of currents in narrow channels due to horizontal diffusion.
- a variety of vertical eddy viscosity formulations are selectable.
- barometric pressure and wind conditions, entered as time series from a number of locations, will be interpolated by the model.
- heat inputs to the water body and thermocline formation can be simulated.
- enhanced bed friction due to wave/current interaction can be selected.

- hot starts are possible so that new runs can commence at any time during a prior simulation.
- 3DD provides for nested simulations.
- bathymetry can be represented on the cell walls (rather than cell mid-points) thereby maximising bathymetric resolution without increasing CPU requirements.
- advection/dispersion can be treated using either a Eulerian scheme or Lagrangian scheme which is coupled to the hydrodynamics. Alternatively, these simulations can be separately undertaken with the Lagrangian model POL3DD.

Model results are presented to the screen at run-time as a diagnostic aid to allow rapid assessment of model behaviour.

A9.2.1 Model equations

3DD (Black, 1995) is a layered 3-dimensional hydrodynamic and transport/dispersion model which incorporates the vertically-averaged model hydrodynamic Model 2DD (Black, 1983). The 3-dimensional equations are,

$$\frac{\partial u}{\partial t}+\frac{u\partial u}{\partial x}+\frac{v\partial u}{\partial y}+\frac{w\partial u}{\partial z}-fv=-\frac{g\partial \varsigma}{\partial x}-\frac{1\partial P}{\rho\partial x}+A_H\left(\frac{\partial^2 u}{\partial x^2}+\frac{\partial^2 u}{\partial y^2}\right)+\frac{\partial}{\partial z}\left(N_z\frac{\partial u}{\partial z}\right)+S_b \quad \text{(A9.14)}$$

$$\frac{\partial v}{\partial t}+\frac{u\partial v}{\partial x}+\frac{v\partial v}{\partial y}+\frac{w\partial v}{\partial z}+fu=-\frac{g\partial \varsigma}{\partial y}-\frac{1\partial P}{\rho\partial y}+A_H\left(\frac{\partial^2 v}{\partial x^2}+\frac{\partial^2 v}{\partial y^2}\right)+\frac{\partial}{\partial z}\left(N_z\frac{\partial v}{\partial z}\right)+S_b \quad \text{(A9.15)}$$

$$w=-\frac{\partial}{\partial x}\int_{-h}^{z} u\,dz-\frac{\partial}{\partial y}\int_{-h}^{z} v\,dz \quad \text{(A9.16)}$$

t is the time, u, v are velocities in the x, y directions respectively, w the vertical velocity in the z direction (positive upward) at the top of each layer, h the depth, g the gravitational acceleration, ζ the sea level above a horizontal datum, f the Coriolis parameter, P the pressure, ρ the density of water, A_H the horizontal eddy viscosity coefficient, and N_z the vertical eddy viscosity coefficient. S_b represents Boussinesq terms, discussed below, and other forcing terms including radiation stress calculated from the wave height spatial gradients and body forces.

The pressure at depth z is:

$$P = P_{atm} + g\int_{z}^{o} \rho \, dz \tag{A9.17}$$

where P_{atm} is the atmospheric pressure. The conservation equations for temperature and salinity may be written as:

$$\frac{\partial T}{\partial t} + \frac{u\,\partial T}{\partial x} + \frac{v\,\partial T}{\partial y} + \frac{w\,\partial T}{\partial z} = \frac{\partial}{\partial z}\left(K_z \frac{\partial T}{\partial z}\right) + K_H\left(\frac{\partial^2 T}{\partial x^2} + \frac{\partial^2 T}{\partial y^2}\right) \tag{A9.18}$$

$$\frac{\partial S}{\partial t} + \frac{u\,\partial S}{\partial x} + \frac{v\,\partial S}{\partial y} + \frac{w\,\partial S}{\partial z} = \frac{\partial}{\partial z}\left(K_z \frac{\partial S}{\partial z}\right) + K_H\left(\frac{\partial^2 S}{\partial x^2} + \frac{\partial^2 S}{\partial y^2}\right) \tag{A9.19}$$

where T is temperature, S is salinity, and K_H, K_Z are the horizontal and vertical coefficients of eddy diffusivity.

Using the temperature and salinity, the density is computed according to an equation of state of the form,

$$\rho = \rho(T,S,z) \tag{A9.20}$$

that is,

$$\begin{aligned} T_K &= T + 2.7 \\ \rho &= 1000(1 - 3.7\times10^{-6} T_K^2 + 8.13\times10^{-4} S) \end{aligned} \tag{A9.21}$$

Surface boundary conditions at $z = 0$ are:

$$\rho N_z \frac{\partial u}{\partial z} = \tau_x^s \tag{A9.22}$$

$$\rho N_z \frac{\partial v}{\partial z} = \tau_y^s \tag{A9.23}$$

$$\frac{\partial \varsigma}{\partial t} + u\frac{\partial \varsigma}{\partial x} + v\frac{\partial \varsigma}{\partial y} = w^s \qquad \text{(A9.24)}$$

where τ_x^s, τ_y^s denote the components of wind stress and

$$\begin{aligned} \tau_x^s &= \frac{\rho_a}{\rho}\gamma |W|\ W_x \\ \tau_y^s &= \frac{\rho_a}{\rho}\gamma |W|\ W_y \end{aligned} \qquad \text{(A9.25)}$$

ρ is the water density, W the wind speed at 10 m above sea level with W_x and W_y its x and y components, γ is the wind drag coefficient, ρ_a the density of air.

Surface boundary conditions for temperature and salinity are,

$$\rho N_z \frac{\partial S}{\partial z} = S_l \qquad \text{(A9.26)}$$

$$\rho N_z \frac{\partial T}{\partial z} = T_l$$

where

$$S_l = S(0)\,(E_l - P_l)/\rho \qquad \text{(A9.27)}$$

$$T_1 = Q/c$$

and $S(0)$ is the surface salinity, E_1 is the net evaporation, P_1 is the net precipitation mass flux of fresh water, Q is the net ocean heat flux and c is the water heat capacity.

At the sea bed, $z = -h$, we have

$$\rho N_z \frac{\partial u}{\partial z} = \tau_x^h \qquad \text{(A9.28)}$$

$$\rho N_z \frac{\partial v}{\partial z} = \tau_y^h \qquad \text{(A9.29)}$$

where τ_x^h, τ_y^h denotes the components of bottom stress. Applying a quadratic law at the sea bed,

$$\tau_x^h = g u_h (u_h^2 + v_h^2)^{1/2} / C^2 \qquad \text{(A9.30)}$$

$$\tau_y^h = g v_h (u_h^2 + v_h^2)^{1/2} / C^2 \qquad \text{(A9.31)}$$

with u_h, v_h being the bottom currents and C is Chezy's C. For a logarithmic profile,

$$C = 18 \log_{10}(0.37 h/z_o) \qquad \text{(A9.32)}$$

where z_o is the roughness length.

Also,

$$\frac{\partial S}{\partial z} = 0$$

$$\frac{\partial T}{\partial z} = 0 \qquad \text{(A9.33)}$$

$$w_h = -u_h \frac{\partial h}{\partial x} - v_h \frac{\partial h}{\partial y} \qquad \text{(A9.34)}$$

to ensure no transport of mass, salinity or temperature through the bed.

The form of the horizontal eddy viscosity term results when the depth is presumed constant before taking the derivative of the horizontal shear stresses. The term, as

presented, behaves as a velocity smoothing algorithm. The horizontal eddy viscosity coefficient is a variable in space in the model.

A staggered finite difference grid is utilised similar to that applied which places the v and u components on “north” and “east” walls respectively. w is located in the centre of the "top" wall. The sea level replaces w in the top layer. The solution is found by time stepping with an explicit scheme.

Boussinesq terms

For short surface wave applications, the momentum equations for depth-averaged velocity require additional ("Boussinesq") terms. Including these terms, the 2-dimensional form of equations A9.14 and A9.15 may be written

$$u_t = F^{(u)} + \frac{D}{2}\left[(hu_t)_x + (hv_t)_y\right]_x - \frac{Dh}{6}\left[u_{xt} + v_{yt}\right]_x \qquad \text{(A9.35)}$$

$$v_t = F^{(v)} + \frac{D}{2}\left[(hu_t)_x + (hv_t)_y\right]_y - \frac{Dh}{6}\left[u_{xt} + v_{yt}\right]_y \qquad \text{(A9.36)}$$

where $F^{(u)}$ and $F^{(v)}$ represent the terms previously considered, and h is the mean still-water depth. Subscripts x, y, t denote partial derivatives. In the original form $D = h$, but a version in which D is the net depth $h + \zeta$ is also considered; both forms are supported for 2-dimensional modelling in 3DD.

On the eastern wall of cell (i,j), the depth $h^{(u)}_{i,j}$ and the x component of velocity $U_{i,j}^{(n)}$ at time step n are defined, while the depth $h^{(v)}_{i,j}$ and the y component of velocity $V_{i,j}^{(n)}$ at time step n are located on the northern wall. Defining the velocities at the next step as the standard 3DD prediction (ie: solving (A9.35, A9.36) with $\vec{S} = 0$), plus a Boussinesq correction:

$$U_{i,j}^{(n+1)} = U_{i,j}^{(n)} + F^{(u)}_{i,j}\delta t + \hat{U}_{i,j}\ , \qquad \text{(A9.37)}$$

$$V_{i,j}^{(n+1)} = V_{i,j}^{(n)} + F^{(v)}_{i,j}\delta t + \hat{V}_{i,j}\ , \qquad \text{(A9.38)}$$

the momentum equations may be written in difference form as

$$\hat{U}_{i,j} - \frac{D_{i,j}}{\delta x^2}\left[\tfrac{1}{2}(h^{(u)}{}_{i+1,j}\hat{U}_{i+1,j} - 2h^{(u)}{}_{i,j}\hat{U}_{i,j} + h^{(u)}{}_{i-1,j}\hat{U}_{i-1,j}) - \tfrac{1}{6}h^{(u)}{}_{i,j}(\hat{U}_{i+1,j} - 2\hat{U}_{i,j} + \hat{U}_{i-1,j})\right]$$

$$= \frac{D_{i,j}}{\delta x^2}\left[\tfrac{1}{2}(h^{(u)}{}_{i+1,j}F^{(u)}{}_{i+1,j} - 2h^{(u)}{}_{i,j}F^{(u)}{}_{i,j} + h^{(u)}{}_{i-1,j}F^{(u)}{}_{i-1,j}) - \tfrac{1}{6}h^{(u)}{}_{i,j}(F^{(u)}{}_{i+1,j} - 2F^{(u)}{}_{i,j} + F^{(u)}{}_{i-1,j})\right]$$

$$- \frac{D_{i,j}}{\delta x\,\delta y}\left[\tfrac{1}{2}(h^{(v)}{}_{i+1,j}\hat{V}_{i+1,j} - h^{(v)}{}_{i,j}\hat{V}_{i,j} - h^{(v)}{}_{i+1,j-1}\hat{V}_{i+1,j-1} + h^{(v)}{}_{i,j-1}\hat{V}_{i,j-1}) - \tfrac{1}{6}h^{(u)}{}_{i,j}(\hat{V}_{i+1,j} - \hat{V}_{i,j} - \hat{V}_{i+1,j-1} + \hat{V}_{i,j-1})\right]$$

(A9.39)

and

$$\hat{V}_{i,j} - \frac{D_{i,j}}{\delta y^2}\left[\tfrac{1}{2}(h^{(v)}{}_{i,j+1}\hat{U}_{i,j+1} - 2h^{(v)}{}_{i,j}\hat{V}_{i,j} + h^{(v)}{}_{i,j-1}\hat{V}_{i,j-1}) - \tfrac{1}{6}h^{(v)}{}_{i,j}(\hat{V}_{i,j+1} - 2\hat{V}_{i,j} + \hat{V}_{i,j-1})\right]$$

$$= \frac{D_{i,j}}{\delta y^2}\left[\tfrac{1}{2}(h^{(v)}{}_{i,j+1}F^{(v)}{}_{i,j+1} - 2h^{(v)}{}_{i,j}F^{(v)}{}_{i,j} + h^{(v)}{}_{i,j-1}F^{(v)}{}_{i,j-1}) - \tfrac{1}{6}h^{(v)}{}_{i,j}(F^{(v)}{}_{i,j+1} - 2F^{(v)}{}_{i,j} + F^{(v)}{}_{i,j-1})\right]$$

$$- \frac{D_{i,j}}{\delta x\,\delta y}\left[\tfrac{1}{2}(h^{(u)}{}_{i,j+1}\hat{U}_{i,j+1} - h^{(u)}{}_{i,j}\hat{U}_{i,j} - h^{(u)}{}_{i-1,j+1}\hat{U}_{i-1,j+1} + h^{(u)}{}_{i-1,j}\hat{U}_{i-1,j}) - \tfrac{1}{6}h^{(v)}{}_{i,j}(\hat{U}_{i,j+1} - \hat{U}_{i,j} - \hat{U}_{i-1,j+1} + \hat{U}_{i-1,j})\right]$$

(A9.40)

To solve these, $\hat{U}$ and $\hat{V}$ are first set to zero, and (A9.39) is solved for $\hat{U}$ by a tridiagonal algorithm along each row of constant j. $\hat{V}$ is found similarly from (A9.40). This process is iterated with updated $\hat{V}$ terms in the $\hat{U}$ equation and vice-versa until convergence is reached. Typically around 5 iterations are required for 1% precision.

APPENDIX 10: Sflux Data

SFLUX 1

TIME	CURSPD	CURDIR	WAVEORB	PERIOD	C0	SSLOAD	VOLFLUX	VOL CROSS	VOL LONG	SUM CROSS	SUM LONG
DAYS	M/S	DEG	M/S	SECS	KG/M3	KG/M/S	M3/M	M3/M	M3/M	M3/M	M3/M
Note that	the M3 v	Note that the M3 volumes do not include pore spaces									
162.6729	0.068	-43.85	0.363	10.27	1.5000	0.0043	0.0057	-0.0022	0.0053	-0.0022	0.0053
162.7146	0.09	-79.52	0.404	10.4	2.2100	0.0085	0.0113	-0.0096	0.0059	-0.0118	0.0112
162.7563	0.091	-57.17	0.405	10.52	2.2000	0.0086	0.0114	-0.0067	0.0092	-0.0186	0.0204
162.798	0.045	-85.77	0.377	11.2	1.6400	0.0032	0.0042	-0.0038	0.0018	-0.0224	0.0222
162.8397	0.023	-34.44	0.371	11.24	1.5300	0.0015	0.0020	-0.0005	0.0019	-0.0228	0.0241
162.8814	0.057	-83.5	0.389	12.43	1.7300	0.0042	0.0056	-0.0049	0.0026	-0.0278	0.0267
162.9231	0.045	-52.56	0.367	12.12	1.4000	0.0027	0.0036	-0.0019	0.0031	-0.0296	0.0297
162.9648	0.027	-8.89	0.359	12.22	1.2800	0.0015	0.0020	0.0004	0.0019	-0.0292	0.0316
163.0065	0.051	-58.9	0.319	11.69	0.7940	0.0017	0.0023	-0.0014	0.0018	-0.0306	0.0335
163.0482	0.042	-42.43	0.319	12.16	0.7750	0.0014	0.0019	-0.0007	0.0017	-0.0313	0.0352
163.0899	0.036	-46.37	0.339	11.85	1.0300	0.0016	0.0021	-0.0009	0.0019	-0.0322	0.0371
163.1316	0.032	-63.65	0.365	11.69	1.4000	0.0019	0.0026	-0.0018	0.0019	-0.0340	0.0390
163.1733	0.036	-34.85	0.406	11.43	2.1200	0.0032	0.0043	-0.0010	0.0042	-0.0350	0.0431
163.215	0.04	-56.96	0.358	10.91	1.3600	0.0023	0.0031	-0.0018	0.0025	-0.0368	0.0457
163.2567	0.108	-36.29	0.371	10.83	1.5800	0.0073	0.0097	-0.0026	0.0093	-0.0394	0.0550
163.2984	0.063	-79.76	0.338	10.53	1.1000	0.0030	0.0039	-0.0034	0.0020	-0.0427	0.0570
163.3401	0.01	-53.83	0.301	10.11	0.6830	0.0003	0.0004	-0.0002	0.0003	-0.0429	0.0573
163.3818	0.026	49.57	0.358	10.88	1.3600	0.0015	0.0020	0.0019	0.0007	-0.0410	0.0580
163.4235	0.027	106.4	0.319	12.31	0.7700	0.0009	0.0012	0.0009	-0.0007	-0.0401	0.0573
163.4652	0.022	-3.49	0.292	12.49	0.4910	0.0005	0.0006	0.0002	0.0006	-0.0399	0.0579
163.5069	0.017	2.56	0.3	11.82	0.5920	0.0004	0.0006	0.0002	0.0005	-0.0397	0.0584
163.5486	0.103	-81.05	0.316	11.31	0.7820	0.0035	0.0046	-0.0040	0.0023	-0.0436	0.0607
163.5903	0.089	-83.65	0.342	10.06	1.1900	0.0045	0.0060	-0.0054	0.0028	-0.0490	0.0634
163.632	0.089	266.8	0.364	10.27	1.5100	0.0058	0.0077	-0.0073	0.0023	-0.0563	0.0658
163.6737	0.043	-86.18	0.351	6.66	1.7200	0.0032	0.0042	-0.0038	0.0018	-0.0601	0.0676
163.7154	0.069	-82.47	0.366	5.21	2.3500	0.0069	0.0092	-0.0081	0.0044	-0.0682	0.0720
163.7571	0.141	-87.38	0.346	4.43	2.1400	0.0129	0.0171	-0.0157	0.0069	-0.0839	0.0788
163.7988	0.152	265.8	0.299	4.11	1.3400	0.0087	0.0115	-0.0110	0.0033	-0.0949	0.0821
163.8405	0.134	-86.82	0.312	6.24	1.1400	0.0065	0.0087	-0.0079	0.0036	-0.1030	0.0857
163.8822	0.094	264.6	0.26	10.86	0.2880	0.0012	0.0015	-0.0015	0.0004	-0.1040	0.0861
163.9239	0.033	-84.8	0.263	11.83	0.2810	0.0004	0.0005	-0.0005	0.0002	-0.1050	0.0863
163.9656	0.039	-54.72	0.245	10.23	0.2100	0.0003	0.0005	-0.0003	0.0004	-0.1050	0.0867

164.0073	0.024	-25.73	0.279	6.55	0.6800	0.0007	0.0009	-0.0001	0.0009	-0.1050	0.0876
164.049	0.105	-75.86	0.39	6.07	2.6500	0.0120	0.0159	-0.0130	0.0091	-0.1180	0.0968
164.0907	0.115	269.4	0.457	4.93	4.9900	0.0245	0.0325	-0.0305	0.0113	-0.1490	0.1080
164.1324	0.048	-70.4	0.46	4.88	5.1200	0.0105	0.0139	-0.0106	0.0091	-0.1590	0.1170
164.1741	0.034	-59.69	0.433	4.86	4.2500	0.0063	0.0083	-0.0052	0.0065	-0.1640	0.1240
164.2158	0.018	27.81	0.407	4.75	3.5500	0.0027	0.0036	0.0027	0.0024	-0.1620	0.1260
164.2575	0.026	-5.65	0.481	4.8	5.9300	0.0066	0.0088	0.0023	0.0085	-0.1590	0.1350
164.2992	0.032	11.21	0.588	4.83	10.8000	0.0148	0.0197	0.0105	0.0166	-0.1490	0.1510
164.3409	0.117	-44.63	0.538	4.82	8.3000	0.0414	0.0550	-0.0220	0.0504	-0.1710	0.2020
164.3826	0.048	-86.35	0.512	5.32	6.8100	0.0139	0.0184	-0.0167	0.0077	-0.1880	0.2090
164.4243	0.007	86.04	0.465	5.28	5.0700	0.0015	0.0020	0.0019	-0.0006	-0.1860	0.2090
164.466	0.003	-55.05	0.472	5.24	5.3600	0.0007	0.0010	-0.0005	0.0008	-0.1860	0.2100
164.5077	0.019	-15.89	0.45	5.9	4.3300	0.0034	0.0045	0.0004	0.0045	-0.1860	0.2140
164.5494	0.061	260.2	0.468	6.34	4.7000	0.0122	0.0163	-0.0160	0.0032	-0.2020	0.2170
164.5911	0.056	-86.84	0.44	6.31	3.8600	0.0093	0.0123	-0.0112	0.0050	-0.2130	0.2220
164.6328	0.038	-68.43	0.373	6.55	2.1600	0.0035	0.0047	-0.0035	0.0032	-0.2160	0.2250
164.6745	0.029	-73.63	0.392	7.05	2.4800	0.0031	0.0041	-0.0032	0.0025	-0.2200	0.2280
164.7162	0.037	-66.55	0.437	5.71	4.0000	0.0064	0.0084	-0.0060	0.0059	-0.2260	0.2340
164.7579	0.063	-81.71	0.577	5.67	9.4200	0.0251	0.0334	-0.0291	0.0163	-0.2550	0.2500
164.7996	0.055	-65	0.697	6.1	15.7000	0.0366	0.0487	-0.0338	0.0350	-0.2890	0.2850
164.8413	0.047	-84.6	0.74	6.37	18.3000	0.0370	0.0492	-0.0441	0.0219	-0.3330	0.3070
164.883	0.064	-89.9	0.812	6.91	23.1000	0.0627	0.0833	-0.0778	0.0300	-0.4110	0.3370
164.9247	0.034	-66.06	0.765	7.14	19.3000	0.0276	0.0367	-0.0260	0.0259	-0.4370	0.3630
164.9664	0.025	-72.13	0.726	6.92	16.8000	0.0183	0.0243	-0.0189	0.0152	-0.4550	0.3780
165.0081	0.055	-78.2	0.709	7.24	15.3000	0.0359	0.0478	-0.0402	0.0259	-0.4960	0.4040
165.0498	0.054	-62.95	0.645	7.32	11.6000	0.0269	0.0358	-0.0239	0.0266	-0.5200	0.4310
165.0915	0.07	-65.71	0.671	7.78	12.7000	0.0379	0.0504	-0.0355	0.0358	-0.5550	0.4670
165.1332	0.059	-69.21	0.689	7.49	13.9000	0.0349	0.0464	-0.0346	0.0309	-0.5900	0.4980
165.1749	0.06	-54.57	0.723	7.29	16.2000	0.0412	0.0548	-0.0303	0.0456	-0.6200	0.5430
165.2166	0.065	-57.08	0.702	7.29	14.9000	0.0410	0.0545	-0.0321	0.0440	-0.6520	0.5870
165.2583	0.059	-51.92	0.766	6.68	19.8000	0.0497	0.0661	-0.0340	0.0567	-0.6860	0.6440
165.3	0.078	-40.43	0.795	7.23	21.4000	0.0711	0.0945	-0.0314	0.0891	-0.7170	0.7330
165.3417	0.08	-44.53	0.707	7.15	15.3000	0.0525	0.0699	-0.0279	0.0640	-0.7450	0.7970
165.3834	0.053	-54.91	0.725	6.82	16.8000	0.0383	0.0509	-0.0284	0.0423	-0.7740	0.8390
165.4251	0.027	-32.32	0.608	7.08	9.8900	0.0115	0.0153	-0.0030	0.0150	-0.7770	0.8540
165.4668	0.036	-29.31	0.591	7.01	9.1600	0.0139	0.0185	-0.0027	0.0183	-0.7790	0.8730

165.5085	0.031	-62.51	0.569	6.97	8.2000	0.0108	0.0144	-0.0096	0.0108	-0.7890	0.8830
165.5502	0.023	-63.73	0.53	7.59	6.3300	0.0062	0.0082	-0.0056	0.0060	-0.7940	0.8890
165.5919	0.069	-76.42	0.539	7.47	6.7200	0.0199	0.0265	-0.0218	0.0150	-0.8160	0.9040
165.6336	0.059	-75.59	0.56	7.86	7.3700	0.0187	0.0249	-0.0203	0.0144	-0.8370	0.9190
165.6753	0.078	-70.42	0.482	7.52	4.7400	0.0157	0.0209	-0.0159	0.0136	-0.8520	0.9320
165.717	0.068	-68.01	0.551	8.03	6.9500	0.0203	0.0270	-0.0197	0.0184	-0.8720	0.9510
165.7587	0.069	-64.7	0.565	8.05	7.4900	0.0220	0.0293	-0.0202	0.0212	-0.8920	0.9720
165.8004	0.059	-46.71	0.599	8.63	8.6700	0.0220	0.0293	-0.0127	0.0264	-0.9050	0.9980
165.8421	0.159	-11.7	0.604	8.58	8.8900	0.0603	0.0802	0.0130	0.0792	-0.8920	1.0800
165.8838	0.075	-61.48	0.669	8.68	12.0000	0.0383	0.0509	-0.0330	0.0387	-0.9250	1.1200
165.9255	0.028	-74.92	0.581	9.16	7.6800	0.0090	0.0120	-0.0097	0.0071	-0.9350	1.1200
165.9672	0.035	-52.04	0.575	9.68	7.2800	0.0109	0.0145	-0.0075	0.0124	-0.9420	1.1400
166.0089	0.043	-29.66	0.547	8.9	6.4900	0.0118	0.0156	-0.0024	0.0155	-0.9450	1.1500
166.0506	0.039	-32.7	0.59	9.43	7.9400	0.0134	0.0178	-0.0036	0.0174	-0.9480	1.1700
166.0923	0.035	-60.95	0.572	9.45	7.2200	0.0108	0.0144	-0.0093	0.0110	-0.9580	1.1800
166.134	0.057	-72.61	0.604	9.59	8.5000	0.0208	0.0277	-0.0217	0.0172	-0.9790	1.2000
166.1757	0.051	-63.49	0.572	9.27	7.2900	0.0160	0.0213	-0.0144	0.0157	-0.9940	1.2100
166.2174	0.048	-59.36	0.6	9.06	8.5100	0.0174	0.0232	-0.0144	0.0182	-1.0100	1.2300
166.2591	0.057	-57.96	0.676	8.97	12.2000	0.0300	0.0399	-0.0240	0.0319	-1.0300	1.2600
166.3008	0.075	-63.53	0.778	8.22	19.1000	0.0610	0.0811	-0.0548	0.0598	-1.0900	1.3200
166.3425	0.087	-64.44	0.757	8.09	17.7000	0.0661	0.0878	-0.0604	0.0638	-1.1500	1.3900
166.3842	0.077	-68.13	0.705	8.09	14.4000	0.0476	0.0633	-0.0464	0.0431	-1.1900	1.4300
166.4259	0.113	-42.2	0.737	8.4	16.2000	0.0780	0.1040	-0.0375	0.0967	-1.2300	1.5300
166.4676	0.066	-68.97	0.737	8.35	16.2000	0.0454	0.0604	-0.0449	0.0404	-1.2800	1.5700
166.5093	0.034	-53.75	0.628	8.29	10.2000	0.0147	0.0195	-0.0106	0.0164	-1.2900	1.5800
166.551	0.055	-78.63	0.614	8.64	9.3100	0.0219	0.0291	-0.0246	0.0156	-1.3100	1.6000
166.5927	0.047	-71.99	0.647	8.6	10.9000	0.0221	0.0293	-0.0228	0.0185	-1.3300	1.6200
166.6344	0.059	-72.87	0.624	8.52	9.8700	0.0250	0.0332	-0.0261	0.0205	-1.3600	1.6400
166.6761	0.065	-61.47	0.605	8.41	9.0300	0.0251	0.0334	-0.0216	0.0254	-1.3800	1.6600
166.7178	0.067	-62.39	0.583	8.34	8.0900	0.0230	0.0305	-0.0202	0.0229	-1.4000	1.6900
166.7595	0.059	-72.68	0.643	8.08	11.0000	0.0277	0.0368	-0.0289	0.0228	-1.4300	1.7100
166.8012	0.052	-60.35	0.651	8.14	11.4000	0.0253	0.0336	-0.0213	0.0260	-1.4500	1.7300
166.8429	0.048	-52.78	0.624	7.7	10.3000	0.0212	0.0282	-0.0148	0.0240	-1.4700	1.7600
166.8846	0.081	-63.47	0.696	7.74	14.1000	0.0488	0.0649	-0.0438	0.0479	-1.5100	1.8100
166.9263	0.122	-29.58	0.598	7.97	8.9500	0.0467	0.0621	-0.0093	0.0614	-1.5200	1.8700
166.968	0.061	-76.51	0.528	8.01	6.1200	0.0161	0.0213	-0.0176	0.0121	-1.5400	1.8800

167.0097	0.036	-78.83	0.522	8.34	5.7700	0.0089	0.0118	-0.0100	0.0063	-1.5500	1.8900
167.0514	0.036	-88.56	0.513	8.4	5.4400	0.0083	0.0110	-0.0102	0.0042	-1.5600	1.8900
167.0931	0.056	-61.84	0.455	8.5	3.6800	0.0087	0.0116	-0.0076	0.0088	-1.5700	1.9000
167.1348	0.075	-58.74	0.48	8.63	4.3600	0.0139	0.0185	-0.0113	0.0146	-1.5800	1.9100
167.1765	0.071	-64.06	0.454	8.36	3.6900	0.0112	0.0149	-0.0102	0.0109	-1.5900	1.9200
167.2182	0.062	-69.36	0.432	8.18	3.1600	0.0084	0.0112	-0.0084	0.0074	-1.6000	1.9300
167.2599	0.048	-77.52	0.435	7.36	3.4200	0.0069	0.0092	-0.0077	0.0051	-1.6000	1.9400
167.3016	0.04	-56.66	0.456	6.24	4.3600	0.0074	0.0098	-0.0057	0.0080	-1.6100	1.9400
167.3433	0.038	-55.09	0.607	5.83	10.8000	0.0174	0.0231	-0.0130	0.0192	-1.6200	1.9600
167.385	0.068	-69.91	0.761	5.03	22.0000	0.0643	0.0855	-0.0644	0.0562	-1.6900	2.0200
167.4267	0.074	-47.53	0.771	5.25	22.4000	0.0706	0.0938	-0.0419	0.0840	-1.7300	2.1000
167.4684	0.05	-87.11	0.788	5.32	23.7000	0.0506	0.0673	-0.0615	0.0272	-1.7900	2.1300
167.5101	0.029	-60.5	0.784	5.51	23.0000	0.0288	0.0383	-0.0244	0.0296	-1.8100	2.1600
167.5518	0.035	-34.5	0.811	5.31	25.7000	0.0380	0.0505	-0.0118	0.0491	-1.8300	2.2100
167.5935	0.058	-55.69	0.847	5.6	28.4000	0.0706	0.0938	-0.0534	0.0772	-1.8800	2.2900
167.6352	0.064	-39.27	0.863	5.65	29.8000	0.0808	0.1070	-0.0337	0.1020	-1.9100	2.3900
167.6769	0.093	-72.93	0.894	5.58	33.0000	0.1310	0.1740	-0.1370	0.1070	-2.0500	2.5000
167.7186	0.046	-65.75	1.028	5.75	47.9000	0.0945	0.1260	-0.0885	0.0892	-2.1400	2.5900
167.7603	0.083	-79.01	0.951	6.05	37.8000	0.1340	0.1790	-0.1510	0.0946	-2.2900	2.6800
167.802	0.085	-76.75	0.998	5.99	43.4000	0.1570	0.2090	-0.1730	0.1180	-2.4600	2.8000
167.8437	0.091	-68.92	1.201	6.03	72.1000	0.2790	0.3710	-0.2750	0.2490	-2.7400	3.0500
167.8854	0.104	-63.18	1.133	5.93	61.9000	0.2740	0.3640	-0.2450	0.2700	-2.9800	3.3200
167.9271	0.169	-52.53	1.212	5.85	74.8000	0.5390	0.7160	-0.3750	0.6110	-3.3600	3.9300
167.9688	0.107	-61.74	1.054	5.96	50.6000	0.2320	0.3080	-0.2010	0.2340	-3.5600	4.1600
168.0105	0.138	-83.86	1.16	6.17	65.0000	0.3830	0.5090	-0.4530	0.2320	-4.0100	4.3900
168.0522	0.192	-88.01	1.082	6.49	52.7000	0.4320	0.5740	-0.5290	0.2240	-4.5400	4.6200
168.0939	0.241	265.9	1.07	6.67	50.6000	0.5200	0.6920	-0.6620	0.2010	-5.2000	4.8200
168.1356	0.197	-88.06	1.063	6.72	49.5000	0.4160	0.5530	-0.5090	0.2160	-5.7100	5.0300
168.1773	0.137	-76.79	0.966	6.99	37.4000	0.2180	0.2900	-0.2400	0.1630	-5.9500	5.2000
168.219	0.12	-82.66	1.089	7.24	51.5000	0.2640	0.3510	-0.3090	0.1670	-6.2600	5.3600
168.2607	0.112	-65.59	1.137	6.8	59.4000	0.2830	0.3760	-0.2640	0.2680	-6.5200	5.6300
168.3024	0.095	-56.75	1.086	7	51.7000	0.2090	0.2790	-0.1630	0.2260	-6.6900	5.8600
168.3441	0.095	-44.9	1.067	6.99	49.3000	0.2000	0.2660	-0.1080	0.2430	-6.7900	6.1000
168.3858	0.111	-43.17	1.217	6.13	74.3000	0.3530	0.4690	-0.1770	0.4340	-6.9700	6.5300
168.4275	0.094	-45.7	1.127	6.53	58.8000	0.2360	0.3130	-0.1310	0.2850	-7.1000	6.8200
168.4692	0.136	-22.42	1.211	6.44	72.0000	0.4170	0.5540	-0.0137	0.5540	-7.1200	7.3700

168.5109	0.134	-28.37	1.045	6.65	47.4000	0.2700	0.3590	-0.0461	0.3560	-7.1600	7.7300
168.5526	0.067	-73.58	1.03	7.45	43.6000	0.1240	0.1650	-0.1310	0.1000	-7.2900	7.8300
168.5943	0.062	-57.89	0.982	6.98	39.2000	0.1030	0.1380	-0.0826	0.1100	-7.3800	7.9400
168.636	0.059	-69.25	0.895	6.85	30.5000	0.0774	0.1030	-0.0768	0.0685	-7.4500	8.0100
168.6777	0.106	-64.48	1.054	7.1	47.4000	0.2140	0.2850	-0.1960	0.2060	-7.6500	8.2100
168.7194	0.071	-74.63	0.952	7.18	35.6000	0.1070	0.1420	-0.1150	0.0845	-7.7600	8.3000
168.7611	0.064	-57.83	1.009	6.87	42.5000	0.1160	0.1540	-0.0923	0.1230	-7.8500	8.4200
168.8028	0.092	-61.67	1.11	6.41	56.8000	0.2240	0.2980	-0.1940	0.2260	-8.0500	8.6500
168.8445	0.094	-59.25	1.035	6.2	47.4000	0.1900	0.2520	-0.1560	0.1980	-8.2100	8.8500
168.8862	0.088	-31.33	1.308	5.49	94.3000	0.3540	0.4710	-0.0844	0.4630	-8.2900	9.3100
168.9279	0.122	-0.79	1.302	5.4	93.7000	0.4870	0.6470	0.2240	0.6070	-8.0700	9.9200
168.9696	0.22	-19.04	1.419	5.7	116.0000	1.0900	1.4500	0.0496	1.4500	-8.0200	11.4000
169.0113	0.134	-36.11	1.396	6.36	107.0000	0.6110	0.8130	-0.2120	0.7850	-8.2300	12.2000
169.053	0.105	-76.68	1.353	7.09	94.3000	0.4210	0.5600	-0.4630	0.3160	-8.6900	12.5000
169.0947	0.079	-63.42	1.37	6.76	99.2000	0.3340	0.4440	-0.3000	0.3280	-8.9900	12.8000
169.1364	0.079	-55.9	1.243	7.51	73.2000	0.2470	0.3290	-0.1880	0.2700	-9.1800	13.1000
169.1781	0.069	-58.67	1.282	7.18	81.0000	0.2370	0.3150	-0.1930	0.2490	-9.3700	13.3000
169.2198	0.096	-60.25	1.344	7.35	91.4000	0.3760	0.4990	-0.3160	0.3870	-9.6900	13.7000
169.2615	0.102	-56.56	1.391	7.24	101.0000	0.4380	0.5820	-0.3380	0.4730	-10.0000	14.2000
169.3032	0.095	-52.72	1.375	6.89	99.5000	0.4040	0.5380	-0.2830	0.4570	-10.3000	14.6000
169.3449	0.087	3.58	1.336	6.36	94.7000	0.3500	0.4650	0.1930	0.4230	-10.1000	15.1000
169.3866	0.107	-1.02	1.4	6.07	109.0000	0.5020	0.6670	0.2280	0.6270	-9.8900	15.7000
169.4283	0.097	-16.57	1.541	5.06	152.0000	0.6300	0.8380	0.0647	0.8350	-9.8200	16.5000
169.47	0.239	10.86	1.477	5.42	132.0000	1.3400	1.7900	0.9440	1.5200	-8.8800	18.0000
169.5117	0.175	-25.57	1.423	5.28	120.0000	0.9010	1.2000	-0.0954	1.1900	-8.9700	19.2000
169.5534	0.096	-63.16	1.33	6.04	95.3000	0.3910	0.5190	-0.3490	0.3850	-9.3200	19.6000
169.5951	0.084	-45.97	1.336	5.96	96.9000	0.3490	0.4650	-0.1960	0.4210	-9.5200	20.0000
169.6368	0.052	-23.39	1.221	6.29	74.3000	0.1640	0.2180	-0.0091	0.2180	-9.5300	20.3000
169.6785	0.053	-36.76	1.298	6.44	87.1000	0.1980	0.2630	-0.0714	0.2530	-9.6000	20.5000
169.7202	0.125	-72.06	1.19	7.21	65.9000	0.3520	0.4690	-0.3640	0.2940	-9.9600	20.8000
169.7619	0.079	-54.6	1.228	6.49	74.6000	0.2520	0.3360	-0.1860	0.2800	-10.1000	21.1000
169.8036	0.093	-36.17	1.333	5.69	98.0000	0.3880	0.5160	-0.1350	0.4980	-10.3000	21.6000
169.8453	0.099	-23.14	1.373	6.14	103.0000	0.4350	0.5780	-0.0216	0.5770	-10.3000	22.2000
169.887	0.113	-28.4	1.486	6	129.0000	0.6210	0.8260	-0.1060	0.8190	-10.4000	23.0000
169.9287	0.13	5.03	1.504	5.39	139.0000	0.7700	1.0200	0.4490	0.9190	-9.9600	23.9000
169.9704	0.117	-10.74	1.526	5.77	141.0000	0.7050	0.9370	0.1670	0.9220	-9.8000	24.8000

170.0121	0.204	18.46	1.554	6.37	143.0000	1.2400	1.6500	1.0500	1.2700	-8.7500	26.1000
170.0538	0.175	-34.89	1.398	6.2	108.0000	0.8090	1.0800	-0.2580	1.0400	-9.0100	27.1000
170.0955	0.135	-40.42	1.436	6.6	114.0000	0.6570	0.8740	-0.2910	0.8240	-9.3000	28.0000
170.1372	0.079	-48.99	1.374	7.56	96.2000	0.3240	0.4310	-0.2020	0.3810	-9.5000	28.3000
170.1789	0.096	-55.62	1.32	7.91	84.8000	0.3490	0.4640	-0.2640	0.3820	-9.7600	28.7000
170.2206	0.091	-50.54	1.433	7.35	109.0000	0.4250	0.5640	-0.2780	0.4910	-10.0000	29.2000
170.2623	0.147	-57.84	1.503	7.75	122.0000	0.7680	1.0200	-0.6120	0.8170	-10.7000	30.0000
170.304	0.131	-59.05	1.49	7.6	120.0000	0.6690	0.8890	-0.5480	0.7000	-11.2000	30.7000
170.3457	0.142	-46.23	1.374	7.32	97.3000	0.5890	0.7830	-0.3340	0.7080	-11.5000	31.4000
170.3874	0.166	-7.22	1.842	5.84	234.0000	1.6600	2.2100	0.5250	2.1400	-11.0000	33.6000
170.4291	0.274	27.5	1.919	4.99	276.0000	3.2200	4.2900	3.2100	2.8400	-7.8000	36.4000
170.4708	0.458	58.27	1.934	4.58	290.0000	5.6700	7.5300	7.4000	1.4000	-0.3980	37.8000
170.5125	0.757	60.02	2.124	3.77	399.0000	12.9000	17.2000	17.0000	2.6800	16.6000	40.5000
170.5542	0.589	58.13	1.956	3.76	321.0000	8.0700	10.7000	10.5000	2.0200	27.1000	42.5000
170.5959	0.297	43.8	1.869	4.81	260.0000	3.3000	4.3800	3.9700	1.8700	31.0000	44.4000
170.6376	0.16	-10.25	1.692	6.32	181.0000	1.2400	1.6400	0.3060	1.6100	31.4000	46.0000
170.6793	0.155	-43.07	1.552	7.47	135.0000	0.8900	1.1800	-0.4450	1.1000	30.9000	47.1000
170.721	0.129	-63.4	1.603	7	151.0000	0.8290	1.1000	-0.7430	0.8140	30.2000	47.9000
170.7627	0.125	-54.23	1.464	7.26	116.0000	0.6190	0.8220	-0.4510	0.6880	29.7000	48.6000
170.8044	0.13	-62.35	1.6	7.85	144.0000	0.7980	1.0600	-0.7010	0.7960	29.0000	49.4000
170.8461	0.139	-66.47	1.569	7.71	137.0000	0.8150	1.0800	-0.7730	0.7600	28.2000	50.2000
170.8878	0.149	-60.65	1.553	6.61	141.0000	0.8930	1.1900	-0.7580	0.9140	27.5000	51.1000
170.9295	0.18	-51.64	1.541	6.14	141.0000	1.0900	1.4500	-0.7380	1.2500	26.7000	52.3000
170.9712	0.221	30.41	1.815	4.83	240.0000	2.2600	3.0000	2.3500	1.8700	29.1000	54.2000
171.0129	0.25	17.07	1.642	5.02	180.0000	1.9200	2.5500	1.5800	2.0100	30.7000	56.2000
171.0546	0.228	7.37	1.765	5.3	215.0000	2.1000	2.7900	1.3200	2.4500	32.0000	58.7000
171.0963	0.162	-22.2	1.734	4.87	211.0000	1.4600	1.9400	-0.0406	1.9400	32.0000	60.6000
171.138	0.141	-65.31	1.527	6.5	135.0000	0.8160	1.0800	-0.7580	0.7760	31.2000	61.4000
171.1797	0.156	-62.02	1.386	7.24	100.0000	0.6660	0.8850	-0.5810	0.6680	30.6000	62.0000
171.2214	0.135	-54.07	1.21	8.32	65.5000	0.3770	0.5020	-0.2740	0.4210	30.3000	62.5000
171.2631	0.113	-60.58	1.236	8.65	68.6000	0.3310	0.4400	-0.2800	0.3390	30.1000	62.8000
171.3048	0.097	-56.65	1.194	8.86	61.8000	0.2550	0.3390	-0.1980	0.2760	29.9000	63.1000
171.3465	0.099	-58.87	1.064	9.35	44.0000	0.1860	0.2470	-0.1520	0.1950	29.7000	63.3000
171.3882	0.107	-74.07	1.094	8.12	50.0000	0.2280	0.3040	-0.2430	0.1820	29.5000	63.4000
171.4299	0.129	-51.56	1.226	7.16	71.7000	0.3930	0.5230	-0.2660	0.4500	29.2000	63.9000
171.4716	0.141	-52.43	1.228	7.15	72.0000	0.4330	0.5750	-0.3000	0.4910	28.9000	64.4000

171.5133	0.131	-19.99	1.434	5.09	124.0000	0.6990	0.9290	0.0164	0.9290	28.9000	65.3000
171.555	0.208	-30.36	1.394	5.95	109.0000	0.9680	1.2900	-0.2090	1.2700	28.7000	66.6000
171.5967	0.205	-34.72	1.338	5.96	97.3000	0.8530	1.1300	-0.2690	1.1000	28.4000	67.7000
171.6384	0.141	-66.34	1.225	7.25	71.2000	0.4270	0.5680	-0.4040	0.3990	28.0000	68.1000
171.6801	0.064	-55.28	1.01	7.8	40.6000	0.1110	0.1480	-0.0832	0.1220	28.0000	68.2000
171.7218	0.049	-74.15	0.938	9.03	31.3000	0.0648	0.0862	-0.0689	0.0517	27.9000	68.3000
171.7635	0.067	-64.13	0.868	8.97	25.2000	0.0718	0.0954	-0.0652	0.0696	27.8000	68.3000
171.8052	0.08	-62.33	0.863	9.7	24.0000	0.0818	0.1090	-0.0718	0.0817	27.8000	68.4000
171.8469	0.103	-72.7	0.882	9.61	25.7000	0.1130	0.1500	-0.1170	0.0928	27.6000	68.5000
171.8886	0.113	-63.18	0.839	8.69	23.1000	0.1120	0.1490	-0.0999	0.1100	27.5000	68.6000
171.9303	0.123	-63.01	0.969	8.14	35.6000	0.1870	0.2490	-0.1670	0.1850	27.4000	68.8000
171.972	0.099	-60.21	0.929	8.71	30.9000	0.1310	0.1740	-0.1100	0.1350	27.3000	68.9000
172.0137	0.143	-53.3	1.107	6.8	55.1000	0.3370	0.4480	-0.2400	0.3790	27.0000	69.3000
172.0554	0.135	-47.45	1.146	6.97	60.1000	0.3470	0.4610	-0.2050	0.4120	26.8000	69.7000
172.0971	0.19	-30.37	1.07	7.02	49.6000	0.4030	0.5360	-0.0873	0.5290	26.7000	70.3000
172.1388	0.106	-68.11	1.068	7.03	49.3000	0.2230	0.2970	-0.2180	0.2020	26.5000	70.5000
172.1805	0.05	-57.74	0.912	8.57	29.5000	0.0629	0.0836	-0.0500	0.0670	26.5000	70.5000
172.2222	0.028	-26.35	0.798	8.66	20.1000	0.0242	0.0322	-0.0030	0.0321	26.5000	70.6000
172.2639	0.049	-38.77	0.782	9.24	18.4000	0.0389	0.0517	-0.0158	0.0492	26.4000	70.6000
172.3056	0.064	-49.81	0.78	9.85	17.9000	0.0486	0.0646	-0.0311	0.0566	26.4000	70.7000
172.3473	0.07	-57.44	0.807	9.78	19.8000	0.0592	0.0786	-0.0467	0.0633	26.4000	70.7000
172.389	0.108	-50.65	0.858	10.67	22.8000	0.1050	0.1400	-0.0691	0.1210	26.3000	70.9000
172.4307	0.091	-55.03	0.861	9.48	24.1000	0.0937	0.1250	-0.0698	0.1030	26.2000	71.0000
172.4724	0.104	-56.06	0.814	8.86	21.1000	0.0935	0.1240	-0.0714	0.1020	26.2000	71.1000
172.5141	0.086	-63.66	0.914	8.5	29.8000	0.1090	0.1450	-0.0979	0.1060	26.1000	71.2000
172.5558	0.08	-44.94	0.925	8.13	31.2000	0.1060	0.1410	-0.0573	0.1290	26.0000	71.3000
172.5975	0.109	-48.96	1.059	7.62	46.7000	0.2180	0.2900	-0.1360	0.2560	25.9000	71.5000
172.6392	0.157	-31.19	0.865	9.19	24.7000	0.1660	0.2210	-0.0390	0.2170	25.8000	71.8000
172.6809	0.162	-33.04	0.98	8.54	36.1000	0.2490	0.3320	-0.0692	0.3240	25.8000	72.1000
172.7226	0.054	-70.86	0.894	9.37	26.9000	0.0620	0.0824	-0.0630	0.0531	25.7000	72.1000
172.7643	0.079	-69.85	0.771	9.99	17.2000	0.0576	0.0766	-0.0577	0.0504	25.6000	72.2000
172.806	0.104	-66.15	1.028	9.55	39.6000	0.1750	0.2330	-0.1650	0.1640	25.5000	72.4000
172.8477	0.099	-63.33	0.955	10.54	31.1000	0.1310	0.1750	-0.1180	0.1290	25.3000	72.5000
172.8894	0.111	-71.16	0.936	10.82	29.1000	0.1380	0.1840	-0.1410	0.1180	25.2000	72.6000
172.9311	0.105	-60.75	0.852	10	22.9000	0.1020	0.1360	-0.0871	0.1050	25.1000	72.7000
172.9728	0.104	-62.52	0.963	10.71	31.6000	0.1410	0.1870	-0.1240	0.1400	25.0000	72.8000

173.0145	0.088	-62.25	0.983	9.58	34.9000	0.1310	0.1740	-0.1150	0.1310	24.9000	73.0000
173.0562	0.09	-59.35	1.051	8.09	44.8000	0.1720	0.2280	-0.1420	0.1790	24.7000	73.2000
173.0979	0.111	-49.33	1.071	8.38	46.6000	0.2200	0.2930	-0.1390	0.2570	24.6000	73.4000
173.1396	0.14	-57.02	0.968	8.38	35.1000	0.2090	0.2780	-0.1640	0.2250	24.4000	73.6000
173.1813	0.179	-40.09	0.962	8.64	34.1000	0.2600	0.3460	-0.1130	0.3270	24.3000	74.0000
173.223	0.057	-80.26	0.85	8.98	23.7000	0.0572	0.0761	-0.0654	0.0389	24.3000	74.0000
173.2647	0.063	-71.45	0.837	9.94	21.8000	0.0586	0.0778	-0.0600	0.0496	24.2000	74.1000
173.3064	0.075	-60.27	0.817	10.21	20.2000	0.0644	0.0856	-0.0542	0.0663	24.1000	74.1000
173.3481	0.1	-73.88	0.904	10.05	27.1000	0.1150	0.1530	-0.1220	0.0926	24.0000	74.2000
173.3898	0.098	-81.26	0.8	9.73	19.3000	0.0804	0.1070	-0.0928	0.0530	23.9000	74.3000
173.4315	0.113	-70.3	0.937	9.48	30.6000	0.1480	0.1970	-0.1500	0.1290	23.8000	74.4000
173.4732	0.114	-64.88	0.969	9.1	34.1000	0.1660	0.2200	-0.1530	0.1590	23.6000	74.6000
173.5149	0.101	-51.99	1.053	8.1	45.0000	0.1940	0.2590	-0.1330	0.2220	23.5000	74.8000
173.5566	0.081	-53.37	0.991	8	38.1000	0.1310	0.1740	-0.0934	0.1470	23.4000	74.9000
173.5983	0.108	-52.72	1.046	7.76	44.9000	0.2060	0.2740	-0.1440	0.2330	23.3000	75.2000
173.64	0.096	-52.74	1.171	6.73	64.6000	0.2650	0.3530	-0.1860	0.3000	23.1000	75.5000
173.6817	0.197	-27.03	1.228	7.4	71.2000	0.5980	0.7950	-0.0835	0.7910	23.0000	76.2000
173.7234	0.146	-52.7	1.045	7.23	45.9000	0.2860	0.3810	-0.2000	0.3240	22.8000	76.6000
173.7651	0.068	-73.35	0.949	9.05	32.2000	0.0935	0.1240	-0.0984	0.0759	22.7000	76.6000
173.8068	0.056	-51.19	0.856	9.35	23.8000	0.0563	0.0749	-0.0377	0.0647	22.6000	76.7000
173.8485	0.047	-53.22	0.854	9.11	23.9000	0.0476	0.0633	-0.0337	0.0535	22.6000	76.8000
173.8902	0.058	-61.97	0.817	9.76	20.5000	0.0510	0.0678	-0.0445	0.0512	22.6000	76.8000
173.9319	0.113	-58.97	0.809	9.61	20.0000	0.0962	0.1280	-0.0787	0.1010	22.5000	76.9000
173.9736	0.121	-49.94	0.791	9.46	18.9000	0.0977	0.1300	-0.0628	0.1140	22.4000	77.0000
174.0153	0.092	-56.18	0.787	8.48	19.4000	0.0764	0.1020	-0.0585	0.0830	22.4000	77.1000

FLUX 1 = 80.28804

SFLUX 2	TIME	CURSPD	CURDIR	WAVEORB	PERIOD	C0	SSLOAD	VOLFLUX	VOL CROSS	VOL LONG	SUM CROSS	SUM LONG
	DAYS	M/S	DEG	M/S	SECS	KG/M3	KG/M/S	M3/M	M3/M	M3/M	M3/M	M3/M
	Note that	the M3 v	Note that the M3 volumes do not include pore spaces									
	162.7531	0.079	-60.79	0.292	11.17	0.7460	0.0025	0.0067	-0.0043	0.0052	0.00	0.01
	162.8365	0.037	165.9	0.264	11.21	0.4470	0.0007	0.0019	-0.0002	-0.0019	0.00	0.00
	162.9199	0.032	243.9	0.368	12.53	1.8000	0.0025	0.0066	-0.0066	-0.0006	-0.01	0.00
	163.0033	0.026	247.4	0.272	12.59	0.4730	0.0005	0.0014	-0.0014	0.0000	-0.01	0.00
	163.0867	0.036	240.6	0.288	12.64	0.6360	0.0010	0.0026	-0.0026	-0.0004	-0.02	0.00
	163.1701	0.018	256.2	0.314	12.35	0.9620	0.0007	0.0020	-0.0020	0.0002	-0.02	0.00
	163.2535	0.058	-60.57	0.286	12.01	0.6380	0.0016	0.0042	-0.0027	0.0032	-0.02	0.01
	163.3369	0.038	134.7	0.252	12.52	0.3090	0.0005	0.0013	0.0005	-0.0012	-0.02	0.00
	163.4203	0.061	117.7	0.294	12.68	0.6940	0.0018	0.0048	0.0032	-0.0036	-0.02	0.00
	163.5037	0.035	84.29	0.231	12.41	0.1680	0.0003	0.0007	0.0007	-0.0002	-0.02	0.00
	163.5871	0.059	246.8	0.308	13.38	0.8270	0.0021	0.0055	-0.0055	-0.0002	-0.02	0.00
	163.6705	0.04	228.6	0.254	12.63	0.3180	0.0005	0.0014	-0.0014	-0.0005	-0.02	0.00
	163.7539	0.075	251.4	0.256	10.83	0.3930	0.0013	0.0033	-0.0033	0.0001	-0.03	0.00
	163.8373	0.17	264.1	0.263	12.99	0.3820	0.0028	0.0074	-0.0071	0.0019	-0.03	0.00
	163.9207	0.005	101.7	0.198	11.39	0.0319	0.0000	0.0000	0.0000	0.0000	-0.03	0.00
	164.0041	0.017	83.01	0.207	12.71	0.0493	0.0000	0.0001	0.0001	0.0000	-0.03	0.00
	164.0875	0.064	-88.9	0.256	10.06	0.4160	0.0011	0.0030	-0.0028	0.0011	-0.04	0.00
	164.1709	0.007	172	0.224	6.84	0.2810	0.0001	0.0002	-0.0001	-0.0002	-0.04	0.00
	164.2543	0.02	82.78	0.268	7.74	0.6590	0.0006	0.0015	0.0014	-0.0003	-0.03	0.00
	164.3377	0.12	-17.19	0.309	7.85	1.2100	0.0062	0.0166	0.0011	0.0165	-0.03	0.02
	164.4211	0.03	119.1	0.253	8.16	0.4760	0.0006	0.0016	0.0010	-0.0012	-0.03	0.02
	164.5045	0.015	104	0.264	9.02	0.5430	0.0004	0.0010	0.0008	-0.0005	-0.03	0.02
	164.5879	0.043	227.2	0.271	8.82	0.6310	0.0012	0.0031	-0.0029	-0.0011	-0.03	0.02
	164.6713	0.026	221.3	0.266	9.52	0.5370	0.0006	0.0016	-0.0014	-0.0007	-0.04	0.02
	164.7547	0.041	255.6	0.402	6.97	3.3600	0.0058	0.0155	-0.0154	0.0018	-0.05	0.02
	164.8381	0.047	235.4	0.564	8.12	9.0300	0.0180	0.0479	-0.0465	-0.0113	-0.10	0.01
	164.9215	0.011	240.6	0.546	8.8	7.9200	0.0038	0.0100	-0.0099	-0.0015	-0.11	0.00
	165.0049	0.032	236.6	0.455	9.12	4.4100	0.0060	0.0159	-0.0155	-0.0034	-0.12	0.00
	165.0883	0.048	260	0.431	9.19	3.6600	0.0076	0.0202	-0.0198	0.0039	-0.14	0.00
	165.1717	0.022	-86.28	0.543	9.14	7.6700	0.0072	0.0191	-0.0173	0.0080	-0.16	0.01
	165.2551	0.022	-58.32	0.538	8.65	7.6300	0.0070	0.0186	-0.0113	0.0148	-0.17	0.03
	165.3385	0.07	260.5	0.549	8.61	8.1400	0.0243	0.0647	-0.0634	0.0129	-0.23	0.04
	165.4219	0.001	113.8	0.411	8.09	3.3600	0.0002	0.0005	0.0004	-0.0003	-0.23	0.04

165.5053	0.021	217.6	0.38	8.87	2.4400	0.0022	0.0058	-0.0049	-0.0030	-0.24	0.04
165.5887	0.049	245.1	0.353	9.99	1.7500	0.0037	0.0097	-0.0097	-0.0007	-0.25	0.04
165.6721	0.03	266.5	0.369	9.51	2.1200	0.0028	0.0073	-0.0070	0.0022	-0.26	0.04
165.7555	0.028	-82.73	0.422	9.4	3.3900	0.0041	0.0110	-0.0097	0.0052	-0.27	0.04
165.8389	0.155	-17.05	0.436	9.54	3.7500	0.0248	0.0659	0.0045	0.0658	-0.26	0.11
165.9223	0.011	220.5	0.463	10.23	4.4100	0.0020	0.0054	-0.0047	-0.0026	-0.27	0.11
166.0057	0.023	-74.6	0.451	10.12	4.0700	0.0040	0.0107	-0.0086	0.0064	-0.27	0.11
166.0891	0.048	252.4	0.445	10.14	3.8900	0.0079	0.0211	-0.0210	0.0013	-0.30	0.12
166.1725	0.031	246.3	0.474	10.21	4.7700	0.0063	0.0166	-0.0166	-0.0008	-0.31	0.11
166.2559	0.011	-75.8	0.503	10.05	5.7900	0.0028	0.0074	-0.0061	0.0043	-0.32	0.12
166.3393	0.025	-48.01	0.587	10.13	9.3000	0.0098	0.0260	-0.0118	0.0231	-0.33	0.14
166.4227	0.122	-31.32	0.61	9.96	10.5000	0.0547	0.1450	-0.0260	0.1430	-0.36	0.28
166.5061	0.014	243.3	0.474	9.87	4.8400	0.0029	0.0076	-0.0076	-0.0008	-0.36	0.28
166.5895	0.027	250.1	0.518	10.31	6.2900	0.0072	0.0192	-0.0192	0.0004	-0.38	0.28
166.6729	0.027	264.6	0.417	9.5	3.2300	0.0037	0.0099	-0.0095	0.0027	-0.39	0.29
166.7563	0.028	257	0.442	9.26	3.9800	0.0047	0.0126	-0.0125	0.0018	-0.40	0.29
166.8397	0.041	256.1	0.506	9.26	6.1200	0.0109	0.0289	-0.0286	0.0036	-0.43	0.29
166.9231	0.126	-23.34	0.409	8.87	3.1400	0.0169	0.0450	-0.0018	0.0449	-0.44	0.34
167.0065	0.026	229	0.389	8.98	2.6400	0.0029	0.0077	-0.0073	-0.0026	-0.44	0.33
167.0899	0.03	256.1	0.347	9.24	1.7000	0.0022	0.0057	-0.0057	0.0007	-0.45	0.34
167.1733	0.076	270	0.35	9.24	1.7600	0.0057	0.0152	-0.0142	0.0054	-0.46	0.34
167.2567	0.053	235.8	0.334	9.77	1.4400	0.0033	0.0086	-0.0084	-0.0020	-0.47	0.34
167.3401	0.026	234.9	0.408	8.19	3.2600	0.0036	0.0095	-0.0092	-0.0023	-0.48	0.34
167.4235	0.064	-51.44	0.441	6.76	4.6100	0.0126	0.0336	-0.0170	0.0290	-0.50	0.37
167.5069	0.002	190.3	0.449	7.65	4.5900	0.0004	0.0011	-0.0006	-0.0009	-0.50	0.36
167.5903	0.008	-16.89	0.46	8.22	4.7900	0.0017	0.0044	0.0003	0.0044	-0.50	0.37
167.6737	0.065	-88.27	0.505	8.09	6.4700	0.0180	0.0478	-0.0441	0.0185	-0.54	0.39
167.7571	0.072	259.7	0.587	7.82	10.4000	0.0320	0.0852	-0.0837	0.0158	-0.63	0.40
167.8405	0.058	263	0.792	7.96	24.5000	0.0606	0.1610	-0.1560	0.0390	-0.78	0.44
167.9239	0.172	-57.58	0.879	8.23	32.5000	0.2380	0.6340	-0.3780	0.5090	-1.16	0.95
168.0073	0.152	268.6	0.81	8.24	25.8000	0.1670	0.4430	-0.4180	0.1490	-1.58	1.10
168.0907	0.329	253.7	0.69	9.59	15.4000	0.2160	0.5740	-0.5720	0.0470	-2.15	1.15
168.1741	0.24	260.6	0.688	9.46	15.3000	0.1570	0.4170	-0.4090	0.0839	-2.56	1.23
168.2575	0.118	-86.38	0.809	10.06	23.8000	0.1200	0.3180	-0.2890	0.1330	-2.85	1.36
168.3409	0.081	-45.07	0.742	9.58	18.9000	0.0656	0.1740	-0.0712	0.1590	-2.92	1.52
168.4243	0.063	-45.48	0.779	9.07	22.3000	0.0595	0.1580	-0.0656	0.1440	-2.98	1.67

168.5077	0.134	-23.18	0.792	10.2	22.3000	0.1280	0.3400	-0.0129	0.3400	-3.00	2.01
168.5911	0.031	262.4	0.7	10.39	15.5000	0.0206	0.0547	-0.0532	0.0127	-3.05	2.02
168.6745	0.04	258	0.695	10.19	15.3000	0.0258	0.0687	-0.0679	0.0108	-3.12	2.03
168.7579	0.026	263.4	0.722	9.39	17.6000	0.0199	0.0529	-0.0512	0.0132	-3.17	2.04
168.8413	0.023	-66.23	0.703	8.77	16.8000	0.0162	0.0431	-0.0306	0.0303	-3.20	2.07
168.9247	0.032	-18.53	0.888	8.55	33.0000	0.0446	0.1190	0.0051	0.1180	-3.19	2.19
169.0081	0.056	-50.14	0.924	8.98	36.2000	0.0859	0.2280	-0.1110	0.1990	-3.30	2.39
169.0915	0.038	237.1	0.943	8.78	38.7000	0.0635	0.1690	-0.1650	-0.0348	-3.47	2.36
169.1749	0.047	-83.86	0.932	9.87	35.9000	0.0720	0.1920	-0.1700	0.0874	-3.64	2.44
169.2583	0.052	-75.27	0.975	10.23	40.3000	0.0899	0.2390	-0.1940	0.1400	-3.83	2.58
169.3417	0.054	31.03	0.912	9.46	34.3000	0.0785	0.2090	0.1640	0.1280	-3.67	2.71
169.4251	0.058	32.64	1.073	9.26	54.5000	0.1350	0.3580	0.2890	0.2130	-3.38	2.92
169.5085	0.126	-28.49	1.012	8.81	47.1000	0.2530	0.6730	-0.0878	0.6680	-3.47	3.59
169.5919	0.057	251.9	0.891	8.82	33.0000	0.0805	0.2140	-0.2140	0.0108	-3.68	3.60
169.6753	0.043	228.3	0.877	9.19	31.0000	0.0576	0.1530	-0.1430	-0.0542	-3.83	3.55
169.7587	0.089	259.8	0.807	8.57	25.1000	0.0953	0.2530	-0.2490	0.0475	-4.08	3.60
169.8421	0.036	-21.74	0.929	9.07	36.7000	0.0559	0.1490	-0.0019	0.1490	-4.08	3.74
169.9255	0.045	-9.58	1.081	8.59	57.1000	0.1100	0.2930	0.0581	0.2870	-4.02	4.03
170.0089	0.114	48.01	1.05	9.09	51.7000	0.2510	0.6670	0.6230	0.2390	-3.40	4.27
170.0923	0.096	257.6	1.026	9.29	48.1000	0.1970	0.5250	-0.5190	0.0785	-3.91	4.35
170.1757	0.004	267.7	1.023	10.43	45.8000	0.0078	0.0208	-0.0197	0.0067	-3.93	4.36
170.2591	0.092	-74.48	1.016	10.76	44.5000	0.1750	0.4650	-0.3740	0.2770	-4.31	4.63
170.3425	0.084	-85.07	0.972	10.39	39.7000	0.1420	0.3770	-0.3390	0.1650	-4.65	4.80
170.4259	0.065	-28.86	1.347	10.1	99.7000	0.2750	0.7310	-0.1000	0.7240	-4.75	5.52
170.5093	0.502	68	1.583	8.64	164.0000	3.5100	9.3300	9.3200	0.1630	4.58	5.68
170.5927	0.354	69.19	1.315	9.8	94.2000	1.4200	3.7900	3.7900	-0.0126	8.36	5.67
170.6761	0.074	-78.42	1.079	11.46	51.5000	0.1620	0.4310	-0.3630	0.2320	8.00	5.90
170.7595	0.067	260.3	1.163	11.12	64.2000	0.1850	0.4910	-0.4820	0.0963	7.52	6.00
170.8429	0.09	-83.57	1.244	11.75	76.2000	0.2930	0.7780	-0.6910	0.3580	6.83	6.36
170.9263	0.072	-60.09	1.035	10.78	46.8000	0.1440	0.3830	-0.2410	0.2970	6.59	6.66
171.0097	0.166	11.71	1.127	11.09	58.9000	0.4170	1.1100	0.5990	0.9320	7.19	7.59
171.0931	0.097	-53.8	1.251	9.55	82.7000	0.3420	0.9090	-0.4920	0.7640	6.69	8.35
171.1765	0.051	-72.38	0.989	10.93	41.0000	0.0896	0.2380	-0.1860	0.1490	6.51	8.50
171.2599	0.067	250.7	0.918	11.64	32.5000	0.0929	0.2470	-0.2470	0.0073	6.26	8.51
171.3433	0.075	264.3	0.87	10.94	28.5000	0.0918	0.2440	-0.2360	0.0644	6.02	8.57
171.4267	0.074	266.4	0.962	10.55	38.4000	0.1220	0.3230	-0.3080	0.0966	5.72	8.67

171.5101	0.104	-85.8	1.177	9.86	69.1000	0.3050	0.8120	-0.7340	0.3460	4.98	9.01
171.5935	0.11	-82.32	0.996	10.16	42.9000	0.2020	0.5360	-0.4700	0.2570	4.51	9.27
171.6769	0.044	257.1	0.82	10.32	24.5000	0.0460	0.1220	-0.1210	0.0172	4.39	9.29
171.7603	0.044	225.8	0.686	11.13	14.2000	0.0267	0.0710	-0.0652	-0.0280	4.33	9.26
171.8437	0.058	257.9	0.753	11.63	18.4000	0.0454	0.1210	-0.1190	0.0187	4.21	9.28
171.9271	0.071	269.7	0.738	11.02	17.7000	0.0532	0.1420	-0.1320	0.0500	4.07	9.33
172.0105	0.081	-80.61	0.846	10.5	26.7000	0.0919	0.2440	-0.2110	0.1240	3.86	9.45
172.0939	0.172	-39.71	0.808	10.67	23.3000	0.1710	0.4560	-0.1460	0.4320	3.72	9.89
172.1773	0.034	230.7	0.688	9.98	15.0000	0.0215	0.0573	-0.0544	-0.0180	3.66	9.87
172.2607	0.023	213	0.642	11.17	11.7000	0.0114	0.0303	-0.0245	-0.0178	3.64	9.85
172.3441	0.038	251.9	0.653	11.11	12.3000	0.0200	0.0533	-0.0532	0.0027	3.58	9.85
172.4275	0.045	253.4	0.669	12	12.9000	0.0248	0.0659	-0.0657	0.0051	3.52	9.86
172.5109	0.032	261.5	0.703	11	15.3000	0.0206	0.0548	-0.0535	0.0119	3.47	9.87
172.5943	0.067	-80.03	0.763	11.74	19.0000	0.0541	0.1440	-0.1230	0.0740	3.34	9.94
172.6777	0.056	-83.73	0.736	11.99	17.0000	0.0407	0.1080	-0.0963	0.0496	3.25	9.99
172.7611	0.071	236	0.596	12.9	8.8400	0.0268	0.0711	-0.0693	-0.0160	3.18	9.98
172.8445	0.069	262.5	0.741	13.42	16.7000	0.0493	0.1310	-0.1270	0.0306	3.05	10.00
172.9279	0.063	263.8	0.676	12.2	13.1000	0.0356	0.0946	-0.0915	0.0242	2.96	10.00
173.0113	0.049	-86.67	0.728	11.3	16.9000	0.0356	0.0946	-0.0862	0.0390	2.87	10.10
173.0947	0.041	260.8	0.757	11.07	19.0000	0.0329	0.0875	-0.0856	0.0179	2.79	10.10
173.1781	0.126	-66.4	0.779	11.97	20.1000	0.1080	0.2870	-0.2040	0.2010	2.58	10.30
173.2615	0.066	232.4	0.689	12.91	13.6000	0.0382	0.1020	-0.0973	-0.0290	2.48	10.30
173.3449	0.071	241.9	0.594	13.29	8.6100	0.0263	0.0699	-0.0694	-0.0086	2.41	10.30
173.4283	0.088	265.7	0.664	13.5	12.0000	0.0450	0.1200	-0.1150	0.0344	2.30	10.30
173.5117	0.081	-82.62	0.875	11.76	28.3000	0.0983	0.2610	-0.2300	0.1240	2.07	10.40
173.5951	0.06	-73.71	0.816	10.92	23.7000	0.0605	0.1610	-0.1280	0.0975	1.94	10.50
173.6785	0.115	-13.31	0.828	10.37	25.2000	0.1240	0.3290	0.0440	0.3260	1.99	10.80
173.7619	0.101	240.1	0.809	11.81	22.5000	0.0970	0.2580	-0.2550	-0.0399	1.73	10.80
173.8453	0.038	214.1	0.634	12.07	10.9000	0.0176	0.0468	-0.0384	-0.0268	1.69	10.80
173.9287	0.034	251.6	0.592	11.62	9.0100	0.0133	0.0353	-0.0352	0.0016	1.66	10.80
174.0121	0.052	239.2	0.6	10.41	9.8100	0.0217	0.0578	-0.0569	-0.0098	1.60	10.80
174.0955	0.04	266.8	0.698	10.62	15.2000	0.0263	0.0699	-0.0665	0.0214	1.53	10.80
174.1789	0.078	-64.69	0.683	10.66	14.3000	0.0477	0.1270	-0.0876	0.0917	1.45	10.90
174.2623	0.062	230.9	0.593	10.73	9.3700	0.0248	0.0658	-0.0626	-0.0205	1.38	10.90
174.3457	0.036	225.7	0.49	11.58	5.0100	0.0076	0.0203	-0.0186	-0.0080	1.37	10.80

FLUX 2= 10.88655

SFLUX 3

TIME DAYS	CURSPD M/S	CURDIR DEG	WAVEORB M/S	PERIOD SECS	C0 KG/M3	SSLOAD KG/M/S	VOLFLUX M3/M	VOL CROSS M3/M	VOL LONG M3/M	SUM CROSS M3/M	SUM LONG M3/M
Note that the M3 volumes do not include pore spaces											
163.0865	0.035	242.7	0.228	11.54	0.6610	0.0010	0.0053	-0.0053	-0.0006	-0.01	0.00
163.2532	0.104	-1.45	0.223	10.87	0.6150	0.0027	0.0145	0.0049	0.0137	0.00	0.01
163.4199	0.063	122.3	0.23	11.66	0.6880	0.0019	0.0099	0.0059	-0.0079	0.01	0.01
163.5866	0.025	98.56	0.232	12.7	0.6730	0.0007	0.0038	0.0033	-0.0019	0.01	0.00
163.7533	0.044	121.2	0.208	10.84	0.4330	0.0008	0.0043	0.0026	-0.0034	0.01	0.00
163.92	0.012	251.3	0.157	11.29	0.0316	0.0000	0.0001	-0.0001	0.0000	0.01	0.00
164.0867	0.008	-38.21	0.205	7.07	0.5680	0.0002	0.0011	-0.0003	0.0010	0.01	0.00
164.2534	0.042	106.3	0.213	5.4	0.8510	0.0015	0.0082	0.0065	-0.0049	0.02	0.00
164.4201	0.014	108.4	0.198	6.03	0.5560	0.0003	0.0018	0.0014	-0.0012	0.02	-0.01
164.5868	0.049	239.6	0.217	7.09	0.7430	0.0016	0.0083	-0.0082	-0.0014	0.01	-0.01
164.7535	0.046	257.2	0.305	5.91	3.0900	0.0061	0.0325	-0.0322	0.0046	-0.02	0.00
164.9202	0.046	111.8	0.449	7.09	9.6600	0.0188	0.1000	0.0734	-0.0680	0.05	-0.07
165.0869	0.042	256.4	0.356	7.32	4.6500	0.0084	0.0448	-0.0444	0.0058	0.01	-0.06
165.2536	0.018	23.54	0.435	7.25	8.7000	0.0066	0.0350	0.0245	0.0249	0.03	-0.04
165.4203	0.016	59.02	0.367	7.64	5.0000	0.0034	0.0178	0.0176	0.0031	0.05	-0.04
165.587	0.015	228.9	0.302	8.29	2.5200	0.0016	0.0087	-0.0082	-0.0030	0.04	-0.04
165.7537	0.005	-77.77	0.341	7.92	3.9000	0.0008	0.0044	-0.0037	0.0024	0.04	-0.04
165.9204	0.02	22.13	0.403	8.91	6.3000	0.0053	0.0280	0.0192	0.0205	0.06	-0.02
166.0871	0.041	241.1	0.38	9.1	5.2100	0.0092	0.0488	-0.0484	-0.0067	0.01	-0.02
166.2538	0.014	203.5	0.398	9.11	6.0200	0.0037	0.0195	-0.0137	-0.0139	-0.01	-0.04
166.4205	0.062	-6.2	0.5	8.68	12.3000	0.0328	0.1740	0.0445	0.1680	0.04	0.13
166.5872	0.018	241.8	0.449	9.28	8.6700	0.0067	0.0358	-0.0355	-0.0045	0.00	0.13
166.7539	0.019	162.8	0.366	8.67	4.6900	0.0037	0.0197	-0.0013	-0.0197	0.00	0.11
166.9206	0.069	-8.08	0.332	7.7	3.5900	0.0106	0.0562	0.0126	0.0548	0.02	0.16
167.0873	0.019	262.4	0.286	8.24	2.0800	0.0017	0.0089	-0.0086	0.0021	0.01	0.16
167.254	0.084	244.7	0.262	8.43	1.4700	0.0053	0.0280	-0.0279	-0.0021	-0.02	0.16
167.4207	0.068	-42.85	0.331	5.49	4.2300	0.0123	0.0654	-0.0243	0.0607	-0.05	0.22
167.5874	0.006	0.32	0.377	6.03	6.1200	0.0016	0.0086	0.0031	0.0080	-0.04	0.23
167.7541	0.115	261.8	0.46	6	11.2000	0.0550	0.2920	-0.2850	0.0647	-0.33	0.30
167.9208	0.162	-66.59	0.652	6.67	29.3000	0.2030	1.0800	-0.7690	0.7540	-1.10	1.05
168.0875	0.371	256.2	0.532	7.65	15.5000	0.2460	1.3100	-1.3000	0.1640	-2.39	1.21
168.2542	0.21	261.9	0.612	7.53	23.4000	0.2100	1.1200	-1.0900	0.2490	-3.48	1.46
168.4209	0.032	-55.77	0.582	7.22	20.6000	0.0284	0.1510	-0.0861	0.1240	-3.57	1.59

168.5876	0.029	240	0.531	7.55	15.5000	0.0192	0.1020	-0.1010	-0.0160	-3.67	1.57
168.7543	0.018	205.7	0.554	7.24	17.8000	0.0134	0.0713	-0.0519	-0.0489	-3.72	1.52
168.921	0.024	-42.51	0.685	6.7	33.6000	0.0350	0.1860	-0.0682	0.1730	-3.79	1.69
169.0877	0.019	162.4	0.688	7.33	32.9000	0.0266	0.1410	-0.0084	-0.1410	-3.80	1.55
169.2544	0.03	-82.4	0.755	7.88	41.8000	0.0534	0.2840	-0.2490	0.1360	-4.05	1.69
169.4211	0.031	76.07	0.822	6.9	55.6000	0.0736	0.3910	0.3880	-0.0481	-3.66	1.64
169.5878	0.111	245.6	0.761	7.2	44.1000	0.2090	1.1100	-1.1100	-0.0658	-4.77	1.58
169.7545	0.059	263.8	0.619	6.99	24.9000	0.0624	0.3320	-0.3210	0.0848	-5.09	1.66
169.9212	0.029	20.11	0.798	7.7	49.2000	0.0611	0.3250	0.2140	0.2450	-4.87	1.91
170.0879	0.122	256.4	0.835	8.51	54.0000	0.2820	1.5000	-1.4900	0.1930	-6.36	2.10
170.2546	0.087	-78.78	0.874	9.15	59.9000	0.2240	1.1900	-1.0100	0.6350	-7.37	2.73
170.4213	0.059	256.5	0.979	9.04	82.5000	0.2070	1.1000	-1.0900	0.1430	-8.46	2.88
170.588	0.01	62.38	1.029	8.42	97.0000	0.0435	0.2310	0.2300	0.0267	-8.23	2.90
170.7547	0.05	220.5	0.916	9.68	67.1000	0.1430	0.7570	-0.6660	-0.3610	-8.89	2.54
170.9214	0.025	-65.59	0.842	9.59	53.2000	0.0578	0.3070	-0.2160	0.2190	-9.11	2.76
171.0881	0.03	-58.46	1.009	8.2	92.6000	0.1170	0.6230	-0.3790	0.4940	-9.49	3.25
171.2548	0.019	256.7	0.757	10.29	38.4000	0.0310	0.1650	-0.1630	0.0221	-9.65	3.28
171.4215	0.026	218.9	0.773	8.58	43.3000	0.0477	0.2540	-0.2190	-0.1270	-9.87	3.15
171.5882	0.021	40.76	0.748	8.13	40.2000	0.0361	0.1920	0.1690	0.0908	-9.70	3.24
171.7549	0.016	205.1	0.567	9.43	17.2000	0.0117	0.0622	-0.0448	-0.0431	-9.74	3.20
171.9216	0.079	262.1	0.59	9.2	19.5000	0.0656	0.3490	-0.3400	0.0791	-10.10	3.28
172.0883	0.122	-54.11	0.595	8.57	20.6000	0.1070	0.5700	-0.3110	0.4770	-10.40	3.75
172.255	0.027	116.3	0.499	9.14	12.0000	0.0137	0.0728	0.0494	-0.0535	-10.30	3.70
172.4217	0.032	233.7	0.534	9.15	14.6000	0.0197	0.1050	-0.1010	-0.0276	-10.40	3.67
172.5884	0.025	-88.97	0.565	8.25	17.9000	0.0196	0.1040	-0.0963	0.0390	-10.50	3.71
172.7551	0.073	222.2	0.48	9.37	10.6000	0.0330	0.1760	-0.1570	-0.0791	-10.70	3.63
172.9218	0.051	264.3	0.539	8.61	15.4000	0.0332	0.1760	-0.1700	0.0466	-10.90	3.68
173.0885	0.055	264.9	0.593	7.66	21.2000	0.0497	0.2640	-0.2540	0.0724	-11.10	3.75
173.2552	0.109	226.3	0.569	9.92	17.2000	0.0801	0.4260	-0.3930	-0.1640	-11.50	3.59
173.4219	0.121	-89.27	0.507	10.38	12.0000	0.0619	0.3290	-0.3050	0.1220	-11.80	3.71
173.5886	0.058	-55.03	0.603	7.58	22.4000	0.0551	0.2930	-0.1640	0.2430	-12.00	3.95
173.7553	0.02	255.1	0.621	8.38	23.4000	0.0204	0.1090	-0.1080	0.0115	-12.10	3.96
173.922	0.04	225	0.458	9.23	9.2100	0.0157	0.0837	-0.0764	-0.0340	-12.20	3.93
174.0887	0.01	125.3	0.536	9.18	14.8000	0.0061	0.0325	0.0181	-0.0271	-12.20	3.90
174.2554	0.042	166	0.468	8	10.4000	0.0188	0.1000	-0.0122	-0.0993	-12.20	3.80

FLUX 3 = 12.77811

APPENDIX 11: Raw Data on CD